



<https://theses.gla.ac.uk/>

Theses Digitisation:

<https://www.gla.ac.uk/myglasgow/research/enlighten/theses/digitisation/>

This is a digitised version of the original print thesis.

Copyright and moral rights for this work are retained by the author

A copy can be downloaded for personal non-commercial research or study, without prior permission or charge

This work cannot be reproduced or quoted extensively from without first obtaining permission in writing from the author

The content must not be changed in any way or sold commercially in any format or medium without the formal permission of the author

When referring to this work, full bibliographic details including the author, title, awarding institution and date of the thesis must be given

Enlighten: Theses

<https://theses.gla.ac.uk/>  
[research-enlighten@glasgow.ac.uk](mailto:research-enlighten@glasgow.ac.uk)

FLUORIDE ION SUPPORTED ON Y-ALUMINA :

CHARACTERIZATION AND CATALYTIC ACTIVITY

VOLUME ONE

THESIS SUBMITTED TO THE UNIVERSITY OF GLASGOW IN

FULFILMENT OF THE REQUIREMENT OF THE DEGREE OF DOCTOR OF PHILOSOPHY

BY

ABDALLAH BENDADA BSc.

DEPARTMENT OF CHEMISTRY

UNIVERSITY OF GLASGOW

MAY 1990

© ABDALLAH BENDADA

ProQuest Number: 11007364

All rights reserved

INFORMATION TO ALL USERS

The quality of this reproduction is dependent upon the quality of the copy submitted.

In the unlikely event that the author did not send a complete manuscript and there are missing pages, these will be noted. Also, if material had to be removed, a note will indicate the deletion.



ProQuest 11007364

Published by ProQuest LLC (2018). Copyright of the Dissertation is held by the Author.

All rights reserved.

This work is protected against unauthorized copying under Title 17, United States Code  
Microform Edition © ProQuest LLC.

ProQuest LLC.  
789 East Eisenhower Parkway  
P.O. Box 1346  
Ann Arbor, MI 48106 – 1346

## ACKNOWLEDGEMENTS

It is with great pleasure that I would like to express my sincere thanks to my supervisors, Professor G. Webb and Dr J.M. Winfield for the valuable advice, constructive criticism and encouragement provided during the course of this work.

Thanks are also due to the many members of staff who have contributed in some way. In particular, to Dr T. Baird for performing the transmission electron microscopy work and George (Department of Geology) for his assistance with the X-ray diffraction analyses. Pat Gibbs is also acknowledged for her efficient and fast typing of the most difficult part of this thesis, which Mrs Liz Hughes could not complete.

I would also like to thank all my friends and colleagues in the fluorine and catalysis groups for their advice and friendship throughout my period of study.

Ultimately, I am indebted to my parents for my first lessons in understanding the value and importance of education and science.

## SUMMARY

i

CHAPTER ONE

## INTRODUCTION

1.1	Acid-Base Concepts	1
1.1.1	Brønsted-Lowry Definition of Acids and Bases	2
1.1.2	Lewis Acid-Base Definition	3
1.1.3	The Application of Acid-Base Reactions to Heterogeneous Systems	5
1.1.4	The Aims of the Present Work	6
1.2	Some Chemistry of the Reagents	7
1.2.1	Chlorine Monofluoride	8
1.2.2	Anhydrous Hydrogen Fluoride	9
1.2.3	Carbonyl Fluoride	11
1.2.4	Carbon Dioxide	12
1.2.5	Thionyl Fluoride	14
1.2.6	Sulphur Dioxide	15
1.2.7	Sulphur Tetrafluoride	16
1.2.8	Sulphur Chloride Pentafluoride	19
1.2.9	Chlorofluorination of Sulphur Tetrafluoride with Chlorine Monofluoride	20
1.2.10	Alkali Metal Fluorides	23
1.3	Alumina	28
1.3.1	Types of Alumina	28
1.3.2	Preparation of $\gamma$ -Alumina	30
1.3.3	Structure of $\gamma$ -Alumina	31
1.4	Previous Work Using Caesium and Potassium Fluoride Supported on $\gamma$ -Alumina	32

CHAPTER TWO

## EXPERIMENTAL

2.1	Equipment	36
2.1.1	Vacuum Systems	36
2.1.2	Gas Uptake Apparatus	38
2.1.3	Temperature Measurement	39
2.1.4	The Inert Atmosphere Box	39
2.1.5	Infra-Red Spectroscopy	39
2.1.6	Electron Microscopy	40
2.1.7	Raman Spectroscopy	42
2.1.8	Solid State $^{27}\text{Al}$ NMR Spectroscopy	42
2.1.9	X-Ray Diffraction	43
2.2	Preparation and Purification of Reagents	43
2.2.1	Purification of Acetonitrile	43
2.2.2	Purification of Diethyl Ether	44
2.2.3	Purification of Pyridine	44
2.2.4	Purification of Sulphur Dichloride	44
2.2.5	Purification of Carbon and Sulphur Dioxides	45
2.2.6	Preparation and Purification of Chlorine Monofluoride	45
2.2.7	Preparation of Sodium Tetrafluoroborate	46
2.2.8	Preparation and Purification of Boron Trifluoride	46
2.2.9	Preparation and Purification of Iodine Pentafluoride	48
2.2.10	Preparation and Purification of Sulphur Tetrafluoride	49
2.2.11	Preparation and Purification of Sulphur Chloride Pentafluoride	51

2.2.12	Preparation and Purification of Carbonyl Fluoride	51
2.2.13	Preparation and Purification of Thionyl Fluoride	52
2.2.14	Preparation of Penta- and Hexa-fluoroaluminates	53
2.2.15	Preparation of Ammonium Tetrafluoroaluminate	53
2.3	Radiochemical Techniques	54
2.3.1	Isotopic Exchange Reaction	55
2.3.2	Choice of Isotope	58
2.3.3	The Radioisotope [ $^{18}\text{F}$ ]-Fluorine	58
2.3.4	The Radioisotope [ $^{36}\text{Cl}$ ]-Chlorine	60
2.3.5	The Radioisotope [ $^{14}\text{C}$ ]-Carbon	60
2.3.6	The Radioisotope [ $^{35}\text{S}$ ]-Sulphur	61
2.4	Background	61
2.5	Statistical Errors	62
2.6	Counting of [ $^{14}\text{C}$ ]-Carbon, [ $^{36}\text{Cl}$ ]-Chlorine and [ $^{35}\text{S}$ ]-Sulphur Samples	63
2.6.1	Geiger-Müller Counters	63
2.6.2	Plateau Curve	64
2.6.3	Dead Time	64
2.6.4	The Direct Monitoring Geiger-Müller Counters	66
2.6.5	Application of the Technique to Experiments Involving Supported Metal Fluoride	67
2.7	Counting of [ $^{18}\text{F}$ ]-Fluorine Samples	68
2.7.1	Scintillation Counters	68
2.7.2	Decay Correction	70
2.7.3	[ $^{18}\text{F}$ ]-Fluorine Counting Apparatus	71
2.7.4	Application to Reactions Involving Supported Metal Fluoride	71

2.8	Preparation of Radiochemically Labelled Species	72
2.8.1	Preparation of [ <sup>18</sup> F]-Fluorine Labelled Caesium Fluoride	72
2.8.2	Preparation of [ <sup>18</sup> F]-Fluorine Labelled Hydrogen Fluoride, Boron Trifluoride, Carbonyl Fluoride, Sulphur Tetrafluoride and Thionyl Fluoride	73
2.8.3	Preparation of [ <sup>36</sup> Cl]-Dichlorine	75
2.8.4	Preparation and Purification of [ <sup>36</sup> Cl]-Chlorine Labelled Chlorine Monofluoride	76
2.8.5	Preparation and Purification of [ <sup>35</sup> S]-Sulphur Labelled Sulphur Tetrafluoride, Thionyl Fluoride and Sulphur Dioxide	76
2.8.6	Preparation and Purification of [ <sup>35</sup> S]-Sulphur and [ <sup>36</sup> Cl]-Chlorine Labelled Sulphur Chloride Pentafluoride	78
2.8.7	Preparation and Purification of [ <sup>14</sup> C]-Carbon Labelled Carbon Dioxide	79
2.8.8	Preparation of [ <sup>14</sup> C]-Carbon Labelled Carbonyl Fluoride	79

### CHAPTER THREE

#### PREPARATION AND PRETREATMENT OF CATALYSTS

3.1	Preparation of Caesium or Potassium Fluoride Supported on $\gamma$ -Alumina	81
3.1.1	Preparation of Caesium or Potassium Fluoride Supported on $\gamma$ -Alumina from Aqueous Solution	81
3.1.2	Preparation of Caesium or Potassium Fluoride Supported on $\gamma$ -Alumina from Non-Aqueous Solution	82



3.1.3	Dry Preparation of Caesium and Potassium Fluoride Supported on $\gamma$ -Alumina	83
3.2	Treatment of Caesium and Potassium Fluoride Supported on $\gamma$ -Alumina	84
3.2.1	Fluorination of $\gamma$ -Alumina Supported Caesium or Potassium Fluoride with Sulphur Tetrafluoride, Thionyl Fluoride and Carbonyl Fluoride	84
3.2.2	Treatment of $\gamma$ -Alumina Supported Caesium or Potassium Fluoride with Anhydrous Hydrogen Fluoride and Sulphur Dioxide then Anhydrous Hydrogen Fluoride	86
3.3	Fluorination of $\gamma$ -Alumina by Anhydrous Hydrogen Fluoride, Sulphur Tetrafluoride, Thionyl Fluoride and Carbonyl Fluoride	88

#### CHAPTER FOUR

#### THE PHYSICAL EXAMINATION OF $\gamma$ -ALUMINA SUPPORTED CAESIUM OR POTASSIUM FLUORIDE, FLUORINATED $\gamma$ -ALUMINA SUPPORTED CAESIUM OR POTASSIUM FLUORIDE AND FLUORINATED $\gamma$ -ALUMINA

4.1	B.E.T. Area	90
4.1.1	Surface Area Determination by the B.E.T. Method	90
4.1.2	B.E.T. Area of Caesium or Potassium Fluoride Supported on $\gamma$ -Alumina	95
4.1.3	B.E.T. Area of $\gamma$ -Alumina Treated with Anhydrous Hydrogen Fluoride, Sulphur Tetrafluoride, Thionyl Fluoride or Carbonyl Fluoride	100

4.1.4	B.E.T. Area of Caesium or Potassium Fluoride Supported on $\gamma$ -Alumina Treated with Sulphur Tetrafluoride, Thionyl Fluoride Anhydrous Hydrogen Fluoride, Carbonyl Fluoride or Liquid Sulphur Dioxide then Anhydrous Hydrogen Fluoride	101
4.2.	X-Ray Powder Diffraction Study	103
4.2.1	X-Ray Powder Diffraction of Spinel $\gamma$ -Alumina Calcined to 523 K and $\gamma$ -Alumina Treated with Sulphur Tetrafluoride, Thionyl Fluoride, Carbonyl Fluoride or Anhydrous Hydrogen Fluoride	103
4.2.2	X-Ray Powder Diffraction of Caesium or Potassium Fluoride Supported on $\gamma$ -Alumina or Fluorinated $\gamma$ -Alumina Supported Caesium or Potassium Fluoride	105
4.3	Transmission Electron Microscopy	106
4.3.1	Transmission Electron Microscopy of Caesium or Potassium Fluoride Supported on $\gamma$ -Alumina or Fluorinated $\gamma$ -Alumina	107
4.4	Solid State Magic Angle Spinning Aluminium-27 Nuclear Magnetic Resonance	109
4.4.1	Aluminium-27, MAS-NMR Study of $\gamma$ -Alumina Supported Caesium or Potassium Fluoride	109
4.4.2	Aluminium-27, MAS-NMR Study of Caesium or Potassium Fluoride Supported on $\gamma$ -Alumina Treated with Sulphur Tetrafluoride at Room Temperature	111

4.5.1	Infra-Red Spectra of Caesium or Potassium Fluoride Supported on $\gamma$ -Alumina or Fluorinated $\gamma$ -Alumina	112
4.5.2	Raman Spectra of Caesium or Potassium Fluoride Supported on $\gamma$ -Alumina	113

### VOLUM E II

#### CHAPTER FIVE

#### THE REACTIONS OF PROBE MOLECULES WITH ALKALI METAL FLUORIDES SUPPORTED ON $\gamma$ -ALUMINA

5.1	Introduction	114
5.2	Experimental	114
5.3	The Reactions Involving Volatile Sulphur Containing Probe Molecules with Caesium or Potassium Fluoride Supported on $\gamma$ -Alumina	119
5.3.1	Infra-Red Analysis of the Hydrolysis of Sulphur Tetrafluoride over $\gamma$ -Alumina Supported Caesium or Potassium Fluoride	119
5.3.2	Monometric Study of Reactions of Sulphur Tetrafluoride with Caesium or Potassium Fluoride Supported on $\gamma$ -Alumina	121
5.3.3	The Change in the Temperature of Solid Caesium or Potassium Fluoride Supported on $\gamma$ -Alumina During Reaction with Sulphur	122
5.3.4	Reaction of [ $^{35}\text{S}$ ]-Sulphur Labelled Sulphur Tetrafluoride with Caesium or Potassium Fluoride Supported on $\gamma$ -Alumina	122
5.3.5	Infra-Red Analysis of the Hydrolysis of Thionyl Fluoride over $\gamma$ -Alumina Supported Caesium or Potassium Fluoride	124

5.3.6	Manometric Study of Reactions of Thionyl Fluoride with Caesium or Potassium Fluoride Supported on $\gamma$ -Alumina	125
5.3.7	The Change in the Temperature of Solid Caesium or Potassium Fluoride Supported on $\gamma$ -Alumina During Reaction with Thionyl Fluoride	126
5.3.8	Reactions of [ $^{35}\text{S}$ ]-Sulphur Labelled Thionyl Fluoride with Caesium or Potassium Fluoride Supported on $\gamma$ -Alumina	126
5.3.9	Manometric Study of Reactions of Sulphur Dioxide with Caesium or Potassium Fluoride Supported on $\gamma$ -Alumina	128
5.3.10	Reactions of [ $^{35}\text{S}$ ]-Sulphur Labelled Sulphur Dioxide with Caesium or Potassium Fluoride Supported on $\gamma$ -Alumina	129
5.3.11	Reactions of [ $^{18}\text{F}$ ]-Fluorine Labelled Thionyl Fluoride with Caesium or Potassium Fluoride Supported on $\gamma$ -Alumina	131
5.3.12	Reactions of [ $^{18}\text{F}$ ]-Fluorine Labelled Sulphur Tetrafluoride with Caesium or Potassium Fluoride Supported on $\gamma$ -Alumina	133
5.4	The Reactions Involving Volatile Carbon Containing Probe Molecules with Caesium or Potassium Fluoride Supported on $\gamma$ -Alumina	137
5.4.1	Infra-Red Analysis of the Hydrolysis of Carbonyl Fluoride over $\gamma$ -Alumina Supported Caesium or Potassium Fluoride	137
5.4.2	Manometric Study of Reactions of Carbonyl Fluoride with $\gamma$ -Alumina Supported Caesium or Potassium Fluoride	137

5.4.3	Reactions of [ <sup>14</sup> C]-Carbon Labelled Carbonyl Fluoride with Caesium or Potassium Fluoride Supported on $\gamma$ -Alumina	138
5.4.4	Reactions of [ <sup>14</sup> C]-Carbon Labelled Carbon Dioxide with Caesium or Potassium Fluoride Supported on $\gamma$ -Alumina	140
5.4.5	Reactions of [ <sup>18</sup> F]-Fluorine Labelled Carbonyl Fluoride with Caesium or Potassium Fluoride Supported on $\gamma$ -Alumina	141
5.5	Reactions Involving Anhydrous Hydrogen Fluoride with Caesium or Potassium Fluoride Supported on $\gamma$ -Alumina	143
5.5.1	Manometric Study of Reactions of Anhydrous Hydrogen Fluoride with Caesium or Potassium Fluoride Supported on $\gamma$ -Alumina	143
5.5.2	Reactions of [ <sup>18</sup> F]-Fluorine Labelled Anhydrous Hydrogen Fluoride with Caesium or Potassium Fluoride Supported on $\gamma$ -Alumina	144

## CHAPTER SIX

REACTIONS OF PROBE MOLECULES WITH  $\gamma$ -ALUMINA CALCINED  
TO 523 K and  $\gamma$ -ALUMINA FLUORINATED WITH SULPHUR  
TETRAFLUORIDE, THIONYL FLUORIDE, CARBONYL FLUORIDE  
OR ANHYDROUS HYDROGEN FLUORIDE

6.1	Introduction	146
6.2	Experimental	146
6.3	Reaction of Probe Molecules with $\gamma$ -Alumina Previously Calcined to 523 K	147
6.3.1	Reaction of Sulphur Dioxide with $\gamma$ -Alumina	147

6.3.2	Reaction of Thionyl Fluoride with $\gamma$ -Alumina Previously Calcined to 523 K	148
6.3.3	Reaction of Sulphur Tetrafluoride with $\gamma$ -Alumina Previously Calcined to 523 K	150
6.3.4	Reaction of Carbon Dioxide with $\gamma$ -Alumina	152
6.3.5	Reaction of Carbonyl Fluoride with $\gamma$ -Alumina Previously Calcined to 523 K	152
6.3.6	Reaction of Anhydrous Hydrogen Fluoride with $\gamma$ -Alumina Previously Calcined to 523 K	154
6.4	Reactions of Probe Molecules with $\gamma$ -Alumina Fluorinated with Sulphur Tetrafluoride, Thionyl Fluoride, Carbonyl Fluoride or Anhydrous Hydrogen Fluoride	154
6.4.1	Reactions of Carbon Dioxide and Sulphur Dioxide with $\gamma$ -Alumina Fluorinated with Sulphur Tetrafluoride, Thionyl Fluoride, Carbonyl Fluoride or Anhydrous Hydrogen Fluoride	154
6.4.2	Reactions of Carbonyl Fluoride and Thionyl Fluoride with $\gamma$ -Alumina Fluorinated with Sulphur Tetrafluoride, Thionyl Fluoride, Carbonyl Fluoride or Anhydrous Hydrogen Fluoride	155
6.4.3	Reactions of Sulphur Tetrafluoride with $\gamma$ -Alumina Fluorinated with Sulphur Tetrafluoride, Thionyl Fluoride, Carbonyl Fluoride or Anhydrous Hydrogen Fluoride	155
6.4.4	Reaction of [ $^{18}\text{F}$ ]-Fluorine Labelled Anhydrous Hydrogen Fluoride with Fluorinated $\gamma$ -Alumina	157

CHAPTER SEVEN

CATALYTIC ACTIVITY OF CAESIUM OR POTASSIUM FLUORIDE  
SUPPORTED ON  $\gamma$ -ALUMINA FLUORINATED AT ROOM  
TEMPERATURE

7.1	Introduction	159
7.2	Experimental	159
7.3	Reactions of Sulphur and Chlorine Containing Species with Caesium or Potassium Fluoride Supported on Fluorinated $\gamma$ -Alumina	160
7.3.1	Reactions of Sulphur Tetrafluoride with Caesium or Potassium Fluoride Supported on $\gamma$ -Alumina Fluorinated at Room Temperature	161
7.3.2	Reaction of Sulphur Chloride Pentafluoride with Caesium or Potassium Fluoride Supported on Fluorinated $\gamma$ -Alumina	162
7.3.3	Reaction of Chlorine Monofluoride with Caesium or Potassium Fluoride Supported on Fluorinated $\gamma$ -Alumina	163
7.4	The Oxidative Addition of Chlorine Monofluoride to Sulphur Tetrafluoride in the Presence of Metal Fluoride Supported on Fluorinated $\gamma$ -Alumina	165
7.4.1	The Reaction of Sulphur Tetrafluoride with Metal Fluoride Supported on Fluorinated $\gamma$ -Alumina Pretreated with Chlorine Monofluoride	166
7.4.2	The Reaction of Chlorine Monofluoride with Metal Fluoride Supported on Fluorinated $\gamma$ -Alumina Pretreated with Sulphur Tetrafluoride	167

7.4.3	The Reactions of Sulphur Tetrafluoride with Chlorine Monofluoride in the Presence of Metal Fluoride Supported on Fluorinated $\gamma$ -Alumina	169
-------	--	-----

CHAPTER EIGHT      DISCUSSION

8.1	Characterization of the Supported Metal Fluoride	179
8.2	Characterization of Fluorinated $\gamma$ -Alumina	188
8.3	Catalytic Activity of Metal Fluoride Supported on Fluorinated $\gamma$ -Alumina	192
8.4	Physical Examination of Supported Metal Fluoride	197

CHAPTER NINE      CONCLUSION

APPENDIX I		204
------------	--	-----

APPENDIX II		205
-------------	--	-----

REFERENCES		206
------------	--	-----



SUMMARY

Caesium or potassium fluoride supported on  $\gamma$ -alumina have been widely used as solid bases and catalysts in organic synthesis, in the presence of the solvent and under heterogeneous conditions. The nature of the active sites on the surface of these solids was not yet fully understood.

The aim of the present work is to obtain information regarding the nature and the active sites of the supported metal fluoride, using a series of analytical techniques and chemical reactions. The chemical reactions involve the individual interactions of the Lewis acid sulphur tetrafluoride and its hydrolysis products, thionyl fluoride and sulphur dioxide, the Lewis acid carbonyl fluoride and its hydrolysis product carbon dioxide, and anhydrous hydrogen fluoride with the supported metal fluoride. The interactions of the probe molecules described above with  $\gamma$ -alumina pretreated with sulphur tetrafluoride, thionyl fluoride, carbonyl fluoride or anhydrous hydrogen fluoride are also studied.

Terminal hydroxyl groups present on the surface of  $\gamma$ -alumina supported metal fluoride are removed by treatment with sulphur tetrafluoride, thionyl fluoride or sulphur dioxide then anhydrous hydrogen fluoride. The resulting materials caesium or potassium fluoride supported on  $\gamma$ -alumina, are catalytically examined, using the chlorofluorination of sulphur tetrafluoride with chlorine monofluoride at room temperature to give sulphur chloride pentafluoride as a model reaction.

The reactions described above are studied under heterogeneous conditions at room temperature, using the radiotracers [ $^{14}\text{C}$ ]-carbon

(ii)

[<sup>36</sup>Cl]-chlorine, [<sup>18</sup>F]-fluorine and [<sup>35</sup>S]-sulphur labelled compounds. The experiments carried out using [<sup>35</sup>S]-sulphur labelled sulphur tetrafluoride, thionyl fluoride or sulphur dioxide show that there is more than one adsorbed species present on the surface of the supported metal fluoride, these are weakly adsorbed molecules of sulphur tetrafluoride, thionyl fluoride and sulphur dioxide, and permanently retained pentafluorosulphate and fluorosulphite. For each system studied the surface activity is dependent on the metal fluoride loading in the composition range 0.6 - 20.0 mmol g<sup>-1</sup>, and is at a maximum at 5.5 mmol g<sup>-1</sup>. The overall uptake of the volatile sulphur containing probe molecules by the supported metal fluoride is in the order SF<sub>4</sub> > SO<sub>2</sub> ~ SOF<sub>2</sub>. [<sup>18</sup>F]-Fluorine exchange is observed in the sulphur tetrafluoride/supported metal fluoride system but not in the thionyl fluoride/supported metal fluoride system.

[<sup>18</sup>F]-Fluorine exchange is observed between [<sup>18</sup>F]-fluorine labelled carbonyl fluoride and the supported metal fluoride. The trifluoromethoxide anion is detected after each reaction. Experiments carried out using [<sup>14</sup>C]-carbon labelled carbonyl fluoride show that there are two species present on the surface of the supported metal fluoride, weakly adsorbed molecules of carbonyl fluoride and carbon dioxide. The surface activity is at a maximum at 5.5 mmol g<sup>-1</sup>.

The reaction of carbon dioxide and the supported metal fluoride is barely detectable but experiments carried out using [<sup>14</sup>C]-carbon labelled carbon dioxide confirm that weakly adsorbed carbon dioxide occurs.

The uptake of fluorine by calcined γ-alumina during treatment

(iii)

with sulphur tetrafluoride, thionyl fluoride, carbonyl fluoride or anhydrous hydrogen fluoride, is in the order  $SF_4 \sim SOF_2 > COF_2 \sim HF$ . It is found that treatment of  $\gamma$ -alumina with anhydrous hydrogen fluoride or carbonyl fluoride results in labile surface fluorine. However treatment of calcined  $\gamma$ -alumina with sulphur tetrafluoride or thionyl fluoride results in at least two forms of surface fluorine being produced one which is not labile and consisted of ca. 40% of the total fluorine present at the surface.

Caesium or potassium fluoride supported on  $\gamma$ -alumina prepared from aqueous or non-aqueous solution and treated with sulphur tetrafluoride, thionyl fluoride or sulphur dioxide then anhydrous hydrogen fluoride are efficient catalysts for the chlorofluorination of sulphur tetrafluoride by chlorine monofluoride. Catalytic activity is at a maximum at  $5.5 \text{ mmol g}^{-1}$  and poisoning by chlorine monofluoride appears to be less important than was the case for unsupported caesium fluoride. Catalysts prepared by mixing the two salts in the absence of the solvent or those treated with carbonyl fluoride or anhydrous hydrogen fluoride give very poor yields of sulphur chloride pentafluoride.

The B.E.T area of the supported metal fluoride is dependent on the metal fluoride loading in the composition range 0.6 - 20.0  $\text{mmol g}^{-1}$ . The fluorination of  $\gamma$ -alumina results in a decrease in the B.E.T area and is in the order calcined  $\gamma$ -alumina  $> COF_2/\gamma$ -alumina  $\sim HF/\gamma$ -alumina  $> SOF_2/\gamma$ -alumina  $\sim SF_4/\gamma$ -alumina  $\gg$  aluminium(III) fluoride. However the B.E.T areas of the supported metal fluoride prepared from aqueous or non-aqueous solution and treated with sulphur tetrafluoride, thionyl fluoride or sulphur dioxide then anhydrous hydrogen fluoride are equal within

the experimental errors.

The spectroscopic analyses, e.g. infra-red, Raman,  $^{27}\text{Al}$  MAS-NMR, and structural properties, powder x-ray diffraction, of these materials depend on their composition. Transmission electron microscopy is particularly useful; below  $5.5 \text{ mmol g}^{-1}$ , potassium fluoride particles ~~are~~ detected while at higher loadings formation of Al-F phases is observed.

## CHAPTER ONE

## INTRODUCTION

Virtually all chemical technologies in most fields use catalysis as an essential part of the process. The role of the catalyst was first defined in 1836 by Berzelius<sup>1</sup> who identified substances that accelerate chemical reactions without themselves undergoing any chemical change. The total rate of such reactions is proportional to the surface area. It is very important, therefore in heterogeneous reactions, to provide a large contact area between the reactants and the surface. As a consequence, a great deal of effort has been expended to prepare large surface area materials using large surface area carriers such as alumina and silica. In the present work  $\gamma$ -alumina was used as a support for alkali metal fluorides (Solid Base).

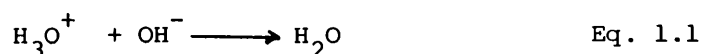
Metal halides can behave as Lewis bases, that is halide ion donors or as Lewis acids, that is halide ion acceptors. Section 1.1 reviews the acid-base definitions.

### 1.1 ACID-BASE CONCEPTS

The classification of substances as acids was first suggested by their sour taste (Latin acidus, sour, acetum, vinegar). Alkalis (Arabic al-kali, ashes of a plant),<sup>2</sup> were defined as those substances that could reverse or neutralize the action of acids. It was thought that an acid must have the element oxygen, as a necessary constituent (Greek Oxus, sour, gennae), but in 1910 Davy<sup>3</sup> demonstrated that hydrochloric acid contained only hydrogen and chlorine. As a result the view was taken, that all acids had hydrogen as an essential constituent.<sup>4</sup>

The more modern Arrhenius definition of acids and bases is that an acid is any substance that can increase the concentration of hydronium ion,  $\text{H}_3\text{O}^+$ , in aqueous solution.<sup>5</sup> On the other hand, a base is a substance that increases the hydroxide ion concentration in water.

In aqueous solution the neutralization of an acid by base can be described by equation 1.1

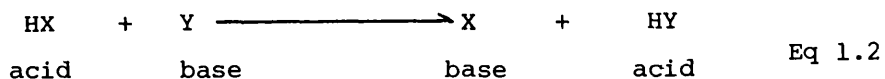


#### 1.1.1 BRØNSTED-LOWRY DEFINITION OF ACIDS AND BASES

The definition of acids and bases in terms of the hydronium and hydroxide ions is limited to acid-base phenomena in aqueous solution. A more powerful and general approach was proposed independently in 1923 by the Danish chemist, J.N. Brønsted and the British chemist, T.M. Lowry<sup>6,7</sup>. They defined an acid as a substance that is able to donate a proton to some other substance and a base as a substance that is able to accept a proton from an acid. In other words, an acid is a proton donor and a base is a proton acceptor. Accordingly the ionization of hydrogen chloride in water is an example of a Brønsted-Lowry acid-base reaction. On losing a proton the acid becomes a base. The base will then tend to regain the proton and revert to the acid. The acid and base arising from this equilibrium are commonly referred to as a conjugate acid-base pair.

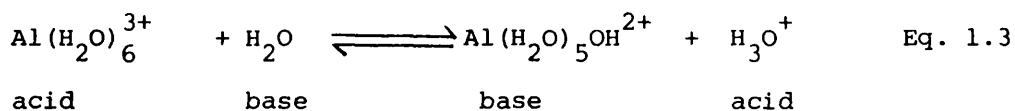
Generally any Brønsted-Lowry acid-base reaction can be

represented by equation 1.2



where acid HX and base X represent one conjugate pair and acid HY and base Y represent the other.

An interesting example of a Brønsted-Lowry acid-base reaction occurs in aqueous solutions which contain metal ions in high positive oxidation states. In an aqueous solution containing  $\text{Al}^{3+}$ , for example, the aluminium ion appears to have six water molecules arranged at the vertices of an octahedron. Even after crystallization, crystals usually contain the octahedral  $\text{Al}(\text{H}_2\text{O})_6^{3+}$ . The high charge on the metal ion draws electron density away from the surrounding water molecules. The oxygen atoms, in turn, draw electron density from the O-H bonds. As a result, a hydrogen is rather easily removed as  $\text{H}^+$  from  $\text{Al}(\text{H}_2\text{O})_6^{3+}$ . Its reaction with water can be viewed as a Brønsted-Lowry acid-base reaction as in equation 1.3.



The Brønsted-Lowry concept is more general than the Arrhenius concept since it can be applied to any reaction which involves *protonic* solutions.

### 1.1.2 LEWIS ACID-BASE DEFINITION

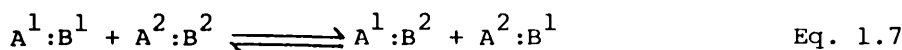
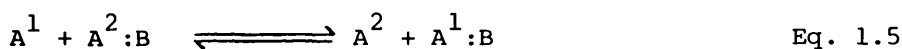
The Brønsted-Lowry concept is restricted in scope, since it limits discussion of acid-base phenomena to proton-transfer



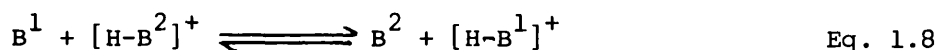
reactions. The approach taken by the American chemist Gilbert N. Lewis further extended the acid-base concept to cover cases where proton transfer was not involved.<sup>8</sup> In the Lewis definition of acids and bases, primary attention is focussed on the base. A Lewis base is defined as a substance that can donate a pair of electrons to form a covalent bond. An acid is a substance that can accept a pair of electrons to form the bond. The acid-base reaction is shown as an equilibrium process in equation 1.4, where A represents the acidic species and B the basic species:-



The heterolytic processes, which follow are given by equations 1.5 - 1.7



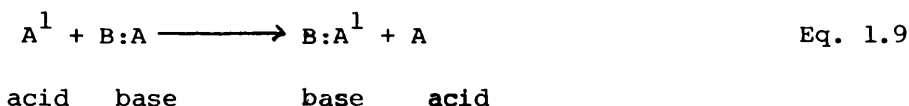
The Lewis definition includes the Brønsted-Lowry acid-base concept. For example, the proton in equation 1.8 is equivalent to the Lewis acid in equation 1.6.



An advantage of the Lewis acid-base concept is that it is comprehensive in its approach. A disadvantage, however, is that the approach cannot be applied quantitatively since acidity and basicity are dependent upon the reaction or method used for their

evaluation. As a result the hard/soft acid/base formalism of R.G. Pearson<sup>9</sup> has been adopted for their evaluation.

Lewis proposed that a strong acid should be able to displace a weaker acid from its acid-base complex. Accordingly the study of a large number of displacement reactions of the type shown in equation 1.9, should allow an ordering of the



strengths of acids towards a particular base.

Within recent years it has been shown that, the order of acid strengths is affected by the reference base chosen.<sup>10,11</sup> For example, the fluoride ion is a commonly used reference base when comparing the acidities of inorganic fluorides in the gas phase.<sup>12-14</sup>

### 1.1.3 THE APPLICATION OF ACID-BASE REACTIONS TO HETEROGENEOUS SYSTEMS

Although the original Lewis definitions were based on homogeneous systems, they can be applied to heterogeneous gas-solid reactions if the acid-base definitions are restated as follows:-

A Lewis acid site on a solid surface is a site which has an unoccupied orbital with a high affinity for an electron pair, so that a decrease in energy results when such a site shares an electron pair donated by an adsorbed base molecule. Lewis base sites on the surface are those which have electron pairs available at a high energy level and a major decrease in the energy is obtained if they share this

electron pair with an adsorbed electron pair acceptor.

It would seem therefore, that the Lewis acid-base definitions are the most suitable for describing heterogeneous gas-solid reactions.

#### 1.1.4 THE AIMS OF THE PRESENT WORK

The aim of the present work was to complete the characterization and the catalytic optimisation of caesium and potassium fluoride supported on  $\gamma$ -alumina prepared by different methods, particularly using radiotracer methods. Some analytical techniques such as, solid state aluminium-27 magic angle spinning-nuclear magnetic resonance spectroscopy, infra-red and Raman spectra and by examination using transmission electron microscopy and powder x-ray diffraction, were undertaken in order to achieve maximum physical characterization of caesium or potassium fluoride supported on  $\gamma$ -alumina at different compositions (0.6 mmol g<sup>-1</sup> - 20.0 mmol g<sup>-1</sup>).

The chemical reactions examined involved the adsorption and retention of {<sup>14</sup>C}-carbon, {<sup>36</sup>Cl}-chlorine and {<sup>35</sup>S}-sulphur labelled Lewis acid probe molecules chlorine monofluoride, carbonyl fluoride, carbon dioxide, sulphur tetrafluoride, thionyl fluoride and sulphur dioxide on variously prepared caesium or potassium fluoride supported on  $\gamma$ -alumina and fluorinated  $\gamma$ -alumina with various inorganic fluorinating agents. The {<sup>18</sup>F}-fluorine radiotracer studies were carried out in order to clarify whether the fluorine associated with these phases is labile with respect to fluorine exchange.

The chlorofluorination of sulphur tetrafluoride with chlorine monofluoride at room temperature to give sulphur chloride pentafluoride, was taken as a model reaction in an attempt to clarify and optimise the catalytic activity of caesium or potassium fluoride supported on  $\gamma$ -alumina fluorinated at room temperature then calcined to 523 K. The reaction examined involved the chemisorption and retention of  $\{^{35}\text{S}\}$ -sulphur labelled sulphur tetrafluoride,  $\{^{36}\text{Cl}\}$ -chlorine labelled chlorine monofluoride and  $\{^{35}\text{S}\}$ -sulphur and  $\{^{36}\text{Cl}\}$ -chlorine labelled sulphur chloride pentafluoride on variously prepared caesium or potassium fluoride supported on  $\gamma$ -alumina fluorinated at room temperature.

## 1.2 SOME CHEMISTRY OF THE REAGENTS

In the present work, the Lewis acid sulphur tetrafluoride and its hydrolysis products thionyl fluoride, sulphur dioxide and hydrogen fluoride and the Lewis acid carbonyl fluoride and its hydrolysis products carbon dioxide and hydrogen fluoride, have been used as probe molecules for the active basic sites of caesium or potassium fluoride supported on  $\gamma$ -alumina prepared by different methods. The chlorofluorination of sulphur tetrafluoride by chlorine monofluoride to yield sulphur chloride pentafluoride has been used to test for the catalysis at caesium or potassium fluoride supported on  $\gamma$ -alumina fluorinated at room temperature then calcined to 523 K. It is therefore appropriate that some of the chemistry of these molecules is discussed below.

### 1.2.1 CHLORINE MONOFLUORIDE

Unlike the monofluorides of bromine and iodine, chlorine monofluoride is stable at room temperature and may be isolated in a pure state by low temperature distillation. The gas is colourless and the liquid, which boils at ca. 173 K, is yellow. The solid which melts at ca. 118 K is colourless.<sup>15</sup>

Pauling has pointed out that, the Cl-F bond in chlorine monofluoride should have a high degree of ionic character.<sup>16</sup> A very precise value of the bond length, 1.628 Å, has been obtained by Gilbert et al.<sup>17</sup>

Chlorine monofluoride is a moderately strong fluorinating agent.<sup>18</sup> It attacks "Pyrex" glass and quartz at elevated temperature and reacts violently with water, forming hydrogen fluoride and chloride oxides.<sup>19</sup> It reacts with sodium, mercury and iron powder when cold; and with magnesium, aluminium, copper zinc, gold and platinum when heated, arsenic, antimony and boron inflame spontaneously apparently forming arsenic pentafluoride, antimony pentafluoride and boron trifluoride.<sup>20</sup>

Christe and Guertin have reported the formation of the compound nitrosyl difluorochlorate by reaction of nitrosyl fluoride with chlorine monofluoride at 195 K.<sup>21</sup> The compound is ionic, with the structure  $\text{NO}^+\text{ClF}_2^-$ . Since only one infra-red active band is observed for  $\text{ClF}_2^-$ , the anion appears to have a linear structure.<sup>21</sup> Since the nitrosyl difluorochlorate is stable only at low temperatures, the replacement of the nitrosyl cation by an alkali metal cation has been investigated.<sup>22</sup> The compounds obtained are colourless solids

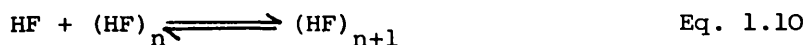
at room temperature, having good thermal stabilities, which decrease in the order caesium difluorochlorate>rubidium difluorochlorate>potassium difluorochlorate. The decrease in cation size and the increase in polarising power from caesium to lithium cations<sup>23</sup> probably accounts for this order of stability.

### 1.2.2 ANHYDROUS HYDROGEN FLUORIDE

As early as 1670, according to some authors, the Nurnberg glassworker Heinrich Schwanhardt made artistic etchings on glass with fumes evolved from the reaction of sulphuric acid with fluorospar.<sup>24</sup> The late chemist-historian J.R. Partington has questioned the validity of this traditional account, and states that, the first authenticated record of this reaction, which produces hydrofluoric acid or hydrogen fluoride (HF), dates from either the year 1720 or 1725.<sup>25</sup> A better understanding by chemists soon followed, and in 1771 the Swede Carl. W. Scheele recognised, in fluorospar, the calcium salt of the new acid, which he called the "acid fluorospar" or fluoric acid.<sup>26</sup>

Anhydrous hydrogen fluoride is a colourless liquid at room temperature with a boiling point of ca. 293 K and a density of ca. 0.96 g cm<sup>-3</sup>.<sup>27</sup> The high boiling point compared with other hydrogen halides is a consequence of the association of anhydrous hydrogen fluoride molecules in the liquid state. The association of hydrogen fluoride molecules is also observed in the gaseous state and there have been contradictory views on whether the species formed from the association of hydrogen fluoride molecules are linear or cyclic.

Two different models have been proposed to account for the polymerisation of hydrogen fluoride monomers in the gas phase; a continuous polymerisation model, first proposed by Strohmeier and Briegleb<sup>28</sup> and a "few species" model involving dimers, tetramers and hexamers. In the continuous polymerisation model a step-wise association of hydrogen fluoride with  $(\text{HF})_n$  is proposed, as shown in equation 1.10



The formation of a cyclic hexamer is also proposed with the decrease in entropy being offset by the additional stability introduced by the extra hydrogen bond. Results from Raman study of hydrogen fluoride dissolved in liquid sulphur hexafluoride provided evidence for a cyclic hexamer in solution<sup>29</sup> and the existence of a cyclic hexamer in the gaseous state has been established by electron diffraction.<sup>30</sup> A relatively recent vapour pressure analysis,<sup>31</sup> where vapour density, heat capacity, excess entropy, excess enthalpy and infra-red data were combined to obtain a non-ideal associated vapour model, concluded that the cyclic hexamer is the most abundant in the temperature range 292.5 - 329 K. A recent study<sup>32</sup> presented evidence for open trimers and tetramers and four cyclic  $(\text{HF})_n$  species,  $n = 3-6$ . In the opinion of the authors,<sup>32</sup> oligomeric species with  $n > 6$  seem unlikely, since no spectroscopic evidence for them could be obtained.

It seems reasonable to suggest, on the basis of the published work, that gaseous hydrogen fluoride adopts a chain structure for  $(\text{HF})_2$ , chain or cyclic structures for  $(\text{HF})_3$

and  $(\text{HF})_4$  and cyclic structures for higher oligomers, notably  $(\text{HF})_5$  and  $(\text{HF})_6$ . The interaction of gaseous hydrogen fluoride with surface, for example,  $\gamma$ -alumina supported caesium or potassium fluoride, could involve stabilization of a hydrogen fluoride chain structure at Lewis acid and Lewis base sites, forming a pseudo-cyclic oligomer.

Ions of the type  $(\text{HF})_n\text{F}^-$  were formed by hydrogen bonding of up to four molecules to a central fluoride ion. The ion  $\text{HF}_2^-$  is a linear species with the proton positioned symmetrically between the two fluorine atoms<sup>33</sup> and the ion  $\text{H}_2\text{F}_3^-$ , on the basis of an infra-red study<sup>34</sup> is assigned a bent structure of  $\text{C}_{2v}$  symmetry, Fig. 1.1. Low temperature infra-red spectroscopy<sup>35</sup> suggests a planar  $\text{D}_{3h}$  configuration for the ion  $\text{H}_3\text{F}_4^-$ . No diffraction data are available to confirm this assignment, but ab-initio calculations<sup>36</sup> found the planar  $\text{D}_{3h}$  structure to be the lowest energy state for  $\text{H}_3\text{F}_4^-$ . The structure of the ion  $\text{H}_4\text{F}_5^-$ , obtained by x-ray crystallography<sup>37</sup> of crystalline  $\text{K}[\text{H}_4\text{F}_5]$ , was that of a slightly distorted tetrahedron.

In common with surface  $(\text{HF})_n$  oligomers, ions of the type  $(\text{HF})_n\text{F}^-$  could adsorb at Lewis acid and Lewis base sites, the proton associated with the fluoride ion interacting with the Lewis base site.

### 1.2.3 CARBONYL FLUORIDE

Carbonyl fluoride is a weak Lewis acid which is a special reagent that falls into the category of fluorinated carbonyl compounds.<sup>38</sup> It can be used in direct fluorination<sup>38</sup> but is



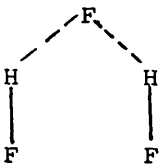
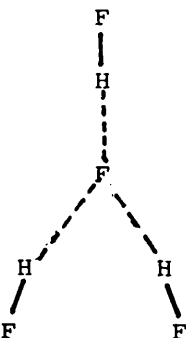
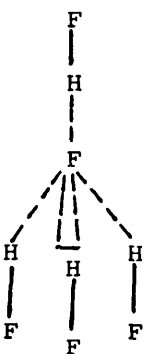
Ion	Symmetry
$[\text{HF}_2]^-$ $[\text{F}-\text{H}-\text{F}]^-$	$D_{\infty h}$
$[\text{H}_2\text{F}_3]^-$ 	$C_{2v}$
$[\text{H}_3\text{F}_4]^-$ 	$D_{3h}$
$[\text{H}_4\text{F}_5]^-$ 	Td

Figure 1.1 Structures of Ions of general  $(\text{HF})_n\text{F}^-$

frequently used to introduce a COF unit.<sup>39</sup> Its reaction with caesium or potassium fluoride, and in the presence of dried acetonitrile, trifluoromethoxide anion was formed.<sup>40,41</sup> In the absence of the solvent no adduct was isolated. Spectroscopic studies of the trifluoromethoxide anion have indicated that, it has  $C_{3v}$  symmetry.<sup>42</sup> Examination of the bond positions indicated that the C-O bond is intermediate between a single and a double bond. This was defined by the x-ray single crystal diffraction analysis of tris(dimethylamino)sulphonium trifluoromethoxide  $TAS^+CF_3O^-$ , Fig. 1.2.<sup>42</sup> This analysis showed, the C-F bonds of the trifluoromethoxide anion are long and the C-O bond short compared with the corresponding gas-phase experimental values for tetrafluoromethoxide. The C-O bond length approaches that for C=O bond in carbonyl fluoride.

The presence of resonance structures is also indicated by the results of Mulliken population analysis which show that each fluorine in the trifluoromethoxide anion carries an additional charge, Fig. 1.3 shows the four hyperconjugative resonance structures which are proposed to contribute to the bonding in the trifluoromethoxide anion.

#### 1.2.4 CARBON DIOXIDE

Reaction of carbon dioxide with bases, either as solvent or solute is one of the most significant effects on carbon dioxide solubility in aqueous media. The solubility of carbon dioxide in aqueous and nonaqueous solutions depends on its partial pressure, on temperature and on acid-base reactions within the solution.<sup>43</sup>

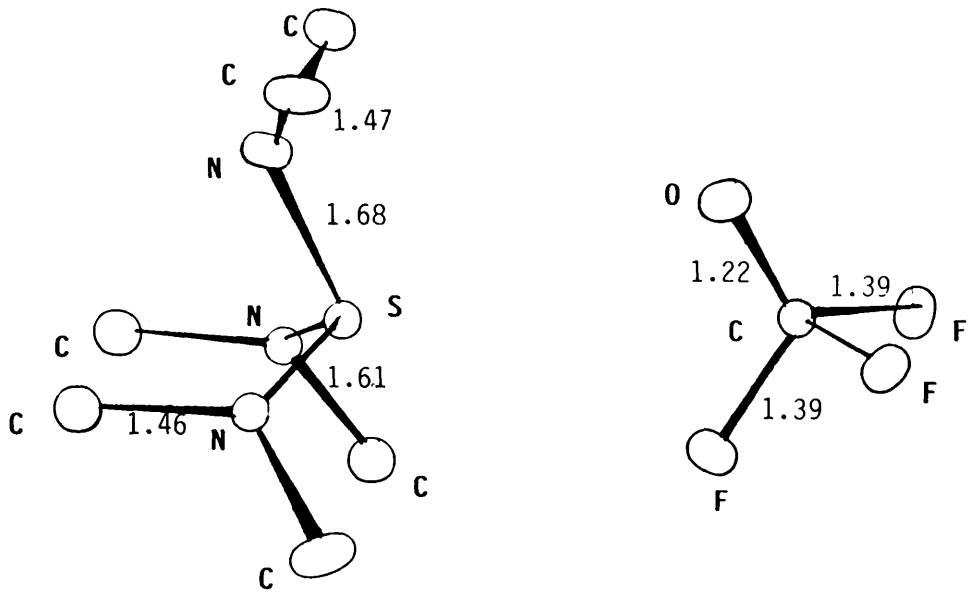
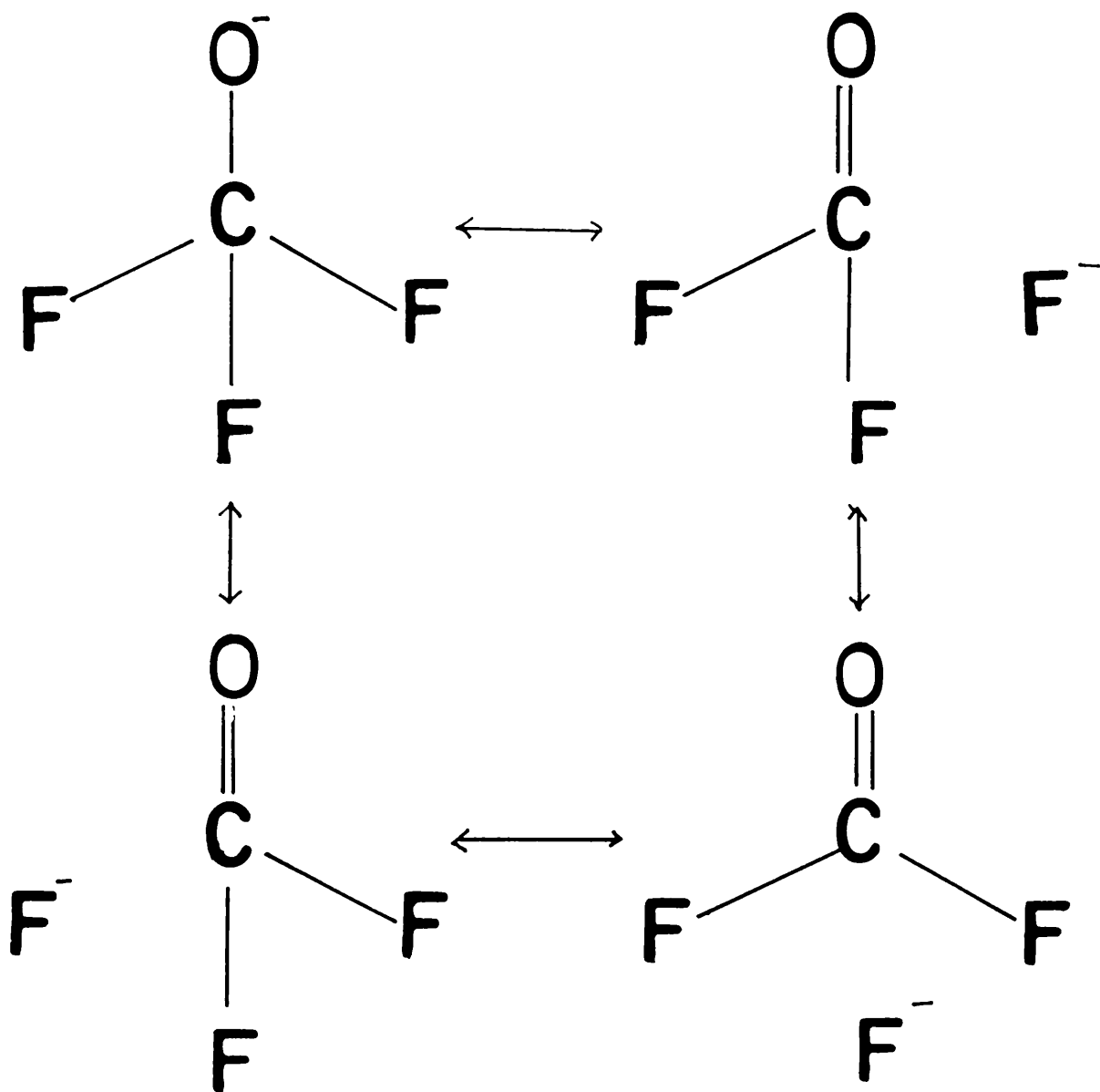


**Figure 1.2** The structure of TAS<sup>+</sup>CF<sub>3</sub>O<sup>-</sup>

TAS = tris(dimethylamino)sulphonium

Figure 1.3  $\text{CF}_3\text{O}^-$  Resonance structure



In aqueous solutions, the equilibria forming  $\text{HCO}_3^-$  and  $\text{CO}_3^{2-}$  depend on pH and ionic strength; the presence of metal ions which form insoluble carbonates may also be a factor. The equilibria are well known for aqueous solutions,<sup>43</sup> but little data have been systematically compiled on acid-base reactions of carbon dioxide in nonaqueous solutions. For example, the published results of the reaction between caesium fluoride and carbon dioxide have aroused a great deal of controversy. In 1971 Martineau and Milne<sup>44</sup> reported the preparation of  $\text{Cs}_2\text{CO}_2\text{F}_2$  from the reaction between caesium fluoride and carbon dioxide in acetonitrile at room temperature. The product was identified spectroscopically and from caesium and fluorine analyses. Subsequent attempts to reproduce these results have not been successful. In 1979 Lawler and Passmore<sup>45</sup> suggested that rather than observing the  $\text{CO}_2\text{F}_2^{2-}$  anion, Martineau and Milne had in fact obtained hydrolysis products caused by the presence of water in their acetonitrile.

Further doubt was cast on the validity of Martineau and Milne's results by David and Ault<sup>46</sup> in 1985. They carried out a matrix isolation study of the  $\text{CO}_2\text{F}_2^{2-}$  anion and their infra-red spectrum data did not agree with that of Martineau and Milne. David and Ault explained this disagreement by suggesting, like Lawler and Passmore in 1979, that Martineau and Milne had obtained an infra-red spectrum of a hydrolysis product rather than that of  $\text{Cs}_2\text{CO}_2\text{F}_2$ . A recent study of the adsorption of [ $^{14}\text{C}$ ]-carbon labelled carbon dioxide on caesium fluoride activated with hexafluoroacetone, suggested that the permanently adsorbed species is most likely to be  $\text{CO}_2\text{F}^-$  rather than  $\text{CO}_2\text{F}_2^{2-}$ .<sup>47</sup> Since David and Ault have shown that the  $\text{CO}_2\text{F}_2^{2-}$  anion has limited

stability even at low temperature.<sup>46</sup>

#### 1.2.5 THIONYL FLUORIDE

Thionyl fluoride is used as a fluorinating agent for, for example, organosilicon compounds,<sup>48</sup> but it usually requires higher temperatures and longer reaction time than those used with sulphur tetrafluoride or carbonyl fluoride. Thionyl fluoride Fig. 1.4 is known to exhibit some Lewis acid character through involvement of the sulphur d-orbitals,<sup>49</sup> but there is no evidence for the anion formed through fluoride ion addition.

As a logical extension of an EPR study of sulphur tetrafluoride<sup>50</sup> reaction of caesium fluoride with thionyl fluoride has been studied<sup>51</sup> by means of Matrix isolation. The EPR spectrum of the solid obtained was assigned to the carrier  $\text{SOF}_3^\bullet$  as shown in Fig. 1.5. The radical  $\text{SOF}_3^\bullet$  is isoelectronic with  $\text{PF}_4$  radical, which has a trigonal bipyramidal structure in which the two apical fluorine nuclei have 282 G hyperfine interactions and the two equatorial fluorine nuclei 59 G interactions. By analogy with the spectrum of  $\text{PF}_4$ , it was therefore assigned the configuration of the  $\text{SOF}_3^\bullet$  is trigonal bipyramidal structure with the two apical fluorine nuclei having 252 G hyperfine interactions and the one equatorial fluorine nucleus 52 G interaction.<sup>51</sup> This configuration is consistent with the observation that in trigonal bipyramidal structures the more electronegative ligands occupy the apical positions.<sup>51</sup> The infra-red spectrum of the product obtained from the reaction between caesium fluoride and thionyl fluoride showed four absorption bands assigned to the

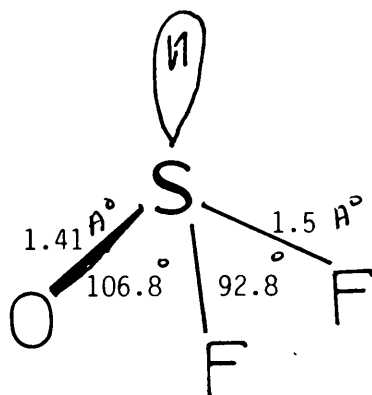


Figure 1.4 The structure of thionyl fluoride

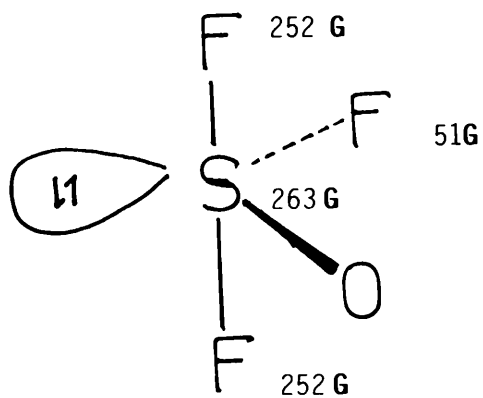
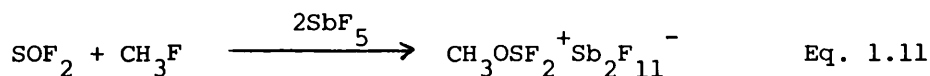


Figure 1.5 The structure of  $\text{SO}_2\text{F}_2^\bullet$

trifluorosulphite anion, in an ion pair with caesium cation.<sup>52</sup>

Thionyl fluoride forms weak oxygen-bridged adducts with the strong Lewis acids arsenic pentafluoride or antimony pentafluoride.<sup>53</sup> In the presence of fluoromethane and antimony pentafluoride, a novel cation was formed according to equation 1.11<sup>54</sup>



#### 1.2.6 SULPHUR DIOXIDE

Sulphur dioxide is a weak reducing agent in aqueous acid solution, but a stronger one in basic solution, where the sulphite ion is formed. Sulphur dioxide is a colourless, poisonous gas with a sharp odour (maximum safe concentration 5 p.p.m). It condenses to a clear liquid at 263.14 K which yields colourless crystals on further cooling to 197.68 K.<sup>55</sup> The bonding in gaseous sulphur dioxide molecule is shown in Fig 1.6. The percentage of individual structures in the molecule is not known for certain, but the mesomeric structure II, represents the ground state of sulphur dioxide best. Both S-O bond distances in sulphur dioxide are equal and according to microwave and electron diffraction spectroscopy, they are 1.432 Å.<sup>56-58</sup> Sulphur in sulphur dioxide molecules acts as an electron acceptor, Lewis acid, as a result of its formal positive charge. One of the most stable adducts formed by reaction with amines is Me<sub>3</sub>N.SO<sub>2</sub> as shown in Fig. 1.7.<sup>59</sup> Alkali metal halides (sodium, potassium, rubidium and caesium) react



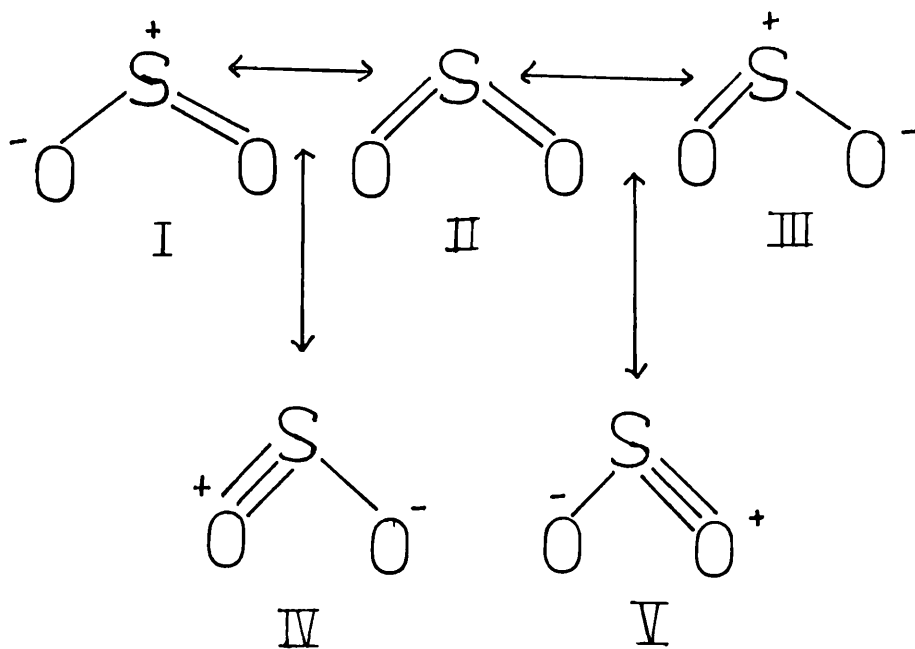


**Figure 1.6** The molecular structure of gaseous SO<sub>2</sub>

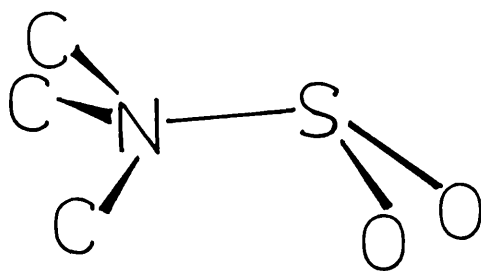
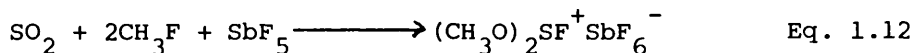


**Figure 1.7** The structure of Me<sub>3</sub>NSO<sub>2</sub>

with sulphur dioxide to form  $\text{MSO}_2\text{X}$ , which are thermally stable, the fluoroanions are water sensitive. The interaction is in the order  $\text{F} > \text{Cl} > \text{Br} > \text{I}$ .<sup>60</sup> The fluoroanions are oxidised at 443 K by sulphur dioxide to fluorosulphates,  $\text{MSO}_3\text{F}$ .<sup>60</sup> Sulphur dioxide undergoes reactions with strong Lewis acids such as antimony pentafluoride or arsenic pentafluoride, forming weak adducts of the type  $\text{SbF}_5 \cdot \text{SO}_2$  as shown in Fig. 1.8, which melts at 330 K with evolution of sulphur dioxide.<sup>61</sup> This adduct is of interest because of the use of sulphur dioxide as a solvent for superacid systems. In the presence of fluoromethane, sulphur dioxide is alkylated to give  $(\text{CH}_3\text{O})_2\text{SF}^+\text{SbF}_6^-$ ,<sup>61</sup> according to equation 1.12.



### 1.2.7 SULPHUR TETRAFLUORIDE

Literature reports concerning sulphur tetrafluoride have appeared sporadically since 1905.<sup>62</sup> There are numerous reactions in which sulphur tetrafluoride is formed, but most of them have poor yields, Fig. 1.9.<sup>63a-g</sup> Sulphur tetrafluoride is a colourless gas (b.p. 165 K) which condenses to a colourless liquid. It solidifies at 152 K. Its critical temperature is 364 K. The heats of hydrolysis<sup>64</sup> and hydrogenation<sup>65</sup> of sulphur tetrafluoride have been measured and lead to values of 176 and 172 kcal/mol respectively. Sulphur tetrafluoride is hydrolysed rapidly and exothermically by aqueous media at all pH values. The primary reaction yields thionyl fluoride and hydrogen fluoride, the

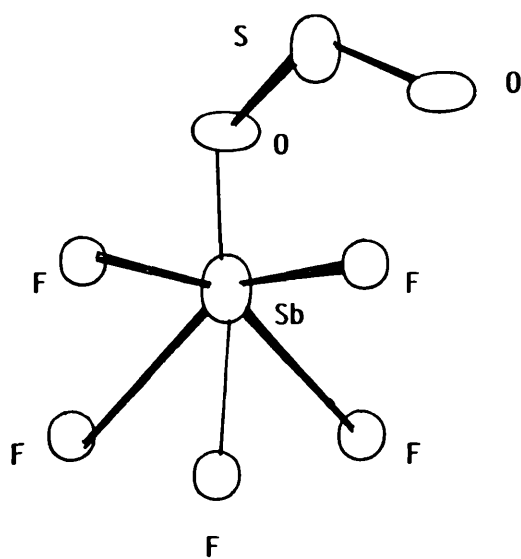
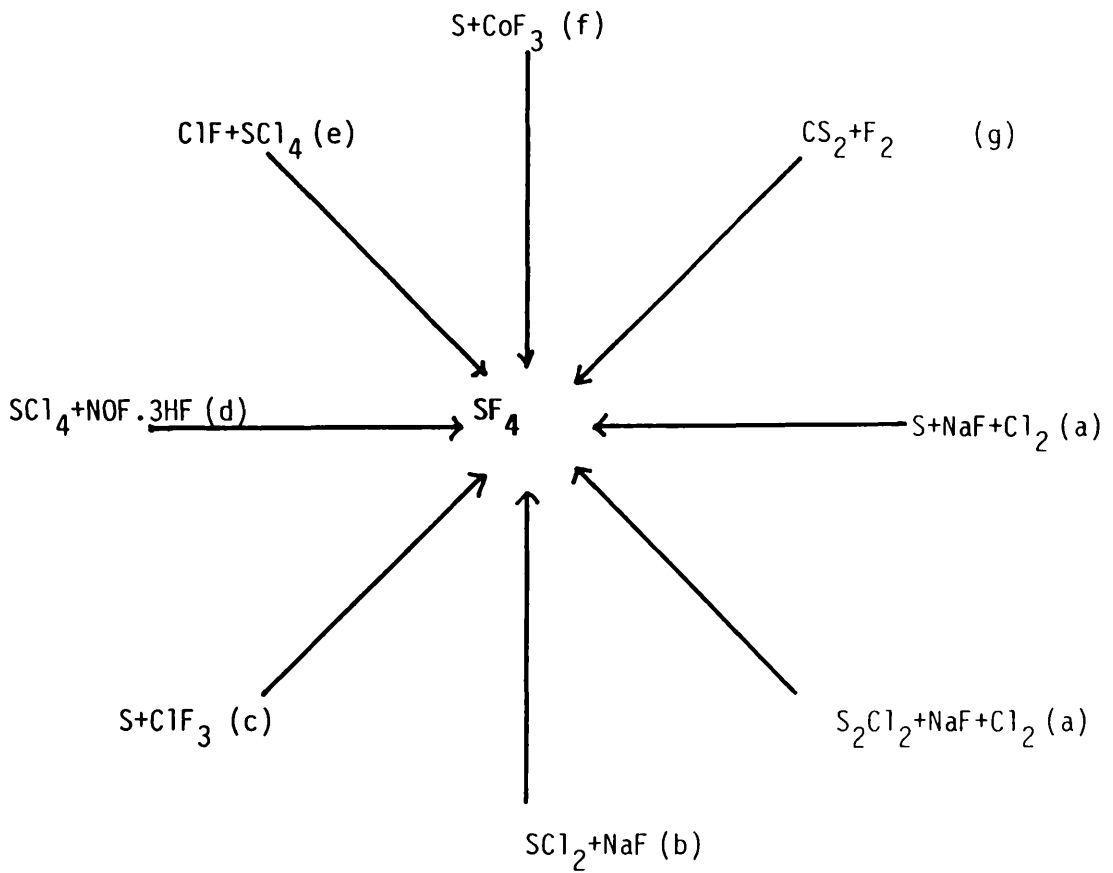


Figure 1.8 The structure of  $\text{SbF}_5 \cdot \text{SO}_2$

Figure 1.9 Preparation of Sulphur Tetrafluoride 63



subsequent hydrolysis of thionyl fluoride taking place somewhat less rapidly. It is for this reason that it is difficult to handle small quantities of sulphur tetrafluoride in any but the most rigorously dried glass apparatus. Stainless steel, copper or nickel are all quite inert to sulphur tetrafluoride at ambient temperature and use of apparatus constructed from these metals greatly simplifies the handling of sulphur tetrafluoride.

The structure of sulphur tetrafluoride has been established by a study of its vibrational <sup>66</sup>, NMR <sup>67</sup> and microwave spectra. <sup>68</sup> The vibrational spectra suggested that the structure has C<sub>2v</sub> symmetry. This led to the proposal that the structure was that of a trigonal bipyramid in which one of the three equatorial atoms was replaced by a lone pair of electrons. The <sup>19</sup>F NMR spectrum of sulphur tetrafluoride consisted of a single sharp line at room temperature. On cooling the line broadened and at 215 K was resolved into two broad lines. At 175 K the spectrum was resolved into two identical triplets, as would be expected for the C<sub>2v</sub> symmetry indicated by the vibrational spectra. From this temperature dependence of the spectra an activation energy of 4.5 ± 0.8 kcal was deduced for fluorine exchange in sulphur tetrafluoride. The microwave spectrum showed that marked deviations occurred from the trigonal bipyramid structure, Fig. 1.10, such that:-

$$d S-F_1 = d S-F_2 = 1.646 \pm 0.003 \text{ \AA}$$

$$d S-F_3 = d S-F_4 = 1.545 \pm 0.003 \text{ \AA}$$

$$L F_2 S F_1 = 186^\circ 56$$

$$L F_4 S F_3 = 101^\circ 33$$

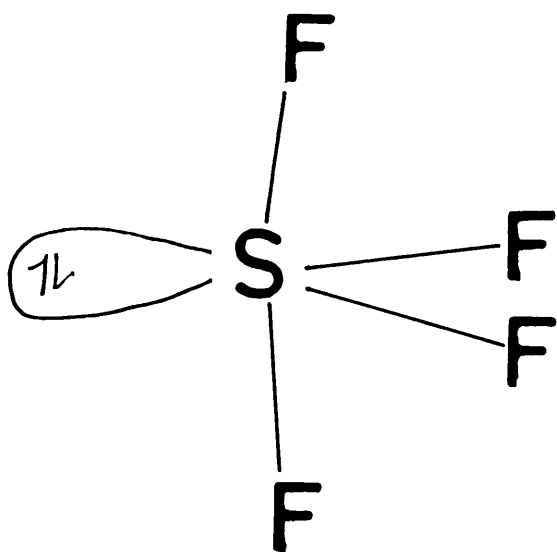


Figure 1.10 The structure of  $\text{SF}_4$

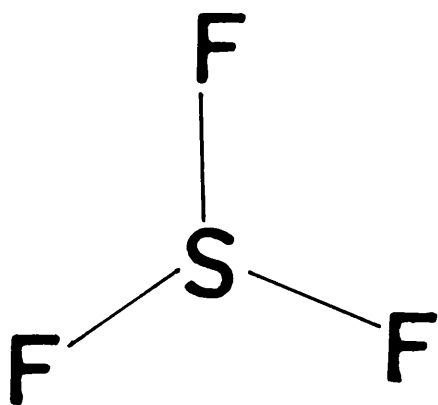


Figure 1.11 The structure of  $\text{SF}_3^+$

Sulphur tetrafluoride can react with inorganic fluorides which are also Lewis acids. These may be written in approximate order of decreasing stability  $\text{SbF}_5 \cdot \text{SF}_4$ ,  $\text{AsF}_5 \cdot \text{SF}_4$ ,  $\text{BF}_3 \cdot \text{SF}_4$ ,  $\text{PF}_5 \cdot \text{SF}_4$ ,  $\text{GeF}_4 \cdot 2\text{SF}_4$  and  $\text{AsF}_3 \cdot \text{SF}_4$ . Bartlett and Robinson<sup>69</sup> first formulated these substances as Lewis acid Lewis base adducts  $\text{SF}_4 \rightarrow \text{BF}_3$ . Seel and Detmer<sup>70</sup> have advanced evidence on the basis of solid infrared spectra that the boron trifluoride adduct should be regarded as  $\text{SF}_3^+ \text{BF}_4^-$ . In contrast to this, solution of sulphur tetrafluoride in excess arsenic trifluoride gave no evidence of the presence of  $\text{SF}_3^+$  or  $\text{AsF}_4^-$ .<sup>71</sup> The  $\text{SF}_3^+$  cation exhibits  $C_{3v}$  symmetry, Fig. 1.11. The crystal structure of the adduct  $\text{SF}_3^+ \text{BF}_4^-$  is shown in Fig. 1.12.

Sulphur tetrafluoride can also act as a weak electron-pair acceptor, Lewis acid. Thus, it reacts with tetramethyl ammonium fluoride<sup>72</sup> or caesium fluoride<sup>73</sup> to form a stable anion, pentafluorosulphate,  $\text{SF}_5^-$ . There are several possible structures for the  $\text{SF}_5^-$  anion which can be described in terms of the  $C_{5v}$ ,  $C_{4v}$ ,  $C_{3v}$ ,  $C_{2v}$ ,  $C_s$  and  $D_{3h}$  point groups. Of these only the  $C_{4v}$  and the  $D_{3h}$  point groups are likely to be reasonable. In the first, the structure is similar to that assumed by the halogen pentafluorides<sup>74</sup> in which the basic framework is a slightly distorted tetragonal pyramid as shown in Fig. 1.13a. An electron pair is localized in one position of an octahedral structure and the repulsive forces between this pair and the electrons surrounding the four equivalent fluorine atoms accounts for the observation that, the central atom is not coplanar with these fluorine atoms. A second structure is based upon a regular trigonal bipyramid, as shown in Fig. 1.13b, in which one could consider a fluorine atom and an electron added

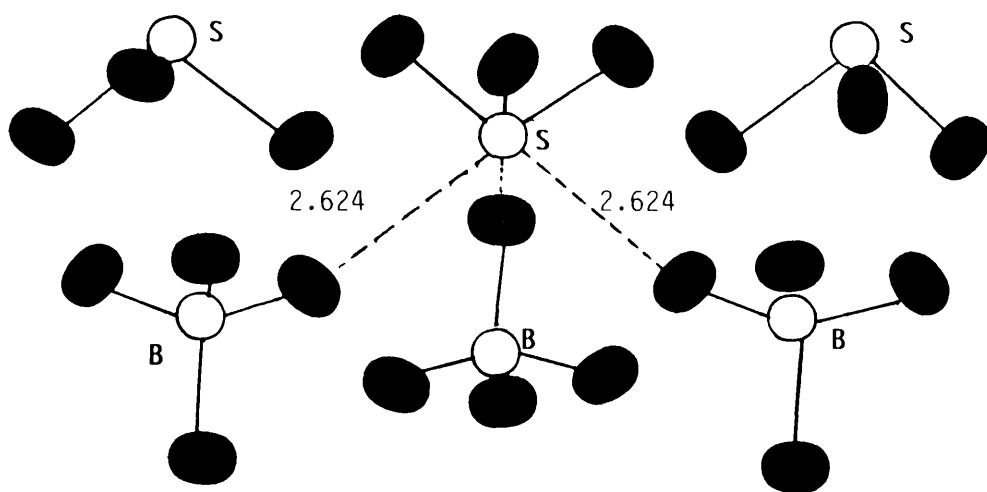
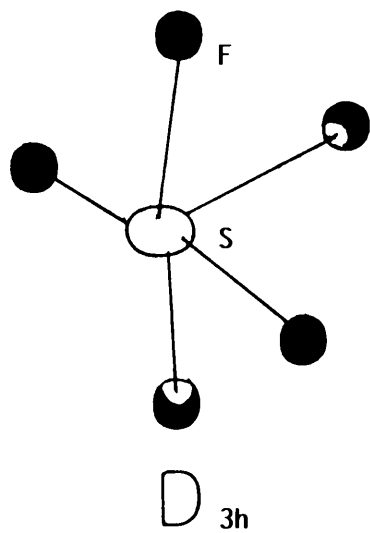
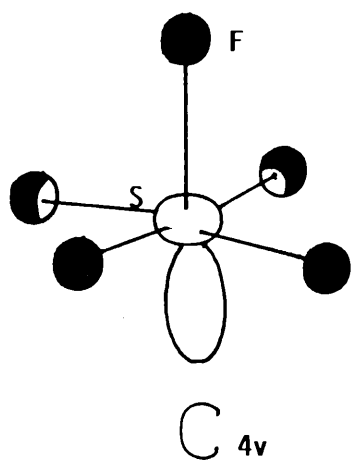


Figure 1.12 The structure of  $\text{SF}_3^+\text{BF}_4^-$





( b )



( a )

Figure 1.13 The structure of  $\text{SF}_5^-$

to sulphur tetrafluoride. The electron would be delocalized over the whole molecule.<sup>75</sup>

In addition to the Lewis acid-base reactions, sulphur tetrafluoride is also widely used as a fluorinating agent for organic chemistry, it will convert C=O and P=O groups smoothly into CF<sub>2</sub> and PF<sub>2</sub> and COOH and POOH groups into CF<sub>3</sub> and PF<sub>3</sub> groups without attack on most other functional or reactive groups which may be present in the molecule. It can also replace halogen by a fluorine atom. Such reactions are summarized in Fig 1.14.<sup>76</sup> a-f Sulphur tetrafluoride undergoes a wide range of inorganic reactions. It is, for example, useful to convert inorganic oxides into fluorides or oxyfluorides as summarized in Fig 1.15.<sup>77</sup> a-e

The above review shows that sulphur tetrafluoride can undergo a wide range of chemical reactions. This, together with the availability of {<sup>18</sup>F}-fluorine and {<sup>35</sup>S}-sulphur radiotracers makes sulphur tetrafluoride a very useful substance for the study of Lewis acid-base reactions under heterogeneous conditions.

#### 1.2.8 SULPHUR CHLORIDE-PENTAFLUORIDE

Sulphur chloride pentafluoride is a colourless gas at room temperature with a boiling point of 258 K and melting point of 109 K. There are many reactions in which sulphur chloride pentafluoride is formed, but the best reported method is the chlorofluorination of sulphur tetrafluoride using caesium fluoride as a catalyst at room temperature.<sup>78</sup> Sulphur chloride pentafluoride is more reactive than sulphur hexafluoride, being attacked by hydroxyl groups and other

Figure 1.14 Reaction of SF<sub>4</sub> in Organic Chemistry 76

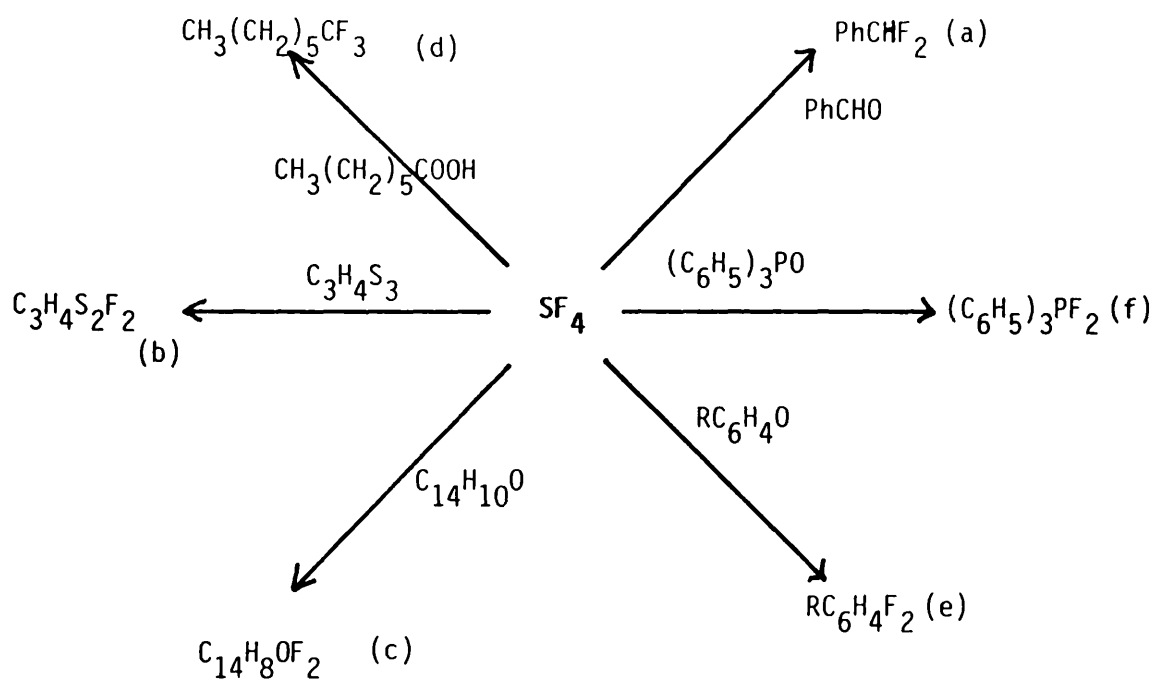
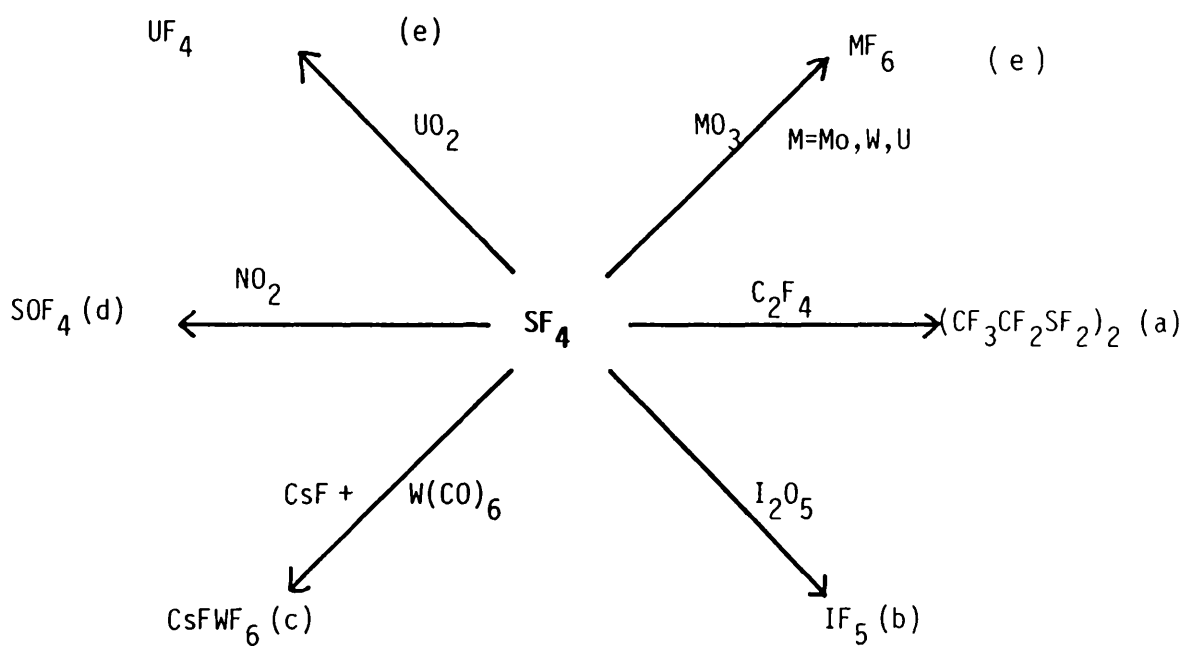
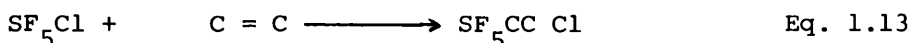


Figure 1.15 Reaction of SF<sub>4</sub> in Inorganic Chemistry [77]

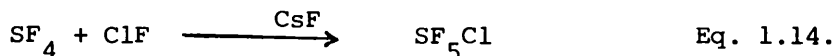


nucleophiles<sup>79</sup> though it is inert to acids. Its hydrolysis and its powerful oxidizing action toward many organic substances are consistent with the charge  $SF_5^{\delta-} - Cl^{\delta+}$ .<sup>79</sup> Sulphur chloride pentafluoride has a rich chemistry<sup>80</sup> for example, it is very good source for  $SF_5^{\cdot}$  radical which is useful in organic chemistry as shown in equation 1.13.<sup>81</sup>



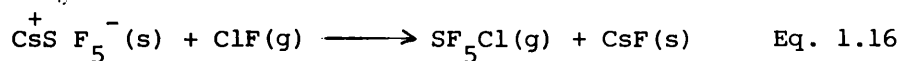
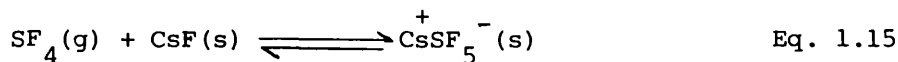
#### 1.2.9 CHLOROFLUORINATION OF SULPHUR TETRAFLUORIDE WITH CHLORINE MONOFLUORIDE.

The reaction between chlorine monofluoride and sulphur tetrafluoride to give sulphur chloride pentafluoride requires high temperature<sup>63c</sup> but in the presence of caesium fluoride, this reaction occurs readily at room temperature with no byproducts as shown in equation 1.14



The role of the metal fluoride in the oxidative addition reactions as in the case of the chlorofluorination of sulphur tetrafluoride or the halogen addition reactions, is not clearly understood. Mechanisms proposed for these reactions have usually involved intermediates related to complex fluoroanions, but in many cases the validity of this approach has been questioned. In 1969 Schack et. al. studied the reaction between

sulphur tetrafluoride and chlorine monofluoride over caesium fluoride to give sulphur chloride pentafluoride at room temperature and reported that, the catalytic effect of caesium fluoride in this reaction probably occurs through polarization of the sulphur tetrafluoride, which makes it readily susceptible to oxidation by the chlorine monofluoride.<sup>82</sup> The formation of caesium pentafluorosulphate can also occur. This salt is then oxidized with chlorine monofluoride to give sulphur chloride pentafluoride.<sup>82</sup> The mechanism proposed is shown in equations 1.15 and 1.16. However, the reaction between sulphur tetrafluoride and caesium

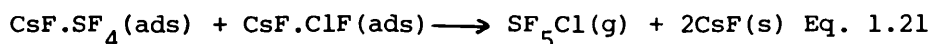
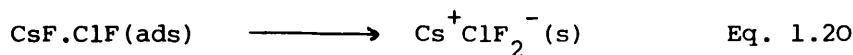
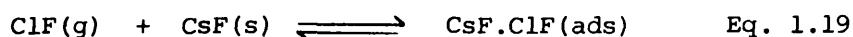
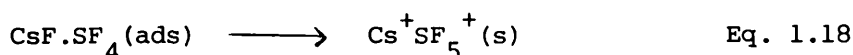
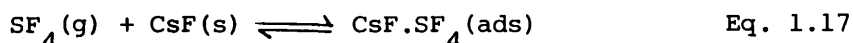


fluoride has been reported<sup>73</sup> to begin only at ca 383 K and even caesium fluoride, pretreated with hexafluoroacetone to increase its surface area showed only a slow adsorption of sulphur tetrafluoride at room temperature. Thus, the oxidative chlorofluorination of sulphur tetrafluoride is much faster than the caesium fluoride-sulphur tetrafluoride complexing reaction. The previous mechanism was shown to be incorrect by Kolta et al. in 1982,<sup>83</sup> in that such a mechanism does not take into account the reaction between chlorine monofluoride and caesium fluoride. The results of radiotracer studies in this Department, involving  $\{^{36}\text{Cl}\}$ -chlorine labelled chlorine monofluoride and  $\{^{35}\text{S}\}$ -sulphur labelled sulphur tetrafluoride showed that there is considerable retention of chlorine monofluoride by the caesium fluoride surface

and that the retained species does not participate to any appreciable extent in reaction with sulphur tetrafluoride.<sup>83</sup>

It is suggested that the caesium difluorochlorate compound is responsible for the observed retention. Similar retention of  $\{^{35}\text{S}\}$  sulphur labelled sulphur tetrafluoride was observed, but the quantities retained were considerably less than those observed for chlorine monofluoride. Furthermore, unlike chlorine monofluoride retention, which led to catalyst poisoning, there was no evidence to suggest that, the retained sulphur tetrafluoride acted as catalyst poison.

Kolta et al. indicated that the formation of sulphur chloride pentafluoride is a true surface reaction involving adsorbed chlorine monofluoride and adsorbed sulphur tetrafluoride, and they interpreted their results by the following equilibria as shown in equations 1.17 - 1.21



where  $\text{CsF} \cdot \text{SF}_4(\text{ads})$  and  $\text{CsF} \cdot \text{ClF}(\text{ads})$  represent the surface adsorbed states of sulphur tetrafluoride and chlorine monofluoride respectively and involve a relatively weak chemical interaction between the substrate and the surface.

These results showed that, mechanisms of reactions

catalysed by ionic fluorides are not as straightforward as was at first thought.

#### 1.2.10 ALKALI METAL FLUORIDES.

Alkali metal fluorides have been widely used as reagents for the substitution of halogens by fluorine for the synthesis of organofluorine compounds.<sup>84,85</sup> At the same time, alkali metal fluorides are rather strong bases in non-aqueous media. The basic properties of alkali metal fluorides have long been known.<sup>86</sup> In 1947 Knunyants et al<sup>87</sup> showed that when heated with potassium fluoride, bornyl chloride is quantitatively converted to camphene. This was the first example of a dehydrohalogenation reaction carried out in the presence of alkali metal fluoride. In the 1950's Yakobson and Vorazhtov investigated the applicability of fluorides of various metals in organic reactions such as the alkylation and the arylation of amino and hydroxy compounds, in Michael, Knoevenagel and other types of reactions, and found caesium fluoride to possess the maximum activity. Lithium and sodium fluorides, as well as calcium, barium and zinc fluorides proved to be inactive in the above mentioned reactions.<sup>88</sup> The activity of alkali metal fluorides was found to decrease in the order<sup>89</sup> caesium fluoride > rubidium fluoride > potassium fluoride > sodium fluoride > lithium fluoride.

The potential ability of the fluoride anion to act as a base might be predicted by considering the strength of the H-F bond  $569 \text{ k J mol}^{-1}$ . On this basis, nucleophilic attack by fluoride toward other nuclei including carbon ( $\text{C-F} = 536 \text{ k J mol}^{-1}$ )

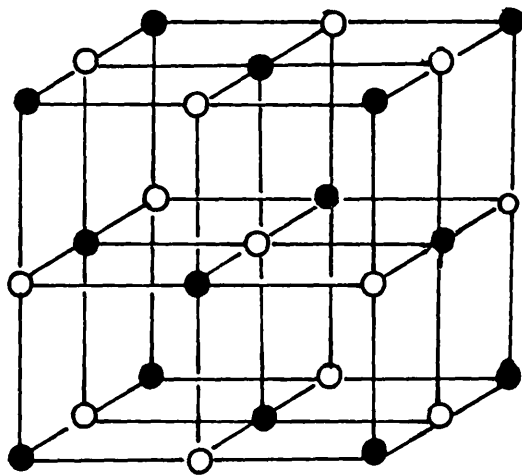


might also be expected to be of possible synthetic value.<sup>90</sup>  
Alkali metal fluorides have a number of advantages over other bases : reactions conducted in their presence give high yields, they proceed quite selectively and without formation of any byproducts, unlike the situation when hydroxides or carbonates of alkali metals are used.<sup>89</sup> It has been suggested that reactions involving alkali metal fluorides usually result in the formation of fluoroanions.<sup>89</sup> The resulting reactive fluoroanions are capable of entering into reactions similar to those of carbenium ions in the chemistry of hydrocarbons.<sup>89</sup> This allows the use of alkali metal fluorides as catalysts in the chemistry of organofluorine compounds.

Most of the more recently reported examples of alkali metal fluorides promoted reactions involve caesium fluoride and potassium fluoride, the former usually being regarded as the most active, although the latter is less hygroscopic and appreciably less expensive. Caesium fluoride and potassium fluoride possess the crystal structure of sodium chloride.<sup>91</sup> In this structure as shown in Fig. 1.16, the M and X atoms alternate in a simple cubic sphere packing. It is the only MX structure in which there is regular octahedral coordination of both atoms. In this lattice each  $M^+$  ion is surrounded by  $6X^-$  ions, and vice versa, at the corners of a regular octahedron. Some physical properties of caesium fluoride and potassium fluoride are given in Table 1.1<sup>92-94</sup>

The use of alkali metal fluorides in Michael and Knoevenagel reactions instead of the traditionally used amines, alkoxides, ammonium salts of organic acids or alkali hydroxides, makes it possible to carry out reactions under milder conditions and increases the yields

Figure 1.16 The unit cell of CsF or KF



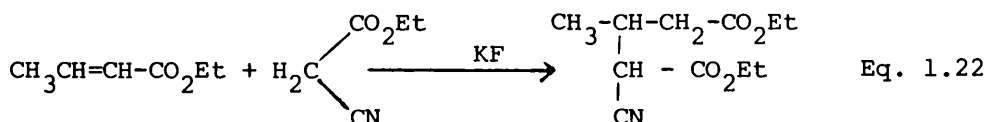
- F
- M = Cs or K

Table 1.1      Physical Properties of MF (M = Cs or K).

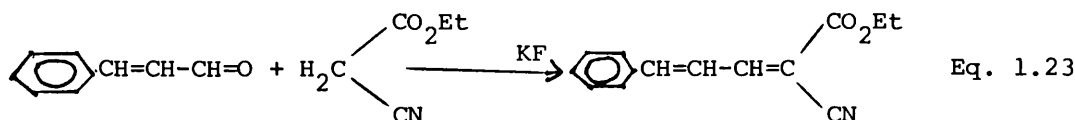
MF	m.p. K	b.p. K	M-F bond A°	a° A°
CsF	703	1253	4.25	6.008
KF	858	1502	3.77	5.347

a° = Length of the unit cell.

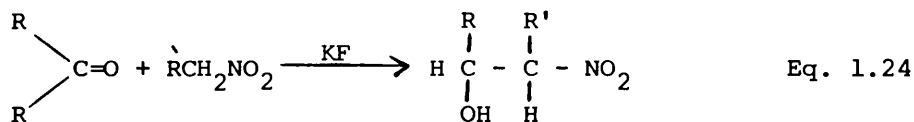
of the reaction products. Midorikawa et al. have found that in the presence of potassium fluoride  $\alpha,\beta$ -unsaturated aliphatic ketones and esters easily interact with active methylene compounds such as ethyl cyanoacetate to give the Michael reaction product<sup>95</sup> shown in equation 1.22



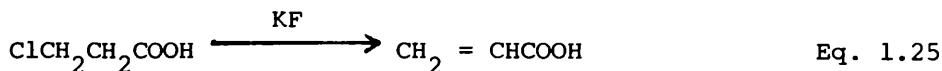
Under similar conditions, cinnamic aldehyde gives a Knoevenagel reaction product as shown in equation 1.23<sup>95</sup>



Addition of an enolate anion to the carbonyl group of an aldehyde or ketone followed by protonation constitutes a reaction known as the Aldol condensation. For example, reactions between aldehydes and nitroalkanes are readily accomplished using potassium fluoride as the basic cataly<sup>96-98</sup> as shown in equation 1.24

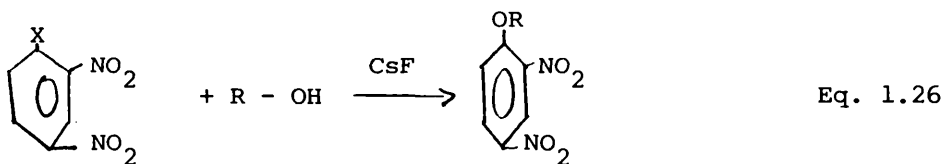


The formation of acrylic acid was observed in the reaction of 3-chloropropanoic acid with potassium fluoride<sup>99</sup> as shown in equation 1.25



Reaction of haloorganics with alcohols or phenols in the presence of alkali metal fluorides leads to the formation of ethers accompanied by the elimination of halide <sup>100</sup> as shown in equation

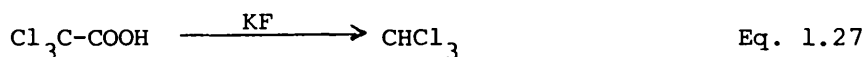
1.26



X = Cl, F, Br

R = CH<sub>3</sub>, C<sub>2</sub>H<sub>5</sub>, C<sub>6</sub>H<sub>5</sub>

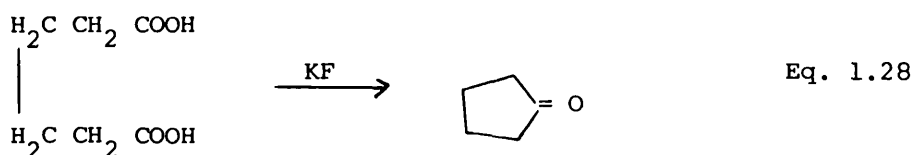
In an attempt to obtain trifluoroacetic acid from trichloroacetic acid in the presence of potassium fluoride, Nesmeyanov et al. <sup>99</sup> isolated chloroform as shown in equation 1.27



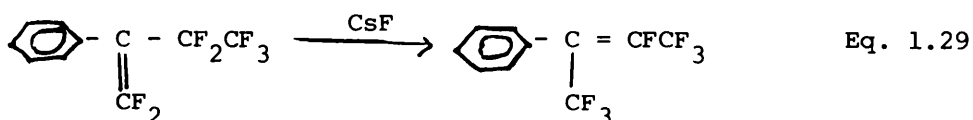
The reaction proved to be applicable to a wide range of acids.

Heating dicarboxylic acid with potassium fluoride in partial decarboxylation which leads to cyclic ketones <sup>101</sup> as shown in equation

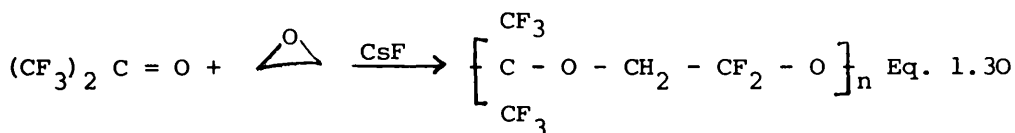
1.28



In the presence of alkali metal fluorides, fluorine containing  $\alpha$ -alkylstyrenes are transformed to more stable isomers <sup>102</sup> as shown in equation 1.29

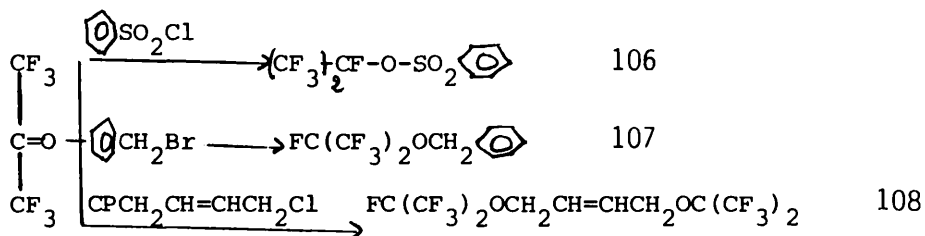


There have been numerous reports in the last thirty years describing the use of ionic fluorides as catalysts in polymerisations<sup>103,104</sup>. For example, hexafluoroacetone reacts with oxiranes in the presence of caesium fluoride to give a linear polymeric product<sup>105</sup> as shown in equation 1.30. In the presence of potassium fluoride hexafluoroacetone undergoes the following



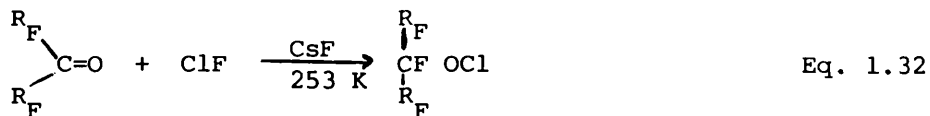
mol mass = 118000

transformation as shown in equation 1.31.

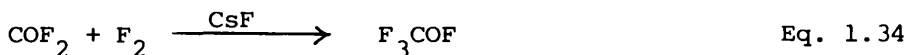
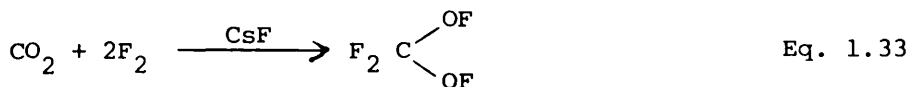


Eq. 1.31

Compounds such as trifluoromethoxychloride, pentafluoroethoxychloride and other similar compounds can be prepared at low temperature by the caesium fluoride catalysed addition of chlorine monofluoride to the appropriate carbonyl compound<sup>109</sup> as shown in equation 1.32. Carbon dioxide and carbonyl fluoride react with



difluorine in the presence of caesium fluoride as shown in equations 1.33 and 1.34



### 1.3 ALUMINA

Aluminas are gaining attention as supports for alumina-based catalysts<sup>110,111</sup> because of their attractiveness for study by modern surface analytical techniques.<sup>112</sup> High surface area aluminas are used commercially as supports in many industrial catalytic processes<sup>113,114</sup> Transition metal sulphides (Co, Ni, Mo, W etc)<sup>115</sup> supported on alumina are catalytically active towards hydronitrogenation, hydrodesulphurisation or hydrodemetallation reactions of heavy petroleum fractions.<sup>116</sup> Supported noble metals are used in reforming reactions<sup>117 119</sup>, whilst supported metal oxides such as iron-oxides are very active for dehydrogenation processes.<sup>120</sup> These various uses of alumina show that, it is far from a passive support, many of the catalysts showing bifunctional properties.

#### 1.3.1 TYPES OF ALUMINA

The behaviour of alumina as a support or catalyst depends on the method of preparation,<sup>121-126</sup> Stoichiometrically there is only one oxide of aluminium, namely, alumina ( $\text{Al}_2\text{O}_3$ ). However this simplicity is compensated by the occurrence of various polymorphs and hydrated species.<sup>127</sup> The classification of polymorphs based upon the crystallographic structures of the aluminas

has been implemented.<sup>128</sup> Three distinct series of alumina have been identified, based on close packed oxygen lattices with aluminium in octahedral and tetrahedral environments. The  $\alpha$ -series with hexagonal close-packed lattices, characterized by the sequence ABAB, is stable at high temperatures and very hard and resistant to hydration and attack by acids. The  $\beta$ -series with alternating close-packed lattices, is characterized by ABAC-ABAC, ABAC-CABA, and the  $\gamma$ -series with cubic close-packed lattices, characterized by the sequence ABC-ABC.<sup>129</sup>

A representative of the first series is  $\alpha$ -alumina with a corundum structure<sup>130</sup> described as face-sharing pairs of octahedra interlinked through edges to form layers of six member rings. The  $\beta$ -series consists of X- and K-alumina, which are products of the decomposition of the true aluminium hydroxide, Gibbsite  $(Al(OH)_3)$ .<sup>131</sup> Members of  $\gamma$ -series are obtained on decomposition of the hydroxides Bayerite, Nordstrandite and Boehmite  $(AlO.OH)$ , and can be divided into a low temperature group ( $\gamma$ - and  $\zeta$ -alumina) and the high temperature group ( $\delta$ - and  $\theta$ -alumina).<sup>132</sup>

In this work we will investigate the properties of the low temperature phase  $\gamma$ -alumina as a support for alkali metal fluorides.

The so-called  $\gamma$ -,  $\zeta$ - and  $\chi$ -aluminas are the most extensively used in heterogeneous catalysis. Their surfaces contain chemical defects caused by dehydroxylation or anion additions, which act either catalytically<sup>133</sup> or as potential binding site for active species. These types of alumina have been classified as either Lewis or Brønsted acids and bases. For example, the incorporation of fluorine in alumina catalysts enhances their activity for acid-



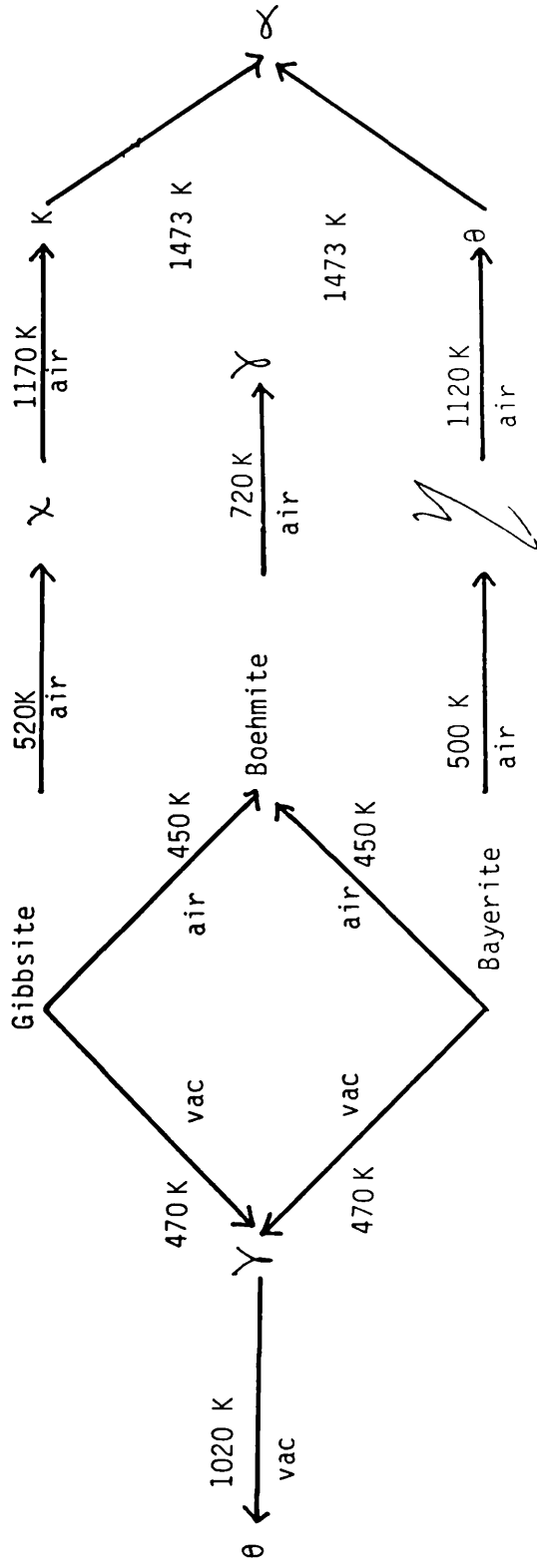
catalysed reactions such as the cracking of dimethylbutane<sup>134</sup> and the olefin polymerisation.<sup>135</sup> The fluorine incorporated replaces surface oxygen or hydroxyl, and because fluorine is very electro-negative it polarizes the lattice more than the groups it replaces. This increases the acidity of both protonic (Brønsted) and non-protonic (Lewis) sites on the surface.<sup>136</sup> However, the impregnation of fluoride ions on to  $\gamma$ -alumina enhances its activity for base-catalysed reactions such as Michael addition<sup>137</sup> as is discussed later in this chapter.

### 1.3.2 PREPARATION OF $\gamma$ -ALUMINA.

When an aqueous solution containing aluminium(III) is neutralised with ammonia, bulky amorphous precipitates containing a large quantity of water are formed.<sup>138</sup> The precipitate is a gel-like substance which gives a diffuse x-ray powder diffraction diagram. The slurry from this precipitate is normally aged at temperatures between 313 and 353 K at a  $pH > 12$ <sup>139</sup> for ca 8h.<sup>140</sup> If the ageing process is prolonged, Bayerite is formed, hence the detail of this ageing procedure is important in determining the properties of the final product. After ageing the precipitate is filtered, washed and dried. The final procedure in the preparation of  $\gamma$ -alumina consists of heating the solid at high temperatures up to 873 K.

During the thermal treatment, alumina passes through various states of hydration and several distinct compounds are observed as shown in Fig. 1.17.<sup>141</sup>

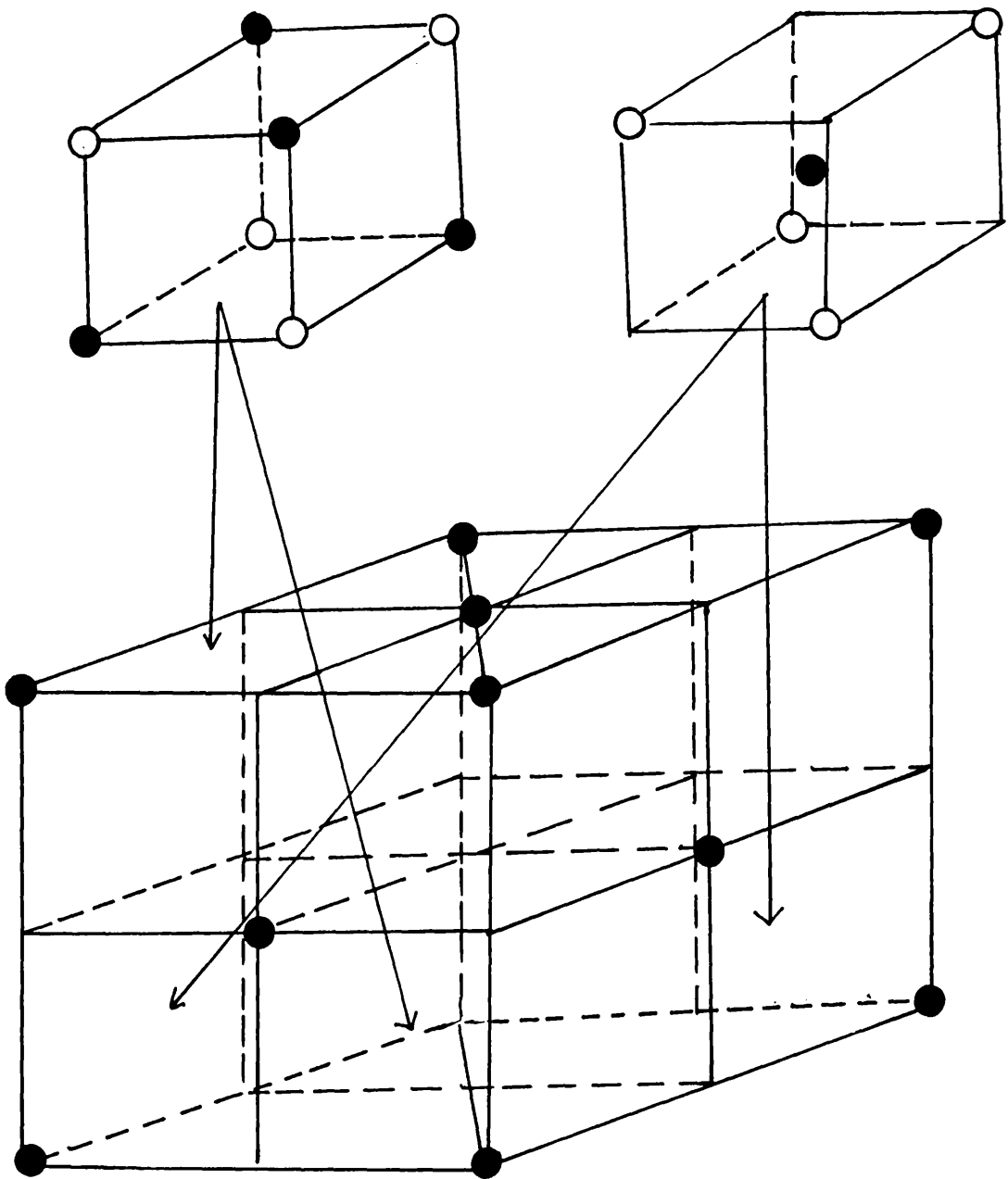
Figure 1.17



### 1.3.3 STRUCTURE OF $\gamma$ -ALUMINA

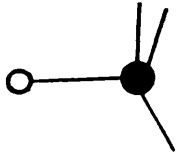
The unit cell of spinel ( $AB_2O_4$ ) is formed by a cubic close packing of 32 oxygen atoms with 16 trivalent atoms in half of the octahedral interstices and 8 divalent atoms in tetrahedral holes<sup>142</sup> as shown in Fig. 1.18. Powder x-ray diffraction has established that,  $\gamma$ -alumina crystallises with a spinel-related structure<sup>130</sup> in which 32 oxygen atoms per unit cell are arranged exactly as in a spinel but with  $21 \frac{1}{3}$  aluminium atoms distributed over the 24 cation positions available.<sup>143</sup> There are in average  $2 \frac{2}{3}$  vacant cation sites per unit cell. Electrical neutrality is partially achieved by the occurrence of these vacant sites. The crystallite surface contains hydroxyl groups in place of oxygen ions which further contribute to the electrical neutrality of the  $\gamma$ -alumina crystallite. Peri<sup>144</sup> had shown by Monte Carlo simulation of the dehydration process of the surfaces of  $\gamma$ -alumina that, there are five types of hydroxyl groups surrounded by different numbers of oxides (exposed O atom) and /or anion vacancies (exposed Al atom), as shown in Fig. 1.19. The stoichiometry of  $\gamma$ -alumina based on the unit cell and the assumption that  $\gamma$ -alumina grains expose only the flat planes, which are locally assigned to (100), (111) and (110) planes is a  $Al_{2.5} \square_{0.5} O_4$ . By taking its fully hydroxylated state into account can be derived a precursor of stoichiometry  $Al_{2.5} \square_{0.5} O_{3.5} (OH)_{0.5}$ . This formula of  $\gamma$ -alumina in its fully hydroxylated state has recently been confirmed.<sup>145</sup> A three dimensional model of the surface of  $\gamma$ -alumina based on (100) phase is shown in Fig. 1.20. In this model, there are five distinct aluminium environments that may occur for terminal hydroxyl groups, and the  $\gamma$ -alumina surface heterogeneous.

Figure 1.18 Spinel unit cell

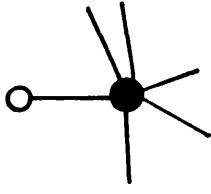


○ oxygen

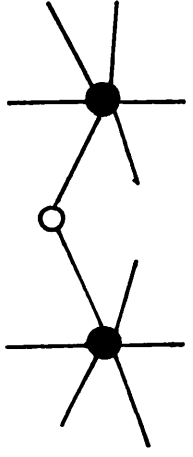
● aluminium



tetrahedral



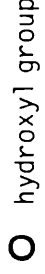
octahedral



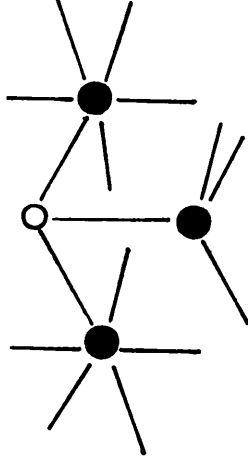
octahedral-o- octahedral



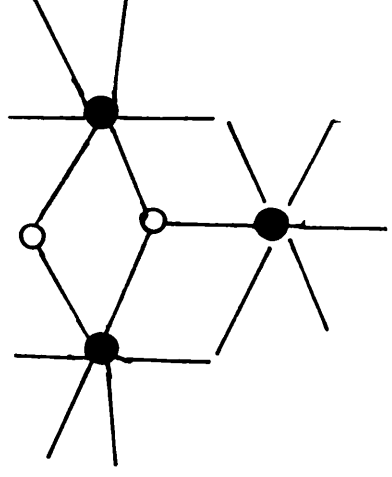
aluminium



hydroxyl group



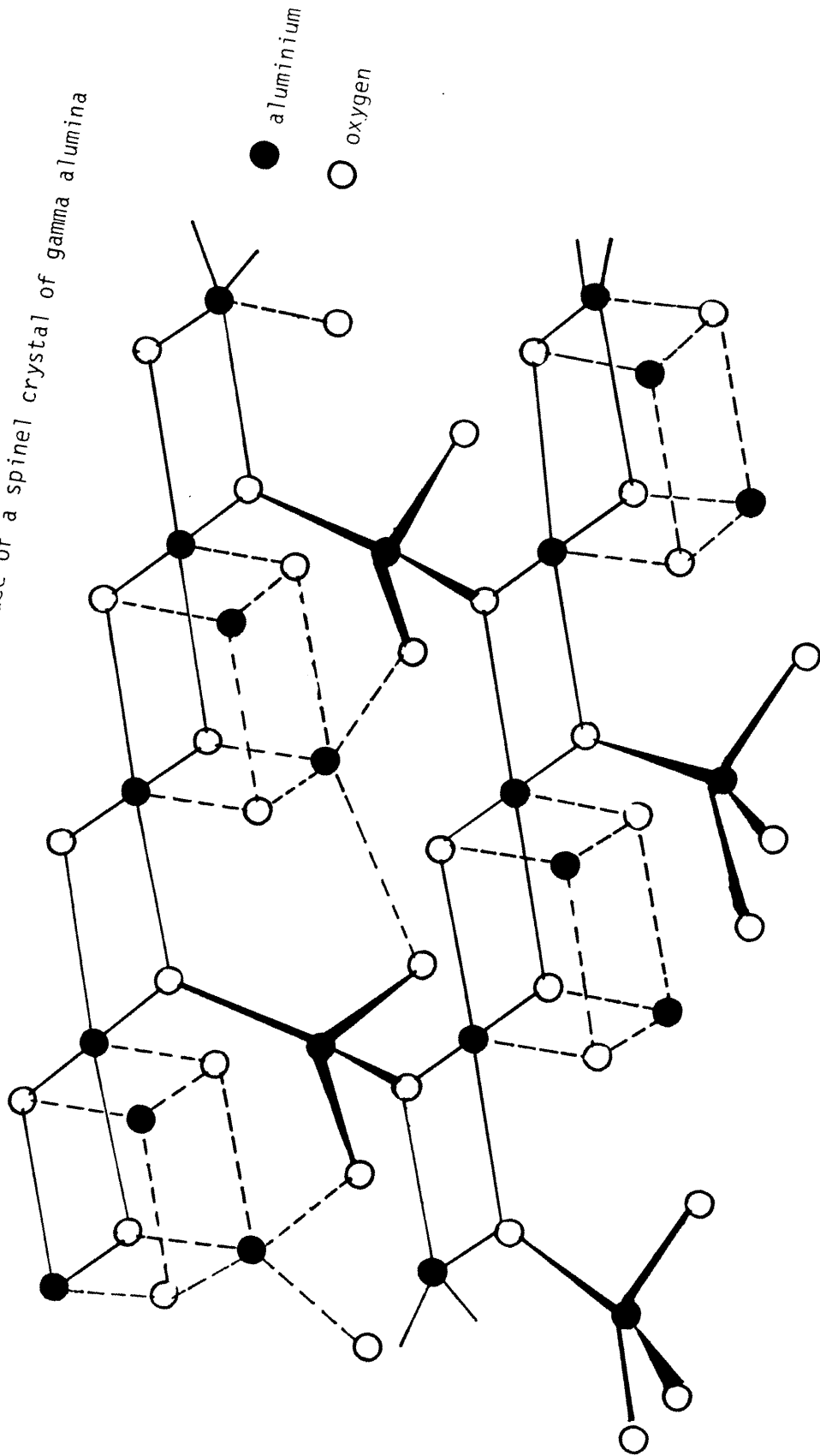
oct-tet  
|  
tet



oct-oct  
|  
tet

**Figure 1.19** Basic cluster of gamma phase alumina

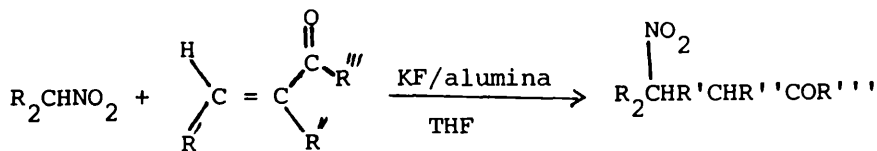
Figure 1.20 (100) face of a spinel crystal of gamma alumina



1.4 PREVIOUS WORK USING CAESIUM AND POTASSIUM FLUORIDES

SUPPORTED ON  $\gamma$ -ALUMINA .

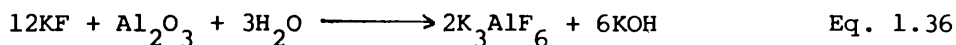
Catalysts and reagents supported on inorganic substrates have received increasing attention in recent years as a means to develop more convenient or selective catalysts or reagents.<sup>146,147</sup> In this context caesium or potassium fluoride supported on various types of metal oxide has been used as a base.<sup>148</sup> Such heterogeneous bases have been known to be effective in both Aldol condensations and Michael addition reactions. The impregnation of caesium or potassium fluoride on to  $\gamma$ -alumina greatly enhances the activity of this base catalyst.<sup>149,150</sup> Other workers have also noted that the use of basic alumina as a support for potassium fluoride leads to moderate yields of Michael addition products under heterogeneous conditions.<sup>151</sup> In solution for example the Michael additions of nitroalkanes to  $\alpha,\beta$ -unsaturated carbonyl compounds using potassium fluoride supported basic alumina in the presence of tetrahydrofuran, can be carried out in large scale<sup>151</sup> as shown in equation 1.35. Several other reports have also highlighted the



Eq. 1.35

utility of this convenient solid base, and some useful applications of it have been published. A recent study has suggested that the nature of the reaction and the role of the basic reagent are important factors to consider in determining appropriate metal fluoride supported on alumina preparation.<sup>152</sup> Reagent loading and drying conditions have been compared for alkali metal fluorides

supported on alumina, by reactions studies and using of analytical techniques such as thermogravimetric analysis and  $^{19}\text{F}$  solid state MAS-NMR.<sup>153</sup> These reactions and analytical studies provided some rationalisation of the reaction results as well as the nature of the active basic species and led to the conclusion that, the formation of free hydroxyl groups on the surface of reagents cannot be entirely responsible for the high basicity of the reagents and it seems that coordinatively unsaturated fluoride ion on the reagent surface plays very important role in the behaviour of the reagents.<sup>153</sup> High metal fluoride loadings and high drying temperatures resulted in significant structural damage of  $\gamma$ -alumina phase with loss in the activity of the reagents. Powder x-ray diffraction and infra-red analysis have clearly indicated the formation of potassium hexafluoroaluminate  $\text{K}_3\text{AlF}_6$ .<sup>153</sup> The formation of hexafluoroaluminate must be accompanied by the formation of hydroxides and/or aluminate according to equation 1.36



Weinstock et al.<sup>154</sup> have recently noted the presence of potassium hexafluoroaluminate in an unspecified sample of potassium fluoride supported on alumina and have stated that fluoride ion has little or no direct role in the enhanced reactivity, but rather potassium hydroxide and/or aluminate are the agents responsible for the catalysis. Further study showed that the free hydroxyl groups alone cannot explain the high activity of potassium fluoride supported on aluminas.<sup>155</sup> Clark et al.<sup>155</sup> suggested that caesium or potassium fluoride supported on aluminas owe their efficient and



versatile reactivity as heterogeneous bases for organic synthesis to at least three possible mechanisms: i) dispersion and increased surface area of caesium or potassium fluoride giving coordinatively unsaturated fluoride ion; (ii) liberation of strong base during preparation and (iii) the cooperative action of fluoride ion and the hydrated alumina surface.

While the applications and advantages of caesium or potassium fluoride supported on  $\gamma$ -alumina as heterogeneous bases for organic synthesis continue to increase, the nature of the active basic sites remain a point of contention.

In the other hand, fluorinated  $\gamma$ -alumina is very active for most of the acid-catalysed hydrocarbon reactions involving skeletal rearrangement.<sup>156</sup> It is, for example, catalytically active for cracking, isomerization, alkylation, polymerisation and disproportionation of alkanes, alkenes and aromatics.<sup>136</sup> There are two common methods of incorporating fluorine in  $\gamma$ -alumina: (i) vapour phase fluorination and (ii) impregnation. In vapour phase fluorination the  $\gamma$ -alumina is maintained in contact with vapours of fluorine-containing compounds at temperatures between 296 - 773 K but the impregnation is carried out by saturating the  $\gamma$ -alumina, usually at room temperature, with an aqueous solution containing an appropriate quantity of the fluorine-containing compounds, as shown in Table 1.2. Although fluorinated aluminas are widely used as promoters for metals, such as platinum, palladium or nickel for hydrocarbon reforming, isomerization or polymerisation processes, no previous work using caesium or potassium fluoride supported on fluorinated

Table 1.2Fluorination of  $\gamma$ -Alumina.

Source of fluorine	Method
HF	Vapour phase
HF	Impregnation
$\text{NH}_4\text{F}$	Impregnation
$\text{NH}_4\text{HF}_2$	Impregnation
$\text{BF}_3$	Vapour phase
$\text{NH}_4\text{AlF}_4$	Impregnation
$\text{FSO}_3\text{H}, \text{SbF}_5$	Impregnation
$\text{FSO}_3\text{H}-\text{SbF}_5$	Impregnation

$\gamma$ -alumina has been reported in the literature.

In this work, metal fluoride supported on fluorinated alumina was studied and the basic sites were characterized.

## CHAPTER TWO

## EXPERIMENTAL

### 2.1 EQUIPMENT

All operations were carried out under the most rigorously water-free conditions available, due to the hygroscopic properties of most of the reactants used in this work. Solids were handled in vacuo ( $10^{-4}$  Torr) or in an inert atmosphere box ( $H_2O < 10$  p.p.m.).

#### 2.1.1 VACUUM SYSTEMS

Manipulations of volatile material were carried out in evacuated systems. Two separate systems were used, Pyrex glass lines for experiments that involved radiochemical counting techniques, and Monel metal lines for handling anhydrous hydrogen fluoride and chlorine monofluoride.

##### (a) THE GLASS VACUUM LINE

Each vacuum line was an enclosed Pyrex glass structure which consisted of a main manifold, a constant volume manometer and a Vacustat. The system was evacuated to a pressure of  $10^{-4}$  Torr by means of a mercury diffusion pump, together with an oil-sealed rotary pump. The Vacustat was used to estimate the pressure achieved. Volatile material was prevented from entering the pumps by a series of glass traps which were cooled in liquid nitrogen. The pumps and waste traps could be isolated from the rest of the line using either a glass or polytetrafluoroethylene (Rotaflon or J. Young) stopcock Fig. 2.1.

The main components of the system were a manometer or pressure gauge (Heise) to measure the pressure of gas or vapour contained in the line to a precision of  $\pm 0.5$  Torr and  $\pm 1$  Torr

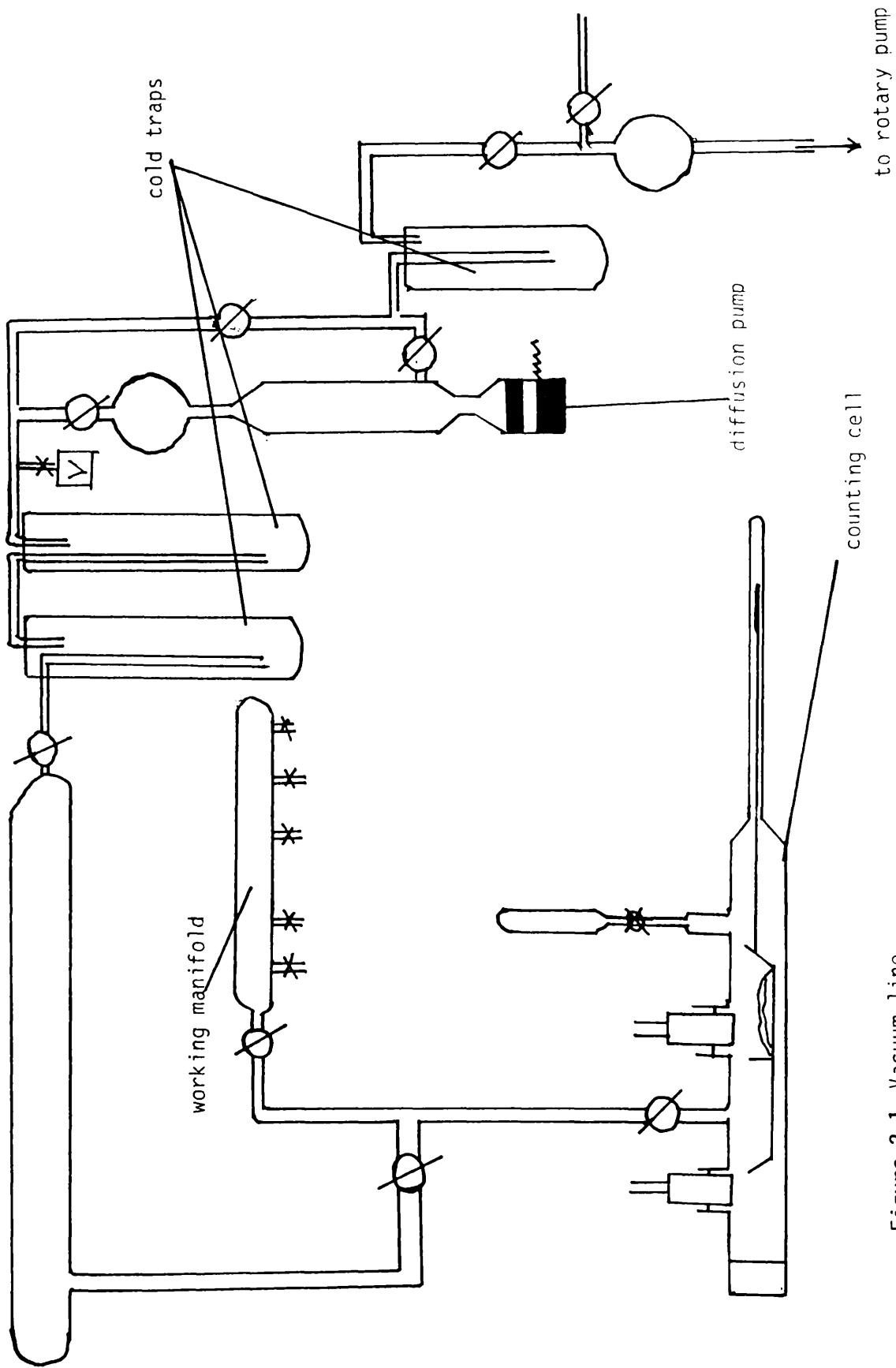


Figure 2.1 Vacuum line

respectively. The type of, <sup>the</sup> main manifold fitted depended on the operation being carried out. The simplest manifold had several B14 ground glass sockets which could be isolated from the system by means of high vacuum stopcocks (J. Young). Vacuum flasks, Fig. 2.2 and dropping vessels Fig. 2.3 equipped with high vacuum stopcocks (J. Young or Rotaflo) and B14 cones, were attached to the sockets of the manifold using Kel-F grease. The glass vessels and the line were flamed out with a gas/oxygen flame while the system was being pumped. Although this process did not remove all moisture adsorbed on the surface of the glass a reduction in the level of adsorbed water was achieved.

(b) MONEL METAL LINE

Monel is an alloy of nickel and copper and was selected for its chemical resistance to corrosive chemicals, particularly fluorides. Each Monel vacuum system was constructed using 2/5 inch O.d. Monel tubing and Monel valves (Autoclave Engineers). Monel metal pressure vessels were attached to the line by means of nipple and collar screw couplings (Autoclave Engineers, high pressure fittings 30VM). The line was equipped with a Budenberg gauge to enable pressure measurements to be made. A lecture bottle of anhydrous hydrogen fluoride, a Monel metal waste trap and a graduated Kel-F tube were also attached to the system, Fig. 2.4. The Monel metal section was connected to waste traps and the vacuum pump via a 1/4 inch glass metal joint.

Chlorine monofluoride was handled in a Monel metal vacuum line, Fig. 2.5. Cylinders of chlorine and chlorine trifluoride were connected via Monel valves. A Monel metal waste trap and

Figure 2.2 Vacuum flask

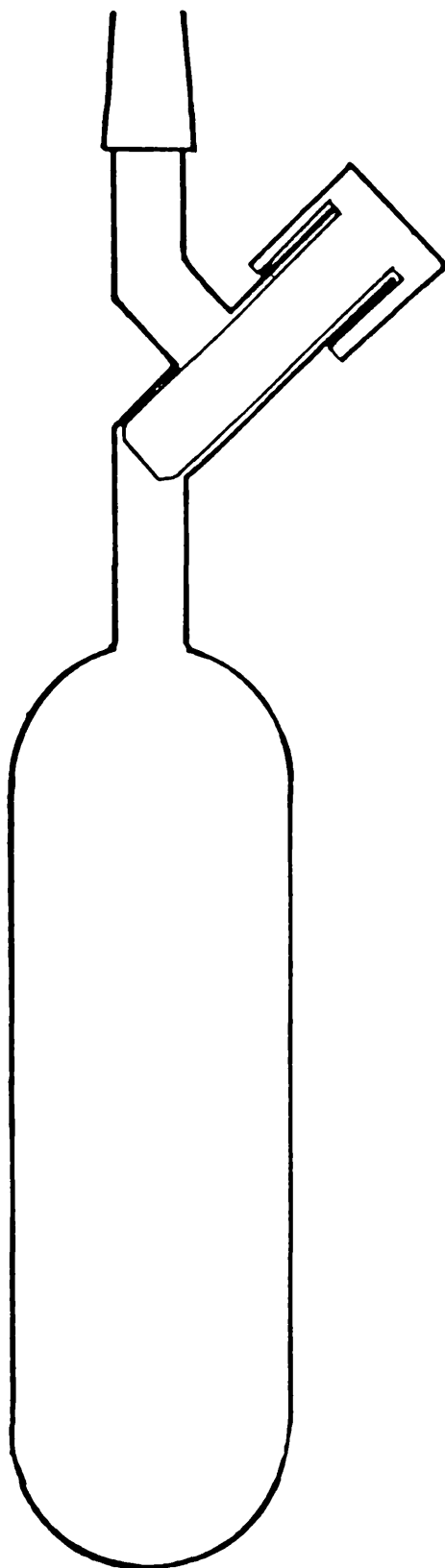
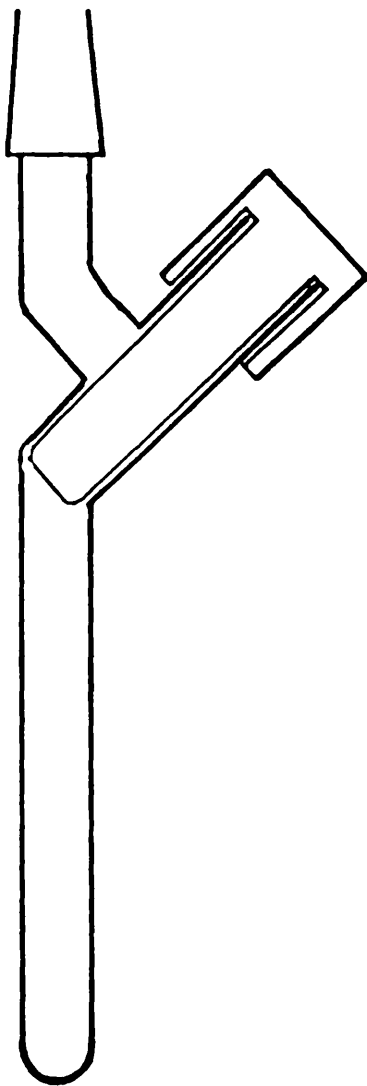




Figure 2.3 Dropping vessel



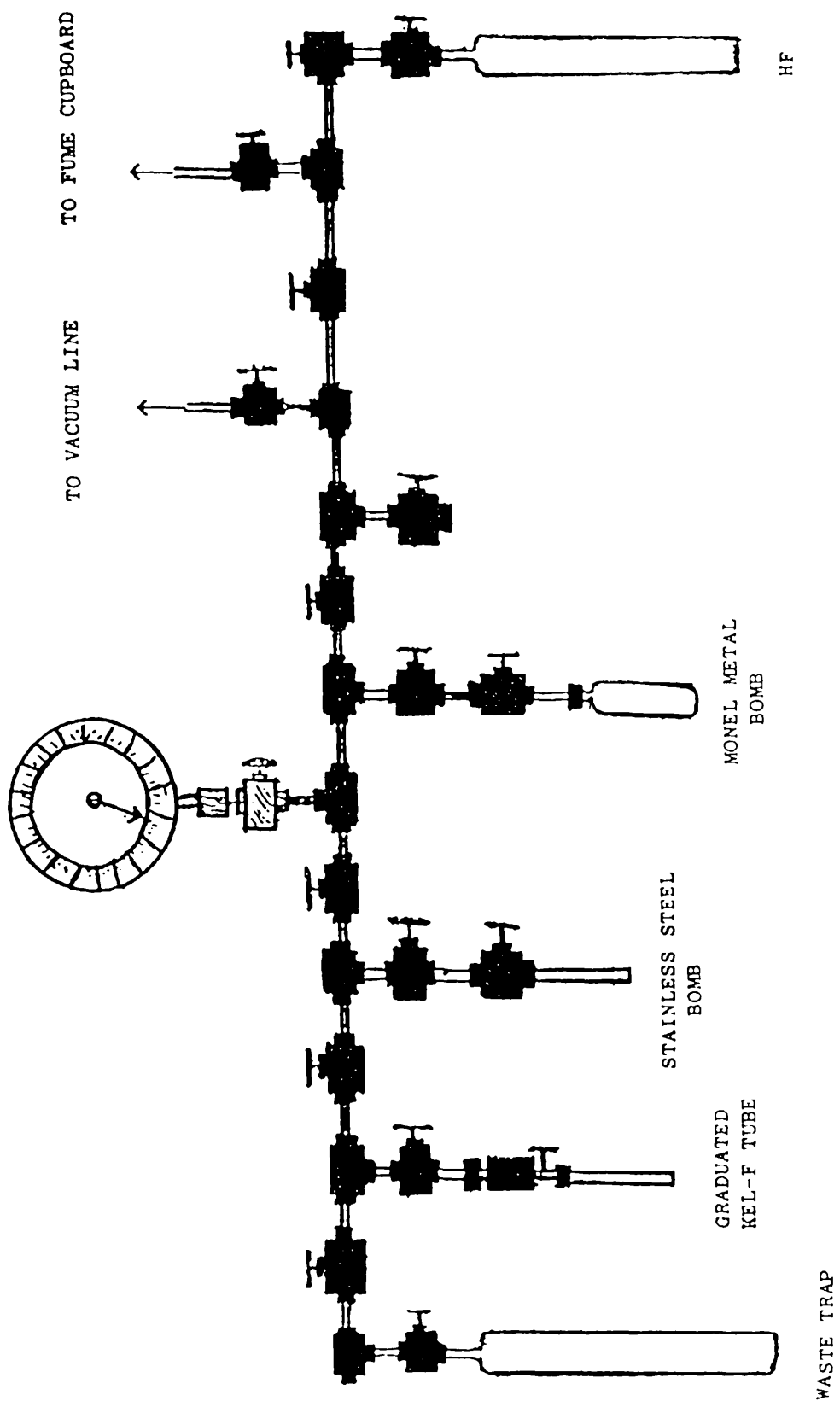


Figure 2.4 Monel metal line for storage of HF

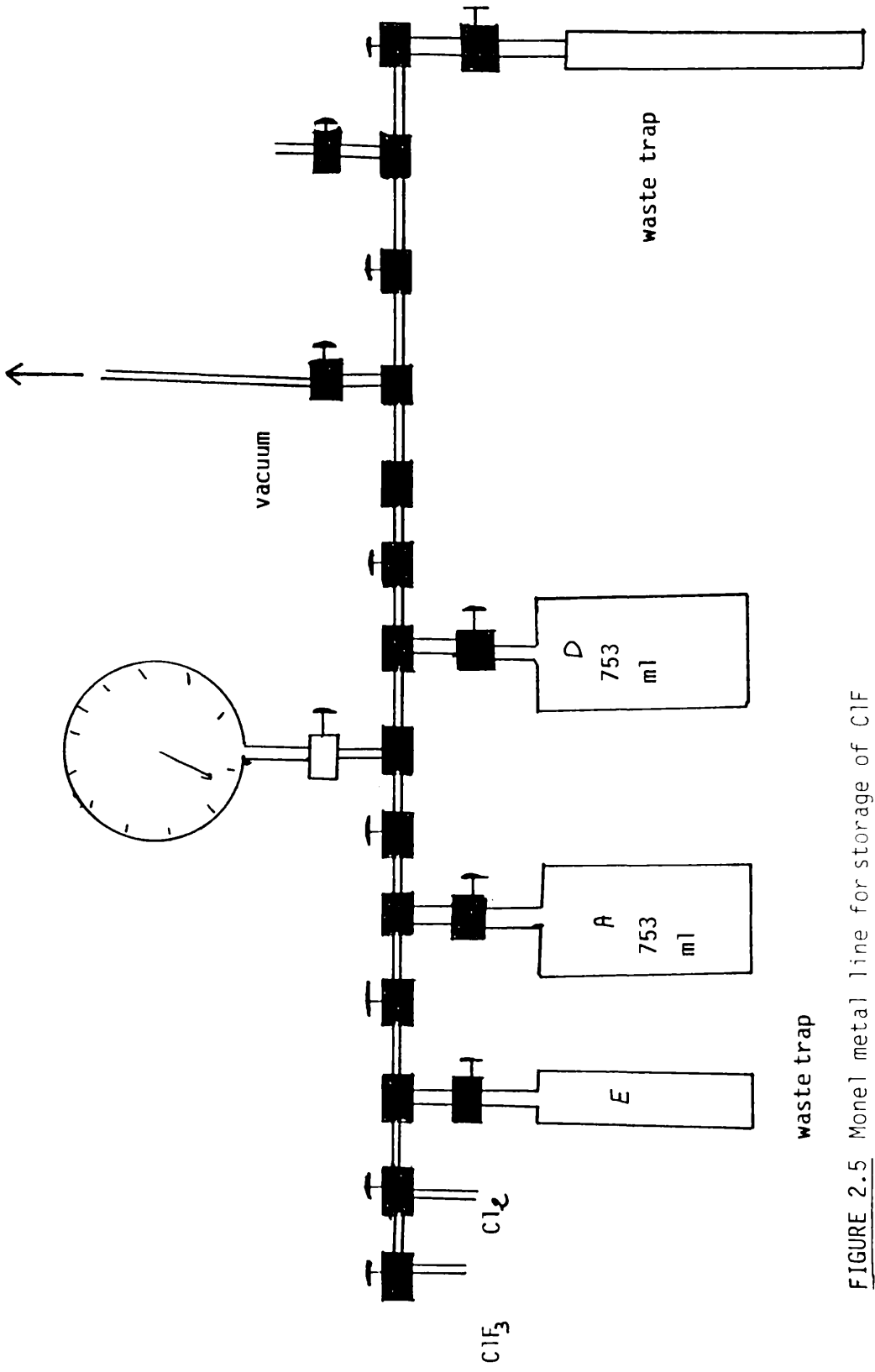


FIGURE 2.5 Metal line for storage of  $\text{ClF}_3$

reaction vessels were also connected by the same means. The metal section was connected via a 2/5 inch glass-metal joint to the traps and the pumps.

#### 2.1.2 GAS UPTAKE APPARATUS

The Pyrex apparatus Fig. 2.6 was used to follow manometrically the uptake of a gas by a solid. The apparatus consisted of a constant volume manometer and a small manifold, a bulb B of known volume and B14 ground sockets to enable ampoules to be attached. The volume of the system was measured accurately before use and changes in pressure were measured using a cathetometer. The constant volume monometer is shown in Fig. 2.7., in more detail. The mercury level was manipulated by admission of air or by evacuating the reservoir using the two way stopcocks, hence the level of the mercury in the left limb could be brought to a constant reference line.

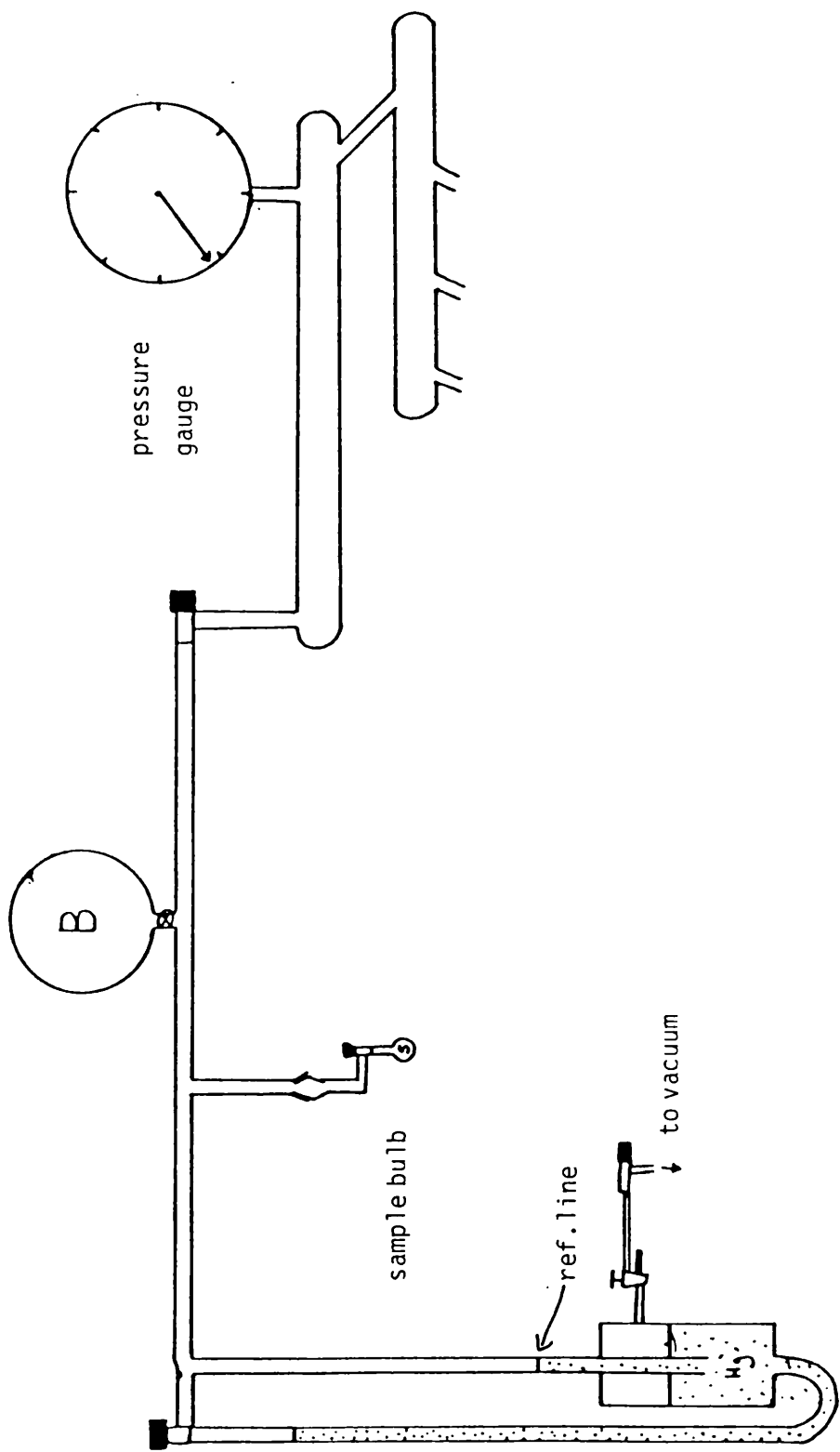
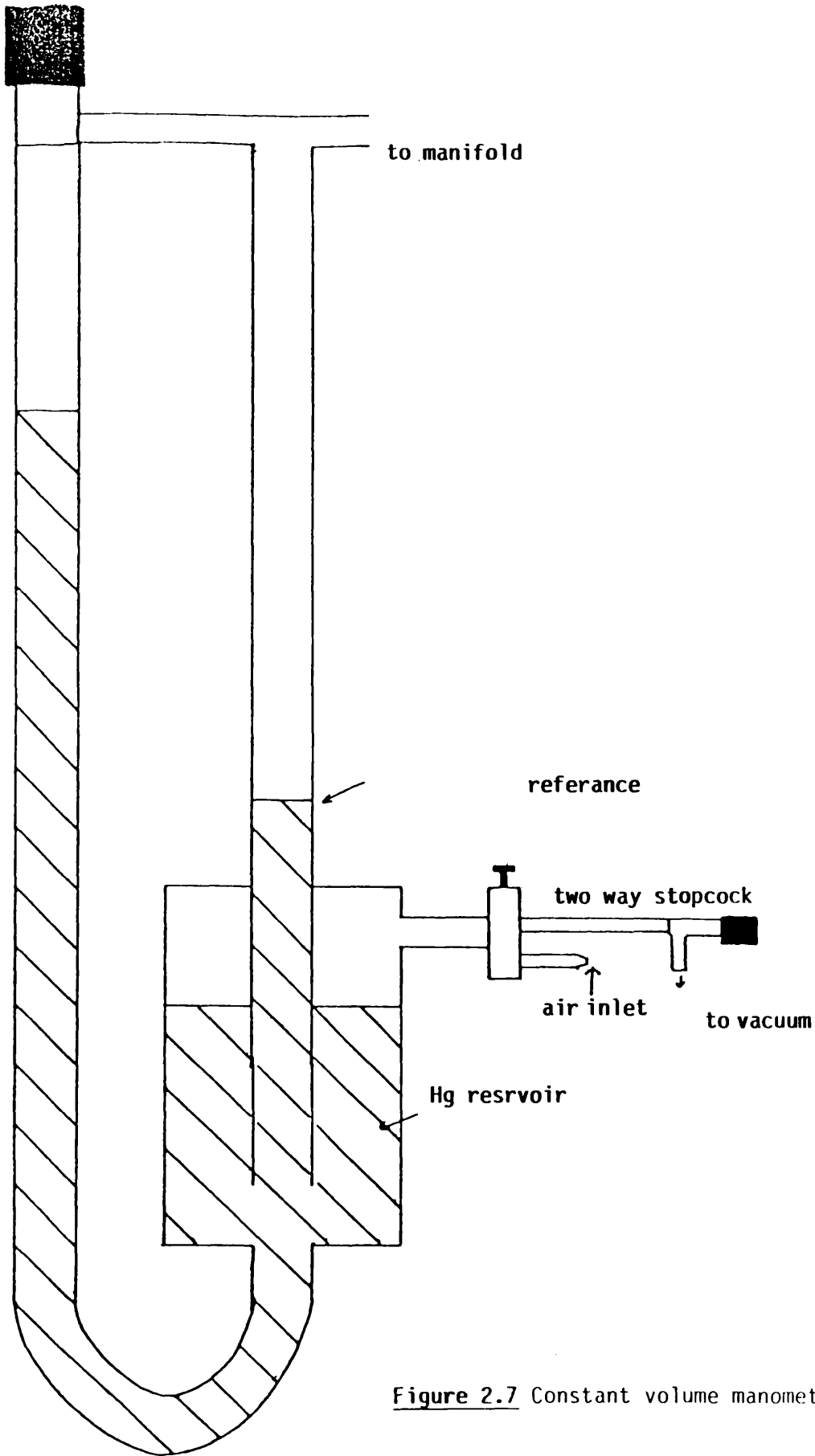


Figure 2.6 Constant volume apparatus



**Figure 2.7** Constant volume manometer

### 2.1.3 TEMPERATURE MEASUREMENT

Some reactions were very exothermic and the apparatus shown in Fig. 2.8 was designed and used to determine the temperature of these reactions at the surface of solids. This apparatus was fitted by a B14 cone to enable it to be attached to the vacuum line, a B14 socket which was used for the attachment of gas sample ampoules. A solid sample was placed in a vessel (2) fitted with a thermocouple and attached to the apparatus via a B24 socket. Before this apparatus was used a series of calibrations was made using different temperatures in the range 195 - 523 K.

### 2.1.4 THE INERT ATMOSPHERE BOX

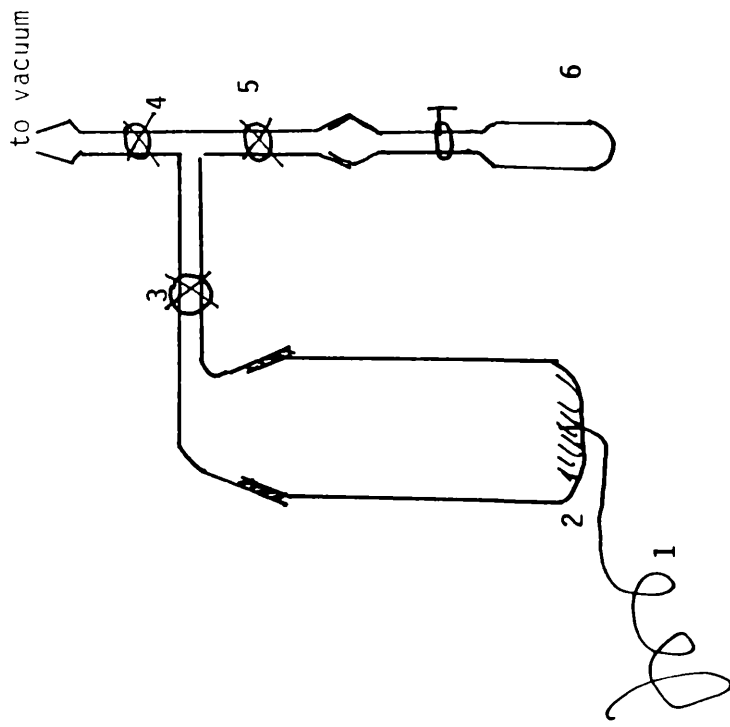
An argon or nitrogen atmosphere Lintott box ( $H_2O < 10$  p.p.m) was used when handling and storing all moisture sensitive samples. Glass flasks were pumped and flamed out before being transferred to the box. The box was equipped with a balance which enabled solid samples to be weighed in this dry atmosphere.

### 2.1.5 INFRA-RED SPECTROSCOPY

Infra-red spectroscopic analyses of the gas phase in the gas/solid systems during and after reactions were carried out using a Perkin Elmer 983 grating infra-red spectrometer. The infra-red cell used is shown in Fig. 2.9 [157] Its path length was 10 cm and either KBr or AgCl windows were used as appropriate. A B14 cone and tap arrangement facilitated attachment to the vacuum line and a B14 socket enabled the attachment of an ampoule containing dry solid. This cell had a volume of  $54.4 \pm 0.6$  cm<sup>3</sup>.

In all gas phase analyses , species were identified by

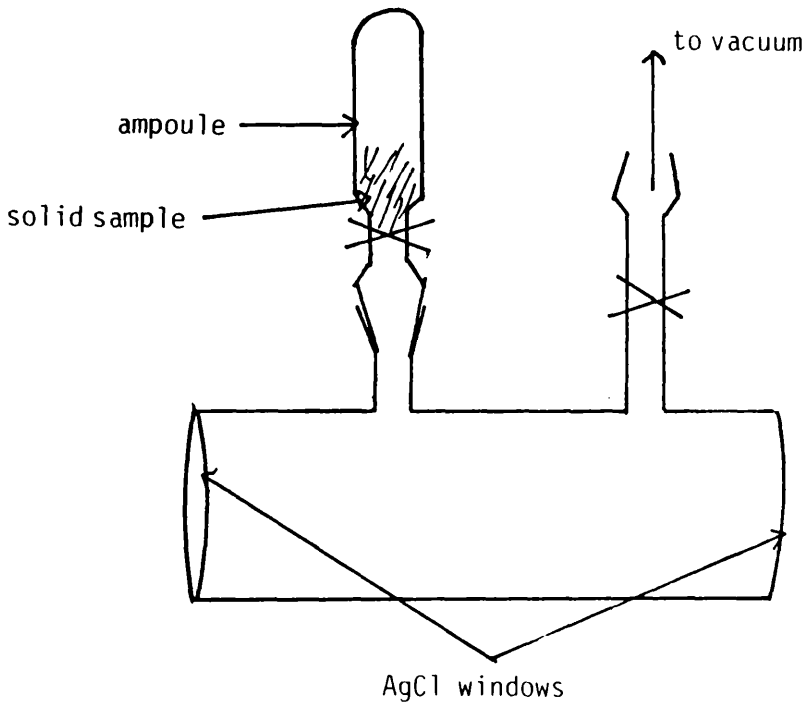
Figure 2.8 Temperature measurement apparatus



- 1) thermocouple
- 2) reaction vessel
- 3, 4, and 5 taps
- 6) Monel bomb containing the gas



Figure 2.9 Infrared gas cell



comparison with standard gas phase spectra. Analytically useful infra-red absorptions of the species studied are tabulated in Table 2.1. Spectra were obtained for various pressures of gaseous sulphur tetrafluoride, thionyl fluoride, sulphur dioxide, carbonyl fluoride and carbon dioxide.

Plots of peak area vs pressure were constructed and those which had correlation coefficients  $> 0.99$  were considered acceptable; details are listed in Table 2.2 and calibration curves are shown in Figs. 2.10 - 2.14.

Spectra of solids were obtained as Nujol mulls, between AgCl plates or as KBr disks. All mulls and disks were prepared in an inert atmosphere box due to their sensitivity to moisture and air.

#### 2.1.6 ELECTRON MICROSCOPY

The idea of using electron beams for microscopy is often assumed to have been a logical consequence of the hypothesis of the nature of the electron [158]. Transmission electron microscopy (T.E.M) was developed in the 1930's and 40's [159]. Modern day commercial electron microscopes, such as the JEOL JEM 1200 EX at Glasgow University, are capable of achieving a resolution of better than 0.3nm routinely. The main features of a modern electron microscope are shown in Fig. 2.15. The JEOL JEM 1200 EX electron microscope has an accelerating voltage of 120 KV.

Electron diffraction patterns (EDP) and microscope images are closely related by the fact that electrons scattered by a specimen

Table 2.1 Infra-red Positions of Volatile Material

Material	Peak Position $\text{cm}^{-1}$
$\text{SF}_4$	892, 860, 730
$\text{SOF}_2$	1308, 801, 721
$\text{SO}_2$	1362, 1151
$\text{COF}_2$	1928, 1249, 963
$\text{CO}_2$	2349, 667

Table 2.2 Analytically Useful Infra-red Peak Positions.

Material	Absorbance $\text{cm}^{-1}$	Assignment
$\text{SF}_4$	860	$\nu_6$
$\text{SOF}_2$	1308	$\nu_1$
$\text{SO}_2$	1151	$\nu_1$
$\text{COF}_2$	963	$\nu_2$
$\text{CO}_2$	2349	$\nu_3$

Figure 2.10 Calibration of sulphur tetrafluoride

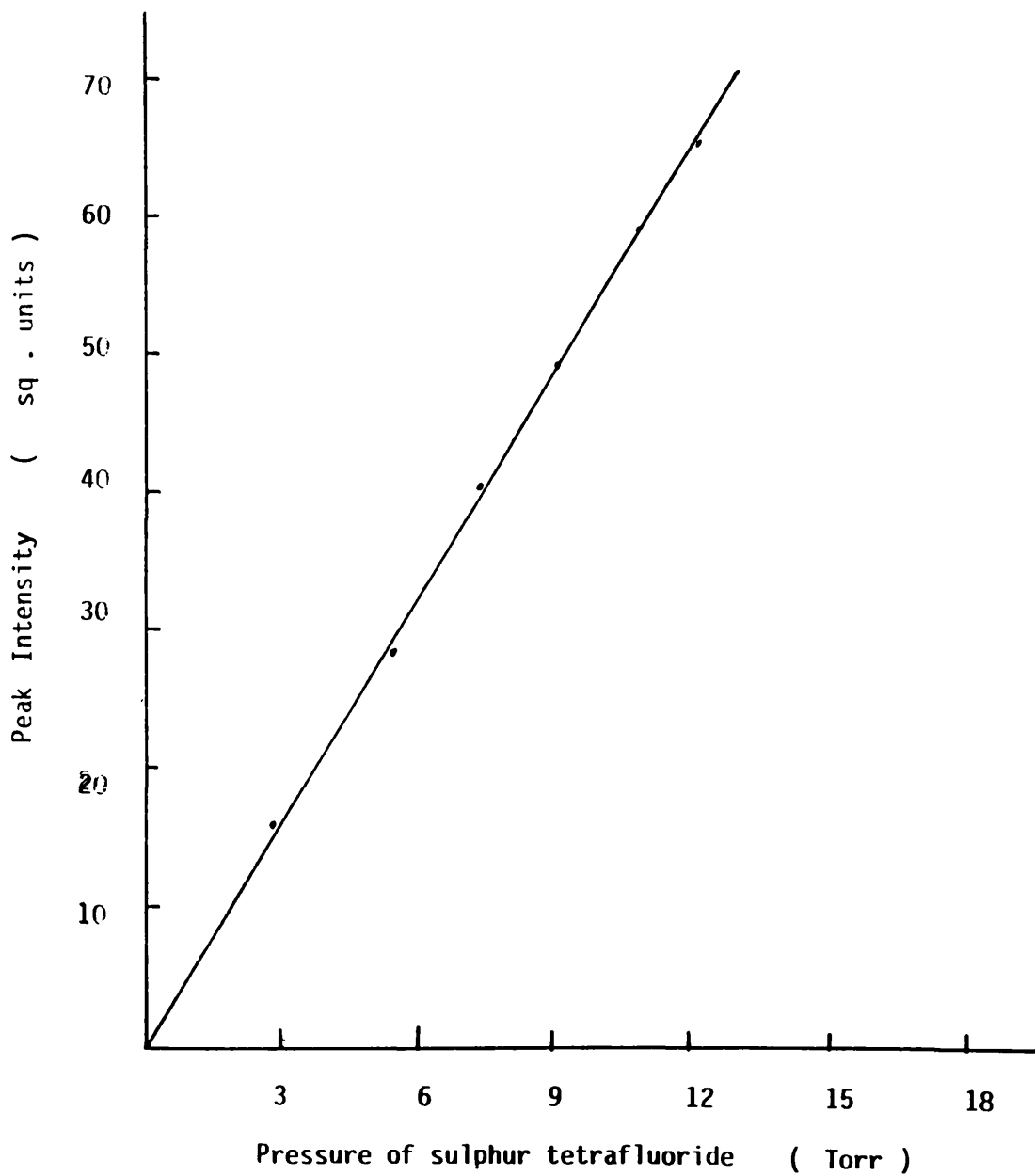


Figure 2.11 Calibration of thionyl fluoride

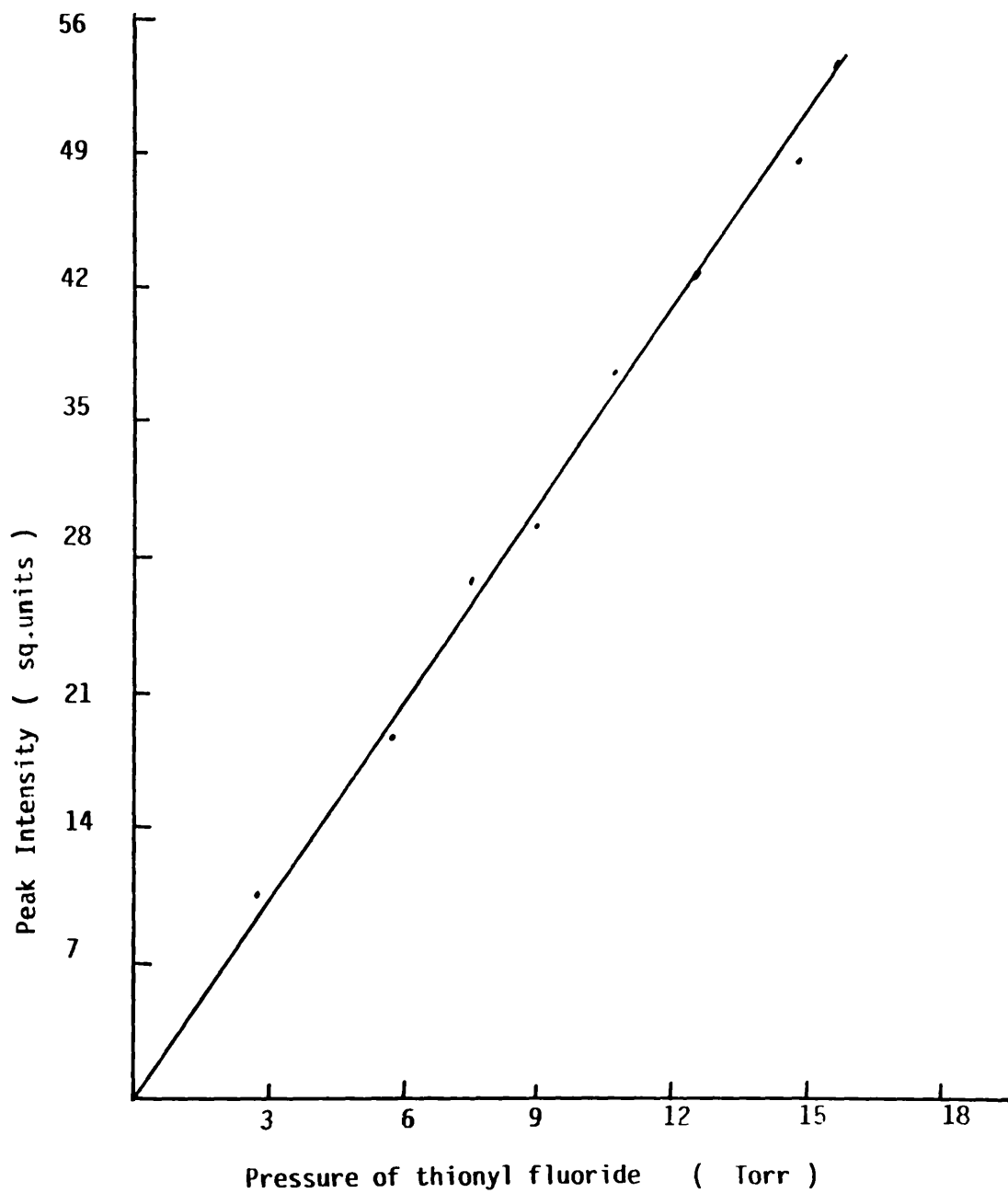


Figure 2.1 2 Calibration of sulphur dioxide

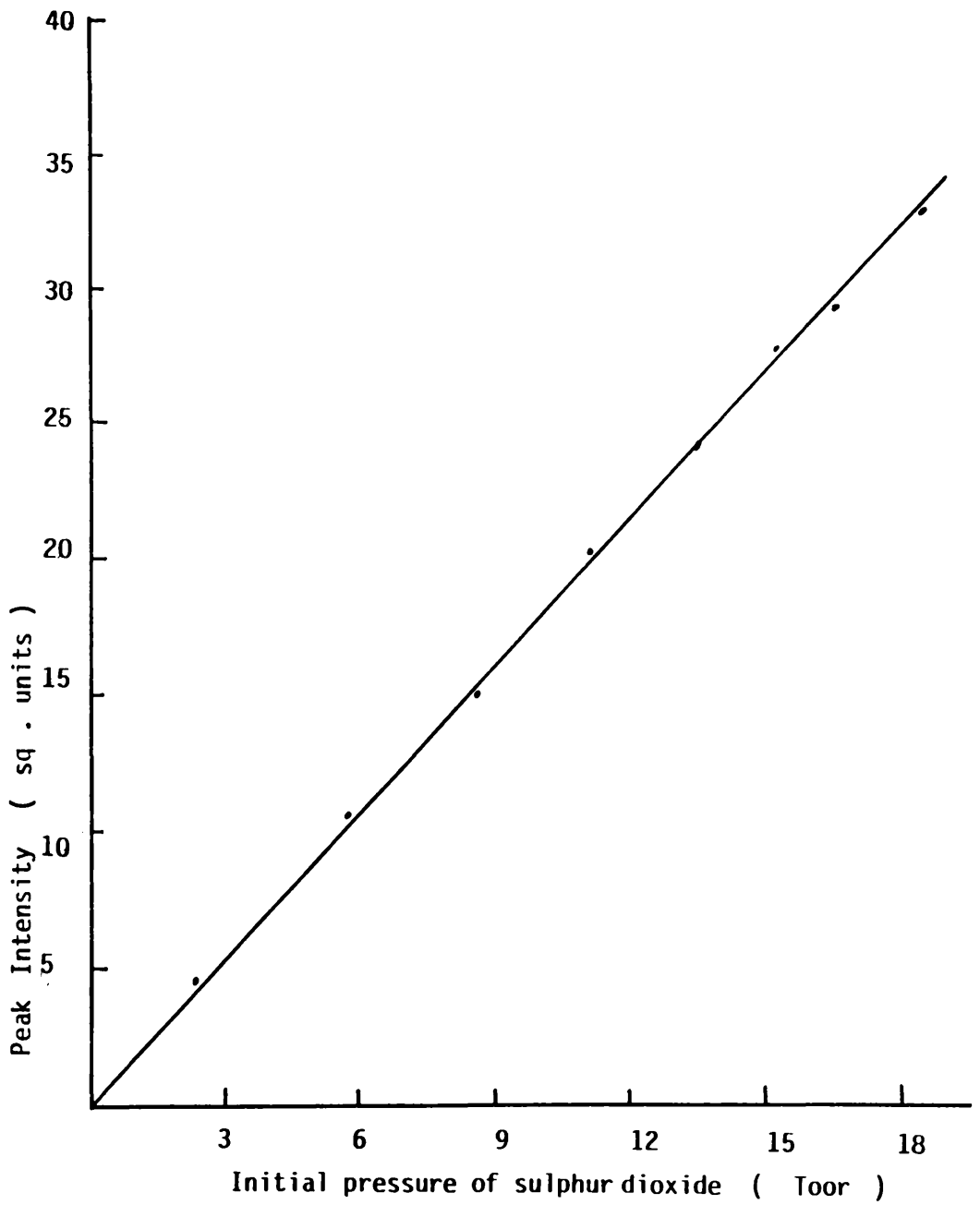


Figure 2.13 Calibration of carbonyl fluoride

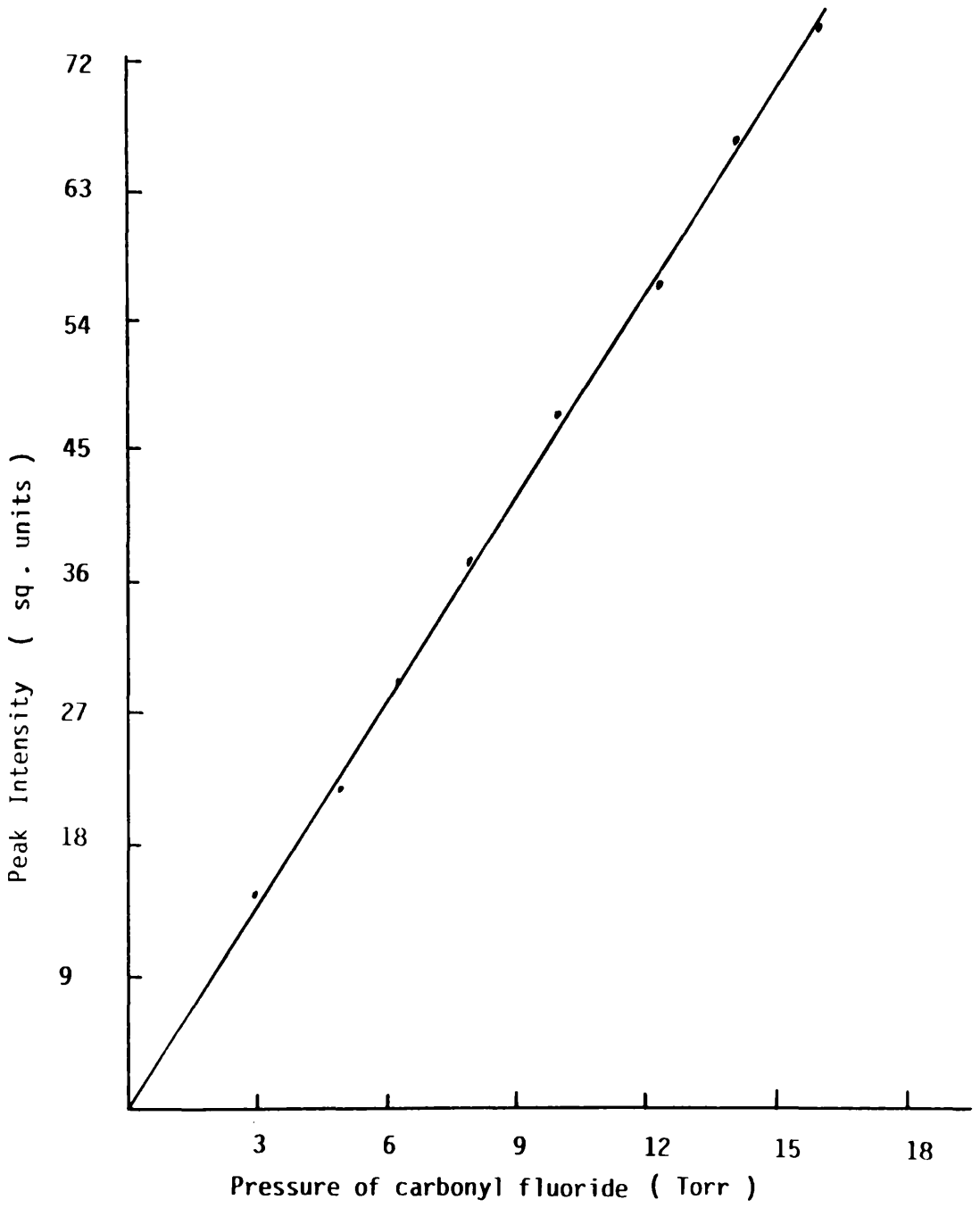
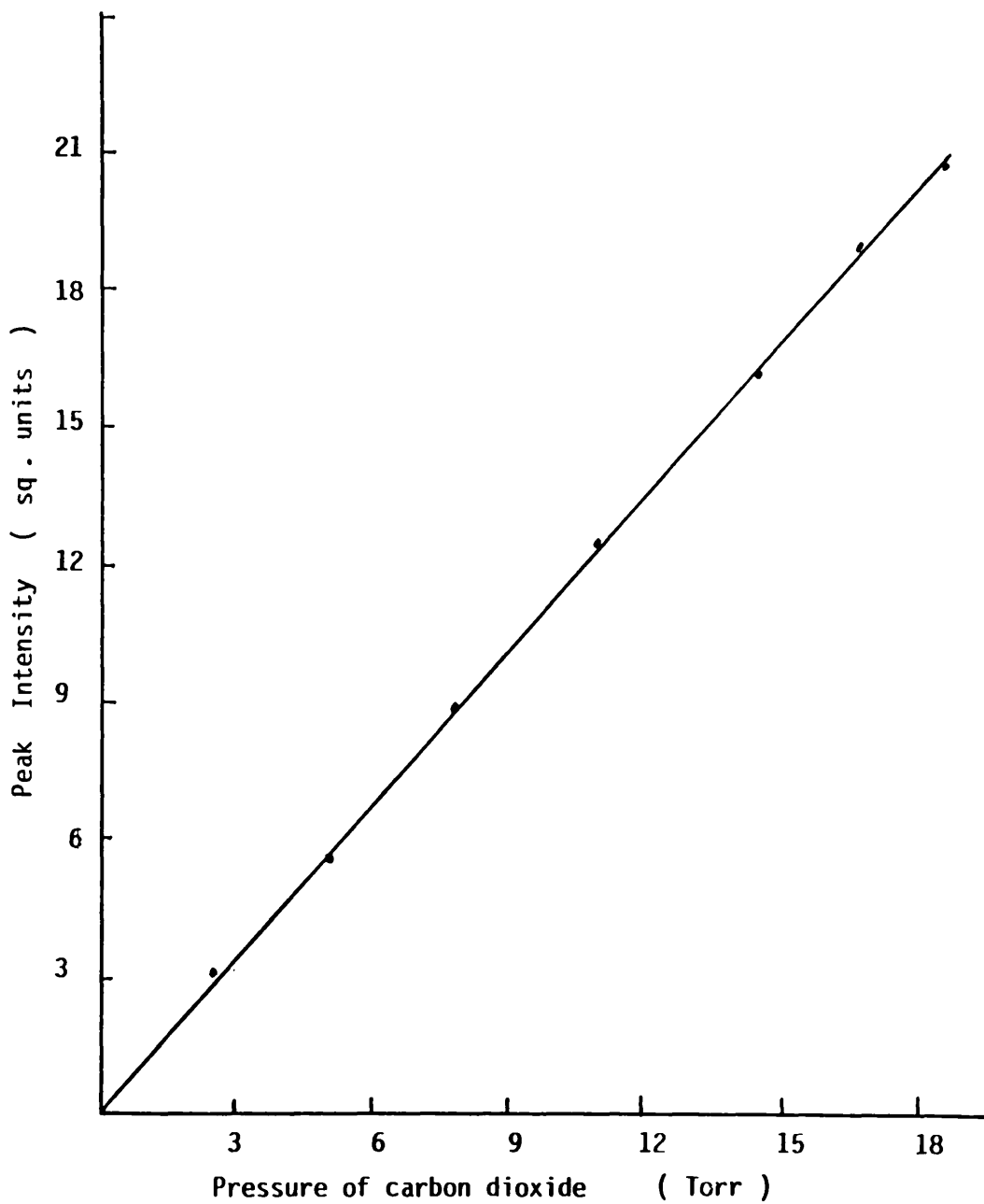


Figure 2.14 Calibration of carbon dioxide





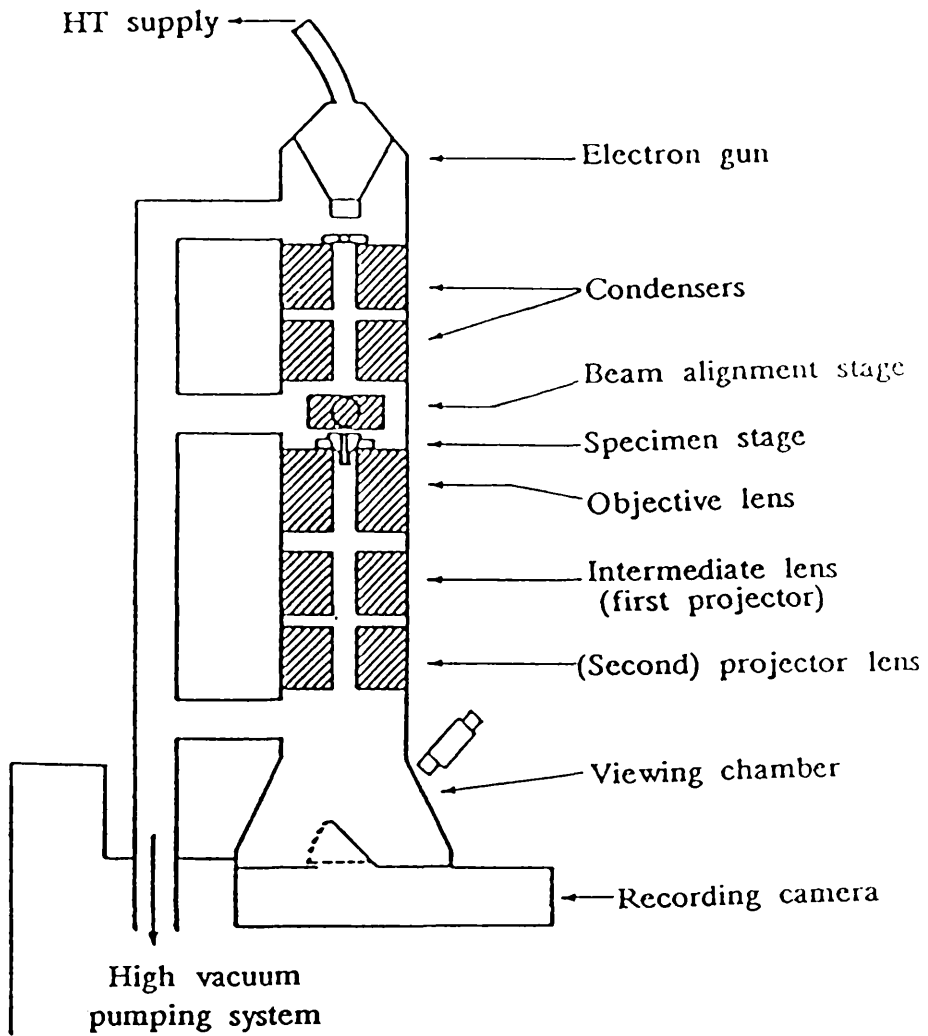


Figure 2.15 Schematic diagram of high resolution transmission electron microscope.

provide EDP at the back-focal plane of the electron lens.

They are in turn Fourier-transformed so as to form images. Thus, the EDP and the intermediate image are always present in the microscope Fig. 2.16., and the intermediate lens setting determines which is projected onto the image plane. If an aperture of diameter  $D$  is placed in the first intermediate image plane Fig. 2.17, only electrons passing through an area  $D/M$  on the specimen can reach the final screen ( $M$  is the magnification of the objective). The formation of EDP is shown diagrammatically in Fig. 2.18 for a set of lattice planes, spacing  $d$ , at an angle  $\theta$  to the electron beam. If  $R$  is the distance between the incident and the diffracted beam at the plane of the photographic plane and  $L$  the camera length, which is dependent upon the lens excitation, the relationship is given in equation 2.1.

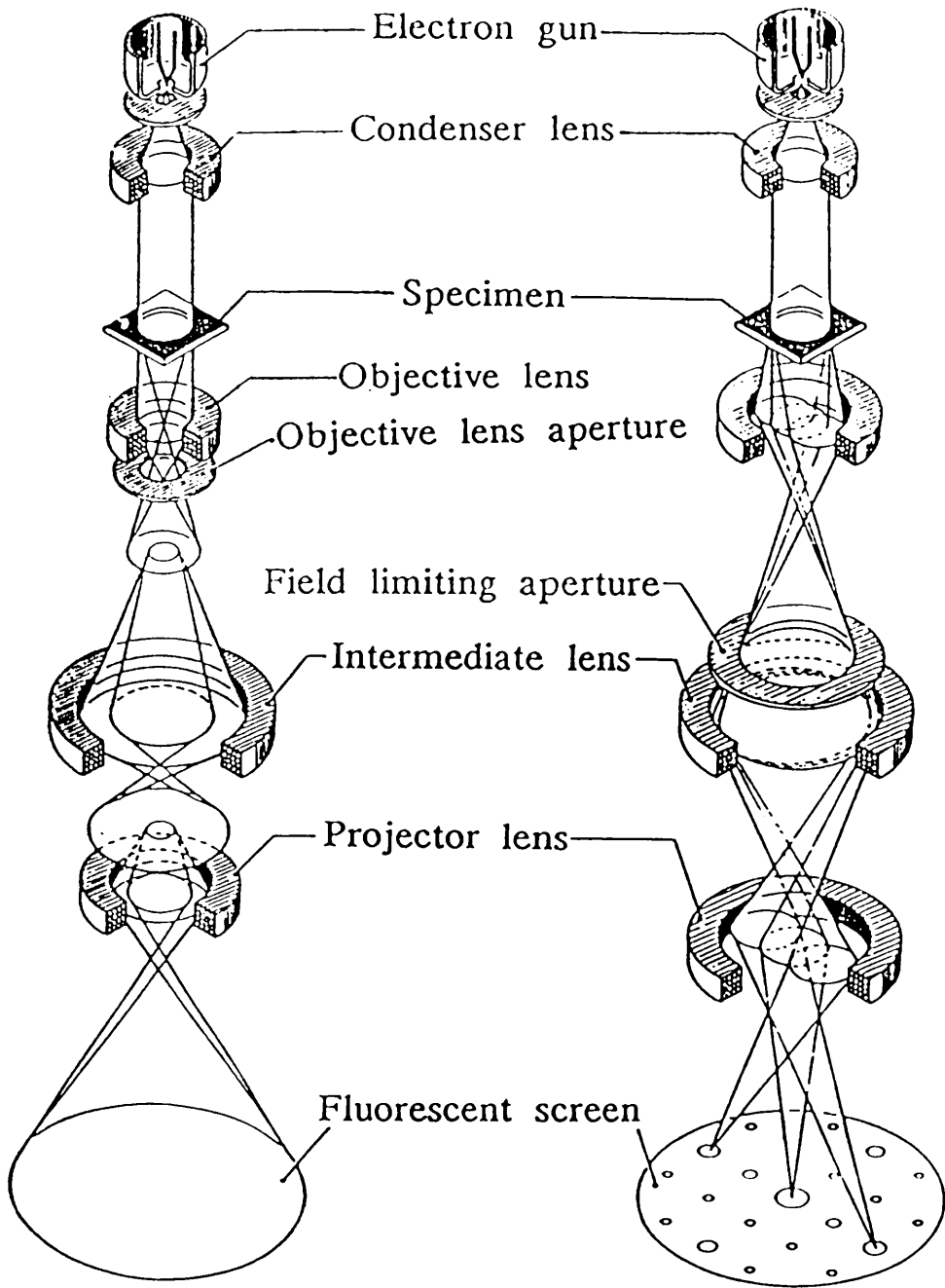
$$R/L = \tan 2\theta \qquad \text{Eq. 2.1}$$

From the Bragg law equation 2.2

$$n\lambda = 2d \sin\theta \qquad \text{Eq. 2.2}$$

for first order diffraction ( $n = 1$ )  $d$  can be calculated assuming that  $\tan\theta = \sin\theta$ .

Specimens of solids for electron microscopy were prepared and run by Dr. Tom Baird (Department of Chemistry, The University of Glasgow). Metal fluorides supported on  $\gamma$ -alumina samples were prepared by dipping an adhesive-coated carbon-filmed grid into the powder and inserted into the microscope within a very short time to prevent any hydrolysis.



**ELECTRON MICROSCOPE IMAGE**

**ELECTRON DIFFRACTION PATTERN**

**Figure 2.16** Comparison between image and electron diffraction pattern formation in the transmission electron microscope.

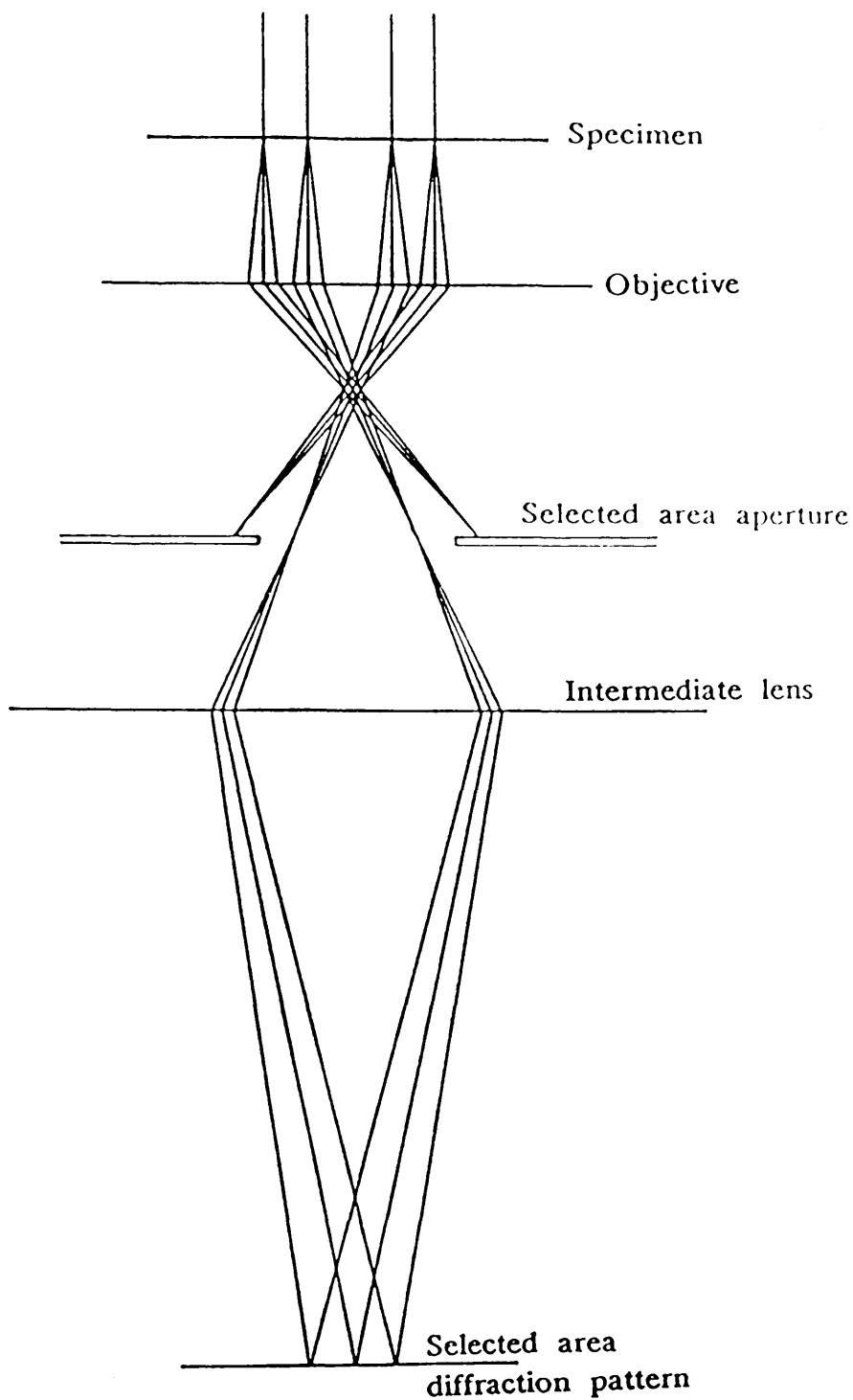


Figure 2.17 The selected-area aperture ensures that only electrons coming from a chosen region in the specimen contribute to the electron diffraction pattern.

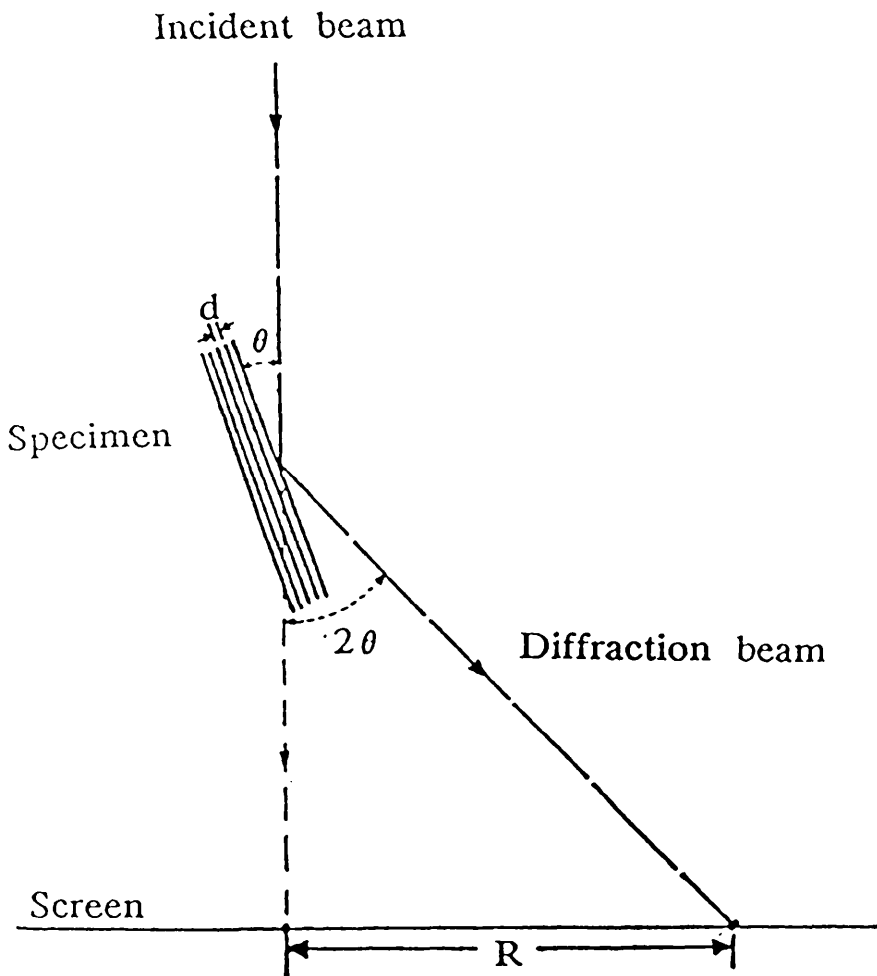


Figure 2.18 The transmission electron microscope as a simple diffraction camera

### 2.1.7 RAMAN SPECTROSCOPY

Spectra were obtained using a Spex Romalog spectrometer, using argon ion (488.0, 514.5 nm) or krypton ion (647.1, 520.8, 568.2 nm) laser sources. Samples of solids were sealed in Pyrex glass capillaries.

### 2.1.8 SOLID STATE <sup>27</sup>Al NMR SPECTROSCOPY

The <sup>27</sup>Al magic angle spinning nuclear magnetic resonance spectroscopy investigation was carried out at the Industrial Research Laboratories of the University of Durham, using a Varian UXR-300/89 NMR spectrometer. This instrument is dedicated to solid-state NMR work and is equipped with a 7 Tesla superconducting magnet with 89 mm vertical bore. It operates at 78.152 MHz for <sup>27</sup>Al nuclei. The MAS-NMR spectra were obtained by way of a pulse of width of 30 degrees and decoupling the protons. Typically 40 μs pulses were used. The spectra were obtained using a probe which was aluminium free and gave no background signal. Chemical shifts were recorded, with an aqueous solution of aluminium(III) chloride serving as an external standard. Samples were contained in a 300 microlitre (μl) zirconia tube. The response of the samples under a single-pulse excitation combined with magic-angle spinning at 12 KHz was used to obtain time domain data which were Fourier transformed for frequency domain information.

### 2.1.9 X-RAY DIFFRACTION

The X-ray diffraction (XRD) equipment used was a Philips diffractometer located in the Department of Geology, University of Glasgow. It consisted of an x-ray generator and a diffractometer unit. The powdered samples were mounted on adhesive tape, rolled into a cylinder in the inert atmosphere box and then placed in the XRD equipment. They were rotated through angles  $3-80^{\circ}$  (two theta values) whilst being exposed to copper  $K\alpha$  radiation ( $\lambda = 0.154$  nm) at 40 Kv and 20 mA. The resulting XRD patterns were recorded on a chart recorder operating at  $400 \text{ count s}^{-1}$ . The lattice spacings were subsequently calculated using the Bragg equation 2.2.

## 2.2 PREPARATION AND PURIFICATION OF REAGENTS

### 2.2.1 PURIFICATION OF ACETONITRILE

Acetonitrile was used as a solvent for some preparative reactions. A number of methods have been used by different workers for the purification of MeCN. The method developed in this Department [160] is an extension of the method of Walter and Ramelay [161]. It consists of a series of refluxes of HPLC grade MeCN (Rathburn Chemicals Ltd) in a Pyrex still equipped with 0.75 m silvered vacuum jacketed separating column. The following sequence of reagents was used; the quantities and times are given in parentheses i) anhydrous  $\text{AlCl}_3$  ( $15 \text{ g dm}^{-3}$ , 1h), ii)  $\text{KMnO}_4 + \text{Li}_2\text{CO}_3$  ( $10 \text{ g dm}^{-3}$  each, 15 min), iii)  $\text{KHSO}_4$  ( $15 \text{ g dm}^{-3}$ , 1h), iv)  $\text{CaH}_2$  ( $20 \text{ g dm}^{-3}$ , 1h), v) and vi)  $\text{P}_2\text{O}_5$  ( $1 \text{ g dm}^{-3}$ , 30 min).

After each reflux, MeCN was distilled rapidly topping and tailing by approximately 3%. During refluxing and distillation,

MeCN was protected from atmospheric moisture by silica gel drying tubes. The distilled MeCN was collected in vessels containing activated alumina (neutral 60 mesh), degassed twice in vacuo and distilled in storage vessels over activated 3A molecular sieves.

### 2.2.2 PURIFICATION OF DIETHYL ETHER

Analar diethyl ether was purified by addition of small pieces of freshly cut sodium metal until no further gas evolution was observed. The Et<sub>2</sub>O was degassed at 77 K under vacuum and stored over activated 3A molecular sieves for 24 hours, then was vacuum distilled onto fresh 3A molecular sieves before use.

### 2.2.3 PURIFICATION OF PYRIDINE

Analar pyridine was purified by degassing several times in vacuo at 77 K then was dried over activated 4A molecular sieves. Before use the dried pyridine was allowed to stand over freshly activated 4A molecular sieves.

### 2.2.4 PURIFICATION OF SULPHUR DICHLORIDE

Analar SCl<sub>2</sub> was purified by distillation in vacuo, first removing Cl<sub>2</sub> by reaction with Hg metal, then degassing at 195 K.

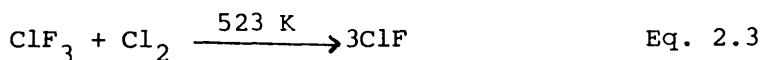


### 2.2.5 PURIFICATION OF CARBON AND SULPHUR DIOXIDES

Carbon and sulphur dioxides were purified by vacuum distillation over  $P_2O_5$  at 77 K. They were allowed to stand over  $P_2O_5$  overnight at room temperature in a Monel metal pressure vessel before use.

### 2.2.6 PREPARATION AND PURIFICATION OF CHLORINE MONOFLUORIDE.

Chlorine monofluoride was prepared according to the method previously used by several authors [162]. The reaction is represented by equation 2.3



Chlorine trifluoride (B.D.H, 98%) was condensed in trap [E] Fig. 2.5 followed by equal quantity of dichlorine (B.D.H Ltd., 99.9%). A measured amount of the  $ClF_3/Cl_2$  mixture (200 Torr) was expanded into the reaction vessel (A) ( $753 \text{ cm}^3$ ) which was placed in a drying oven. The temperature was raised gradually up to 523 K and left overnight, ca. 18 h. The contents of the vessel (A) were distilled into another vessel (D) and separated by fraction distillation. The unreacted materials  $ClF_3$  and  $Cl_2$  were trapped at 143 K using the cooling mixture of n-pentane-liquid nitrogen bath. The purity of  $ClF$  was determined by the vapour pressure at different temperatures [163], Table 2.3.

Table 2.3 Vapour Pressure Data for ClF.

Temperature (K)	Pressure (Torr) This work	Literature[ 163]
134.0	11 ± 2	10
144.2	38 ± 6	40
152.2	103 ± 5	100
166.0	409 ± 7	400
172.2	763 ± 4	760

Table 2.4 Infra-red Spectrum Data for NaBF<sub>4</sub>

This work.	Literature 165	Assignment
518 w	518	
521 vs	522	$\nu_4$
552 vs	551	
770 vw	770	
779 vs	779	$\nu_1$
1036 vw	1036	$\nu_3$

### 2.2.7 PREPARATION OF SODIUM TETRAFLUOROBORATE [164]

Boric acid (6.2 g, 100 mmol) was added slowly to 40% aqueous hydrofluoric acid (25.0 g) at 273 K in a P.T.F.E beaker (500 cm<sup>3</sup>). The mixture was left standing for 6h at room temperature, then cooled in an ice bath and dry Na<sub>2</sub>CO<sub>3</sub> (5.3 g, 50 mmol) was added. The solution was left at room temperature for 30 min, then was heated in a Pt evaporating dish until crystallisation commenced. The salt was washed with cold water several times and dried under vacuum. The yield of sodium tetrafluoroborate (9.9 g, 90 mmol) was 90% based on the boric acid taken. The infra-red spectrum data are given in Table 2.4 [165].

### 2.2.8 PREPARATION OF BORON TRIFLUORIDE [166]

A mixture of 4-chloroaniline (5.16 g, 40 mmol) in hydrochloric acid (35.4 w/w%, 16 cm<sup>3</sup>) was diazotized at 273 K with sodium nitrite (2.9 g, 42 mmol) in water (4.3 cm<sup>3</sup>). The mixture was stirred magnetically for 30 min., and a solution of sodium tetrafluoroborate (7.7 g, 70 mmol) in water (9 cm<sup>3</sup>) was added slowly with constant stirring at 273 K; stirring was continued for another 30 min. The precipitated 4-chlorodiazonium tetrafluoroborate was removed by filtration using a Buchner funnel and flask, then washed several times with EtOH and Et<sub>2</sub>O [167]. It was dried under vacuum and stored in the fridge until required. The yield of 4-Cl-C<sub>6</sub>H<sub>4</sub>N<sub>2</sub>BF<sub>4</sub> (9.24, 40 mmol) was quantitative based on 4-Cl-C<sub>6</sub>H<sub>4</sub>NH<sub>2</sub>.

Boron trifluoride was liberated by thermal decomposition of 4-chlorodiazonium tetrafluoroborate using a Pyrex glass reactor, shown in Fig.2.19. It consisted of a reaction vessel (A) (50 cm<sup>3</sup>)

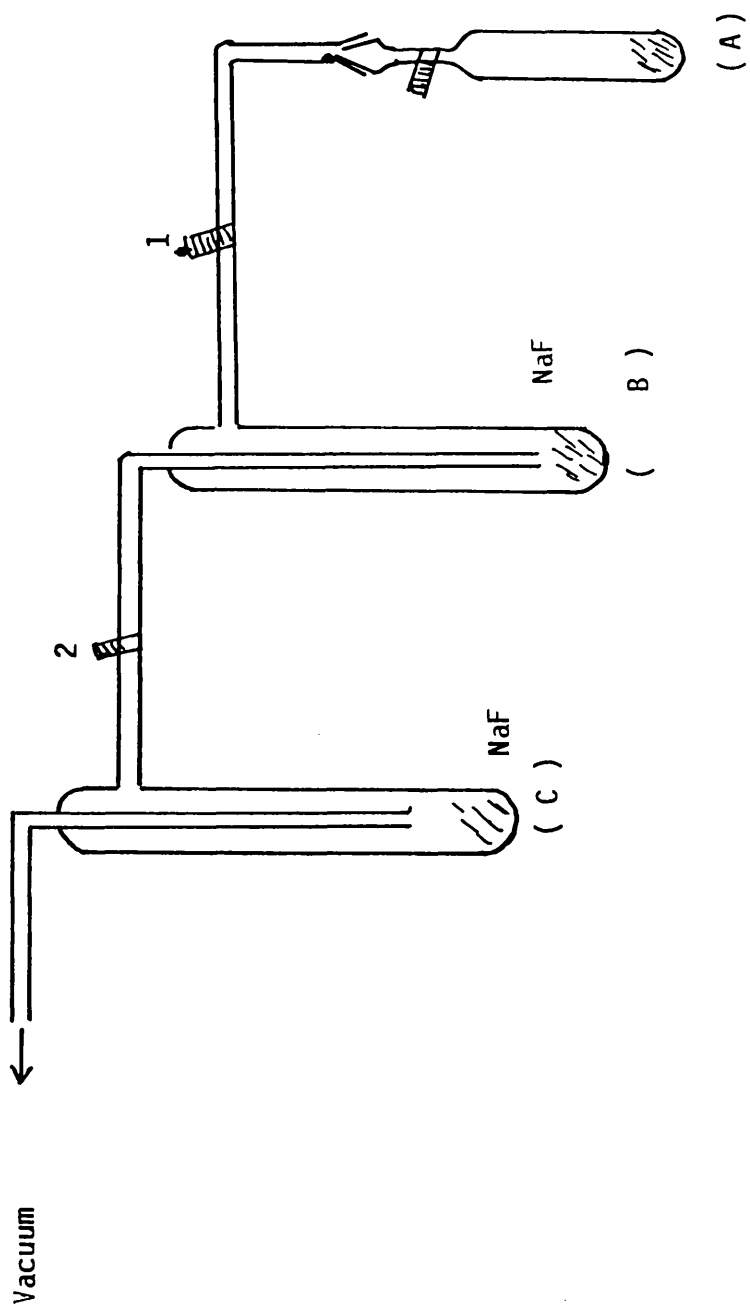


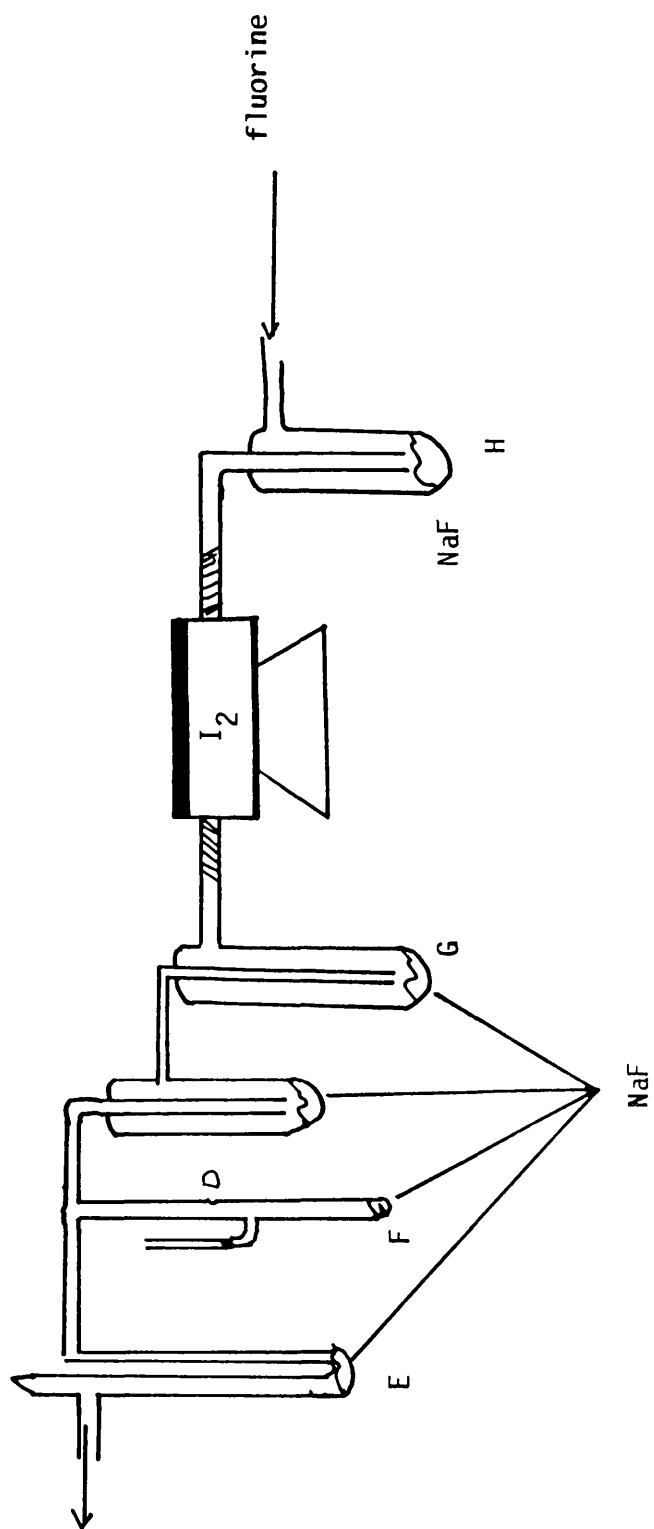
Figure 2.19 Preparation apparatus of boron trifluoride

### 2.2.9 PREPARATION AND PURIFICATION of IF<sub>5</sub> [169]

Pure iodine (5 g) was placed in a small nickel boat and spread out as much as possible. The boat containing the iodine was placed inside the nickel reaction tube. The Swagelok couplings were replaced and the tube and glass apparatus, which contained NaF in traps, E, F G and H were attached to the tube using the Swagelok couplings and P.T.F.E. ferrules. The apparatus was attached to the fluorine gas cylinder and control valves and the whole apparatus was flushed several times with nitrogen, while traps E (for trapping moisture from air), F (for collecting IF<sub>5</sub>), G (for trapping IF<sub>5</sub>) and H (for trapping trace of HF) were cooled to 195 K, using dry ice/dichloromethane slush baths Fig. 2.20.

The fluorine cylinder was opened and the cylinder head pressure gauge was adjusted to 40 psi. Difluorine diluted with N<sub>2</sub> to give 1:2 ratio by volume of difluorine/nitrogen was passed through the system at a rate of 100 cm<sup>3</sup> min<sup>-1</sup>. The product was trapped in trap G and after approximately one hour the reaction was complete and the main fluorine supply was shut off. Iodine pentafluoride was transferred to trap F and sealed at point D. It was purified by trap to trap distillation over activated NaF with occasional pumping at 195 K to remove any excess of SiF<sub>4</sub>. The IF<sub>5</sub> was shaken at room temperature with Hg metal for a short time to remove I<sub>2</sub> and stored over NaF at 77 K in a sealed vessel.

Figure 2.20  $\text{IF}_5$  Preparation apparatus

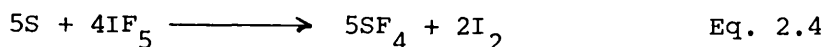


### 2.2.10 PREPARATION AND PURIFICATION of SF<sub>4</sub>

Sulphur tetrafluoride was prepared by two methods:

a) The fluorination of elemental sulphur [170].

Sulphur tetrafluoride was prepared by the fluorination of elemental sulphur with iodine pentafluoride, equation 2.4



Purified iodine pentafluoride (9.95 g, 44.84 mmol) was transferred to a glass vessel which had been flamed out immediately before the preparation process. The required amount of the elemental sulphur (1.794 g, 56.05 mmol) according to equation 2.4 was transferred to a Monel pressure vessel and evacuated. The pre-weighed IF<sub>5</sub> was condensed into the bomb at 77 K, and then heated at 373 K for 5 hours, followed by 473 K for 48 hours. The bomb was cooled to 195 K and volatile material was distilled into another bomb containing activated NaF. The pressure of the crude SF<sub>4</sub> was determined in a calibrated vacuum manifold and similar amount of BF<sub>3</sub> was added at 77 K forming the adduct, SF<sub>3</sub><sup>+</sup>BF<sub>4</sub><sup>-</sup> [70]. The bomb was warmed to 195 K and held at this temperature for 0.5h. Unreacted material was removed at 195 K. This consisted of unreacted BF<sub>3</sub> and impurities, mainly SOF<sub>2</sub>.

The adduct was decomposed by adding a stoichiometric amount of dried Et<sub>2</sub>O and SF<sub>4</sub> was recovered in a highly pure state. The infra-red spectrum and molecular weight were obtained for each batch prepared. Details are summarised in Tables 2.6 and 2.7.

Table 2.6 The Infra-red Spectrum for SF<sub>4</sub>

This work.	Literature [ 66 ]	Assignment
887 s	892	$\nu_1$ (A <sub>1</sub> )
860 s	867	$\nu_6$ (B <sub>1</sub> )
730 vs	730	$\nu_8$ (B <sub>2</sub> )
550 w	558	$\nu_2$ (A <sub>1</sub> )
530 w	532	$\nu_7$ (B <sub>1</sub> )
	475	$\nu_3$ (A <sub>1</sub> )
	353	$\nu_9$ (B <sub>2</sub> )

Table 2.7 Molecular Weight Determination for SF<sub>4</sub>

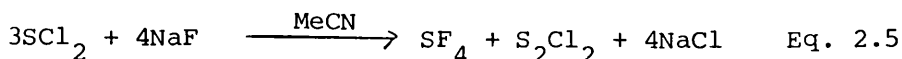
Pressure (Torr)	Sample Weight (g)	Molecular Weight (g mol <sup>-1</sup> ).
184.59	0.1095	109.5
276.88	0.1625	108.3
369.17	0.2159	107.9
424.55	0.2457	106.8
461.46	0.2726	109.1

Required value 108 g mol<sup>-1</sup>

Calculated value 108.3 ± 2.8 g mol<sup>-1</sup>



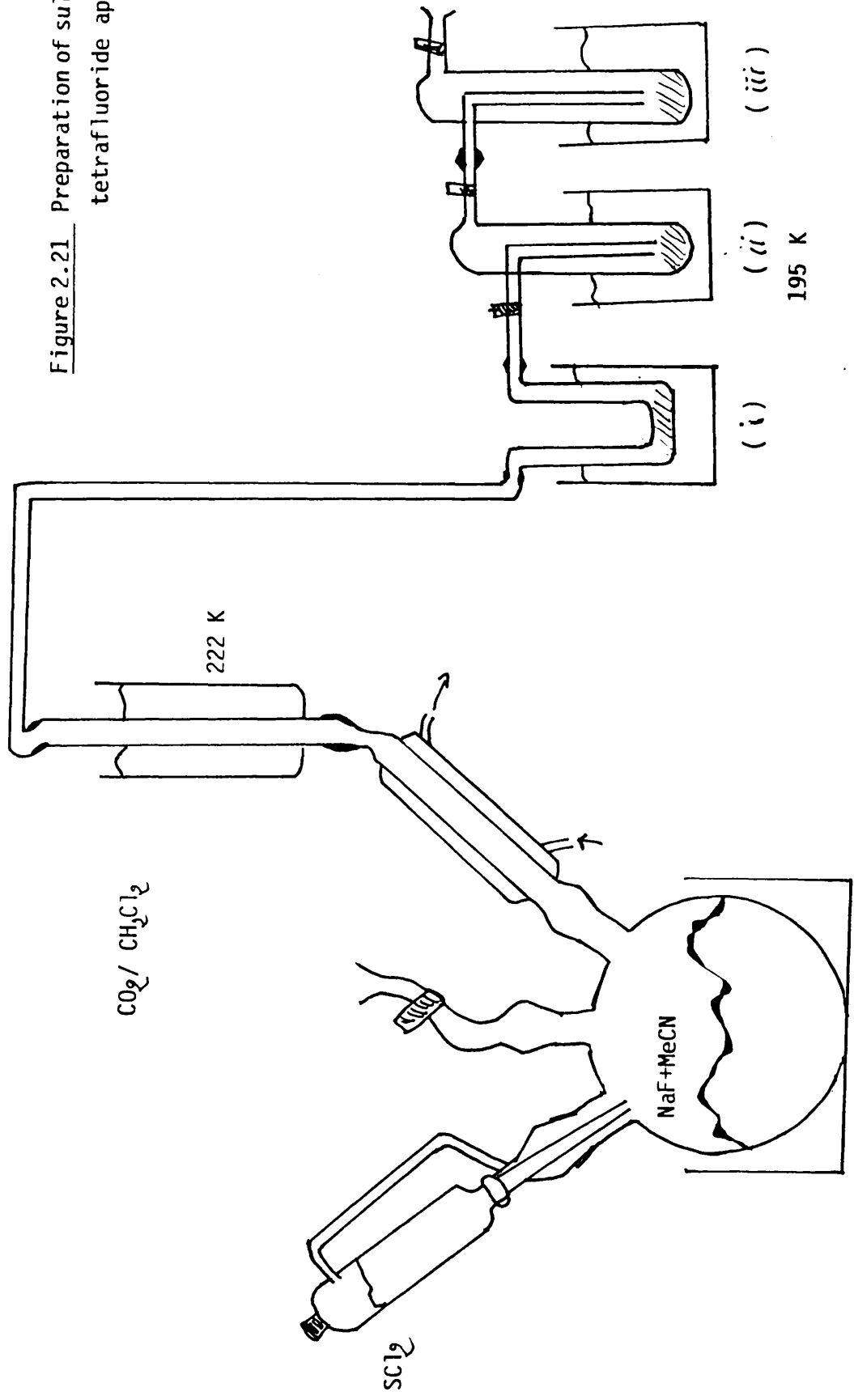
b) Halogen exchange reaction [63b] equation 2.5



The apparatus used for this method of preparation is shown in Fig. 2.21. This consisted of a three necked flask provided with a pressure-equalised dropping funnel to contain  $\text{SCl}_2$ , a water condenser to which a 222 K (solid  $\text{CO}_2/\text{CH}_2\text{Cl}_2$  slush) condenser was directly attached and magnetic stirrer for mixing the slurry  $\text{NaF}/\text{MeCN}/\text{SCl}_2$ . The outlet from the 222 K condenser was connected via flexible polyethylene tubing and standard glass joints to the collection vessel. The latter consisted of three parts (i) a U tube, (ii) and (iii) traps equipped with P.T.F.E/Pyrex stopcocks. The U tube and trap (ii) contained small quantities of  $\text{NaF}$  and was used to condense  $\text{SF}_4$ . Trap (iii) was used to trap moisture from the atmosphere. All traps (i) to (iii) inclusive were cooled to 195 K using solid  $\text{CO}_2/\text{CH}_2\text{Cl}_2$  slush baths.

Predried analar  $\text{NaF}$  (21.0 g, 500 mmol) was placed in a dry 3 necked flask (1000  $\text{cm}^3$ ) followed by purified and dried  $\text{MeCN}$  (300  $\text{cm}^3$ ). Sulphur dichloride was added from the dropping funnel in small quantities to the stirred slurry of  $\text{NaF}/\text{MeCN}$  over 0.5 h. When the addition was complete, the heat was supplied until the  $\text{MeCN}$  refluxes gently. Reflux was continued for 2h while the crude  $\text{SF}_4$  was collected, mainly in trap (i) then transferred to trap (ii) by warming trap (i) to room temperature. The crude  $\text{SF}_4$  was transferred to the vacuum line and purified as described above.

Figure 2.21 Preparation of sulphur tetrafluoride apparatus



### 2.2.11 PREPARATION AND PURIFICATION OF SF<sub>5</sub>Cl

The best methods reported for the synthesis of sulphur chloride pentafluoride, utilize reactions of SF<sub>4</sub> and ClF [63c] or SF<sub>4</sub> with Cl<sub>2</sub> and CsF . These reactions require elevated temperatures which must be controlled closely to obtain good comparisons. An improved, simplified synthesis of SF<sub>5</sub>Cl has been found [78] which employs the ambient temperature reaction of SF<sub>4</sub> and ClF in the presence of caesium fluoride, equation 2.6.



In a typical preparation a Monel metal pressure vessel (100 cm<sup>3</sup>) was loaded with activated CsF (2 g) with hexafluoroacetone in an inert atmosphere box. The evacuated vessel was charged with a mixture of purified SF<sub>4</sub> (20 mmol) and ClF (20 mmol) at 77 K. The vessel was then allowed to warm to ambient temperature and the mixture allowed to react for 5h. Vacuum fractionation of the vessel contents after this time revealed that nearly quantitative conversion into SF<sub>5</sub>Cl (18.4 mmol) had occurred. The identity of the product was confirmed by its i.r. spectrum and the molecular weight data [171]; results are reported in Tables 2.8 and 2.9.

### 2.2.12 PREPARATION AND PURIFICATION OF CARBONYL FLUORIDE [172]

Carbonyl fluoride was prepared by the halogen exchange reaction between carbonyl chloride (phosgene) and activated NaF in dried acetonitrile. Typically a Monel metal pressure vessel (200 cm<sup>3</sup>)

Table 2.8 The Infra-red Spectrum of SF<sub>5</sub>Cl

This work $\nu_{\max}$	Literature $\nu_{\max}$ 171	Assignment
573	578	$\nu_9$ (c)
603	602	$\nu_3$ (a <sub>1</sub> )
709	706	$\nu_2$ (a <sub>1</sub> )
813	805	A <sub>1</sub>
861	856	$\nu_1$ (a <sub>1</sub> )
910	908	$\nu_8$ (c)

Table 2.9 Molecular Weight Determination for SF<sub>5</sub>Cl

Pressure (Torr)	Sample Weight (g)	Molecular Weight (g mol <sup>-1</sup> )
184.59	0.1639	163.9
276.88	0.2416	161.0
369.17	0.3258	162.9
424.55	0.3756	163.3
461.46	0.4057	162.2

Required value 162.5 g mol<sup>-1</sup>

Calculated value 162.7 ± 2.0 g mol<sup>-1</sup>

was loaded with NaF (32 g, 720 mmol). The evacuated vessel was charged with dried MeCN (60 ml) followed by  $\text{COCl}_2$  (6.0 g, 60.8 mmol). The reactants were left at room temperature for 48h with occasional shaking. Carbonyl fluoride (3.6 g, 59.6 mmol) was removed and purified by trap to trap distillation at 195 K, then was stored in a Monel pressure vessel over NaF. Tables 2.10 and 2.11 list the i.r. spectrum and molecular weight data obtained.

### 2.2.13 PREPARATION AND PURIFICATION OF THIONYL FLUORIDE [174]

Several methods can be used for the production of thionyl fluoride. The simplest method is the halogen exchange reaction between  $\text{SOCl}_2$  and activated NaF in MeCN. In a typical preparation  $\text{SOCl}_2$  (30 mmol) was condensed into a stainless steel pressure vessel ( $200 \text{ cm}^3$ ) containing activated NaF (50 g) and MeCN ( $50 \text{ cm}^3$ ). The vessel was shaken for 36h at room temperature. Thionyl fluoride (30 mmol) was collected at 195 K and stored over activated NaF until required. Tables 2.12 and 2.13 list the i.r. and molecular weight data obtained.

Table 2.10 The IR Spectrum of  $\text{COF}_2$

This work	Literature 173	Assignment 173
	584	$\nu_3$ ( $A_1$ )
633	626	$\nu_5$ ( $B_2$ )
775	774	$\nu_6$ ( $B_1$ )
967	965	$\nu_2$ ( $A_1$ )
1246	1249	$\nu_4$ ( $B_2$ )
1931	1928	$\nu_1$ ( $A_1$ )

Table 2.11 Molecular Weight Determination for COF<sub>2</sub>

Pressure (Torr)	Sample Weight (g)	Molecular Weight (g mol <sup>-1</sup> )
184.50	0.0693	69.3
276.88	0.1034	68.9
369.17	0.1327	66.4
424.55	0.1558	67.7
461.46	0.1703	68.1

Required value    66 g mol<sup>-1</sup>

Calculated value    68.1 ± 1.6 g mol<sup>-1</sup>

Table 2.12 The IR Spectrum of SOF<sub>2</sub>

This work	Literature	175	Assignment
1318	1308		$\nu_1$ (A')
807	801		$\nu_2$ (A')
730	721		$\nu_5$ (A'')
527	526		$\nu_3$ (A')
393	393		$\nu_6$ (A'')

Table 2.13 Molecular Weight Determination for SOF<sub>2</sub>

Pressure (Torr)	Sample Weight (g)	Molecular Weight (g mol <sup>-1</sup> )
184.59	0.0871	87.1
276.88	0.1336	89.1
369.17	0.1721	86.3
424.55	0.1956	85.7
461.46	0.2173	86.9

Required value 86 g mol<sup>-1</sup>

Calculated value 87.0 ± 1.1 g mol<sup>-1</sup>

#### 2.2.14 PREPARATION OF PENTA AND HEXA FLUOROALUMINATES

In all cases reactions were carried out by the addition of aluminium bromide in methanol solution to a rapidly stirred saturated solution of metal fluoride in water in a polyethylene container. The volume of aluminium bromide to be added was according to Table 2.14 based on the molarity of the solution ( $0.5 \text{ mol dm}^{-3}$ ) of the saturated MF ( $M = \text{K or NH}_4$ ) solution. The products were filtered using a Buchner funnel and flask and washed on the filter with cold methanol until a test of the washings with aqueous silver nitrate showed them to be free from bromide. The precipitate was washed with anhydrous diethyl ether and dried under vacuum overnight [176]. The infra-red spectra for  $\text{K}_3\text{AlF}_6$ ,  $(\text{NH}_4)_3\text{AlF}_6$ , and  $\text{K}_2\text{AlF}_5 \cdot \text{H}_2\text{O}$  are given in Tables 2.15 - 2.17. The XRD data were obtained and d values calculated Tables 2.18 - 2.20

#### 2.2.15 PREPARATION OF $\text{NH}_4\text{AlF}_4$

Ammonium tetrafluoroaluminate was prepared by the thermal decomposition of  $(\text{NH}_4)_3\text{AlF}_6$  under specific conditions. A nickel boat containing  $(\text{NH}_4)_3\text{AlF}_6$  (20.0 g, 103 mmol) was placed in a Pyrex glass tube. Dry nitrogen gas was introduced and the whole device was heated in a furnace to 573 K for 2h, Fig. 2.22 shows the apparatus. The volatile product was collected either in the cooler part of the reaction boat or in a cooled trap attached to the reaction tube. The remaining solid was washed several times with cold water, methanol and anhydrous diethylether. Pure  $\text{NH}_4\text{AlF}_4$  (12 g, 103 mmol) was collected. Infra-red and the XRD data were obtained and are listed in Tables 2.21 and 2.22 .



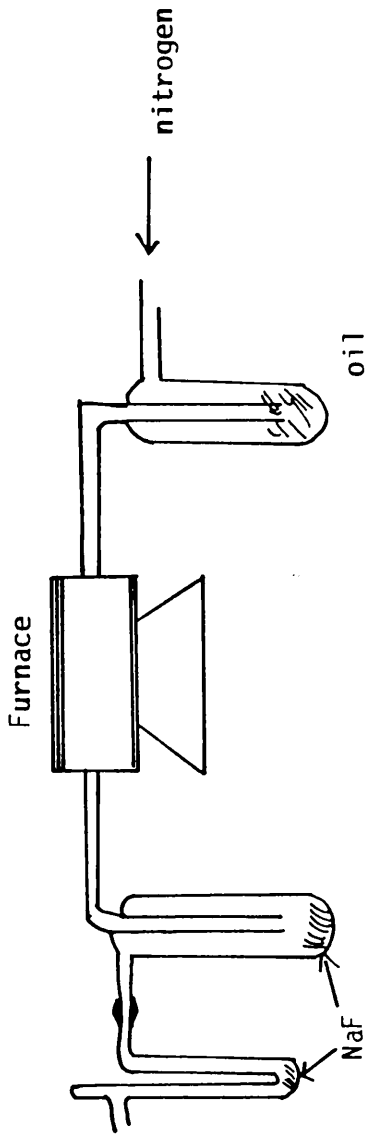


Figure 2.22  $\text{NH}_4\text{AlF}_6$  preparation apparatus.

Table 2.14 Preparation Conditions of Fluoroaluminate.

Amount of Reactants	Compound		
	$K_3AlF_6$	$K_2AlF_5$	$(NH_4)_3AlF_6$
MF (g) M = K or $NH_4$	34.8	29	22.2
Water (cm <sup>3</sup> )	300	200	300

$AlBr_3$  used 26.7 g

Table 2.15 Infra-red Spectrum for  $(NH_4)_3AlF_6$

This work $\nu_{max}$ cm <sup>-1</sup>	Literature [177 ]	Assignment
3256	3250	$\nu_3$
3053	3060	$\nu_2 + \nu_4$
1429	1428	$\nu_4$
583	570	$\nu_3$

Table 2.16 Infra-red Spectrum Data for  $K_3AlF_6$

This work $\nu_{\max} \text{ cm}^{-1}$	Literature [ 177 ]
633	630
569	570
381	382

Table 2.17 Infra-red Spectrum Data for  $K_2AlF_5 \cdot 2H_2O$

This work $\nu_{\max} \text{ cm}^{-1}$	Literature [ 177 ]
744	744
656	655
523	524
406	405
396	395
	340

Table 2.18 X-Ray Powder Diffraction Data for  $K_3AlF_6$

This work			Literature [ 178]			
$2\theta^\circ$	$d(\text{\AA})$	$I/I_0$	$2\theta^\circ$	$d(\text{\AA})$	hkl	$I/I_0$
18.33	4.89	16	17.92	4.95	111	13
			20.75	4.28	200	8
28.04	3.11	100	29.79	3.00	220	100
			35.19	2.55	311	5
37.69	2.41	39	36.68	2.45	222	42
43.08	2.08	63	42.86	2.11	400	67
			46.83	1.94	331	5
54.21	1.68	37	53.26	1.72	422	33
			56.45	1.63	511, 333	10
61.18	1.51	33	62.83	1.49	440	37
			65.24	1.43	531	3
			66.28	1.41	600	5
71.96	1.28	15	70.24	1.34	620	13

Table 2.19 X-Ray Powder Diffraction Data for  $(\text{NH}_4)_3\text{AlF}_6$

This work			Literature [ 179]			
$2\theta^\circ$	$d(\text{A}^\circ)$	$I/I_0$	$2\theta^\circ$	$d(\text{A}^\circ)$	hkl	$I/I_0$
17.59	4.98	100	17.50	5.2	111	100
18.93	4.51	63	19.88	4.47	200	60
29.43	3.07	59	28.42	3.14	220	60
34.66	2.59	31	34.91	2.57	222	30
43.12	2.11	98	41.02	2.22	400	100
			44.64	2.03	331	4
			45.58	1.99	420	4
			50.12	1.82	422	12
51.58	1.77	23	53.58	1.71	511, 333	25
59.30	1.49	15	58.40	1.58	440	16
			61.84	1.50	531	12
			62.78	1.48	600, 442	4
67.39	1.43	15	66.29	1.41	620	14
			69.06	1.36	533	4
			73.40	1.29	444	6
			76.16	1.25	711	8
82.08	1.13	15	80.02	1.19	642	12
			83.30	1.16	731	6

Table 2.20 X-Ray Powder Diffraction Data for  $K_2AlF_6 \cdot H_2O$

This work			Literature [ 180 ]			
$2\theta^\circ$	d (Å)	$I/I_0$	$2\theta^\circ$	d(Å)	hkl	$I/I_0$
24.8	3.59	60	24.86	3.58	021	60
28.14	3.17	60	27.96	3.19	112	80
37.32	2.41	100	38.12	2.36	222	100
38.64	2.33	60	39.16	2.3	113,400	80
45.34	2.0	80	45.26	2.03	040,330	80
48.14	1.89	60	48.74	1.87	004	80
51.02	1.79	30	50.56	1.8	241	60
59.0	1.56	70	60.4	1.53	600	60
65.60	1.42	30	63.99	1.46	513	60

Table 2.21 Infra-red Spectrum Data for  $\text{NH}_4\text{AlF}_6$

This work $\nu_{\text{max}} \text{ cm}^{-1}$	Literature [177 ]	Assignment
3241	3230	$\nu_3$
3106	3120	$\nu_2 + \nu_4$
2889	2905	$2\nu_4$
1816	1800	$\nu_4 + \nu_6$
1435	1435	$\nu_4$
715	705	-
609	610	$\nu_3$
373	375	-
351	350	-

Table 2.22 X-Ray Powder Diffraction Data for  $\text{NH}_4\text{AlF}_6$

$2\theta^\circ$	This work		$2\theta^\circ$	Literature [181]		
	d(A $^\circ$ )	I/I $_0$		d(A $^\circ$ )	hkl	I/I $_0$
13.7	6.46	100	13.96	6.346	001	100
24.94	3.57	83	24.84	3.585	100	80
28.8	3.1	78	28.6	3.128	101	80
34.8	2.57	33	35.42	2.534	110	30
37.8	2.38	38	38.06	2.364	102	40

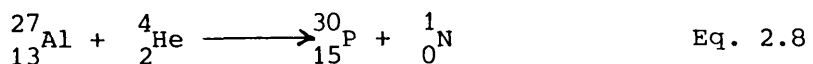


### 2.3 RADIOCHEMICAL TECHNIQUES

Radioactive isotopes have wide applications in research, Neutron activation, isotope dilution, radiometric titration, surface catalysed processes. In some cases, radioisotopes make experiments possible which could not be carried out in any other way. In others they offer a more convenient and a simpler procedure than conventional methods.

The basic assumption in all tracer work is that the radioactive isotope behaves chemically in an identical manner to a non-radioactive isotope. This assumption is valid in the great majority of cases although hydrogen and some of the lighter elements are exceptions. Owing to large differences in relative atomic mass, isotopes of lighter elements have different velocities leading to considerable differences in kinetic studies.

Before 1934 the applications of radioactivity were limited to the use of naturally occurring isotopes but at the beginning of that year artificial radioactivity was discovered by Curie and Joliot [182]. They found that aluminium foil which had been bombarded with  $\alpha$  particles gave off radiation after the bombardment had ceased, equation 2.8.



This finding, the successful operation of nuclear reactors and the development of particle accelerators since 1945 led to the production of artificial radioactive isotopes of nearly all the elements with half lives ranging from microseconds to many millions of years.

The particle accelerator has removed most of the restrictions on the systems which could be examined and exchange reactions have provided much information on a wide variety of topics, for example, the study of reaction mechanisms, reactions of high energy atoms, and molecular structure [183,184]

### 2.3.1 ISOTOPIC EXCHANGE REACTIONS

Perhaps the most extensive chemical application of artificial radioisotopes as indicators has been to the study of exchange reactions. The first exchange reaction experiments were performed by Hevesey et.al [185], who used the naturally occurring radioactive lead isotope to demonstrate a rapid exchange between the lead atoms in aqueous lead nitrate and lead chloride.

In exchange experiments the atoms of an element in one of its valence forms, are labelled by admixture with isotopes of the element which is in the same form. The presence of radioactivity in the second chemical form after it has been separated from the first, shows that an effective exchange of atoms between the two different states of the element has taken place. Complete exchange has been attained when the radioactivity has distributed itself between the two chemical forms in the same ratio as the amounts of element in the two forms. An isotopic exchange reaction can be defined by equation 2.9



In all exchange reactions, regardless of the order, the rate varies with time according to the law for first-order reversible reactions, since the chemical composition of the reaction mixture remains unchanged [186].

To carry out quantitative investigations of exchange reactions, the results are expressed in terms of the fraction of activity exchanged (f) where (f) is defined by equation 2.10 [187,188] .

$$f = \frac{\text{Fraction of activity in the initially labelled compound}}{\text{Fraction of fluorine(mg-atom)in the initially unlabelled compound}}$$

Eq. 2.10

f is determined experimentally using either equation 2.11 or 2.12

$$f = \frac{A_1}{A_1 + A_2} \bigg/ \frac{xm_1}{xm_1 + ym_2} \quad \text{Eq. 2.11}$$

$$f = \frac{S_o - S_t}{S_o - S_\alpha} \quad \text{Eq. 2.12}$$

where  $A_1$  and  $A_2$  count  $\text{min}^{-1}$  are the count rates, corrected for decay, after exchange between  $m_1$  and  $m_2$  mmol of reactants (1 being inactive initially) containing respectively x and y F atoms.

$S_o$ ,  $S_t$  and  $S_\alpha$  count  $\text{min}^{-1} (\text{mg atom F})^{-1}$  are the specific count rate of reactant 2 (being active initially) before the exchange, after the exchange, and when exchange is complete respectively.

Equation 2.11 and 2.12 should in theory give the same answer providing that the radiochemical balance is > 95%, thus is

$A_o = A_1 + A_2$ . In practice this is not always the case since

four possible, complications could arise.

1-Fluorine exchange with neither retention nor hydrolysis of the gas by the solid. In this case either equation can be applied and the value  $f$  obtained indicates the level to which exchange has occurred. A value of  $f = 0$  corresponds to no exchange and  $f = 1$  corresponds to complete exchange, that is a random distribution of activity.

2-Retention of the gas by solid with neither hydrolysis nor fluorine exchange taking place, Equation (2.11) would give a value  $f \neq 0$  and equation (2.12) would give a value  $f = 0$ . If an uptake of gas occurs therefore equation (2.11) becomes invalid and equation (2.12) must be applied.

3-Fluorine exchange and retention with no hydrolysis of the gas by solid. In this case equation (2.11) will give a value of  $f > 1$ . Since equation (2.12) depends on the specific count rate of the gas before and after reaction, a true measure of the fraction exchanged will be obtained if this equation is used.

4-Retention and hydrolysis of the gas by the solid both occur. In this case both equations will give a value of  $f > 1$ . Since equation 2.12 depends on the specific count rate of the gas before and after exchange, an accurate value of  $f$  can be obtained if the composition of the gas can be established by independent means.

### 2.3.2 CHOICE OF ISOTOPE

In general, the least radiotoxic isotope available and the minimum activity consistent with obtaining good counting statistics at the end of the experiment should be used. The choice of the isotope is determined by the following factors:-

1. The ease of handling and detection.
2. The availability of the isotope
3. Its half life.

The radioisotopes used in the present work were  $\{^{14}\text{C}\}$ -carbon,  $\{^{36}\text{Cl}\}$ -chlorine,  $\{^{18}\text{F}\}$ -fluorine and  $\{^{35}\text{S}\}$ -sulphur, the longest lived radioactive isotope of each element in each case. All of them are detectable using either Geiger-Müller counter for detecting  $^{14}\text{C}$ ,  $^{36}\text{Cl}$  and  $^{35}\text{S}$ ,  $\beta^-$  emitters and scintillation counter for  $^{18}\text{F}$ ,  $\gamma$  emitter.

### 2.3.3 THE RADIOISOTOPE $\{^{18}\text{F}\}$ -FLUORINE

Naturally occurring fluorine is monoisotopic  $\{^{19}\text{F}\}$ -fluorine with a spin quantum number  $I = \frac{1}{2}$ . This makes it useful in n.m.r. studies. The element has artificially produced radioisotopes ( $^{17}\text{F}$  —  $^{23}\text{F}$ ) of which  $\{^{18}\text{F}\}$ -fluorine has the longest half life. The most recently determined value for its half life is  $109 \pm 0.6$  min [189].

During the process of decay of  $\{^{18}\text{F}\}$ -fluorine to  $\{^{18}\text{O}\}$ -oxygen an emission of a positron  $\beta^+$ , that is a positively charged electron, takes place. This results in the decrease of the atomic number by one but leaves the mass number of the element unchanged. The kinetic energy of the emitted positron is

reduced through interactions with surrounding particles and collides with an electron resulting in a mutual annihilation and an emission of 0.511 MeV  $\gamma$ -photons.

$\{^{18}\text{F}\}$ -Fluorine is an attractive radiotracer as its  $\gamma$ -radiation is easily detected. Since its discovery in 1937 [190]  $\{^{18}\text{F}\}$ -fluorine has been used in inorganic and organic chemistry [191] and due to the strong C-F bond ( $477 \text{ K j mol}^{-1}$ ) it has been extensively used in biological and medical studies [192].

Due to its short half life  $\{^{18}\text{F}\}$ -labelled compounds are not commercially available. Hence they must be produced and used during one working day. After six half lives only 1-2% of the starting activity is left and therefore correction for radioactive decay during an experiment is required.  $\{^{18}\text{F}\}$ -Fluorine can be produced by different methods but in general an accelerator, a cyclotron or a nuclear reactor is required. Table 2.23 gives some examples of cyclotron produced  $\{^{18}\text{F}\}$ -fluorine.

The incorporation of  $\{^{18}\text{F}\}$ -fluorine in the desired compound competes with its radioactive decay, Fig. 2.23 represents the relationship between the degree of incorporation, time and radioactive decay of  $\{^{18}\text{F}\}$ -fluorine. For a good radiochemical yield the incorporation time must not be longer than  $t_{\text{limit}}$ .

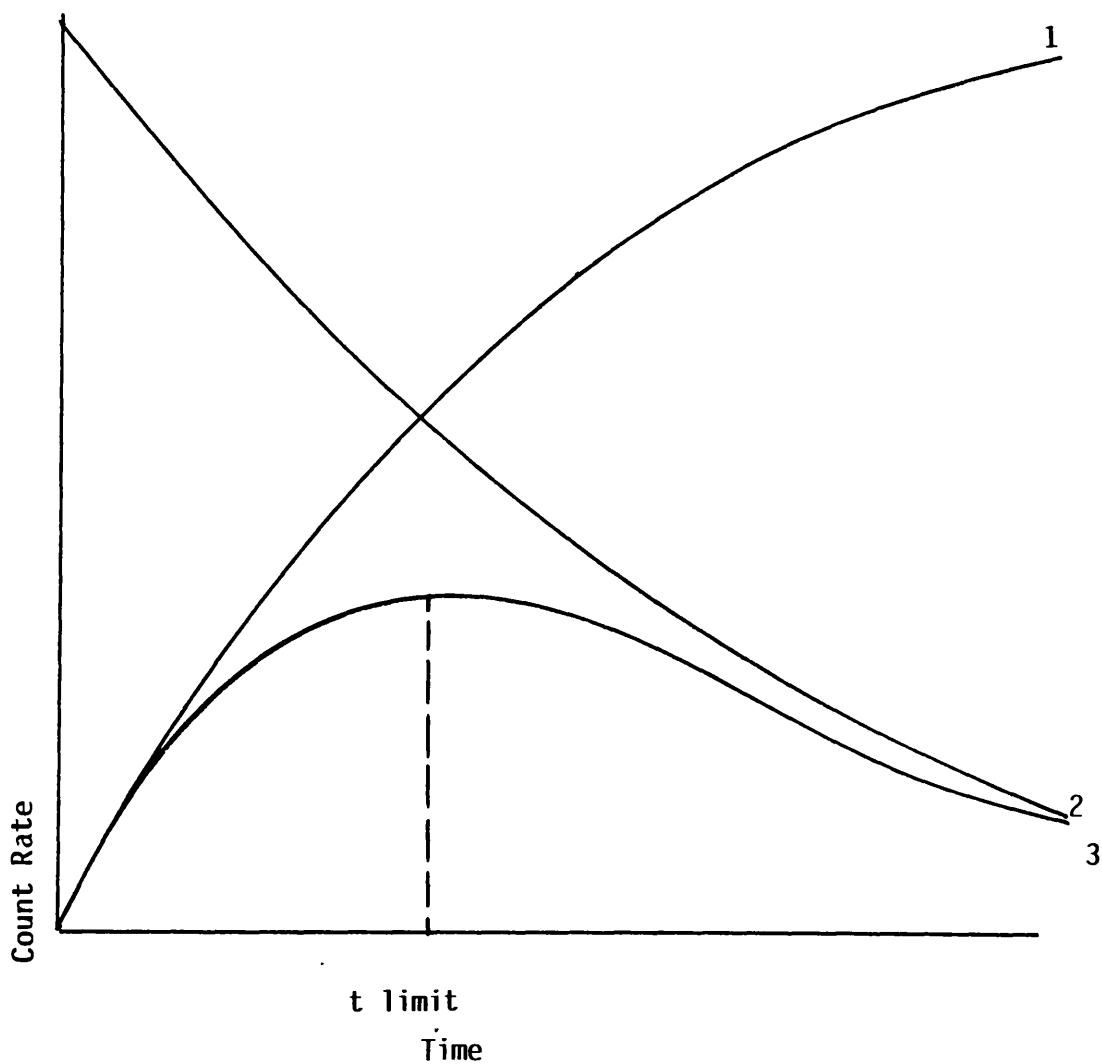
The purity of radiotracers is of considerable importance. Two principal types of impurity exist.

- (i) Radionuclidic impurity where radioactive nuclides other than those desired are present.

Table 2.23 Cyclotron Production of  $^{18}\text{F}$ -Fluorine

Reaction	Target Material	Energy Range	Ref
$^{16}\text{O}(\alpha, d)^{18}\text{F}$	$\text{SiO}_2; \text{H}_2\text{O}$	20 $\rightarrow$ 0	193
$^{20}\text{Ne}(d, \alpha)^{18}\text{F}$	Ne/ $\text{H}_2$ gas	30 $\rightarrow$ 0	193, 194
$^{19}\text{F}(p, pn)^{18}\text{F}$	$\text{F}_2$ gas	31 $\rightarrow$ 7	195
$^{19}\text{F}(p, 2n)^{18}\text{Ne}$			
$^{18}\text{Ne} \xrightarrow[1.55]{\beta^+} ^{18}\text{F}$	$\text{F}_2$ gas	31 $\rightarrow$ 7	195

**Figure 2.23** Kinetic relationship between incorporation and decay of fluorine-18



1= product formation

2=decay curve of fluorine-18

3=incorporation of fluorine-18 in the labelled product



- (ii) Radiochemical impurity where the nuclide of interest is also present in a chemical form differing from the one specifically needed.

The former can be checked by determining the half life and, where possible, the energy of the emitted particle by the radionuclide of interest. The latter can be checked by conventional methods, e.g. vibrational spectroscopy.

#### 2.3.4 THE RADIOISOTOPE $\{^{36}\text{Cl}\}$ - CHLORINE

$\{^{36}\text{Cl}\}$ -Chlorine decays by  $\beta^-$  emission with a half life of  $3 \times 10^5$  y and a  $\beta$  max of 0.714 MeV. The isotope was supplied as an aqueous solution of  $\text{Na}^{36}\text{Cl}$  (Amersham International plc) and was diluted with concentrated hydrochloric acid to give a solution with a specific  $\{^{36}\text{Cl}\}$ -chlorine activity of ca  $9.3 \times 10^5$   $\text{Bq cm}^{-3}$ .

#### 2.3.5 THE RADIOISOTOPE $\{^{14}\text{C}\}$ -CARBON

$\{^{14}\text{C}\}$ -Carbon isotope is a  $\beta^-$  emitter with a half life of 5730 y that can be produced by neutron bombardment of  $^{14}\text{N}$ ,  $^{14}\text{N}(n,p)^{14}\text{C}$ . The isotope was supplied as a solid of  $\text{Ba}^{14}\text{CO}_3$  with activity of  $5.7 \text{ mCi mmol}^{-1}$  (Amersham International plc.)

### 2.3.6 THE RADIOISOTOPE $^{35}\text{S}$ -SULPHUR

Sulphur-35 is a radiotracer which is widely used [196]. Its half life ( $t_{1/2}$  87.39  $\pm$  0.10 d) [197] makes it easy to handle. Its use does not require correction for decay to be made when experiments of a short duration are involved as was the case in this project, and it is commercially available (Amersham International plc). However, due to its low  $\beta$  energy ( $\beta$  max 0.167 MeV), when counted as a solid, correction for self-absorption is required. Its detection requires the use of sensitive counting devices, e.g., liquid scintillation counter, or proportional counter. In this work a direct monitoring technique with internally mounted Geiger-Müller counters was used.

### 2.4 BACKGROUND

Any radioactive counter will register some counts in the absence of a radioactive source. In laboratory environments these counts are due primarily to cosmic radiation and radiation from materials used in the construction of the laboratory. An average background count must be subtracted from all counts in radiochemical counting experiments to correct for this effect.

$$C_t = C_o - C_b$$

where  $C_t$  is the true count

$C_o$  is the observed count

$C_b$  is the background count

The background registered by any counter can be reduced by enclosing the system and the sample to be counted in a lead walled container. The radioisotopes  $^{14}\text{C}$ ,  $^{36}\text{Cl}$  and  $^{35}\text{S}$  containing species

were counted in a glass reaction vessel, which could not be shielded and consequently a higher background count was recorded in these experiments. The scintillation counter used for counting  $^{18}\text{F}$  samples was contained in a lead castle for the same reason.

## 2.5 STATISTICAL ERRORS

Radioactive decay is a random process. This means that if a source of constant activity is measured in a way that excludes all other errors in measurement, the number of disintegrations observed in successive periods of fixed duration will not be constant. The probability,  $W_m$ , of obtaining  $m$  disintegrations in time  $t$  from  $N_0$  radioactive atoms is given by the expression, equation 2.13

$$W_m = \frac{N_0!}{(N_0-m)!m!} P^m (1-P)^{N_0-m} \quad \text{Eq. 2.13}$$

where  $P$  is the probability of a disintegration occurring within the time of observation. From this expression, it can be shown that the expected standard deviation for radioactive disintegration,  $\sigma$  is given by equation 2.14 [198]. In practice, observation time  $t$  is short compared with  $t_{1/2}$ , so  $\lambda t$  is small and

$$\sigma = \sqrt{m} e^{-\lambda t} \quad \text{Eq. 2.14}$$

equation 2.15 can be involved. The error on a result is often quoted as  $\pm \sigma$  on this convention has been adopted

$$\sigma = \sqrt{m} \quad \text{Eq. 2.15}$$

throughout this work. All errors quoted on radiochemical measurements were from the combination of the radiochemical error and the uncertainty

in physical measurements such as the measurement of the pressure of a gas or the weight of a sample.

## 2.6 COUNTING OF $^{14}\text{C}$ , $^{36}\text{Cl}$ and $^{35}\text{S}$ SAMPLES.

### 2.6.1 GEIGER-MÜLLER COUNTERS

$\{^{14}\text{C}\}$ -Carbon,  $\{^{36}\text{Cl}\}$ -chlorine and  $\{^{35}\text{S}\}$ -sulphur are  $\beta^-$  emitters. In this type of decay process the mass number A remains unchanged but the atomic number is increased by unit.

A Geiger-Müller tube was used for counting  $^{14}\text{C}$ ,  $^{36}\text{Cl}$  and  $^{35}\text{S}$  labelled compounds. The Geiger-Müller counter, in which the gas amplification factor is between  $10^7$ - $10^{10}$ , is commonly used instrument for both detection and counting. It is filled with a noble gas such as argon, generally at pressure of one-fifth of an atmosphere, and also contains a 'quenching' agent such as ethanol or bromine which has a lower ionization potential than the noble gas. When an ionizing particle enters the tube through a thin mica window, a large number of electrons are produced, the discharge spreading along the entire length of the tube. A positively charged electrode is suspended along the centre of the tube. The electrical pulses are recorded by an electronic scaler which produces an output that is proportional to the strength of the initial ionising radiation.

### 2.6.2 PLATEAU CURVE

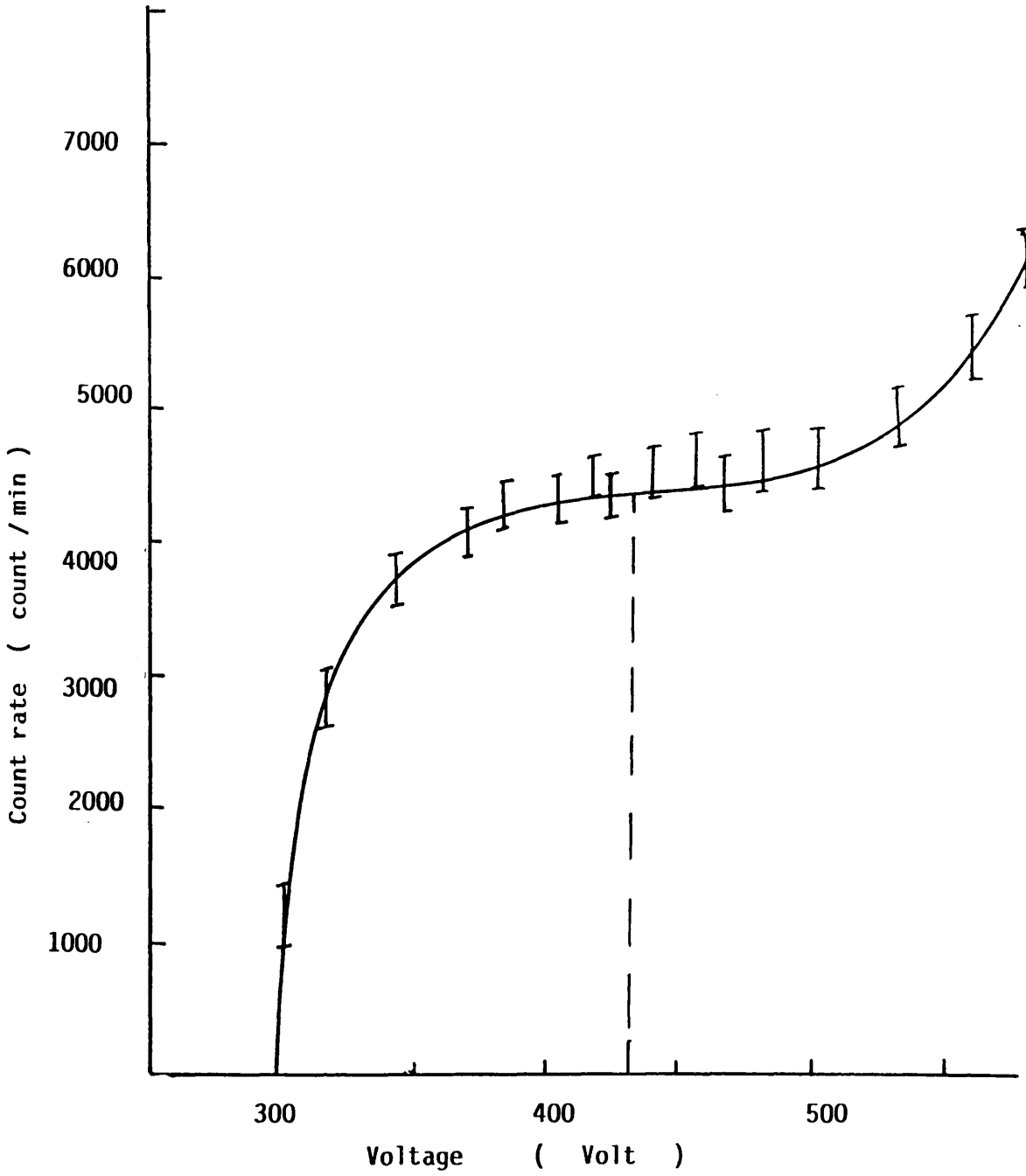
No event will be recorded by a Geiger-Müller tube until the applied voltage potential is large enough to attract the free electrons to the anode. When the voltage is applied, the count rate begins to arise rapidly until a plateau region is reached in which the counting rate caused by a given radiation source is independent of the applied voltage. Geiger-Müller counters typically have plateaus of several hundred volts with slopes of  $< 1$ . This is due to the generation inside the counter of spurious discharges caused by secondary electron emission. This occurs when the positive ion produced in the initial ionisation reaches the cathode and causes secondary electron emission from the surface. This secondary electron emission is usually suppressed by the addition of an organic quench gas such as  $\text{CH}_4$ . As the potential increases, the quench gas cannot cope with the large number of spurious discharges and the count rate begins to rise rapidly until the counter begins to discharge.

The plateau curve was determined for each Geiger-Müller counter using a solid Cobalt-60 source by sweeping through the voltage region whilst monitoring the count obtained. A typical example is shown in Fig. 224 and the mid point of the plateau was taken as the operating voltage.

### 2.6.3 DEAD TIME

In a Geiger-Müller counter, the negative ions formed (mostly free electrons) reach the central wire very quickly, typically in about  $5 \times 10^{-7}$  s; however, the sheath of positive ions that now

Figure 2.24 The plateau curve of the G.M tube



surrounds the wire reduces the voltage gradient below the voltage necessary for ion multiplication, and the counter cannot record another event until the positive ions reach the cathode, in about 100-500  $\mu$ s. As a result each pulse from the Geiger-Müller tube is followed by a period during which no particles can be detected. This insensitive period is known as the dead time of the G.M. tube. A correction for counts lost in such periods must be applied especially if the counting rate is high. The true count rate  $N_t$  is defined by the following equation (2.16)

$$N_t = N_o / (1 - N_o \tau) \quad \text{Eq. 2.16}$$

where  $N_o$  is the observed count rate

$\tau$  is the dead time

The dead time of each Geiger-Müller counter was determined using samples of  $\text{Cs}^{18}\text{F}$  which were counted repeatedly over a period of three half lives. Equation 2.17 describes the decay of a radioisotope

$$A_t = A_o e^{-\lambda t} \quad \text{Eq. 2.17}$$

where  $\lambda$  = decay constant in  $\text{s}^{-1}$

$A_t$  = count rate of sample at time  $t$  (count  $\text{min}^{-1}$ )

$A_o$  = count rate of sample at time  $t = 0$  (count  $\text{min}^{-1}$ )

Thus a plot of  $\ln A_t$  versus time should be linear with a gradient  $-\lambda$  and intercept  $\ln A_o$ . Plots of this type were constructed for  $\text{Cs}^{18}\text{F}$  counts. When  $\ln A_t$  versus time was plotted, a linear relationship was obtained for  $t > 250$  min, but showed curvature at  $t < 250$  min. This is due to the effect of the dead time at higher counting rates. The linear portion of the graph was extrapolated

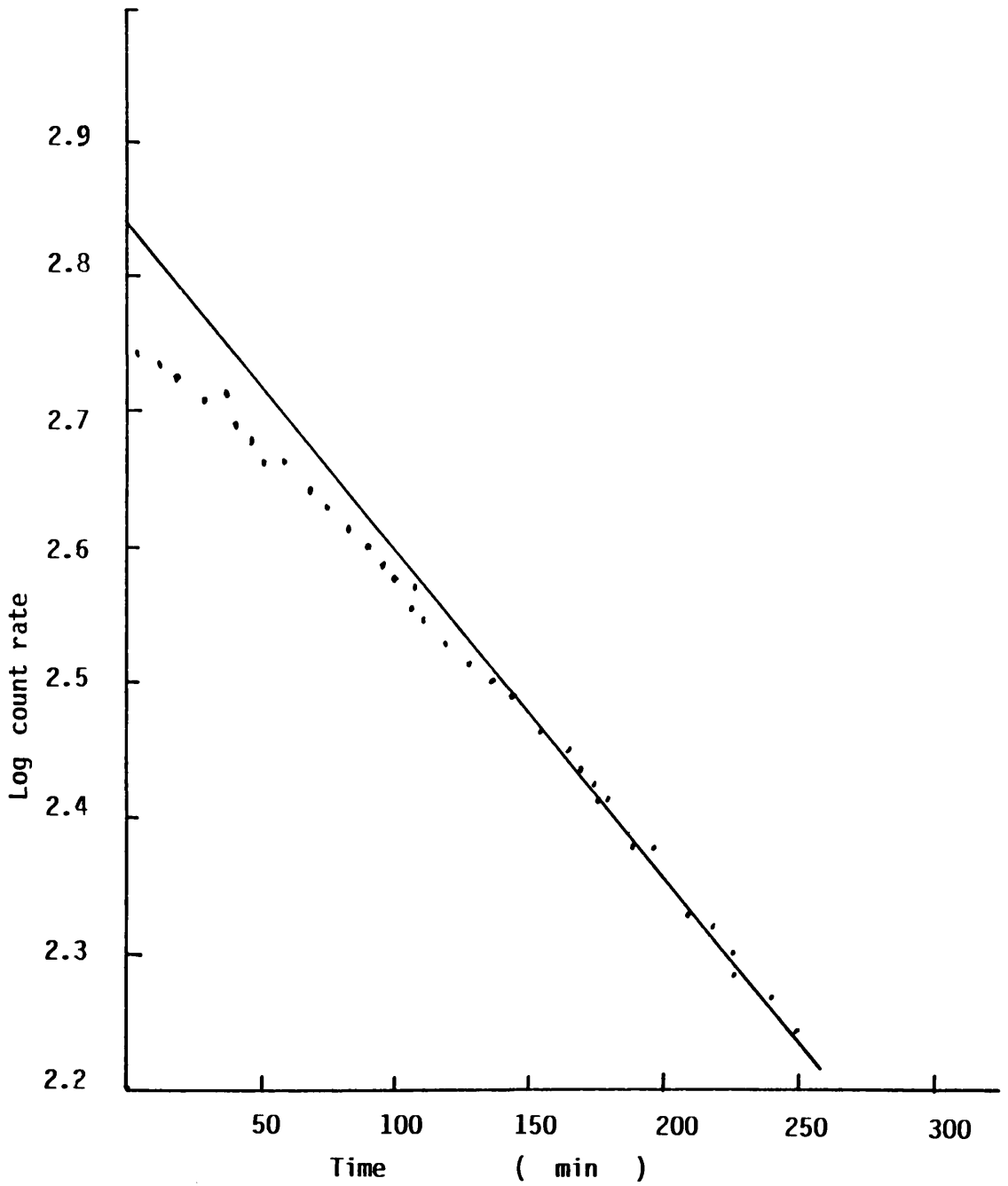
to  $t = 0$  using the known half life of  $\{^{18}\text{F}\}$ -fluorine. This line gave  $N_t$ , the calculated true count rate at any time  $t$ , which is related to  $N_0$ , the observed count rate at time  $t$ , by equation 2.16, where  $\tau$  is the dead time. A computer programme was used to calculate  $\tau$  from  $N_t$  and  $N_0$  for the first twenty points after  $t = 0$ , and the mean value of  $\tau$  was taken to be the dead time of the Geiger-Müller counter. Fig. 2.25 shows a typical plot. A typical value of the dead time was  $3.98 \times 10^{-4} \text{ s}^{-1}$ .

#### 2.6.4 THE DIRECT MONITORING GEIGER-MÜLLER COUNTERS.

The direct monitoring G.M. radiochemical counting technique was developed by Thomson, and modified by Al-Ammar and Webb [199] to determine surface radioactivity on solids exposed to radio-labelled gases. The technique has been successfully used to detect both weakly and strongly adsorbed species in a variety of situations [83] and has proved to be a powerful tool in the elucidation of mechanism in heterogeneous catalysis. This apparatus Fig. 2.26 consists of two intercalibrated G.M. detectors in an accurately calibrated, evacuable glass cell which enables the surface radioactivity to be determined directly. Both G.M. tubes are positioned at the same height to ensure identical counting geometry. A solid sample is placed in a Pyrex glass boat by dropping the solid into the boat and positioning under either G.M. detector. The G.M. tubes were tested for counting only the active solid beneath it; the counts from both G.M. tubes were monitored with  $^{60}\text{Co}$  source placed directly under one of the tubes. The tube which was above the source gave a large



Figure 2.25 The dead time of the G.M tube ; decay of fluorine-18



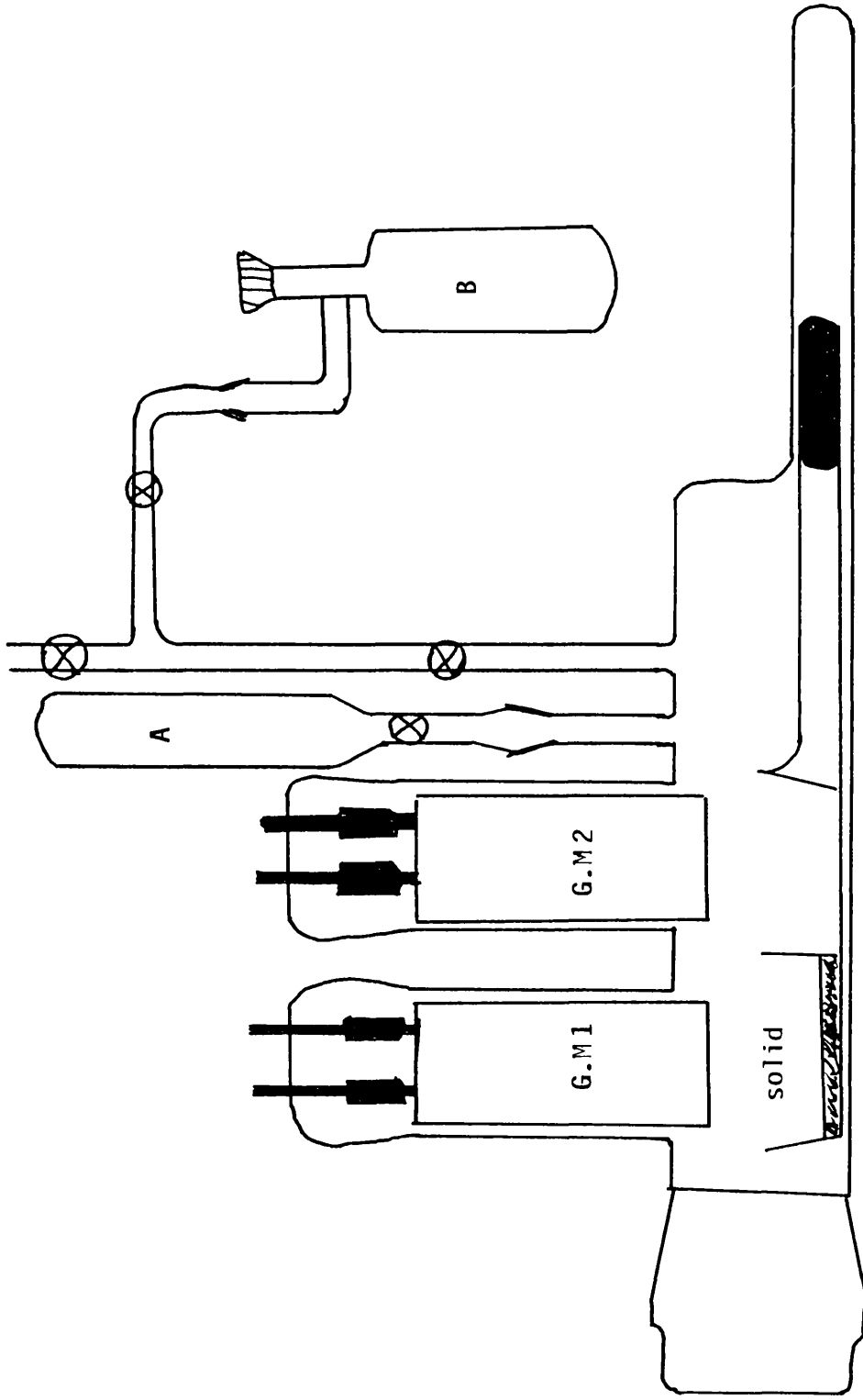


Figure 2.26 Counting Cell

count, but the other tube gave only the background count rate, Table 2.24.

The count rate of the same source varies slightly from G.M. tube to another, so the two tubes contained in the counting cell were intercalibrated regularly. Various pressures of radioactive gas were counted and a plot of the count rate from GMI versus the count rate from GMII was constructed. A set of results obtained using  $\{^{35}\text{S}\}\text{-SF}_4$  is given in Table 2.25. A linear relationship was obtained for GMI count rate versus GMII count rate plot with a gradient of 1.02 which was taken as the intercalibration coefficient of the GM tubes, Fig. 2.27.

#### 2.6.5 APPLICATION FOR THE TECHNIQUE TO EXPERIMENTS INVOLVING MF / $\gamma$ -ALUMINA

The procedure was as follows; the dropping vessel (A) was evacuated and flamed out then transferred to an inert atmosphere box and loaded with an accurately weighed amount of the required solid. The dropping vessel was attached to the vacuum line and evacuated before being re-attached to the counting cell which was then pumped and flamed out. After one hour an accurately measured pressure of a radioactive gas, for example,  $^{35}\text{SF}_4$ , was admitted to the counting cell and three 100 second counts were taken. The average was taken as the count rate of the gas before reaction. The radioactive gas was then removed from the counting cell by condensing into vessel B. The dropping vessel was opened and the sample of the solid dropped into the right hand portion of the glass boat. The boat was then moved, so that, the right hand portion was directly under Geiger-Müller I

Table 2.24 OBSERVED COUNT RATES FROM THE GM TUBES

Position of $^{60}\text{Co}$ source.	GMI count $\text{s}^{-1}$	GMI count $\text{s}^{-1}$
Background	0.43	0.47
$^{60}\text{Co}$ under I	43	0.42
$^{60}\text{Co}$ under I	45	0.45
$^{60}\text{Co}$ under I	44	0.49
$^{60}\text{Co}$ under II	0.39	51
$^{60}\text{Co}$ under II	0.43	49
$^{60}\text{Co}$ under II	0.41	50

Table 2.25  $^{35}\text{SF}_4$  Pressure vs Count Rate

Pressure (Torr)	Count Rate GMI (count min <sup>-1</sup> )	Count Rate GMII (count min <sup>-1</sup> )
10.3 ± 1	8389 ± 17	8556 ± 18
22 ± 1	16790 ± 23	17126 ± 25
42.1 ± 1	33541 ± 27	34211 ± 29
60.7 ± 1	50317 ± 32	51323 ± 33
80.8 ± 1	67085 ± 35	68426 ± 37
103 ± 1	83878 ± 37	85556 ± 38
143 ± 1	117406 ± 41	119754 ± 43
200 ± 1	167949 ± 48	171308 ± 50
263 ± 1	218120 ± 53	222482 ± 55
281 ± 1	234955 ± 58	239654 ± 61
300 ± 1	251736 ± 63	256771 ± 64

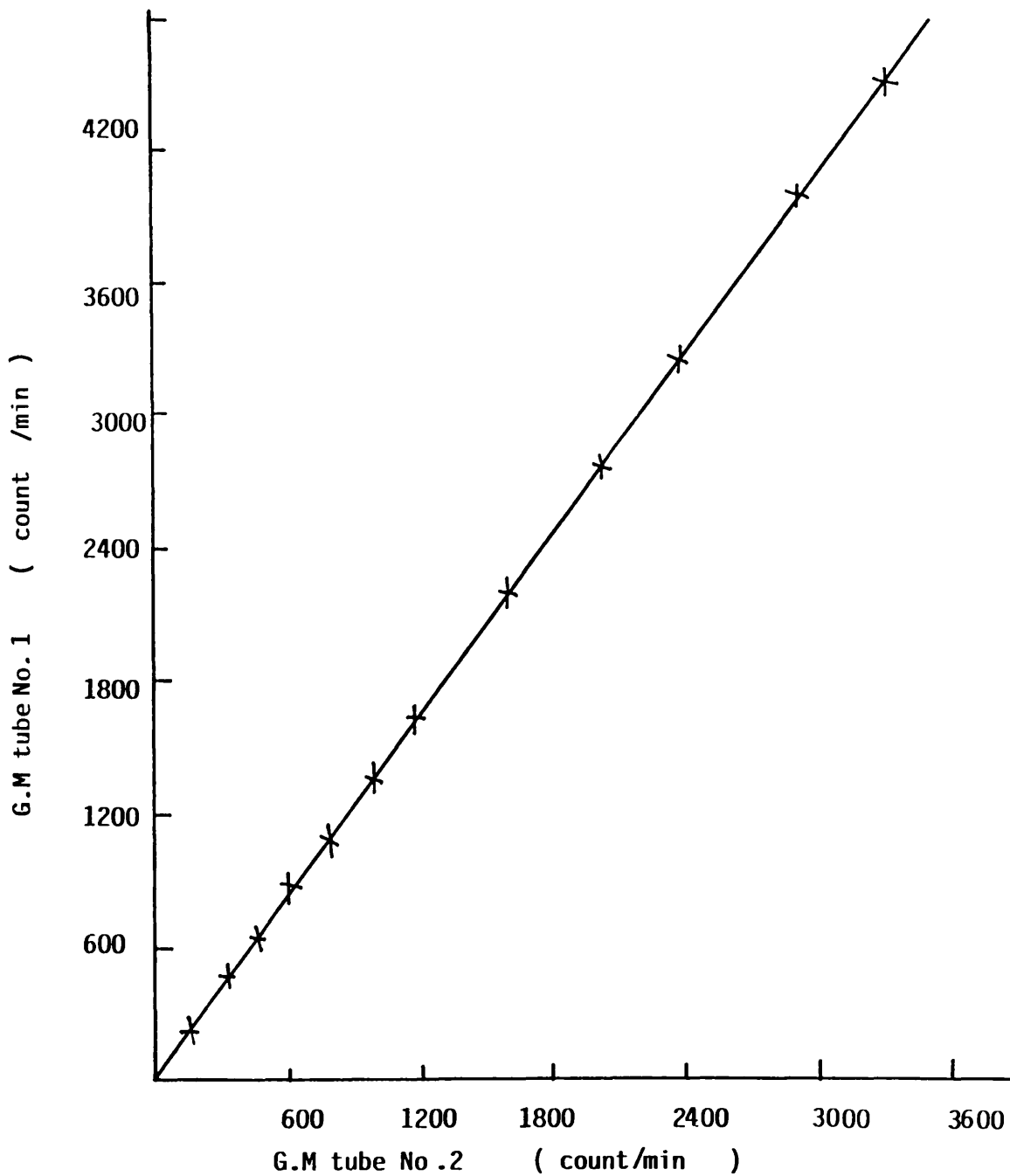


Figure 2.27 Intercalibration of G.M tubes using various pressures of  $^{35}\text{SF}_4$

and the empty left-hand portion was directly under Geiger-Müller II. Counts were taken from both GM tubes with time. Counts registered from GM counter I were from gas and solid, whilst those from GM counter II were from the gas alone. The reaction was followed by monitoring the counts from both tubes over a period of time. The counts from both GM tubes were corrected for dead-time, background and intercalibration. The difference represented the surface count rate. The overall drop in gas count rate that is the difference between the count rate of gas before reaction and the last point in the reaction, gave a measure of the total uptake of the gas by the solid. Pressures were measured by three different ways according to the chemical properties of the involved material. Details are given in Table 2.26.

## 2.7 COUNTING OF $^{18}\text{F}$ SAMPLES

### 2.7.1 Scintillation Counters

{ $^{18}\text{F}$ }-Fluorine decays by the emission of a positron ( $\beta^+$ ).

A positron is a positively charged electron which is ejected from the nucleus. This occurs when the balance between protons and neutrons is adjusted by the transformation within the nucleus of a proton into a neutron



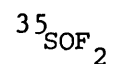
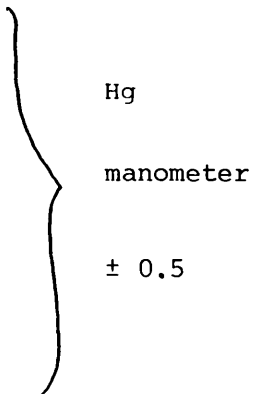
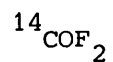
The emission of  $\beta^+$  leaves the mass number of the isotope unchanged but the atomic number decreases by one. The emitted positrons interact with surrounding atoms in a manner very similar to that of an ordinary electron, and hence the range of positrons and

Table 2.26

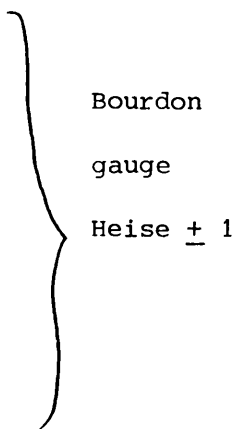
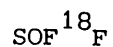
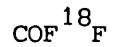
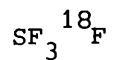
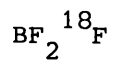
The Measurement of Volatile Materials.

Material

Measurement of Pressure



Oil manometer ± 0.5





the ionisation produced is almost identical to that of a negatively charged electron of the same energy. At the end of its range where the positron has lost its initial kinetic energy, it combines with a negative electron, and annihilation of both particles occurs. The rest mass energy appears as two photons of electromagnetic radiation moving in opposite directions. This annihilation radiation emitted by  $\{^{18}\text{F}\}$ -fluorine results in the emission of  $\gamma$  radiation with a  $\gamma$  max of 0.51 MeV. The  $\gamma$  rays produced in the annihilation process of positron interacting with a negative electron were counted using a Tl/NaI scintillation counter (NE electronics instruments).

Among the inorganic scintillators NaI activated with 0.1-0.2% thallium is by far the most widely used. The high density ( $3.7 \text{ g cm}^{-3}$ ) of NaI and the high Z of iodine make this a very efficient  $\gamma$  ray detector.

Approximately 30 eV of energy deposition in a NaI(Tl) crystal is required to produce one light photon, and it takes on the average about 10 photons to release one photoelectron at the photo-cathode of the multiplier. These photoelectrons are then accelerated by a potential to the first electrode where each one produces another four or so electrons. These secondary electrons are similarly accelerated, so that in a 10 stage tube there is again  $10^4$ . The resulting pulse is then fed to an amplifier and then to a scaler where it is recorded.

To achieve a maximum pulse the scintillator crystal is surrounded by a reflector, and the space between the crystal and the photomultiplier filled with paraffin oil or silicone oil of high viscosity to improve the light transmission.

The scintillation counter and the scaler were calibrated before use by a standard  $^{137}\text{Cs}$   $\gamma$  emitter source and then with  $^{60}\text{Co}$  source which emits  $\gamma$  rays of energy of 1.33 MeV.

In each case  $\gamma$ -ray spectrum was obtained by monitoring the counts from the source while varying the applied threshold. The  $\gamma$ -ray spectrum obtained for  $^{137}\text{Cs}$  source is shown in Fig. 2.28. Absolute intensities of  $\gamma$  rays in moderately complex spectra can usually be determined to about  $\pm 5\%$ . The  $\gamma$ -ray spectra obtained from  $\text{Cs}^{18}\text{F}$ ,  $\text{SF}_3^{18}\text{F}$ .Pyridine,  $\text{CsCOF}_2^{18}\text{F}$ .MeCN and  $\text{CsHF}^{18}\text{F}$  are in Figs. 2.29 - 2.32.

### 2.7.2 DECAY CORRECTION

The disintegration of a given radioactive species decays according to equation 2.17. The half life  $t_{1/2}$  is the time interval required for A (measured activity) decreases to one half of its original value. The half life is conveniently determined from a plot of  $\ln A$  versus  $t$  and is related to the decay constant by equation 2.18 and Fig. 2.33

$$t_{1/2} = \frac{\ln 2}{\lambda} = \frac{0.69315}{\lambda} \quad \text{Eq. 2.18}$$

Since significant decay occurred in the time taken to carry out one experiment, all data obtained must be corrected to the zero time before being analysed. Results obtained from  $\{^{18}\text{F}\}$ -fluorine work were corrected to the activity at time of the last count rate using equation 2.17. A microcomputer programme was used to carry out these calculations

Figure 2.28 Gamma ray spectrum of  $^{137}\text{Cs}$

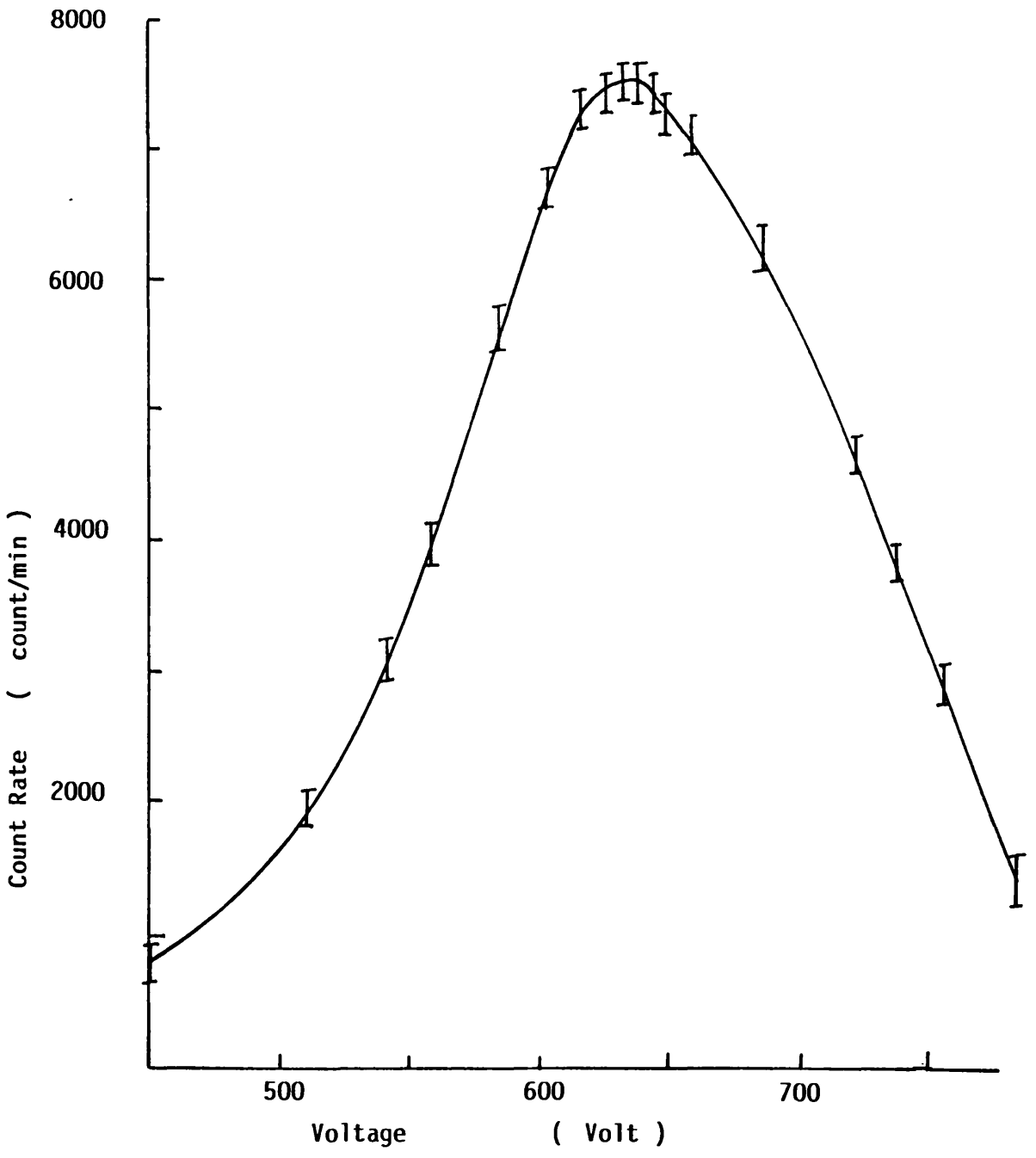


Figure 2.29 Gamma ray spectrum of Cs<sup>18</sup>F

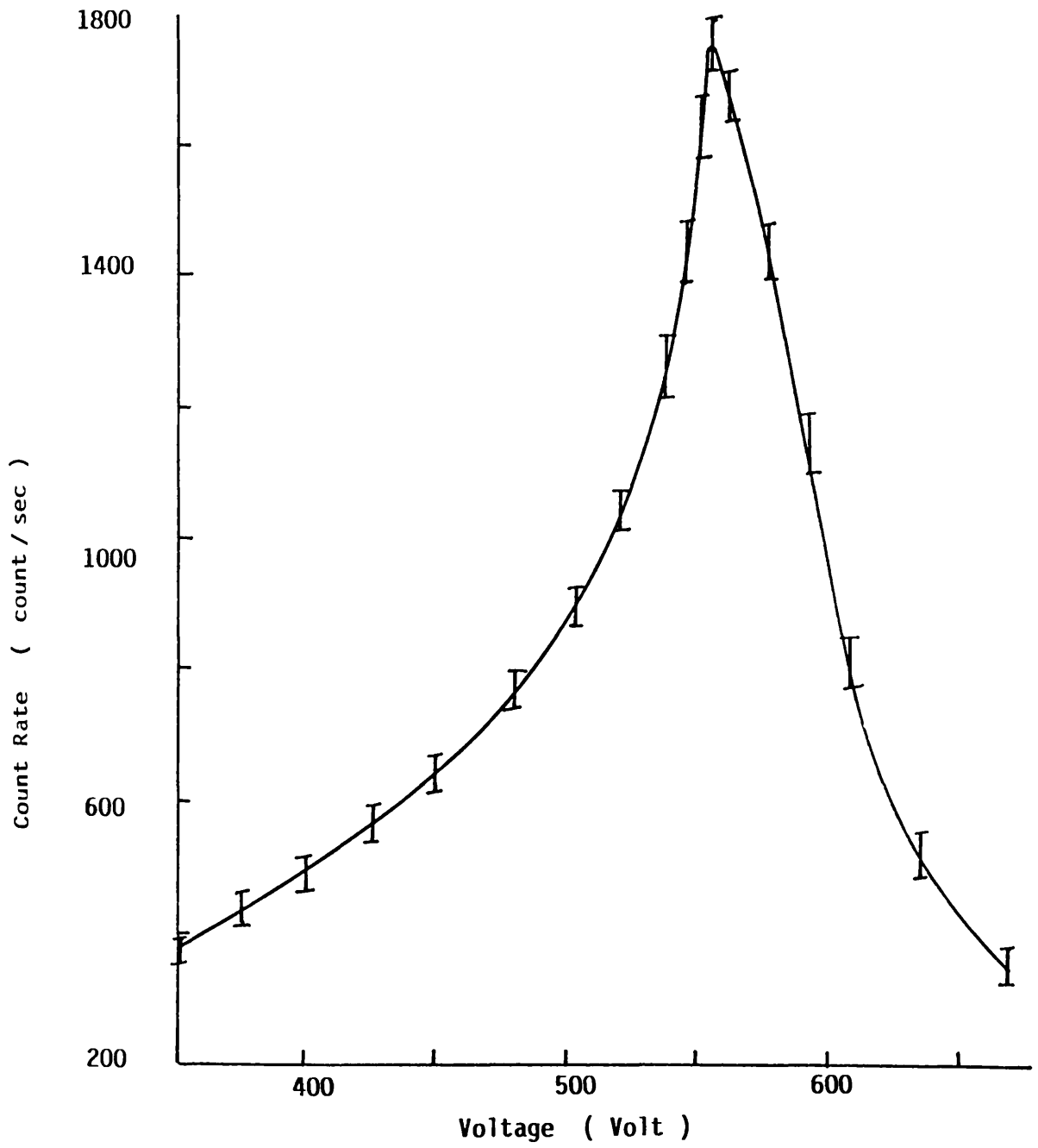


Figure 2.30 Gamma ray spectrum of SF<sub>3</sub><sup>18</sup>F

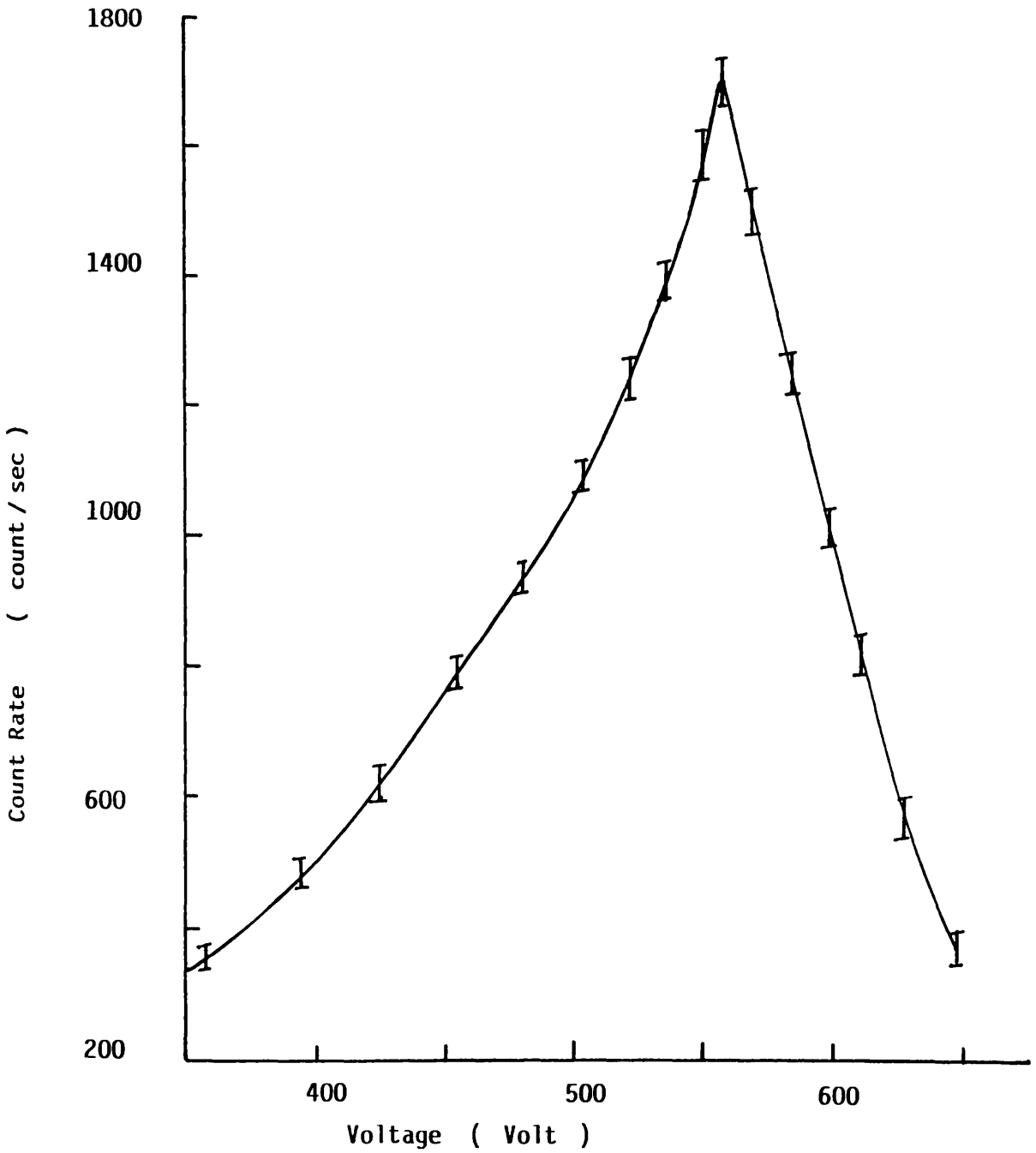


Figure 2.31 Gamma ray spectrum of COF<sup>18</sup>F

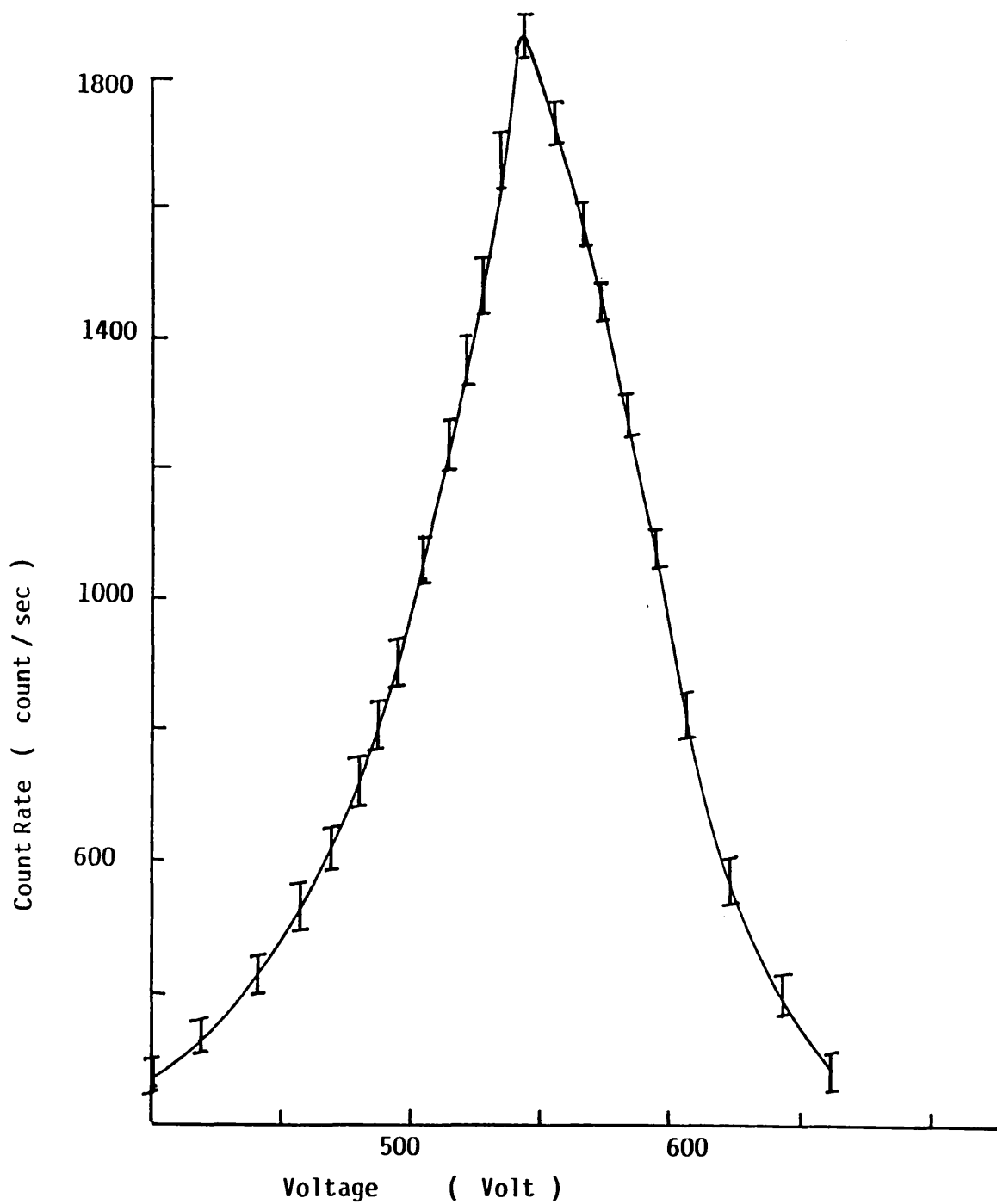


Figure 2.32 Gamma ray spectrum of  $H^{18}F$

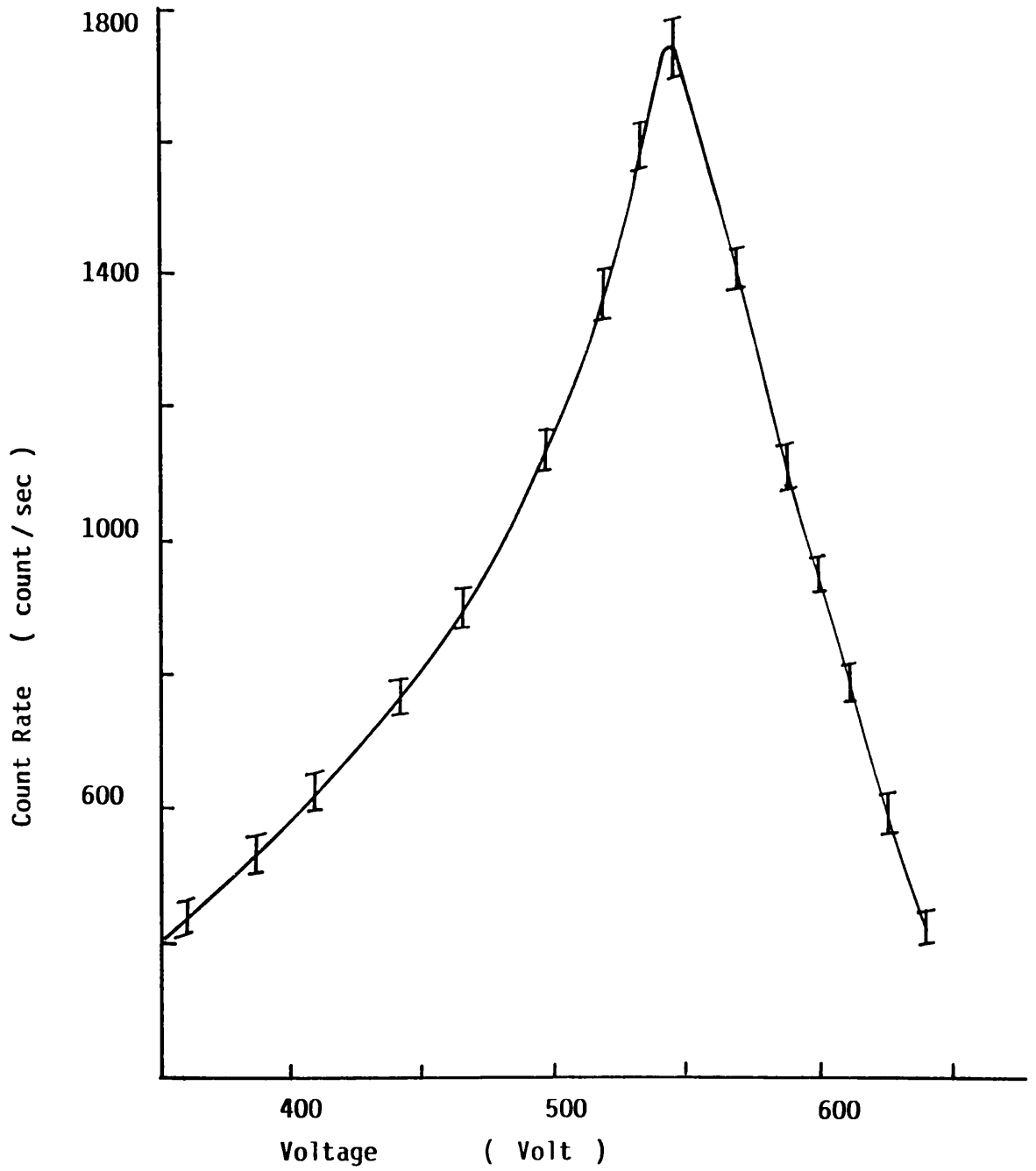
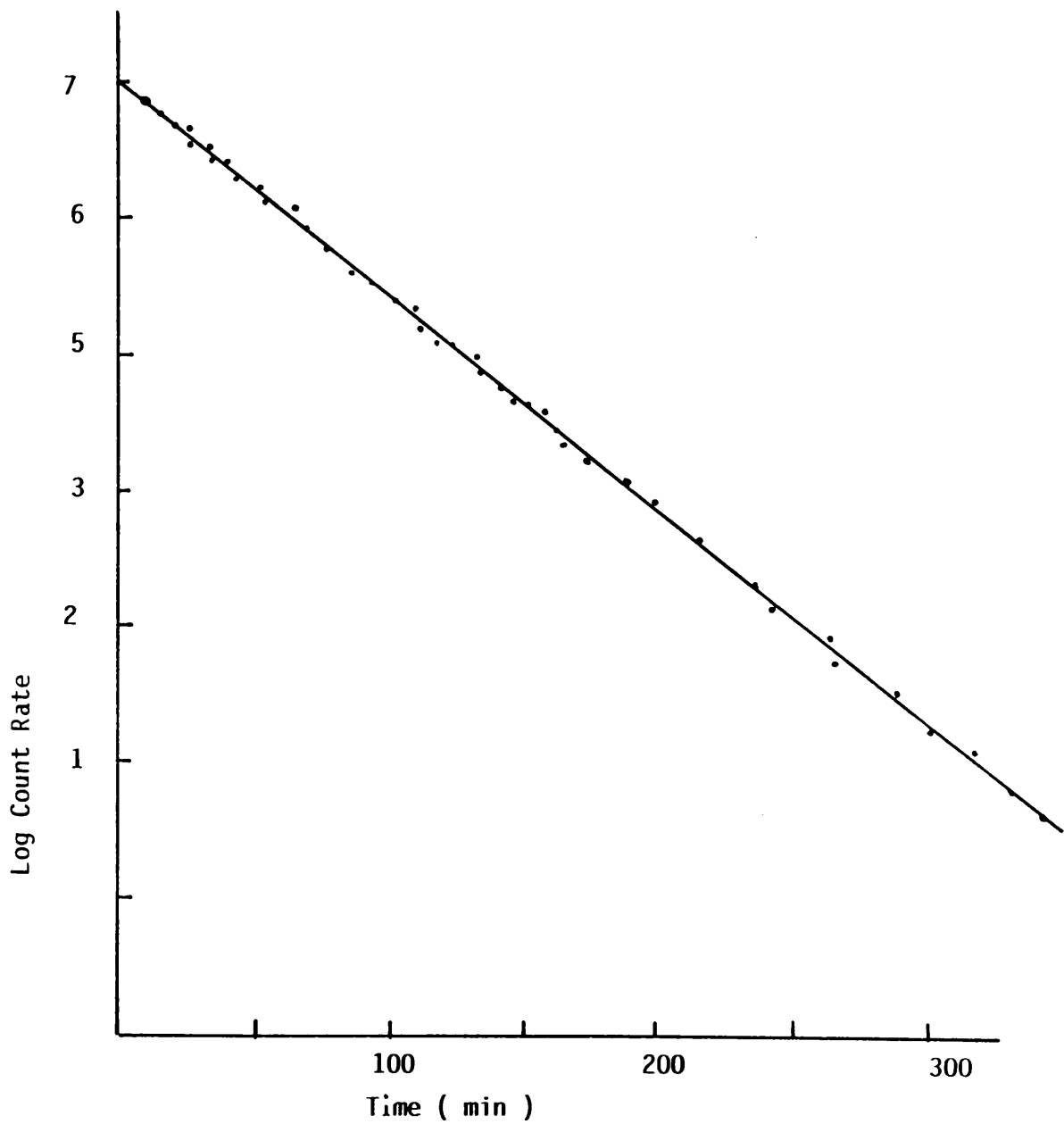


Figure 2.33 The half life of  $\text{Cs}^{18}\text{F}$





### 2.7.3 {<sup>18</sup>F}-FLUORINE COUNTING APPARATUS

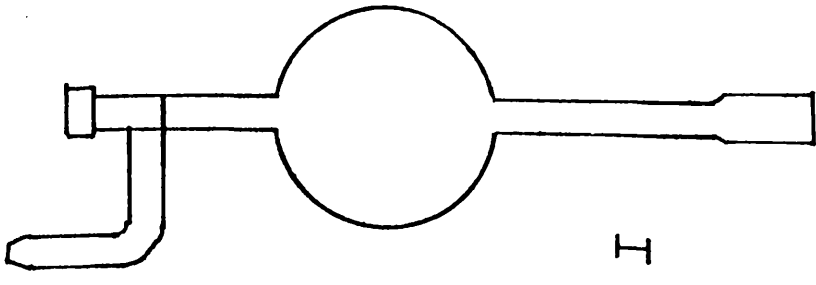
Reactions involving {<sup>18</sup>F}-fluorine labelled SF<sub>4</sub>, SOF<sub>2</sub> and COF<sub>2</sub> were monitored using the counting vessels shown in Fig. 2.34; vessel I was used to count gas samples and vessel II was used to follow the reaction between SF<sub>4</sub>, SOF<sub>2</sub> or COF<sub>2</sub>, isotopically labelled gases with {<sup>18</sup>F}-fluorine and MF/γ-alumina solid samples (M = Cs, K).

### 2.7.4 APPLICATION TO REACTIONS WITH MF/γ-ALUMINA

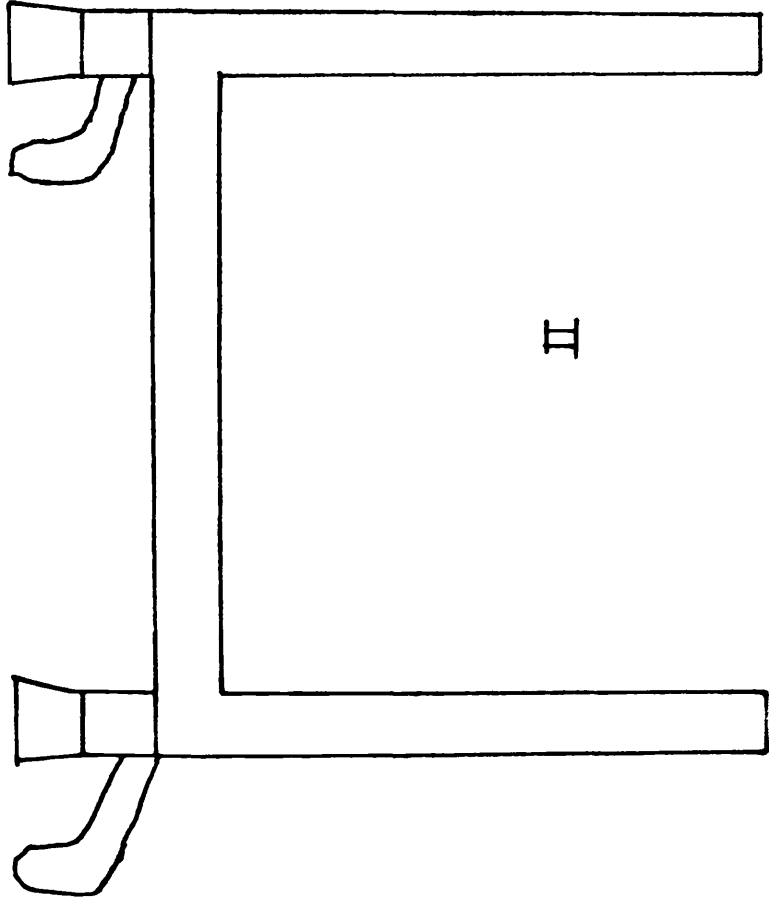
Counting vessel II was evacuated, flamed out for 0.5h then was transferred to an inert atmosphere box where a weighed amount of the required solid was placed in one limb of the vessel. The vessel was then transferred to the vacuum system and evacuated for two hours. A measured pressure of {<sup>18</sup>F}-fluorine labelled gas was admitted to the vessel and the reaction followed by counting each limb alternately over a period of time. After reaction the data were corrected for decay and background.

At the end of the reaction the gas phase was transferred from the double limbed vessel to another pre-weighed flask of type I and its specific count rate calculated. The specific count rates of the gas before and after reaction were compared in order to determine whether the growth of activity in the solid was due to {<sup>18</sup>F}-fluorine exchange between the gas phase and the solid or the retention of gas by the solid, or was it due to the hydrolysis of gas.

Reactions involving {<sup>18</sup>F}-fluorine labelled anhydrous hydrogen fluoride were followed using vessel (A) and reactor (B) in Fig. 2.35. The reactor was evacuated and transferred to an inert atmosphere box



I



II

Figure 2.34 Fluorine-18 Counting vessels

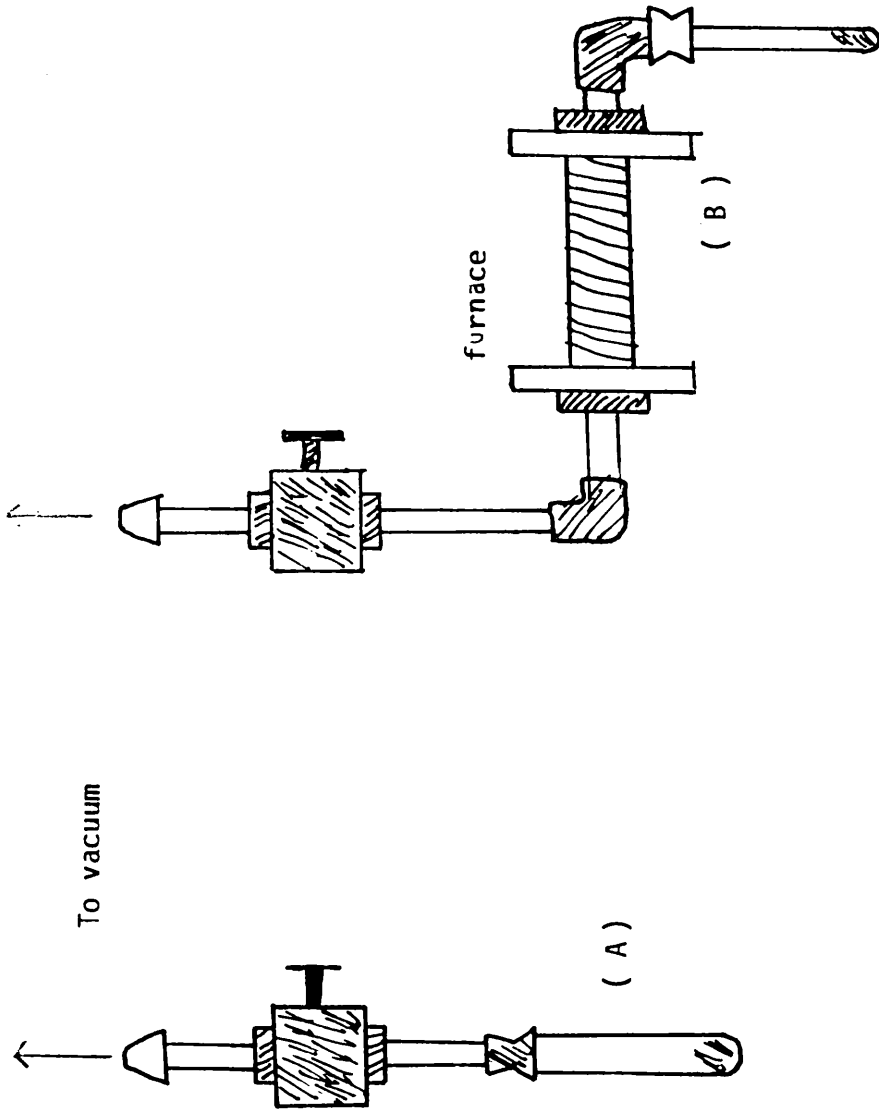


Figure 2.35  $\text{H}^{18}\text{F}$  Counting vessels

where a weighed amount of the required solid was placed in the (P.T.F.E) tube. The reactor was then evacuated and an amount of  $H^{18}F$  was admitted, followed by counting the solid over a period of time. After reaction the gas phase was removed and condensed in another vessel type (A) and its specific count rate was calculated.

Fluorine-18 labelled samples were counted using a well scintillation counter. The efficiency of the gas phase counting is less than these of solid or liquid since only the amount of material which is in the well of the counter will be counted. For this reason  $SF_3^{18}F$  was counted as its adduct with pyridine [200],  $SOF^{18}F$  was counted as solid at 77 K,  $COF^{18}F$  was counted as solid with  $CsF$  and  $MeCN$  and  $H^{18}F$  was counted as a complex with  $CsF$ . These methods of counting were tested before being applied, counting vessels were filled with varying amounts of labelled gas and the adduct allowed to be formed followed by monitoring; a linear relationship between the amount of gas in the flask and the count rate recorded was obtained in each case.

## 2.8 PREPARATION OF RADIOCHEMICALLY LABELLED SPECIES.

### 2.8.1 Preparation of $Cs^{18}F$

{ $^{18}F$ }-Fluorine labelled caesium fluoride was prepared by irradiating lithium carbonate ca. 2.0g in the central core of the Scottish Universities Research and Reactor Centre (S.U.R.R.C) at East Kilbride using the sequence



Typical irradiation conditions are tabulated in Table 2.27. The sample of  $Li_2CO_3$  (BDH Analar) was contained within an aluminium

Table 2.27 Irradiation Conditions of  $^{18}\text{F}$  Preparation.

Sample weight (g)	Number of Pellets	Irradiation Time (min)	System	Activity Measured ( $\mu\text{Ci}$ )
2	Powder	30	C C	35-36
2	10	30	L R	10
2	10	40	L R	15
2	10	30	L R	20
2	15	40	L R	30
2	25	30	L R	40
2.5	25	40	L R	40-75

C C = central core

L R = Large Rabbit

screw-top can (height, 8cm; diameter 3cm). A graphite rod (length 7cm; diameter 1.5cm) inside the aluminium acted as neutron moderator, slowing the neutrons to improve the probability of collision with lithium nuclei. However, some contamination arose in the working area using this procedure and the method was modified. The modification involved the use of reactor Rabbit system and pellets rather than powder to minimise contamination. Lithium carbonate pellets were spread carefully on the surface of a P.T.F.E. vial so that each was subject to an identical neutron flux. The plastic vial was placed in a P.T.F.E. bag which was placed in the "Rabbit". The Rabbit, Fig 2.36, is a cylindrical plastic screw-top container which is transferred between the laboratory and the reactor by an evacuated loop. Irradiation conditions are given in Table 2.27. The  $\text{Li}^{18}\text{F}$  produced in the irradiation was converted to  $\text{H}^{18}\text{F}$  by reaction with sulphuric acid ( $\text{H}_2\text{SO}_4:\text{H}_2\text{O} = 1.1$  by volume). The  $\text{H}^{18}\text{F}$  was distilled into a solution of  $\text{CsOH}$  at 273 K. Neutralisation of the solution by addition of aqueous  $\text{HF}$  was followed by evaporation to dryness using a hot plate to give  $\text{Cs}^{18}\text{F}$  as a finely divided white powder.

#### 2.8.2 Preparation of $\text{H}^{18}\text{F}$ , $\text{BF}_2^{18}\text{F}$ , $\text{BF}_3^{18}\text{F}$ , $\text{FFCO}^{18}\text{F}$ , $\text{SF}_3^{18}\text{F}$ and $\text{FFSO}^{18}\text{F}$ .

{ $^{18}\text{F}$ }-Fluorine labelled anhydrous hydrogen fluoride, boron trifluoride and carbonyl fluoride were prepared by temperature exchange with  $\text{Cs}^{18}\text{F}$  in a Monel metal pressure vessel. Previous work has been shown that  $\text{Cs}^{18}\text{F}$  undergoes high temperature fluorine exchange more readily than any group I fluoride [ 188 ]. Various reaction conditions were used in order to determine those which gave the greatest incorporation of  $^{18}\text{F}$ . The results of these experiments for each type of gas labelled are listed in Tables 2.28 - 2.30.

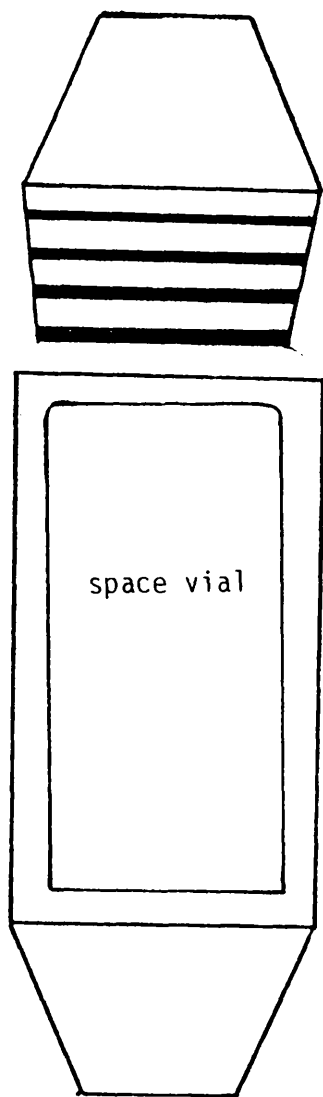


Figure 2.36 Rabbit and space vial used in the bombardment of  $\text{Li}_2\text{CO}_3$

Table 2.28 Labelling Conditions of H<sup>18</sup>F

Temp (K)	Exchange Time (min)	Activity of Cs <sup>18</sup> F	Count min <sup>-1</sup> mmol <sup>-1</sup> H <sup>18</sup> F
373	30	45 μCi	1513
423	30	45 μCi	1913
523	30	45 μCi	5915

Using 3 cm<sup>3</sup> HF.

Table 2.29 Labelling Conditions of BF<sub>2</sub><sup>18</sup>F

Pressure of BF <sub>3</sub> (Torr)	Temp K	Exchange Time (min)	Activity of Cs <sup>18</sup> F	Count min <sup>-1</sup> mmol <sup>-1</sup> of BF <sub>2</sub> <sup>18</sup> F
760	398	60	45 μCi	2467
760	398	60	35 μCi	1906
1010	398	60	55 μCi	6690
1010	398	60	55 μCi	6203



Table 2.30 Labelling Conditions of COF<sup>18</sup>F

Pressure of F <sub>2</sub> CO (Torr)	Temp (K)	Exchange Time (min)	Activity of Cs <sup>18</sup> F	Count min <sup>-1</sup> mmol <sup>-1</sup> Gas phase
760	373	60	65 μCi	9876
1010	373	60	60 μCi	11499
1010	373	60	65 μCi	11898

Plots of the count rate vs pressure for each type of gas are shown in Figs. 2.37 and 2.38 .

$\{^{18}\text{F}\}$ -Fluorine labelled  $\text{SF}_4$  prepared by this method had a specific count rate which was too low to be used. Sulphur tetrafluoride labelled with  $\{^{18}\text{F}\}$ -fluorine was therefore prepared from inactive  $\text{SF}_4$  by means of the adduct  $\text{SF}_3^+ \text{BF}_3^- \text{F}^{18}$ , formation of which was responsible for complete  $\{^{18}\text{F}\}$ -fluorine exchange between  $\text{BF}_2 \text{F}^{18}$  and  $\text{SF}_4$  [ 70 ].  $\{^{18}\text{F}\}$ -Fluorine labelled  $\text{SF}_4$  was liberated from the adduct at 195 K by adding a measured quantity of dried diethyl ether as described in section 2.2.10 .

Several methods were attempted in order to prepare  $\{^{18}\text{F}\}$ -fluorine labelled  $\text{SOF}_2$  with a suitable working specific count rate. The first was that of Azeem and Gillespie [201] Thionyl fluoride was condensed onto  $\text{Cs}^{18}\text{F}$  in a stainless steel pressure vessel at 77 K which was kept at 223 K for 1 hour. Under those conditions material of very low specific count rate was obtained. In an effort to improve this, the  $\text{Cs}^{18}\text{F}$  was pretreated with  $(\text{CF}_3)_2\text{CO}$  by condensing  $(\text{CF}_3)_2\text{CO}$  (15 mmol, 1110 Torr) into the pressure vessel containing  $\text{Cs}^{18}\text{F}$ . The vessel was kept at room temperature for 30 min and then heated at 393 K for another 30 min.

This procedure also resulted in a negligible activity of  $\text{SOF}^{18}\text{F}$ . Attempts to label  $\text{SOF}_2$  by high temperature exchange with  $\text{Cs}^{18}\text{F}$  were also unsuccessful.

The third method tried was the reaction between  $\text{SOCl}_2$  and  $\text{Cs}^{18}\text{F}$  in the presence of MeCN at room temperature using a stainless steel pressure vessel (90 cm<sup>3</sup>). The mixture was shaken for one hour which

Figure 2.37 Calibration of  $\text{H}^{18}\text{F}$

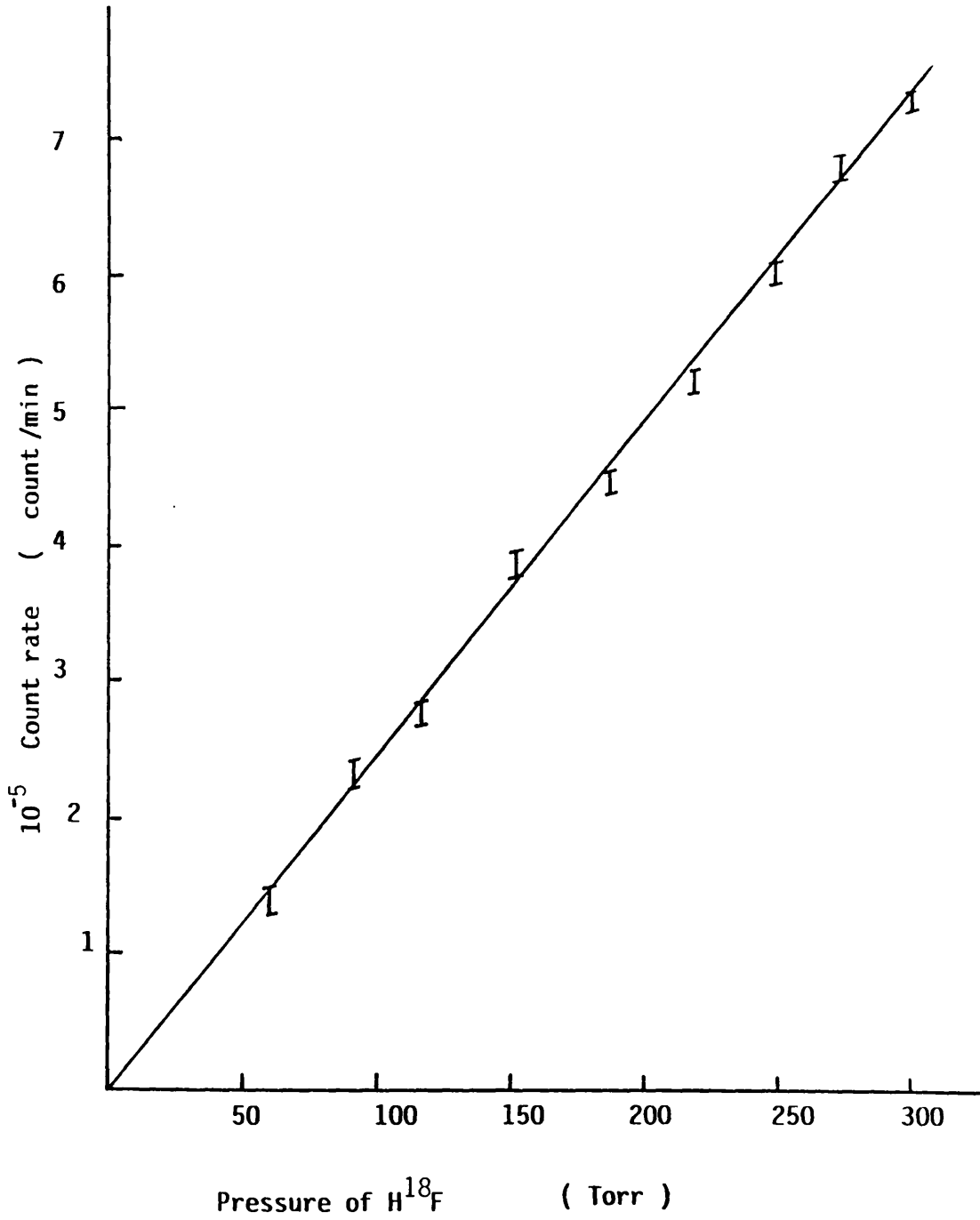
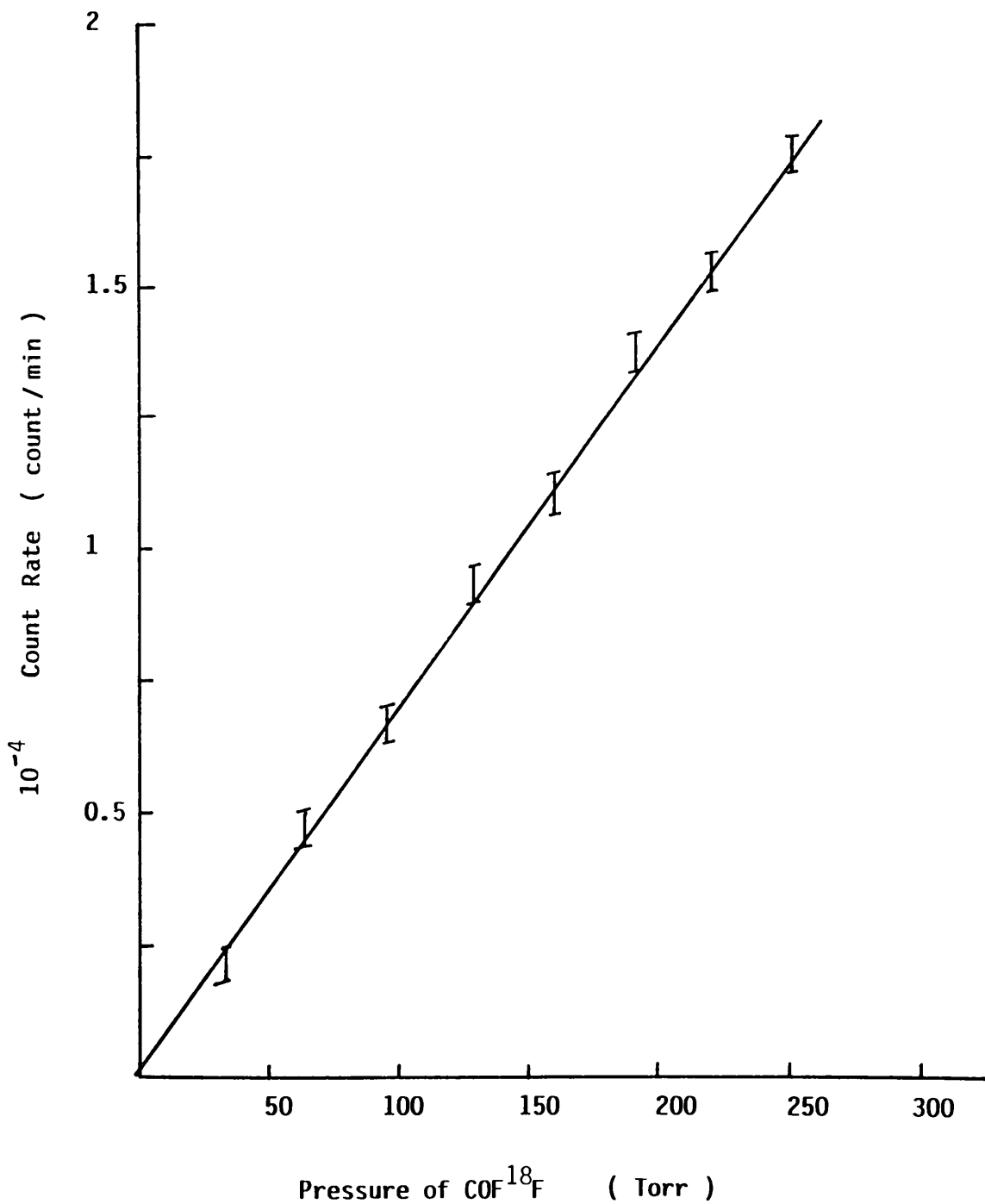


Figure 2.38 Calibration of COF<sup>18</sup>F

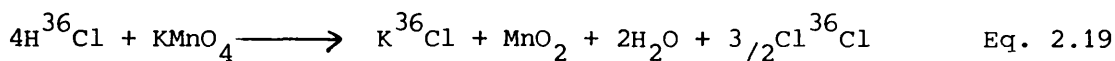


was the maximum allowance time. This preparation resulted in a reasonable activity but with very low chemical yield. The best method and that finally adopted was to prepare  $\text{SOF}^{18}\text{F}$  by the hydrolysis of  $\text{SF}_3^{18}\text{F}$  at room temperature over calcined  $\gamma$ -alumina. Conversion of  $\text{SF}_3^{18}\text{F}$  to  $\text{SOF}^{18}\text{F}$  was quantitative for optimum conditions. Figs 2.39 and 2.40 plot the count rate vs pressure.

### 2.8.3 Preparation of $\{^{36}\text{Cl}\}$ -Dichlorine

The main consideration in the preparation of  $\{^{36}\text{Cl}\}$ -chlorine labelled dichlorine was to produce anhydrous  $^{36}\text{Cl}_2$  with a high specific activity. The preparation of  $^{36}\text{Cl}_2$  was carried out by the following procedure using the apparatus shown in Fig.2.41, .

$\{^{36}\text{Cl}\}$ -Chlorine labelled dichlorine was prepared from the reaction of  $\{^{36}\text{Cl}\}$ -chlorine labelled hydrochloric acid with potassium permanganate solution, according to equation 2.19



$\{^{36}\text{Cl}\}$ -Chlorine labelled  $\text{Cl}_2$  was generated in a round bottomed flask Fig. 2.41 vessel (A) to which a series of cooled traps was attached. Traps (B) and (C) contained solid  $\text{KMnO}_4$  to remove  $\text{HCl}$ , and were cooled to 195 K in dichloromethane/solid  $\text{CO}_2$  baths. Traps (D) and (E) contained solid phosphorus pentoxide to remove moisture, and were cooled to 195 K. The collection vessel (F) was equipped with high vacuum stopcocks (J. Young) in order that it could be isolated from the rest of the apparatus. The ground-glass joints in the apparatus were sealed with Kel-F grease and the whole system, apart from the three necked flask, was evacuated before the reaction. The

Figure 2.39 Calibration of SF<sub>3</sub><sup>18</sup>F

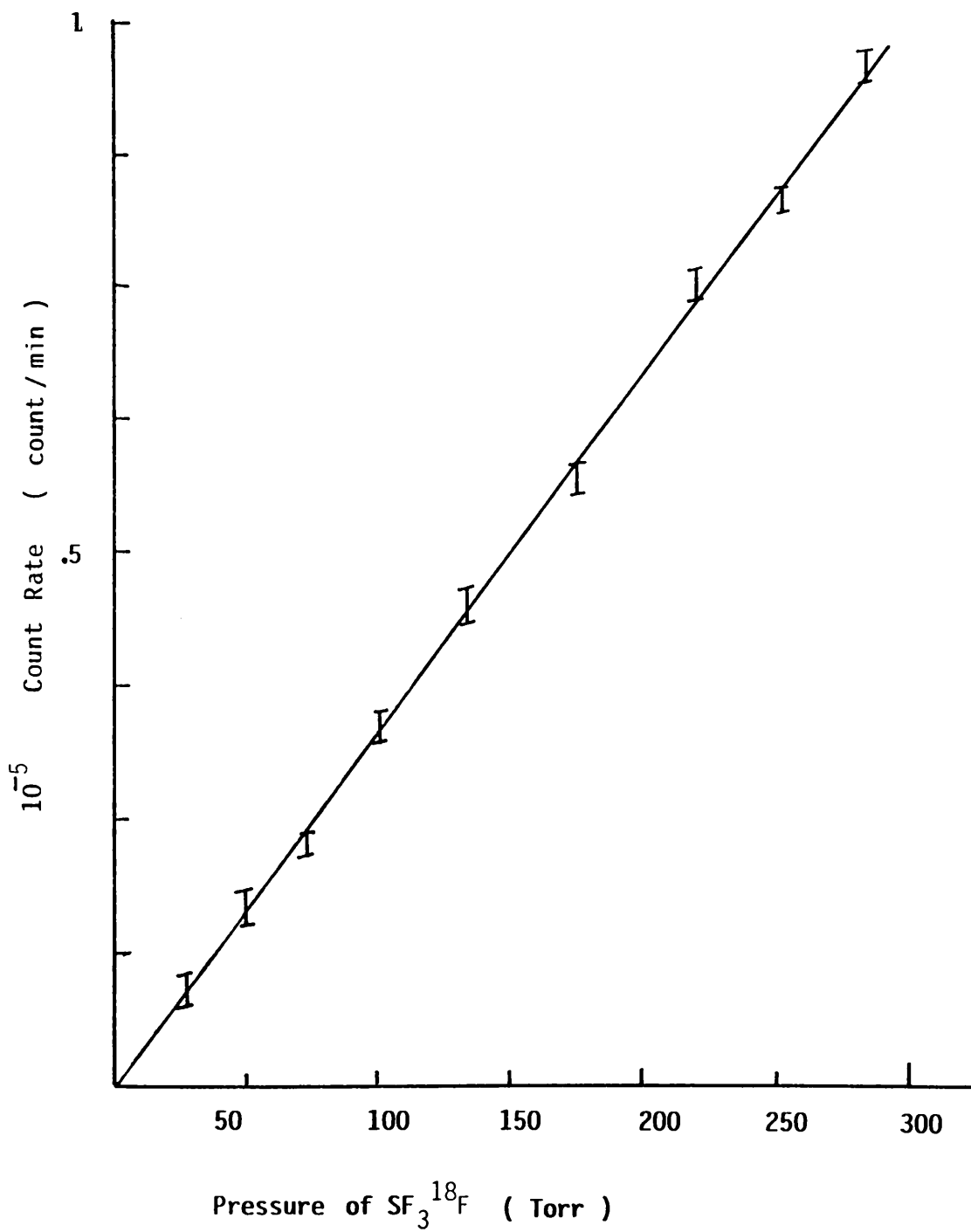
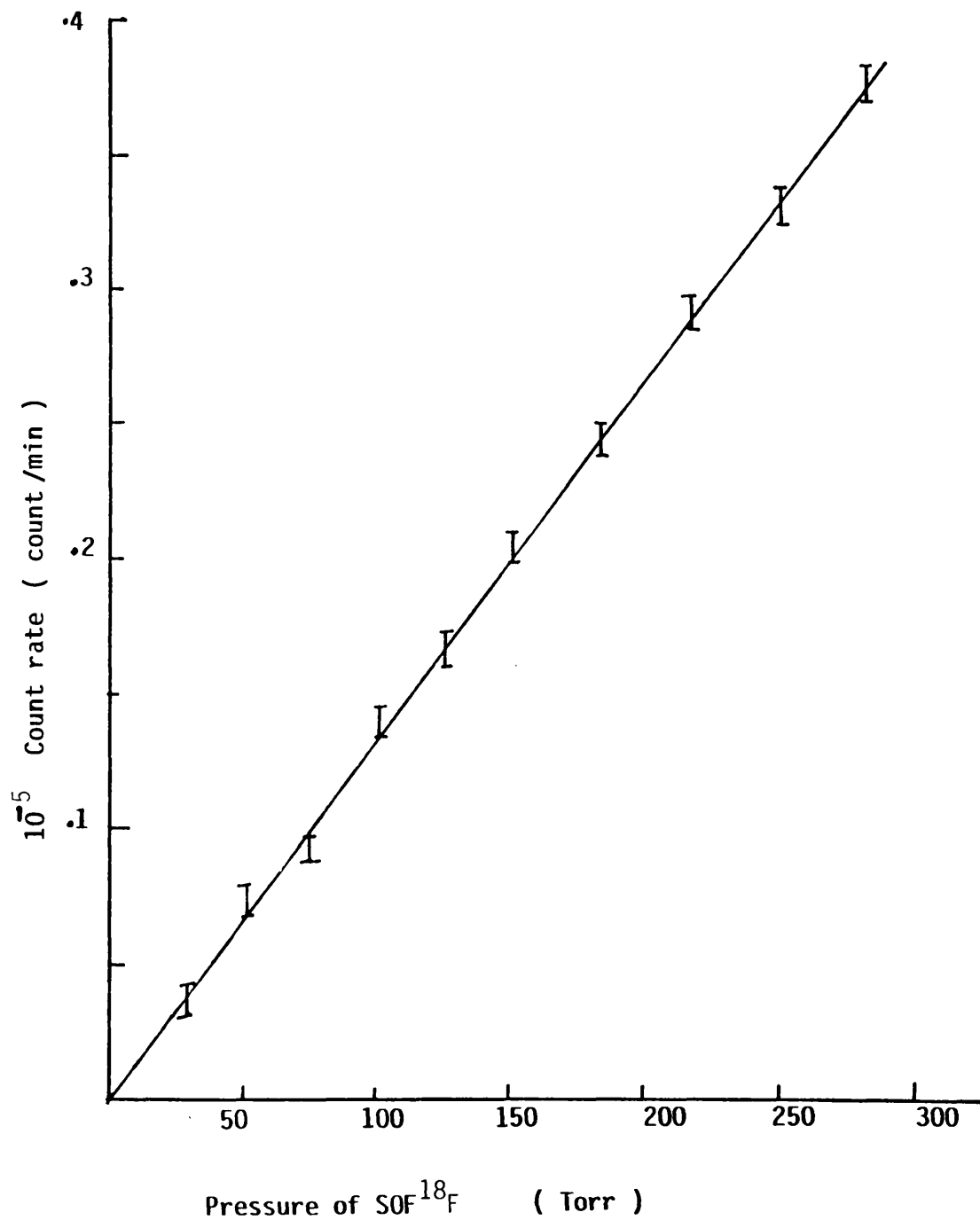


Figure 2.40 Calibration of  $\text{SO}_2^{18}\text{F}$



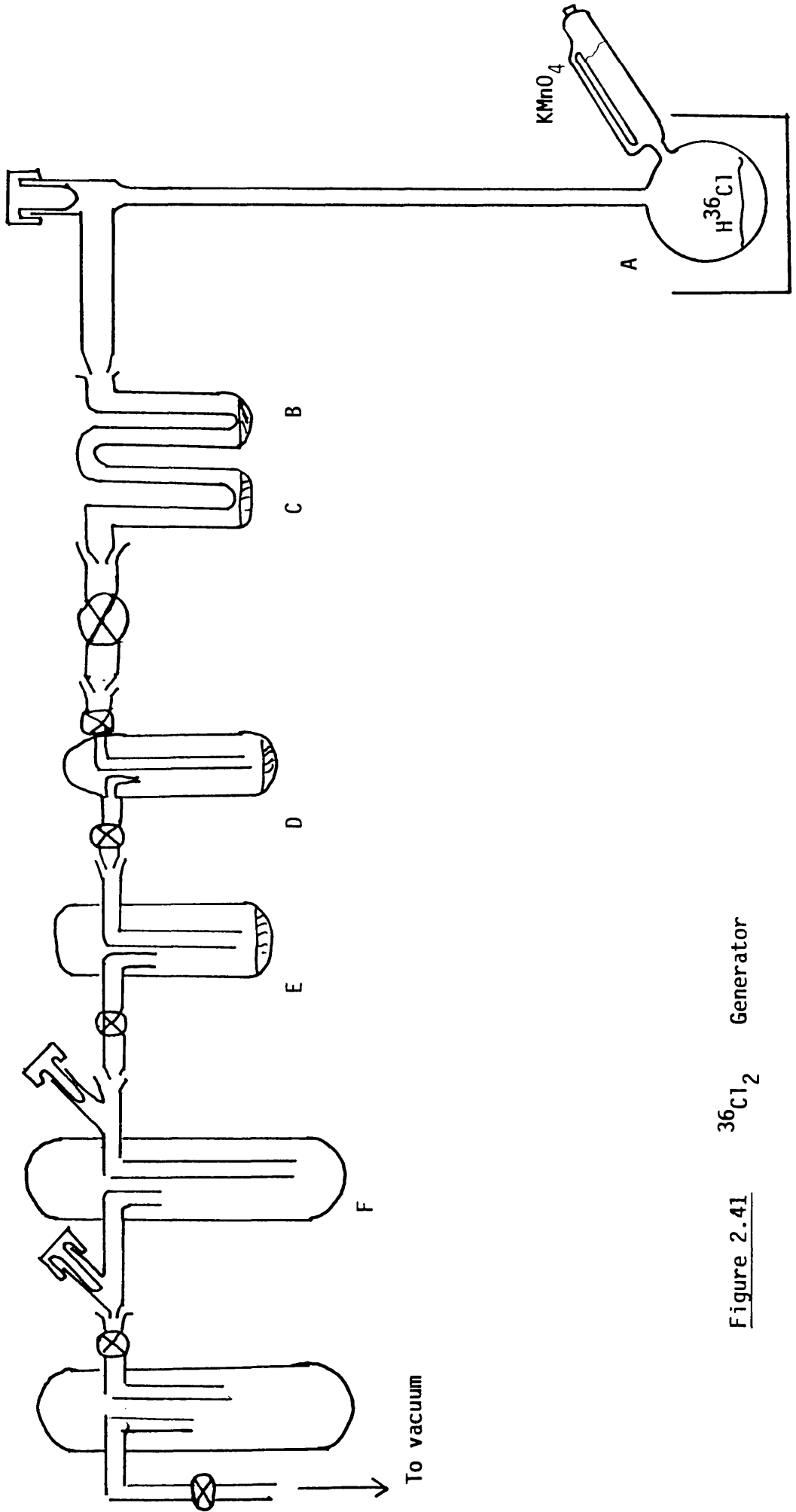


Figure 2.41  $^{36}\text{Cl}_2$  Generator



operations were carried out in dry air at reduced pressure.

Aqueous  $\{^{36}\text{Cl}\}$ -NaCl (4.8 ml, 120  $\mu\text{Ci}$ , Amersham International plc) was added to hydrochloric acid (35.4%, w/n, 30  $\text{cm}^3$  Hay's Chemicals) in (A) which was heated to 333 K in a water bath. A saturated solution of  $\text{KMnO}_4$  (32.0g  $\text{KMnO}_4/60$  ml  $\text{H}_2\text{O}$ ) was added dropwise with stirring. The  $\{^{36}\text{Cl}\}$ - $\text{Cl}_2$  liberated was distilled through traps (B) to (E) and collected in (F) at 195 K. Trap (F) was transferred to a vacuum line where the  $\{^{36}\text{Cl}\}$ - $\text{Cl}_2$  was degassed and stored over, phosphorus pentoxide in a Monel pressure vessel.

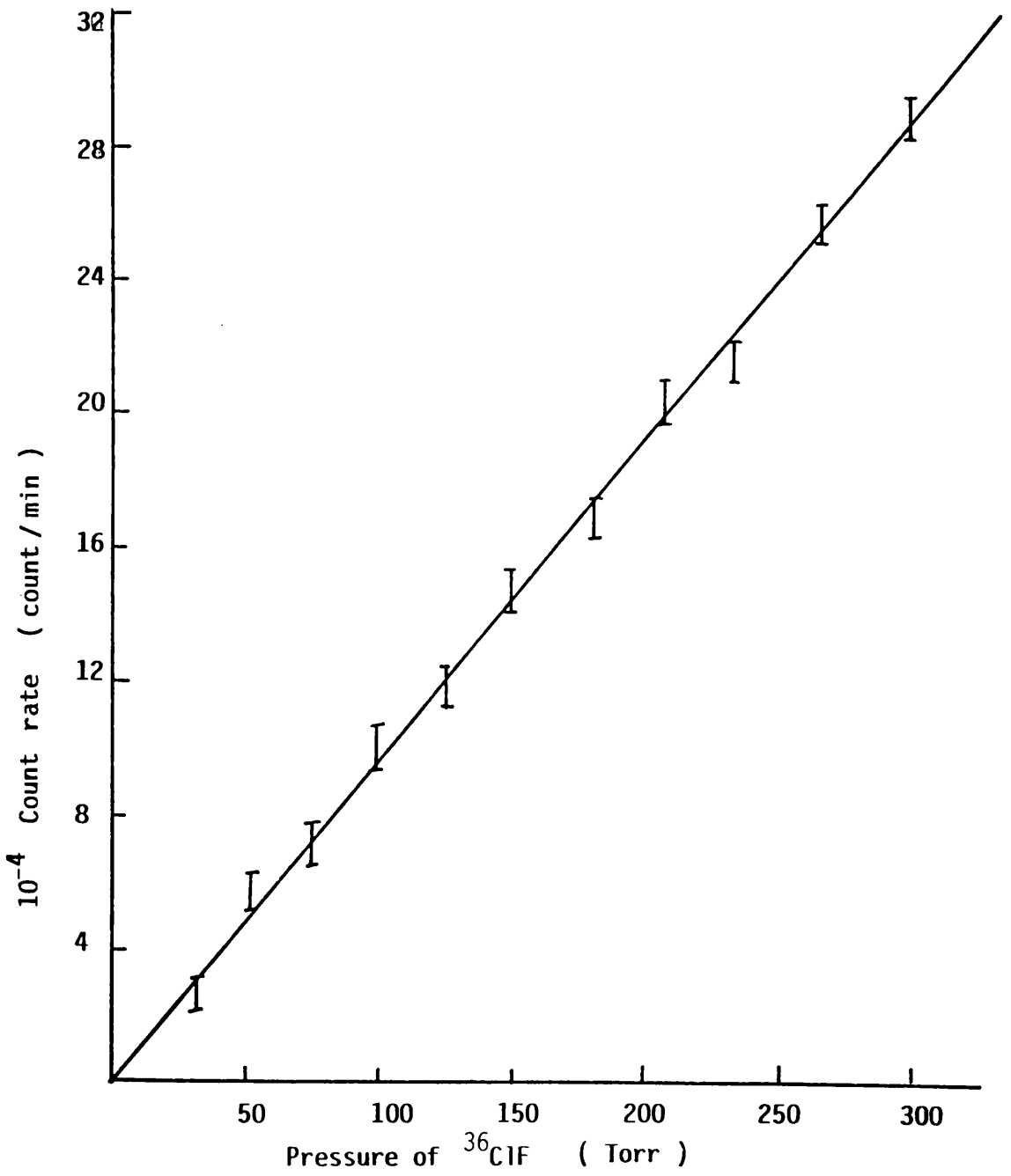
#### 2.8.4 Preparation and Purification of $^{36}\text{ClF}$ [162]

A measured amount of an equimolar mixture of  $\{^{36}\text{Cl}\}$ - $\text{Cl}_2$  and  $\text{ClF}_3$  was condensed into a Monel metal pressure vessel held at 77 K. After warming to ambient temperature, the reactor was heated slowly to the final temperature ca 425 K and left for 18 hours. The contents were separated by fractional condensation. A trap cooled to 143 K (isopentane/liq  $\text{N}_2$ ) was used to retain impurities such as  $^{36}\text{Cl}_2$ ,  $^{36}\text{ClF}_3$ ,  $^{36}\text{ClO}_2$ , while the  $\{^{36}\text{Cl}\}$ - $\text{ClF}$  was condensed in a trap held at 77 K. The purity of  $\{^{36}\text{Cl}\}$ - $\text{ClF}$  was determined by checking the vapour pressure. A linear relationship was found when the  $^{36}\text{Cl}$  count rate was plotted versus pressure Fig. 2.42 .

#### 2.8.5 Preparation and Purification of $^{35}\text{SF}_4$ , $^{35}\text{SOF}_2$ and $^{35}\text{SO}_2$

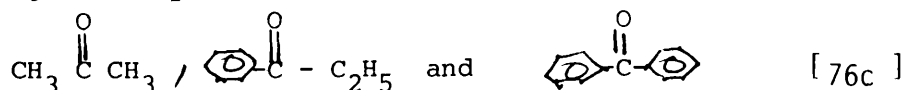
$\{^{35}\text{S}\}$ -Sulphur labelled  $\text{SF}_4$  was prepared from elemental sulphur and  $\text{IF}_5$  according to equation 2.4 . Rhombic  $\{^{35}\text{S}\}$ -sulphur (1 mCi,  $S_{\text{p.at}} < 30$  mCi ( $\text{mg atom}^{-1}$  Amersham International plc) was diluted with inactive  $\text{S}_8$  (5 mmol) by dissolution in dry carbon

Figure 2.42 Calibration of  $^{36}\text{ClF}$



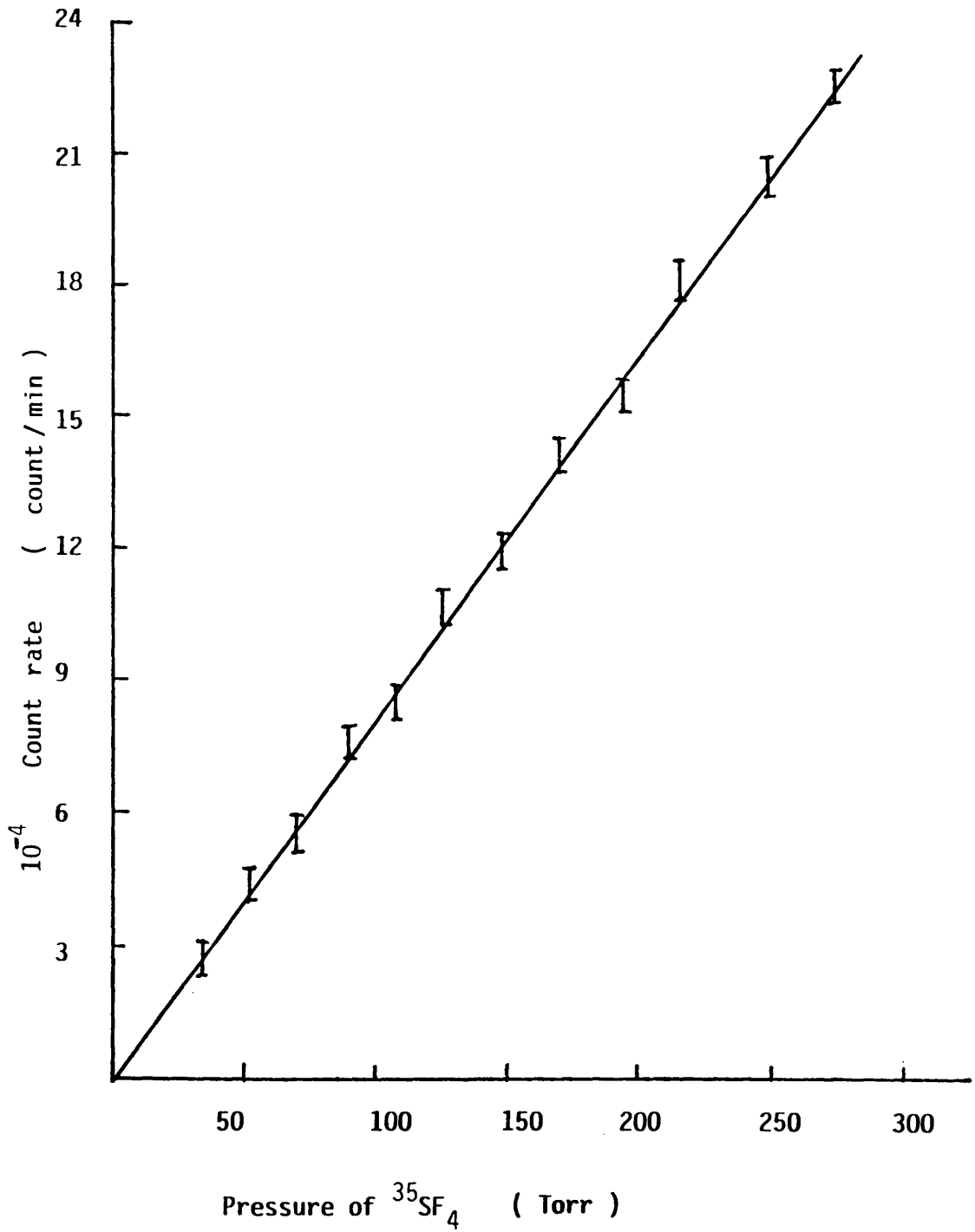
disulphide in a Monel metal pressure vessel (90 cm). The CS<sub>2</sub> was removed under vacuum and purified iodine pentafluoride (35.0 mmol) added by vacuum distillation. The mixture was allowed to react at 373 K for 12 hours followed by 473 K for 48 hours. After reaction volatile material was removed at 195 K and condensed in a similar Monel pressure vessel containing activated NaF. The yield of {<sup>35</sup>S}-SF<sub>4</sub> at this stage was 68% (23.8 mmol). The crude product was purified by reaction with BF<sub>3</sub> at 195 K forming the adduct <sup>35</sup>SF<sub>3</sub><sup>+</sup>BF<sub>4</sub><sup>-</sup>. Unreacted material was removed by pumping at this temperature. {<sup>35</sup>S}-Sulphur labelled SF<sub>4</sub> (17.85 mmol) was liberated from the adduct by adding the calculated amount of Et<sub>2</sub>O. The infra-red spectrum and the molecular weight data were obtained and found in good agreement with the literature. The specific count rate of this material was very high so that a dilution was made by adding inactive SF<sub>4</sub> (89.25 mmol) to give a working specific count rate of 525 ± 33 count s<sup>-1</sup> mmol<sup>-1</sup>. A linear count rate versus pressure relationship was obtained over the range 10 - 300 Torr, Fig. 2.43.

Several methods were tried in order to prepare <sup>35</sup>SOF<sub>2</sub> in which <sup>35</sup>SF<sub>4</sub> is a starting material for {<sup>35</sup>S}-sulphur radiotracer reactions. The first method was that of the fluorination of inorganic compounds by <sup>35</sup>SF<sub>4</sub> such as I<sub>2</sub>O<sub>5</sub>, P<sub>4</sub>O<sub>10</sub>, HgO, B<sub>2</sub>O<sub>3</sub>, SO<sub>2</sub> and MO<sub>3</sub> (M = U, W, Mo or Bi) [77b] or organic compounds such as



Although the volatile products in each case contained thionyl fluoride as a major compound, they were a mixture of SF<sub>4</sub>, SO<sub>2</sub>, SF<sub>6</sub> and SiF<sub>4</sub>. A better method was the hydrolysis of {<sup>35</sup>S}-SF<sub>4</sub> at room temperature over γ-alumina. Typically <sup>35</sup>SF<sub>4</sub> (23 mmol) was condensed over

Figure 2.43 Calibration of  $^{35}\text{SF}_4$



$\gamma$ -alumina 5 g in a stainless steel pressure vessel (90 cm<sup>3</sup>). Highly pure {<sup>35</sup>S}-SOF<sub>2</sub> (23 mmol) was collected after 25 min at room temperature. The i.r. spectrum was obtained and showed no bands attributable to SF<sub>4</sub>, SO<sub>2</sub> or SiF<sub>4</sub>. A linear relationship was obtained when the <sup>35</sup>S count rate was plotted versus pressure Fig. 2.44. The specific count rate was 525 ± 49 count s<sup>-1</sup> mmol<sup>-1</sup>.

{<sup>35</sup>S}-Sulphur labelled SO<sub>2</sub> was prepared by a similar method of that described for <sup>35</sup>SOF<sub>2</sub>. A sample of SF<sub>4</sub> (23 mmol) was condensed at 77 K in a Monel metal pressure vessel (90 cm<sup>3</sup>) containing  $\gamma$ -alumina (5g). The reactants were heated at 423 K for 25 min. Volatile material was removed and condensed onto a similar pressure vessel containing Hg metal. The contents were shaken at room temperature for 48 hours, to remove any <sup>35</sup>SOF<sub>2</sub> that might be present in the product. {<sup>35</sup>S}-Sulphur labelled SO<sub>2</sub> (17 mmol) was removed by distillation. Its i.r. spectrum gave no evidence for bands due to SF<sub>4</sub>, SOF<sub>2</sub> or SiF<sub>4</sub>. The <sup>35</sup>S count rate varied linearly with pressure, Fig. 2.45. The specific count rate of <sup>35</sup>SO<sub>2</sub> was 525 ± 19 count s<sup>-1</sup> mmol<sup>-1</sup>.

#### 2.8.6 Preparation and Purification of <sup>35</sup>SF<sub>5</sub>Cl and SF<sub>5</sub><sup>36</sup>Cl

Sulphur chloride pentafluoride labelled with {<sup>36</sup>Cl}-chlorine or {<sup>35</sup>S}-sulphur was prepared from SF<sub>4</sub> and ClF over CsF at room temperature [ 82]. A mixture of SF<sub>4</sub> (20.0 mmol) and ClF (20.0 mmol) was condensed onto a Monel metal pressure vessel containing CsF (5.0 g) at 77 K. The mixture was allowed to react at room temperature for 5h. Sulphur chloride pentafluoride was condensed at 195 K and volatile at

Figure 2.44 Calibration of  $^{35}\text{SOF}_2$

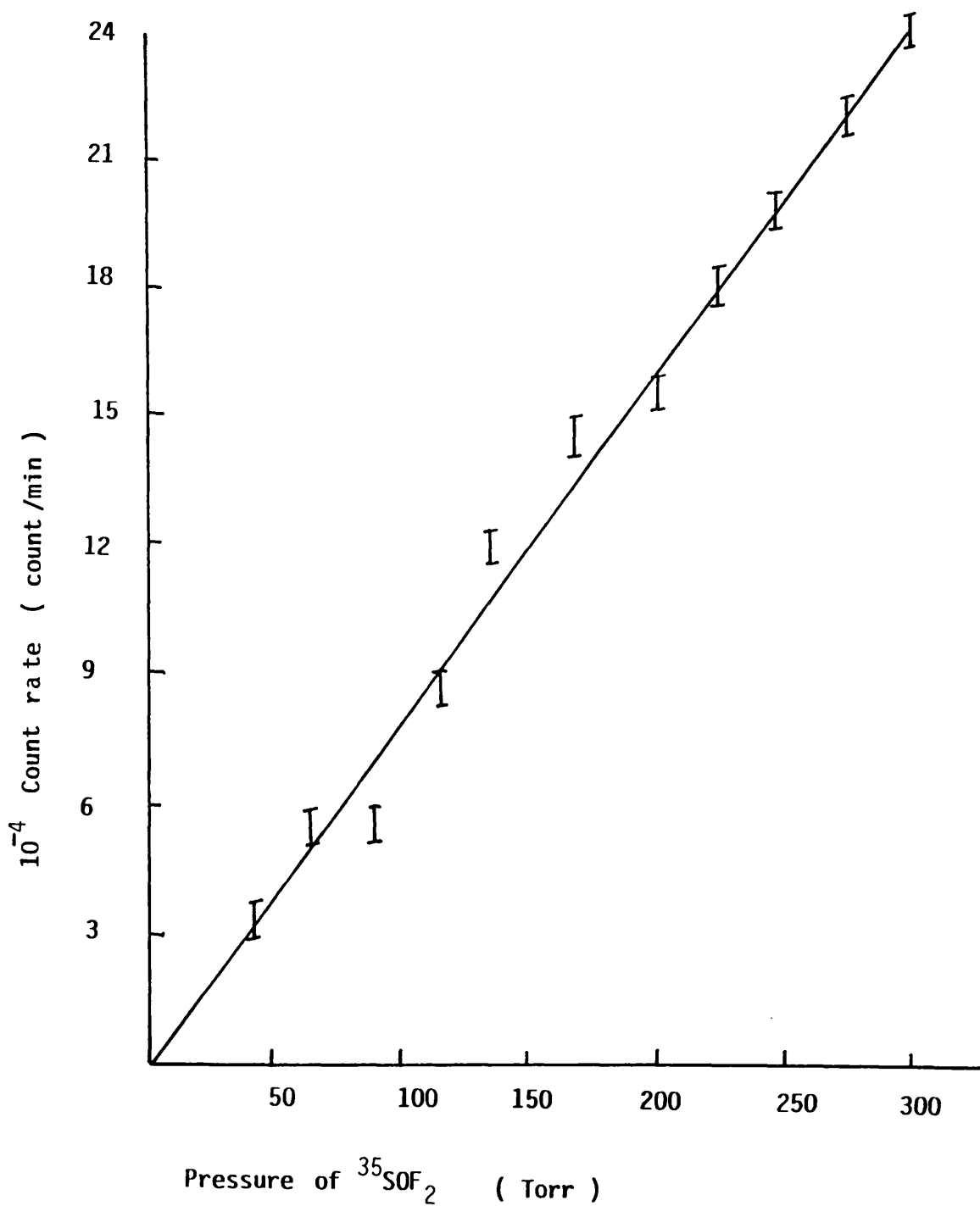
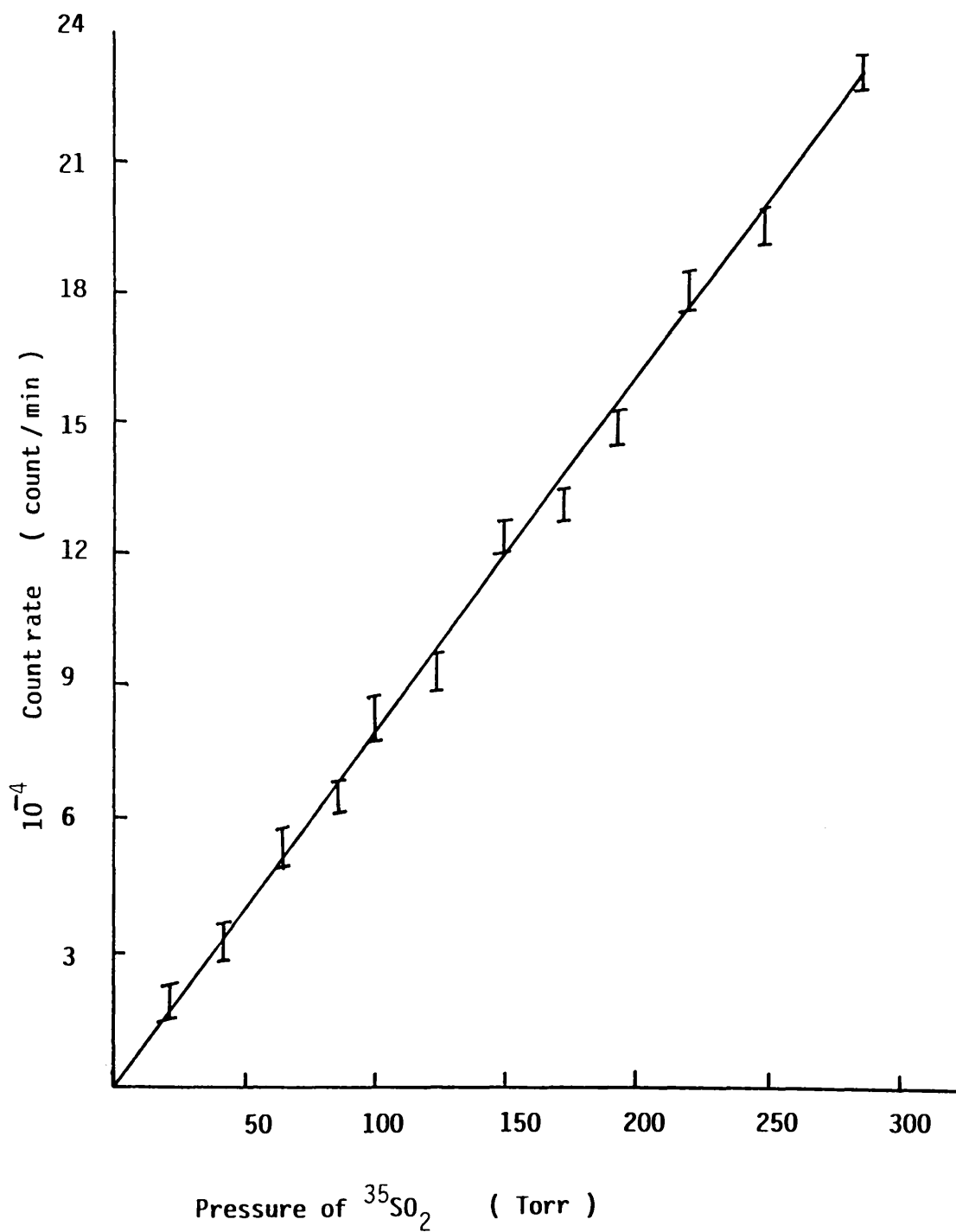


Figure 2.45 Calibration of  $^{35}\text{SO}_2$



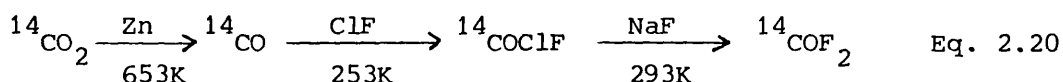
this temperature was removed. Linear relationships were found between the  $^{35}\text{S}$ - and  $^{36}\text{Cl}$ - count rates versus pressure, Figs 2.46 and 2.47.

### 2.8.7 Preparation and Purification of $^{14}\text{CO}_2$

$\{^{14}\text{C}\}$ -Carbon labelled  $\text{CO}_2$  (1 mCi, 2 mmol) was prepared by the addition of hydrochloric acid (35.4 w/w %) to a sample of  $\{^{14}\text{C}\}$ -carbon labelled barium carbonate ( $\text{Ba}^{14}\text{CO}_3$ ) ( $29.0 \mu\text{Ci mg}^{-1}$ ). It was dried by low temperature distillation over  $\text{P}_2\text{O}_5$  and was then diluted by dry  $\text{CO}_2$  to give a working count rate of  $330 \pm 18 \text{ count s}^{-1} \text{ mmol}^{-1}$ . A linear relationship between the count rate and pressure was obtained Fig. 2.48.

### 2.8.8 Preparation of $^{14}\text{COF}_2$ [202]

$\{^{14}\text{C}\}$ -Carbon labelled carbonyl fluoride was prepared according to equation 2.20



$\{^{14}\text{C}\}$ -Carbon monoxide was prepared by reduction of  $\{^{14}\text{C}\}$ - $\text{CO}_2$  ( $1 \text{ mCi mmol}^{-1}$ ) with metallic zinc [203]. The apparatus, which was used for the reduction process, is shown in Fig. 2.49. It contained small pellets, each of about 5 mm diameter, which were made from a moistened mixture composed of 95% (w/w) zinc mixed with aerosil silica, the silica being used to increase the porosity and to prevent clogging. The zinc pellets were dried at 393 K in an air oven for about 24 hours before being introduced into the reactor. With the



Figure 2.46 Calibration of  $^{35}\text{SF}_5\text{Cl}$

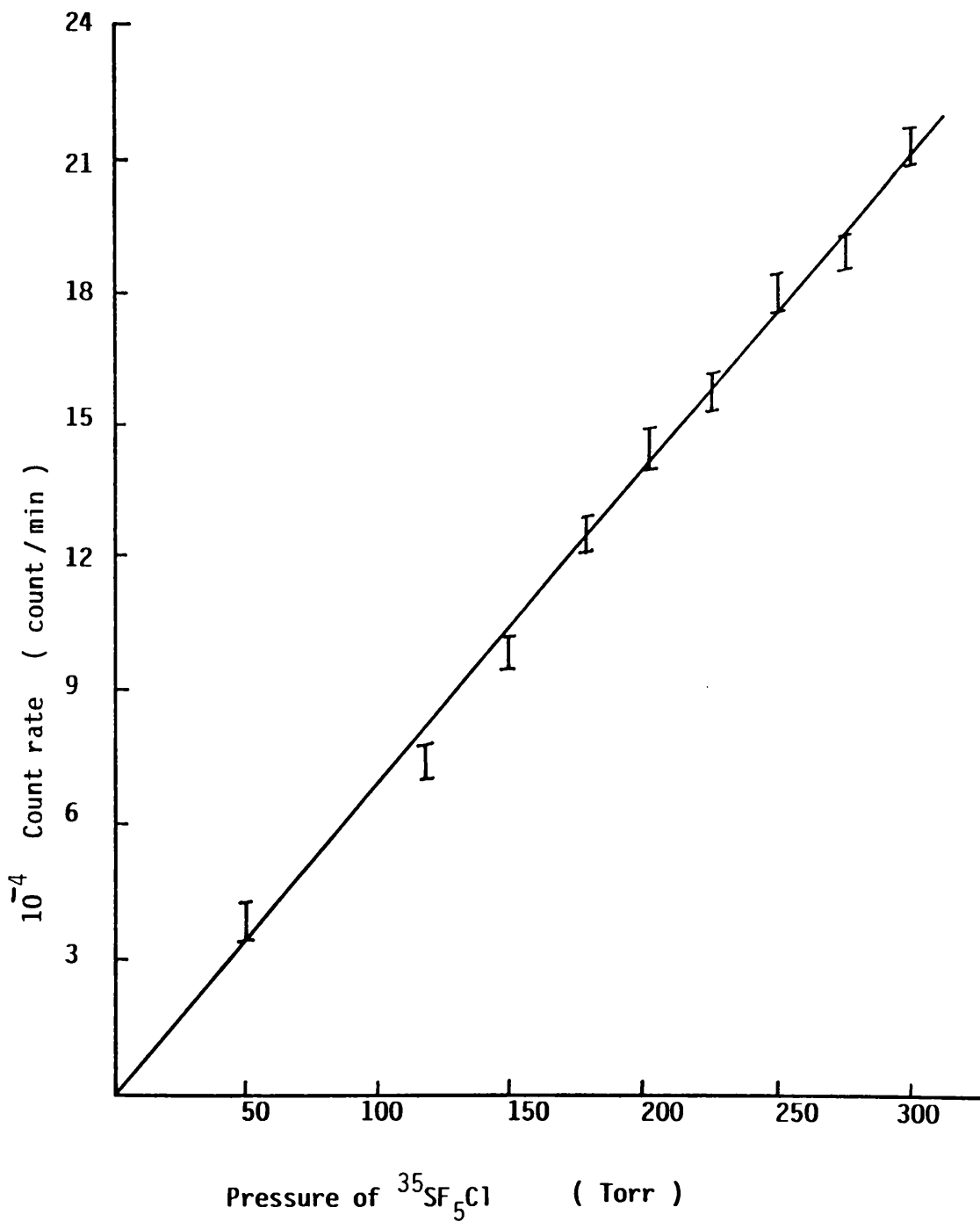


Figure 2.47 Calibration of SF<sub>5</sub><sup>36</sup>Cl

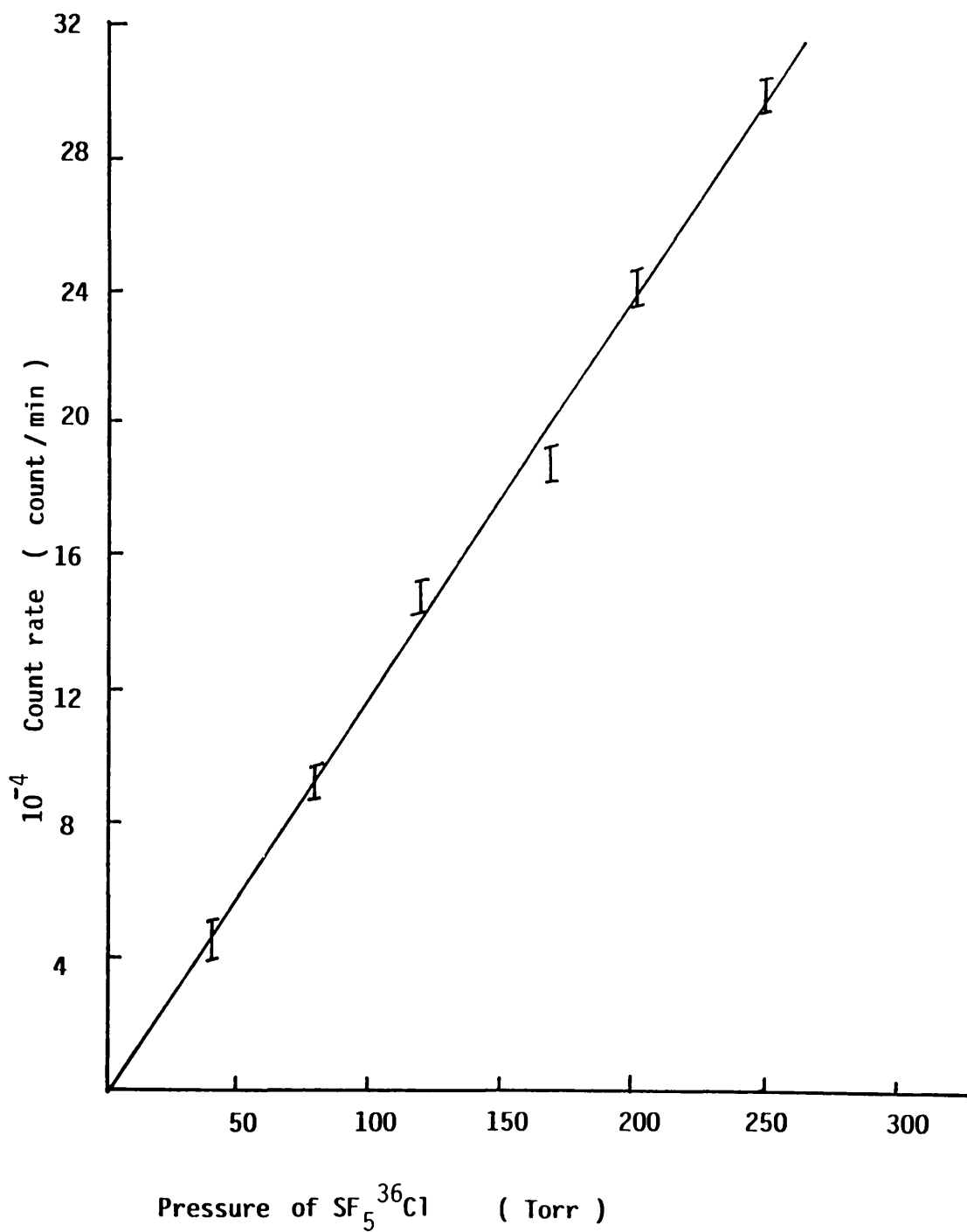
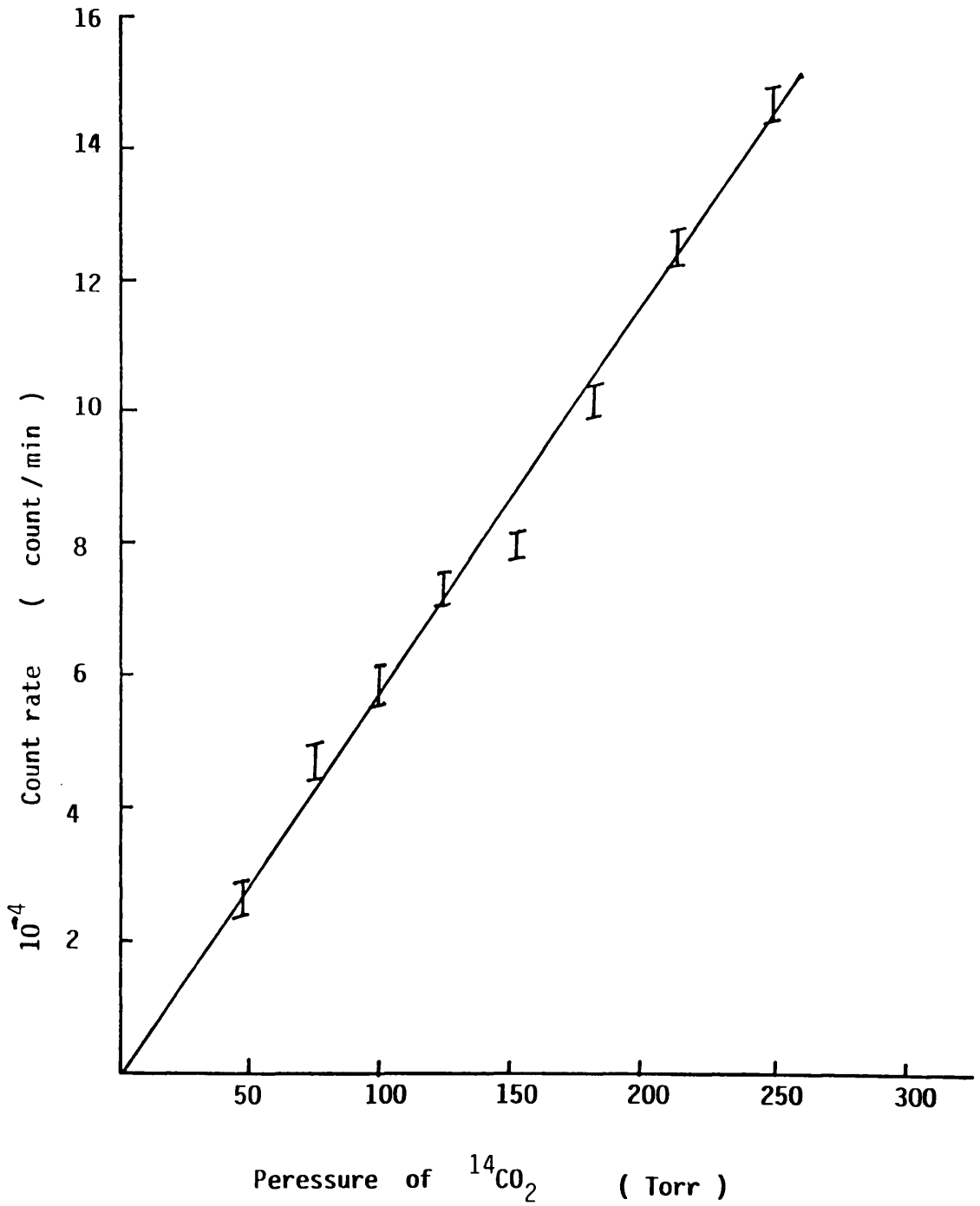


Figure 2.48 Calibration of  $^{14}\text{CO}_2$



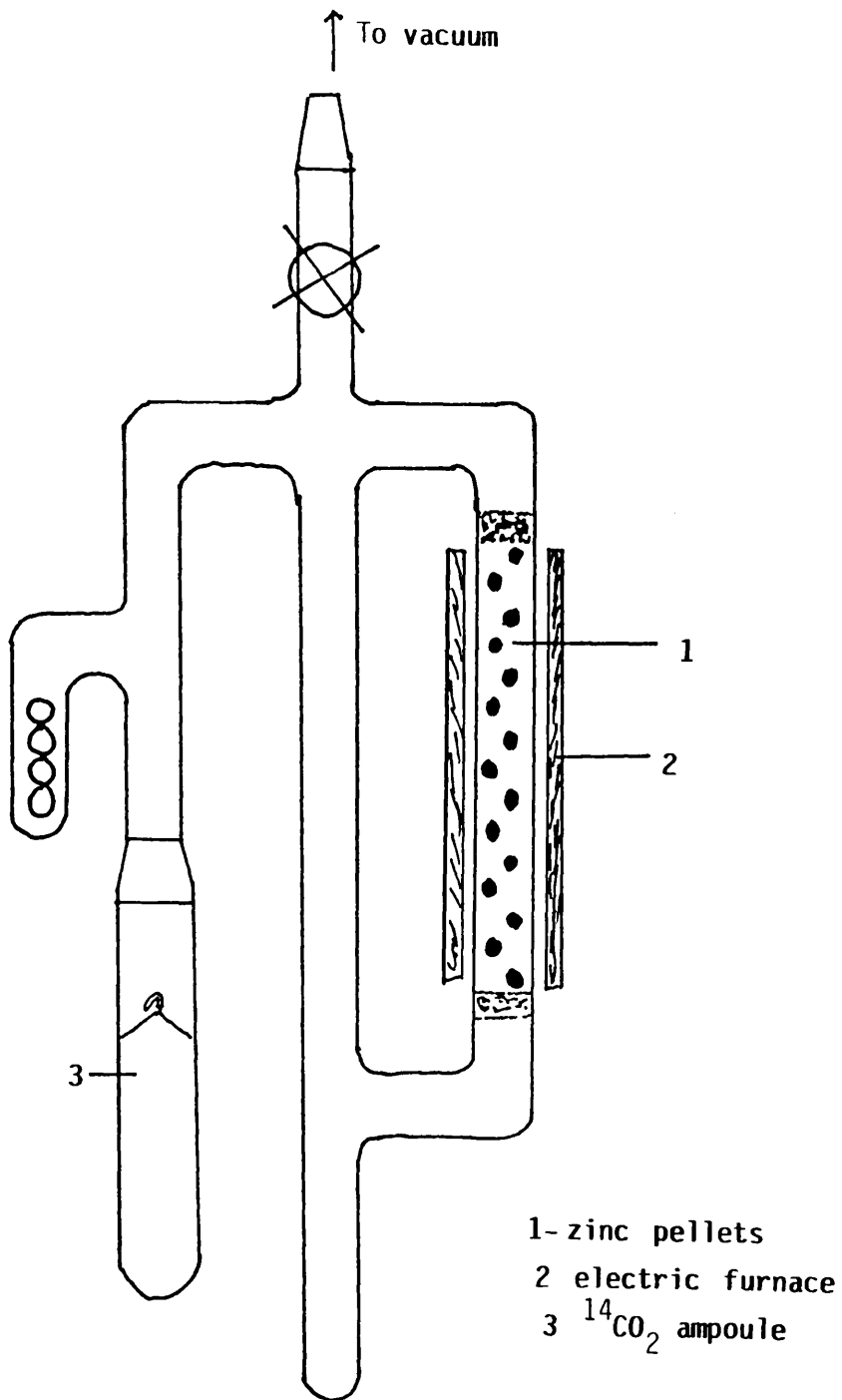


Figure 2.49  $^{14}\text{CO}$  Generator

$\{^{14}\text{C}\}$ -carbon dioxide sample attached to the B14 joint, the converter was degassed for 24 hours at 593 K, by surrounding the part of the converter containing the zinc pellets with an electric furnace. The  $\{^{14}\text{C}\}$ - $\text{CO}_2$  was introduced into the converter by rupturing the break seal of the ampoule using stainless steel balls and an external magnet. The conversion of  $\{^{14}\text{C}\}$ - $\text{CO}_2$  with zinc pellets at ca 653 K was completed in about 72 hours. The  $\{^{14}\text{C}\}$ -CO was allowed to expand into 250 ml storage bulb and diluted four times (1:4) with inactive carbon monoxide (Air Products Ltd) in a Monel metal line Fig.2.50 The  $^{14}\text{CO}$  was mixed with a stream of ClF at 255 K in a Monel metal reactor. The rate of the mixture was slow to achieve the maximum yield. Product gases were condensed in a trap cooled to 77 K, Fig.2.50 After the reaction was finished the yellow product was repeatedly passed over Sb powder and finally distilled over Sb and left overnight. The colourless product ( $\text{COF}_2$  :  $\text{COClF}$  :  $\text{COCl}_2$  ; 5 : 90 : 5%) (20 mmol) was then condensed in a Monel metal pressure vessel containing NaF (10 g, 225 mmol) and MeCN (10 ml). The vessel was left at room temperature with occasional shaking for 36 hours.  $\{^{14}\text{C}\}$ -Carbon labelled carbonyl fluoride was removed at 195 K and purified by trap to trap distillation. The  $^{14}\text{COF}_2$  had a specific count rate of  $330 \pm 29$  count  $\text{s}^{-1}$   $\text{mmol}^{-1}$ . A linear relationship was obtained when the  $^{14}\text{C}$  count rate was plotted vs pressure, Fig. 2. 51

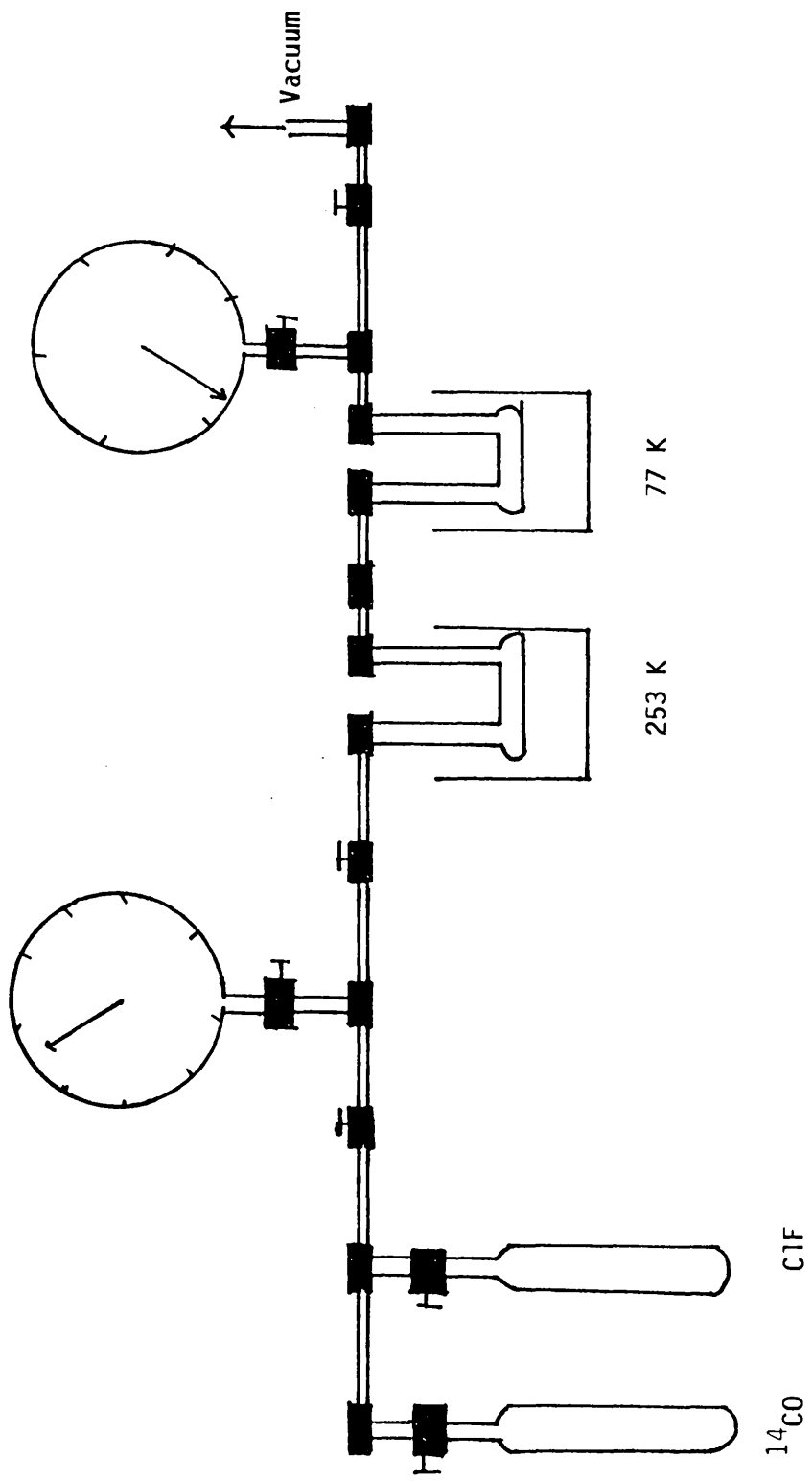
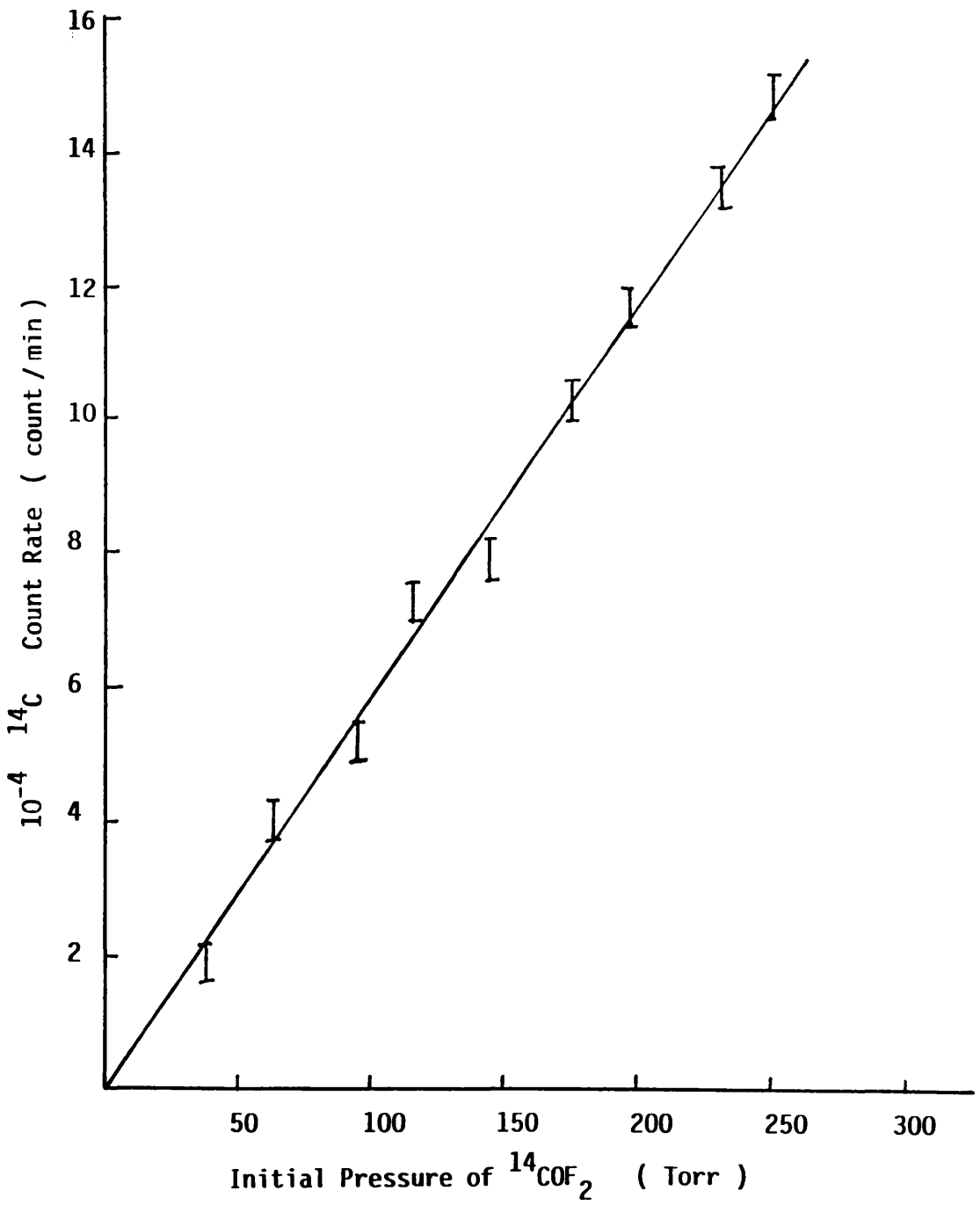


Figure 2.50 COCIF preparation apparatus

Figure 2.51 Calibration of  $^{14}\text{COF}_2$



CHAPTER THREE



## Preparation and Pretreatment of Catalysts

### 3.1 Preparation of Caesium or Potassium Fluoride Supported on $\gamma$ -Alumina,

Caesium or potassium fluoride supported on  $\gamma$ -alumina was prepared in the same way as described in the literature by the impregnation of MF (M = Cs or K) onto  $\gamma$ -alumina (Pural Sb90 or Aluminium Oxide Degussa) from aqueous solution, non-aqueous solution, or grinding the alkali metal fluoride and  $\gamma$ -alumina together under dry conditions. [148]

#### 3.1.1 Preparation of Caesium and Potassium Fluoride Supported on $\gamma$ -Alumina from Aqueous Solution.

Caesium or potassium fluoride was impregnated onto  $\gamma$ -alumina from an aqueous solution containing the appropriate amount of fluoride at room temperature. The impregnated material was then dried and calcined above room temperature .

Typically potassium fluoride (2.552g, 44 mmol, BDH Optran grade) was dissolved in water (ca 130 ml) in a Buchi flask.  $\gamma$ -Alumina (10g) was then added and the solution was stirred for 1h. The bulk of the water was removed by rotary evaporation at ca 333 K. The sample was calcined under vacuum at 523 K for 5h. Table 3.1 lists the conditions and amounts of reactants. After drying, all materials were kept under dry nitrogen in an inert atmosphere box.

Table 3.1 : The Preparation Conditions for MF/ $\gamma$ -Alumina Materials.

Composition of Material			
KF (g)	W/W %	mmol MF(g $\gamma$ -alumina) <sup>-1</sup>	CsF (g)
0.348	1.14	0.6	0.918
0.580	2.10	1.1	1.683
1.160	3.80	2.0	3.060
2.552	8.37	4.4	6.732
2.900	9.51	5.0	7.650
3.140	10.46	5.5	8.415
3.480	11.41	6.0	9.181
3.770	12.36	6.5	9.945
4.350	14.26	7.5	11.475
5.104	16.74	8.8	13.464
6.220	19.02	10.0	15.295
8.200	28.53	15.0	22.951
11.600	38.00	20.0	30.600

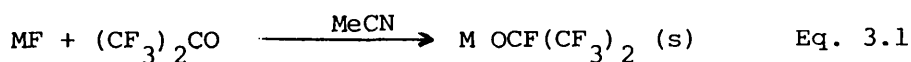
using 10g  $\gamma$ -alumina

130cm<sup>3</sup> water

### 3.1.2 Preparation of Caesium and Potassium Fluoride Supported on $\gamma$ -Alumina from Non-aqueous Solution.

This method of preparation has not been reported previously in the literature. It involves the preparation of the materials from non-aqueous solution to minimise hydroxyl groups on the surface of the MF/ $\gamma$ -alumina. However, due to the low solubility of alkali metal fluorides in most of non-aqueous solvents, the direct preparation of this material was not possible. A better method was preparation via the decomposition of the appropriate alkali metal heptafluoroisopropoxide.

The alkali metal heptafluoroisopropoxide ( $M^+(CF_3)_2COF^-$ ) was prepared according to the reaction scheme shown below using a variation of the method described by Redwood and Willis[204] equation 3.1.



Caesium fluoride (4.0g, 26 mmol, BDH Optran grade) was ground in an agate mortar and pestle in the inert atmosphere box and placed in a stainless steel pressure vessel (Hoke Inc.) together with four stainless steel ball bearings. The vessel was sealed and evacuated and hexafluoroacetone (30 mmol) together with acetonitrile (5 ml) added by vacuum distillation. The vessel was allowed to warm to room temperature and shaken for 12h, then the acetonitrile and unreacted hexafluoroacetone were removed by vacuum distillation. The infra-red spectrum of the product at this stage consisted of ten bands Table 3.2; the infra-red spectrum of  $(CF_3)_2CO$  is listed in Table 3.3 for comparison.

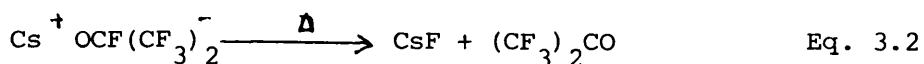
Table 3.2 : The infra-red spectrum of  $\text{CsOCF}(\text{CF}_3)_2$

$\nu$ max	Literature [47]	Assignment [47 ]
1459 (m)	1450 (m)	$\nu$ CO
1343 (w)	1350 (w)	$\nu$ CF
1256 (s)	1250 (s)	$\nu$ CF
1211 (s)	1210 (s)	$\nu$ CF
1136 (s)	1150 (s)	$\nu$ CF
1103 (s)	1100 (s)	$\nu$ CF
969 (w)	960 (s)	$\nu$ CC
763 (w)	780 (w)	$\nu$ CF
731 (w)	730 (w)	SCF
636 (w)	630 (w)	SF

Table 3.3 : The vibrational spectrum of  $(\text{CF}_3)_2\text{CO}$

$\nu$ max	Literature[205]	Assignment[205]
1813 (m)	1805	$\nu$ (CO) $A_1$
1351 (sh)	1340	$\nu$ (CF) $B_1$
1269 (w)	1265	$\nu$ (CF) $B_1$
1253 (s)	1250	$\nu$ (CF) $A_1$
963 (s)	970	$\nu$ (CC) $B_1$
783 (s)	780	$\nu$ (CC) $A_1$
721 (sh)	720	$\delta$ (CF) $B_1$
633 (w)	640	$\delta$ (CF) $A_1$

Alkali metal fluorides supported on  $\gamma$ -aluminas were then prepared by dissolving a weighed quantity of a heptafluoroisopropoxide in dried acetonitrile in an inert atmosphere box. Previously calcined  $\gamma$ -alumina was then added. The contents were shaken vigorously in a Monel metal pressure vessel for 2h, then acetonitrile was removed under vacuum at room temperature. The infra-red spectrum of this material contained the same bands as those listed in Table 3.2. The vessel was heated under vacuum at 398 K for 16h to decompose the adduct formed. The amount of hexafluoroacetone collected was equivalent to a 1:1 mole ratio  $\text{CsF}:(\text{CF}_3)_2\text{CO}$  according to equation 3.2



The  $\gamma$ -alumina supported alkali metal fluorides were calcined at 523 K under vacuum for 5h and were then transferred to an inert atmosphere box until required. The infra-red spectrum contained no bands due to heptafluoroisopropoxide. The quantities used in various preparation are given in Table 3.4.

### 3.1.3 Dry Preparation of Caesium and Potassium Fluoride Supported On $\gamma$ -Alumina.

This method of preparation was carried out in order to establish the role of the solvent (water or acetonitrile) in the impregnation process. The preparations involved grinding calculated weights of dried MF (M = Cs or K) and  $\gamma$ -alumina under a dry nitrogen atmosphere in an inert atmosphere box. The material was calcined at 523 K in

Table 3.4 : Preparation Conditions for MF/ $\gamma$ -Alumina from Non-Aqueous Solution.

KOCF(CF <sub>3</sub> ) <sub>2</sub> (g)	Composition		CsOCF(CF <sub>3</sub> ) <sub>2</sub> (g)
	W/W % MF/ $\gamma$ -alumina	mmol g <sup>-1</sup> MF/ $\gamma$ -alumina	
0.648	1.14	0.6	0.93
4.752	8.37	4.4	6.82
5.94	10.46	5.5	8.525
9.504	16.74	8.8	13.64
10.86	19.02	10.0	15.50

Using 5.0 g calcined  $\gamma$ -alumina at 523 K, and 20 cm<sup>3</sup> dried acetonitrile.

Table 3.5 : Dry Preparation Conditions for MF/ $\gamma$ -Alumina.

KF (g)	Composition		CsF (g)
	W/W %	mmol g <sup>-1</sup>	
1.276	8.37	4.4	3.366
2.552	16.74	8.8	6.732

Using 5.0g  $\gamma$ -alumina calcined at 523K.

a Monel metal pressure vessel for 5h under vacuum, then kept under dry nitrogen in an inert atmosphere box. Table 3.5 lists the quantities of reactants used.

### 3.2 Treatment of Caesium and Potassium Fluorides Supported on $\gamma$ -Alumina

The aluminas used in this work were high surface area (ca 130  $\text{m}^2\text{g}^{-1}$ ) materials which have a maximum surface hydroxy coverage in the range 3.6 - 14.5 hydroxyl groups  $\text{nm}^{-2}$ . These values represent the estimated total assuming the surface to comprise [100], [111] and [110] planes of the defect spinel formula structure (145). Several studies of surface hydration have shown the average OH densities to be within the range 8-9 surface hydroxy groups  $\text{nm}^{-2}$  (144)

Most of the materials used are very hygroscopic, so that, their use is limited by the presence of OH groups which would initiate hydrolysis. Samples of CsF or KF supported on  $\gamma$ -alumina were therefore treated to remove the hydroxyl groups from the surface by a fluorination process. The vapour phase fluorination method is the best method of removing surface hydroxyl groups.

#### 3.2.1 Fluorination of Caesium and Potassium Fluoride Supported on $\gamma$ -Alumina with Sulphur Tetrafluoride, Thionyl Fluoride and Carbonyl Fluoride.

Sulphur tetrafluoride, thionyl fluoride and carbonyl fluoride are well known fluorinating reagents in inorganic chemistry. Their general reaction involves the replacement of oxygen or hydroxyl groups by fluorine. Thionyl fluoride has the advantage over  $\text{SF}_4$

of ease of preparation and handling, but usually longer reaction times are necessary. Reactions using carbonyl fluoride as a fluorinating reagent usually require high temperatures due to the strength of the C-F bond. In order to prevent any structural changes to the bulk of  $\gamma$ -alumina, the use of high temperatures was not advisable. Fluorination of  $\gamma$ -alumina supported caesium or potassium fluoride was, therefore, carried out at room temperature.

A sample of CsF/ $\gamma$ -alumina (5.0g) was placed in a Monel metal pressure vessel (139 cm<sup>3</sup>) in an inert atmosphere box. The vessel was transferred to the vacuum line and evacuated for 1h. A measured pressure of the required fluorinating material ( $\text{SF}_4$ ,  $\text{SOF}_2$  or  $\text{COF}_2$ ) was condensed into the bomb at 77 K, and the mixture was allowed to warm, very slowly in the case of  $\text{SF}_4$  or  $\text{SOF}_2$ , to room temperature by surrounding the vessel by a cold Dewar flask to minimise the temperature increases due to exothermic reactions. The vessel was left at room temperature for 6h. In each case volatile products were removed and analysed spectroscopically. This sequence was repeated until no hydrolysis of  $\text{SF}_4$ ,  $\text{SOF}_2$  and  $\text{COF}_2$ , to yield  $\text{SOF}_2$  and  $\text{SO}_2$ ,  $\text{SO}_2$  or  $\text{CO}_2$  respectively, was observed. The total amount of each fluorinating reagent was calculated by means of i.r. spectroscopic analyses of the volatile material after reaction with the MF/ $\gamma$ -alumina. Tables (3.6 - 3.8), (3.9 - 3.11) and 3.12 list the amounts of  $\text{SF}_4$ ,  $\text{SOF}_2$  and  $\text{COF}_2$  used for the respective fluorination processes. Plots of amounts of material used for the fluorination of various compositions of MF/ $\gamma$ -alumina are shown in Figs. 3.1, 3.2 and 3.3 for  $\text{SF}_4$ ,  $\text{SOF}_2$  and  $\text{COF}_2$  respectively. In each case the infra-red spectrum of the solid product was recorded and showed bands due to pentafluorosulphate,  $\text{SF}_5^-$  and fluorosulphite,  $\text{SO}_2\text{F}^-$  anions



Table 3.6 : Sulphur Tetrafluoride used for the Fluorination of MF/ $\gamma$ -Alumina which had been Prepared from Aqueous Solution.

Material Composition MF/ $\gamma$ -alumina mmol g <sup>-1</sup>	Total quantity of SF <sub>4</sub> used to fluorinate the surface (mmol)	
	M = Cs	M = K
0.6	12.3	15.4
1.1	10.9	14.2
2.0	9.0	10.7
4.4	8.9	10.5
5.0	8.7	10.5
5.5	8.7	10.4
6.0	8.3	9.9
6.5	7.7	9.4
7.5	6.7	8.7
8.8	5.7	7.6
10.0	4.8	6.7
15.0	1.4	2.9

Table 3.7 : Sulphur Tetrafluoride used for the Fluorination of MF/ $\gamma$ -alumina which had been Prepared from Non-Aqueous Solution.

Material Composition MF/ $\gamma$ -alumina mmol g <sup>-1</sup>	Total SF <sub>4</sub> used to Fluorinate the Surface (mmol)	
	M = Cs	M = K
0.6	5.8	7.4
2.0	4.1	4.9
4.4	4.1	4.8
5.5	4.0	5.0
8.8	2.8	3.7
10.0	2.2	3.2

Table 3.8 : Total Quantity of SF<sub>4</sub> used for Fluorination of the Dry Prepared MF/ $\gamma$ -Alumina

Material Composition MF/ $\gamma$ -alumina mmol g <sup>-1</sup>	Total quantities of SF <sub>4</sub> used to Fluorinate Surface (mmol)	
	M = Cs	M = K
4.4	3.4, 5.9	4.2, 6.3
8.8	2.2, 4.1	1.3, 5.8

Table 3.9 : Quantities of SOF<sub>2</sub> used for the Fluorination of MF/γ-alumina which had been Prepared from Aqueous Solution.

Material Composition MF/γ-alumina mmol g <sup>-1</sup>	Total quantity of SOF <sub>2</sub> used to Fluorinate Surface (mmol)	
	M = Cs	M = K
0.6	17.1	19.8
1.1	15.9	18.7
2.0	13.9	17.0
4.4	13.7	16.7
5.0	13.7	16.8
5.5	13.6	16.5
6.0	13.1	15.6
6.5	12.7	15.4
7.5	11.1	14.3
8.8	10.4	12.8
10.0	9.0	11.5
15.0	3.6	6.2

Table 3.10 : Quantity of SOF<sub>2</sub> used for the Fluorination of MF/γ-alumina which had been Prepared from Non-Aqueous Solution

Material Composition MF/γ-alumina mmol g <sup>-1</sup>	Total quantity of SOF <sub>2</sub> used to fluorinate Surface (mmol)	
	M = Cs	M = K
0.6	7.9	9.0
2.0	6.7	8.0
4.4	6.4	7.9
5.5	6.4	7.8
8.8	5.2	6.2
10.0	4.1	5.3

Table 3.11 : Quantity of SOF<sub>2</sub> used for the Fluorination of the Dry Prepared MF/γ-Alumina

Material Composition MF/γ-alumina mmol g <sup>-1</sup>	Total quantity of SOF <sub>2</sub> used to fluorinate Surface (mmol)	
	M = Cs	M = K
4.4	11.4, 5.1	7.7, 13.1
8.8	1.9, 4.9	2.0, 6.3

Table 3.12 : Quantity of COF<sub>2</sub> used to Fluorinate the Surface of MF/γ-alumina which had been prepared from Aqueous Solution.

Material Composition MF/γ-alumina mmol g <sup>-1</sup>	Total quantity of COF <sub>2</sub> used to fluorinate surface. (mmol)	
	M = Cs	M = K
0.6	4.2	5.5
2.0	3.7	4.9
4.4	2.9	4.3
5.5	2.6	4.0
8.8	2.0	3.2
10.0	1.7	2.9
15.0	0.8	1.9

Figure 3.1 Fluorination of MF/ $\gamma$ -alumina with SF<sub>4</sub>  
( prepared from aqueous solution )

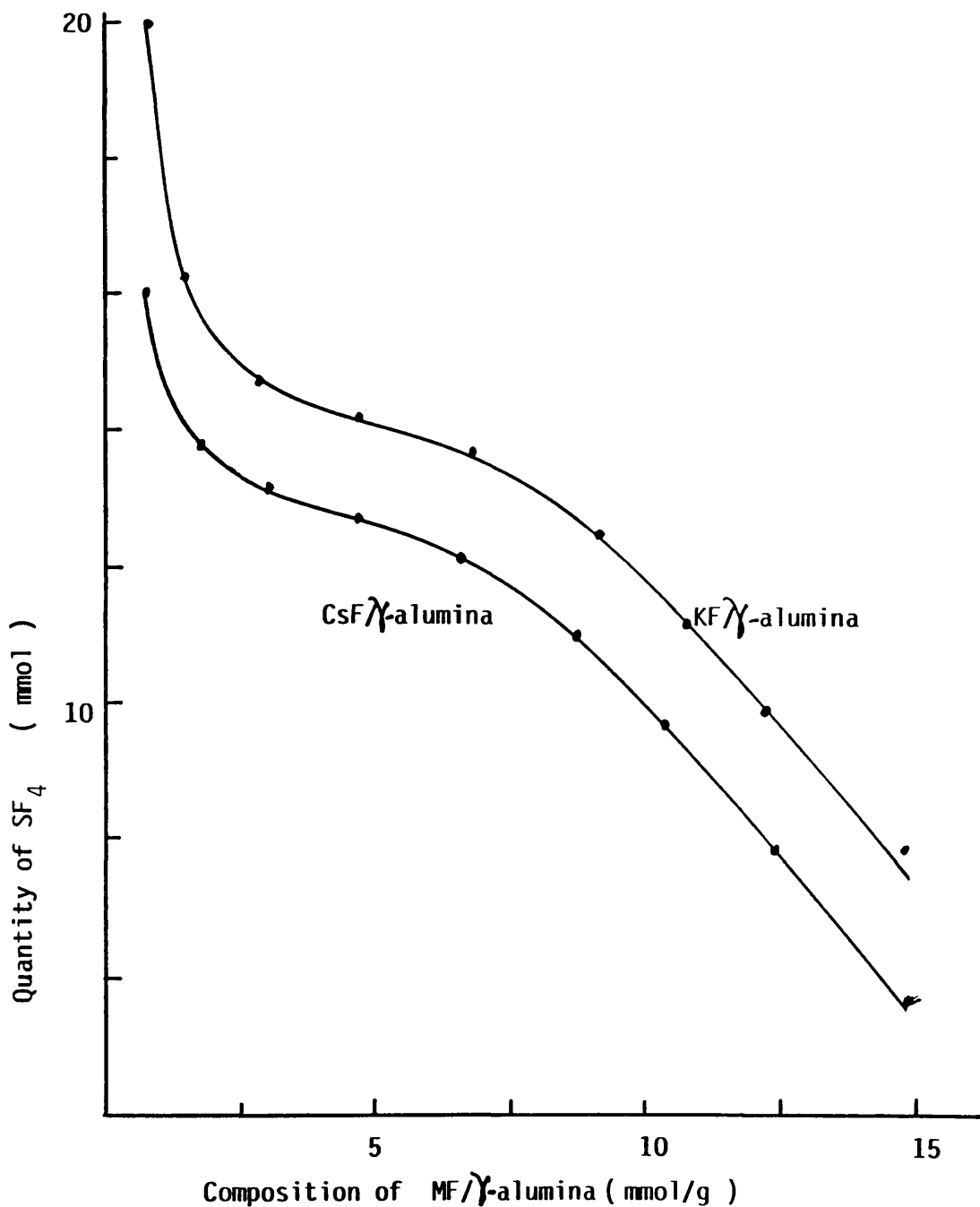


Figure 3.2 Fluorination of MF $\gamma$ -alumina with SOF<sub>2</sub>  
( prepared from aqueous solution )

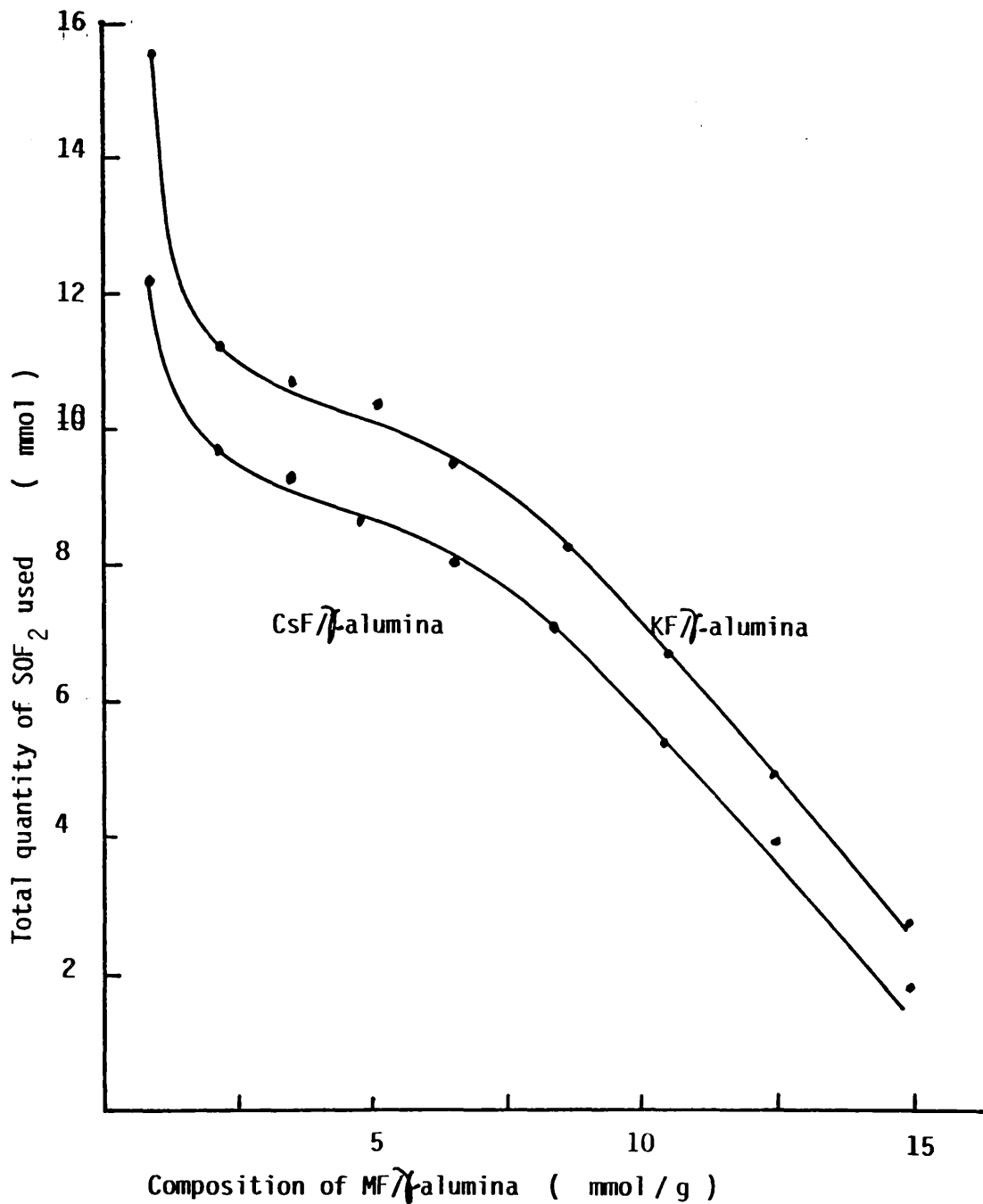
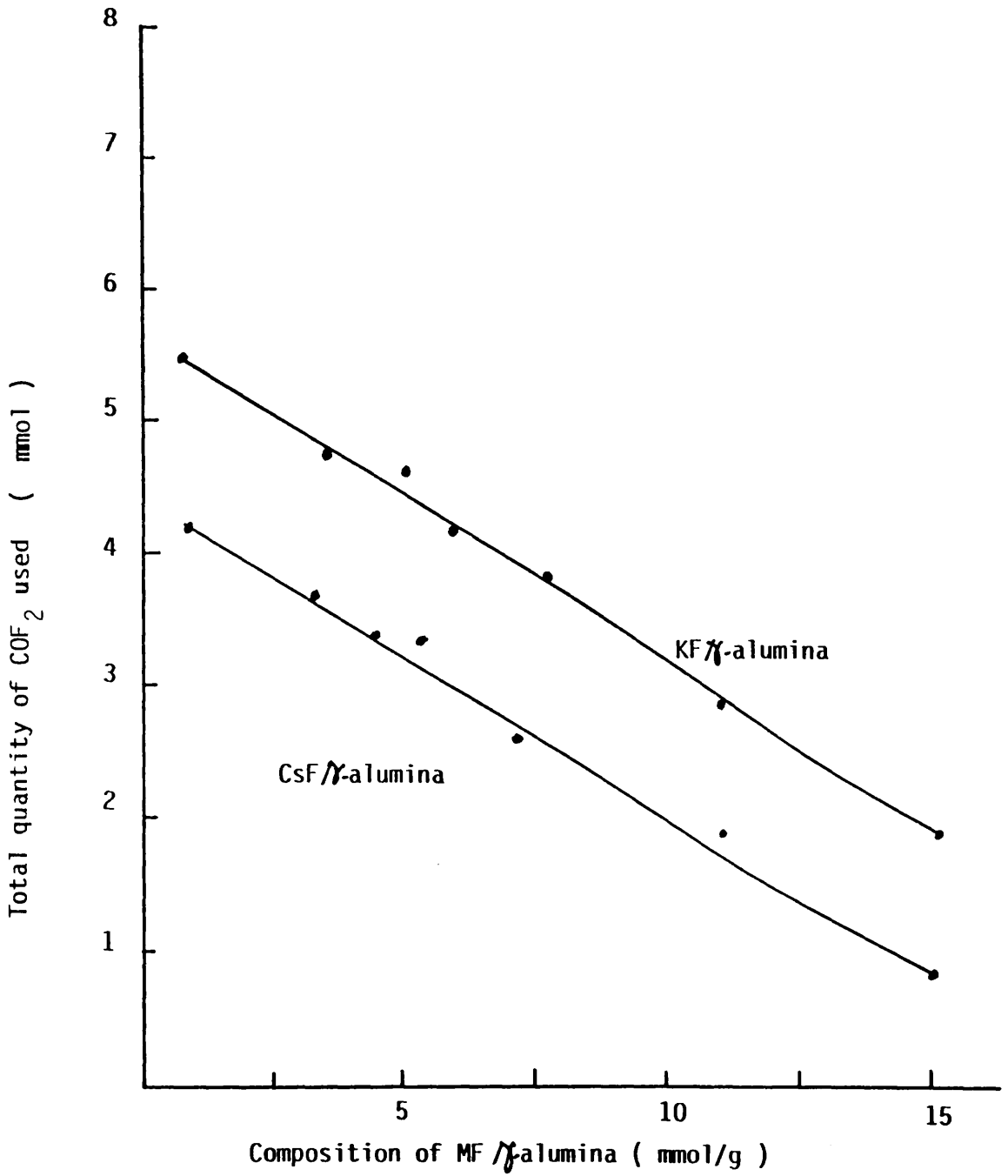


Figure 3.3 Fluorination of MF/ $\gamma$ -alumina with  $\text{COF}_2$   
( prepared from aqueous solution )





using  $\text{SF}_4$ , Table 3.13. The latter anion  $\text{SO}_2\text{F}^-$  was recorded for solid MF/ $\gamma$ -alumina fluorinated with  $\text{SOF}_2$ . In the case of  $\text{COF}_2$ , the infra-red spectrum of the solid product showed bands due to the trifluoromethoxide,  $\text{COF}_3^-$  anion, Table 3.14.

Decomposition of the adducts formed was carried out by heating the material at high temperatures under vacuum. A sample of the fluorinated MF supported on  $\gamma$ -alumina (5.0g) was placed in a stainless steel pressure vessel equipped with a valve and heated under vacuum at 433 K for 3h, followed by 523 K for 5h. The vessel was allowed to cool down to room temperature and transferred to an inert atmosphere box. Infra-red examination of the solid product showed that the anions were no longer present.

### 3.2.2 Treatment of Caesium and Potassium Fluoride Supported on $\gamma$ -Alumina with Anhydrous Hydrogen Fluoride and Sulphur Dioxide Followed by Anhydrous Hydrogen Fluoride.

Anhydrous hydrogen fluoride is widely used as a fluorinating reagent. It reacts, for example, with most metal oxides to give the corresponding metal fluoride or oxyfluoride. Fluorination using HF was attempted in order to compare its behaviour with that of  $\text{SF}_4$ ,  $\text{SOF}_2$  and  $\text{COF}_2$ .

Caesium fluoride supported on  $\gamma$ -alumina (5.0g) was placed in a F.E.P tube equipped with a Monel metal valve in an inert atmosphere box. The vessel was attached to the vacuum line used for the handling of anhydrous hydrogen fluoride, and evacuated for 1h. A measured pressure of HF was admitted to the solid CsF/ $\gamma$ -alumina at room temperature and left for 0.5h. This sequence was

Table 3.13 : Infra-red Spectrum of CsF/ $\gamma$ -alumina after Reaction with SF<sub>4</sub>.

This work $\nu_{\max}$ cm <sup>-1</sup>	Literature CsSF <sub>5</sub> [75]	Literature SO <sub>2</sub> FCs [60]
1193		1178 $\nu_5$
1107		1100 $\nu_1$
793	793 A <sub>1</sub> $\nu_1$	
598		598 $\nu_2$
588	590 E $\nu_1$	
	520 A <sub>1</sub> $\nu_2$	
470		471 $\nu_3$
456	466 A <sub>1</sub> $\nu_3$	
	430 E $\nu_8$	

Table 3.14 : Infra-red Spectrum of Solid CsF/ $\gamma$ -alumina after  
Reaction with  $\text{COF}_2$

This work	$\nu_{\text{max}}$ $\text{cm}^{-1}$	Literature CsCOF <sub>3</sub> [ 41 ]	Assignment
1561		1560	$\nu_1$ A <sub>1</sub> CO str
962		960	$\nu_4$ E CF <sub>3</sub> asym str
813		813	$\nu_2$ A <sub>1</sub> CF <sub>3</sub> sym str
596		595	$\nu_3$ A <sub>1</sub> sy CF <sub>3</sub> def
570		574	$\nu_5$ E OCF, def
420		423	$\nu_6$ asym CF <sub>3</sub>

repeated three or four times until the solid was saturated. The excess HF was removed and the tube evacuated for 2h. The infra-red spectrum of the product at this stage was obtained and showed bands attributable to the  $\text{HF}_2^-$  anion, Table 3.15.

The material was transferred to an inert atmosphere box and ground, then placed in a Monel metal pressure vessel. The bomb was attached to the Monel vacuum line and evacuated for 1h, then heated at 523 K under vacuum for 2h. The bomb was allowed to cool down to room temperature, and the infra-red spectrum was obtained. All bands present were attributable to the  $\text{HF}_2^-$  anion. The bomb was heated at a high temperature, 673 K for 5h. In each case bands due to the  $\text{HF}_2^-$  anion were present. Attempts to decompose the complex by increasing the heating time, 18h, were also unsuccessful. As a result no further attempts were made and the material was used in this state for catalytic examination.

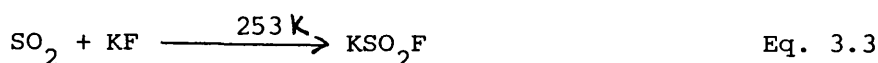
A better method for the fluorination of  $\gamma$ -alumina supported alkali metal fluorides by anhydrous hydrogen fluoride, consisted of a two step process. This has been done by the protection of fluoride ions by reaction with sulphur dioxide to form fluorosulphite, then the fluorination of  $\gamma$ -alumina by anhydrous hydrogen fluoride to remove the surface hydroxyl groups.

Potassium fluoride supported on  $\gamma$ -alumina (5.0g) was placed in a Pyrex glass vessel equipped with a high vacuum stopcock (J. Young) in an inert atmosphere box. The vessel was transferred to the vacuum line and evacuated for 1h, then a quantity of  $\text{SO}_2$  slightly larger than that required for stoichiometric reaction between KF and  $\text{SO}_2$  was added in small portions at 77 K. When the addition was

Table 3.15 : Infra-red Spectrum of Solid CsF/ $\gamma$ -alumina after the Exposure to Anhydrous HF

This work.	Literature $\text{KHF}_2$ [ 34 ]	Assignment
2043	2060	$\nu_3 + \nu_1$
1843	1870	$\nu_2 + \nu_1$
1468	1425	$\nu_3$
1230	1230	$\nu_2$

complete, the contents were allowed to react at 253 K for 2h. The excess SO<sub>2</sub> was removed by distillation, and the product pumped for 0.5h at room temperature, then transferred to an inert atmosphere box. The infra-red spectrum of the solid contained bands attributed to potassium fluorosulphite. Experimentally, the quantity of SO<sub>2</sub> reacted was equivalent to a 1:1 mole ratio SO<sub>2</sub>:KF according to equation 3.3.



The fluorination to remove the terminal hydroxyl groups present on the surface of  $\gamma$ -alumina was performed using anhydrous hydrogen fluoride and the same procedure as that described earlier in this section. The infra-red spectrum of the product was obtained and showed no bands attributable to the HF<sub>2</sub><sup>-</sup> anion. All bands present were due to the fluorosulphite anion. This material was then heated in a Monel bomb under vacuum at 453 K for 5h, followed by 523 K for another 5h. During the first stage of heating the SO<sub>2</sub> collected was equivalent to a SO<sub>2</sub>:KF mole ratio of 1:1.

The vessel was allowed to cool and the infra-red spectrum of the solid showed that the fluorosulphite anion was no longer present.

### 3.3 Fluorination of $\gamma$ -Alumina by Anhydrous Hydrogen Fluoride, Sulphur Tetrafluoride, Thionyl Fluoride and Carbonyl Fluoride.

Calcined  $\gamma$ -alumina at 523 K was fluorinated by each of the fluorinating agents (HF, SF<sub>4</sub>, SOF<sub>2</sub> and COF<sub>2</sub>) at room temperature using the same method as that described in sections 3.2.1 and 3.2.2. The

fluorinated aluminas were then recalcined at 523 K to remove excess hydrogen fluoride and water from the surface.

All fluorinated and non-fluorinated materials were kept under nitrogen in an inert atmosphere box in either glass or P.T.F.E. vials until required.

## CHAPTER FOUR



THE PHYSICAL EXAMINATION OF  $\gamma$ -ALUMINA SUPPORTED CAESIUM AND  
POTASSIUM FLUORIDE, FLUORINATED  $\gamma$ -ALUMINA SUPPORTED CAESIUM  
AND POTASSIUM FLUORIDE AND FLUORINATED  $\gamma$ -ALUMINA.

The rational use of caesium or potassium fluoride supported on  $\gamma$ -alumina under heterogeneous conditions requires a knowledge of their physical properties. This was achieved by the measurement of their B.E.T. areas, their  $^{27}\text{Al}$  MAS-NMR and vibrational spectra and by examination using transmission electron microscopy and powder x-ray diffraction. The latter two methods played a very important role in the physical characterization of these materials.

#### 4.1 B.E.T. Area

Gas adsorption is a widely used technique for the measurement of the surface area of a solid. The quantity of gas adsorbed at a given temperature as a function of pressure is a measure of the surface area. When the surface area to be measured is large, that is above  $5 \text{ m}^2 \text{ g}^{-1}$ , as is the case for  $\gamma$ -alumina, the change in pressure can be measured manometrically. The radioisotope Krypton-85 can be used as an adsorbate for measuring small surface areas, that is below  $5 \text{ m}^2 \text{ g}^{-1}$ , in unsupported alkali metal fluoride MF (M = Cs or K). The advantage of using a radioactive gas is that small changes in pressure can be determined relatively rapidly and precisely [206].

##### 4.1.1 Surface Area Determination by the B.E.T. Method.

When a gas is allowed to come into contact with the surface

of a solid, the gas may be adsorbed by the surface depending upon the experimental conditions. This adsorption may be either chemical (chemisorption) or physical in nature, depending upon the type of bond formed between the gas molecule (the adsorbate) and the solid surface (the adsorbent). Chemisorption involves the formation of chemical bonds between the adsorbate and the adsorbent. As a consequence, chemisorption is limited to the formation of a mono-molecular layer at the surface; furthermore, it is limited to certain activated solids and gases, for example transition metals and hydrogen[207]. In contrast, physical adsorption can, in principle, occur between all gases and all solids provided the temperature is not considerably in excess of the boiling point of the adsorbate. In physical adsorption, no chemical bonds are formed between the adsorbate and the adsorbent; forces similar to those responsible for the cohesive properties of liquids; i.e. van der Waals forces, are involved. Physical adsorption is not restricted to a mono-molecular layer, and multi-layers may be built up on the surface.

If a method of determining when the adsorbed monolayer is complete can be found, and the cross sectional area of the gas molecule in the adsorbed state is known, the total surface of the adsorbent presented to the gas phase can be calculated. Since chemisorption is limited to a monolayer on the surface, it offers the best opportunity of determining a surface area. However, because of the restrictions on the type of solids which will partake in chemisorption, very often physical adsorption must be employed.

The first equation which described the relationship between the quantity of gas adsorbed and the equilibrium pressure of gas at a constant temperature was developed by Langmuir.[208]. The basic assumption in his approach was that adsorption was limited to the formation of a uni-molecular layer. Langmuir visualised an adsorption equilibrium as a dynamic process. The gas molecules strike the surface, most of them become adsorbed and stay on the surface for a short time, then they acquire enough energy to leave the surface. At equilibrium the quantity adsorbed has a definite value and the rate of adsorption should be equal to the rate of desorption. The rate at which the gaseous species is adsorbed is proportional to the number of molecules colliding with the solid surface, which in turn is proportional to the partial pressure  $P_a$ , at a fixed temperature. The adsorption rate must also be proportional to the number of empty sites, assuming that the surface is energetically uniform. If the fraction of the sites covered is  $\theta$ , then  $R_a$ , the rate of adsorption per unit surface area may be written by equation 4.1.

$$R_a = K_a P_a (1-\theta) \quad \text{Eq. 4.1}$$

where  $K_a$  is the rate constant for adsorption.

$R_d$ , the rate of desorption of the adsorbed species, is proportional to the quantity of adsorbate on the surface. Thus equation 4.2

$$R_d = K_d \theta \quad \text{Eq. 4.2}$$

where  $K_d$  is the rate constant of desorption.

At equilibrium, the opposing rates are equal, equation 4.3

$$K_a P_a (1-\theta) = K_d \theta \quad \text{Eq. 4.3}$$

and the solution of equation 4.3 for  $\theta$  gives the Langmuir adsorption isotherm, equation 4.4

$$\theta = bP/(1+bP) \quad \text{Eq. 4.4}$$

Langmuir's derivative applies only to adsorption which is confined to a monolayer and which occurs on an energetically uniform surface and there is no interactions among the adsorbed molecules.

The major difficulty to be overcome with physical adsorption is that because of its close similarity with the liquifaction of gases adsorbed layers begin to form on top of the first layer. As the pressure of gas is increased, there is a progressive build up of several adsorbed layers without a sharp discontinuity when the first layer is complete.

Brunauer, Emmett and Teller<sup>(209)</sup> postulated that layers of adsorbate molecules are adsorbed on these already on the surface of the adsorbent. They made two simplifying assumptions:-

(i) The molecules or atoms in successive layers are in dynamic equilibrium and the quantity adsorbed in each layer when full, is the same.

(ii) The heats of adsorption for all but the first layer are equal to each other and to  $E_L$ , the heat of liquefaction of the adsorbate.

This is equivalent to saying that the evaporation/condensation properties of the second and higher adsorbed layers are the same as those of the liquid state.

Using these postulates, Brunauer, Emmett and Teller were able to derive an equation, now called the "B.E.T. equation", which fits the data for types II and III adsorptions, equation 4.5

$$V = \frac{V_m C}{1-x} \cdot \frac{x}{(1+(C-1)x)} \quad \text{Eq. 4.5}$$

where  $V$  = volume reduced to standard conditions of gas adsorbed per unit mass of adsorbent at a given pressure,  $P$ , and constant temperature  $T$ .

$x = P/P_0$  where  $P_0$  is the saturated vapour pressure at the experimental temperature.

$V_m$  = volume, reduced to standard conditions of gas adsorbed per unit mass of adsorbent when the surface is covered by a uni-molecular layer of adsorbate.

$C = e^{(E_1 - E_L)/RT}$  where  $E_1$  is the heat of adsorption in the first layer and  $E_L$  is the heat of liquefaction of adsorbate.

Type II isotherms are given by equation 4.5 when  $E_1 > E_L$  i.e.  $C > 1$

Type III isotherms are given by equation 4.5 when  $E_1 < E_L$  i.e.  $C < 1$

$E_1 > E_L$  when the attractive forces between the adsorbent and adsorbate are greater than those between the adsorbate molecules in the liquified state and  $E_1 < E_L$  when the attractive forces between the adsorbent and adsorbate are small in comparison with those between the adsorbate molecules in the liquid state.

The B.E.T. Equation can be rearranged to the form shown in equation 4.6

$$\frac{P}{V(P_0 - P)} = \frac{1}{V_m C} + \frac{1}{V_m} \cdot \frac{P}{P_0} \quad \text{Eq. 4.6}$$

and was used in this form throughout this work.

4.1.2 B.E.T. Area of Caesium and Potassium Fluoride  
Supported on  $\gamma$ -Alumina .

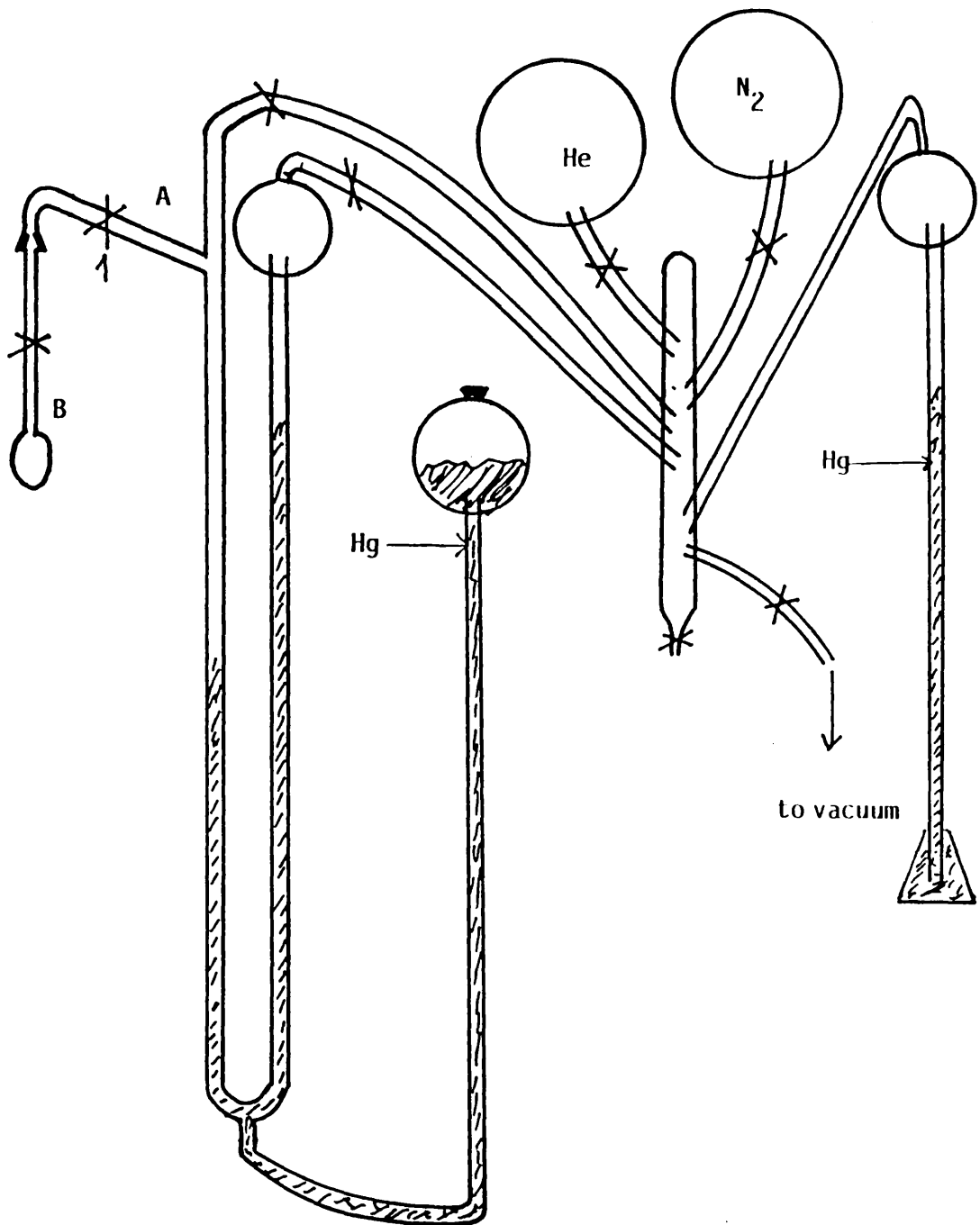
All experiments were carried out under the most rigorously water-free conditions available, due to the hygroscopic properties of the solids. Samples were handled in an inert atmosphere box. Surface areas of caesium or potassium fluoride supported on  $\gamma$ -aluminas were determined by the B.E.T. method using the apparatus shown in Fig. 4.1. This consisted of a calibrated system connected to a standard vacuum line system. The calibrated section, constructed from Pyrex glass consisted of dinitrogen and helium storage bulbs, an U-tube connected to a mercury reservoir and a B14 socket for the attachment of the adsorbent sample bulb. This apparatus was used in conjunction with dinitrogen as the adsorbate gas. The quantity of dinitrogen adsorbed was determined by the difference between the measured volume of gas in the manometer and the volume expected according to the gas laws if there had been no adsorption. For this purpose the volume of the dead space, sections A and B in Fig. 4.1, was determined using helium gas, since it is not adsorbed to any appreciable extent even at low temperatures (77 K) and the application of the gas laws, equations 4.7 and 4.8

$$V + A = K \frac{T}{P} \quad \text{Eq. 4.7}$$

$$V+A+B = K \frac{T}{P} \quad \text{Eq. 4.8}$$

$K$  ( $\text{cm}^3 \text{ Torr}^{-1} \text{ K}^{-1}$ ) is a constant whose value depends on the quantity of the helium admitted and was determined experimentally.

Figure 4.1 The B.E.T Apparatus



A (cm<sup>3</sup>) is the dead space above the zero mark on the burette.

B (cm<sup>3</sup>) is the effective volume of section B.

T (K) is the temperature.

P (Torr) is the pressure and was determined from the difference between the two levels of mercury in the burette.

Plots of V versus  $\frac{T}{P}$  gave straight lines with slope K and intercepts -A and -(A+B) for the room temperature and the 77 K isotherms respectively using helium.

The application of equations 4.7 and 4.8 for dinitrogen at room temperature and 77 K gave 2 further plots of V versus  $\frac{T}{P}$  with different slopes but intercepts identical to the corresponding helium determinations. On the basis of helium adsorption at 77 K the corresponding data for dinitrogen should fit a line parallel to the room temperature isotherm for dinitrogen with an intercept -(A+B). At any pressure the difference  $\Delta V$  between the volume coordinate on this line and that on the experimental line is the volume adsorbed measured at the appropriate pressure. The quantity adsorbed, x, is given by equation 4.9

$$x = P \frac{\Delta V}{T} \cdot \frac{N}{R} \quad \text{Eq. 4.9}$$

P (Torr) is the pressure.

$\Delta V$  (cm<sup>3</sup>) the change in volume.

T (K) the temperature.

N (mol<sup>-1</sup>) the Avogadro number.

R (cm<sup>3</sup> Torr K<sup>-1</sup> mol<sup>-1</sup>) the gas constant.

A plot of  $\frac{P}{x(P_0 - P)}$  versus  $\frac{P}{P_0}$  equation 4.6, gives a



straight line of slope  $\frac{1}{x_m}$ . The quantity ( $x_m$ ) of gas required to form a monolayer was calculated and hence, the surface area by assuming that each nitrogen molecule occupied  $16.2 \text{ \AA}^2$  of surface.

Calcined  $\gamma$ -alumina supported caesium or potassium fluorides (typically 0.2 g) were loaded in the dry box into a preweighed dry capillary sample holder by means of a side arm on the sample bulb. The weight of the calcined material was accurately determined before removal of the side arm, sealing the sample bulb under vacuum. The calcined material was degassed for 30 min, tap (1) closed and a quantity of helium was admitted. A set of readings of V versus P was obtained by adjusting the height of the mercury reservoir to vary the level of mercury in the U-tube. A second set of readings was obtained, with tap (1) open and the sample bulb immersed in liquid nitrogen. This procedure was repeated for dinitrogen at room temperature and at 77 K. The results of a surface area determination on a sample of CsF/ $\gamma$ -alumina (composition  $4.4 \text{ mmol g}^{-1}$ ) are presented in Tables 4.1 and 4.2. Plots of V versus  $\frac{T}{P}$  under various conditions used and  $\frac{P}{x(P_0 - P)}$  versus  $\frac{P}{P_0}$  are shown in Figs. 4.2 and 4.3 respectively. From Fig. 4.3 the gradient,  $\frac{1}{x_m} = 1.63 \times 10^{-20} \text{ (molecule)}^{-1}$  and hence,  $x_m = 0.61 \times 10^{20}$  molecule. For a sample of 0.1604 g, this is equivalent to a surface area

$$0.61 \times 10^{20} \times \frac{16.2 \times 10^{-20}}{0.1604} = 62 \text{ m}^2 \text{ g}^{-1}$$

For each composition at least seven BET area determinations were made using separate samples of  $\gamma$ -alumina supported caesium or potassium fluoride in each case. Normally the samples

Table 4.1 Surface Area Determination of CsF/ $\gamma$ -Alumina (4.4 mmol g<sup>-1</sup>)

Run	Temp (K)	Volume (cm <sup>3</sup> )	H <sub>1</sub> (Torr)	H <sub>2</sub> (Torr)	P (Torr)	T/P (K Torr <sup>-1</sup> )
Heat RT	295.6	90.0	518.38	358.31	160.07	1.84
	295.6	77.0	612.55	428.50	184.05	1.6
	296.1	63.6	726.45	506.60	219.85	1.34
	296.1	51.0	850.49	580.20	270.29	1.09
Heat 77 K	296.2	91.2	424.01	345.01	79.0	3.74
	296.2	69.8	560.28	470.80	89.48	3.3
	296.0	51.8	678.49	577.16	101.33	2.42
	295.8	31.0	801.77	685.41	116.36	2.54
N <sub>2</sub> at RT	295.9	88.0	595.6	364.6	231	1.28
	296.1	80.6	659.5	407.9	251.6	1.17
	295.9	71.0	728.82	452.41	276.41	1.07
	295.9	61.8	841.08	511.67	329.41	0.89
N <sub>2</sub> at 77 K	295.7	76.3	538.5	432.1	106.7	2.77
	296.1	61.0	639.18	521.77	117.41	2.52
	296.1	47.4	730.1	601.0	129.1	2.29
	295.7	32.6	830.92	688.24	142.68	2.07

Table 4.2 The BET Area of CsF/ $\gamma$ -Alumina (4.4 mmol g<sup>-1</sup>)

$\Delta V$ (cm)	T/P (K/Torr)	P (Torr)	x (molecule) 10 <sup>-20</sup>	$\frac{P}{x(P_0-P)}$ 10 <sup>22</sup> (molecule) <sup>-1</sup>	$\frac{P}{P_0}$ 10 <sup>2</sup>
18.0	2.2	134.5	0.78	27.56	17.69
19.0	2.4	123.24	0.76	25.47	16.22
21.0	2.6	113.80	0.77	22.87	14.97
22.5	2.8	105.67	0.77	20.97	13.90
23.5	3.0	98.63	0.75	19.88	12.97

Figure 4.2 Volume  $V$  (  $T/P$  )

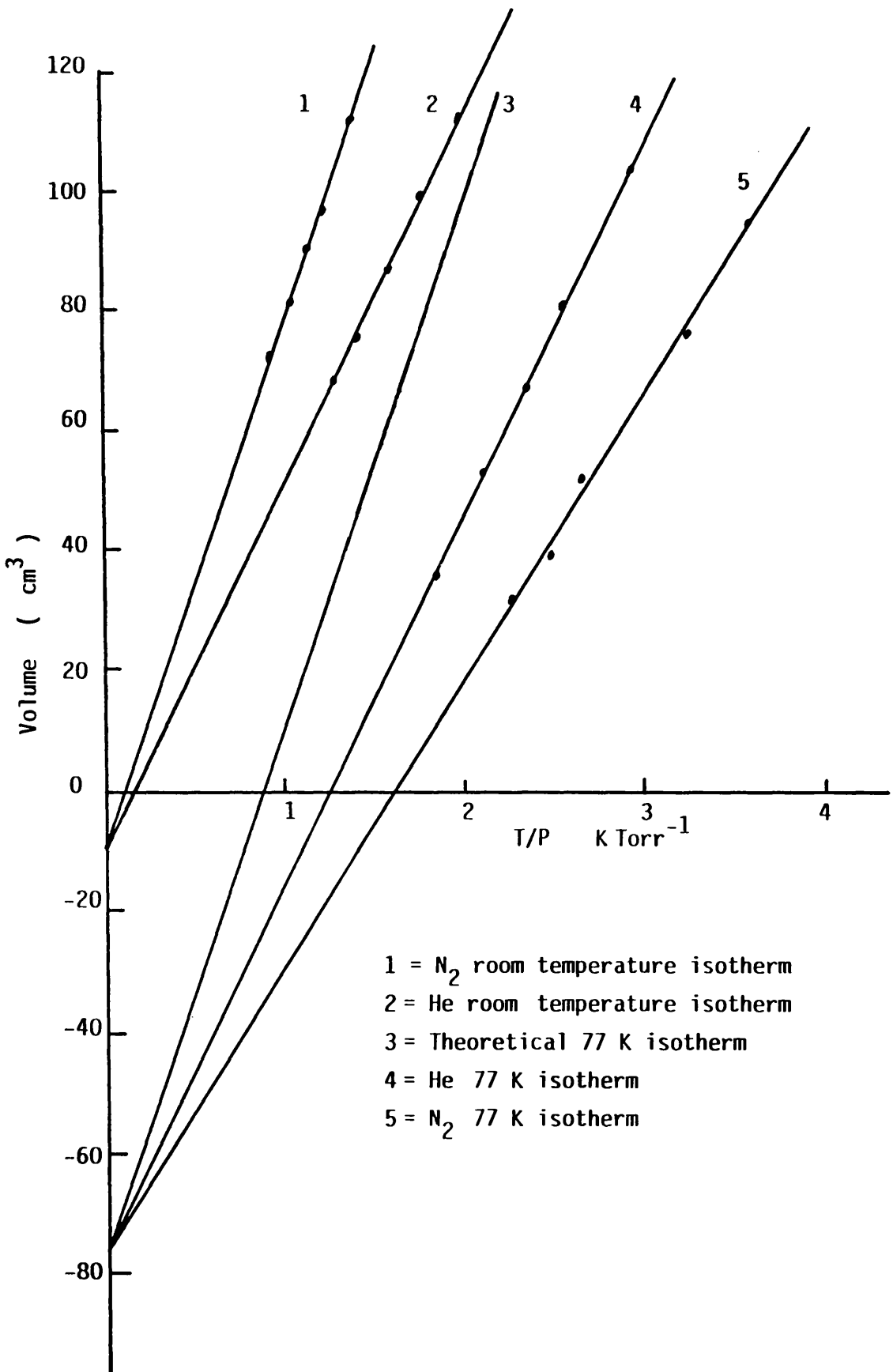
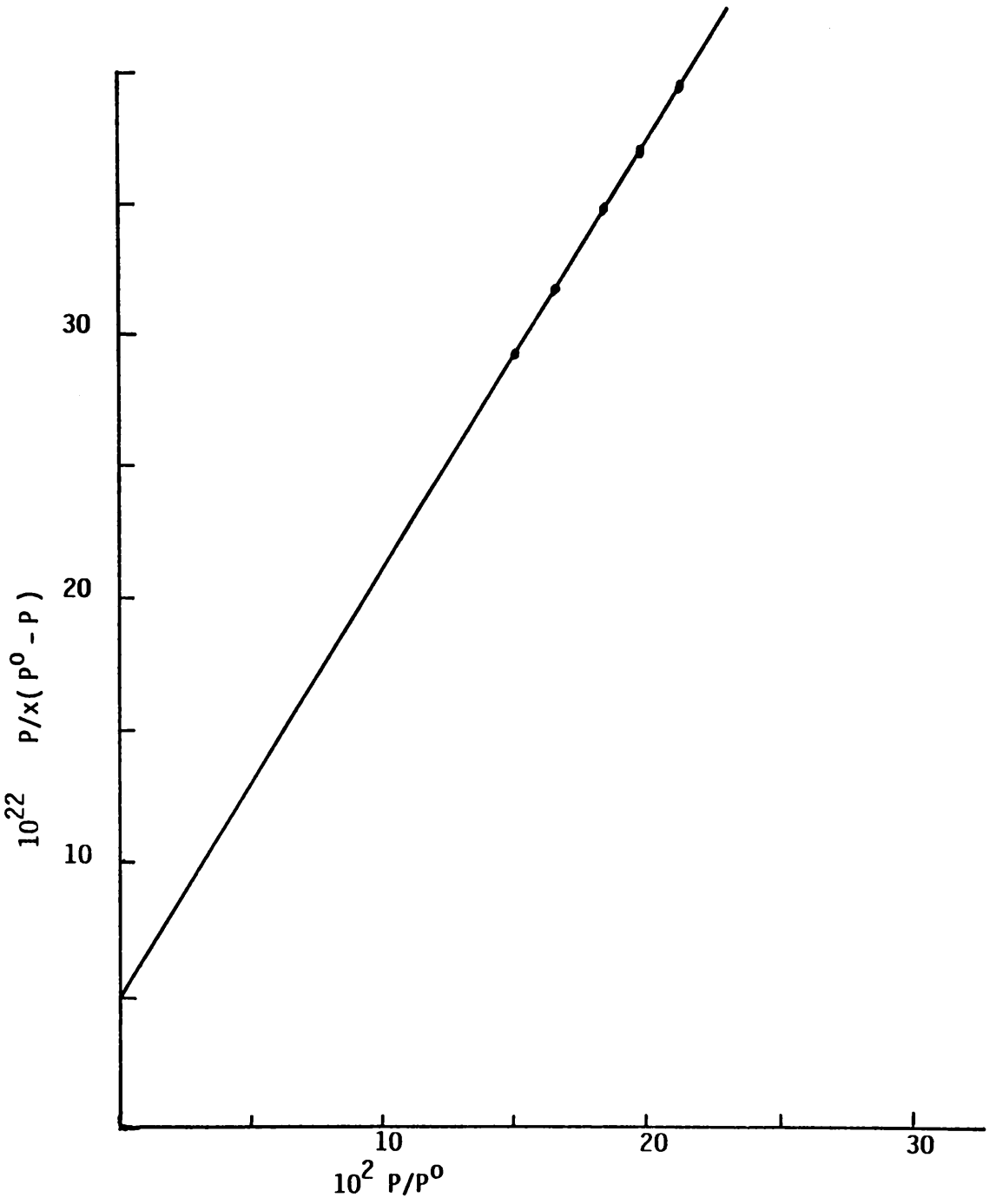


Figure 4.3  $P/x(P^0 - P) \sim P/P^0$



originated from different batches in order to examine whether or not the BET area of  $\gamma$ -alumina supported caesium or potassium fluoride is reproducible. The results of ten determinations for CsF/ $\gamma$ -alumina ( $4.4 \text{ mmol g}^{-1}$ ) and a similar number for KF/ $\gamma$ -alumina ( $4.4 \text{ mmol g}^{-1}$ ) are listed in Table 4.3. The mean values are  $60$  and  $96 \text{ m}^2 \text{ g}^{-1}$  for CsF/ $\gamma$ -alumina and KF/ $\gamma$ -alumina respectively. The standard deviation on the mean are  $6$  for CsF/ $\gamma$ -alumina and  $9$  for KF/ $\gamma$ -alumina. This approach leads to values for the surface area of CsF/ $\gamma$ -alumina of  $60 \pm 6 \text{ m}^2 \text{ g}^{-1}$  and of KF/ $\gamma$ -alumina of  $96 \pm 9 \text{ m}^2 \text{ g}^{-1}$ . However, from a small number of data points it cannot be assumed that the true value corresponds to the mean. It is better therefore to determine an interval within which the probability of finding the true value is high. This interval, the reliability interval,  $L$ , is given by equation 4.10

$$L_{1,2} = X \pm K_n R \quad \text{Eq. 4.10}$$

where  $L_1$  is the lower limit of the reliability interval

$L_2$  is the upper limit of the reliability interval

$X$  is the mean value

$K_n$  is the reliability coefficient, the probability of finding the true value

$R$  is the range of results.

For the ten results obtained for CsF/ $\gamma$ -alumina ( $4.4 \text{ mmol g}^{-1}$ ), the reliability interval within which the result lies with a probability of 95% is  $55-65 \text{ m}^2 \text{ g}^{-1}$ . Application of equation 4.10 to the surface area data for KF/ $\gamma$ -alumina ( $4.4 \text{ mmol g}^{-1}$ ) Table 4.3 results are in the range  $91-101 \text{ m}^2 \text{ g}^{-1}$ . A similar treatment was

Table 4.3 The Mean Values of the BET Area of CsF/ $\gamma$ -Alumina and KF/ $\gamma$ -Alumina (4.4 mmol g<sup>-1</sup>)

Batch	Sample	Surface Area m <sup>2</sup> g <sup>-1</sup>	
		CsF/ $\gamma$ -alumina	KF/ $\gamma$ -alumina
1	1	62	99
	2	71	101
2	3	53	89
	4	55	106
	5	67	109
3	6	54	88
	7	50	90
4	8	66	87
	9	57	86
5	10	66	106

used throughout this work. The results for  $\gamma$ -alumina,  $\gamma$ -alumina calcined at 523 K and  $\gamma$ -alumina supported caesium or potassium fluoride over the composition range 1.1-20.0 mmol g<sup>-1</sup> are given in Table 4.4 and Fig. 4.4. The BET area of CsF/ $\gamma$ -alumina and KF/ $\gamma$ -alumina prepared from non-aqueous solution, using heptafluoroisopropoxide salts, were also determined with 95% confidence limits and are tabulated in Table 4.5 and shown schematically in Fig. 4.5.

The BET areas of caesium or potassium fluoride supported on  $\gamma$ -alumina prepared by mixing the two solids together (MF and  $\gamma$ -alumina), were not reproducible. For each composition (4.4 and 8.8 mmol g<sup>-1</sup>) 12 BET area determinations were made on separate samples of  $\gamma$ -alumina supported caesium or potassium fluoride, originating from 3 different batches. The BET area of CsF/ $\gamma$ -alumina (4.4 mmol g<sup>-1</sup>) from batch 1 (Sample 1 Batch 1 was 41 m<sup>2</sup>g<sup>-1</sup>, other results were for S<sub>2</sub>B<sub>1</sub> = 113 m<sup>2</sup>g<sup>-1</sup>, S<sub>1</sub>B<sub>2</sub> = 19 m<sup>2</sup>g<sup>-1</sup>, S<sub>2</sub>B<sub>3</sub> = 169 m<sup>2</sup>g<sup>-1</sup>), the complete set of results is given in Table 4.6. Based on these results the preparation of supported materials simply by mixing the components is not satisfactory. The use of this method was therefore discontinued.

Calcination of  $\gamma$ -alumina to 523 K under vacuum resulted in an increase in its BET area, but the impregnation of  $\gamma$ -alumina with caesium or potassium fluoride resulted in a decrease in the BET area of the material. A reduction in the BET area for the reagents with increasing the quantity of caesium or potassium fluoride loading was observed. Heating the samples to 773 K under vacuum for 5 h resulted in a very marked decrease in the



Table 4.4 The BET Area of  $\gamma$ -alumina and Caesium or Potassium fluoride Supported on  $\gamma$ -alumina (Dugossa)

Composition (mmol g <sup>-1</sup> )	Surface Area m <sup>2</sup> g <sup>-1</sup>	
	CsF/ $\gamma$ -alumina	KF/ $\gamma$ -alumina
1.1	124 - 135	140 - 156
2.0	76 - 88	104 - 116
4.4	55 - 65	91 - 101
5.5	51 - 61	76 - 88
6.0	42 - 56	69 - 81
8.8	33 - 45	51 - 65
15.0	15 - 27	29 - 39
20.0	11 - 18	19 - 29
$\gamma$ -Alumina Sb Pural 90		114 - 133
Calcined $\gamma$ -alumina Sb Pural 90 at 523 K		203 - 217
$\gamma$ -Alumina Degossa Aluminium Oxide 'C'		129 - 161
$\gamma$ -Alumina Degossa Aluminium Oxide 'C'		
Calcined at 523 K		220 - 249

Figure 4.4 B.E.T Area of MF/ $\gamma$ -alumina Prepared from aqueous solution

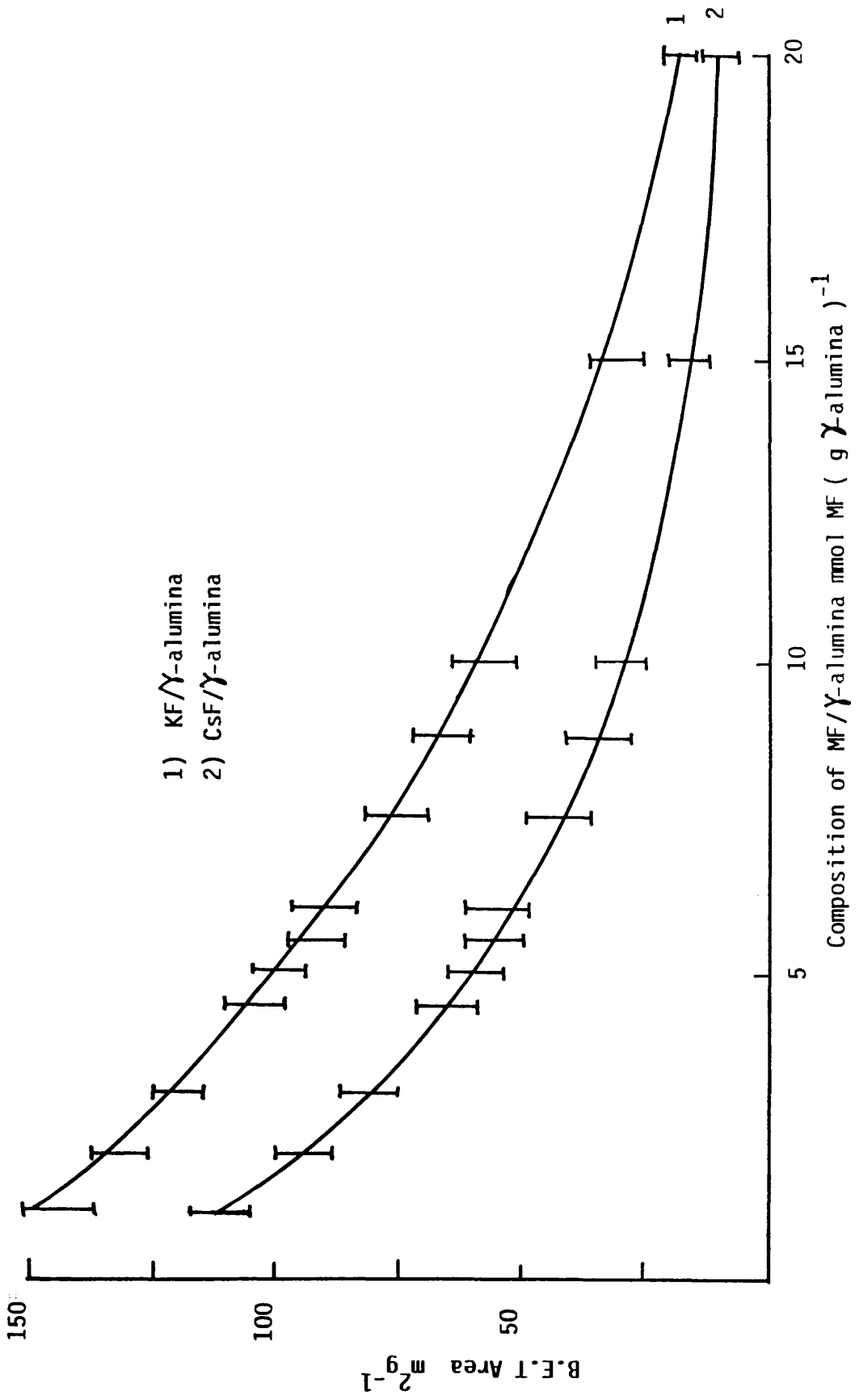


Table 4.5 Surface Area of MF/ $\gamma$ -alumina prepared from  
Non-Aqueous Solution.

Composition mmol g <sup>-1</sup>	Surface Area m <sup>2</sup> g <sup>-1</sup>	
	CsF/ $\gamma$ -alumina	KF/ $\gamma$ -alumina
2.0	62 - 73	80 - 93
4.4	40 - 50	68 - 81
5.5	31 - 47	51 - 69
6.0	24 - 32	47 - 54
8.8	19 - 26	32 - 41
15.0	10 - 19	17 - 25
4.4 calcined at 773 K	16 - 20	17 - 23
8.8 calcined at 773 K	17 - 24	18 - 24

Figure 4.5 B.E.T Area of MF/ $\gamma$ -alumina prepared from non-aqueous solution

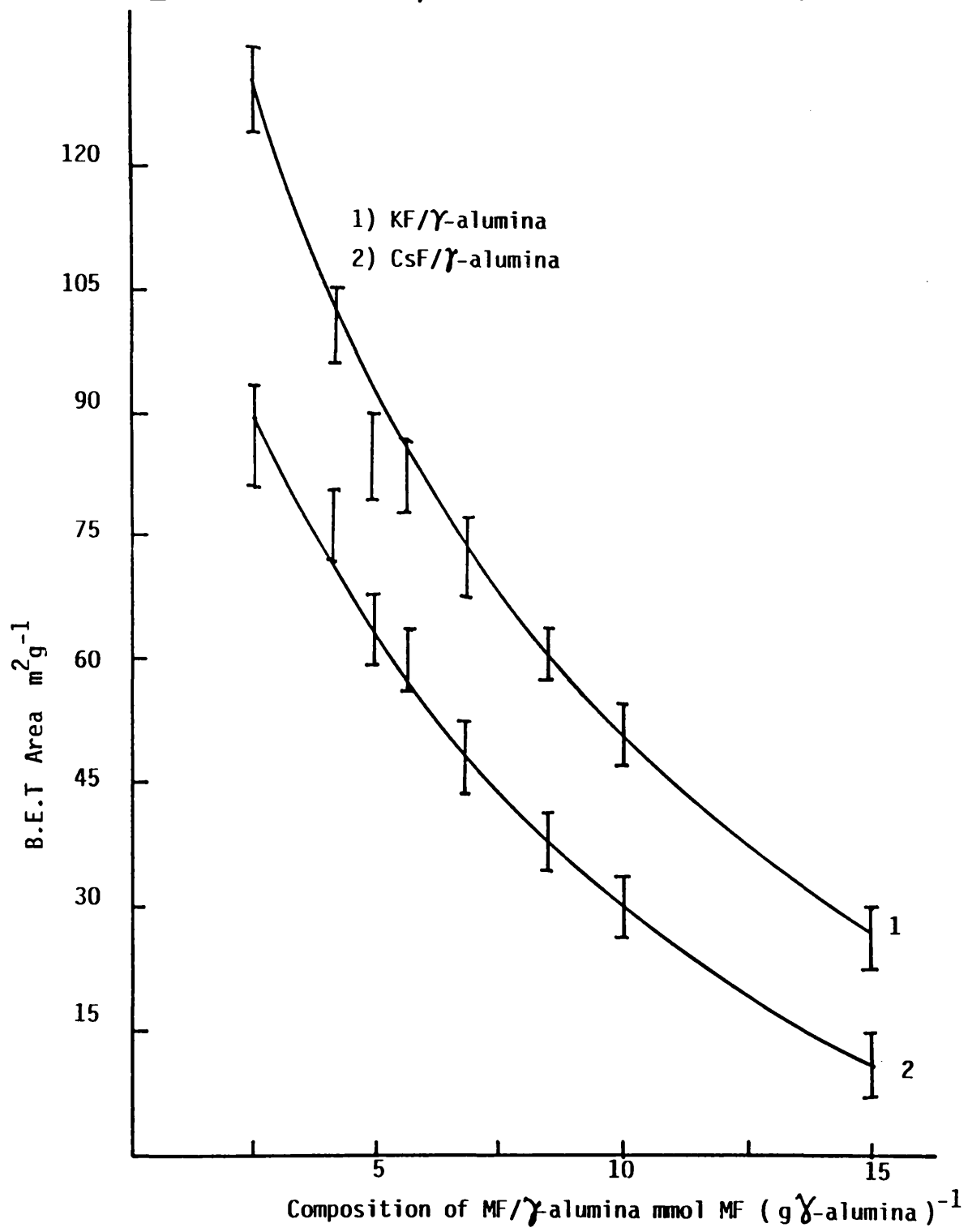


Table 4.6 BET Area of  $\gamma$ -alumina supported Caesium  
or Potassium fluoride prepared from dry reactions  
at room temperature.

Composition mmol g <sup>-1</sup>	Batch	Surface area (m <sup>2</sup> g <sup>-1</sup> )	
		CsF/ $\gamma$ -alumina	KF/ $\gamma$ -alumina
4.4	1	43 - 51	52 - 73
	2	141 - 189	114 - 119
	3	96 - 114	163 - 204
8.8	1	45 - 67	23 - 29
	2	17 - 33	83 - 96
	3	120 - 133	39 - 52

BET area for both 4.4 and 8.8 mmol g<sup>-1</sup> to 16-24 m<sup>2</sup>g<sup>-1</sup>, Table

4.5. The results showed that potassium fluoride supported on  $\gamma$ -alumina has a larger BET area than caesium fluoride supported on  $\gamma$ -alumina at a given composition, although both materials behave similarly as a function of composition. The BET areas of the  $\gamma$ -alumina supported caesium or potassium fluoride prepared from aqueous solution were larger than those prepared from heptafluoroisopropoxide for a given composition across the range 1.1-20.0 mmol g<sup>-1</sup>.

4.1.3 B.E.T. Areas of  $\gamma$ -Alumina Treated with Hydrogen Fluoride, Gaseous Sulphur Tetrafluoride, Thionyl Fluoride or Carbonyl Fluoride.

The procedure used to measure the BET areas of  $\gamma$ -alumina fluorinated by various inorganic fluorinating agents was the same as that described in section 4.1.2.

The results for the BET area determination of  $\gamma$ -alumina calcined to 523 K then treated with various inorganic fluorinating agents at room temperature are presented in Table 4.7 and shown schematically in Fig. 4.6.  $\gamma$ -Alumina calcined to 523 K then treated with anhydrous gaseous hydrogen fluoride, sulphur tetrafluoride, thionyl fluoride or carbonyl fluoride at room temperature resulted in a smaller decrease in the BET area compared with that of the unfluorinated materials. The BET areas of  $\gamma$ -alumina calcined to 523 K then fluorinated with either gaseous sulphur tetrafluoride or thionyl fluoride at room temperature were equal within experimental error. The overall order of the BET area was  $\gamma$ -alumina calcined to 523 K > COF<sub>2</sub>/ $\gamma$ -alumina ~ HF/ $\gamma$ -alumina

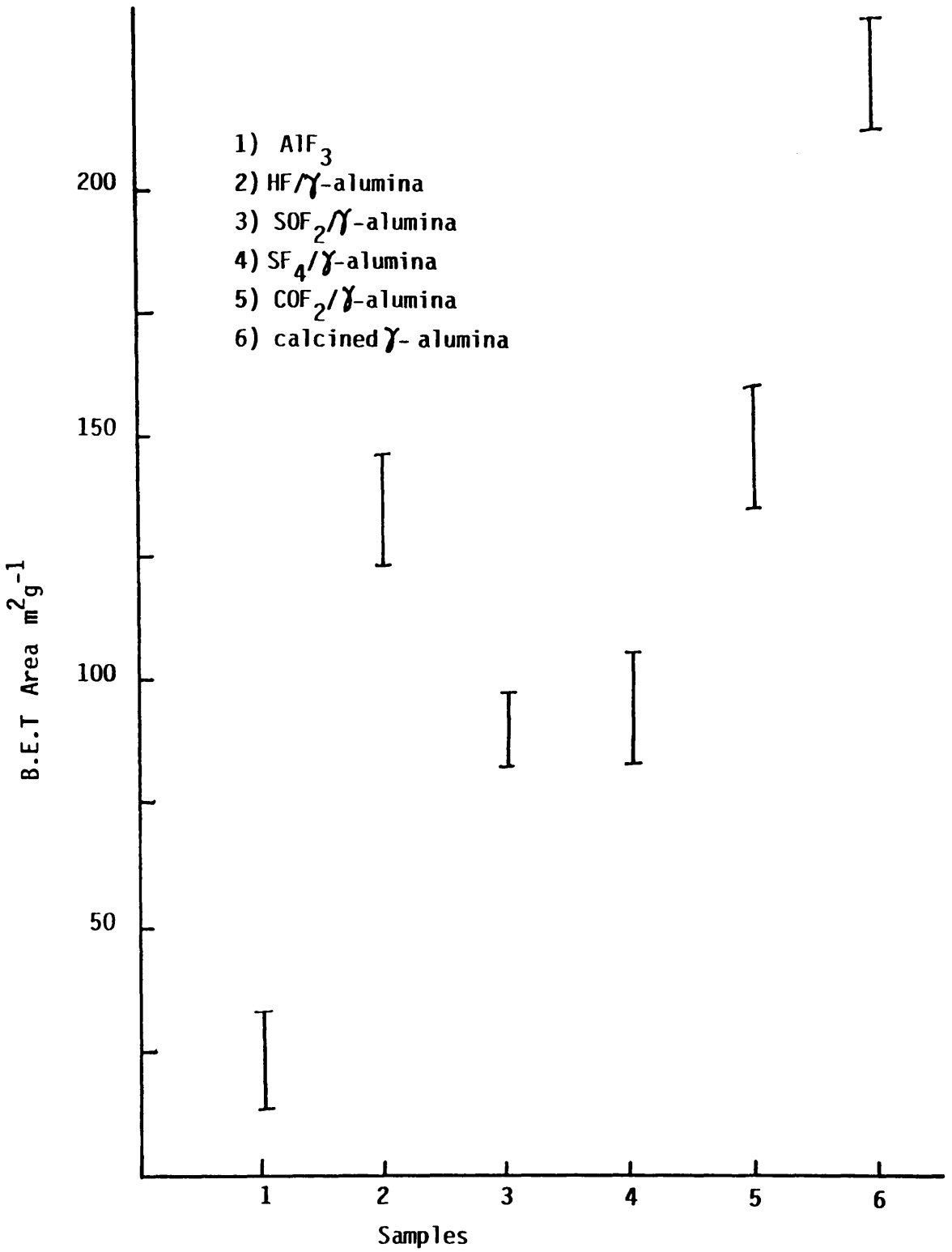
Table 4.7 The BET Areas of Fluorinated  $\gamma$ -Alumina at room Temperature.

---

Fluorinating Agent.	Surface area of fluorinated $\gamma$ -alumina $\text{m}^2 \text{g}^{-1}$
Anhydrous hydrogen fluoride	132 - 148
Sulphur tetrafluoride	80 - 94
Thionyl fluoride	78 - 88
Carbonyl fluoride	138 - 153

---

Figure 4.6 B.E.T Area of fluorinated  $\gamma$ -alumina





> sulphur tetrafluoride treated  $\gamma$ -alumina, thionyl fluoride treated  $\gamma$ -alumina  $\gg$

anhydrous aluminium(III) fluoride activated at 373 K under vacuum for 5h.

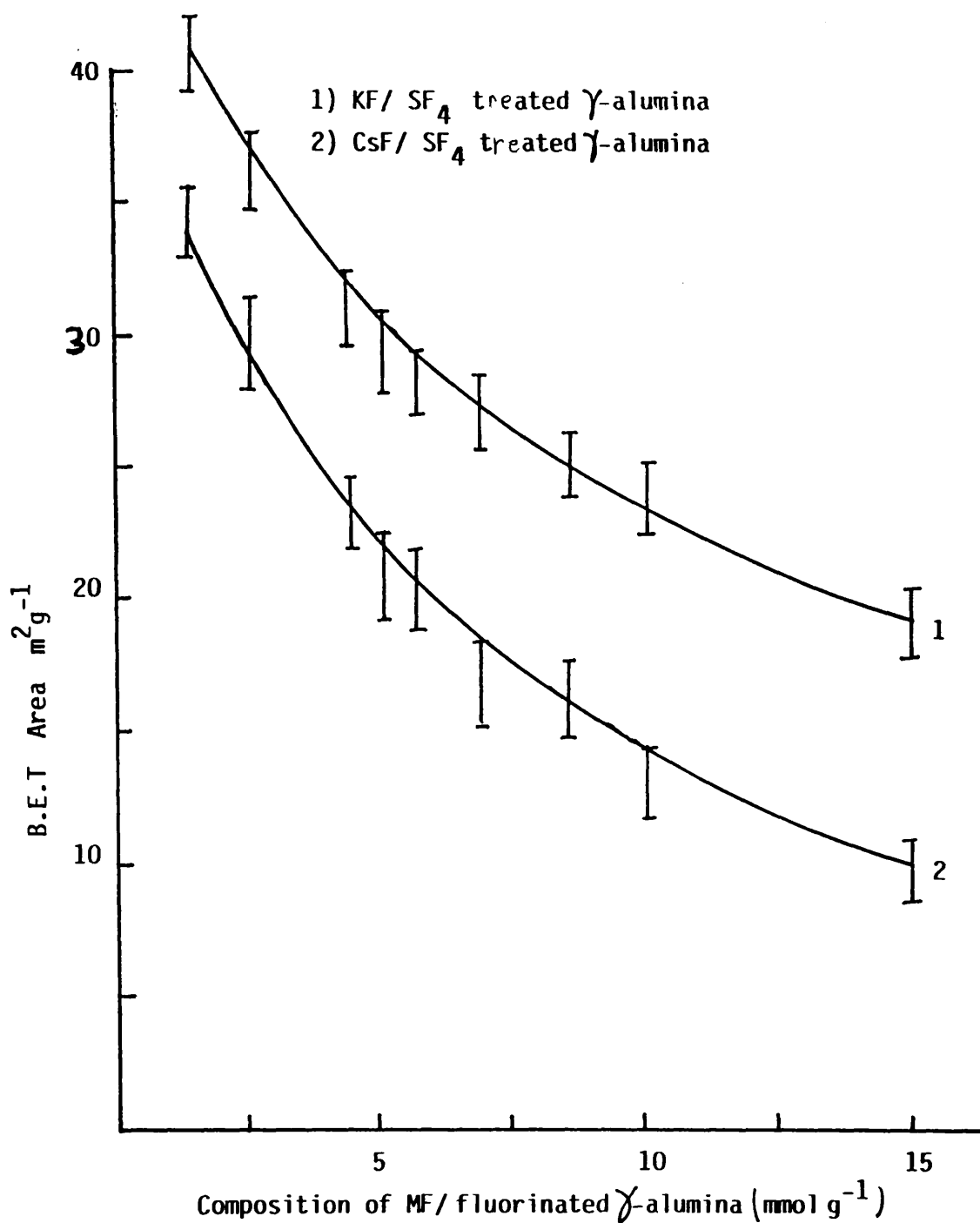
4.1.4 B.E.T. Areas of Caesium or Potassium Fluoride Supported on  $\gamma$ -Alumina Treated with Sulphur Tetrafluoride, Thionyl Fluoride, Anhydrous Hydrogen Fluoride, Carbonyl Fluoride or Liquid Sulphur Dioxide then Anhydrous Hydrogen Fluoride at Room Temperature.

The procedure used in these measurements was the same as that described in section 4.1.2. The results of the BET area determinations of caesium or potassium fluoride supported on  $\gamma$ -alumina prepared from aqueous solution or from heptafluoroisopropoxide salts, then treated with gaseous sulphur tetrafluoride at room temperature are summarized in Table 4.8 and shown schematically in Fig 4.7. The treatment of  $\gamma$ -alumina supported caesium or potassium fluoride prepared from aqueous solution or from heptafluoroisopropoxide salts, with gaseous sulphur tetrafluoride at room temperature resulted in a uniform reduction in the BET area across the composition range 1.1-15.0 mmol g<sup>-1</sup>. The extent of the reduction in the BET area of the  $\gamma$ -alumina supported caesium or potassium fluoride caused by gaseous sulphur tetrafluoride treatment expressed by the ratio of the BET area of caesium or potassium fluoride supported on gaseous sulphur tetrafluoride treated  $\gamma$ -alumina to the BET area of caesium or potassium fluoride supported on unfluorinated  $\gamma$ -alumina, is

Table 4.8 The B.E.T. Area of MF/ $\gamma$ -alumina pretreated with Sulphur Tetrafluoride.

Composition mmol g <sup>-1</sup>	Aqueous Solution Preparation.		Surface Area (m <sup>2</sup> g <sup>-1</sup> )	
	CsF/ $\gamma$ -alumina	KF/ $\gamma$ -alumina	Non-Aqueous Solution Preparation CsF/ $\gamma$ -alumina	KF/ $\gamma$ -alumina
1.1	32 - 36	36 - 44	33 - 37	37 - 46
2.0	22 - 26	29 - 33	22 - 25	29 - 31
4.4	19 - 22	27 - 31	19 - 23	27 - 30
5.0	17 - 21	26 - 30	17 - 20	27 - 30
5.5	17 - 20	26 - 29	17 - 21	26 - 30
8.8	14 - 17	18 - 22	14 - 18	19 - 22
15.0	8 - 12	16 - 21	8 - 11	16 - 20

Figure 4.7 B.E.T Area of MF/fluorinated  $\gamma$ -alumina, prepared from aqueous solution and pretreated with  $SF_4$



shown diagrammatically across the composition range, Fig.

4.8. The treatment of  $\gamma$ -alumina supported caesium or potassium fluoride with gaseous thionyl fluoride or liquid sulphur dioxide then anhydrous hydrogen fluoride, exhibited similar characteristics as that described above, in that, the BET area of those materials was equal to the BET area of the caesium or potassium fluoride supported on gaseous sulphur tetrafluoride treated  $\gamma$ -alumina across the composition range. Results are summarized in Tables 4.9 and 4.10 and shown in Figs. 4.9 and 4.10.

The BET area of caesium or potassium fluoride supported on anhydrous gaseous hydrogen fluoride treated  $\gamma$ -alumina was smaller than those treated with gaseous sulphur tetrafluoride Table 4.11, whereas the BET area of caesium or potassium fluoride supported on gaseous carbonyl fluoride treated  $\gamma$ -alumina was larger, Table 4.11.

In summary the BET areas for caesium or potassium fluoride supported on unfluorinated  $\gamma$ -alumina and fluorinated  $\gamma$ -alumina as a function of composition are shown in Figs. 4.11 and 4.12. The order of the BET area overall was  $\gamma$ -alumina calcined to 523 K > potassium fluoride supported on carbonyl fluoride treated  $\gamma$ -alumina > caesium fluoride supported on carbonyl fluoride treated  $\gamma$ -alumina > potassium fluoride supported on sulphur tetrafluoride, thionyl fluoride, sulphur dioxide then anhydrous hydrogen fluoride treated  $\gamma$ -alumina > caesium fluoride supported on sulphur tetrafluoride, thionyl fluoride or sulphur dioxide then anhydrous hydrogen fluoride treated  $\gamma$ -alumina > potassium fluoride supported

Figure 4.8 Ratio MF/fluorinated  $\gamma$ -alumina To MF/  $\gamma$ -alumina ,B.E.T Area

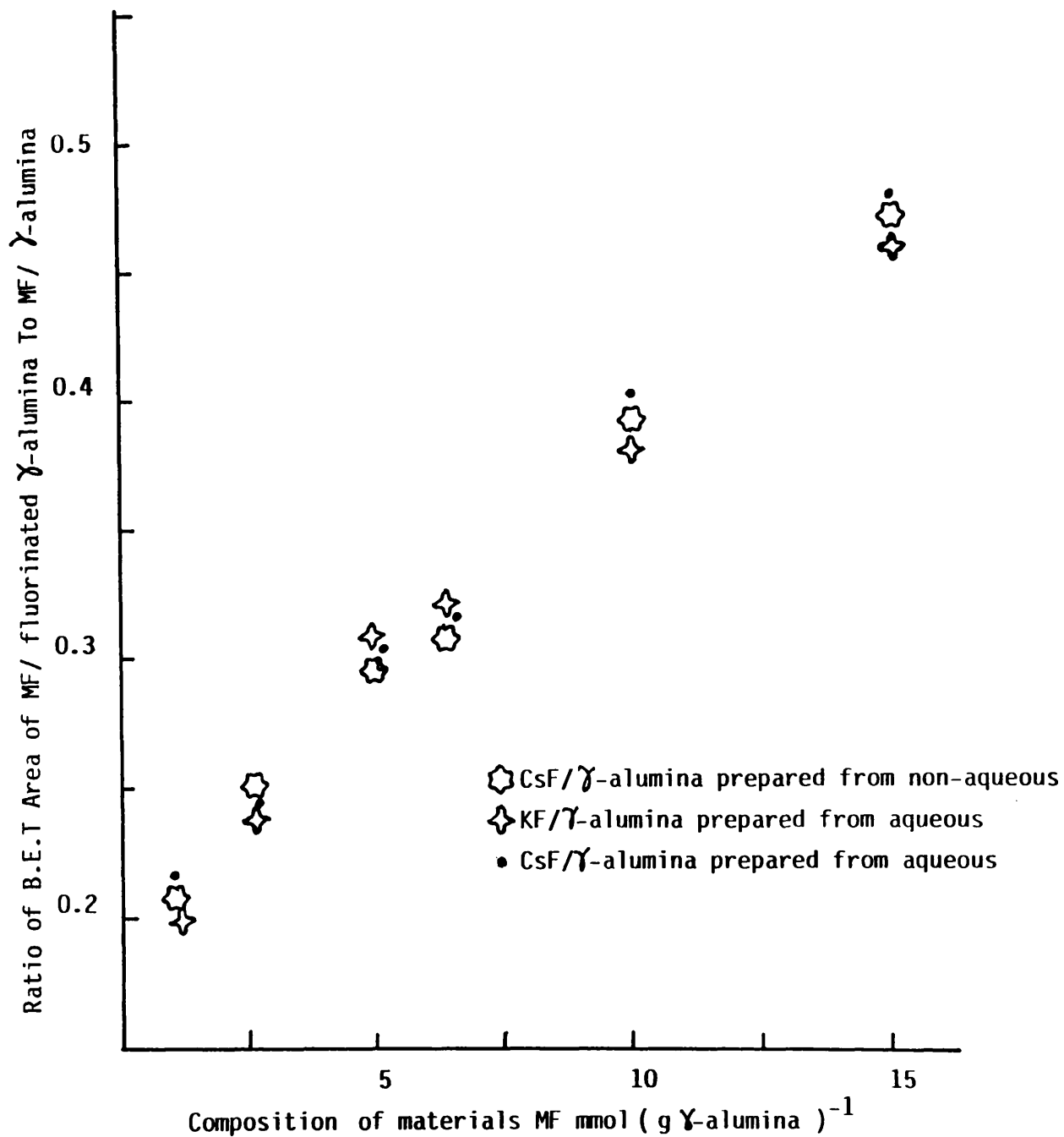


Table 4.9 The B.E.T. Area of MF/ $\gamma$ -alumina pretreated with Thionyl Fluoride.

Composition mmol g <sup>-1</sup>	Surface Area of the Fluorinated Materials.			
	Aqueous Solution Preparation CsF/ $\gamma$ -alumina	KF/ $\gamma$ -alumina	Non-Aqueous Solution Preparation CsF/ $\gamma$ -alumina	KF/ $\gamma$ -alumina
1.1	31 - 35	38 - 43	32 - 36	37 - 46
2.0	22 - 27	30 - 34	23 - 26	29 - 33
4.4	20 - 23	27 - 32	19 - 24	28 - 30
5.5	17 - 21	26 - 30	18 - 22	26 - 29
8.8	13 - 17	19 - 23	14 - 17	20 - 23
15.0	8 - 11	15 - 20	8 - 12	16 - 21

Figure 4.9 B.E.T Area of MF/ fluorinated  $\gamma$ -alumina with  $\text{SOF}_2$

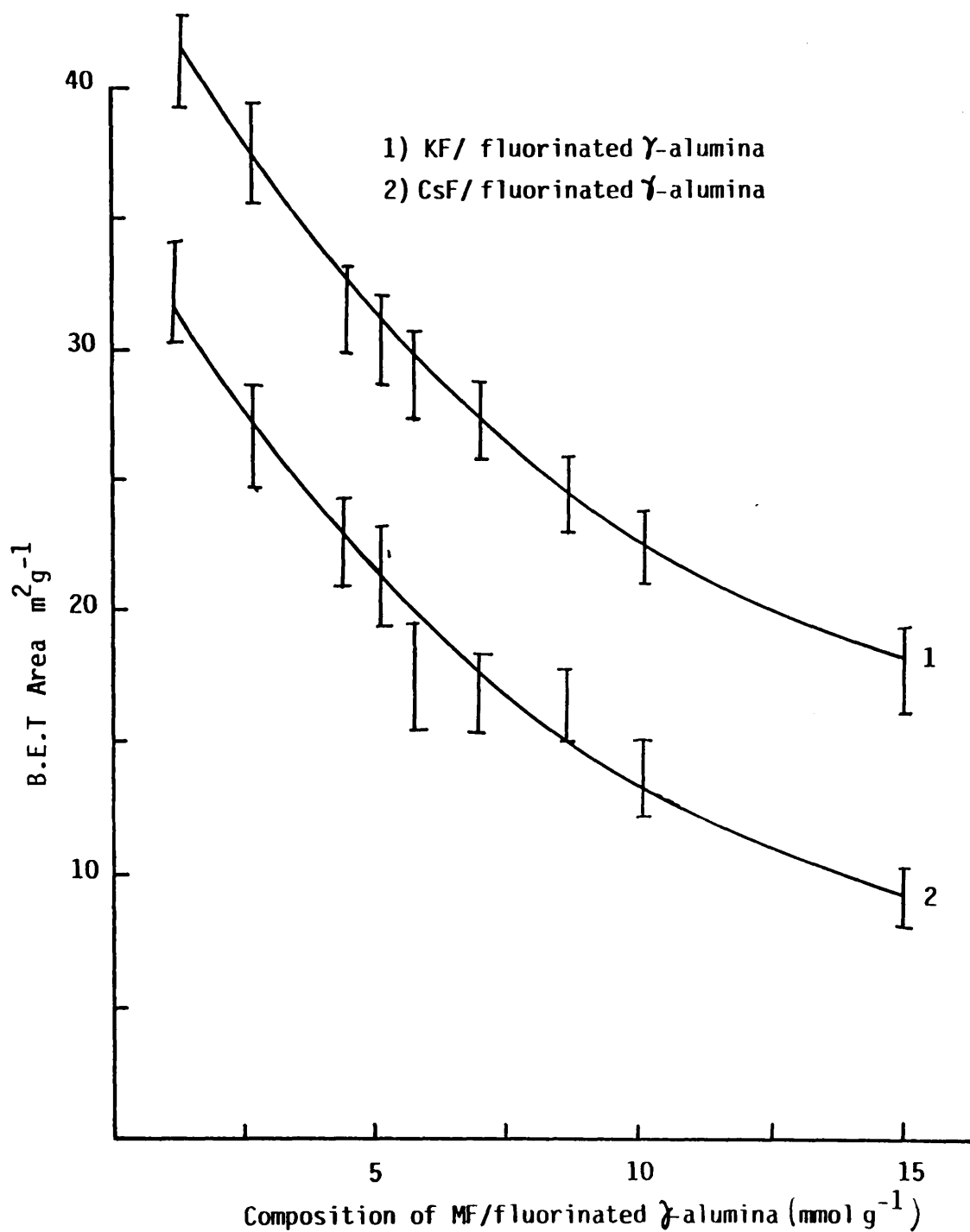


Table 4.10 The B.E.T. Area of  $\alpha$ -alumina Pretreated with Sulphur Dioxide then Anhydrous Hydrogen Fluoride

Composition	Surface Area of Fluorinated Materials					
	Aqueous Solution Preparation		Non-Aqueous Solution Preparation			
	CsF/ $\alpha$ -alumina	KF/ $\alpha$ -alumina	CsF/ $\alpha$ -alumina	KF/ $\alpha$ -alumina	CsF/ $\alpha$ -alumina	KF/ $\alpha$ -alumina
1.1	33 - 37	40 - 46	34 - 39	42 - 50		
2.0	23 - 28	32 - 36	23 - 28	32 - 37		
4.4	20 - 24	28 - 33	21 - 25	27 - 30		
5.5	18 - 22	26 - 31	19 - 23	26 - 30		
8.8	14 - 18	20 - 24	14 - 19	19 - 23		
15.0	8 - 12	16 - 20	8 - 11	17 - 21		



Figure 4.10 B.E.T Area of MF/ fluorinated  $\gamma$ -alumina with  $\text{SO}_2$  then HF

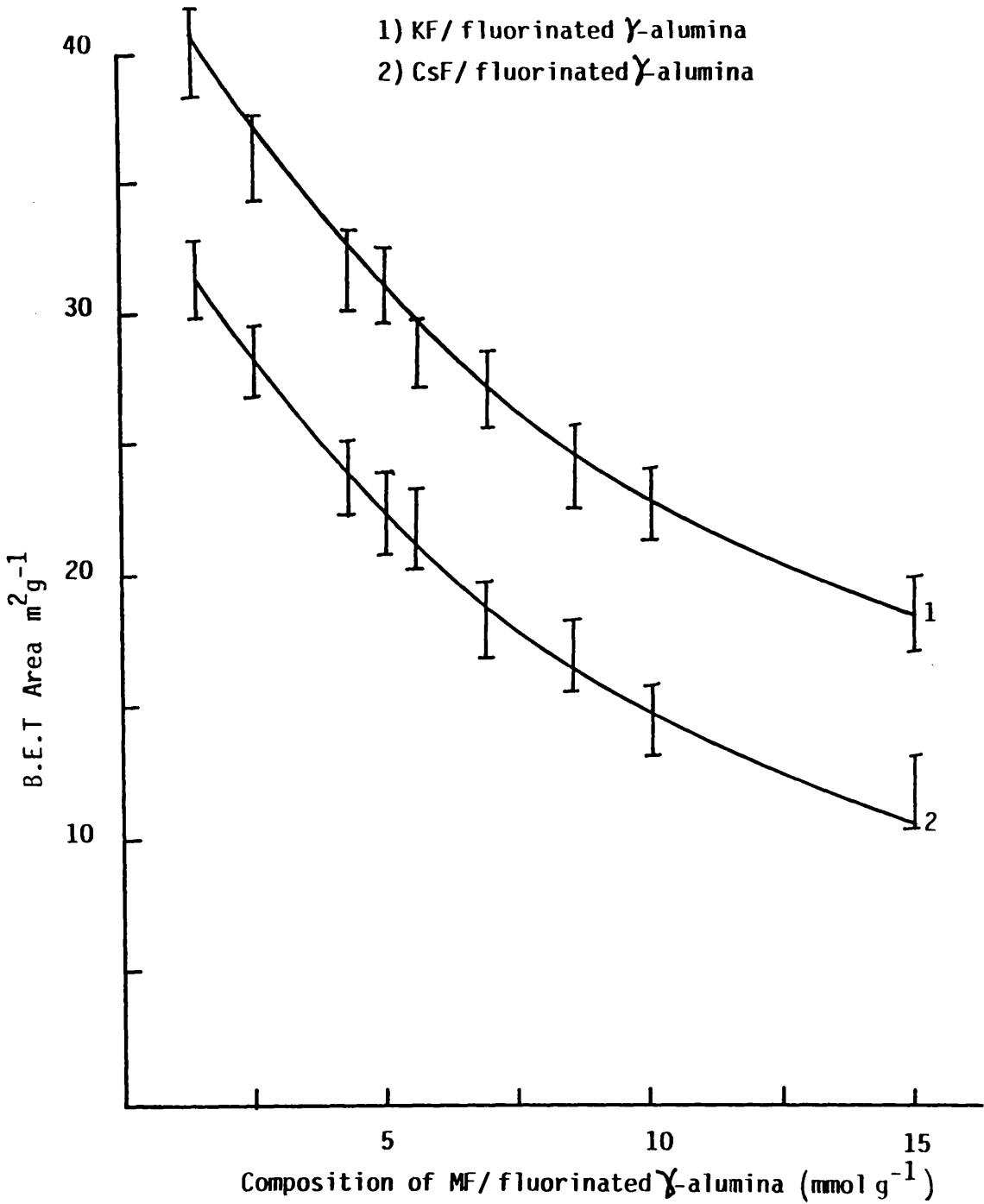


Figure 4.11 B.E.T Area of CsF/ $\gamma$ -alumina prepared from,

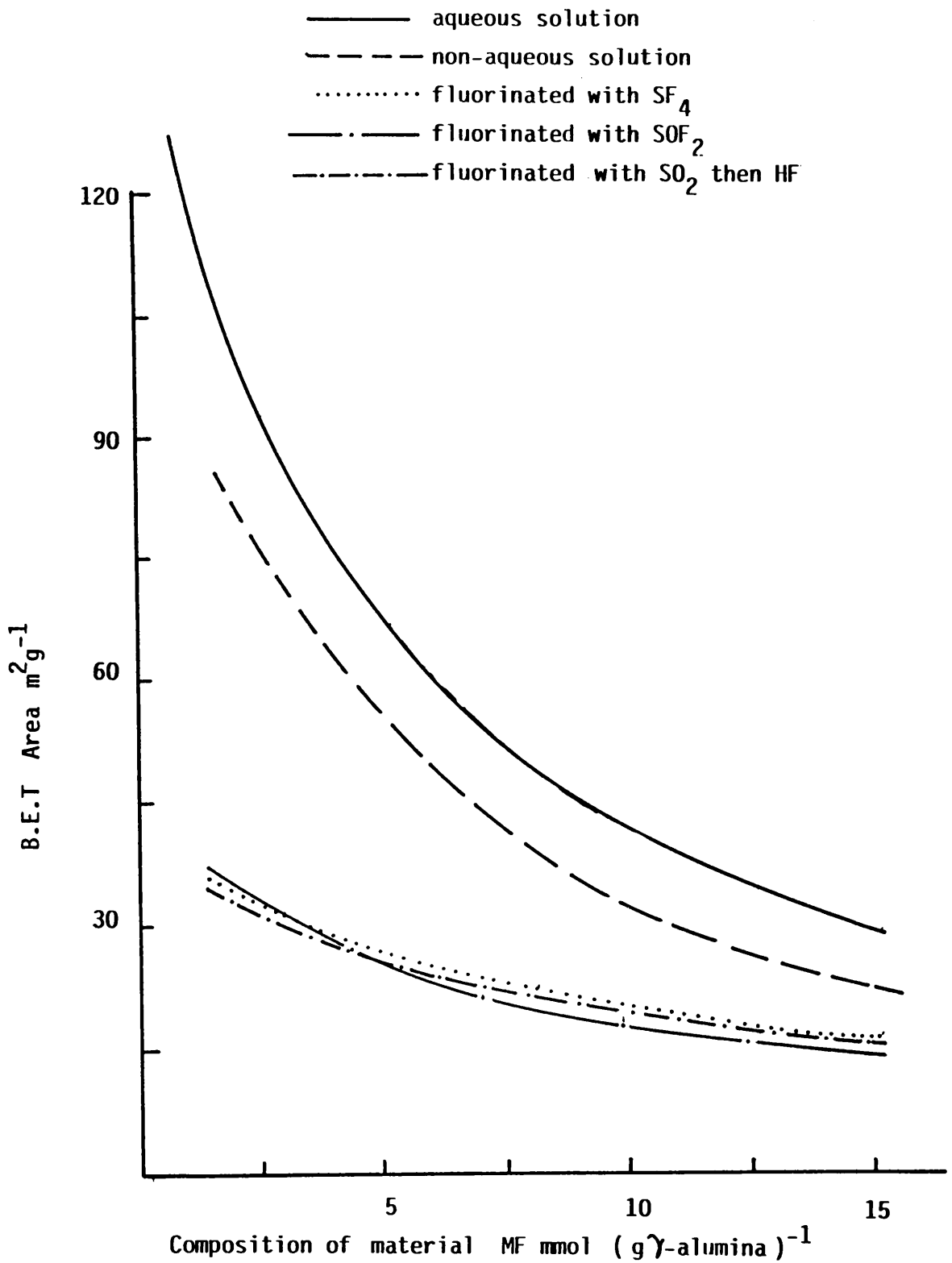
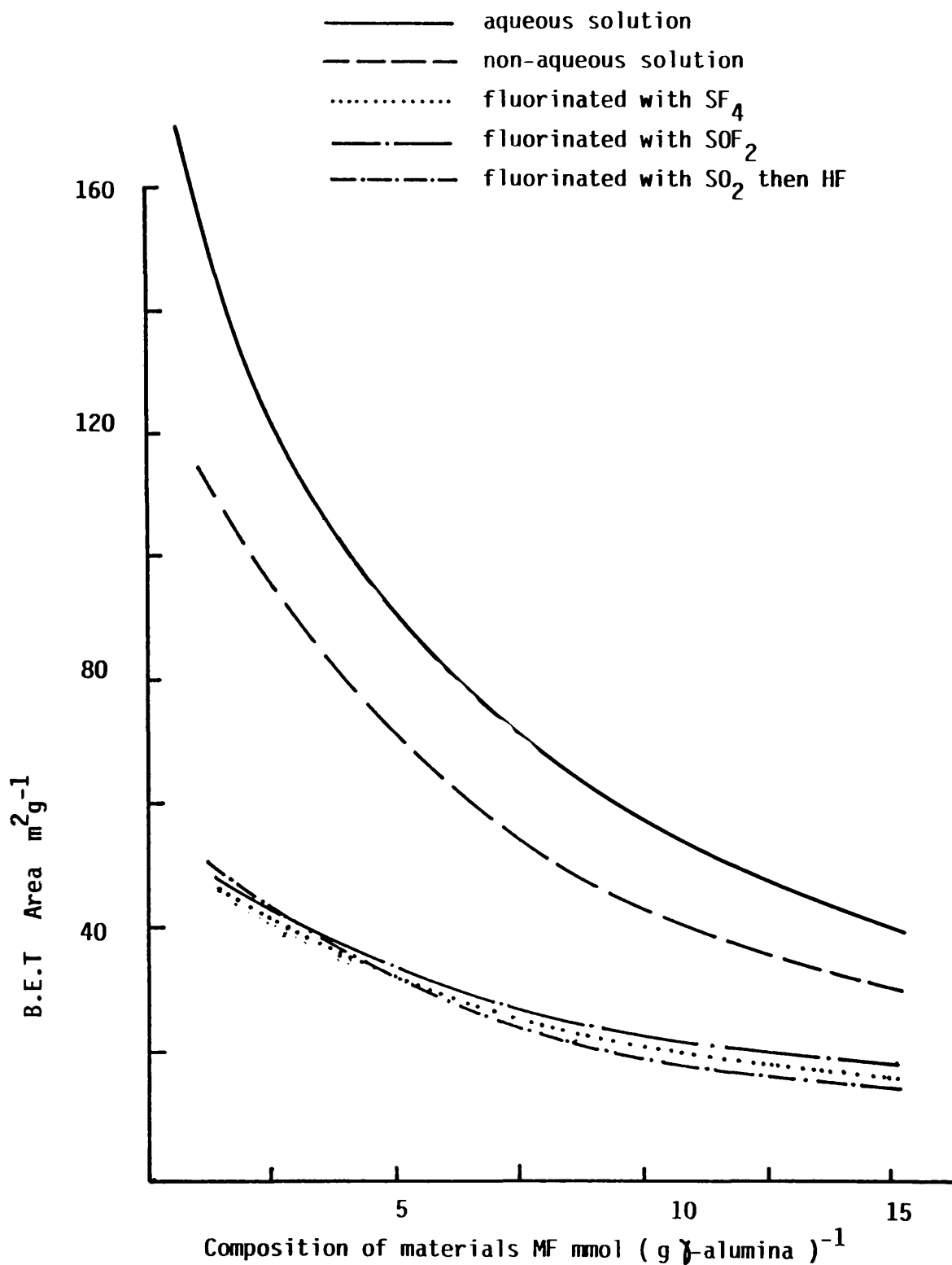


Figure 4.12 B.E.T Area of KF/ $\gamma$ -alumina, prepared from,



**Table 4.11 BET Area of Metal Fluoride Supported on  $\gamma$ -alumina Fluorinated with HF or COF<sub>2</sub>**

---

Composition mmolg <sup>-1</sup>	BET m <sup>2</sup> g <sup>-1</sup>	
	KF/HF- $\gamma$ -alumina	KF/COF <sub>2</sub> - $\gamma$ -alumina
4.4	10 - 15	47 - 52
8.8	6 - 10	39 - 45

---

on anhydrous hydrogen fluoride treated  $\gamma$ -alumina > caesium fluoride supported on anhydrous hydrogen fluoride treated  $\gamma$ -alumina > anhydrous aluminium(III) fluoride activated at 373 K.

#### 4.2 X-RAY POWDER DIFFRACTION STUDY

Prior to examination for any phase changes, the interatomic bond distances were required for the  $\gamma$ -alumina calcined to 523 K, and the d-spacings for  $\gamma$ -alumina or fluorinated  $\gamma$ -alumina supported caesium or potassium fluoride. This was achieved by the x-ray powder diffraction studies on the crystalline materials.

##### 4.2.1 X-Ray Powder-Diffraction of Spinel $\gamma$ -Alumina Calcined to 523 K and $\gamma$ -Alumina Treated with Sulphur Tetrafluoride, Thionyl Fluoride, Carbonyl Fluoride or Anhydrous Hydrogen Fluoride at Room Temperature.

The data obtained from the x-ray powder-diffraction, using a Cu  $K_{\alpha}$  source ( $1.5405 \text{ \AA}$ ) for  $\gamma$ -alumina calcined to 523 K, are presented in Table 4.12. From the small number of the absorption bands obtained, it was found that, the  $\gamma$ -alumina has a face centred cubic lattice the  $h^2+k^2+l^2$  series is specific for F.C.C with a length of  $12.456 \pm 0.19 \text{ \AA}$ . According to the Rooksby classification of aluminas<sup>127b</sup>, d-spacings of 1.971 and  $1.415 \text{ \AA}$  are specific to  $\gamma$ -alumina. In Fig. 1.18, it was shown that, the  $\gamma$ -alumina Spinel structure consisted of an outer face centred cubic lattice with inner cubes consisting of alternating octahedrally arranged aluminium and tetrahedrally

Table 4.12 X-Ray Powder-Diffraction for  $\gamma$ -Alumina

$2\theta$	$d$	$\sin^2$	Empirical	$h^2+k^2+l^2$	$2\sin$	$d_{ClO}$
12.4	6.2	0.0117	1	3(100)	7.13	12.34
13.8	6.9	0.0144	1.23	4(200)	6.41	12.82
28.4	14.2	0.0612	5.23	16(400)	3.14	12.56
38.1	19.65	0.1065	9.20	27(333)	2.36	12.26
46.1	23.05	0.1527	13.05	40(620)	1.971	12.46
47.8	23.9	0.1641	14.02	43(533)	1.90	12.46
65.9	32.95	0.2958	25.28	76(662)	1.415	12.29

$$d = \frac{a}{\sqrt{h^2 + k^2 + l^2}} = 12.45 \pm 0.2 \text{ \AA}$$

arranged aluminium atoms. The (200) face of the unit cell cuts through the face centred aluminium atoms at  $6.228 \text{ \AA}^{\circ}$  and hence the octahedrally arranged aluminium cube is contained in a volume of  $18.339 \text{ \AA}^3$ . The base of this cube has the Miller indices (161) and hence the d-spacing for the face was at  $2.02 \text{ \AA}^{\circ}$  from the (100) face. Similarly, all the faces of the cube were sited at  $2.02 \text{ \AA}^{\circ}$  from the (100) or (200) faces resulting in the dimensions of the octahedral cube being  $2.188 \text{ \AA}^{\circ}$  cubed. Therefore the octahedral Al-O distance in the cube was  $2.188 \text{ \AA}^{\circ}$ . The tetrahedral aluminium cube had sides of the same dimension which resulted in the tetrahedral Al-O bond length of  $1.89 \text{ \AA}^{\circ}$ . The bond distance from the aluminium atoms that made up the face centred cubic unit cell to the oxygen atoms at the corners of the inner cubes are contained in the (660) face and resulted in a d-spacing for the face of  $1.467 \text{ \AA}^{\circ}$ , making this Al-O bond distance  $2.49 \text{ \AA}^{\circ}$ .

The x-ray powder diffraction data obtained from  $\gamma$ -alumina fluorinated with anhydrous hydrogen fluoride, carbonyl fluoride sulphur tetrafluoride or thionyl fluoride at room temperature, showed typical d-spacings due to  $\gamma$ -alumina at  $1.981$  and  $1.393 \text{ \AA}^{\circ}$ . There was no evidence for d-spacings due to anhydrous aluminium(III) fluoride in any of the samples examined. The d-spacing values for  $\gamma$ -alumina treated with anhydrous hydrogen fluoride at room temperature are presented in Table 4.13, together with typical d-spacing values for thermally activated at 373 K anhydrous aluminium(III) fluoride.

**Table 4.13** The X-ray Powder Diffraction Data for  $\gamma$ -Alumina Fluorinated with Anhydrous Gaseous Hydrogen

Anhydrous Aluminium (III) Fluoride

This Work						Literature [210]			
Fluorinated $\gamma$ -Alumina		AlF <sub>3</sub>		$\gamma$ -Alumina		AlF <sub>3</sub>			
2 $\theta$ <sup>o</sup>	d(A <sup>o</sup> )	2 $\theta$ <sup>o</sup>	d(A <sup>o</sup> )	2 $\theta$ <sup>o</sup>	d(A <sup>o</sup> )	hkl	2 $\theta$ <sup>o</sup>	d(A <sup>o</sup> )	hkl
19.68	4.51	25.16	3.539	19.48	4.56	111	25.30	3.52	110
31.72	2.82	-	-	31.96	2.80	220	-	-	-
37.80	2.38	-	-	37.60	2.39	311	-	-	-
39.70	2.27	42.80	2.113	39.40	2.28	222	44.89	2.019	210
45.8	1.981	49.36	1.839	45.90	1.977	400	51.98	1.759	220
60.96	1.521	56.34	1.633	60.94	1.52	511	58.12	1.587	321
67.20	1.393	-	-	67.18	1.395	440	-	-	-



#### 4.2.2 X-Ray Powder-Diffraction of Caesium or Potassium Fluoride Supported on $\gamma$ -Alumina or Fluorinated $\gamma$ -Alumina.

The caesium or potassium fluoride supported on  $\gamma$ -alumina or fluorinated  $\gamma$ -alumina gave x-ray powder diffraction patterns typical of  $\gamma$ -alumina with very sharp lines corresponding to the d-spacing of 1.981 and 1.393 Å. In addition to  $\gamma$ -alumina d-spacings, the x-ray powder diffraction data for the low caesium or potassium fluoride loading, that is  $\leq 5.5 \text{ mmol g}^{-1}$ , showed d-spacing due to the metal fluoride. There was no evidence for the d-spacings due to  $\text{M}_3\text{AlF}_6$ ,  $\text{M}_2\text{AlF}_5 \cdot \text{H}_2\text{O}$  or  $\text{MAlF}_4$ . Typical d-spacings for CsF/ $\gamma$ -alumina and KF/ $\gamma$ -alumina  $4.4 \text{ mmol g}^{-1}$  are given in Tables 4.14 and 4.15 respectively. The d-spacing values 3.0 and 2.671 Å are typical values for caesium fluoride and potassium fluoride respectively. These two d-spacing values correspond to the very sharp lines of the  $2\theta$  angles at  $29.71^\circ$  and  $33.54^\circ$  in the x-ray powder diffraction spectrum for CsF/ $\gamma$ -alumina and KF/ $\gamma$ -alumina. The x-ray powder diffraction for the high metal fluoride loading,  $> 5.5 \text{ mmol g}^{-1}$  clearly showed very sharp lines of the  $2\theta$  angles attributed to the metal hexafluoroaluminate,  $\text{M}_3\text{AlF}_6$ , at  $42.86^\circ$ . The corresponding d-spacing is 2.11 Å. The x-ray powder diffraction data obtained for the supported metal fluorides,  $8.8 \text{ mmol g}^{-1}$  are listed in Tables 4.16 and 4.17 respectively. The data obtained from the x-ray powder diffraction for the supported metal fluoride,  $20.0 \text{ mmol g}^{-1}$ , did not show any evidence for the caesium or potassium fluoride in the samples examined, but lines due to  $\gamma$ -alumina and hexafluoroaluminate were observed.

Table 4.14 The XRD Data for CsF/ $\gamma$ -Alumina (4.4 mmol g<sup>-1</sup>)

This Work					Literature [211]		
$\gamma$ -Alumina					CsF		
2 $\theta$ <sup>o</sup>	d(A <sup>o</sup> )	2 $\theta$ <sup>o</sup>	d(A <sup>o</sup> )	hkl	2 $\theta$ <sup>o</sup>	d(A <sup>o</sup> )	hkl
19.70	4.51	19.45	4.56	111	-	-	-
25.84	3.451	-	-	-	25.67	3.469	111
29.98	3.00	-	-	-	29.76	3.003	200
31.72	2.82	31.96	2.00	220	-	-	-
37.80	2.38	37.63	2.39	311	-	-	-
39.70	2.27	39.52	2.28	222	-	-	-
42.72	2.116	-	-	-	42.44	2.125	220
45.82	1.981	45.96	1.977	400	-	-	-
53.33	1.8130	-	-	-	50.32	1.8131	311
60.90	1.521	60.94	1.520	511	-	-	-
67.26	1.392	67.10	1.395	440	-	-	-

**Table 4.15** The XRD Data for KF/ $\gamma$ -Alumina (4.4 mmol g<sup>-1</sup>)

This Work					Literature [212]		
$\gamma$ -Alumina					KF		
$2\theta^\circ$	$d(\text{Å}^\circ)$	$2\theta^\circ$	$d(\text{Å}^\circ)$	hkl	$2\theta^\circ$	$d(\text{Å}^\circ)$	hkl
19.70	4.51	19.46	4.56	111	-	-	-
29.98	3.061	-	-	-	28.92	3.087	111
31.72	2.82	31.96	2.80	220	-	-	-
33.94	2.64	-	-	-	33.56	2.671	200
37.80	2.38	37.63	2.39	311	-	-	-
39.70	2.27	39.52	2.28	222	-	-	-
45.82	1.981	45.96	1.977	400	-	-	-
48.68	1.87	-	-	-	48.14	1.89	220
60.90	1.5210	60.94	1.520	511	-	-	-
67.20	1.393	67.10	1.3950	440	-	-	-

Table 4.16 The XRD Data for CsF/ $\gamma$ -Alumina (8.8 mmolg<sup>-1</sup>)

This Work					Literature [178]					
$\gamma$ -Alumina					CsF			Cs <sub>3</sub> AlF <sub>6</sub>		
2 $\theta$ <sup>o</sup>	d(A <sup>o</sup> )	2 $\theta$ <sup>o</sup>	d(A <sup>o</sup> )	hkl	2 $\theta$ <sup>o</sup>	d(A <sup>o</sup> )	hkl	2 $\theta$ <sup>o</sup>	d(A <sup>o</sup> )	hkl
17.32	5.12	-	-	-	-	-	-	17.04	5.2	111
19.70	4.51	19.46	4.56	111	-	-	-	-	-	-
20.07	4.42	-	-	-	-	-	-	19.88	4.47	200
25.84	3.451	-	-	-	25.67	3.469	111	-	-	-
28.60	3.12	-	-	-	-	-	-	28.44	3.14	220
29.97	3.03	-	-	-	29.71	3.003	200	-	-	-
31.72	2.82	31.96	2.80	220	-	-	-	-	-	-
34.48	2.60	-	-	-	-	-	-	34.91	2.57	222
37.80	2.38	37.63	2.39	311	-	-	-	-	-	-
39.70	2.27	39.25	2.28	222	-	-	-	-	-	-
40.43	2.23	-	-	-	-	-	-	41.08	2.22	400
42.72	2.116	-	-	-	42.44	2.125	220	-	-	-
45.82	1.981	42.96	1.977	400	-	-	-	-	-	-
53.33	1.813	-	-	-	53.33	1.8131	311	-	-	-

**Table 4.17** The XRD Data for KF/ $\gamma$  - Alumina (8.8 mmol g<sup>-1</sup>)

This Work					Literature [178]					
$\gamma$ -Alumina					KF			K <sub>3</sub> AlF <sub>6</sub>		
2 $\theta$ <sup>o</sup>	d(A <sup>o</sup> )	2 $\theta$ <sup>o</sup>	d(A <sup>o</sup> )	hkl	2 $\theta$ <sup>o</sup>	d(A <sup>o</sup> )	hkl	2 $\theta$ <sup>o</sup>	d(A <sup>o</sup> )	hkl
17.76	4.99	-	-	-	-	-	-	17.87	4.95	111
19.70	4.51	19.46	4.56	111	-	-	-	-	-	-
29.98	3.061	-	-	-	28.93	3.087	111	-	-	-
30.70	2.93	-	-	-	-	-	-	29.98	3.00	220
31.72	2.82	31.96	2.80	220	-	-	-	-	-	-
33.94	2.64	-	-	-	33.45	2.671	200	-	-	-
36.36	2.47	-	-	-	-	-	-	38.19	2.45	222
37.86	2.38	37.63	2.39	311	-	-	-	-	-	-
39.70	2.27	39.25	2.28	222	-	-	-	-	-	-
43.28	2.09	-	-	-	-	-	-	42.86	2.11	400
45.82	1.981	42.96	1.977	400	-	-	-	-	-	-
48.68	1.87	-	-	-	84.14	1.89	220	-	-	-
53.92	1.70	-	-	-	-	-	-	53.24	1.72	422
60.90	1.521	60.94	1.52	511	-	-	-	-	-	-
62.78	1.48	-	-	-	-	-	-	62.30	1.49	440
67.20	1.393	67.10	1.395	440	-	-	-	-	-	-

The x-ray powder-diffraction data for the metal fluoride supported on  $\gamma$ -alumina fluorinated at room temperature, showed  $2\theta$  lines and d-spacing values identical to those for the supported metal fluoride.

The x-ray powder-diffraction data obtained for the metal fluoride supported on  $\gamma$ -alumina fluorinated at room temperature and exposed to sulphur tetrafluoride and chlorine monofluoride mixture at 373 K, clearly showed very sharp lines of  $2\theta$  at  $28.99^\circ$  and  $51.36^\circ$ . These two  $2\theta$  values were attributed to the metal tetrafluoroaluminate ( $\text{MAlF}_4$ ). The lines due to caesium or potassium fluoride were no longer present in the samples examined. Results of the supported potassium fluoride on  $\gamma$ -alumina fluorinated and reacted at 373 K are given in Table 4.18.

#### 4.3 TRANSMISSION ELECTRON MICROSCOPY

High resolution transmission electron microscopy (TEM) is well known as a tool for the microstructural studies of metal oxide supported metals. The use of the transmission electron microscopy frequently involves the correlation of information present in both images and diffraction patterns.

Samples used for the examination were prepared as described in Section 2.1.6. The disadvantage of the preparation method is that, the material was exposed to the moisture and water vapour before insertion into the microscope.

**Table 4.18** The XRD Data for KF/ $\gamma$ -Alumina (4.4 mmol g<sup>-1</sup>) which had been exposed to a mixture of (SF<sub>6</sub> + ClF) Al 373K

This Work		Literature [181]					
		Alumina			KAlF <sub>4</sub>		
2 $\theta$	d(A $^\circ$ )	2 $\theta$	d(A $^\circ$ )	hkl	2 $\theta$	d(A $^\circ$ )	hkl
19.70	4.51	19.45	4.56	111	-	-	-
28.99	3.08	-	-	-	28.99	3.08	101,102
31.72	2.82	31.96	2.80	220	-	-	-
32.21	2.59	-	-	-	32.65	2.52	110
37.86	2.38	37.63	2.39	311	-	-	-
39.70	2.27	39.25	2.28	222	-	-	-
39.33	2.30	-	-	-	38.82	2.32	111,102
45.82	1.981	45.96	1.977	400	-	-	-
51.36	1.78	-	-	-	51.36	1.779	200,103
60.90	1.52	-	-	-	60.08	1.54	211,202
67.20	1.393	67.10	1.395	440	-	-	-

4.3.1 TRANSMISSION ELECTRON MICROSCOPY OF CAESIUM OR POTASSIUM  
FLUORIDE SUPPORTED ON  $\gamma$ -ALUMINA OR FLUORINATED  $\gamma$ -ALUMINA.

Potassium fluoride supported on  $\gamma$ -alumina or fluorinated  $\gamma$ -alumina samples were examined by transmission electron microscopy and electron diffraction patterns across the composition range 0.2 - 8.8 mmol g<sup>-1</sup>. Typical TEM micrograph for the supported potassium fluoride is shown in Fig. 4.13. Potassium fluoride particles were clearly observed, and were dispersed homogeneously on the surface of  $\gamma$ -alumina, at low potassium fluoride loading, that is,  $\leq$  5.5 mmol g<sup>-1</sup>. In some micrographs, fractions of potassium fluoride particles were clustered together in the form of aggregates. The particle size of potassium fluoride on the samples examined was measured and was ca. 25, 33 and 40 Å for 2.0, 4.4 and 5.5 mmol g<sup>-1</sup> materials. The TEM micrograph of the supported potassium fluoride, 8.8 mmol g<sup>-1</sup>, did not show any evidence for the potassium fluoride particles in all areas examined on the surface of  $\gamma$ -alumina, but an 'Al-F' phase was observed.

The electron diffraction patterns of potassium fluoride supported on  $\gamma$ -alumina or fluorinated  $\gamma$ -alumina were obtained and are shown in Figs. 4.14 and 4.15. All the supported potassium fluoride samples gave electron diffraction patterns typical for  $\gamma$ -alumina and the d-spacing values measured, using a graphite standard, are listed in Table 4.19. The electron diffraction data for previously calcined  $\gamma$ -alumina to 523 K did



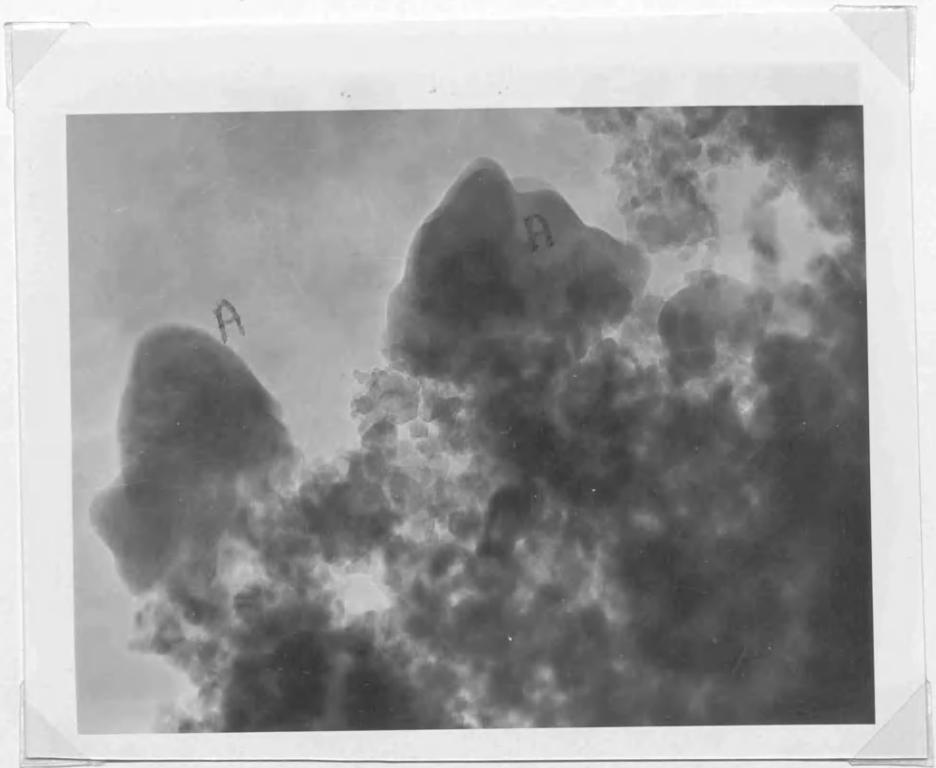


Figure 4.13 TEM Micrograph of KF/ $\gamma$ -alumina, 4.4 mmol/g  
A= KF particle

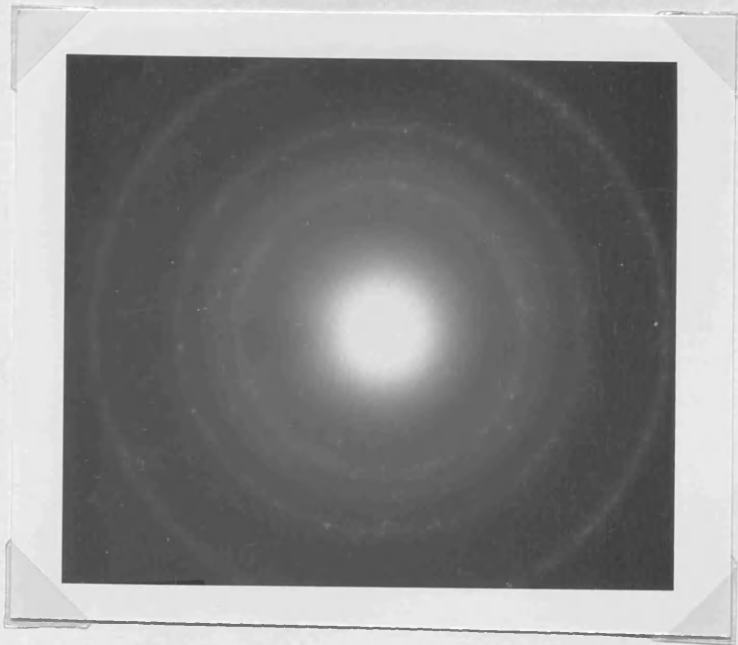
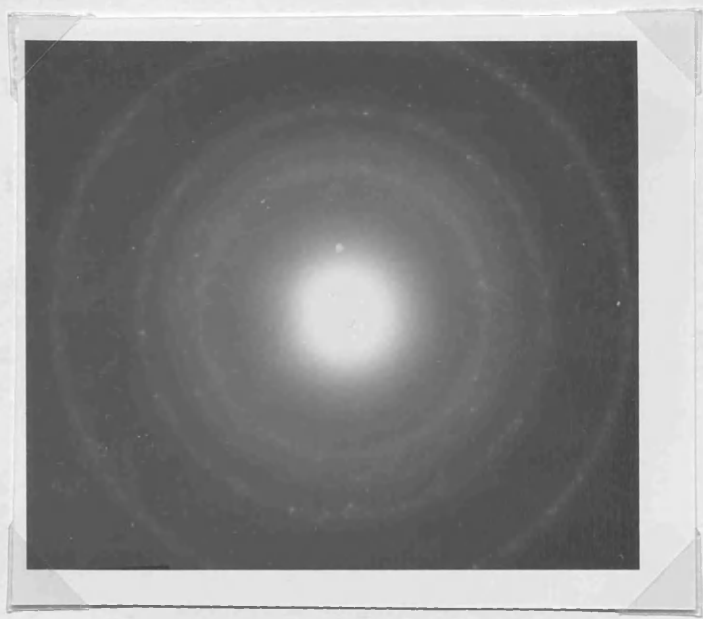


Figure 4.14 EDP Micrograph of KF/ $\gamma$ -alumina

Thin Spot	Alumina	127b
100	100	100
200	200	200
300	300	300
400	400	400
500	500	500
600	600	600
700	700	700
800	800	800
900	900	900
1000	1000	1000

Figure 4.15 EPD Micrograph of KF/ fluorinated  $\gamma$ -alumina



**Table 4.19** EDP Data for  $\gamma$ -Alumina calcined to 523K

<b>This Work</b>		<b>Literature 127b</b>		
<b><math>2\theta^\circ</math></b>	<b>d(A<sup>o</sup>)</b>	<b><math>2\theta^\circ</math></b>	<b>d(A<sup>o</sup>)</b>	<b>hkl</b>
19.49	4.51	19.46	4.56	111
31.94	2.81	31.96	2.80	220
37.61	2.40	37.63	2.39	311
39.48	2.30	39.52	2.28	222
45.95	1.98	45.96	1.977	400
61.03	1.51	60.94	1.520	511
67.04	1.40	67.10	1.395	440
85.13	1.13	85.10	1.14	444

not show any evidence for Boehmite  $\text{AlO}(\text{OH})$  or other aluminium oxides or hydroxides and hence, no structural damage or phase changes had occurred due to the thermal treatment. In addition to  $\gamma$ -alumina spacings, the low potassium fluoride loading, that is  $\leq 5.5 \text{ mmol g}^{-1}$ , gave rather broad diffraction rings corresponding to potassium fluoride particles, typical measured d-spacings are given in Table 4.20. Diffraction rings due to potassium fluoride were observed in most areas examined indicating perhaps well dispersed particles throughout the surface of  $\gamma$ -alumina. There was no evidence for potassium pentafluoroaluminate or hexafluoroaluminate in the areas examined, but some quite large crystals of potassium fluoride were formed under the influence of the electron beam showing that, the potassium fluoride was mobile on the surface of  $\gamma$ -alumina. Apart from the formation of the potassium fluoride crystals,  $\gamma$ -alumina calcined to 523 K and supported potassium fluoride, that is,  $\leq 5.5 \text{ mmol g}^{-1}$ , were indistinguishable. The electron diffraction patterns for the supported potassium fluoride,  $8.8 \text{ mmol g}^{-1}$ , did not show any evidence for potassium fluoride particles in any areas examined, not even under the influence of the electron beam. The data obtained for potassium fluoride supported on  $\gamma$ -alumina fluorinated with sulphur tetrafluoride,  $4.4$  and  $8.8 \text{ mmol g}^{-1}$ , were identical to those obtained for supported potassium fluoride as appropriate.

The TEM micrograph of potassium fluoride supported on  $\gamma$ -alumina treated with sulphur tetrafluoride at room temperature  $4.4 \text{ mmol g}^{-1}$ , which had been exposed to sulphur tetrafluoride and chlorine monofluoride mixture at 373 K, clearly showed the presence

Table 4.20 EDP Data for KF/ $\gamma$ -Alumina (4.4 mmolg<sup>-1</sup>)

This Work			Literature	212	
$\gamma$ -Alumina			Potassium Fluoride		
d(A°)	d(A°)	hkl	d(A°)	hkl	
4.51	4.56	111	3.087	111	
2.81	2.80	220	-	-	
2.64	-	-	2.671	200	
2.35	2.39	311	-	-	
1.98	1.977	400	-	-	
1.86	-	-	1.84	220	
1.40	1.40	444	-	-	

of potassium tetrafluoroaluminate, but potassium fluoride was no longer present in the sample examined, Fig. 4.16. The electron diffraction data showed the presence of potassium tetrafluoroaluminate with a diameter size of ca 23 Å, d-spacings are tabulated in Table 4.21 and shown in Fig. 4.17.

#### 4.4 SOLID-STATE MAGIC-ANGLE SPINNING ALUMINIUM-27 NUCLEAR MAGNETIC RESONANCE.

High resolution NMR spectroscopy of solids is now a well recognised structural tool.<sup>213</sup> Specifically Al exists in both octahedral and tetrahedral coordination and, when the ligands are oxygen, the chemical shift of <sup>27</sup>Al differs by 55-80 ppm for the different coordination.<sup>214</sup> Thus, <sup>27</sup>Al nmr can, in principle, be very useful for following the chemical shifts as a function of the temperature treatment on the composition of the solid.

##### 4.4.1 ALUMINIUM-27 MAS-NMR STUDY OF $\gamma$ -ALUMINA SUPPORTED CAESIUM OR POTASSIUM FLUORIDE.

The <sup>27</sup>Al NMR results of calcined  $\gamma$ -alumina at 523 K showed a main broad peak at 6.944 ppm attributed to the octahedral aluminium environment of calcined  $\gamma$ -alumina, Fig 4.18. A smaller broad peak at 73.1 ppm was attributed to the tetrahedral aluminium environment. Both these peaks were consistent with the values reported for the octahedral and tetrahedral aluminium environments of  $\gamma$ -alumina. Spinning side bands at 47.1 ppm and 34.1 ppm were observed and were shifted when the spin rate was



Figure 4.16 TEM Micrograph of KF/ $\gamma$ -alumina which had been exposed to (  $\text{SF}_4 + \text{ClF}$  ) at 373 K

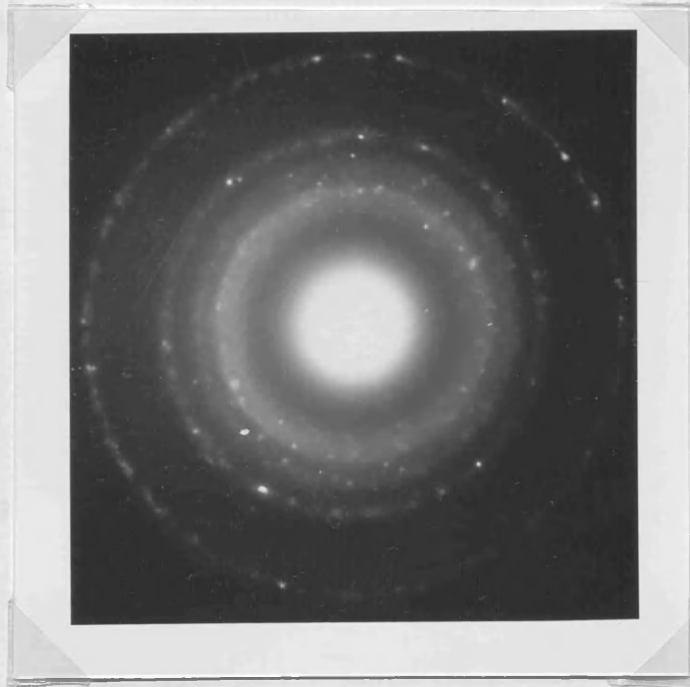


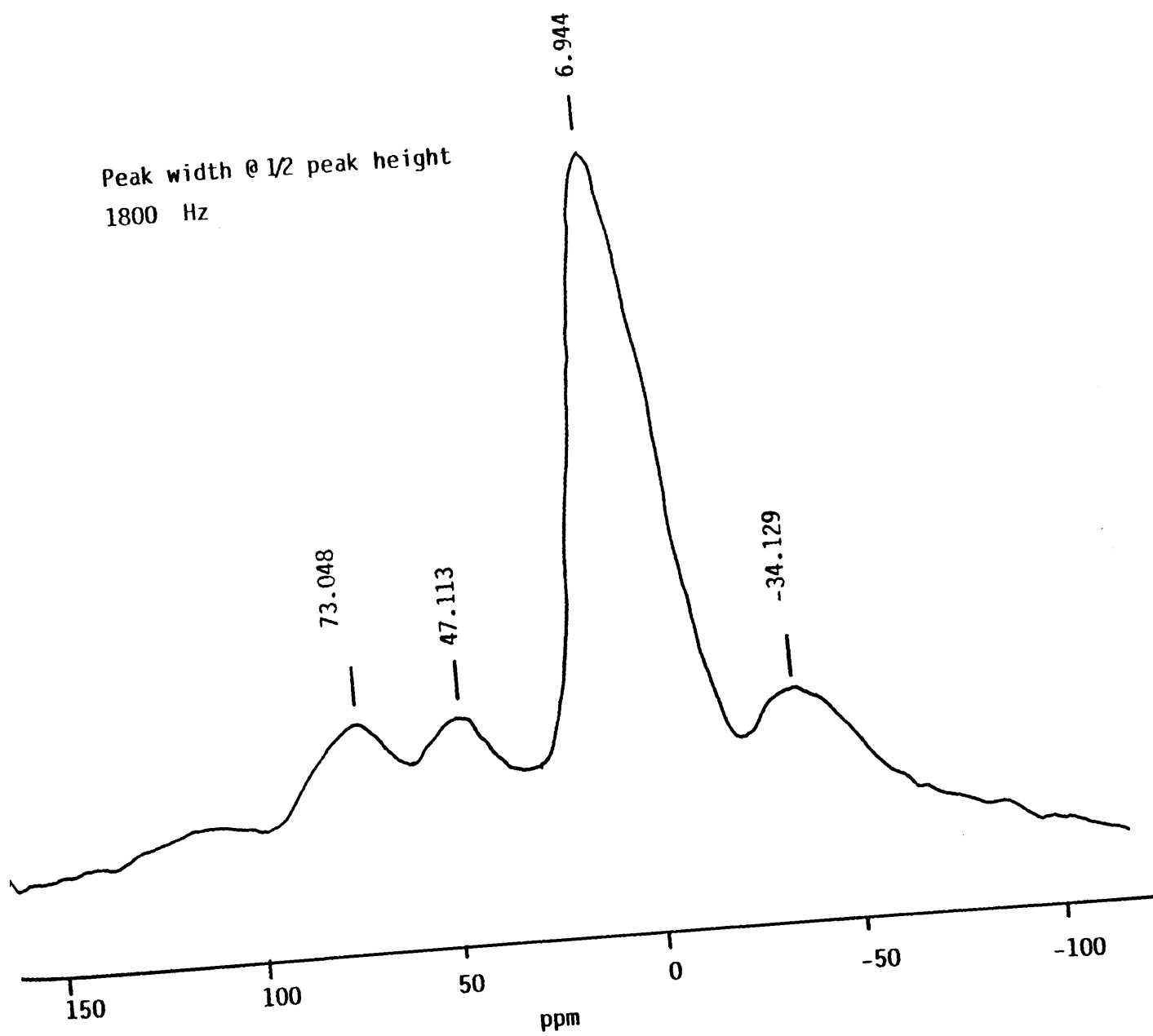
Figure 4.17 EPD Micrograph of KF/ $\gamma$ -alumina which had been exposed to (  $\text{SF}_4 + \text{ClF}$  ) at 373 K

Table 4.21 EDP Data for KF/ $\gamma$ -Alumina ( $4.4 \text{ mmol g}^{-1}$ ) which had been exposed to  $(\text{SF}_6 + \text{ClF})$  mixture at 373K

This Work			Literature [181]		
$\gamma$ -Alumina			KAlF <sub>4</sub>		
d(A°)	d(A°)	hkl	d(A°)	hkl	
4.51	4.56	111	-	-	
3.04	-	-	3.08	101,002	
2.51	2.80	220	-	-	
2.52	-	-	2.52	110	
2.35	2.39	311	-	-	
2.32	-	-	2.32	111,102	
1.98	1.977	400	-	-	
1.74	-	-	1.54	211,202	
1.53	-	-	1.538	004	
1.40	1.395	440	-	-	
1.30	-	-	1.258	220,213	



Figure 4.18  $^{27}\text{Al}$  MAS NMR of  $\gamma$ -alumina calcined to 523K Single pulse  
Spin rate 2950 Hz



raised to 4 K Hz, Fig. 4.19 . The  $\gamma$ -alumina sample calcined to 523 K, contained a peak, width at half peak height for the octahedral aluminium environments at 1.8 K Hz.

The solid-state  $^{27}\text{Al}$  MAS-NMR spectra of the supported caesium fluoride are shown in Figs 4.20 and 4.21 . for the 4.4 and 20.0 mmol  $\text{g}^{-1}$  samples respectively. Two signals were observed due to the octahedral aluminium environment at low caesium fluoride loading, that is,  $\leq 10.0$  mmol  $\text{g}^{-1}$ , and one signal at the high loading, 20.0 mmol  $\text{g}^{-1}$ , and are given in Table 4.22 across the composition range 4.4 - 20.0 mmol  $\text{g}^{-1}$ . These signals were shifted upfield from the comparable signals obtained from  $\gamma$ -alumina calcined to 523 K. The chemical shifts attributed to the tetrahedral aluminium environment for the supported caesium fluoride were also shifted upfield comparable with the corresponding signals obtained for  $\gamma$ -alumina, and are given in Table 4.22. The absolute intensities of the  $^{27}\text{Al}$  MAS-NMR spectra for the supported caesium fluoride across the composition range are shown in Fig 4.22 .

The  $^{27}\text{Al}$  MAS-NMR spectra obtained for the supported potassium fluoride are shown in Figs. 4.23 and 4.24 , for the 4.4 and 20.0 mmol  $\text{g}^{-1}$  samples respectively. Two signals were observed due to the octahedral aluminium environment at the low potassium fluoride loading, that is,  $\leq 10.0$  mmol  $\text{g}^{-1}$  and one signal only at 20.0 mmol  $\text{g}^{-1}$ , and they are given in Table 4.22. The negative signals were shifted downfield compared to the corresponding supported caesium fluoride chemical shifts, but

**Table 4.22** The 27 Al Chemical Shifts of MF/ $\gamma$ -Alumina

Chemical Shifters				
Composition $\text{mmol g}^{-1}$	C <sub>6</sub> F/ $\gamma$ -Alumina (ppm)		KF/ $\gamma$ -Alumina (ppm)	
	Al Octahedral	Al Tetrahedral	Al Octahedral	Al Tetrahedral
4.4	-1.562, 5.381	54.3	-0.694, 4.93	59.3
8.8	-1.632, 5.242	61.626	-1.18, 4.756	59.924
10.0	-1.562, 4.761	60.549	-1.25, 3.993	58.675
20.0	-1.840	55.238	-1.319	71.17

**Table 4.23** The 27 Al Chemical Shifts of (Al-F) Compounds

Compound	Chemicals Shifts ppm
AlF <sub>3</sub>	-16.63
NH <sub>4</sub> AlF <sub>4</sub>	-40.1174 and -18.592
K <sub>2</sub> AlF <sub>5</sub> H <sub>2</sub> O	-2.3436
K <sub>3</sub> AlF <sub>6</sub>	-6.413 and -1.2756

Fig. 4.19

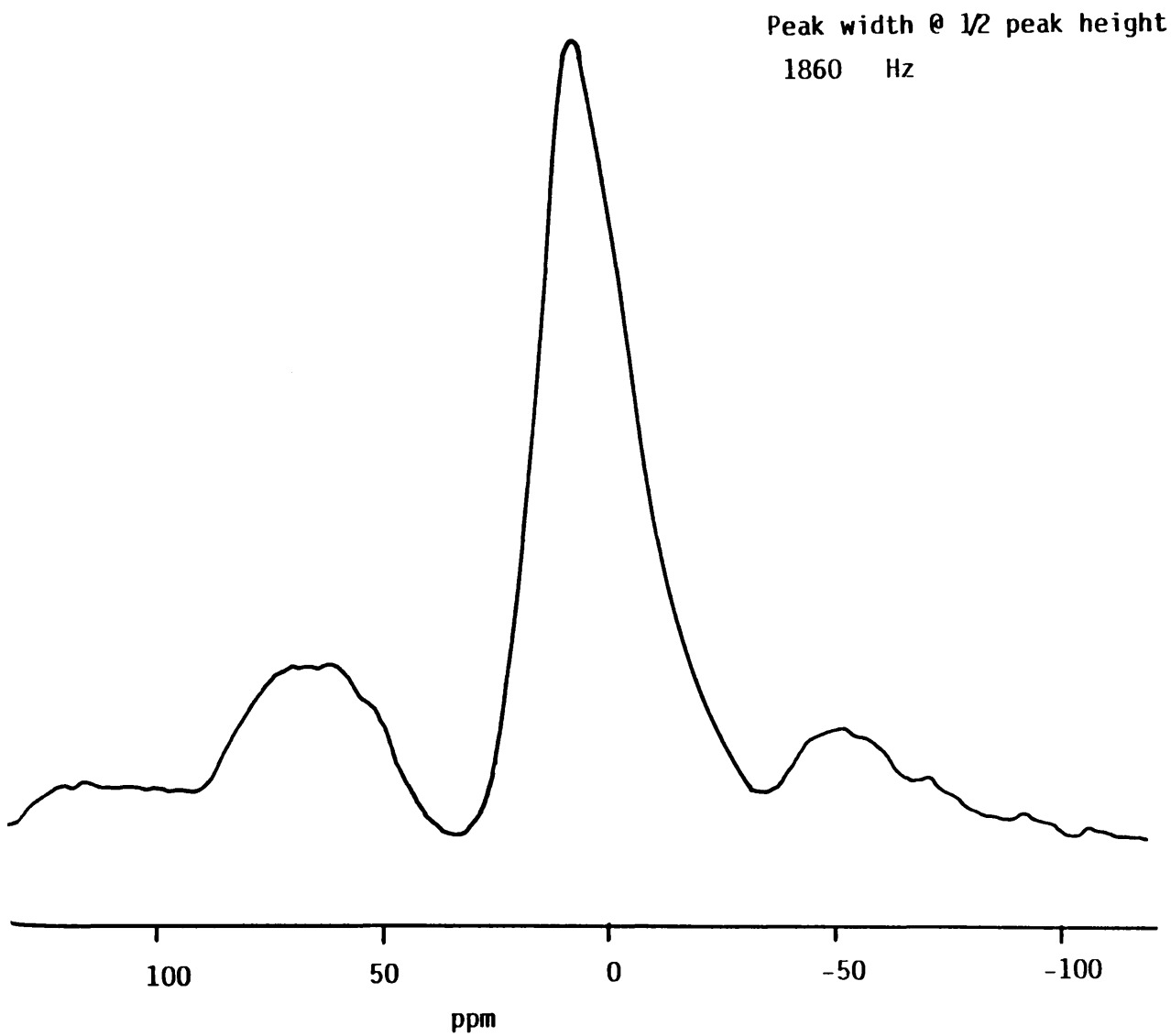


Figure 4.20  $^{27}\text{Al}$  MAS NMR of CsF/ $\gamma$ -alumina,  $4.4 \text{ mmol g}^{-1}$   
Spin rate 12 KHz

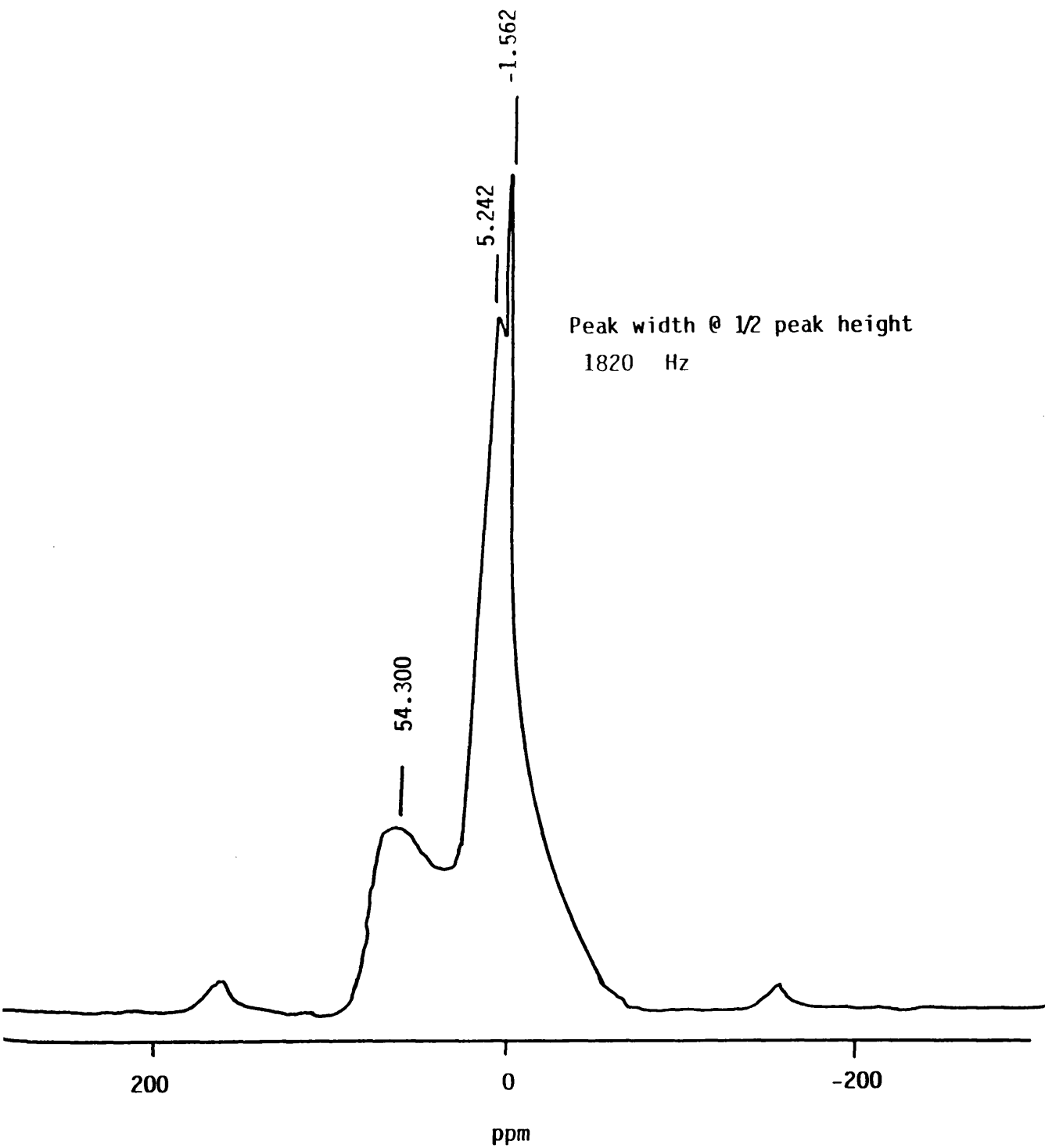


Figure 4.21  $^{27}\text{Al}$  MAS NMR of  $\text{CsF}/\gamma$ -alumina,  $20.0 \text{ mmol g}^{-1}$   
Spin rate 10 KHz

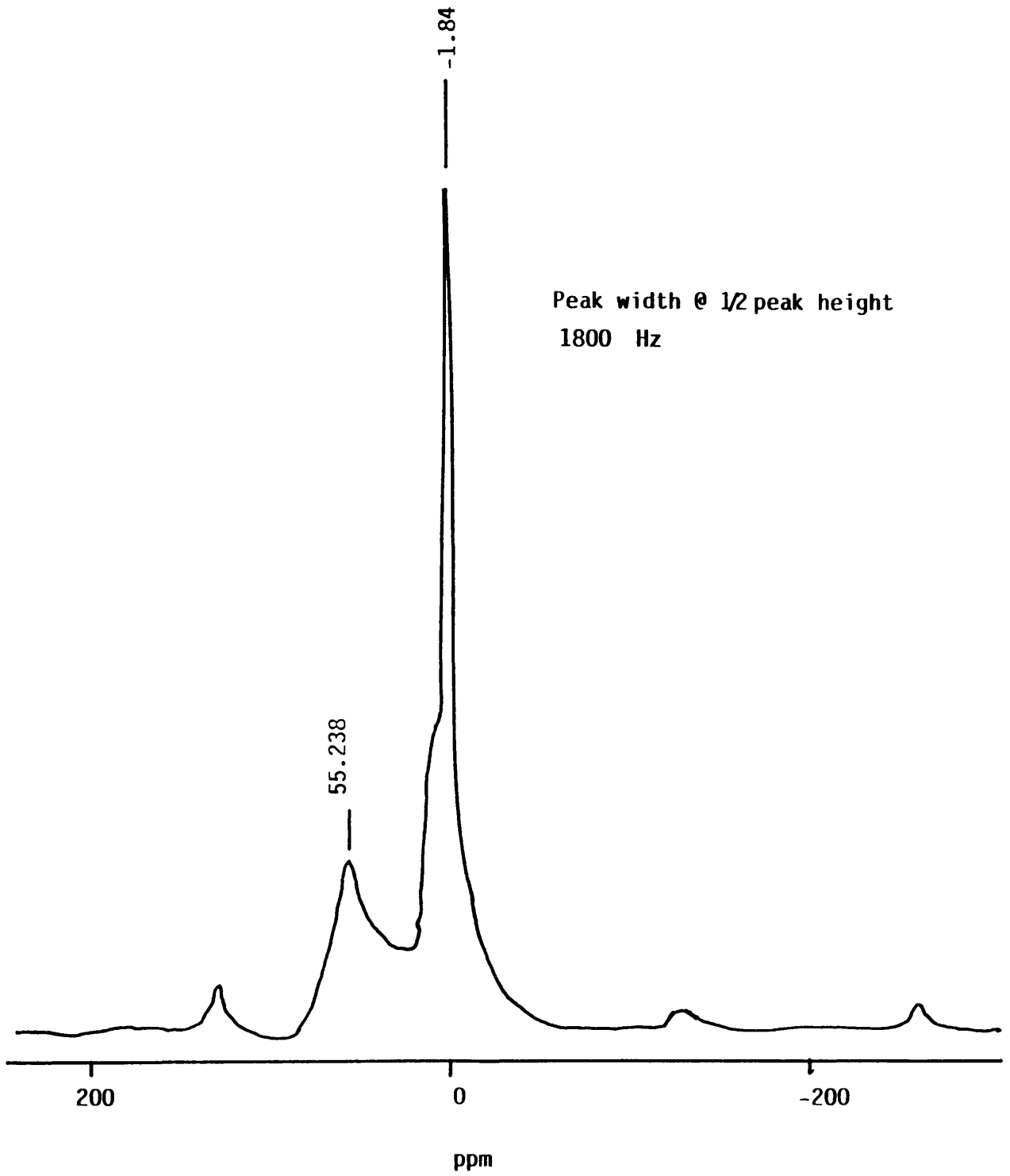


Figure 4.22

$^{27}\text{Al}$  MAS NMR of CsF/ $\gamma$ -alumina , 4.4 – 20.0 mmol g $^{-1}$

Absolute intensities

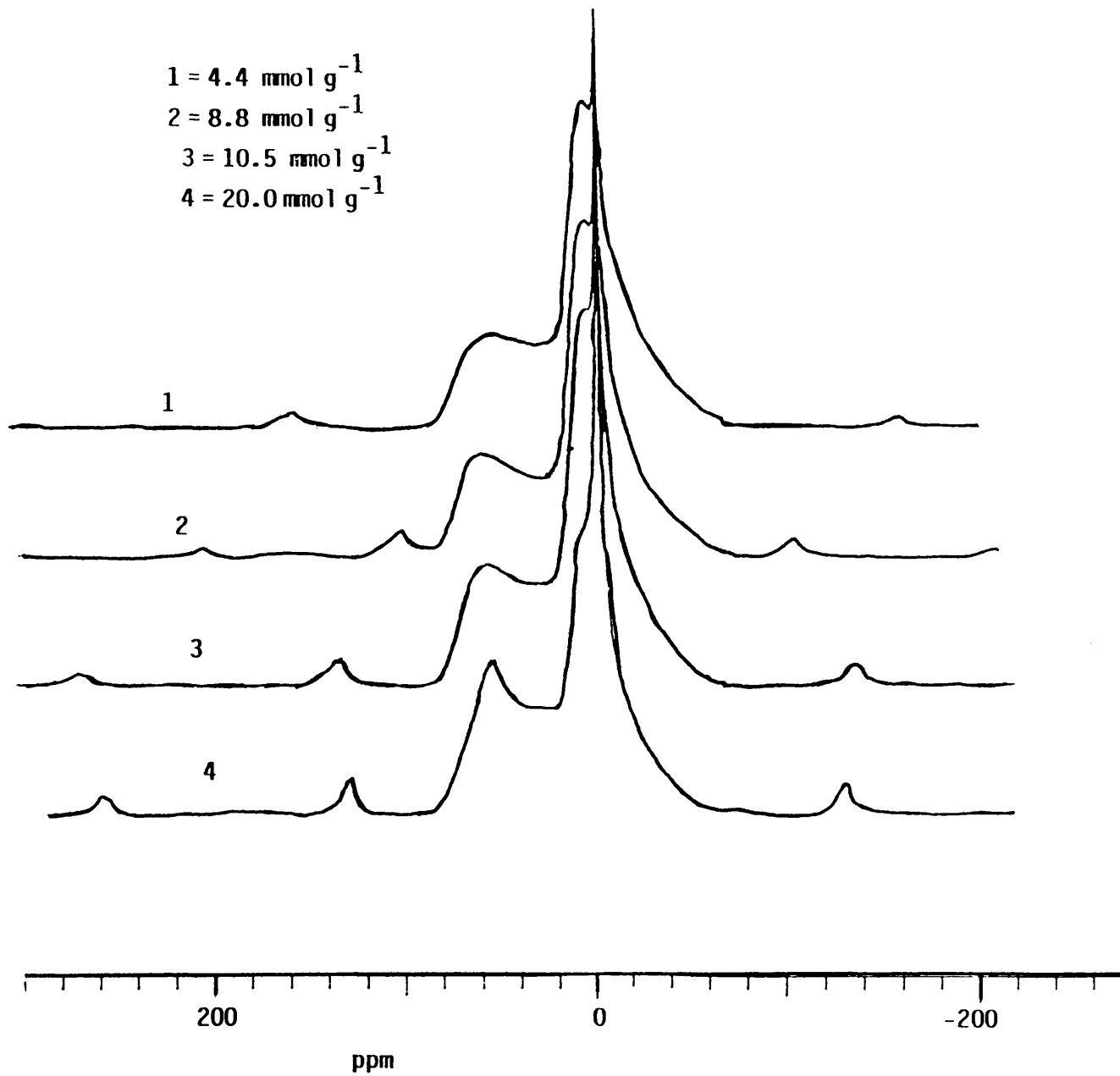


Figure 4.23  $^{27}\text{Al}$  MAS NMR of KF/ $\gamma$ -alumina,  $4.4 \text{ mmol g}^{-1}$   
Spin rate 11 KHz

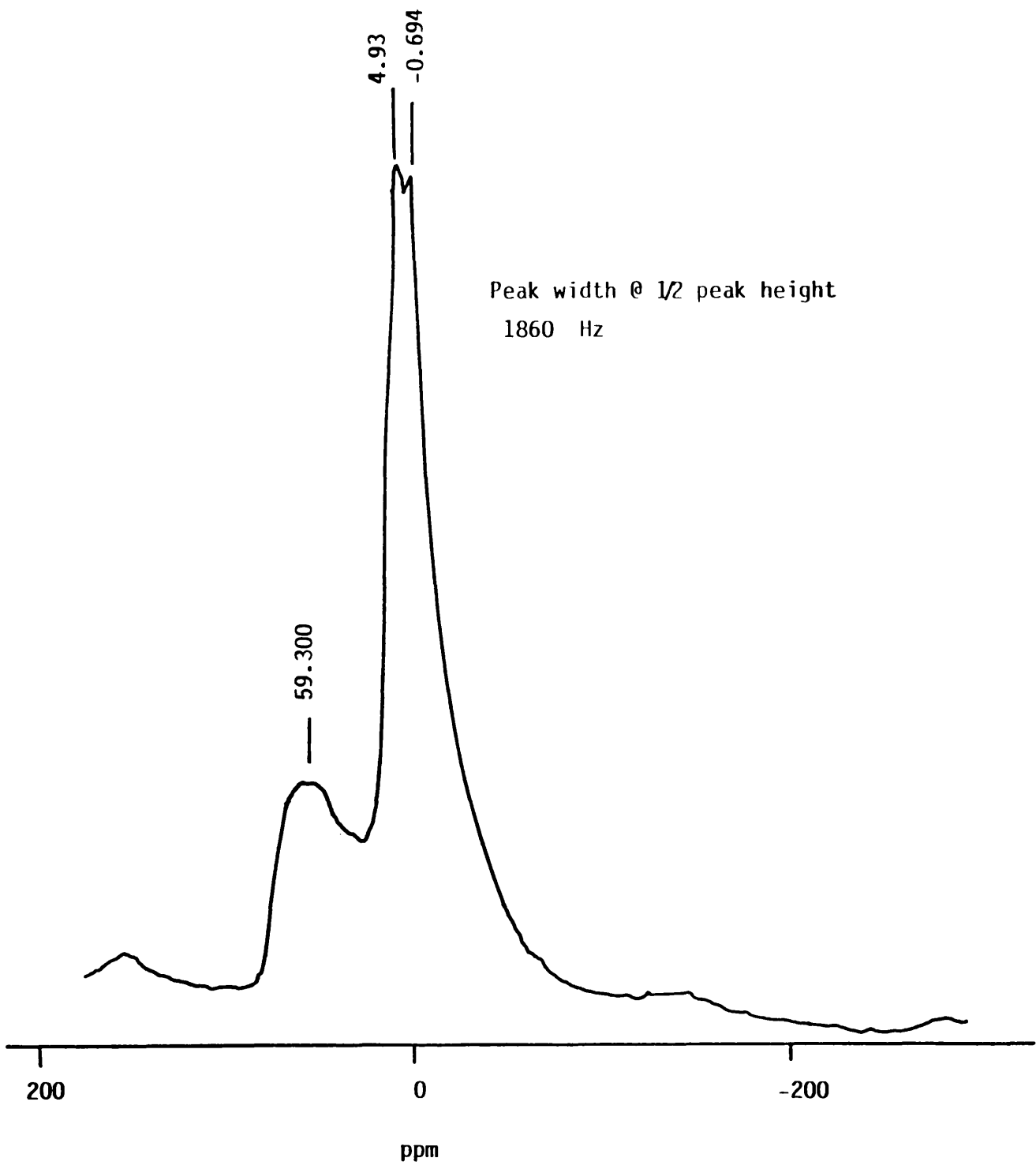
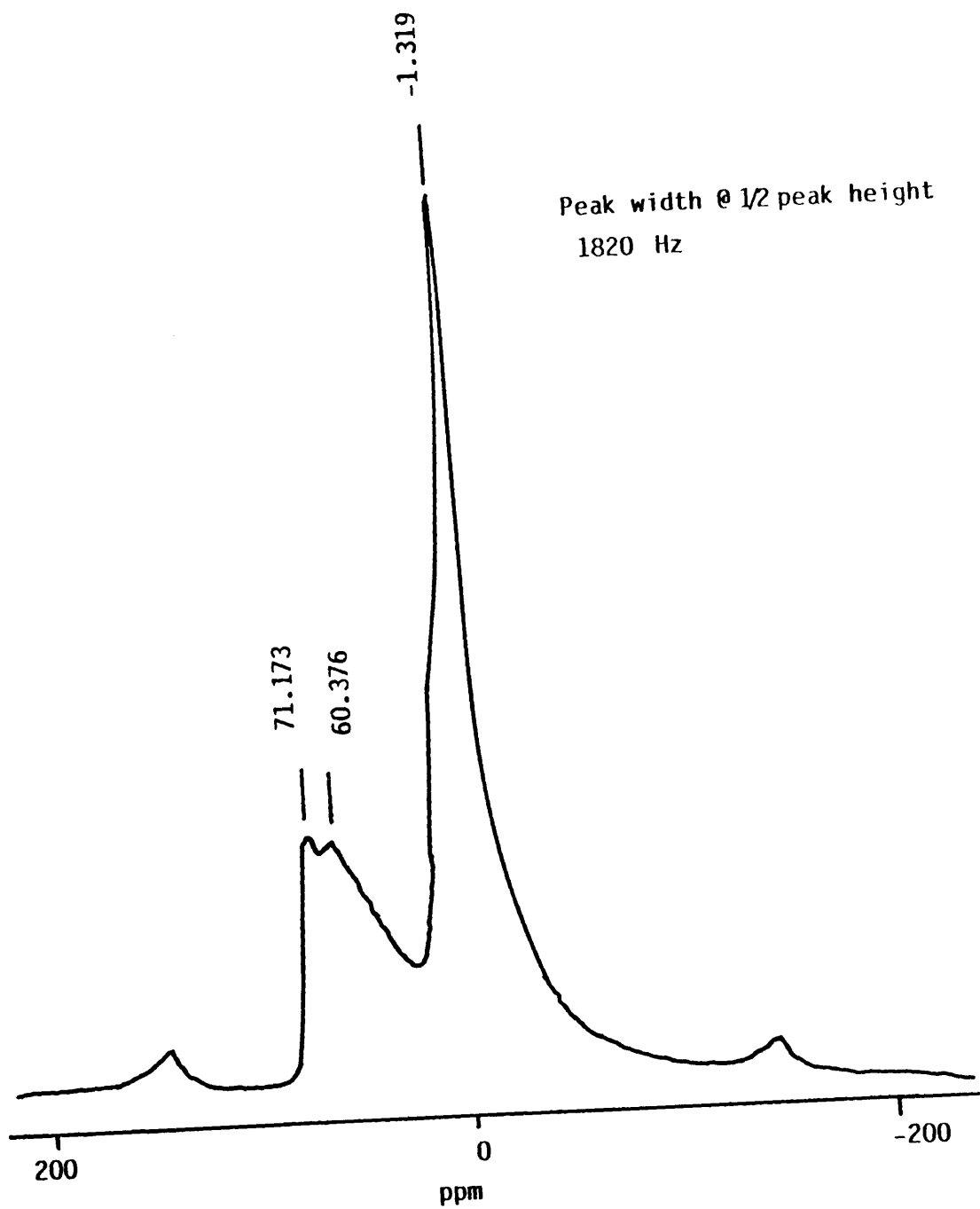




Figure 4.24  $^{27}\text{Al}$  MAS NMR of KF/ $\gamma$ -alumina,  $20.0\text{ mmol g}^{-1}$   
Spin rate 11 KHz



the positive signals were shifted upfield. The signals due to the tetrahedral aluminium environment for the supported potassium fluoride were identical to those obtained for the supported caesium fluoride and are given in Table 4.22.

The  $^{27}\text{Al}$  MAS-NMR spectrum for anhydrous aluminium(III) fluoride, potassium hexafluoroaluminate, potassium pentafluoroaluminate hydrate and ammonium tetrafluoroaluminate were obtained for comparison, and are tabulated in Table 4.23.

4.4.2 ALUMINIUM-27 MAS-NMR STUDY OF CAESIUM OR POTASSIUM  
FLUORIDE SUPPORTED ON  $\gamma$ -ALUMINA TREATED WITH SULPHUR  
TETRAFLUORIDE AT ROOM TEMPERATURE.

The  $^{27}\text{Al}$  MAS-NMR spectra for caesium fluoride supported on  $\gamma$ -alumina and treated with sulphur tetrafluoride at room temperature are presented in Fig 4.25 and 4.26 . Two signals were observed due to the octahedral aluminium environment for the supported caesium fluoride on fluorinated  $\gamma$ -alumina, 4.4 and 8.8 mmol g<sup>-1</sup>. The signals attributed to the tetrahedral aluminium environment were shifted upfield compared with the corresponding signals obtained from the supported caesium fluoride. The chemical shifts obtained are given in Table 4.24

The  $^{27}\text{Al}$  MAS-NMR spectra for potassium fluoride supported on  $\gamma$ -alumina and treated with sulphur tetrafluoride at room temperature were obtained. Two signals were observed due to the octahedral aluminium environment. The peaks attributed to the

Figure 4.25  $^{27}\text{Al}$  MAS NMR of CsF/ fluorinated  $\gamma$ -alumina ,  $4.4 \text{ mmol g}^{-1}$   
Spin rate 12 KHz

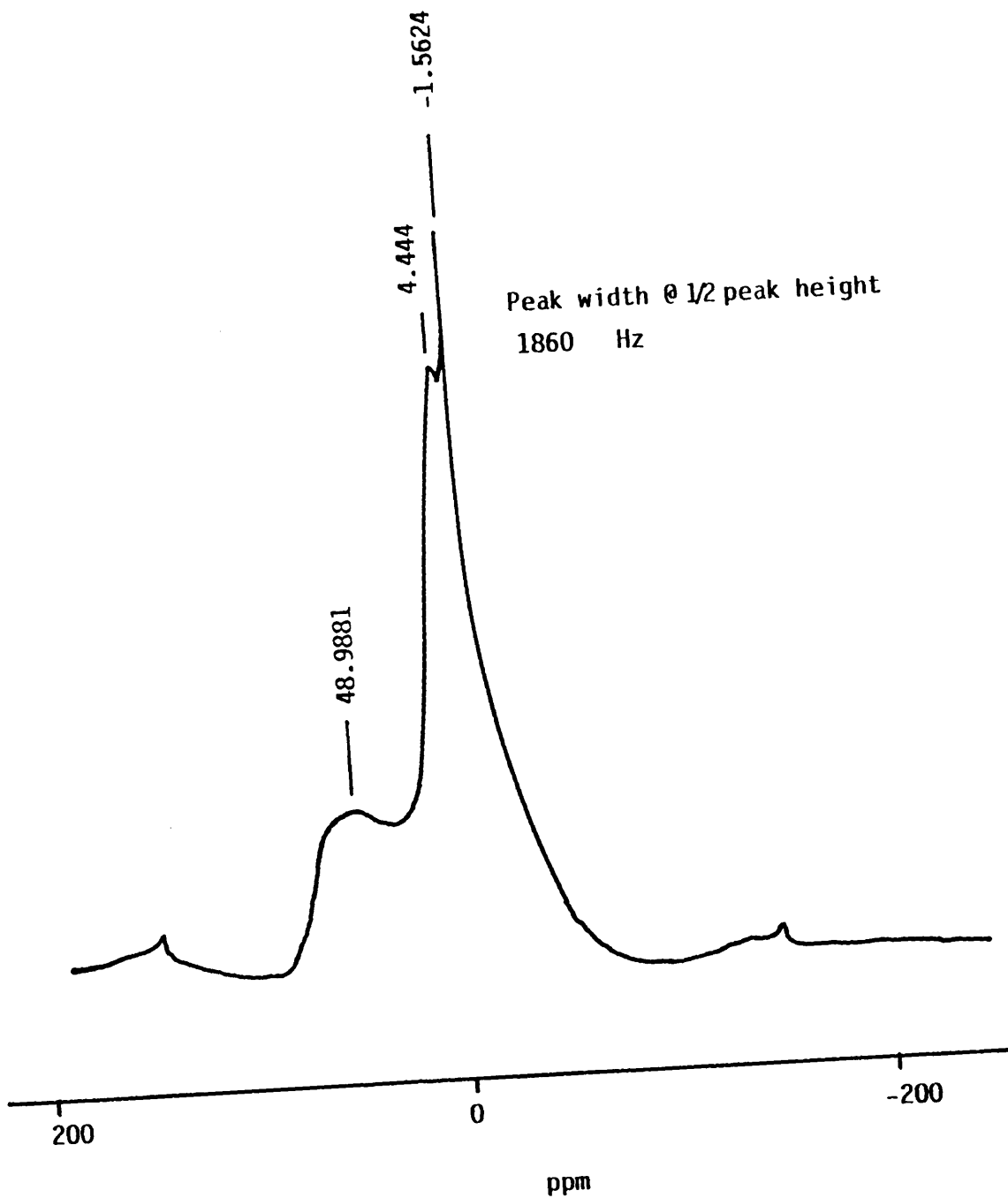


Figure 4.26  $^{27}\text{Al}$  MAS NMR of CsF/ fluorinated  $\gamma$ -alumina,  $8.8 \text{ mmol g}^{-1}$

Spin rate 11 KHz

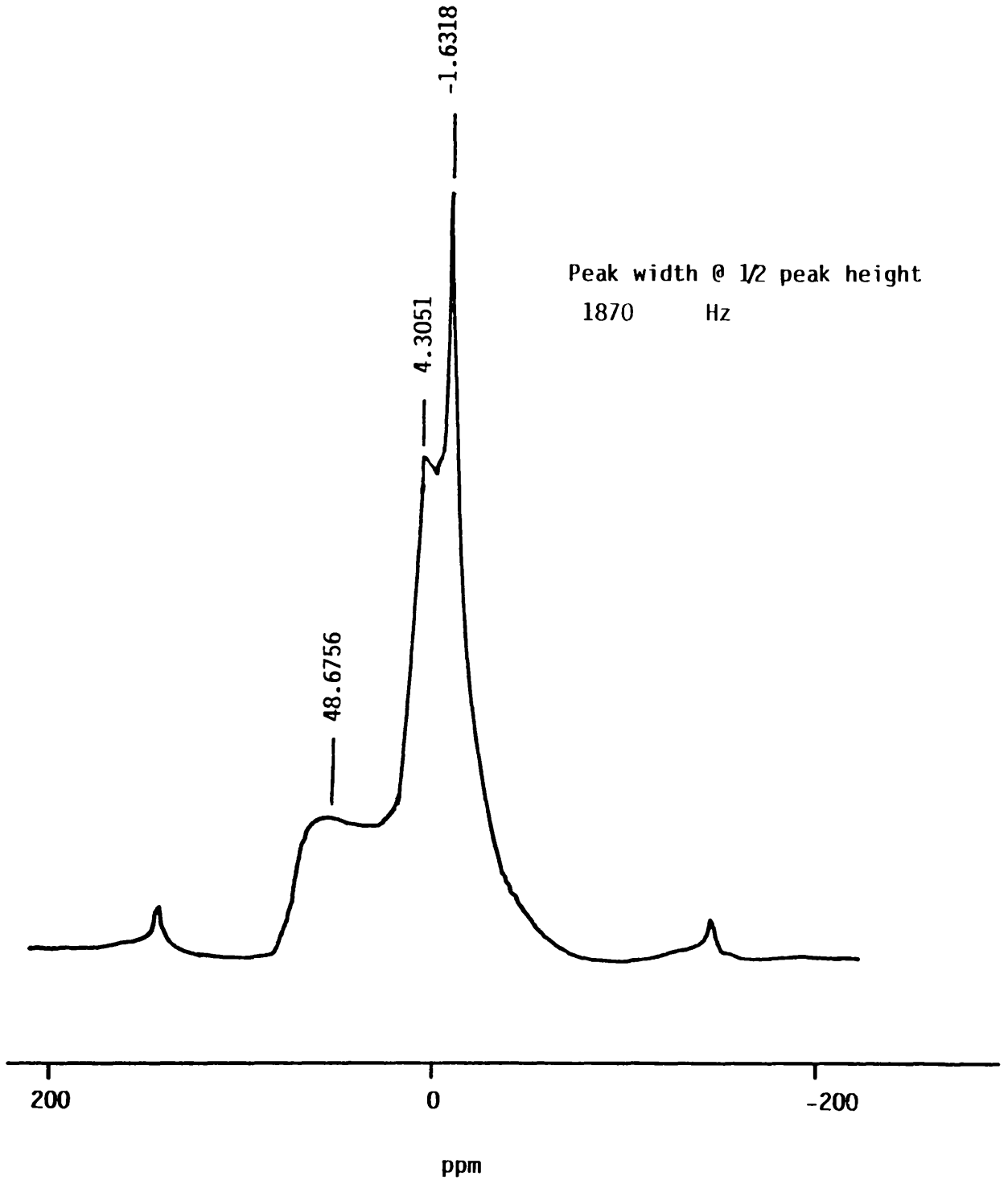


Table 4.24 The  $^{27}\text{Al}$  Chemical Shifts of  $\text{MF}/\text{SF}_6$   $\gamma$ -Alumina

Chemical Shifts ppm				
Composition $\text{mmol g}^{-1}$	$\text{C}_5\text{F}/\text{SF}_6$ - $\gamma$ Alumina		$\text{KF}/\text{SF}_6$ - $\gamma$ Alumina	
	Al Octahedral	Al Tetrahedral	Al Octahedral	Al Tetrahedral
4.4	-1.5624 & 4.4444	48.9881	-1.1805 & 5.3813	48.6756
8.8	-1.6318 & 4.3051	48.6756	-1.5624 & 4.3052	51.1753

tetrahedral aluminium environment were identical to those obtained for the supported caesium fluoride on fluorinated  $\gamma$ -alumina, and are given in Table 4.24

The  $^{27}\text{Al}$  MAS-NMR spectra for the supported metal fluoride on fluorinated  $\gamma$ -alumina  $4.4 \text{ mmol g}^{-1}$ , which had been exposed to sulphur tetrafluoride and chlorine monofluoride mixture at 373 K are shown in Fig 4.27 and 4.28. The chemical shifts obtained for the octahedral and tetrahedral aluminium environment are given in Table 4.25

#### 4.5.1 INFRA-RED SPECTRA OF CAESIUM OR POTASSIUM FLUORIDE SUPPORTED ON $\gamma$ -ALUMINA OR FLUORINATED $\gamma$ -ALUMINA.

The infra-red spectra of the materials studied were recorded on a Perkin-Elmer 983 recording spectrometer, with samples prepared as KBr discs in an inert atmosphere box as described in Section 2.3.1. The infra-red spectra of the supported metal fluoride at high metal fluoride loading, that is, above  $5.5 \text{ mmol g}^{-1}$ , had 3 characteristic bands at 395, 580 and  $760\text{-}850 \text{ cm}^{-1}$  as shown in Fig 4.29. The strong bands at 395 and  $580 \text{ cm}^{-1}$  are similar to the broad Al-F band of potassium hexafluoroaluminate Table 2.16. The broad band  $760\text{-}850 \text{ cm}^{-1}$  was due to the Al-OH stretch. However, there was no evidence for the absorption bands at 395 or  $580 \text{ cm}^{-1}$  at low metal fluoride loading, that is,  $\leq 5.5 \text{ mmol g}^{-1}$ , and a very broad band was observed at  $600 \text{ cm}^{-1}$ . In all infra-red spectra recorded across the composition range  $0.6 - 20.0 \text{ mmol g}^{-1}$ , the O-H

Figure 4.27  $^{27}\text{Al}$  MAS NMR of CsF/ fluorinated  $\gamma$ -alumina,  $4.4 \text{ mmol g}^{-1}$  which had been exposed to (  $\text{ClF} + \text{SF}_4$  ) at 373 K  
Spin rate 11 KHz

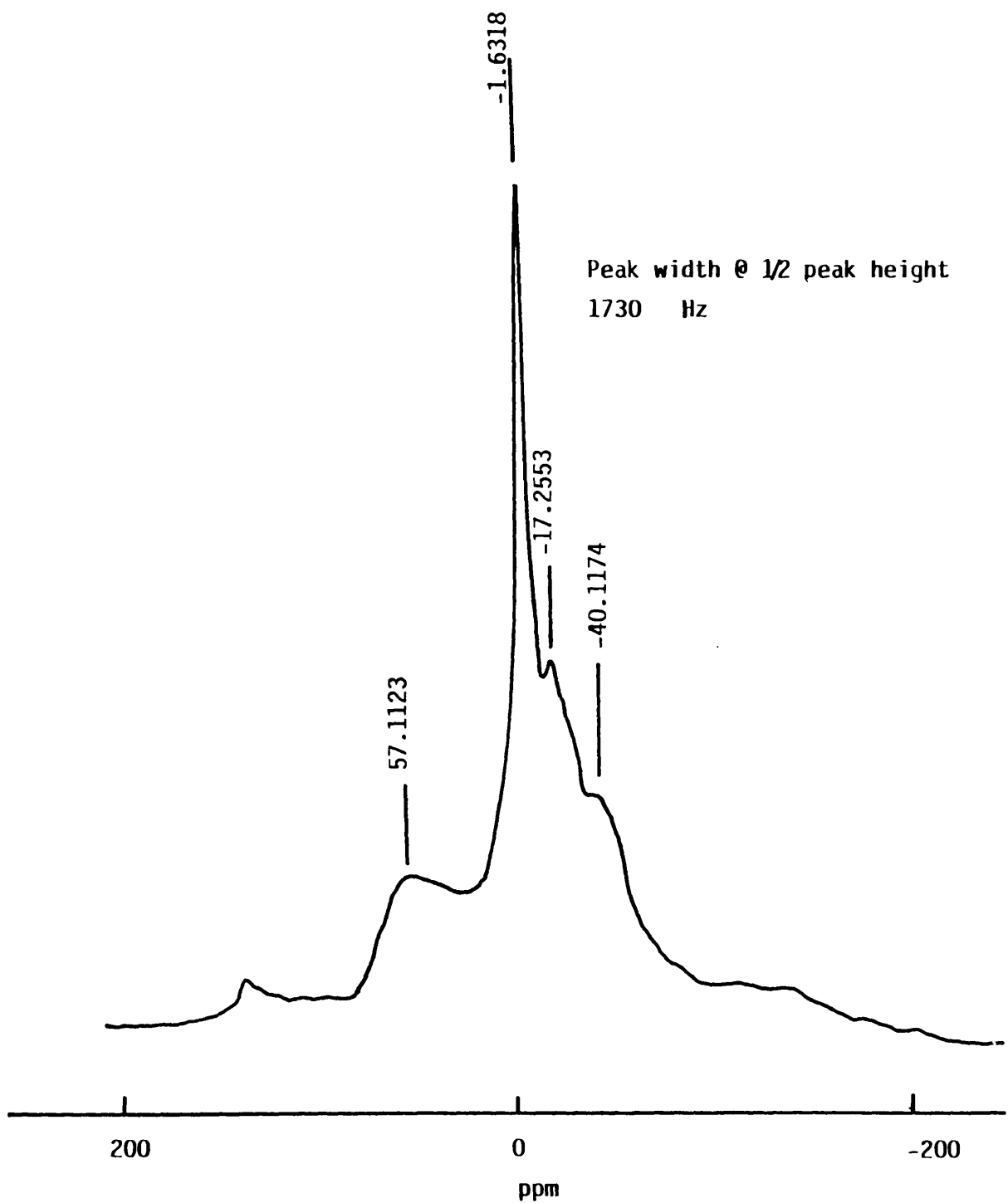
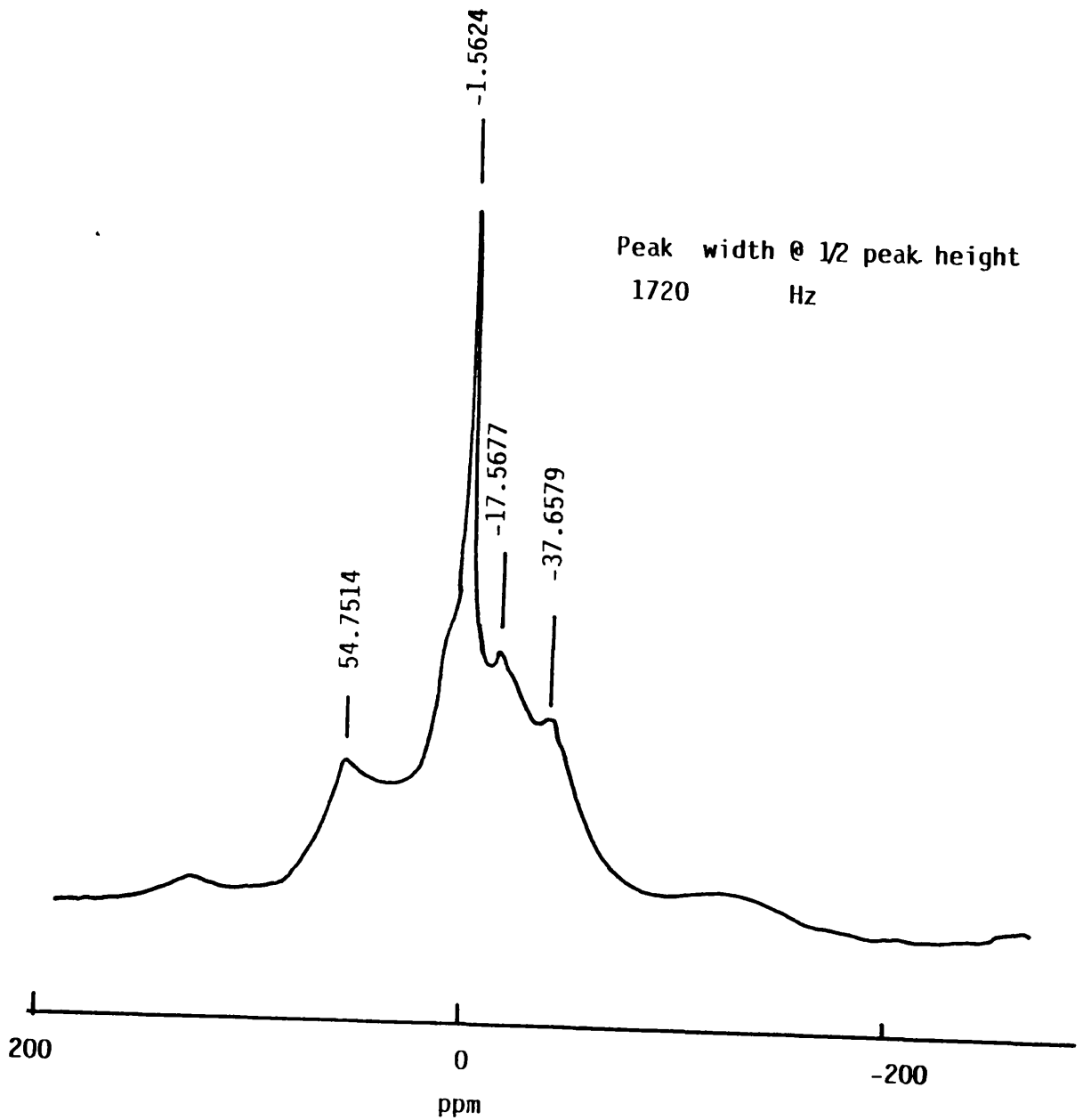


Figure 4.28  $^{27}\text{Al}$  MAS NMR of KF/ fluorinated  $\gamma$ -alumina,  $4.4 \text{ mmol g}^{-1}$  which had been exposed to ( ClF + SF<sub>4</sub> ) at 373 K

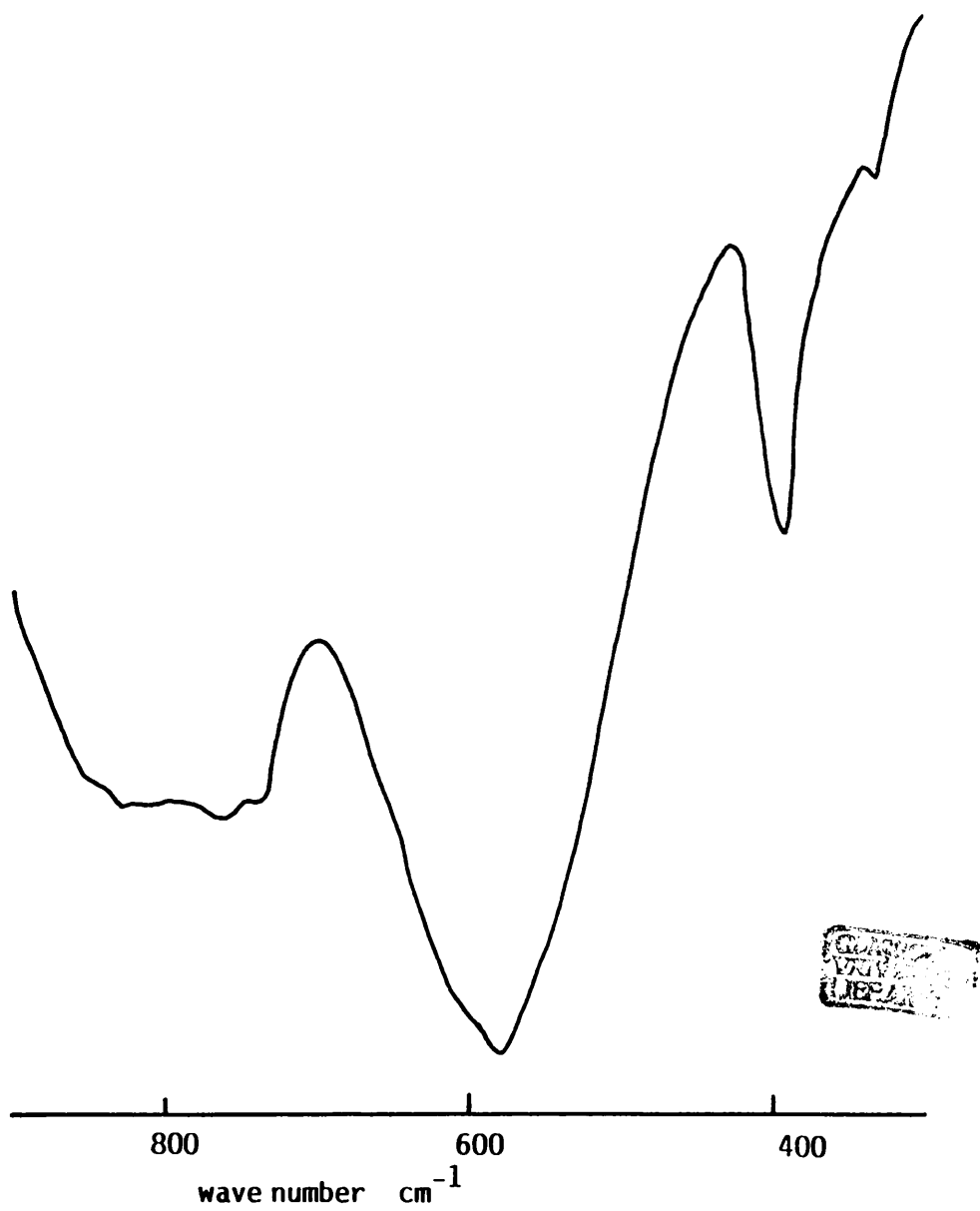




**Table 4.25** The 27 Al Chemical Shifts of MF/SF<sub>4</sub> γ-Alumina (4.4 mmolg<sup>-1</sup>) which had been treated with (SF<sub>6</sub> + ClF) mixture at 373K

Sample	Chemical Shifts ppm	
	Al Octahedral	Al Tetrahedral
C <sub>5</sub> F/SF <sub>4</sub> -γAlumina	-1.5624, -17.5677 & 39.936	54.7514
KF/SF <sub>4</sub> -γ-Alumina	-1.631, -17.2553 & 39.7183	57.1123

Figure 4.29 Intra-red spectrum of CsF/ $\gamma$ -alumina, 8.8 mmol g<sup>-1</sup>



deformation region at  $1640\text{ cm}^{-1}$  was well defined and the band at  $1400\text{ cm}^{-1}$  was broad with 2 minima, 1406 and 1438, the latter disappeared at loadings above  $8.8\text{ mmol g}^{-1}$ .

The infra-red spectra of the supported metal fluoride on fluorinated  $\gamma$ -alumina showed similar absorption bands, but after the exposure to sulphur tetrafluoride and chlorine monofluoride mixture at 373 K, new bands at 363, 610 and  $630\text{ cm}^{-1}$  were observed. These bands are similar to those obtained for ammonium tetrafluoroaluminate.

#### 4.5.2 RAMAN SPECTRA OF CAESIUM OR POTASSIUM FLUORIDE SUPPORTED ON $\gamma$ -ALUMINA.

Raman spectra for the supported metal fluoride at loadings above  $6.0\text{ mmol g}^{-1}$  showed a very broad absorption band at  $596\text{ cm}^{-1}$ . This band is similar to that obtained for potassium hexafluoroaluminate, there was, however, no evidence for this band at the low metal fluoride loading, that is,  $\leq 5.5\text{ mmol g}^{-1}$ .

FLUORIDE ION SUPPORTED ON  $\gamma$ -ALUMINA :

CHARACTERIZATION AND CATALYTIC ACTIVITY

VOLUME TWO

THESIS SUBMITTED TO THE UNIVERSITY OF GLASGOW IN

FULFILMENT OF THE REQUIREMENT OF THE DEGREE OF DOCTOR OF PHILOSOPHY

BY

ABDALLAH BENDADA BSc.

DEPARTMENT OF CHEMISTRY

UNIVERSITY OF GLASGOW

MAY 1990

© ABDALLAH BENDADA

## CONTENTS

VOLUME I

Page

## SUMMARY

i

CHAPTER ONE

## INTRODUCTION

1.1	Acid-Base Concepts	1
1.1.1	Brønsted-Lowry Definition of Acids and Bases	2
1.1.2	Lewis Acid-Base Definition	3
1.1.3	The Application of Acid-Base Reactions to Heterogeneous Systems	5
1.1.4	The Aims of the Present Work	6
1.2	Some Chemistry of the Reagents	7
1.2.1	Chlorine Monofluoride	8
1.2.2	Anhydrous Hydrogen Fluoride	9
1.2.3	Carbonyl Fluoride	11
1.2.4	Carbon Dioxide	12
1.2.5	Thionyl Fluoride	14
1.2.6	Sulphur Dioxide	15
1.2.7	Sulphur Tetrafluoride	16
1.2.8	Sulphur Chloride Pentafluoride	19
1.2.9	Chlorofluorination of Sulphur Tetrafluoride with Chlorine Monofluoride	20
1.2.10	Alkali Metal Fluorides	23
1.3	Alumina	28
1.3.1	Types of Alumina	28
1.3.2	Preparation of $\gamma$ -Alumina	30
1.3.3	Structure of $\gamma$ -Alumina	31
1.4	Previous Work Using Caesium and Potassium Fluoride Supported on $\gamma$ -Alumina	32

CHAPTER TWO

## EXPERIMENTAL

2.1	Equipment	36
2.1.1	Vacuum Systems	36
2.1.2	Gas Uptake Apparatus	38
2.1.3	Temperature Measurement	39
2.1.4	The Inert Atmosphere Box	39
2.1.5	Infra-Red Spectroscopy	39
2.1.6	Electron Microscopy	40
2.1.7	Raman Spectroscopy	42
2.1.8	Solid State $^{27}\text{Al}$ NMR Spectroscopy	42
2.1.9	X-Ray Diffraction	43
2.2	Preparation and Purification of Reagents	43
2.2.1	Purification of Acetonitrile	43
2.2.2	Purification of Diethyl Ether	44
2.2.3	Purification of Pyridine	44
2.2.4	Purification of Sulphur Dichloride	44
2.2.5	Purification of Carbon and Sulphur Dioxides	45
2.2.6	Preparation and Purification of Chlorine Monofluoride	45
2.2.7	Preparation of Sodium Tetrafluoroborate	46
2.2.8	Preparation and Purification of Boron Trifluoride	46
2.2.9	Preparation and Purification of Iodine Pentafluoride	48
2.2.10	Preparation and Purification of Sulphur Tetrafluoride	49
2.2.11	Preparation and Purification of Sulphur Chloride Pentafluoride	51

2.2.12	Preparation and Purification of Carbonyl Fluoride	51
2.2.13	Preparation and Purification of Thionyl Fluoride	52
2.2.14	Preparation of Penta- and Hexa-fluoroaluminate	53
2.2.15	Preparation of Ammonium Tetrafluoroaluminate	53
2.3	Radiochemical Techniques	54
2.3.1	Isotopic Exchange Reaction	55
2.3.2	Choice of Isotope	58
2.3.3	The Radioisotope [ $^{18}\text{F}$ ]-Fluorine	58
2.3.4	The Radioisotope [ $^{36}\text{Cl}$ ]-Chlorine	60
2.3.5	The Radioisotope [ $^{14}\text{C}$ ]-Carbon	60
2.3.6	The Radioisotope [ $^{35}\text{S}$ ]-Sulphur	61
2.4	Background	61
2.5	Statistical Errors	62
2.6	Counting of [ $^{14}\text{C}$ ]-Carbon, [ $^{36}\text{Cl}$ ]-Chlorine and [ $^{35}\text{S}$ ]-Sulphur Samples	63
2.6.1	Geiger-Müller Counters	63
2.6.2	Plateau Curve	64
2.6.3	Dead Time	64
2.6.4	The Direct Monitoring Geiger-Müller Counters	66
2.6.5	Application for the Technique to Experiments Involving Supported Metal Fluoride	67
2.7	Counting of [ $^{18}\text{F}$ ]-Fluorine Samples	68
2.7.1	Scintillation Counters	68
2.7.2	Decay Correction	70
2.7.3	[ $^{18}\text{F}$ ]-Fluorine Counting Apparatus	71
2.7.4	Application to Reactions Involving Supported Metal Fluoride	71

2.8	Preparation of Radiochemically Labelled Species	72
2.8.1	Preparation of [ $^{18}\text{F}$ ]-Fluorine Labelled Caesium Fluoride	72
2.8.2	Preparation of [ $^{18}\text{F}$ ]-Fluorine Labelled Hydrogen Fluoride, Boron Trifluoride, Carbonyl Fluoride, Sulphur Tetrafluoride and Thionyl Fluoride	73
2.8.3	Preparation of [ $^{36}\text{Cl}$ ]-Dichlorine	75
2.8.4	Preparation and Purification of [ $^{36}\text{Cl}$ ]-Chlorine Labelled Chlorine Monofluoride	76
2.8.5	Preparation and Purification of [ $^{35}\text{S}$ ]-Sulphur Labelled Sulphur Tetrafluoride, Thionyl Fluoride and Sulphur Dioxide	76
2.8.6	Preparation and Purification of [ $^{35}\text{S}$ ]-Sulphur and [ $^{36}\text{Cl}$ ]-Chlorine Labelled Sulphur Chloride Pentafluoride	78
2.8.7	Preparation and Purification of [ $^{14}\text{C}$ ]-Carbon Labelled Carbon Dioxide	79
2.8.8	Preparation of [ $^{14}\text{C}$ ]-Carbon Labelled Carbonyl Fluoride	79

### CHAPTER THREE

#### PREPARATION AND PRETREATMENT OF CATALYSTS

3.1	Preparation of Caesium or Potassium Fluoride Supported on $\gamma$ -Alumina	81
3.1.1	Preparation of Caesium or Potassium Fluoride Supported on $\gamma$ -Alumina from Aqueous Solution	81
3.1.2	Preparation of Caesium or Potassium Fluoride Supported on $\gamma$ -Alumina from Non-Aqueous Solution	82



3.1.3	Dry Preparation of Caesium and Potassium Fluoride Supported on $\gamma$ -Alumina	83
3.2	Treatment of Caesium and Potassium Fluoride Supported on $\gamma$ -Alumina	84
3.2.1	Fluorination of $\gamma$ -Alumina Supported Caesium or Potassium Fluoride with Sulphur Tetrafluoride, Thionyl Fluoride and Carbonyl Fluoride	84
3.2.2	Treatment of $\gamma$ -Alumina Supported Caesium or Potassium Fluoride with Anhydrous Hydrogen Fluoride and Sulphur Dioxide then Anhydrous Hydrogen Fluoride	86
3.3	Fluorination of $\gamma$ -Alumina by Anhydrous Hydrogen Fluoride, Sulphur Tetrafluoride, Thionyl Fluoride and Carbonyl Fluoride	88

#### CHAPTER FOUR

#### THE PHYSICAL EXAMINATION OF $\gamma$ -ALUMINA SUPPORTED CAESIUM OR POTASSIUM FLUORIDE, FLUORINATED $\gamma$ -ALUMINA SUPPORTED CAESIUM OR POTASSIUM FLUORIDE AND FLUORINATED $\gamma$ -ALUMINA

4.1	B.E.T. Area	90
4.1.1	Surface Area Determination by the B.E.T. Method	90
4.1.2	B.E.T. Area of Caesium or Potassium Fluoride Supported on $\gamma$ -Alumina	95
4.1.3	B.E.T. Area of $\gamma$ -Alumina Treated with Anhydrous Hydrogen Fluoride, Sulphur Tetrafluoride, Thionyl Fluoride or Carbonyl Fluoride	100

4.1.4	B.E.T. Area of Caesium or Potassium Fluoride Supported on $\gamma$ -Alumina Treated with Sulphur Tetrafluoride, Thionyl Fluoride Anhydrous Hydrogen Fluoride, Carbonyl Fluoride or Liquid Sulphur Dioxide then Anhydrous Hydrogen Fluoride	101
4.2	X-Ray Powder Diffraction Study	103
4.2.1	X-Ray Powder Diffraction of Spinel $\gamma$ -Alumina Calcined to 523 K and $\gamma$ -Alumina Treated with Sulphur Tetrafluoride, Thionyl Fluoride, Carbonyl Fluoride or Anhydrous Hydrogen Fluoride	103
4.2.2	X-Ray Powder Diffraction of Caesium or Potassium Fluoride Supported on $\gamma$ -Alumina or Fluorinated $\gamma$ -Alumina Supported Caesium or Potassium Fluoride	105
4.3	Transmission Electron Microscopy	106
4.3.1	Transmission Electron Microscopy of Caesium or Potassium Fluoride Supported on $\gamma$ -Alumina or Fluorinated $\gamma$ -Alumina	107
4.4	Solid State Magic Angle Spinning Aluminium-27 Nuclear Magnetic Resonance	109
4.4.1	Aluminium-27, MAS-NMR Study of $\gamma$ -Alumina Supported Caesium or Potassium Fluoride	109
4.4.2	Aluminium-27, MAS-NMR Study of Caesium or Potassium Fluoride Supported on $\gamma$ -Alumina Treated with Sulphur Tetrafluoride at Room Temperature	111

4.5.1	Infra-Red Spectra of Caesium or Potassium Fluoride Supported on $\gamma$ -Alumina or Fluorinated $\gamma$ -Alumina	112
4.5.2	Raman Spectra of Caesium or Potassium Fluoride Supported on $\gamma$ -Alumina	113

## VOLUM E II

<u>CHAPTER FIVE</u>	THE REACTIONS OF PROBE MOLECULES WITH ALKALI METAL FLUORIDES SUPPORTED ON $\gamma$ -ALUMINA	
5.1	Introduction	114
5.2	Experimental	114
5.3	The Reactions Involving Volatile Sulphur Containing Probe Molecules with Caesium or Potassium Fluoride Supported on $\gamma$ -Alumina	119
5.3.1	Infra-Red Analysis of the Hydrolysis of Sulphur Tetrafluoride over $\gamma$ -Alumina Supported Caesium or Potassium Fluoride	119
5.3.2	Monometric Study of Reactions of Sulphur Tetrafluoride with Caesium or Potassium Fluoride Supported on $\gamma$ -Alumina	121
5.3.3	The Change in the Temperature of Solid Caesium or Potassium Fluoride Supported on $\gamma$ -Alumina During Reaction with Sulphur	122
5.3.4	Reaction of [ <sup>35</sup> S]-Sulphur Labelled Sulphur Tetrafluoride with Caesium or Potassium Fluoride Supported on $\gamma$ -Alumina	122
5.3.5	Infra-Red Analysis of the Hydrolysis of Thionyl Fluoride over $\gamma$ -Alumina Supported Caesium or Potassium Fluoride	124

5.3.6	Monometric Study of Reactions of Thionyl Fluoride with Caesium or Potassium Fluoride Supported on $\gamma$ -Alumina	125
5.3.7	The Change in the Temperature of Solid Caesium or Potassium Fluoride Supported on $\gamma$ -Alumina During Reaction with Thionyl Fluoride	126
5.3.8	Reactions of [ $^{35}\text{S}$ ]-Sulphur Labelled Thionyl Fluoride with Caesium or Potassium Fluoride Supported on $\gamma$ -Alumina	126
5.3.9	Monometric Study of Reactions of Sulphur Dioxide with Caesium or Potassium Fluoride Supported on $\gamma$ -Alumina	128
5.3.10	Reactions of [ $^{35}\text{S}$ ]-Sulphur Labelled Sulphur Dioxide with Caesium or Potassium Fluoride Supported on $\gamma$ -Alumina	129
5.3.11	Reactions of [ $^{18}\text{F}$ ]-Fluorine Labelled Thionyl Fluoride with Caesium or Potassium Fluoride Supported on $\gamma$ -Alumina	131
5.3.12	Reactions of [ $^{18}\text{F}$ ]-Fluorine Labelled Sulphur Tetrafluoride with Caesium or Potassium Fluoride Supported on $\gamma$ -Alumina	133
5.4	The Reactions Involving Volatile Carbon Containing Probe Molecules with Caesium or Potassium Fluoride Supported on $\gamma$ -Alumina	137
5.4.1	Infra-Red Analysis of the Hydrolysis of Carbonyl Fluoride over $\gamma$ -Alumina Supported Caesium or Potassium Fluoride	137
5.4.2	Monometric Study of Reactions of Carbonyl Fluoride with $\gamma$ -Alumina Supported Caesium or Potassium Fluoride	137

5.4.3	Reactions of [ <sup>14</sup> C]-Carbon Labelled Carbonyl Fluoride with Caesium or Potassium Fluoride Supported on $\gamma$ -Alumina	138
5.4.4	Reactions of [ <sup>14</sup> C]-Carbon Labelled Carbon Dioxide with Caesium or Potassium Fluoride Supported on $\gamma$ -Alumina	140
5.4.5	Reactions of [ <sup>18</sup> F]-Fluorine Labelled Carbonyl Fluoride with Caesium or Potassium Fluoride Supported on $\gamma$ -Alumina	141
5.5	Reactions Involving Anhydrous Hydrogen Fluoride with Caesium or Potassium Fluoride Supported on $\gamma$ -Alumina	143
5.5.1	Monometric Study of Reactions of Anhydrous Hydrogen Fluoride with Caesium or Potassium Fluoride Supported on $\gamma$ -Alumina	143
5.5.2	Reactions of [ <sup>18</sup> F]-Fluorine Labelled Anhydrous Hydrogen Fluoride with Caesium or Potassium Fluoride Supported on $\gamma$ -Alumina	144

## CHAPTER SIX

### REACTIONS OF PROBE MOLECULES WITH $\gamma$ -ALUMINA CALCINED TO 523 K and $\gamma$ -ALUMINA FLUORINATED WITH SULPHUR TETRAFLUORIDE, THIONYL FLUORIDE, CARBONYL FLUORIDE OR ANHYDROUS HYDROGEN FLUORIDE

6.1	Introduction	146
6.2	Experimental	146
6.3	Reaction of Probe Molecules with $\gamma$ -Alumina Previously Calcined to 523 K	147
6.3.1	Reaction of Sulphur Dioxide with $\gamma$ -Alumina	147

6.3.2	Reaction of Thionyl Fluoride with $\gamma$ -Alumina Previously Calcined to 523 K	148
6.3.3	Reaction of Sulphur Tetrafluoride with $\gamma$ -Alumina Previously Calcined to 523 K	150
6.3.4	Reaction of Carbon Dioxide with $\gamma$ -Alumina	152
6.3.5	Reaction of Carbonyl Fluoride with $\gamma$ -Alumina Previously Calcined to 523 K	152
6.3.6	Reaction of Anhydrous Hydrogen Fluoride with $\gamma$ -Alumina Previously Calcined to 523 K	154
6.4	Reactions of Probe Molecules with $\gamma$ -Alumina Fluorinated with Sulphur Tetrafluoride, Thionyl Fluoride, Carbonyl Fluoride or Anhydrous Hydrogen Fluoride	154
6.4.1	Reactions of Carbon Dioxide and Sulphur Dioxide with $\gamma$ -Alumina Fluorinated with Sulphur Tetrafluoride, Thionyl Fluoride, Carbonyl Fluoride or Anhydrous Hydrogen Fluoride	154
6.4.2	Reactions of Carbonyl Fluoride and Thionyl Fluoride with $\gamma$ -Alumina Fluorinated with Sulphur Tetrafluoride, Thionyl Fluoride, Carbonyl Fluoride or Anhydrous Hydrogen Fluoride	155
6.4.3	Reactions of Sulphur Tetrafluoride with $\gamma$ -Alumina Fluorinated with Sulphur Tetrafluoride, Thionyl Fluoride, Carbonyl Fluoride or Anhydrous Hydrogen Fluoride	155
6.4.4	Reaction of [ $^{18}\text{F}$ ]-Fluorine Labelled Anhydrous Hydrogen Fluoride with Fluorinated $\gamma$ -Alumina	157

CHAPTER SEVEN

CATALYTIC ACTIVITY OF CAESIUM OR POTASSIUM FLUORIDE  
SUPPORTED ON  $\gamma$ -ALUMINA FLUORINATED AT ROOM  
TEMPERATURE

7.1	Introduction	159
7.2	Experimental	159
7.3	Reactions of Sulphur and Chlorine Containing Species with Caesium or Potassium Fluoride Supported on Fluorinated $\gamma$ -Alumina	160
7.3.1	Reactions of Sulphur Tetrafluoride with Caesium or Potassium Fluoride Supported on $\gamma$ -Alumina Fluorinated at Room Temperature	161
7.3.2	Reaction of Sulphur Chloride Pentafluoride with Caesium or Potassium Fluoride Supported on Fluorinated $\gamma$ -Alumina	162
7.3.3	Reaction of Chlorine Monofluoride with Caesium or Potassium Fluoride Supported on Fluorinated $\gamma$ -Alumina	163
7.4	The Oxidative Addition of Chlorine Monofluoride to Sulphur Tetrafluoride in the Presence of Metal Fluoride Supported on Fluorinated $\gamma$ -Alumina	165
7.4.1	The Reaction of Sulphur Tetrafluoride with Metal Fluoride Supported on Fluorinated $\gamma$ -Alumina Pretreated with Chlorine Monofluoride	166
7.4.2	The Reaction of Chlorine Monofluoride with Metal Fluoride Supported on Fluorinated $\gamma$ -Alumina Pretreated with Sulphur Tetrafluoride	167

7.4.3	The Reactions of Sulphur Tetrafluoride with Chlorine Monofluoride in the Presence of Metal Fluoride Supported on Fluorinated $\gamma$ -Alumina	169
-------	--	-----

CHAPTER EIGHT      DISCUSSION

8.1	Characterization of the Supported Metal Fluoride	179
8.2	Characterization of Fluorinated $\gamma$ -Alumina	188
8.3	Catalytic Activity of Metal Fluoride Supported on Fluorinated $\gamma$ -Alumina	192
8.4	Physical Examination of Supported Metal Fluoride	197

CHAPTER NINE      CONCLUSION

APPENDIX I		204
------------	--	-----

APPENDIX II		205
-------------	--	-----

REFERENCES		206
------------	--	-----



## CHAPTER FIVE

THE REACTIONS OF PROBE MOLECULES WITH ALKALI METAL FLUORIDES SUPPORTED ON  $\gamma$ -ALUMINA

5.1 INTRODUCTION

A promising approach for the characterization of a catalyst is the use of suitable probe molecules for the quantitative determination of site density and the description of the nature of the active site. The adsorption of Lewis acids as probe molecules will provide the best test for the presence of fluoride ion. The reaction of the volatile Lewis acid sulphur tetrafluoride and its hydrolysis products, thionyl fluoride and sulphur dioxide, the Lewis acid carbonyl fluoride and its hydrolysis product carbon dioxide and the protic molecule anhydrous hydrogen fluoride are reported in this chapter. These reactions were carried out at room temperature under heterogeneous conditions using [ $^{14}\text{C}$ ]-carbon, [ $^{18}\text{F}$ ]-fluorine and [ $^{35}\text{S}$ ]-sulphur labelled probe molecules as appropriate.

5.2 EXPERIMENTAL

The manometric measurements were carried out using the apparatus described in section 2.1.2 and the following procedure. The sample bulb was loaded with an accurately weighed quantity of, for example, CsF/ $\gamma$ -alumina, 4.4 mmol (0.5g, equivalent to 1.32 mmol of caesium fluoride) in an inert atmosphere box, attached to the vacuum line then evacuated for 30 min. The gas was first admitted into the calibrated system with the sample bulb closed and the pressure was noted. After applying a correction for the volume change on expansion into the bulb, the pressure of gas calculated was taken as the pressure of gas before reaction. The sample bulb

was opened, allowing the reaction to proceed, until no change in pressure was observed. The pressure of gas recorded was taken as the pressure of gas in the presence of the solid, which was a direct measure of the total uptake of gas. The gas was condensed back into the original vessel and the pressure measured with the sample bulb closed. The pressure recorded was taken as the pressure of gas after desorption. The difference between the pressure of gas before and after reaction in the presence of the solid (with sample bulb open) was a direct measure of the total uptake, but the difference in pressure of gas before admission and after desorption of gas (with the sample bulb closed) was a direct measure of the quantity of gas permanently retained by the solid. To illustrate the method, a specimen calculation of the uptake of sulphur tetrafluoride by CsF/ $\gamma$ -alumina,  $4.4 \text{ mmol g}^{-1}$  is presented. The volume of vessel I, which contained sulphur tetrafluoride before reaction was  $61.5 \text{ cm}^3$  and the volume of vessel II, which contained the CsF/ $\gamma$ -alumina (0.5g, 1.32 mmol) was  $61.5 \text{ cm}^3$ . The pressure of sulphur tetrafluoride required to deliver 1.0 mmol into the reaction vessel at room temperature was 300 Torr. The pressure of 300 Torr in the total volume of the apparatus including the vessels ( $336.1 \text{ cm}^3$ ) was equivalent to a pressure of 367.2 Torr in the volume of the main manifold and vessel I ( $274.6 \text{ cm}^3$ ). A measured pressure of sulphur tetrafluoride (367.2 Torr) was therefore expanded into the main manifold at room temperature, then the reaction vessel II was opened. The pressure of gas at this stage would be 300 Torr in total, if there was no adsorption. After a period of 65 min at room temperature the pressure of gas was measured and was 275.8 Torr in the total volume of the apparatus ( $336.1 \text{ cm}^3$ ). The total uptake of sulphur tetrafluoride

by solid CsF/ $\gamma$ -alumina at room temperature was therefore equivalent to a pressure of 24.2 Torr in a volume of 336.1 cm<sup>3</sup> using the gas law, equation 5.1,

$$PV = nRT \quad \text{Eq. 5.1}$$

where P(atm) is the pressure of gas, V(l) the total volume, n(mol) the number of moles taken up, R(atm l mol<sup>-1</sup>K<sup>-1</sup>) the gas constant and T(K) the temperature. The quantity of sulphur tetrafluoride and/or its volatile sulphur containing products taken up was 0.44 mmol. the volatile product was removed from vessel II and condensed in vessel I at 77K. The reaction vessel II was isolated, the volatile products expanded into the main manifold (274.6 cm<sup>3</sup>) at room temperature and the total pressure was determined as 358.1 Torr. The quantity of the gas retained by the solid therefore was equivalent to a pressure of 9.1 Torr in 274.6 cm<sup>3</sup>. Using equation 5.1, the quantity of sulphur tetrafluoride retained by the solid was 0.14 mmol. A similar treatment of data was used throughout this work.

The changes in the temperature of the solid during the reaction were measured as described in section 2.1.3 using the following procedure. A weighed quantity of solid, for example, CsF/ $\gamma$ -alumina, 4.4 mmolg<sup>-1</sup> (0.5g, 1.32 mmol of CsF) was placed in vessel 2, Fig. 2.8, in an inert atmosphere box. the apparatus was evacuated, a measured pressure of gas in the range 50-300 Torr admitted and the change in the temperature recorded using a thermocouple.

Infra-red analysis of the gas phase during the reaction was carried out using the apparatus shown in Fig. 2.9 and the following procedure. A sample of CsF/ $\gamma$ -alumina, 4.4 mmolg<sup>-1</sup> (0.1g, 0.26 mmol of CsF) was placed in a small dropping vessel, fitted to the

infra-red gas cell, then evacuated. Sulphur tetrafluoride was allowed to expand into the gas cell to give a suitable pressure, eg. 15 Torr. Its infra-red spectrum was recorded, the solid sample dropped into the cell and the hydrolysis of sulphur tetrafluoride followed with time.

The composition of the volatile product was determined for each reaction by means of an infra-red spectroscopic analysis. The mole ratio of the materials was calculated from the areas under peaks as described in section 2.1.5. To illustrate the method of determining the composition of the volatile products, a single example of product identification after reaction between sulphur tetrafluoride and CsF/ $\gamma$ -alumina is given below.

Sulphur tetrafluoride (300 Torr, equivalent to 1.0 mmol in the reaction vessel) was admitted into the double limbed vessel, type II, Fig. 2.40, containing CsF/ $\gamma$ -alumina, 8.8 mmol g<sup>-1</sup> (0.5g, 1.88 mmol) and left at room temperature for 65 min. The volatile products were condensed in a vessel which had the same volume, type II, Fig. 2.40. The pressure of the volatile products measured was equivalent to 0.94 mmol. the pressure of the volatile products admitted into the infra-red cell was 16.4 Torr. The areas under the bands at 860, 1308 and 1151 cm<sup>-1</sup> were 8.7, 32.2 and 3.48 area unit, which corresponded to sulphur tetrafluoride, thionyl fluoride and sulphur dioxide respectively. The composition of the volatile products was therefore equivalent to partial pressures of sulphur tetrafluoride, thionyl fluoride and sulphur dioxide which gave 8.7, 32.2 and 3.48 area unit respectively. From the calibration curves, Figs. 2.10-2.12, the area under the peaks obtained was 12:68:20 mole % ratio of sulphur tetrafluoride, thionyl fluoride and sulphur dioxide respectively. This ratio was

equivalent to 0.11, 0.64 and 0.19 mmol of sulphur tetrafluoride, thionyl fluoride and sulphur dioxide respectively. A similar treatment was used throughout this work.

The overall drop in the [ $^{14}\text{C}$ ]-carbon or [ $^{35}\text{S}$ ]-sulphur labelled probe molecule count rate was used as a measure of the total uptake of gas; an example is given as follows. The volume of the counting cell was  $468.9 \pm 7.6 \text{ cm}^3$ . The pressure of [ $^{35}\text{S}$ ]-sulphur labelled sulphur tetrafluoride at room temperature required to deliver 1.0 mmol in the counting cell was 39.5 Torr. The specific count rate was  $31506 \pm 139 \text{ count min}^{-1} \text{ mmol}^{-1}$  [ $^{35}\text{S}$ ]-sulphur labelled sulphur tetrafluoride (330 Torr) with a count rate of  $239241 \pm 496 \text{ count min}^{-1}$ , was admitted into the counting cell containing CsF/ $\gamma$ -alumina  $4.4 \text{ mmol g}^{-1}$ . After ca 60 min, the count rate of the gas phase decreased to  $226021 \pm 475 \text{ count min}^{-1}$ . The total uptake of [ $^{35}\text{S}$ ]-sulphur labelled sulphur tetrafluoride by solid CsF/ $\gamma$ -alumina,  $4.4 \text{ mmol g}^{-1}$  (0.5g, 1.32 mmol) was therefore equivalent to a pressure which gave a count rate of  $13220 \pm 971 \text{ count min}^{-1}$ . From the calibration curve, Fig. 2.53,  $13220 \text{ count min}^{-1}$  was equivalent to a pressure of 16.6 Torr of [ $^{35}\text{S}$ ]-sulphur labelled sulphur tetrafluoride. The quantity of [ $^{35}\text{S}$ ]-sulphur labelled sulphur tetrafluoride taken up by the solid was calculated using the gas law, equation 5.1, and was 0.42 mmol. This method was used throughout this work.

The specific count rates of [ $^{18}\text{F}$ ]-fluorine containing probe molecules before and after reaction with supported metal fluoride were calculated by the combination of the results obtained from the manometric study, the infra-red analysis and the count rate of [ $^{18}\text{F}$ ]-fluorine labelled probe molecules. An example is given below; a quantity of [ $^{18}\text{F}$ ]-fluorine labelled sulphur tetrafluoride

(330 Torr, which is equivalent to 1.0 mmol in the reaction vessel) was counted as an adduct with pyridine. The count rate obtained was taken to be the specific count rate of [ $^{18}\text{F}$ ]-fluorine labelled sulphur tetrafluoride before reaction;  $143820 \pm 243 \text{ count min}^{-1} \text{ mmol}^{-1}$ , this was equivalent to  $35955 \text{ count min}^{-1} (\text{mg atom F})^{-1}$ . [ $^{18}\text{F}$ ]-Fluorine labelled sulphur tetrafluoride (300 Torr, 1.0 mmol) was admitted into the counting vessel, type II, Fig. 2.40, containing CsF/ $\gamma$ -alumina,  $8.8 \text{ mmolg}^{-1}$  (0.5g, 1.88 mmol), the reaction followed with time for 70 min, then the reactants separated by condensing the volatile products into the gas counting vessel, type I, Fig. 2.40. The solid and gas count rates after reaction were obtained and compared with the starting count rate of [ $^{18}\text{F}$ ]-fluorine labelled sulphur tetrafluoride. The solid count rate was  $84903 \pm 93 \text{ count min}^{-1}$  and the count rate of the volatile products held at 77K was  $59598 \pm 153 \text{ count min}^{-1}$ .

$$\text{The radiochemical balance: } \frac{84903 + 59598}{143820} \times 100 = 100\%$$

The composition of the volatile products as determined from the infra-red experiments, using the mole ratio 12:68:20, was 0.11, 0.64 and 0.19 mmol of sulphur tetrafluoride, thionyl fluoride and sulphur dioxide respectively. The specific count rate of [ $^{18}\text{F}$ ]-fluorine containing compounds after reaction were therefore calculated and hence, the fraction exchanged.

### 5.3 THE REACTIONS INVOLVING VOLATILE SULPHUR CONTAINING PROBE MOLECULES WITH CAESIUM OR POTASSIUM FLUORIDE SUPPORTED ON $\gamma$ -ALUMINA

#### 5.3.1 INFRA-RED ANALYSIS OF THE HYDROLYSIS OF SULPHUR TETRAFLUORIDE OVER $\gamma$ -ALUMINA SUPPORTED CAESIUM OR POTASSIUM FLUORIDE

Hydrolysis of sulphur tetrafluoride took place at the surface of  $\gamma$ -alumina supported caesium or potassium fluoride to give thionyl fluoride and sulphur dioxide. The composition of the gas products was dependent upon the metal fluoride loading. For example, no sulphur tetrafluoride was detected in the gas phase after reaction between sulphur tetrafluoride and supported metal fluoride when the loading was  $\leq 5.5 \text{ mmol g}^{-1}$ . In all samples analysed, there was no evidence for anhydrous hydrogen fluoride, the other hydrolysis product expected. If anhydrous HF were to be present in the gas phase, it would react with Pyrex glass to produce silicon tetrafluoride and boron trifluoride. However, neither were observed. Apparently anhydrous hydrogen fluoride was taken up completely by the solid. Bands identified in the infra-red spectrum of the volatile material obtained from the reaction of sulphur tetrafluoride (200 Torr) with CsF/ $\gamma$ -alumina,  $4.4 \text{ mmol g}^{-1}$  (0.2g) are listed in Table 5.1.

The decrease in the partial pressure of sulphur tetrafluoride over the solids with time is shown in Fig. 5.1. Analysis of the data obtained showed that the decrease in sulphur tetrafluoride did not follow a first order process. Second order plots of the data obtained are shown in Fig. 5.2. These plots showed that the decrease in sulphur tetrafluoride in the gas phase was not a second order overall, but two linear portions were obtained before and after  $t = 18 \text{ min}$ , with correlation coefficients in the range 0.993-0.9998.

The composition of the gas products after reaction between sulphur tetrafluoride and the supported metal fluorides  $4.4$  and  $8.8 \text{ mmol g}^{-1}$  were determined and the results are given in Tables



**Table 5.1** The Infra-red Spectrum of the Gas Product obtained from the Reaction between Sulphur Tetrafluoride and CsF/ $\gamma$ -Alumina (4.4 mmol g<sup>-1</sup>)

This Work	Literature		66 , 175
	SF <sub>4</sub>	SOF <sub>2</sub>	SO <sub>2</sub>
393	353 $\nu_9$ 475 $\nu_3$	393 $\nu_6$ -	- -
527	532 $\nu_7$ 558 $\nu_2$	526 $\nu_3$ -	- -
728	730 $\nu_8$	721 $\nu_5$	-
807	867 $\nu_6$ 892 $\nu_1$	801 $\nu_2$ -	- -
1159	-	-	1151 $\nu_1$
1318	-	1308 $\nu_1$	-
1362	-	-	1362 $\nu_3$

Figure 5.1 Partial Pressure of  $SF_4$  over  
as a function with time

- 1) KF /  $\gamma$ -alumina,  $4.4 \text{ mmol g}^{-1}$
- 2) CsF /  $\gamma$ -alumina,  $4.4 \text{ mmol g}^{-1}$
- 3) KF /  $\gamma$ -alumina,  $8.8 \text{ mmol g}^{-1}$
- 4) CsF /  $\gamma$ -alumina,  $8.8 \text{ mmol g}^{-1}$

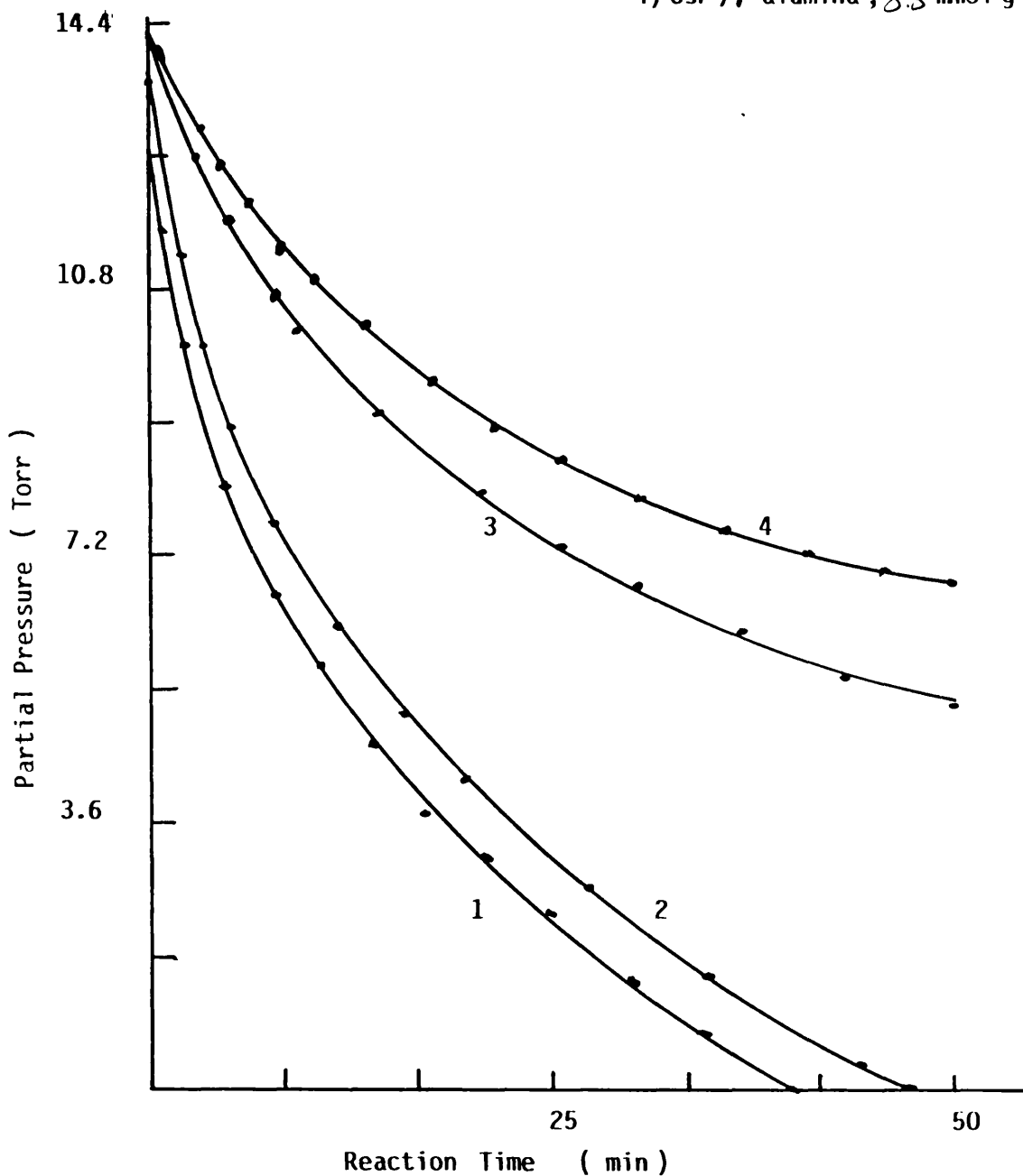
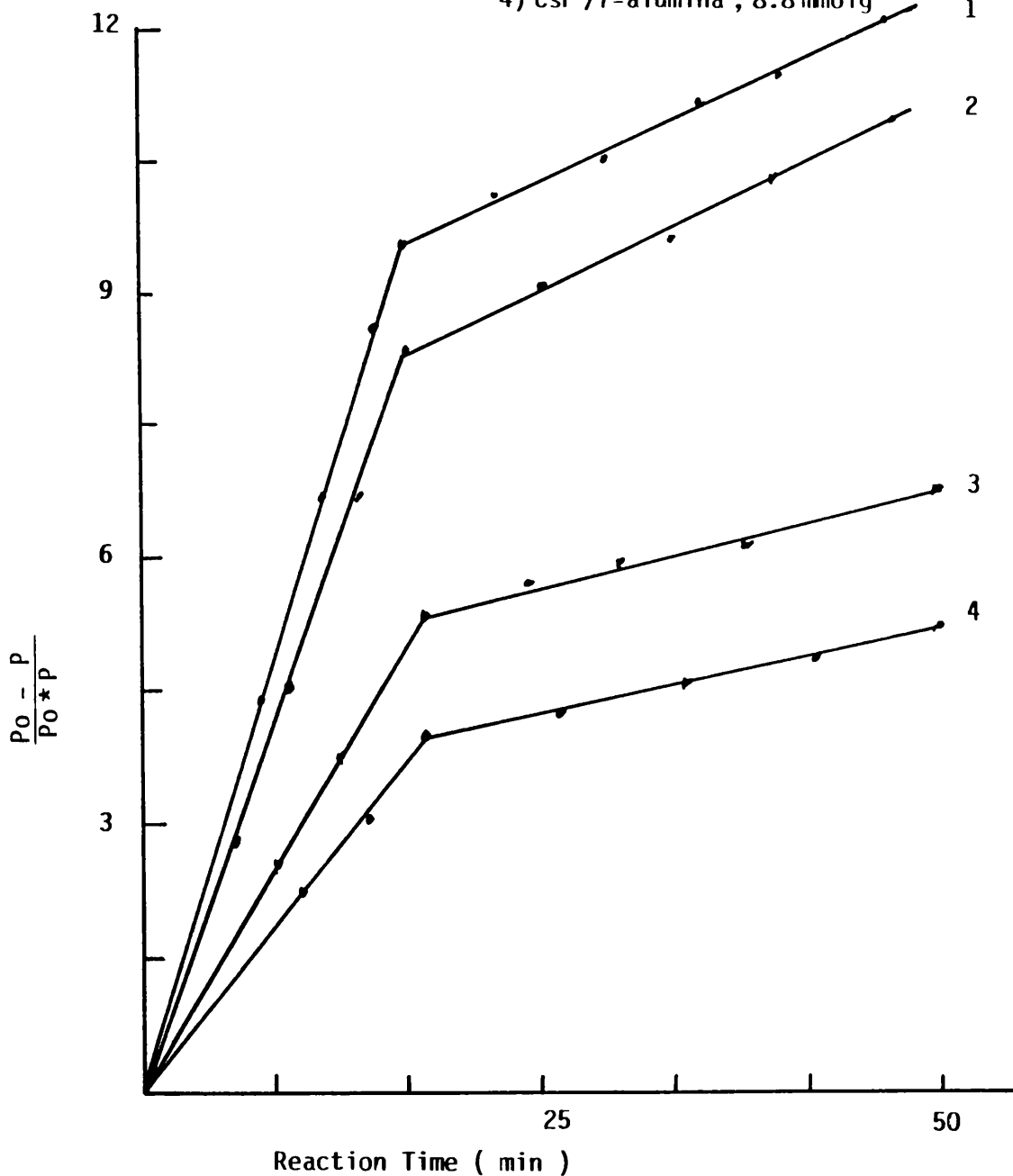


Figure 5.2 Second order plot of the hydrolysis of SF<sub>4</sub> as a function of time over

- 1) KF /  $\gamma$ -alumina , 4.4 mmol g<sup>-1</sup>
- 2) CsF /  $\gamma$ -alumina , 4.4 mmol g<sup>-1</sup>
- 3) KF /  $\gamma$ -alumina , 8.8 mmol g<sup>-1</sup>
- 4) CsF /  $\gamma$ -alumina , 8.8 mmol g<sup>-1</sup>



5.2 and 5.3. The best data were converted to mole ratios and are summarised in Table 5.4.

### 5.3.2 MANOMETRIC STUDY OF REACTIONS OF SULPHUR TETRAFLUORIDE WITH CAESIUM OR POTASSIUM FLUORIDE SUPPORTED ON $\gamma$ -ALUMINA

The uptakes of sulphur tetrafluoride and/or its hydrolysis products thionyl fluoride and sulphur dioxide by supported metal fluorides were studied manometrically across the composition range at different initial pressures of gas. The uptakes of gas by supported metal fluorides 4.4 and 8.8 mmol g<sup>-1</sup> were dependent on the initial pressure of sulphur tetrafluoride in the range 40-300 Torr. The results obtained are given in Table 5.5 and shown schematically in Fig. 5.3. The uptake of volatile sulphur containing compounds was also dependent on the metal fluoride loading, in that, the uptake was increased by increasing the metal fluoride loading in the range 1.1-5.5 mmol g<sup>-1</sup>, then decreased in the range 5.5-15.0 mmol g<sup>-1</sup>. The results obtained are given in Table 5.6 at an initial pressure of sulphur tetrafluoride of 300 Torr. In all reactions studied, the interactions involving supported caesium fluoride were greater than those involving supported potassium fluoride under the same conditions.

In each case the infra-red spectrum of the supported metal fluoride in the range 2-10 mmol g<sup>-1</sup> after reaction with sulphur tetrafluoride showed very strong bands due to pentafluorosulphate (SF<sub>5</sub>)<sup>-</sup> and fluorosulphite (SO<sub>2</sub>F)<sup>-</sup> anions, but there was no evidence for trifluorosulphite (SOF<sub>3</sub>)<sup>-</sup>. The infra-red spectrum of the supported caesium fluoride, 4.4 mmol g<sup>-1</sup> after reaction is given in Table 5.7.

Table 5.2 Results of the Infra-red Analysis of the Gas Products after Reaction between Sulphur Tetrafluoride and Supported Caesium Fluoride prepared from Aqueous Solution

Solid mmolg <sup>-1</sup>	Composition of Gas Products in the Infra-red Cell													
	SF <sub>4</sub>						SOF <sub>2</sub>						SO <sub>2</sub>	
	Torr	mmol	Torr	mmol	Torr	mmol	Torr	mmol	Torr	mmol	Torr	mmol	Torr	mmol
4.4	15.3 ± 0.5	0.044 ± 0.002	-	-	7.9 ± 0.2	0.023 ± 0.0006	7.0 ± 0.2	0.023 ± 0.0006	7.0 ± 0.2	0.023 ± 0.0006	7.0 ± 0.2	0.023 ± 0.0006	0.02 ± 0.0006	
	15.3 ± 0.5	0.044 ± 0.002	-	-	7.5 ± 0.2	0.022 ± 0.0006	6.7 ± 0.2	0.022 ± 0.0006	6.7 ± 0.2	0.022 ± 0.0006	6.7 ± 0.2	0.022 ± 0.0006	0.019 ± 0.0006	
	15.7 ± 0.5	0.045 ± 0.002	-	-	8.3 ± 0.2	0.024 ± 0.0006	7.3 ± 0.2	0.024 ± 0.0006	7.3 ± 0.2	0.024 ± 0.0006	7.3 ± 0.2	0.024 ± 0.0006	0.021 ± 0.0006	
	14.9 ± 0.5	0.043 ± 0.002	-	-	6.8 ± 0.2	0.020 ± 0.0006	6.4 ± 0.2	0.020 ± 0.0006	6.4 ± 0.2	0.020 ± 0.0006	6.4 ± 0.2	0.020 ± 0.0006	0.018 ± 0.0006	
	15.2 ± 0.5	0.044 ± 0.002	-	-	8.0 ± 0.2	0.023 ± 0.0006	7.0 ± 0.2	0.023 ± 0.0006	7.0 ± 0.2	0.023 ± 0.0006	7.0 ± 0.2	0.023 ± 0.0006	0.02 ± 0.0006	
	15.8 ± 0.5	0.046 ± 0.002	-	-	6.9 ± 0.2	0.020 ± 0.0006	6.0 ± 0.2	0.020 ± 0.0006	6.0 ± 0.2	0.020 ± 0.0006	6.0 ± 0.2	0.020 ± 0.0006	0.017 ± 0.0006	
	15.4 ± 0.5	0.045 ± 0.002	-	-	7.8 ± 0.2	0.023 ± 0.0006	6.9 ± 0.2	0.023 ± 0.0006	6.9 ± 0.2	0.023 ± 0.0006	6.9 ± 0.2	0.023 ± 0.0006	0.02 ± 0.0006	
	15.4 ± 0.5	0.045 ± 0.002	-	-	7.8 ± 0.2	0.023 ± 0.0006	6.9 ± 0.2	0.023 ± 0.0006	6.9 ± 0.2	0.023 ± 0.0006	6.9 ± 0.2	0.023 ± 0.0006	0.020 ± 0.0006	
8.8	15.7 ± 0.5	0.045 ± 0.002	1.8 ± 0.2	0.005 ± 0.0006	10.0 ± 0.2	0.029 ± 0.0006	3.3 ± 0.2	0.029 ± 0.0006	3.3 ± 0.2	0.029 ± 0.0006	3.3 ± 0.2	0.029 ± 0.0006	0.095 ± 0.0006	
	16.2 ± 0.5	0.047 ± 0.002	2.0 ± 0.2	0.006 ± 0.0006	11.5 ± 0.2	0.033 ± 0.0006	3.7 ± 0.2	0.033 ± 0.0006	3.7 ± 0.2	0.033 ± 0.0006	3.7 ± 0.2	0.033 ± 0.0006	0.011 ± 0.0006	
	14.9 ± 0.5	0.043 ± 0.002	1.8 ± 0.2	0.005 ± 0.0006	9.2 ± 0.2	0.027 ± 0.0006	2.5 ± 0.2	0.027 ± 0.0006	2.5 ± 0.2	0.027 ± 0.0006	2.5 ± 0.2	0.027 ± 0.0006	0.007 ± 0.0006	
	15.2 ± 0.5	0.044 ± 0.002	1.8 ± 0.2	0.005 ± 0.0006	10.4 ± 0.2	0.030 ± 0.0006	3.2 ± 0.2	0.030 ± 0.0006	3.2 ± 0.2	0.030 ± 0.0006	3.2 ± 0.2	0.030 ± 0.0006	0.009 ± 0.0006	
	15.6 ± 0.5	0.045 ± 0.002	1.8 ± 0.2	0.005 ± 0.0006	10.0 ± 0.2	0.029 ± 0.0006	3.0 ± 0.2	0.029 ± 0.0006	3.0 ± 0.2	0.029 ± 0.0006	3.0 ± 0.2	0.029 ± 0.0006	0.008 ± 0.0006	
	15.7 ± 0.5	0.045 ± 0.002	2.1 ± 0.02	0.006 ± 0.0006	11.4 ± 0.2	0.033 ± 0.0006	3.5 ± 0.2	0.033 ± 0.0006	3.5 ± 0.2	0.033 ± 0.0006	3.5 ± 0.2	0.033 ± 0.0006	0.001 ± 0.0006	
	15.3 ± 0.5	0.044 ± 0.002	1.6 ± 0.02	0.004 ± 0.0006	9.2 ± 0.2	0.027 ± 0.0006	2.7 ± 0.2	0.027 ± 0.0006	2.7 ± 0.2	0.027 ± 0.0006	2.7 ± 0.2	0.027 ± 0.0006	0.007 ± 0.0006	

Table 5.3 Results of the Infra-red Analysis of the Gas Products after Reaction between Sulphur Tetrafluoride and Supported Potassium Fluoride prepared from Aqueous Solution

Solid mmol g <sup>-1</sup>		Composition of Gas Products in the Infra-red Cell									
Gas Admitted to infra-red cell		SF <sub>4</sub>			SOF <sub>2</sub>			SO <sub>2</sub>			
Torr	mmol	Torr	mmol	Torr	mmol	Torr	mmol	Torr	mmol	Torr	mmol
15.6 ± 0.5	0.045 ± 0.002	-	-	1.35 ± 0.2	0.0039 ± 0.0006	13.5 ± 0.2	0.0039 ± 0.0006	13.5 ± 0.2	0.039 ± 0.0006		
15.5 ± 0.5	0.045 ± 0.002	-	-	1.6 ± 0.2	0.0046 ± 0.0006	14.5 ± 0.2	0.0046 ± 0.0006	14.5 ± 0.2	0.042 ± 0.0006		
15.3 ± 0.5	0.044 ± 0.002	-	-	1.38 ± 0.2	0.004 ± 0.0006	13.9 ± 0.2	0.004 ± 0.0006	13.9 ± 0.2	0.040 ± 0.0006		
14.2 ± 0.5	0.041 ± 0.002	-	-	1.64 ± 0.2	0.0047 ± 0.0006	13.4 ± 0.2	0.0047 ± 0.0006	13.4 ± 0.2	0.039 ± 0.0006		
15.9 ± 0.5	0.046 ± 0.002	-	-	1.33 ± 0.2	0.0038 ± 0.0006	13.3 ± 0.2	0.0038 ± 0.0006	13.3 ± 0.2	0.039 ± 0.0006		
14.8 ± 0.5	0.043 ± 0.002	-	-	1.40 ± 0.2	0.0041 ± 0.0006	12.9 ± 0.2	0.0041 ± 0.0006	12.9 ± 0.2	0.037 ± 0.0006		
15.9 ± 0.5	0.046 ± 0.002	-	-	1.8 ± 0.2	0.0052 ± 0.0006	14.7 ± 0.2	0.0052 ± 0.0006	14.7 ± 0.2	0.043 ± 0.0006		
15.7 ± 0.5	0.045 ± 0.002	1.8 ± 0.2	0.005 ± 0.0006	8.5 ± 0.2	0.025 ± 0.0006	4.6 ± 0.2	0.025 ± 0.0006	4.6 ± 0.2	0.013 ± 0.0006		
15.3 ± 0.5	0.044 ± 0.002	2.0 ± 0.2	0.006 ± 0.0006	9.4 ± 0.2	0.027 ± 0.0006	4.8 ± 0.2	0.027 ± 0.0006	4.8 ± 0.2	0.014 ± 0.0006		
14.7 ± 0.5	0.043 ± 0.002	1.8 ± 0.2	0.005 ± 0.0006	8.9 ± 0.2	0.026 ± 0.0006	4.5 ± 0.2	0.026 ± 0.0006	4.5 ± 0.2	0.013 ± 0.0006		
14.9 ± 0.5	0.043 ± 0.002	1.8 ± 0.2	0.005 ± 0.0006	8.8 ± 0.2	0.025 ± 0.0006	4.3 ± 0.2	0.025 ± 0.0006	4.3 ± 0.2	0.012 ± 0.0006		
15.9 ± 0.5	0.046 ± 0.002	1.8 ± 0.2	0.005 ± 0.0006	8.5 ± 0.2	0.025 ± 0.0006	4.3 ± 0.2	0.025 ± 0.0006	4.3 ± 0.2	0.012 ± 0.0006		
16.2 ± 0.5	0.047 ± 0.002	2.1 ± 0.02	0.006 ± 0.0006	10.1 ± 0.2	0.029 ± 0.0006	5.4 ± 0.2	0.029 ± 0.0006	5.4 ± 0.2	0.016 ± 0.0006		
15.3 ± 0.5	0.044 ± 0.002	1.6 ± 0.02	0.004 ± 0.0006	8.8 ± 0.2	0.025 ± 0.0006	4.7 ± 0.2	0.025 ± 0.0006	4.7 ± 0.2	0.014 ± 0.0006		

4.4

8.8

**Table 5.4** The Composition of the Gas Product after Reaction between Sulphur Tetrafluoride and  $\gamma$ -Alumina supported Cesium or Potassium Fluoride

Composition MF/ $\gamma$ -Alumina mmolg <sup>-1</sup>	Composition of Gas Mole %					
	SF <sub>4</sub>		SOF <sub>2</sub>		SO <sub>2</sub>	
	M = Cs	M = K	M = Cs	M = K	M = Cs	M = K
1.1	-	-	13 ± 1	9 ± 2	87 ± 2	91 ± 1
2.0	-	-	27 ± 2	19 ± 2	73 ± 3	81 ± 5
4.4	-	-	53 ± 3	40 ± 4	47 ± 3	60 ± 5
5.0	-	-	56 ± 2	45 ± 7	44 ± 8	55 ± 2
5.5	-	-	59 ± 6	49 ± 7	41 ± 3	51 ± 6
6.5	9 ± 2	7 ± 1	63 ± 3	52 ± 7	28 ± 3	41 ± 6
8.8	12 ± 2	11 ± 2	68 ± 3	58 ± 6	20 ± 1	31 ± 3
15.0	21 ± 1	17 ± 3	73 ± 4	65 ± 7	6 ± 2	18 ± 2

**Table 5.5** Manometric Study of the Uptake of Sulphur Tetrafluoride by  $\gamma$ -Alumina Supported Caesium or Potassium Fluoride  
 A (mmol) uptake of gas  
 B (mmol) total retained

Initial Pressure Torr	CsF/ $\gamma$ -Alumina				KF/ $\gamma$ -Alumina			
	4.4 mmol g <sup>-1</sup>		8.8 mmol g <sup>-1</sup>		4.4 mmol g <sup>-1</sup>		8.8 mmol g <sup>-1</sup>	
	A	B	A	B	A	B	A	B
40 ± 0.5	0.10 ± 0.02	0.033 ± 0.005	0.051 ± 0.002	0.010 ± 0.003	0.061 ± 0.02	0.014 ± 0.004	0.04 ± 0.01	0.006 ± 0.003
60 ± 0.5	0.16 ± 0.02	0.054 ± 0.005	0.069 ± 0.002	0.013 ± 0.003	0.010 ± 0.02	0.022 ± 0.004	0.05 ± 0.01	0.007 ± 0.003
80 ± 0.5	0.20 ± 0.02	0.066 ± 0.005	0.090 ± 0.002	0.018 ± 0.003	0.123 ± 0.02	0.028 ± 0.004	0.014 ± 0.01	0.011 ± 0.003
120 ± 0.5	0.27 ± 0.02	0.086 ± 0.005	0.141 ± 0.002	0.029 ± 0.003	0.180 ± 0.02	0.040 ± 0.004	0.10 ± 0.01	0.015 ± 0.003
140 ± 0.5	0.33 ± 0.02	0.010 ± 0.005	-	-	0.19 ± 0.02	0.044 ± 0.004	-	-
160 ± 0.5	0.34 ± 0.02	0.011 ± 0.005	0.171 ± 0.002	0.033 ± 0.003	0.23 ± 0.02	0.052 ± 0.004	0.149 ± 0.01	0.021 ± 0.003
200 ± 0.5	0.37 ± 0.02	0.012 ± 0.005	0.25 ± 0.002	0.044 ± 0.003	0.26 ± 0.02	0.057 ± 0.004	0.179 ± 0.01	0.027 ± 0.003
240 ± 0.5	0.40 ± 0.02	0.126 ± 0.005	0.27 ± 0.002	0.053 ± 0.003	0.305 ± 0.02	0.067 ± 0.004	0.2 ± 0.01	0.03 ± 0.003
280 ± 0.5	0.42 ± 0.02	0.130 ± 0.005	0.28 ± 0.002	0.06 ± 0.003	0.320 ± 0.02	0.070 ± 0.004	0.22 ± 0.01	0.033 ± 0.003
300 ± 0.5	0.44 ± 0.02	0.136 ± 0.005	0.069 ± 0.002	0.066 ± 0.003	0.34 ± 0.02	0.075 ± 0.004	0.24 ± 0.01	0.036 ± 0.003



Figure 5.3 Total uptake of gas as a function of the initial pressure of  $SF_4$  by

- 1) CsF /  $\gamma$ -alumina ,  $4.4 \text{ mmol g}^{-1}$
- 2) KF /  $\gamma$ -alumina ,  $4.4 \text{ mmol g}^{-1}$
- 3) CsF /  $\gamma$ -alumina ,  $8.8 \text{ mmol g}^{-1}$
- 4) KF /  $\gamma$ -alumina ,  $8.8 \text{ mmol g}^{-1}$

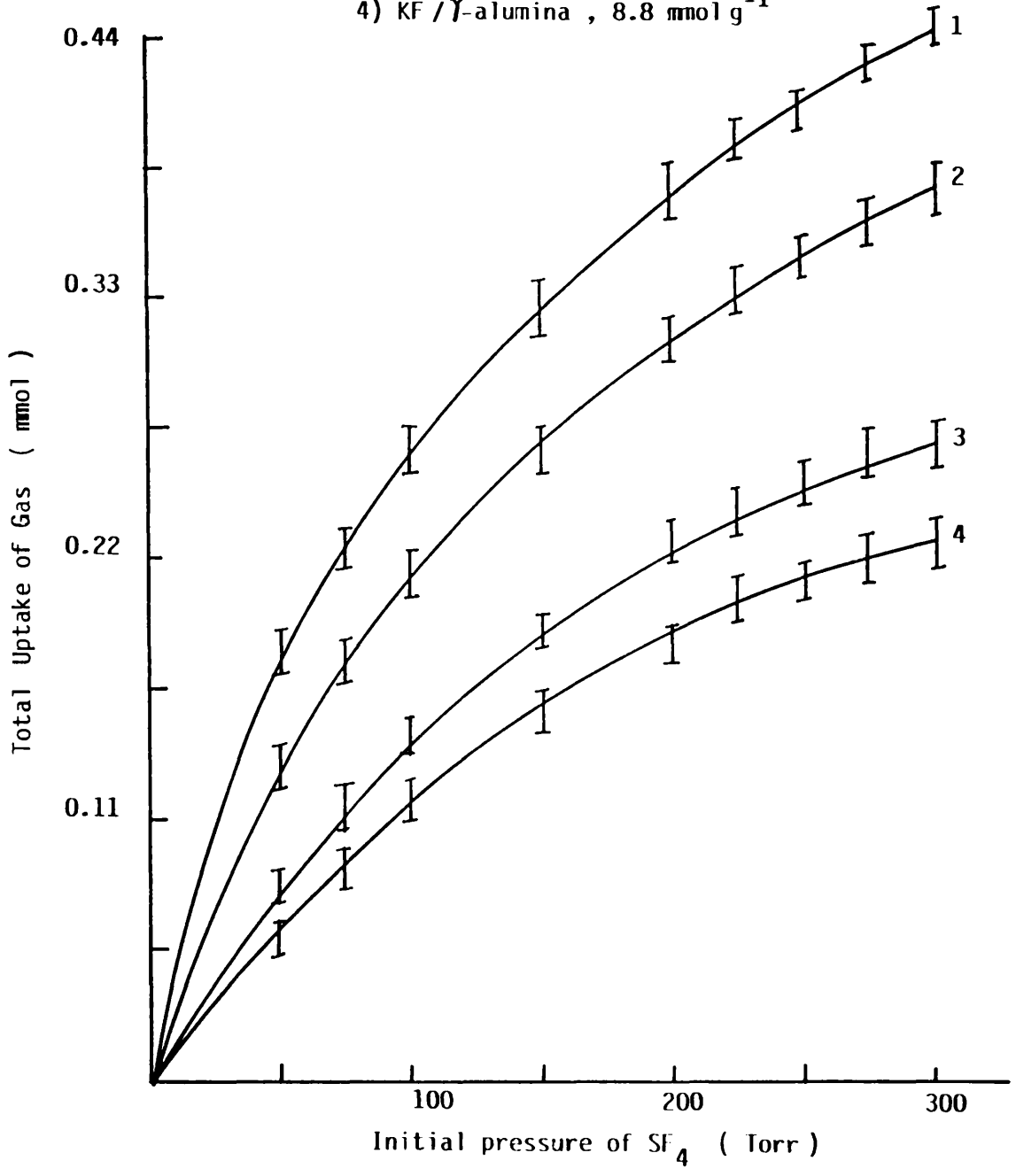


Table 5.6 Manometric Study of the Uptake of Sulphur Tetrafluoride by MF/ $\gamma$ -Alumina across the Composition Range

Composition mmol g <sup>-1</sup>	CsF/ $\gamma$ -Alumina		KF/ $\gamma$ -Alumina	
	Total Uptake (mmol)	Quantity Retained (mmol)	Total Uptake (mmol)	Quantity Retained (mmol)
1.1	0.18 ± 0.01	0.036 ± 0.003	0.13 ± 0.01	0.03 ± 0.003
2.0	0.25 ± 0.01	0.073 ± 0.004	0.19 ± 0.01	0.05 ± 0.004
4.37	0.44 ± 0.02	0.136 ± 0.006	0.34 ± 0.02	0.075 ± 0.003
5.0	0.48 ± 0.02	0.153 ± 0.001	0.37 ± 0.02	0.009 ± 0.003
5.5	0.51 ± 0.03	0.163 ± 0.001	0.39 ± 0.04	0.105 ± 0.003
6.5	0.40 ± 0.03	0.104 ± 0.008	0.37 ± 0.05	0.007 ± 0.003
7.5	0.34 ± 0.02	0.08 ± 0.003	0.28 ± 0.02	0.06 ± 0.003
8.8	0.09 ± 0.01	0.07 ± 0.003	0.24 ± 0.01	0.036 ± 0.003
15.0	0.18 ± 0.01	0.02 ± 0.003	0.05 ± 0.01	0.02 ± 0.003

Initial Pressure of SF<sub>4</sub>, 300 Torr ± 1

**Table 5.7** Infra-Red Spectrum of CsF/ $\gamma$ -Alumina 4.4 mmol g<sup>-1</sup> which had been treated with Gaseous Sulphur Tetrafluoride

<b>This Work</b>	<b>CsSF<sub>5</sub> 73</b>	<b>CsSO<sub>2</sub>F 52</b>
1193	-	1178 $\nu_5$
1107	-	1100 $\nu_1$
793	793 $A_1 \nu_1$	-
598	-	598 $\nu_2$
588	590 $E \nu_1$	-
-	520 $A_1 \nu_2$	-
470	-	471 $\nu_3$
456	466 $A_1 \nu_3$	-
-	430 $E \nu_8$	-

**5.3.3 THE CHANGE IN THE TEMPERATURE OF SOLID CAESIUM OR POTASSIUM  
FLUORIDE SUPPORTED ON  $\gamma$ -ALUMINA DURING REACTION WITH SULPHUR  
TETRAFLUORIDE**

The reactions of sulphur tetrafluoride with supported metal fluorides were very exothermic, with the maximum temperature being recorded 12 min after the admission of sulphur tetrafluoride. The change in the temperature of the supported metal fluoride was recorded and appeared to be dependent on the initial pressure of sulphur tetrafluoride used. For equivalent conditions, composition and initial pressure of sulphur tetrafluoride, reactions of supported potassium fluoride appeared to be more exothermic. The temperatures recorded at the supported metal fluorides, 4.4 and 8.8 mmol g<sup>-1</sup> as a function of the initial pressure (100-300 Torr), are shown in Fig. 5.4. The change in the temperature was also dependent on the composition of the solid in the range 0.6-15.0 mmol g<sup>-1</sup>. A smaller change in the temperatures of the solids during reaction with sulphur tetrafluoride was recorded with increasing metal fluoride loading. The results obtained are shown in Fig. 5.5.

The change in the temperature of the solids during reaction between sulphur tetrafluoride and supported metal fluorides prepared from the heptafluoroisopropoxide salts, exhibited similar characteristics as those described above. However, for equivalent conditions, composition and initial pressure of sulphur tetrafluoride, the reactions involving materials prepared from non-aqueous solution appeared to be less exothermic.

**5.3.4 REACTION OF [<sup>35</sup>S]-SULPHUR LABELLED SULPHUR TETRAFLUORIDE WITH  
CAESIUM OR POTASSIUM FLUORIDE SUPPORTED ON  $\gamma$ -ALUMINA**

Figure 5.4 The change in the temperature of MF /  $\gamma$ -alumina during reaction with  $\text{SF}_4$  as a function of pressure

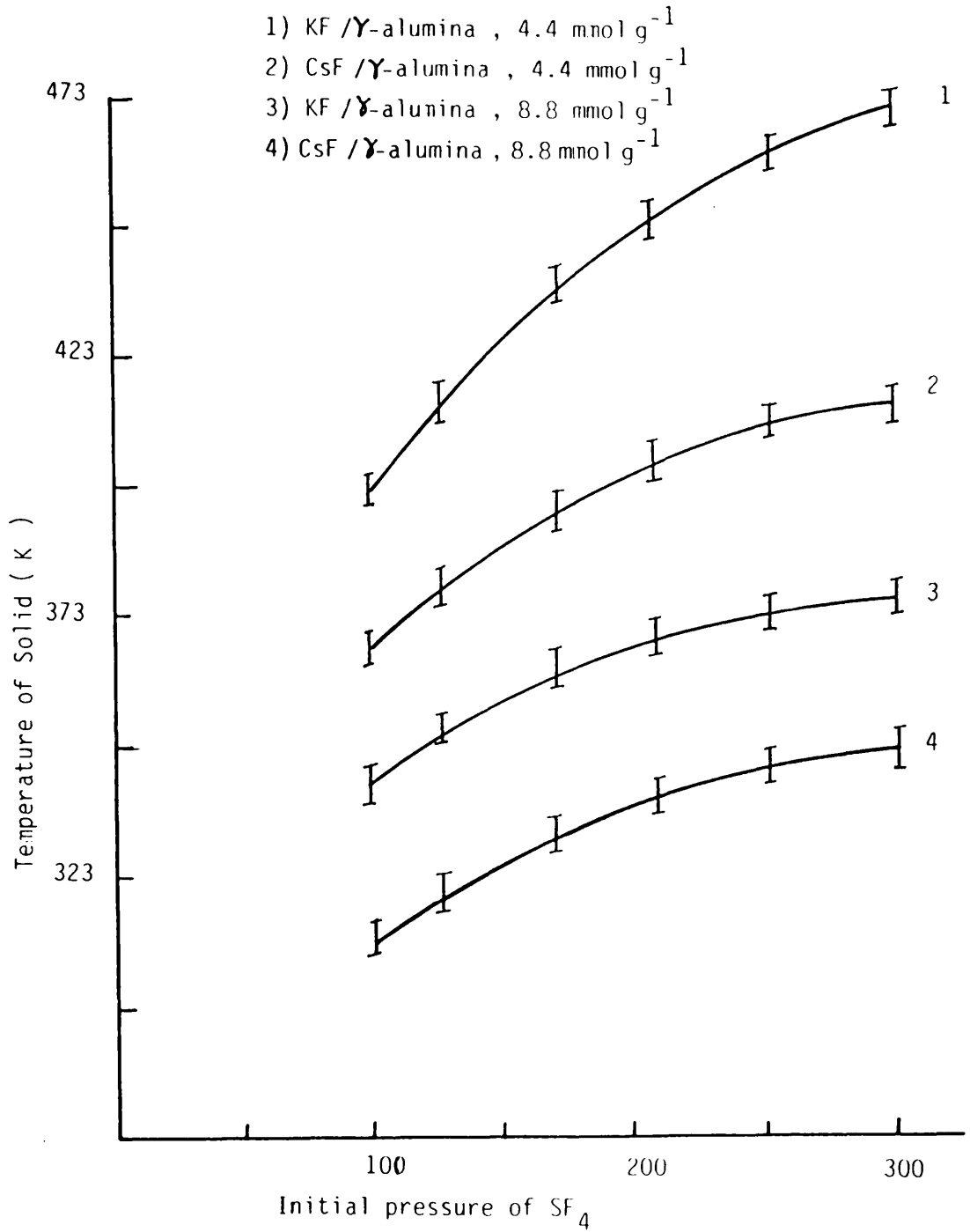
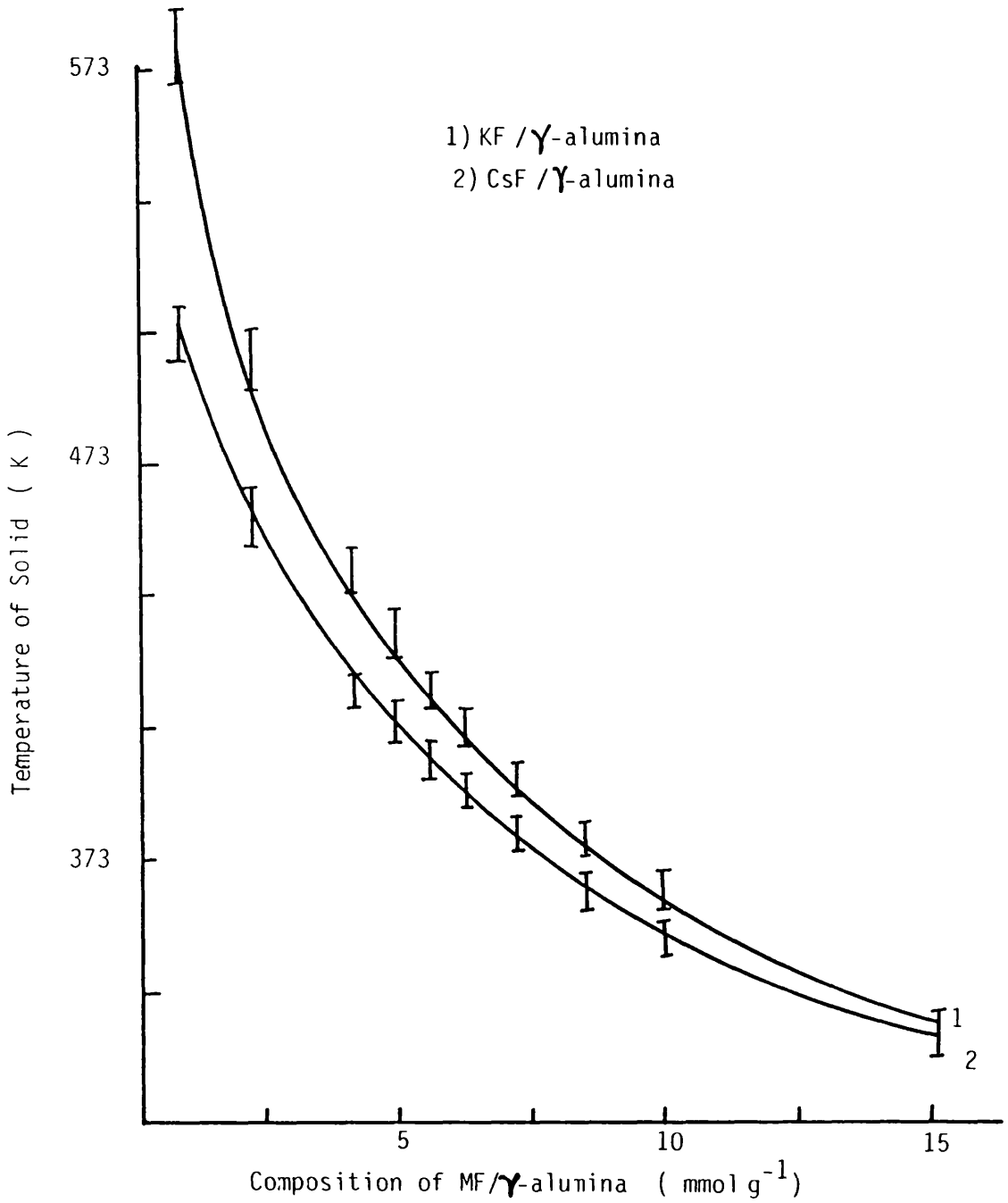


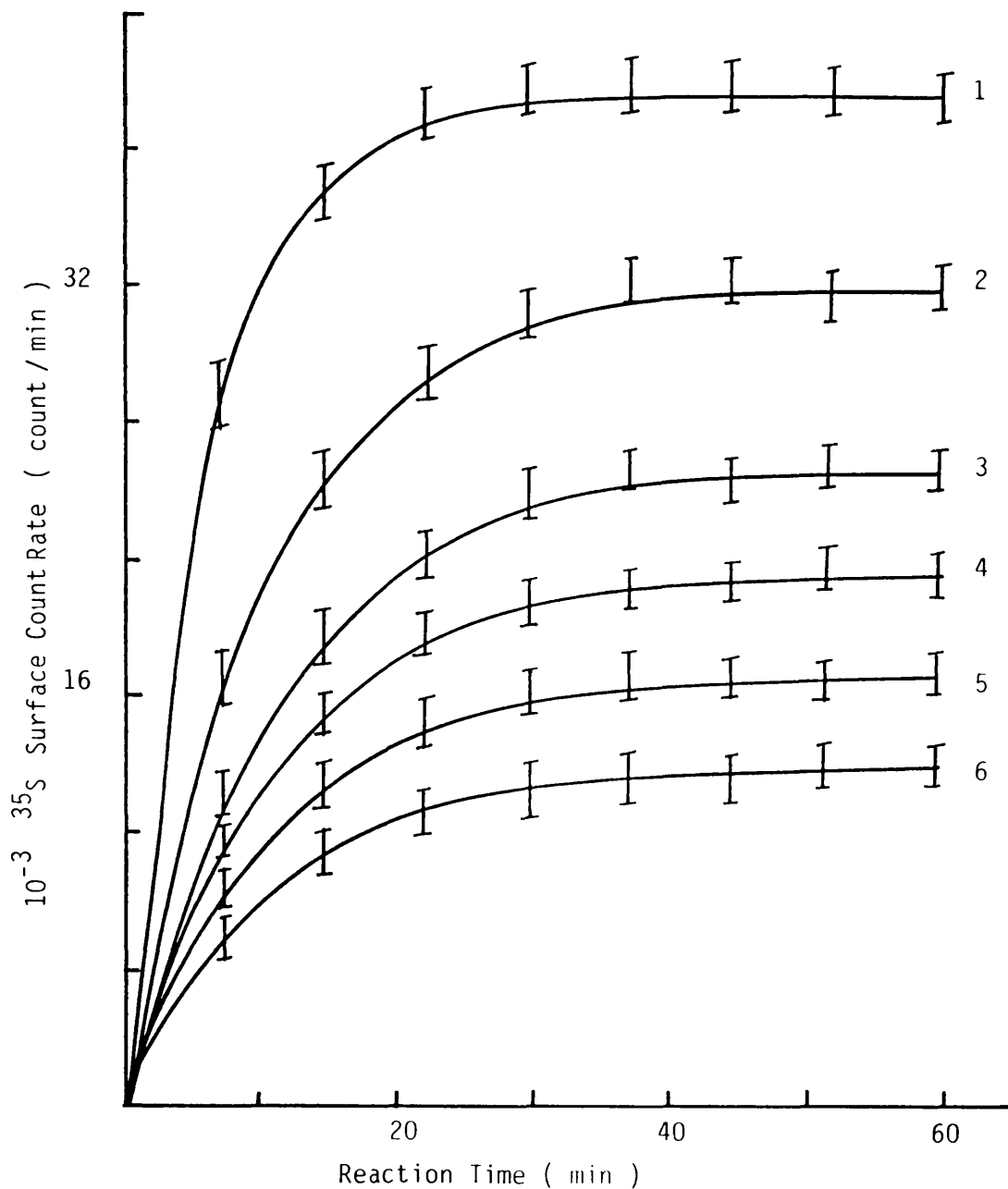
Figure 5.5 The change in the temperature of MF/ $\gamma$ -alumina during reaction with SF<sub>4</sub> as a function of the metal fluoride loading



Information related to the nature and extent of the surface reaction between sulphur tetrafluoride and supported metal fluoride at room temperature was obtained by means of [ $^{35}\text{S}$ ]-sulphur labelling studies. The reaction between [ $^{35}\text{S}$ ]-sulphur labelled sulphur tetrafluoride and supported metal fluorides was studied at different pressures in the range 10-300 Torr across the composition range 0.6-20.0 mmol $\text{g}^{-1}$ . Plots of the surface count rate of the supported metal fluoride 4.4, 5.5 and 8.8 mmol $\text{g}^{-1}$  are shown in Figs. 5.6-5.8, using initial pressures of [ $^{35}\text{S}$ ]-sulphur labelled sulphur tetrafluoride of 60, 160 and 240 Torr. The surface count rate increased rapidly until a constant level was reached after 20 min. When [ $^{35}\text{S}$ ]-sulphur labelled volatile products were removed from the counting cell by condensation at 77K, the surface count rate dropped to ca 30-15% of the original total surface count rate. The major surface species was evidently weakly adsorbed with only ca 30-15% of the total surface count rate being due to a permanently retained species. The results of these reactions are given in Tables 5.8-5.11 and shown schematically in Figs. 5.9-5.11. The surface count rates and the uptake of gas by the supported metal fluoride were pressure dependent. Pumping the solid for 5 days under vacuum after the removal of the gas phase had no effect in the surface count rate, but the [ $^{35}\text{S}$ ]-sulphur surface count rate decreased to background when the solid was heated to 395K under vacuum or was exposed to aliquots of water vapour.

When [ $^{35}\text{S}$ ]-sulphur labelled sulphur tetrafluoride was admitted into the counting cell containing a sample of supported metal fluoride which had been exposed to [ $^{35}\text{S}$ ]-sulphur labelled sulphur tetrafluoride, the surface count rate observed was higher

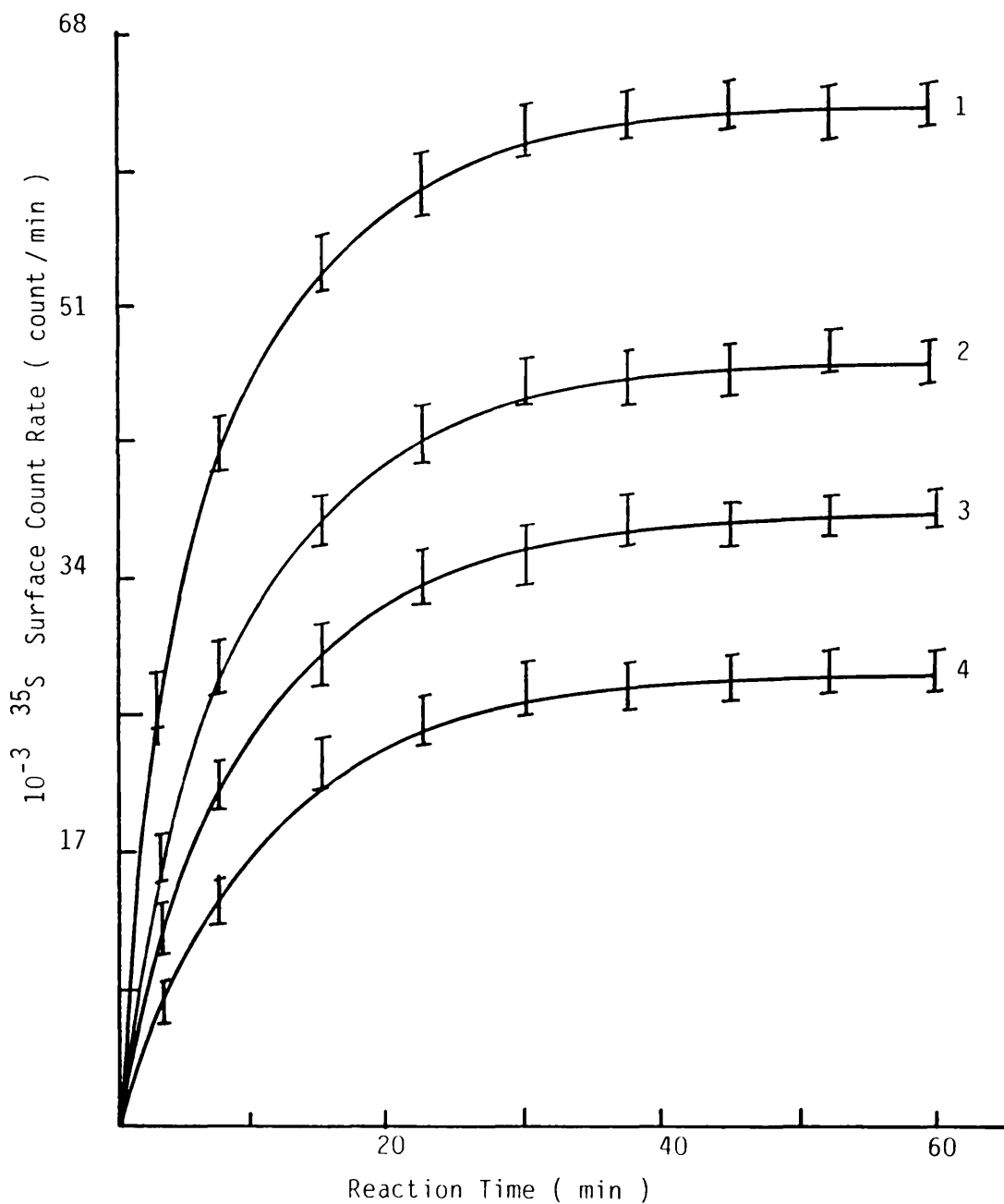
Figure 5.6 Reaction of  $^{35}\text{SF}_4$  With MF /  $\gamma$ -alumina  
 Surface Count Rate  $\nu$  Reaction Time  
 Initial Pressure of  $^{35}\text{SF}_4 = 60$  Torr



KF/ $\gamma$ -alumina	Composition	CsF/ $\gamma$ -alumina
3	$5.5 \text{ mmol g}^{-1}$	1
4	$4.4 \text{ mmol g}^{-1}$	2
6	$8.8 \text{ mmol g}^{-1}$	5

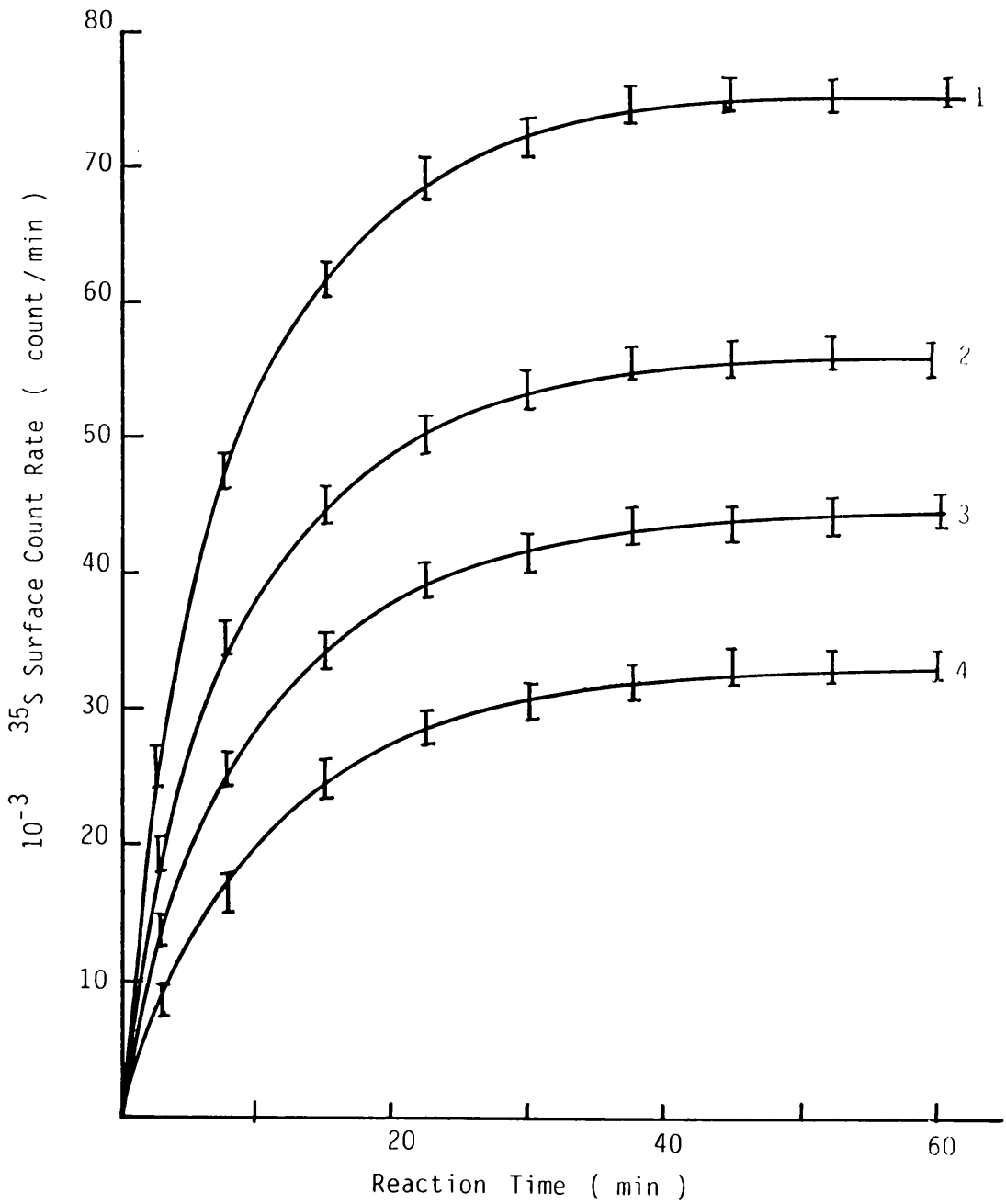


Figure 5.7 Reaction of  $^{35}\text{SF}_4$  with MF /  $\gamma$ -alumina  
 Surface Count Rate v Reaction Time  
 Initial Pressure of  $^{35}\text{SF}_4 = 160$  Torr



KF/ $\gamma$ -alumina	Composition	CsF/ $\gamma$ -alumina
2	$4.4 \text{ mmol g}^{-1}$	1
4	$8.8 \text{ mmol g}^{-1}$	3

Figure 5.8 Reaction of  $^{35}\text{SF}_4$  with MF /  $\gamma$ -alumina  
 Surface Count Rate  $\propto$  Reaction Time  
 Initial Pressure of  $^{35}\text{SF}_4 = 240$  Torr



KF/ $\gamma$ -alumina	Composition	CsF/ $\gamma$ -alumina
2	$4.4 \text{ mmol g}^{-1}$	1
4	$8.8 \text{ mmol g}^{-1}$	3

Table 5.8 Results of Reaction between [<sup>35</sup>S]-Sulphur Labelled Sulphur Tetrafluoride and the Supported Caesium Fluoride, 4.4 mmol g<sup>-1</sup>

Initial Pressure (Torr)	Total Drop in the Gas Count Rate Count min <sup>-1</sup>	Total Uptake of Gas mmol	Surface Count Rate Count min <sup>-1</sup>	Surface Count Rate after Removal of Gas Count min <sup>-1</sup>
10.4 ± 0.5	755 ± 183	0.024 ± 0.006	4936 ± 392	1480 ± 107
20.2 ± 0.5	1417 ± 192	0.045 ± 0.006	9464 ± 462	2936 ± 109
30.7 ± 0.5	2360 ± 213	0.075 ± 0.006	15716 ± 509	4558 ± 111
40.1 ± 0.5	3463 ± 302	0.11 ± 0.006	23700 ± 589	7822 ± 125
60.2 ± 0.5	4784 ± 391	0.15 ± 0.006	31952 ± 672	9266 ± 132
80.6 ± 0.5	6263 ± 417	0.20 ± 0.006	41824 ± 732	12966 ± 142
100.5 ± 0.5	7491 ± 474	0.24 ± 0.006	49606 ± 796	14881 ± 149
120.3 ± 0.5	8624 ± 521	0.27 ± 0.006	55278 ± 812	17688 ± 153
140.7 ± 0.5	9663 ± 586	0.31 ± 0.006	63788 ± 876	19774 ± 167
160.3 ± 0.5	10481 ± 617	0.33 ± 0.006	67274 ± 961	21528 ± 169
180.1 ± 0.5	11111 ± 692	0.35 ± 0.006	74968 ± 1062	23990 ± 163
200.9 ± 0.5	11614 ± 713	0.37 ± 0.006	75250 ± 1089	24024 ± 251
220.7 ± 0.5	11960 ± 790	0.38 ± 0.006	79232 ± 1125	25354 ± 268
240.3 ± 0.5	12244 ± 861	0.39 ± 0.006	79972 ± 1173	25675 ± 326
260.8 ± 0.5	12622 ± 887	0.40 ± 0.006	82626 ± 1198	26440 ± 353
280.6 ± 0.5	12968 ± 931	0.41 ± 0.006	86228 ± 1231	26654 ± 389
300.8 ± 0.5	13220 ± 1092	0.42 ± 0.006	89016 ± 1262	27790 ± 416

Sample Weight 0.5g, 1.32 mmol of CSF.

Table 5.9 Results of Reaction between [<sup>35</sup>S]-Sulphur Labelled Sulphur Tetrafluoride and the Supported Caesium Fluoride, 8.8 mmolg<sup>-1</sup>

Initial Pressure (Torr)	Total Drop in the Gas Count Rate Count min <sup>-1</sup>	Total Uptake of Gas mmol	Surface Count Rate Count min <sup>-1</sup>	Surface Count Rate after Removal of Gas Count min <sup>-1</sup>
10.1 ± 0.5	503 ± 127	0.016 ± 0.006	2962 ± 180	651 ± 93
20.7 ± 0.5	787 ± 149	0.025 ± 0.006	4632 ± 196	886 ± 108
40.9 ± 0.5	1543 ± 163	0.049 ± 0.006	8730 ± 218	1743 ± 127
60.8 ± 0.5	2235 ± 191	0.071 ± 0.006	12526 ± 243	2528 ± 175
80.2 ± 0.5	2896 ± 276	0.092 ± 0.006	16148 ± 289	3294 ± 245
100 ± 0.5	3557 ± 319	0.113 ± 0.006	19969 ± 371	4056 ± 259
120.1 ± 0.5	4343 ± 383	0.14 ± 0.006	22859 ± 407	4650 ± 313
160.4 ± 0.5	5540 ± 471	0.176 ± 0.006	30005 ± 486	6092 ± 347
180.3 ± 0.5	6232 ± 517	0.20 ± 0.006	34158 ± 493	6924 ± 297
200.3 ± 0.5	6767 ± 592	0.20 ± 0.006	37073 ± 541	7566 ± 385
240.4 ± 0.5	7743 ± 637	0.20 ± 0.006	42896 ± 587	8736 ± 407
260.9 ± 0.5	8309 ± 617	0.20 ± 0.006	46062 ± 609	9414 ± 419
280.3 ± 0.5	8656 ± 711	0.27 ± 0.006	48420 ± 637	9834 ± 427
300.8 ± 0.5	9254 ± 757	0.29 ± 0.006	52043 ± 711	10548 ± 439

Sample Weight 0.5g, 1.88 mmol of CsF.

**Table 5.10 Results of Reaction between [<sup>35</sup>S]-Sulphur Tetrafluoride and Supported Potassium Fluoride, 4.4 mmol g<sup>-1</sup>**

Initial Pressure (Torr)	Total Drop in the		Total Uptake of Gas mmol	Surface Count Rate	
	Gas Count Rate Count min <sup>-1</sup>	Count min <sup>-1</sup>		Surface Count Rate Count min <sup>-1</sup>	Surface Count Rate after Removal of Gas Count min <sup>-1</sup>
10.1 ± 0.5	629 ± 123	4102 ± 137	0.02 ± 0.006	4102 ± 137	1022 ± 103
20.9 ± 0.5	1102 ± 147	7055 ± 203	0.035 ± 0.006	7055 ± 203	1792 ± 115
40.3 ± 0.5	3140 ± 168	13950 ± 300	0.068 ± 0.006	13950 ± 300	3486 ± 117
60.1 ± 0.5	3085 ± 192	20027 ± 373	0.098 ± 0.006	20027 ± 373	5019 ± 122
80.3 ± 0.5	3997 ± 263	22815 ± 485	0.13 ± 0.006	22815 ± 485	5698 ± 127
100 ± 0.5	4784 ± 281	28307 ± 593	0.15 ± 0.006	28307 ± 593	7077 ± 132
120.8 ± 0.5	5603 ± 376	34038 ± 677	0.18 ± 0.006	34038 ± 677	8512 ± 143
140.4 ± 0.5	6545 ± 423	40634 ± 725	0.21 ± 0.006	40634 ± 725	10164 ± 162
160.1 ± 0.5	7240 ± 479	45532 ± 792	0.23 ± 0.006	45532 ± 792	11375 ± 176
180.1 ± 0.5	7869 ± 527	49903 ± 837	0.25 ± 0.006	49903 ± 837	12474 ± 189
200.5 ± 0.5	8435 ± 589	53072 ± 889	0.27 ± 0.006	53072 ± 889	13468 ± 252
220.6 ± 0.5	8971 ± 635	57445 ± 942	0.28 ± 0.006	57445 ± 942	14406 ± 289
240.8 ± 0.5	9443 ± 677	59957 ± 989	0.30 ± 0.006	59957 ± 989	15232 ± 333
260.7 ± 0.5	9915 ± 717	64003 ± 1092	0.31 ± 0.006	64003 ± 1092	16058 ± 397
280.3 ± 0.5	10292 ± 789	66845 ± 1109	0.33 ± 0.006	66845 ± 1109	16716 ± 419
300.6 ± 0.5	10576 ± 848	68845 ± 1173	0.34 ± 0.006	68845 ± 1173	17213 ± 489

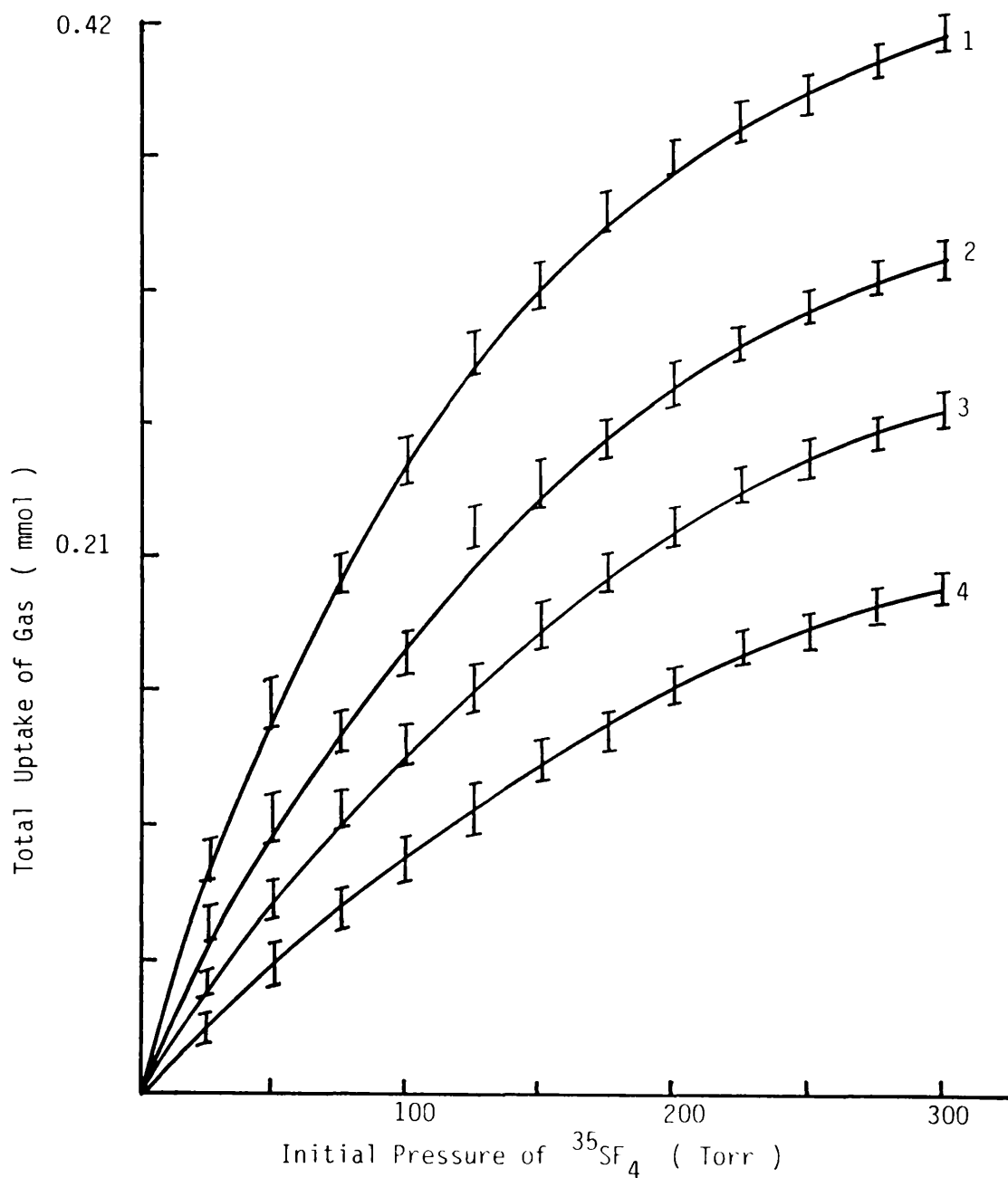
Sample Weight 0.38g, 1.32 mmol of KF.

**Table 5.11 Results of Reaction between [<sup>35</sup>S]-Sulphur Labelled Sulphur Tetrafluoride and Supported Potassium Fluoride, 8.8 mmol g<sup>-1</sup>**

Initial Pressure (Torr)	Total Drop in the Gas Count Rate Count min <sup>-1</sup>	Total Uptake of Gas mmol	Surface Count Rate Count min <sup>-1</sup>	Surface Count Rate after Removal of Gas Count min <sup>-1</sup>
10.9 ± 0.5	378 ± 117	0.012 ± 0.006	1795 ± 112	305 ± 101
20.8 ± 0.5	629 ± 148	0.02 ± 0.006	3010 ± 192	510 ± 112
40.3 ± 0.5	1165 ± 163	0.037 ± 0.006	5509 ± 203	940 ± 117
60.6 ± 0.5	1731 ± 189	0.055 ± 0.006	6655 ± 223	1155 ± 120
80.1 ± 0.5	2266 ± 222	0.072 ± 0.006	9518 ± 249	1610 ± 129
100.2 ± 0.5	2833 ± 277	0.09 ± 0.006	12384 ± 284	2095 ± 132
120.2 ± 0.5	3400 ± 351	0.11 ± 0.006	14836 ± 342	2575 ± 143
160.3 ± 0.5	4532 ± 407	0.144 ± 0.006	20802 ± 372	3540 ± 164
180.7 ± 0.5	5005 ± 452	0.16 ± 0.006	23110 ± 447	3945 ± 189
200.5 ± 0.5	5445 ± 498	0.17 ± 0.006	25313 ± 462	4315 ± 252
240.6 ± 0.5	6358 ± 577	0.20 ± 0.006	29940 ± 500	5090 ± 283
260.6 ± 0.5	6736 ± 528	0.21 ± 0.006	31736 ± 579	5410 ± 327
280.4 ± 0.5	7114 ± 691	0.23 ± 0.006	33580 ± 617	57352 ± 347
300.7 ± 0.5	7403 ± 787	0.24 ± 0.006	35073 ± 689	59808 ± 389

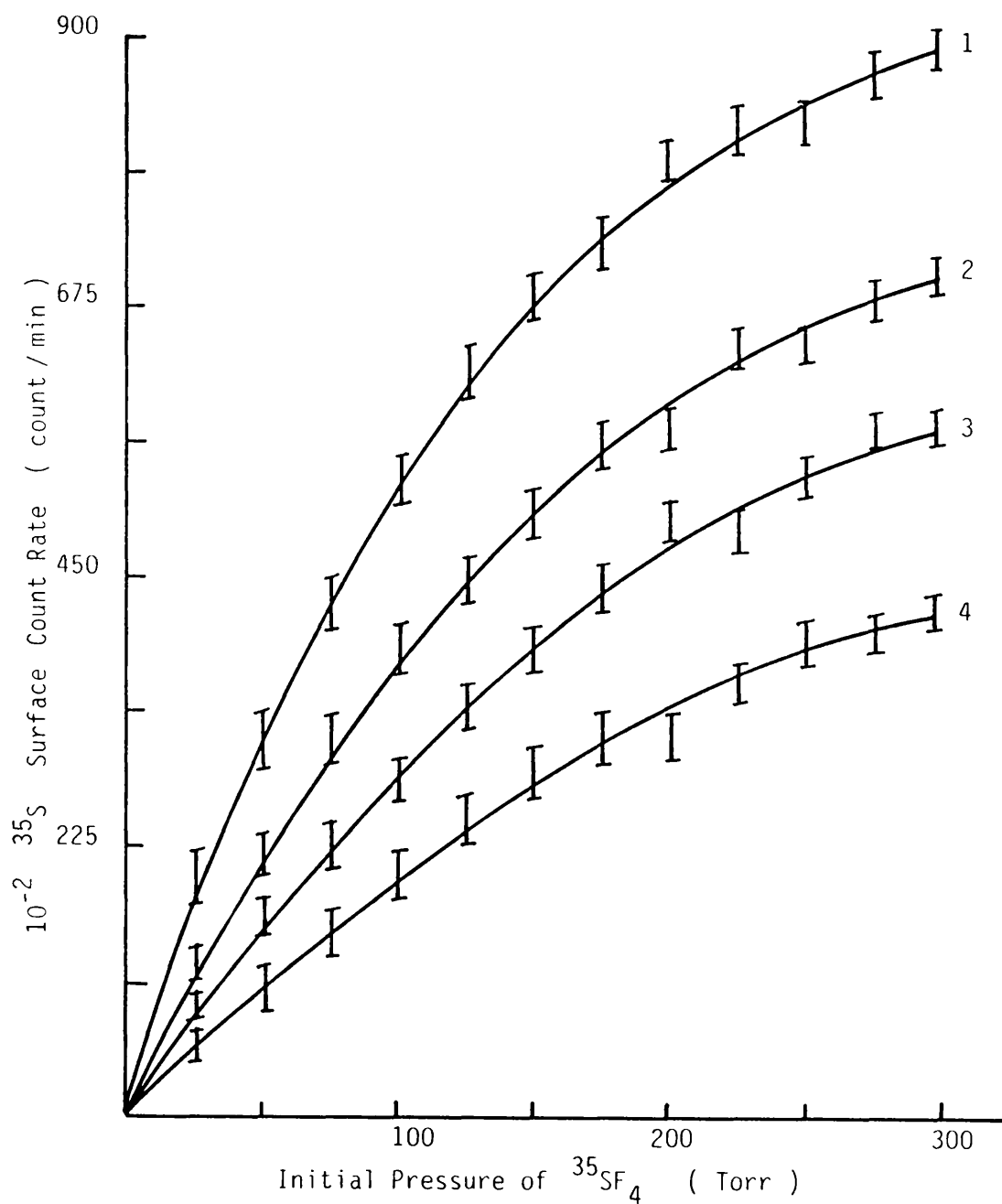
Sample Weight 0.32g, 1.88 mmol of KF.

Figure 5.9 Reaction of  $^{35}\text{SF}_4$  with MF /  $\gamma$ -alumina  
 Total Uptake  $\underline{V}$  Initial Pressure



KF / $\gamma$ -alumina	Composition	CsF / $\gamma$ -alumina
2	4.4 mmol g <sup>-1</sup>	1
4	8.8 mmol g <sup>-1</sup>	3

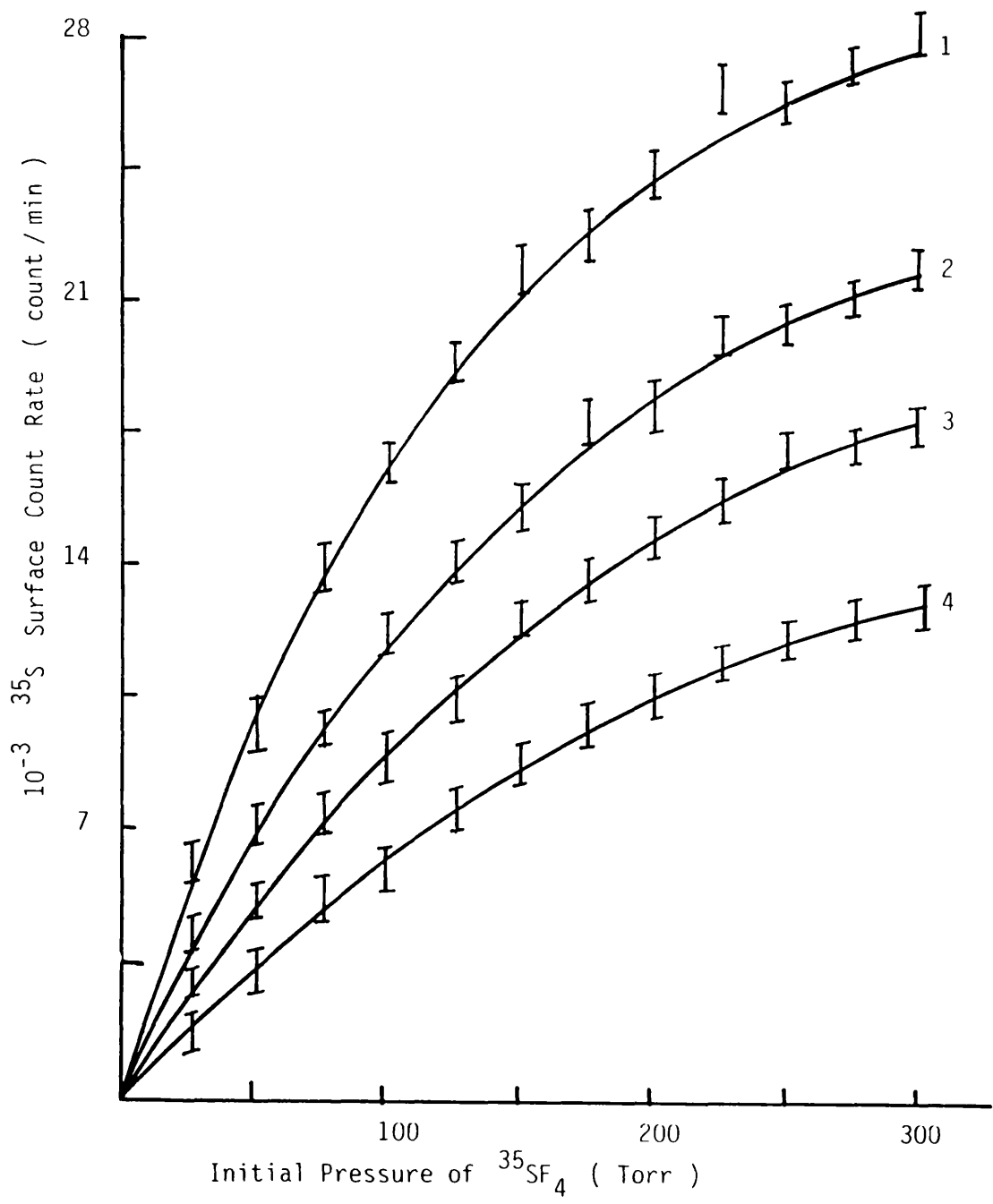
Figure 5.10 Reaction of  $^{35}\text{SF}_4$  with MF /  $\gamma$ -alumina  
 Surface Count Rate  $\nu$  Initial Pressure



KF/ $\gamma$ -alumina	Composition	CsF/ $\gamma$ -alumina
2	$4.4 \text{ mmol g}^{-1}$	1
4	$8.8 \text{ mmol g}^{-1}$	3



Figure 5.11 Reaction of  $^{35}\text{SF}_4$  with MF /  $\gamma$ -alumina  
 Surface Count Rate After Removal of Gas V Initial Pressure



KF/ $\gamma$ -alumina	Composition	CsF/ $\gamma$ -alumina
2	4.4 mmol g $^{-1}$	1
4	8.8 mmol g $^{-1}$	3

than that observed during the first admission, but after the removal of gas at room temperature, the surface count rate returned to its original level. Further adsorption/desorption cycles of [ $^{35}\text{S}$ ]-sulphur labelled sulphur tetrafluoride followed the same patterns. Results obtained for MF/ $\gamma$ -alumina,  $4.4 \text{ mmol g}^{-1}$  are shown in Figs. 5.12-5.15.

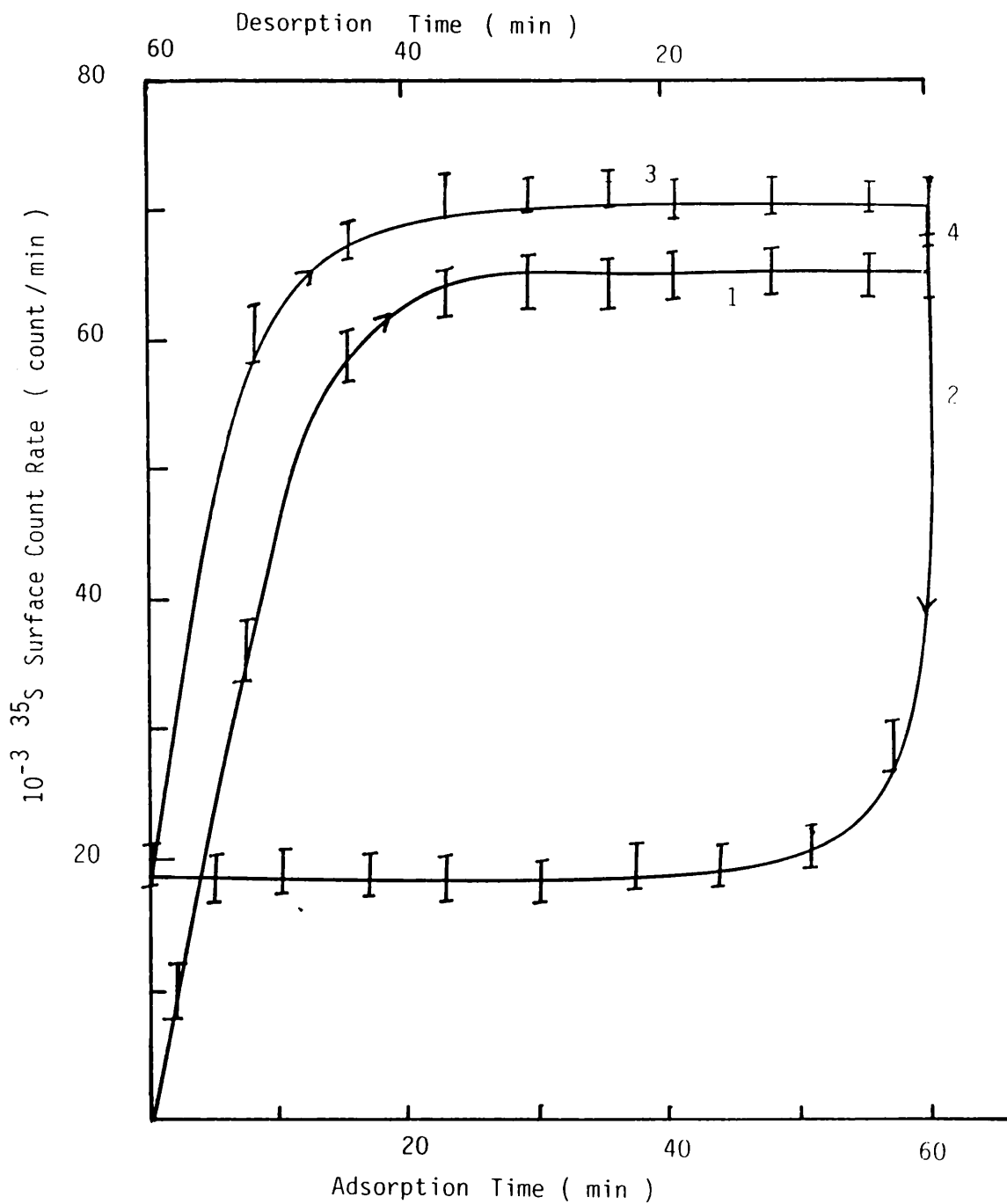
The surface count rate varied with the composition of the solid used, as shown in Fig. 5.16, and was at a maximum for a given pressure at  $5.5 \text{ mmol g}^{-1}$ . The surface count rate of the supported metal fluoride,  $20.0 \text{ mmol g}^{-1}$ , after the removal of the gas phase at room temperature was equivalent to background.

#### 5.3.5 INFRA-RED ANALYSIS OF THE HYDROLYSIS OF THIONYL FLUORIDE OVER $\gamma$ -ALUMINA SUPPORTED CAESIUM OR POTASSIUM FLUORIDE

The infra-red spectrum of the gas products after reaction between thionyl fluoride and the supported metal fluoride showed absorption bands due to sulphur dioxide and thionyl fluoride, but no evidence for anhydrous hydrogen fluoride. Apparently, anhydrous hydrogen fluoride was taken up completely by the solid. Bands identified in the infra-red spectrum of the volatile material obtained from the reaction of thionyl fluoride (200 Torr) with CsF/ $\gamma$ -alumina,  $4.4 \text{ mmol g}^{-1}$  are given in Table 5.12.

The decrease in the partial pressure of thionyl fluoride over the solids,  $4.4$  and  $8.8 \text{ mmol g}^{-1}$  is shown in Fig. 5.17. Analysis of the data obtained showed that the decrease in thionyl fluoride did not follow a first order process. Second order plots of the data obtained are shown in Fig. 5.18. The plots showed that the decrease in the thionyl fluoride in the gas phase was a second order at  $t > 12 \text{ min}$ .

Figure 5.12 Adsorption/Desorption cycle of  $^{35}\text{SF}_4$  over KF/ $\gamma$ -alumina  
 $4.4 \text{ mmol g}^{-1}$



1 = 1st adsorption    2 = 1st desorption  
 3 = 2nd adsorption    4 = 2nd desorption

Figure 5.13 Adsorption/Desorption Cycle of  $^{35}\text{SF}_4$  over  $\text{KF}/\gamma\text{-alumina}$   
 $8.8 \text{ mmol g}^{-1}$

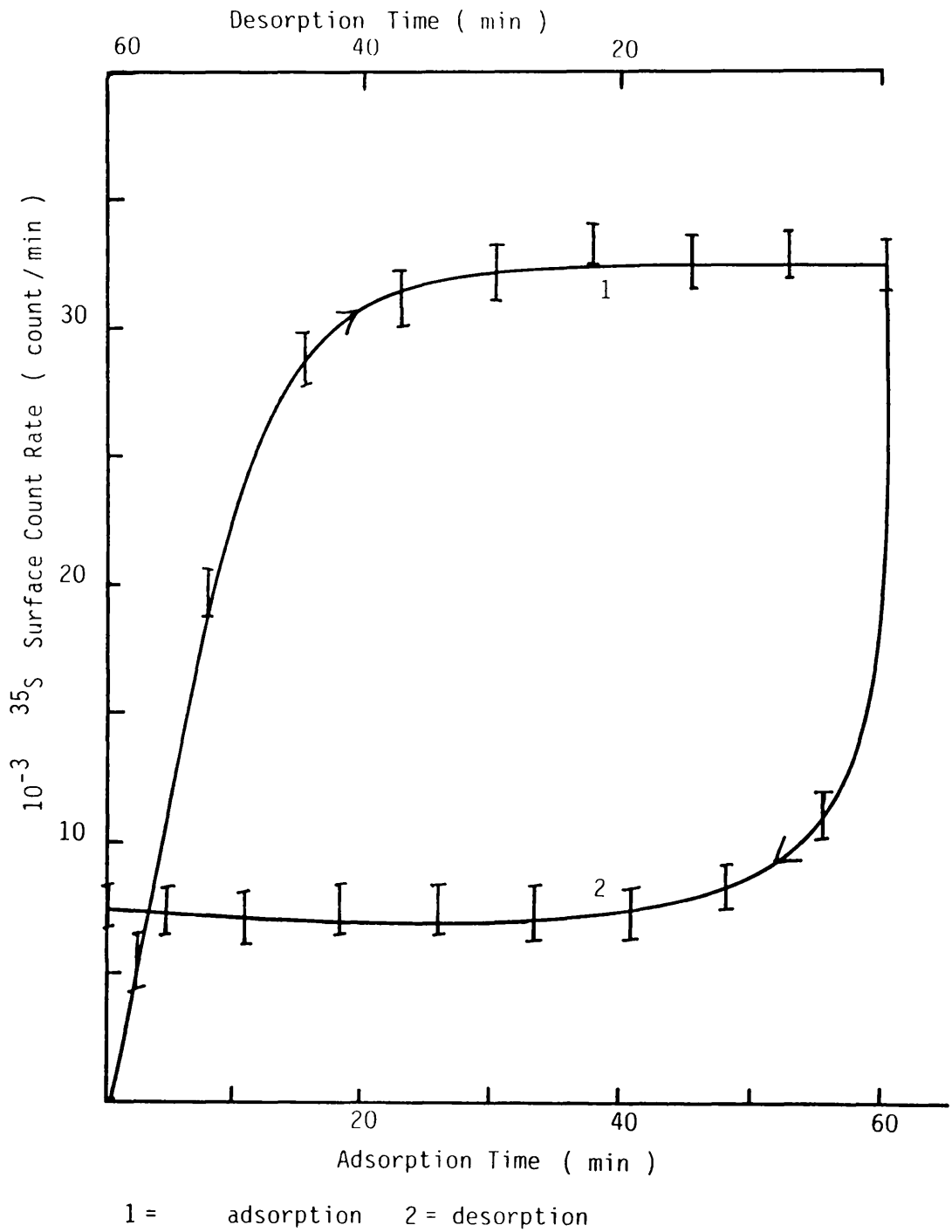
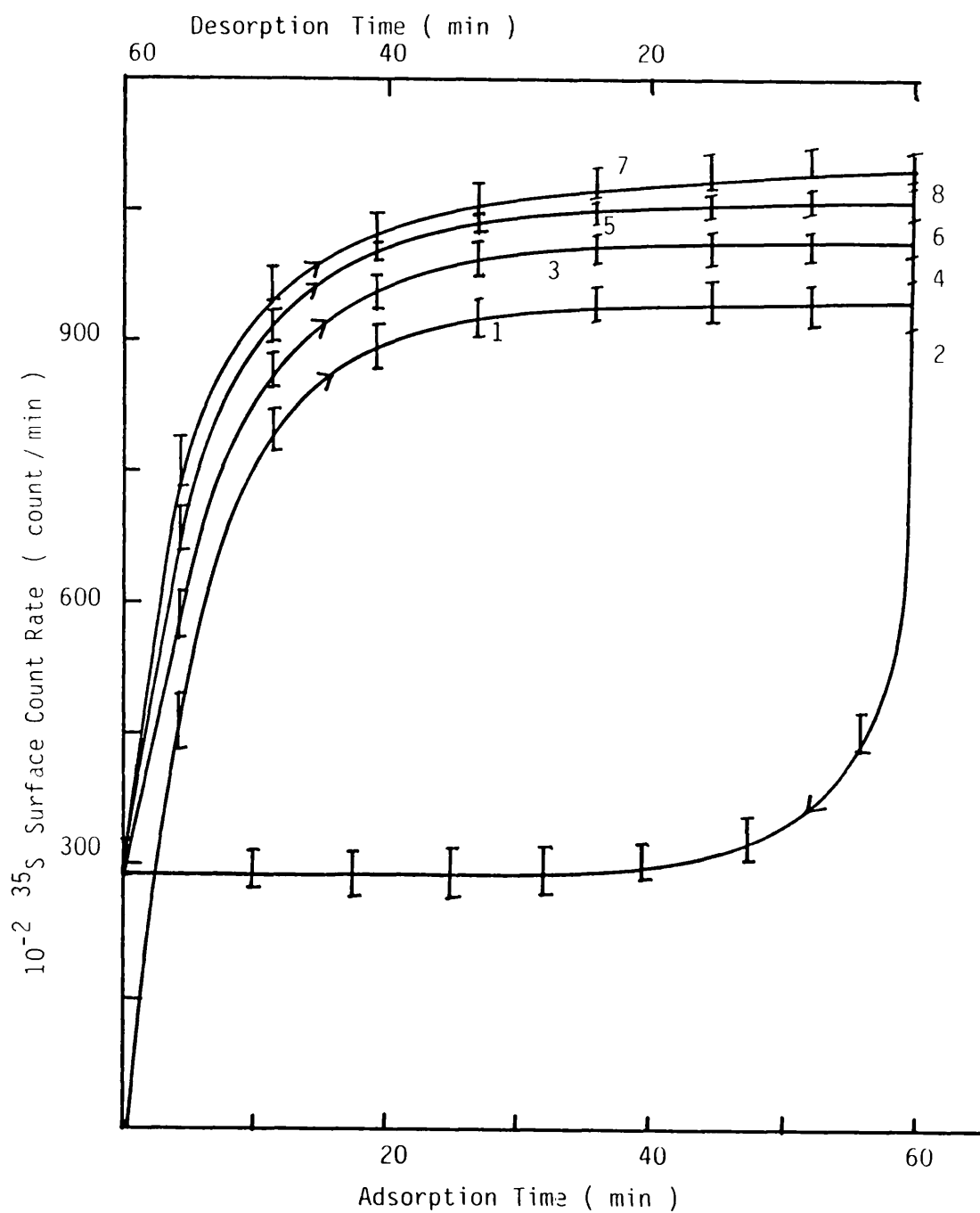


Figure 5.14 Adsorption/Desorption Cycles of  $^{35}\text{SF}_4$  over  $\text{CsF}/\gamma$ -alumina  
 $4.4 \text{ mmol g}^{-1}$



1,3,5,7 = Adsorptions

2,4,6,8 = Desorptions

Initial Pressure of  $^{35}\text{SF}_4 = 310 \text{ Torr}$

Figure 5.15 Adsorption/Desorption Cycle of  $^{35}\text{SF}_4$  over CsF/ $\gamma$ -alumina  
 $8.8 \text{ mmol g}^{-1}$

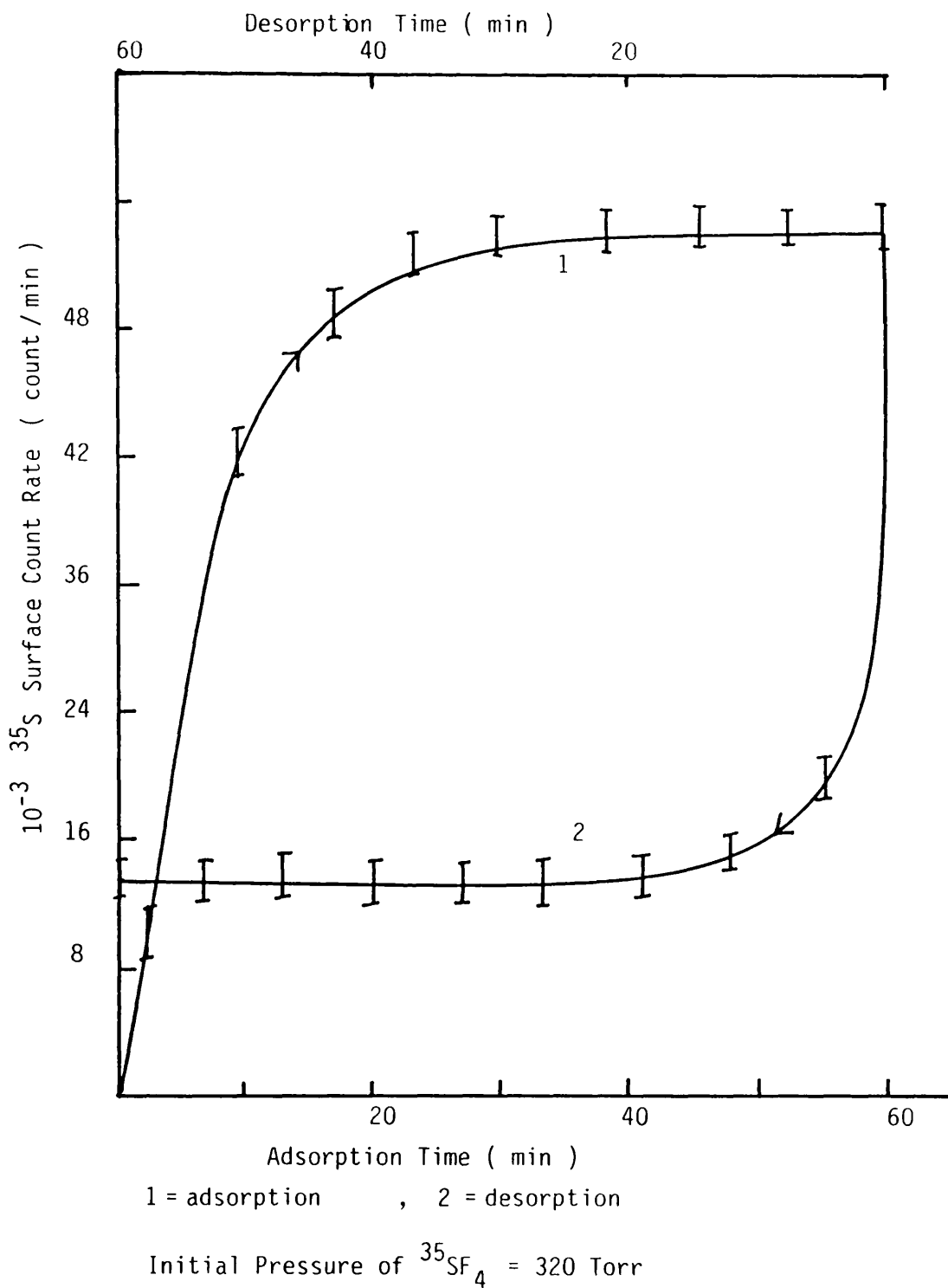
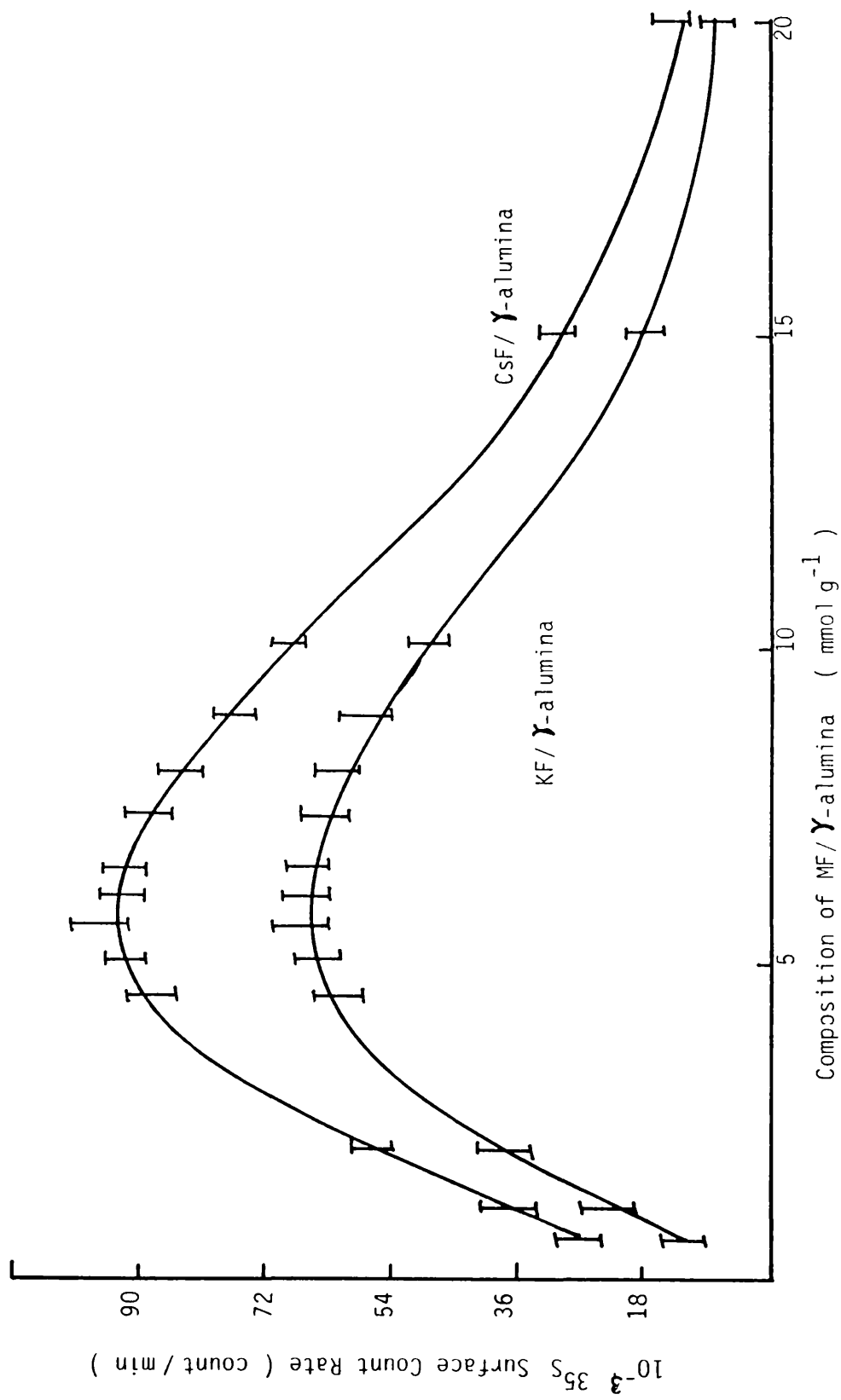


Figure 5.16 Reaction of  $^{35}\text{SF}_4$  with MF/ $\gamma$ -alumina as a function of metal fluoride loading  
Initial Pressure of  $^{35}\text{SF}_4 = 300$  Torr



**Table 5.12** Infra-Red Spectrum of the Volatile Products obtained from the Reaction between Thionyl Fluoride and Supported Potassium Fluoride, 4.4 mmolg<sup>-1</sup>

This Work	Literature 175	
	SOF <sub>2</sub>	SO <sub>2</sub>
393	393 ν <sub>6</sub>	
527	526 ν <sub>3</sub>	
728	721 ν <sub>5</sub>	
807	801 ν <sub>2</sub>	
1159	721 ν <sub>5</sub>	1151 ν <sub>1</sub>
1318	1308 ν <sub>1</sub>	
1369	1308 ν <sub>1</sub>	1362 ν <sub>3</sub>



Figure 5.17

Decrease in the Partial Pressure of  $\text{SOF}_2$  over  
with time

- 1)  $\text{KF}/\gamma\text{-alumina}$ ,  $4.4 \text{ mmol g}^{-1}$
- 2)  $\text{CsF}/\gamma\text{-alumina}$ ,  $4.4 \text{ mmol g}^{-1}$
- 3)  $\text{KF}/\gamma\text{-alumina}$ ,  $8.8 \text{ mmol g}^{-1}$
- 4)  $\text{CsF}/\gamma\text{-alumina}$ ,  $8.8 \text{ mmol g}^{-1}$

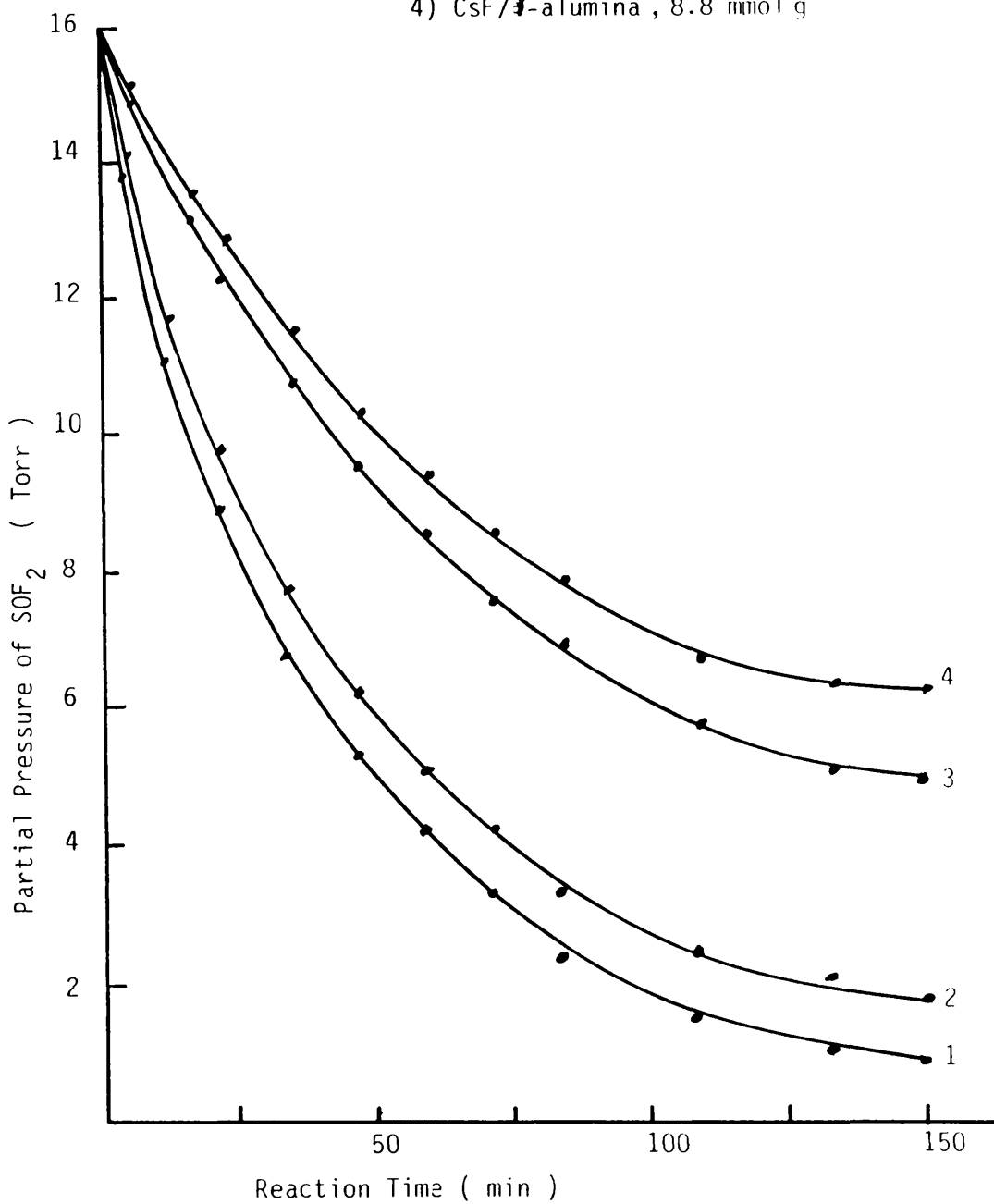
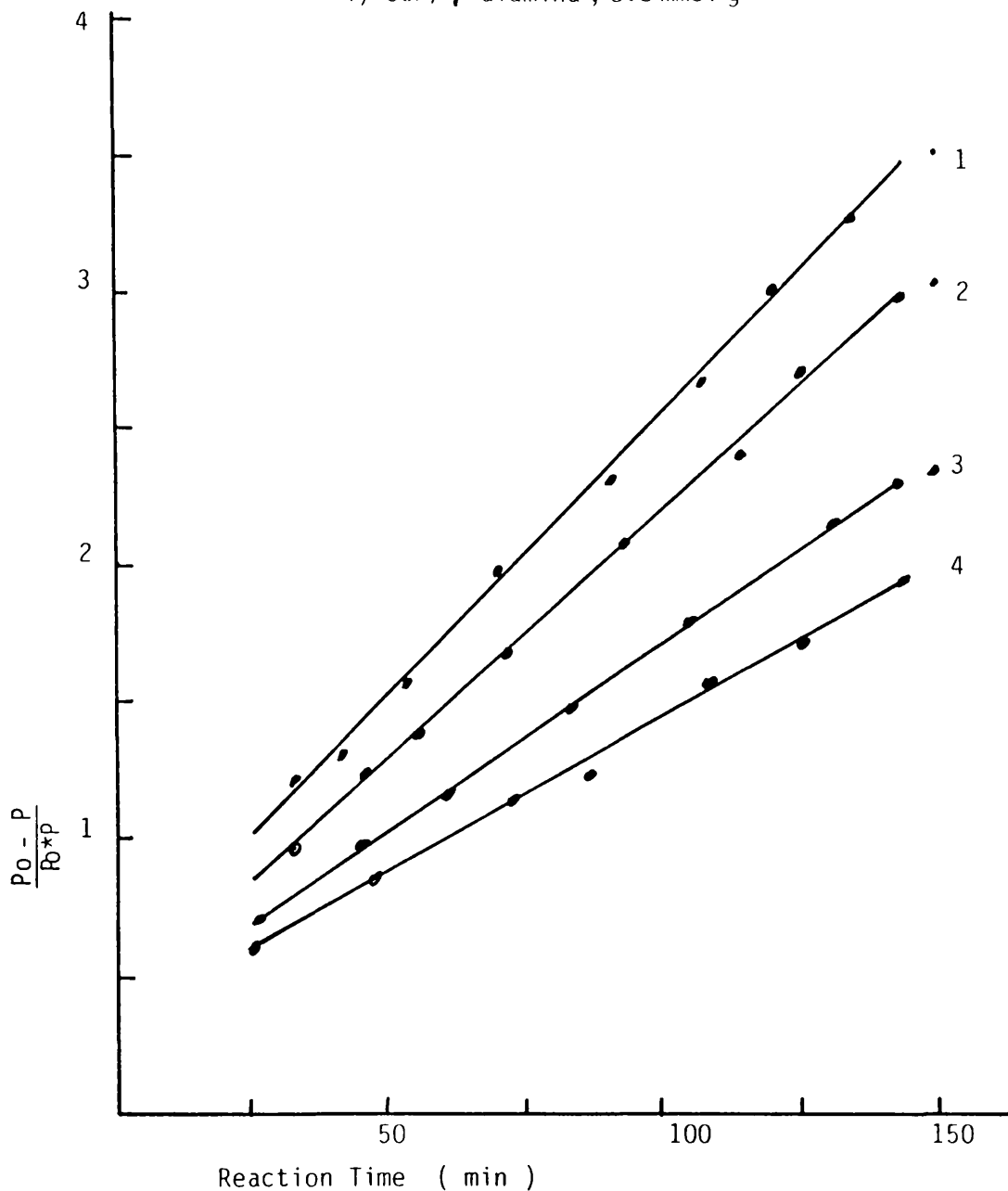


Figure 5.18 Second order plot of the hydrolysis of  $\text{SOF}_2$  with time over

- 1)  $\text{KF}/\gamma$ -alumina,  $4.4 \text{ mmol g}^{-1}$
- 2)  $\text{CsF}/\gamma$ -alumina,  $4.4 \text{ mmol g}^{-1}$
- 3)  $\text{KF}/\gamma$ -alumina,  $8.8 \text{ mmol g}^{-1}$
- 4)  $\text{CsF}/\gamma$ -alumina,  $8.8 \text{ mmol g}^{-1}$



The composition of the gas products after reaction between thionyl fluoride and the supported metal fluoride was dependent on the metal fluoride loadings in the range 1.1-15.0 mmol $g^{-1}$ . The results obtained for the 4.4 and 8.8 mmol $g^{-1}$  samples are given in Tables 5.13 and 5.14. The best data obtained were converted into ratios and are summarised in Table 5.15.

#### 5.3.6 MANOMETRIC STUDY OF REACTIONS OF THIONYL FLUORIDE WITH CAESIUM OR POTASSIUM FLUORIDE SUPPORTED ON $\gamma$ -ALUMINA

The uptakes of thionyl fluoride and/or its hydrolysis product, sulphur dioxide by the supported metal fluoride were studied manometrically across the composition range 1.1-15.0 mmol $g^{-1}$  at different initial pressures of gas in the range 60-300 Torr. The uptakes of thionyl fluoride by the supported metal fluoride, 4.4 and 8.8 mmol $g^{-1}$  were pressure dependent. The results obtained are given in Table 5.16 and shown schematically in Fig. 5.19. The uptake was also dependent on the metal fluoride loading, in that, the uptake was increased by increasing the metal fluoride loading in the range 1.1-5.5 mmol $g^{-1}$ , then decreased thereafter. The results obtained are given in Table 5.17 and shown in Fig. 5.20 at an initial pressure of thionyl fluoride of 300 Torr. At all pressures studied, the interactions involving supported caesium fluoride were greater than those involving supported potassium fluoride under the same conditions.

In each case the infra-red spectrum of the supported metal fluoride in the range 2-10 mmol $g^{-1}$ , after reaction with thionyl fluoride, showed very strong bands at 594 and 1193  $cm^{-1}$ . These two bands were attributed to the fluorosulphite,  $SO_2F^-$  anion, but there was no evidence for trifluorosulphite. The infra-red

Table 5.13 Results of the Infra-red Analysis of the Gas Products after Reaction between Thionyl Fluoride and Supported Caesium Fluoride prepared from Aqueous Solution

Solid mmolg <sup>-1</sup>	Gas Admitted to infra-red cell	Composition of Gas Products in the Infra-red Cell					
		SOF <sub>2</sub>			SO <sub>2</sub>		
Torr	mmol	Torr	mmol	Torr	mmol	Torr	mmol
15.1 ± 0.5	0.043 ± 0.002	3.2 ± 0.2	0.009 ± 0.0006	11.5 ± 0.2	0.0033 ± 0.0006		
14.6 ± 0.5	0.042 ± 0.002	3.6 ± 0.2	0.01 ± 0.0006	11.3 ± 0.2	0.0032 ± 0.0006		
16.2 ± 0.5	0.047 ± 0.002	3.9 ± 0.2	0.011 ± 0.0006	12.6 ± 0.2	0.0036 ± 0.0006		
17.2 ± 0.5	0.049 ± 0.002	3.9 ± 0.2	0.011 ± 0.0006	12.8 ± 0.2	0.0037 ± 0.0006		
15.2 ± 0.5	0.044 ± 0.002	3.9 ± 0.2	0.011 ± 0.0006	11.1 ± 0.2	0.0032 ± 0.0006		
16.3 ± 0.5	0.047 ± 0.002	7.7 ± 0.2	0.022 ± 0.0006	8.3 ± 0.2	0.0024 ± 0.0006		
15.7 ± 0.5	0.045 ± 0.002	8.0 ± 0.2	0.023 ± 0.0006	8.1 ± 0.2	0.0023 ± 0.0006		
14.2 ± 0.5	0.041 ± 0.002	6.9 ± 0.2	0.020 ± 0.0006	6.7 ± 0.2	0.0020 ± 0.0006		
15.8 ± 0.5	0.045 ± 0.002	8.1 ± 0.2	0.023 ± 0.0006	8.5 ± 0.2	0.0024 ± 0.0006		
16.2 ± 0.5	0.047 ± 0.002	8.3 ± 0.2	0.024 ± 0.0006	8.6 ± 0.2	0.0025 ± 0.0006		

Table 5.14 Results of the Infra-red Analysis of the Gas Products after Reaction between Thionyl Fluoride and Supported Potassium Fluoride prepared from Aqueous Solution

Solid mmol <sup>-1</sup>	Gas Admitted to infra-red cell		Composition of Gas Products in the Infra-red Cell			
	Torr	mmol	Torr	mmol	Torr	mmol
4.4	15.9 ± 0.5	0.046 ± 0.002	3.2 ± 0.2	0.009 ± 0.0006	12.1 ± 0.2	0.0035 ± 0.0006
	14.2 ± 0.5	00.41 ± 0.002	3.7 ± 0.2	0.01 ± 0.0006	11.5 ± 0.2	0.0033 ± 0.0006
	16.3 ± 0.5	0.047 ± 0.002	3.4 ± 0.2	0.01 ± 0.0006	11.6 ± 0.2	0.0033 ± 0.0006
	15.3 ± 0.5	00.44 ± 0.002	3.2 ± 0.2	0.009 ± 0.0006	11.8 ± 0.2	0.0034 ± 0.0006
	17.1 ± 0.5	0.049 ± 0.002	3.3 ± 0.2	0.009 ± 0.0006	12.7 ± 0.2	0.0036 ± 0.0006
8.8	16.8 ± 0.5	00.48 ± 0.002	6.7 ± 0.2	0.019 ± 0.0006	10.9 ± 0.2	0.0031 ± 0.0006
	14.2 ± 0.5	0.041 ± 0.002	5.5 ± 0.2	0.016 ± 0.0006	9.3 ± 0.2	0.0027 ± 0.0006
	15.3 ± 0.5	00.44 ± 0.002	6.0 ± 0.2	0.017 ± 0.0006	10.1 ± 0.2	0.0029 ± 0.0006
	17.2 ± 0.5	00.49 ± 0.002	6.2 ± 0.2	0.018 ± 0.0006	11.5 ± 0.2	0.0033 ± 0.0006
	15.4 ± 0.5	0.044 ± 0.002	5.8 ± 0.2	0.017 ± 0.0006	10.1 ± 0.2	0.0029 ± 0.0006

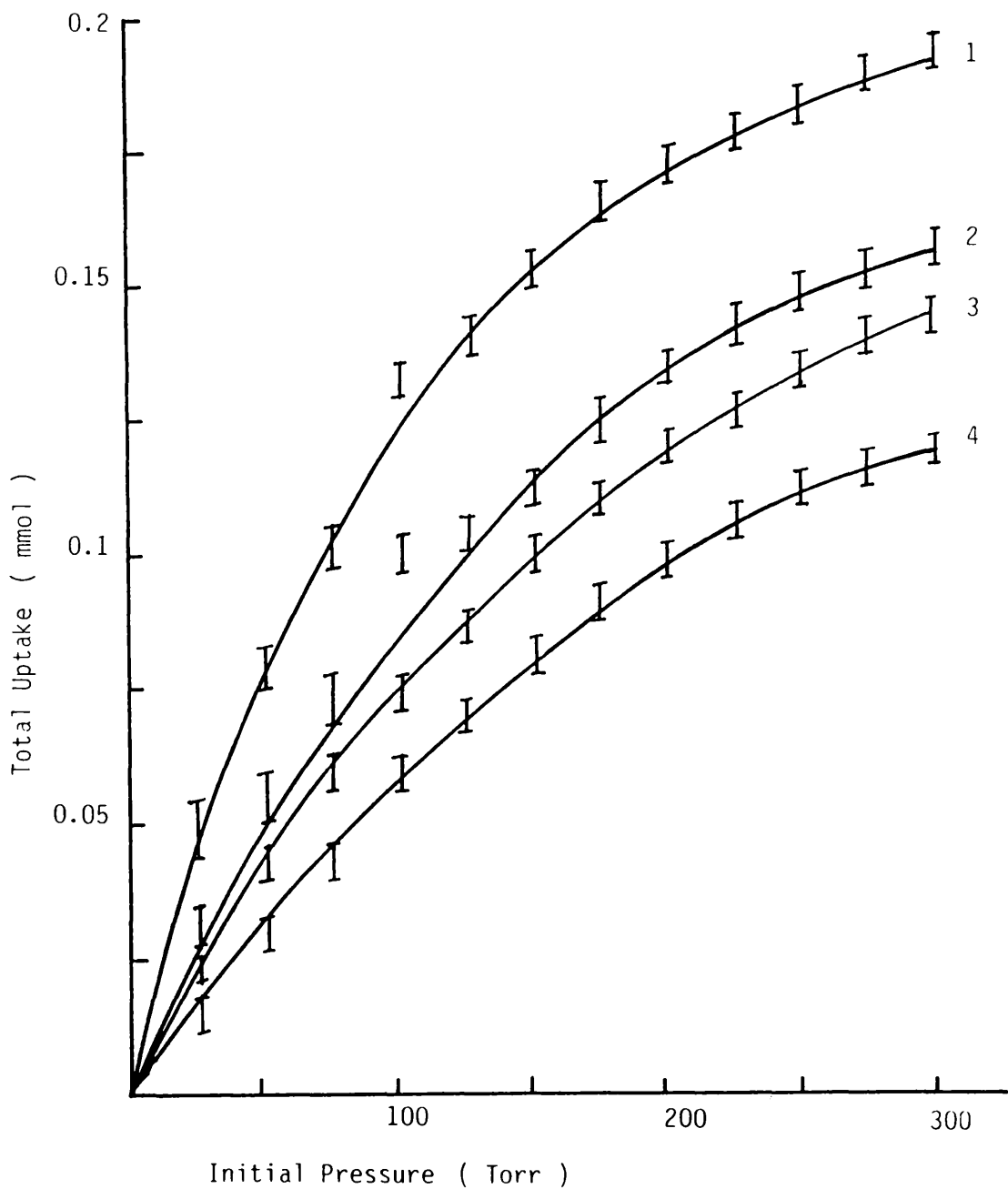
Table 5.15 The Composition of the Gas Products after Reaction between Thionyl Fluoride and Supported Metal Fluoride

Composition of Solid $\text{mmol g}^{-1}$ MF/ $\gamma$ -Alumina	Composition of Gas Products mole %			
	SOF <sub>2</sub>		SO <sub>2</sub>	
	M = Cs	M = K	M = Cs	M = K
1.1	12 ± 3	10 ± 2	88 ± 3	40 ± 2
2.0	19 ± 6	16 ± 7	81 ± 6	84 ± 3
4.4	24 ± 4	21 ± 4	76 ± 3	79 ± 4
5.0	28 ± 2	25 ± 3	72 ± 7	75 ± 4
8.8	48 ± 4	37 ± 3	52 ± 5	63 ± 5
15.0	61 ± 5	49 ± 6	39 ± 6	51 ± 4

**Table 5.16** Manometric Study of Reaction of Thionyl Fluoride with Cesium or Potassium Fluoride Supported on  $\gamma$ -Alumina  
**A** (mmol) total uptake  
**B** (mmol) retained gas

Initial Pressure Torr	CsF/ $\gamma$ -Alumina		KF/ $\gamma$ -Alumina					
	4.4 mmolg <sup>-1</sup>	8.8 mmolg <sup>-1</sup>	4.4 mmolg <sup>-1</sup>	8.8 mmolg <sup>-1</sup>				
40 ± 0.5	0.03 ± 0.006	0.008 ± 0.002	0.022 ± 0.005	0.004 ± 0.001	0.03 ± 0.006	0.008 ± 0.002	0.017 ± 0.05	0.003 ± 0.001
80 ± 0.5	0.071 ± 0.006	0.018 ± 0.002	0.04 ± 0.005	0.007 ± 0.001	0.06 ± 0.006	0.017 ± 0.002	0.038 ± 0.05	0.005 ± 0.001
120 ± 0.5	0.104 ± 0.006	0.028 ± 0.002	0.06 ± 0.005	0.01 ± 0.001	0.07 ± 0.006	0.019 ± 0.002	0.050 ± 0.05	0.008 ± 0.001
160 ± 0.5	0.12 ± 0.006	0.032 ± 0.002	0.08 ± 0.005	0.014 ± 0.001	0.09 ± 0.006	0.025 ± 0.002	0.06 ± 0.05	0.01 ± 0.001
200 ± 0.5	0.16 ± 0.006	0.042 ± 0.002	0.10 ± 0.005	0.018 ± 0.001	0.12 ± 0.006	0.033 ± 0.002	0.07 ± 0.05	0.012 ± 0.001
260 ± 0.5	0.18 ± 0.006	0.043 ± 0.002	0.12 ± 0.005	0.020 ± 0.001	0.15 ± 0.006	0.037 ± 0.002	0.09 ± 0.05	0.015 ± 0.001
280 ± 0.5	0.19 ± 0.006	0.058 ± 0.002	0.13 ± 0.005	0.023 ± 0.001	0.16 ± 0.006	0.039 ± 0.002	0.11 ± 0.05	0.020 ± 0.001
300 ± 0.5	0.20 ± 0.006	0.065 ± 0.002	0.15 ± 0.005	0.025 ± 0.001	0.17 ± 0.006	0.047 ± 0.002	0.12 ± 0.05	0.022 ± 0.001

Figure 5.19 Reaction of  $\text{SOF}_2$  with MF/ $\gamma$ -alumina  
 Total Uptake  $\underline{V}$  Initial Pressure



KF/ $\gamma$ -alumina	Composition	CsF/ $\gamma$ -alumina
2	4.4 mmol g <sup>-1</sup>	1
4	8.8 mmol g <sup>-1</sup>	3

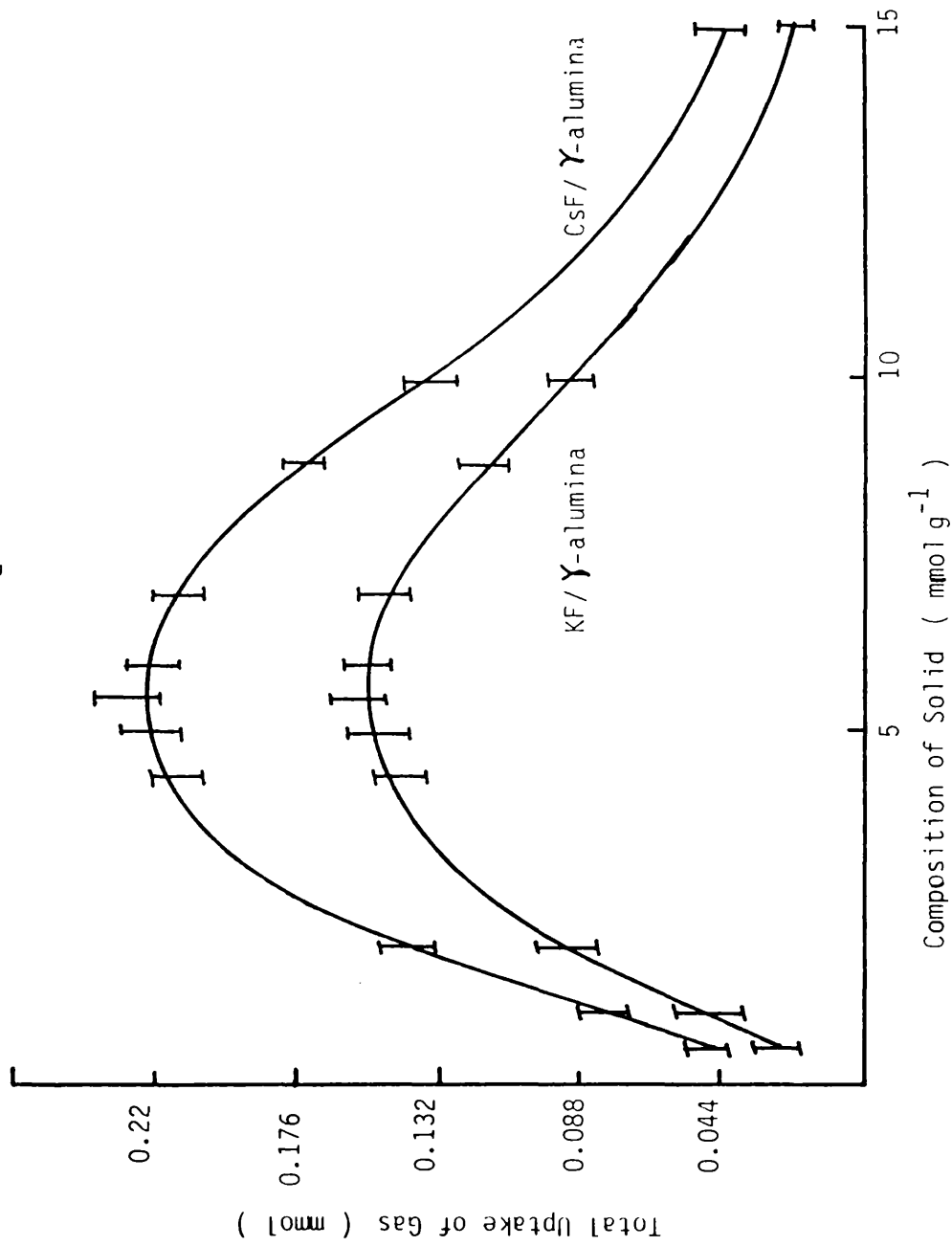


Table 5.17 Summary of the Manometric Results of the Reaction of Thionyl Fluoride with Supported Metal Fluoride

Composition mmol g <sup>-1</sup>	CsF/ $\gamma$ -Alumina		KF/ $\gamma$ -Alumina	
	Total Uptake (mmol)	Retained Gas (mmol)	Total Uptake (mmol)	Retained Gas (mmol)
1.1	0.08	0.016	0.065	0.013
2.0	0.12	0.036	0.095	0.025
4.4	0.20	0.065	0.17	0.047
5.0	0.21	0.07	0.18	0.050
8.8	0.15	0.025	0.12	0.022
15.0	0.04	0.008	0.025	0.01

Initial pressure of thionyl fluoride 300 Torr.

Figure 5.20 Reaction of  $\text{SOF}_2$  with MF/ $\gamma$ -alumina, Total uptake  $\gamma$  Metal Fluoride Loading  
 Initial Pressure of  $\text{SOF}_2 = 310$  Torr



spectrum of KF/ $\gamma$ -alumina 10.0 mmol g<sup>-1</sup> after reaction with thionyl fluoride at room temperature, is given in Table 5.18.

### **5.3.7 THE CHANGE IN THE TEMPERATURE OF SOLID CAESIUM OR POTASSIUM FLUORIDE SUPPORTED ON $\gamma$ -ALUMINA DURING REACTION WITH THIONYL FLUORIDE**

The reactions between thionyl fluoride and the supported metal fluoride were also very exothermic. The change in the temperature of the supported metal fluoride was obtained and appeared to be dependent on the initial pressure used, under the same conditions, reactions involving supported potassium fluoride appeared to be more exothermic. The change in the temperature for a given initial pressure was dependent on the metal fluoride loading in the range 0.6-15.0 mmol g<sup>-1</sup>. A small change in the temperatures of the supported metal fluoride during reaction with thionyl fluoride was recorded with increasing metal fluoride loading. The results obtained are shown in Fig. 5.21.

The change in the temperatures of the supported metal fluoride prepared from heptafluoroisopropoxide salts, during reaction with thionyl fluoride exhibited similar characteristics as those described above. However, for equivalent conditions, the reactions involving materials prepared from non-aqueous solution appeared to be less exothermic, as shown in Fig. 5.21.

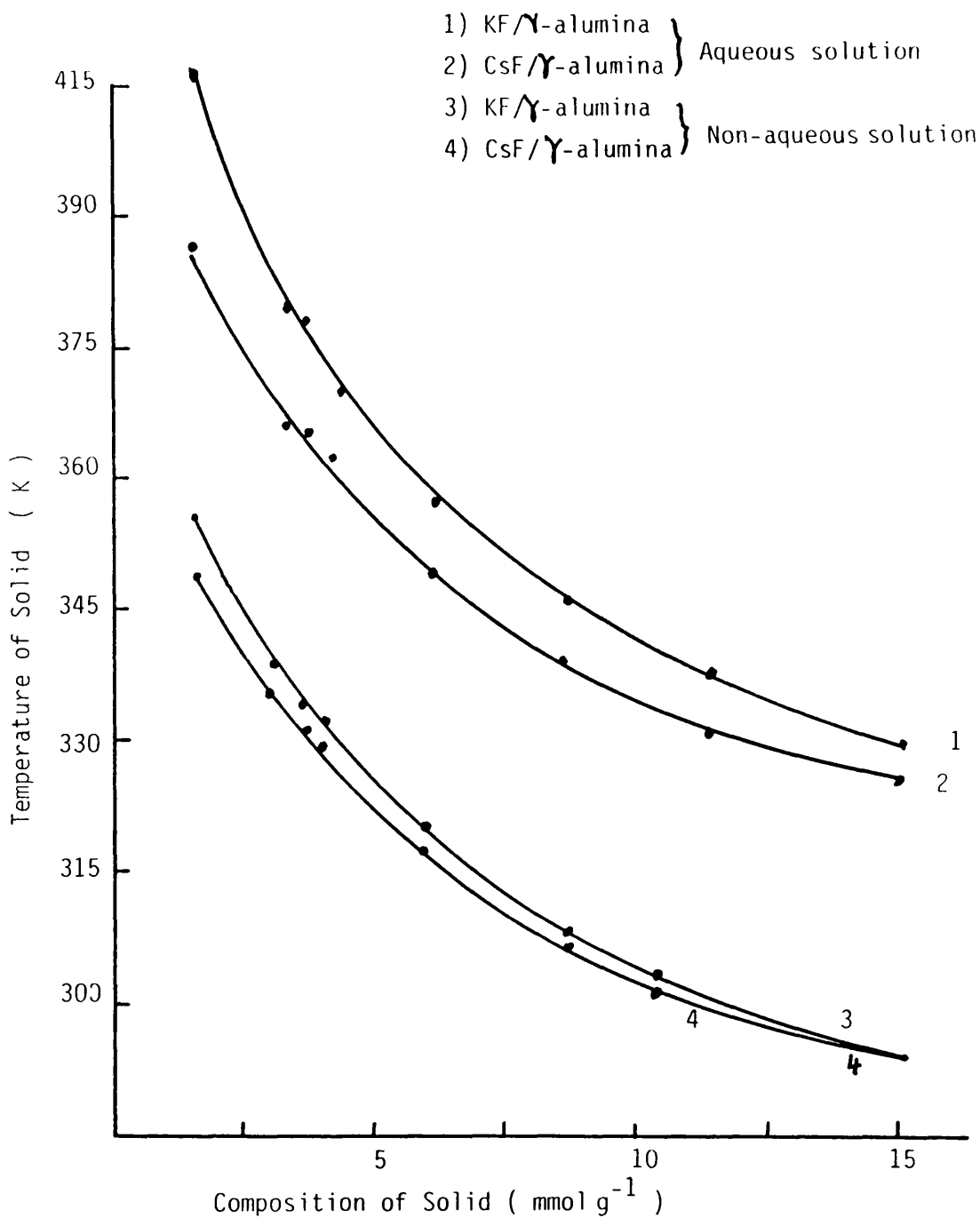
### **5.3.8 REACTIONS OF [<sup>35</sup>S]-SULPHUR LABELLED THIONYL FLUORIDE WITH CAESIUM OR POTASSIUM FLUORIDE SUPPORTED ON $\gamma$ -ALUMINA**

The reaction between [<sup>35</sup>S]-sulphur labelled thionyl fluoride and supported metal fluorides was studied at different initial pressures in the range 10-300 Torr across the composition range

Table 5.18 Infra-Red Spectrum of KF/ $\gamma$ -Alumina 10.0 mmolg<sup>-1</sup> after Reaction with Thionyl Fluoride

This Work	Literature	52
SOF <sub>2</sub> CsF	KSO <sub>2</sub> F	
1264 $\nu_1$		
1193	1178 $\nu_5$	
1109	1100 $\nu_1$	
695 $\nu_2$		
667 $\nu_7$		
623 $\nu_4$		
594	598 $\nu_2$	
470	471 $\nu_3$	

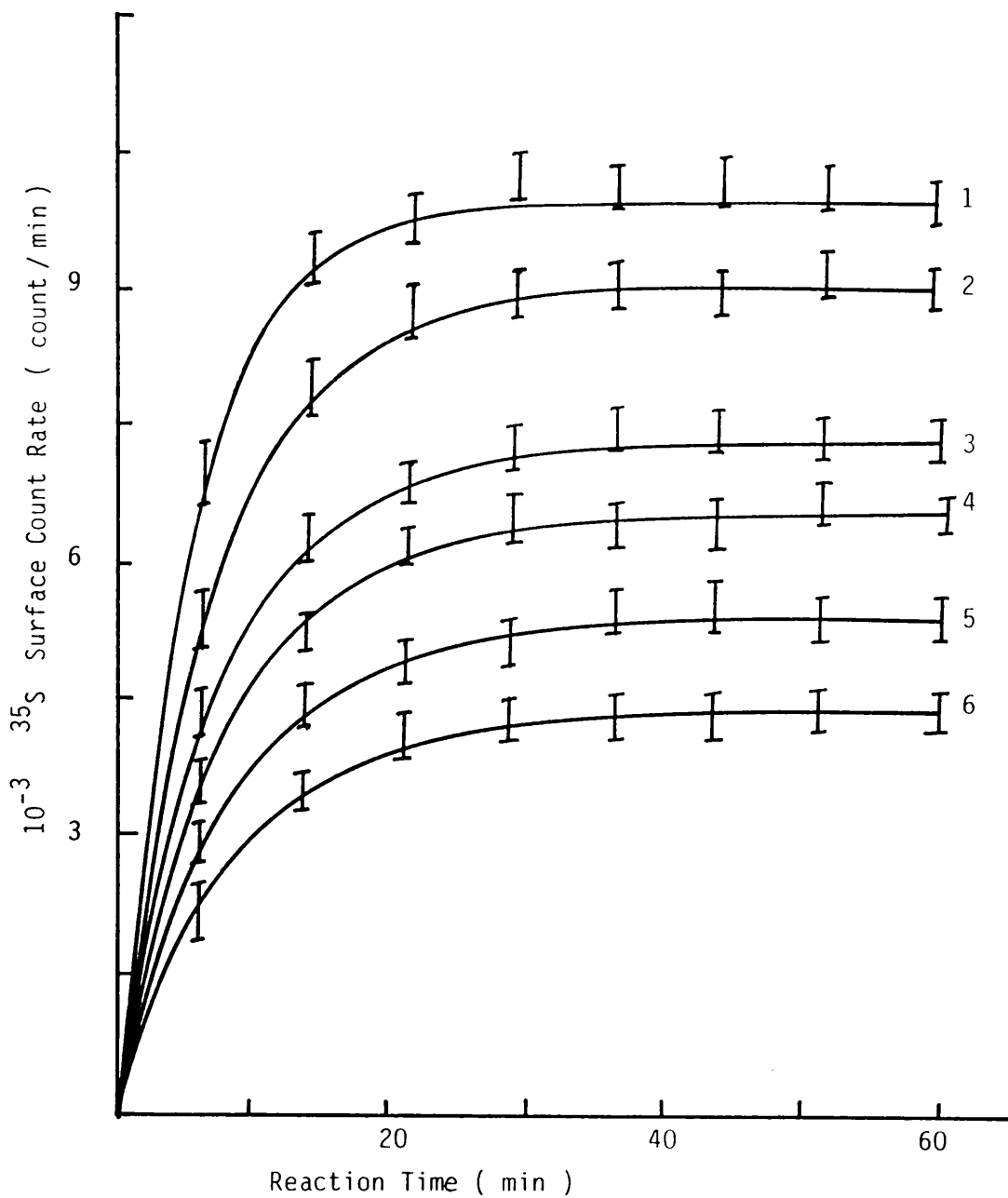
Figure 5.21 Change in temperature of MF/ $\gamma$ -alumina during reaction with  $\text{SOF}_2$  as a function of metal fluoride loading



0.6-20.0 mmol g<sup>-1</sup>. Surface count rates were measured directly and the overall drop in the gas phase count rate was used as a measure of the total uptake. Each reaction was followed for 60 min before removing the [<sup>35</sup>S]-sulphur labelled volatile materials from the counting cell to determine the surface count rate of the supported metal fluoride in the absence of gas. Plots of the surface count rate of the supported metal fluoride, 4.4, 5.5 and 8.8 mmol g<sup>-1</sup> versus time at initial pressures of [<sup>35</sup>S]-sulphur labelled thionyl fluoride of 60, 160 and 240 Torr, are shown in Figs. 5.22-5.24. There was a rapid initial increase in the surface count rate until a constant level was reached after 20 min. The removal of the [<sup>35</sup>S]-sulphur labelled volatile products from the counting vessel by condensation at 77K, resulted in a drop of ca 74-85% of the original [<sup>35</sup>S]-sulphur surface count rate of the supported metal fluoride, 4.4-8.8 mmol g<sup>-1</sup>. The major surface species was evidently weakly adsorbed with only 26-15% of the total surface count rate being due to a permanently retained species. The results obtained from these reactions are summarised in Tables 5.19-5.22 and shown schematically in Figs. 5.25-5.27. The [<sup>35</sup>S]-sulphur surface count rates of the supported metal fluoride in the presence of gas and after pumping at room temperature and the total uptake of gas, were dependent on the initial pressure of [<sup>35</sup>S]-sulphur labelled thionyl fluoride. Pumping the solid for 2 days under vacuum at room temperature after the removal of the gas phase had no effect in the surface count rate, but the [<sup>35</sup>S]-sulphur surface count rate decreased to background when the solid was heated to 373K under vacuum or was exposed to aliquots of water vapour.

The re-admission of [<sup>35</sup>S]-sulphur labelled thionyl fluoride

Figure 5.22 Reaction of  $^{35}\text{SOF}_2$  with MF/ $\gamma$ -alumina  
 Surface Count Rate  $\bar{V}$  Reaction Time  
 Initial Pressure of  $^{35}\text{SOF}_2 = 60$  Torr



KF/ $\gamma$ -alumina	Composition	CsF/ $\gamma$ -alumina
3	$5.5 \text{ mmol g}^{-1}$	1
4	$4.4 \text{ mmol g}^{-1}$	2
6	$8.8 \text{ mmol g}^{-1}$	5

Figure 5.23 Reaction of  $^{35}\text{SOF}_2$  with MF/ $\gamma$ -alumina  
 Surface Count Rate  $\propto$  Reaction Time  
 Initial Pressure of  $^{35}\text{SOF}_2 = 160$  Torr

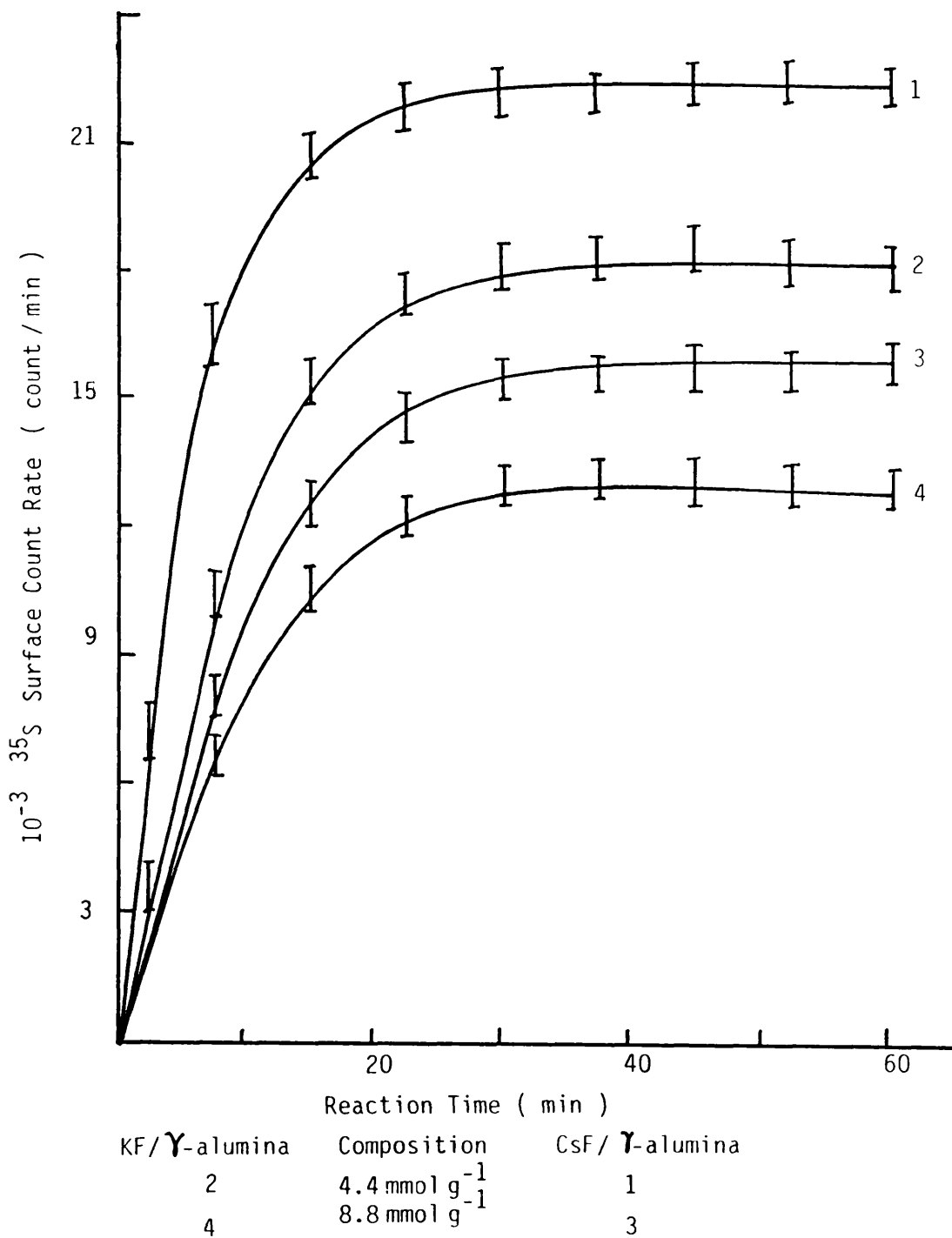
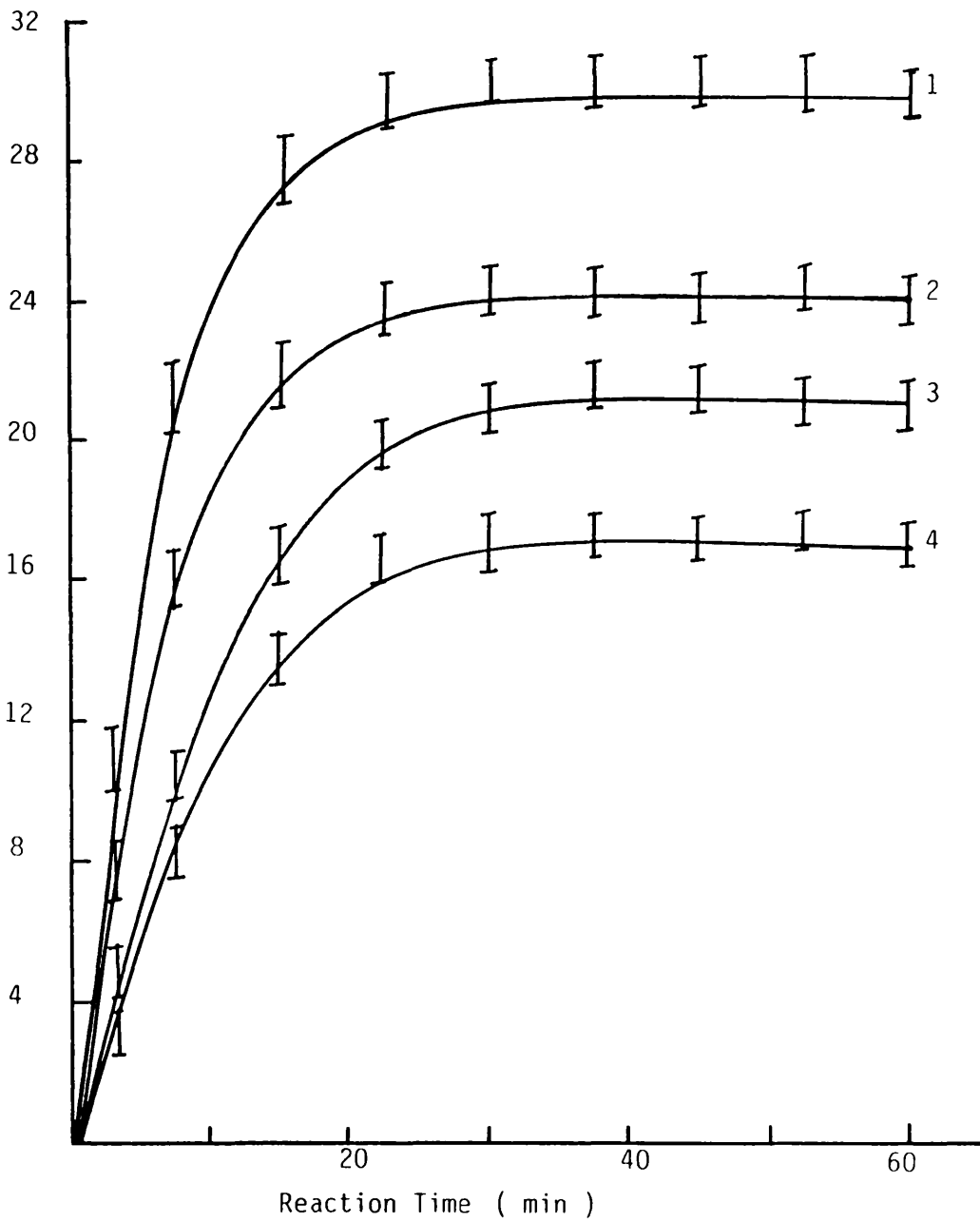




Figure 5.24 Reaction of  $^{35}\text{SOF}_2$  with MF/  $\gamma$ -alumina  
 Surface Count Rate  $\nu$  Reaction Time  
 Initial Pressure of  $^{35}\text{SOF}_2 = 240$  Torr



KF/ $\gamma$ -alumina	Composition	CsF/ $\gamma$ -alumina
2	$4.4 \text{ mmol g}^{-1}$	1
4	$8.8 \text{ mmol g}^{-1}$	3

Table 5.19 Results of Reaction between [<sup>35</sup>S]-Sulphur Labelled Thionyl Fluoride with Supported Caesium Fluoride, 4.4 mmol g<sup>-1</sup>

Initial Pressure (Torr)	Total Drop in the Gas Count Rate Count min <sup>-1</sup>	Total Uptake of Gas mmol	Surface Count Rate Count min <sup>-1</sup>	Surface Count Rate after Removal of Gas Count min <sup>-1</sup>
10.3 ± 0.5	314 ± 113	0.01 ± 0.006	1898 ± 103	494 ± 107
20.6 ± 0.5	535 ± 119	0.017 ± 0.006	3277 ± 149	839 ± 119
40.2 ± 0.5	1102 ± 179	0.035 ± 0.006	6654 ± 163	1729 ± 127
60.3 ± 0.5	1574 ± 152	0.05 ± 0.006	9095 ± 202	2360 ± 134
80.8 ± 0.5	2046 ± 189	0.065 ± 0.006	11145 ± 272	3088 ± 167
100.5 ± 0.5	2581 ± 215	0.082 ± 0.006	14801 ± 347	3854 ± 189
120.6 ± 0.5	3022 ± 273	0.096 ± 0.006	16751 ± 389	4355 ± 197
140.6 ± 0.5	3463 ± 301	0.11 ± 0.006	19553 ± 457	5103 ± 217
160.7 ± 0.5	3871 ± 319	0.12 ± 0.006	22584 ± 541	5792 ± 281
180.4 ± 0.5	4312 ± 389	0.14 ± 0.006	25220 ± 679	6546 ± 299
200.9 ± 0.5	4721 ± 417	0.15 ± 0.006	27753 ± 717	7287 ± 318
220.8 ± 0.5	5099 ± 456	0.16 ± 0.006	30203 ± 789	7865 ± 342
240.7 ± 0.5	5434 ± 483	0.17 ± 0.006	32606 ± 829	8405 ± 357
260.4 ± 0.5	5760 ± 500	0.18 ± 0.006	34920 ± 899	8983 ± 387
280.5 ± 0.5	6075 ± 519	0.19 ± 0.006	36476 ± 973	9516 ± 389
300.1 ± 0.5	6346 ± 543	0.20 ± 0.006	38292 ± 1091	9971 ± 407

Sample Weight 0.5g, 1.32 mmol of CsF.

Table 5.20 Results of Reaction between [<sup>35</sup>S]-Sulphur Labelled Thionyl Fluoride with Supported Caesium Fluoride, 8.8 mmol g<sup>-1</sup>

Initial Pressure (Torr)	Total Drop in the Gas Count Rate Count min <sup>-1</sup>	Total Uptake of Gas mmol	Surface Count Rate Count min <sup>-1</sup>	Surface Count Rate after Removal of Gas Count min <sup>-1</sup>
10.1 ± 0.5	188 ± 103	0.007 ± 0.006	792 ± 109	138 ± 102
20.7 ± 0.5	346 ± 112	0.011 ± 0.006	1481 ± 142	253 ± 119
40.4 ± 0.5	661 ± 123	0.021 ± 0.006	2795 ± 183	485 ± 127
60.7 ± 0.5	944 ± 152	0.03 ± 0.006	3998 ± 205	694 ± 145
80.5 ± 0.5	1291 ± 179	0.041 ± 0.006	5502 ± 275	948 ± 173
100.0 ± 0.5	1605 ± 207	0.051 ± 0.006	6650 ± 317	1157 ± 198
120.4 ± 0.5	2014 ± 213	0.064 ± 0.006	8172 ± 389	1388 ± 211
160.4 ± 0.5	2707 ± 247	0.086 ± 0.006	11081 ± 417	1922 ± 229
180.3 ± 0.5	2710 ± 301	0.086 ± 0.006	11192 ± 483	2060 ± 238
200.9 ± 0.5	3305 ± 319	0.105 ± 0.006	13840 ± 510	2385 ± 253
240.8 ± 0.5	3903 ± 348	0.124 ± 0.006	16601 ± 547	2848 ± 264
260.3 ± 0.5	4155 ± 411	0.132 ± 0.006	17867 ± 583	3044 ± 298
280.2 ± 0.5	4343 ± 422	0.138 ± 0.006	18667 ± 607	3164 ± 302
300.8 ± 0.5	4438 ± 484	0.141 ± 0.006	19016 ± 647	3230 ± 317

Sample Weight 0.5g, 1.88 mmol of CsF.

Table 5.21 Results of Reaction between [<sup>35</sup>S]-Sulphur Labelled Thionyl Fluoride with Supported Potassium Fluoride, 4.4 mmol g<sup>-1</sup>

Initial Pressure (Torr)	Total Drop in the Gas Count Rate Count min <sup>-1</sup>	Total Uptake of Gas mmol	Surface Count Rate Count min <sup>-1</sup>	Surface Count Rate after Removal of Gas Count min <sup>-1</sup>
10.9 ± 0.5	311 ± 126	0.009 ± 0.006	1827 ± 123	403 ± 107
20.7 ± 0.5	472 ± 147	0.015 ± 0.006	2761 ± 146	611 ± 127
40.4 ± 0.5	850 ± 183	0.027 ± 0.006	4985 ± 152	1096 ± 143
60.5 ± 0.5	1227 ± 217	0.039 ± 0.006	5492 ± 171	1210 ± 167
80.6 ± 0.5	1637 ± 283	0.052 ± 0.006	8074 ± 189	1777 ± 182
100.3 ± 0.5	1951 ± 319	0.062 ± 0.006	10054 ± 202	2211 ± 189
120.1 ± 0.5	2360 ± 353	0.075 ± 0.006	12652 ± 222	2778 ± 213
140.1 ± 0.5	2707 ± 379	0.086 ± 0.006	14809 ± 247	3257 ± 231
160.7 ± 0.5	3116 ± 416	0.099 ± 0.006	17438 ± 349	3824 ± 238
180.7 ± 0.5	3462 ± 472	0.11 ± 0.006	19568 ± 398	4309 ± 249
200.8 ± 0.5	3777 ± 493	0.12 ± 0.006	21554 ± 459	4745 ± 279
220.4 ± 0.5	4060 ± 506	0.13 ± 0.006	23342 ± 598	5135 ± 289
240.7 ± 0.5	4406 ± 537	0.14 ± 0.006	25561 ± 619	5613 ± 302
260.8 ± 0.5	4658 ± 583	0.15 ± 0.006	27105 ± 773	5972 ± 319
280.2 ± 0.5	4847 ± 621	0.154 ± 0.006	28299 ± 891	6224 ± 329
300.2 ± 0.5	5067 ± 649	0.16 ± 0.006	29685 ± 992	6533 ± 371

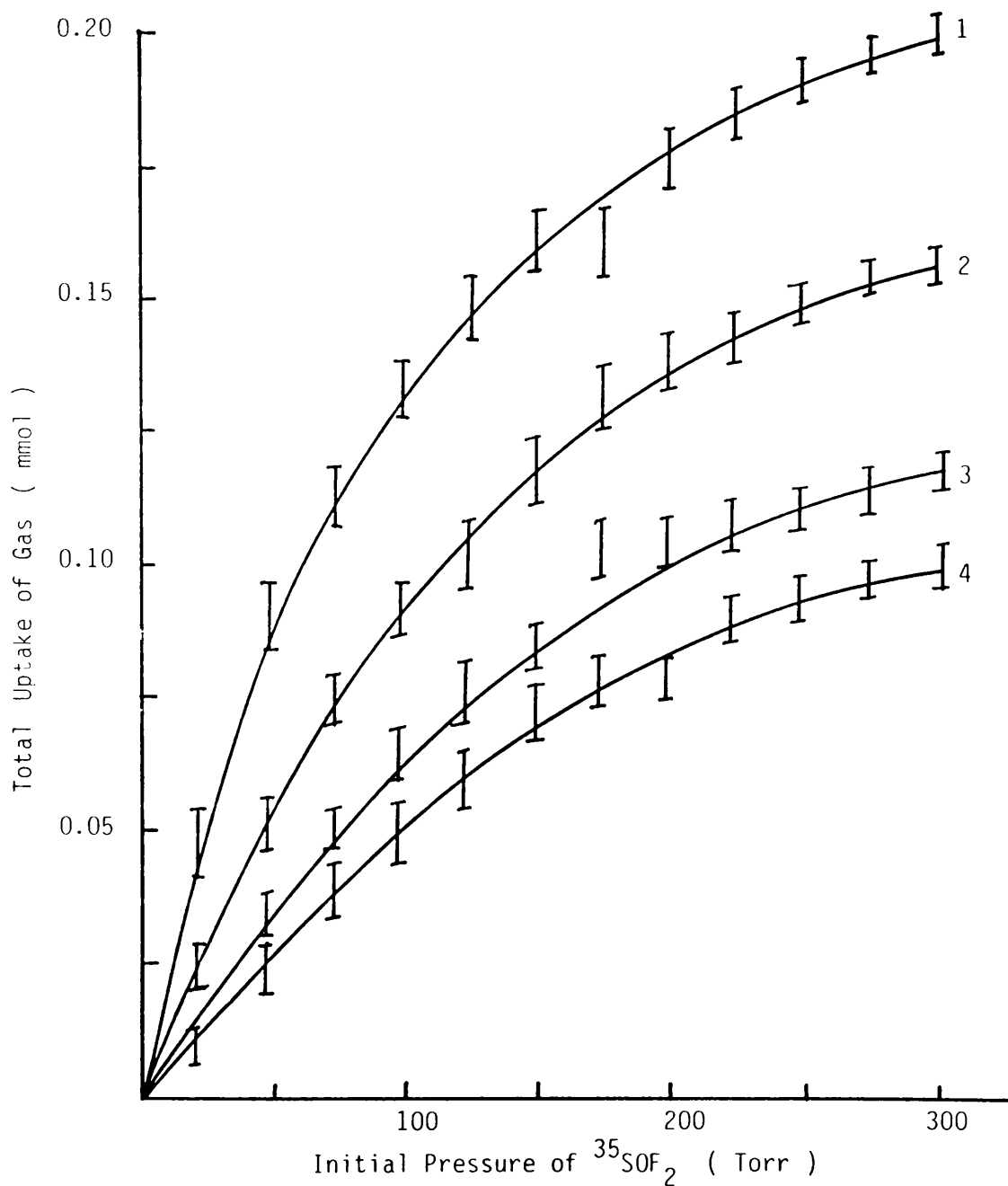
Sample Weight 0.38g, 1.32 mmol of KF.

Table 5.22 Results of Reaction between [ $^{35}\text{S}$ ]-Sulphur Labelled Thionyl Fluoride with Supported Potassium Fluoride, 8.8 mmol g $^{-1}$

Initial Pressure (Torr)	Total Drop in the Gas Count Rate Count min $^{-1}$	Total Uptake of Gas mmol	Surface Count Rate Count min $^{-1}$	Surface Count Rate after Removal of Gas Count min $^{-1}$
10.4 ± 0.5	125 ± 101	0.006 ± 0.006	476 ± 107	72 ± 65
20.1 ± 0.5	308 ± 117	0.01 ± 0.006	1166 ± 120	176 ± 82
40.8 ± 0.5	566 ± 123	0.018 ± 0.006	2159 ± 132	324 ± 97
60.9 ± 0.5	787 ± 149	0.025 ± 0.006	2988 ± 151	448 ± 107
80.3 ± 0.5	1039 ± 179	0.033 ± 0.006	3433 ± 173	516 ± 119
100.4 ± 0.5	1259 ± 189	0.04 ± 0.006	4312 ± 221	648 ± 131
120.8 ± 0.5	1574 ± 213	0.05 ± 0.006	5668 ± 262	836 ± 143
140.4 ± 0.5	1794 ± 243	0.057 ± 0.006	6398 ± 283	972 ± 157
160.8 ± 0.5	2046 ± 269	0.065 ± 0.006	7453 ± 317	1120 ± 161
180.9 ± 0.5	2360 ± 303	0.075 ± 0.006	8709 ± 354	1308 ± 173
200.0 ± 0.5	2581 ± 343	0.082 ± 0.006	9608 ± 389	1444 ± 182
220.2 ± 0.5	2833 ± 387	0.09 ± 0.006	10620 ± 444	1592 ± 190
240.4 ± 0.5	3053 ± 412	0.097 ± 0.006	11459 ± 492	1724 ± 197
260.6 ± 0.5	3242 ± 468	0.103 ± 0.006	15277 ± 557	1840 ± 203
280.6 ± 0.5	3400 ± 493	0.108 ± 0.006	13072 ± 589	1932 ± 207
300.2 ± 0.5	3557 ± 511	0.113 ± 0.006	13472 ± 623	2028 ± 211

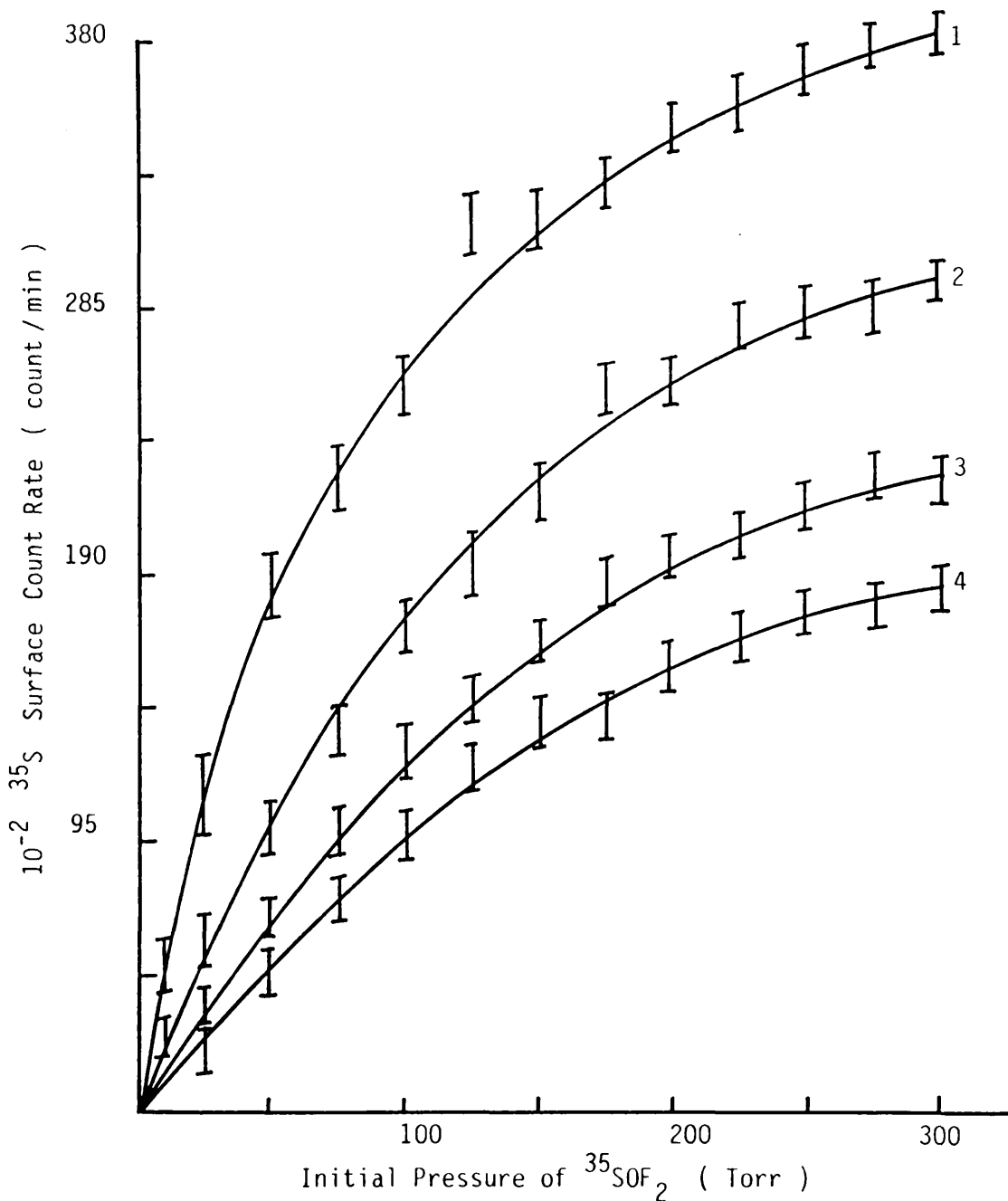
Sample Weight 0.38g, 1.32 mmol of KF.

Figure 5.25 Reaction of  $^{35}\text{SOF}_2$  with MF/ $\gamma$ -alumina  
 Total Uptake V Initial Pressure of  $^{35}\text{SOF}_2$



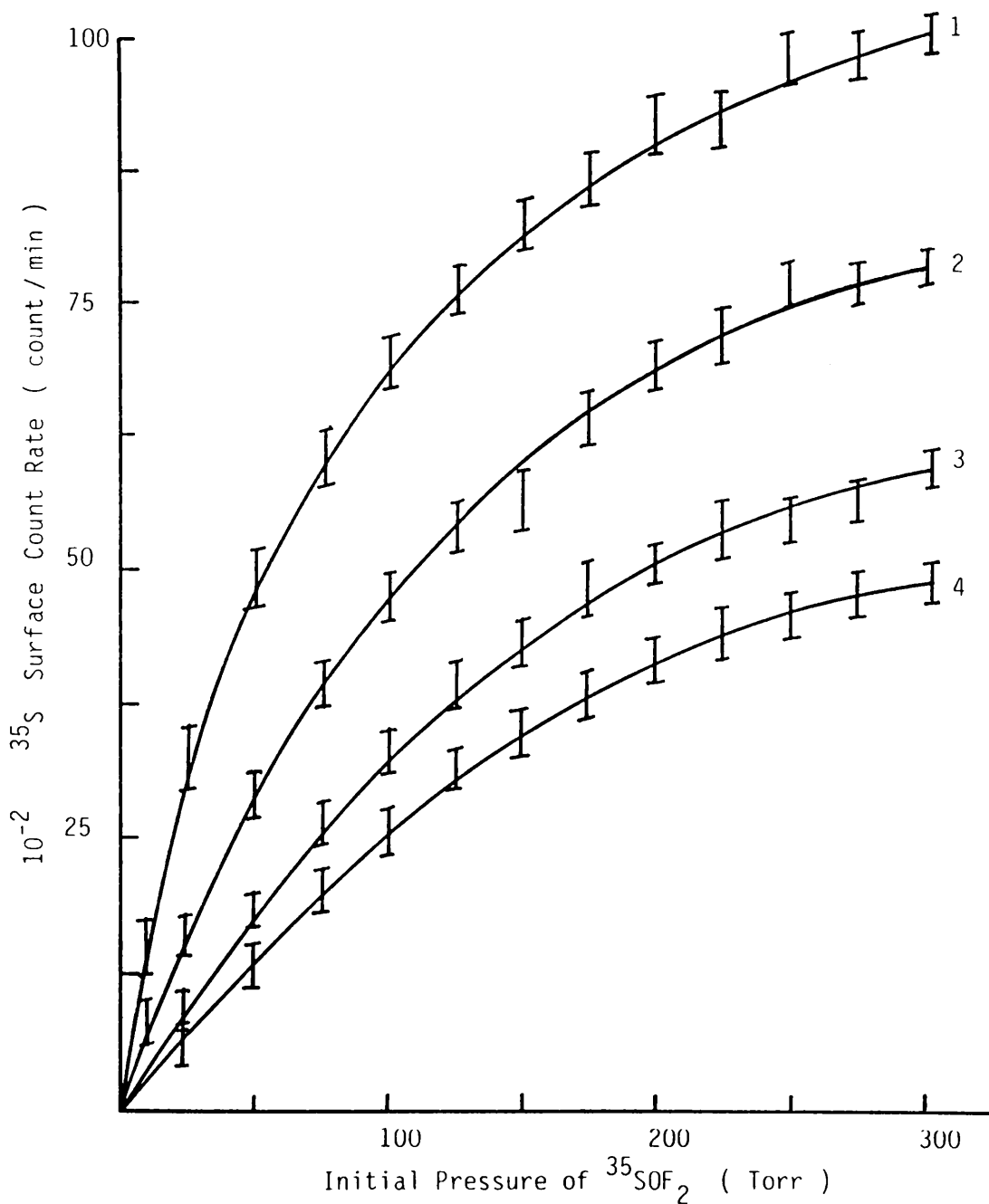
KF/ $\gamma$ -alumina	Composition	CsF/ $\gamma$ -alumina
2	4.4 mmol g <sup>-1</sup>	1
4	8.8 mmol g <sup>-1</sup>	3

Figure 5.26 Reaction of  $^{35}\text{SOF}_2$  with MF/ $\gamma$ -alumina  
 Surface Count Rate  $\vee$  Initial Pressure of  $^{35}\text{SOF}_2$



KF/ $\gamma$ -alumina	Composition	CsF/ $\gamma$ -alumina
2	$4.4 \text{ mmol g}^{-1}$	1
4	$8.8 \text{ mmol g}^{-1}$	3

Figure 5.27 Reaction of  $^{35}\text{SOF}_2$  with MF/ $\gamma$ -alumina  
 Surface Count Rate after removal of gas V Initial Pressure



KF/ $\gamma$ -alumina	Composition	CsF/ $\gamma$ -alumina
2	$4.4 \text{ mmol g}^{-1}$	1
4	$8.8 \text{ mmol g}^{-1}$	3



into the counting cell containing a sample of supported metal fluoride, which had been exposed to [ $^{35}\text{S}$ ]-sulphur labelled thionyl fluoride, led to the return of the surface count rate to its original value during the first admission, after the removal of gas at room temperature, the surface count rate dropped to its original level. Further adsorption/desorption cycles of [ $^{35}\text{S}$ ]-sulphur labelled thionyl fluoride exhibited the same behaviour. Results obtained for the supported metal fluoride,  $4.4 \text{ mmol g}^{-1}$  are given in Figs. 5.28 and 5.29.

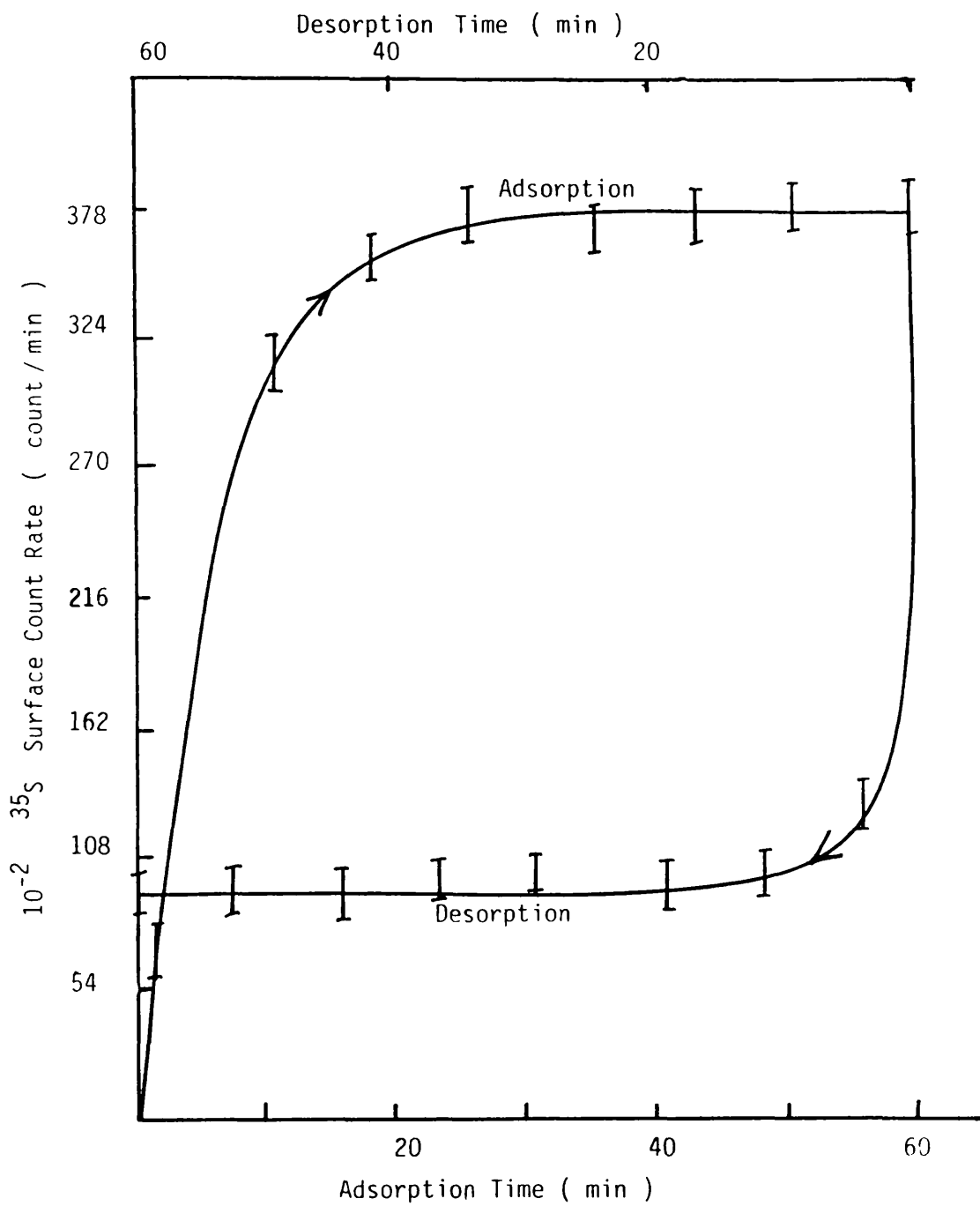
The surface count rate varied with the composition of the supported metal fluoride as shown in Figs. 5.30 and was at a maximum for a given pressure at  $5.5 \text{ mmol g}^{-1}$ . The surface count rate of the supported metal fluoride  $20.0 \text{ mmol g}^{-1}$  recorded after the removal of the gas phase at room temperature was equivalent to background.

### 5.3.9 MANOMETRIC STUDY OF REACTIONS OF SULPHUR DIOXIDE WITH CAESIUM OR POTASSIUM FLUORIDE SUPPORTED ON $\gamma$ -ALUMINA

The uptakes of sulphur dioxide by the supported metal fluoride across the composition range  $2.0\text{-}15.0 \text{ mmol g}^{-1}$  were studied manometrically at different initial pressures. The uptakes of sulphur dioxide by the supported metal fluoride,  $4.4$  and  $8.8 \text{ mmol g}^{-1}$  were dependent on the initial pressure in the range  $50\text{-}300 \text{ Torr}$ . The uptake was increased by increasing the initial pressure of sulphur dioxide as shown in Fig. 5.31. The uptake of sulphur dioxide was also dependent on the metal fluoride loading, in that, the uptake was at a maximum for a given pressure at  $5.5 \text{ mmol g}^{-1}$ . The results obtained are shown in Fig. 5.32 for an initial pressure of sulphur dioxide of  $300 \text{ Torr}$ . In all

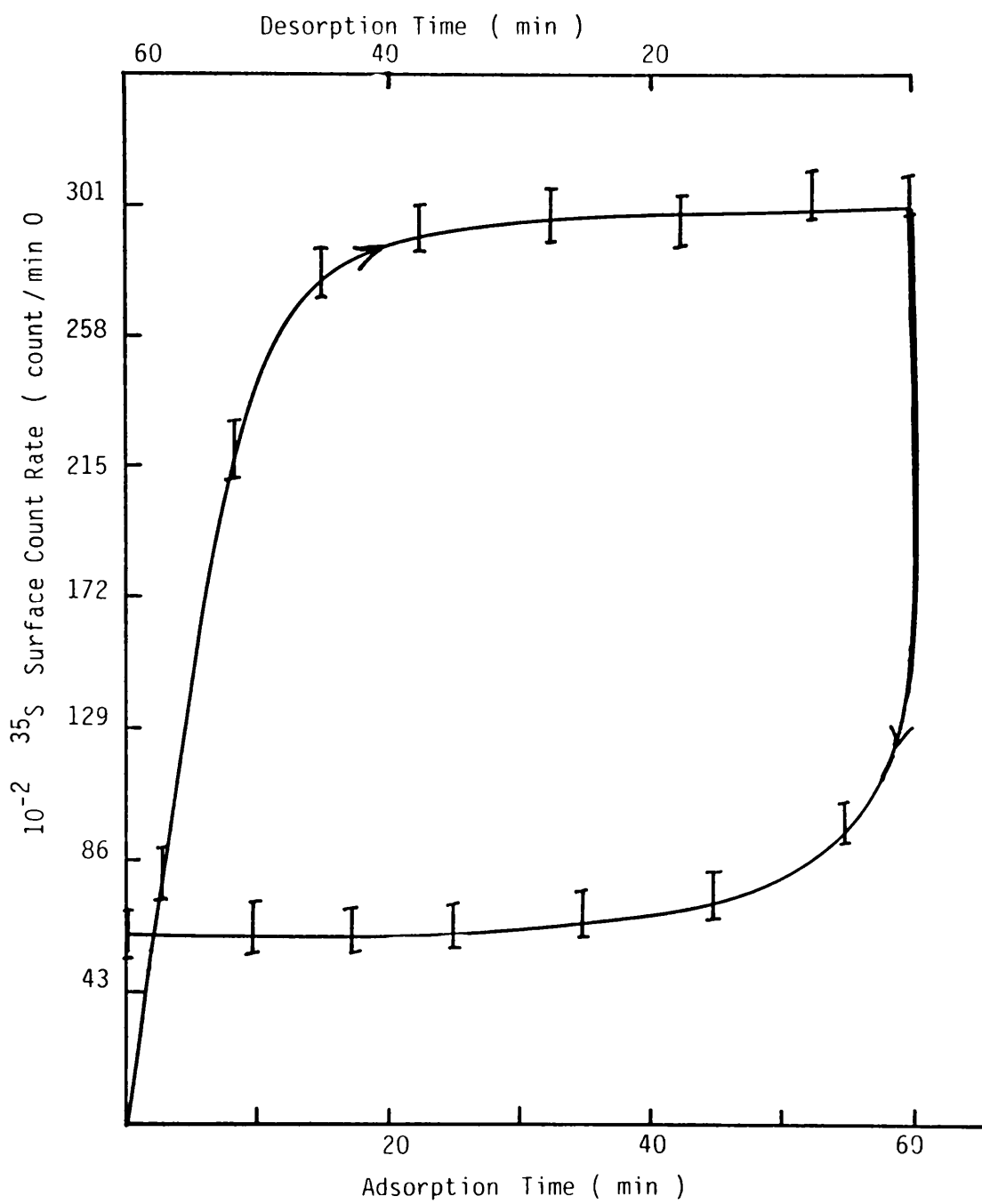
^  
Table 5.23,

Figure 5.28 Adsorption/Desorption Cycle of  $^{35}\text{SOF}_2$  over CsF/ $\gamma$ -alumina  
 $4.4 \text{ mmol g}^{-1}$



Initial Pressure of  $^{35}\text{SOF}_2 = 300 \text{ Torr}$

Figure 5.29 Adsorption/Desorption Cycle of  $^{35}\text{SOF}_2$  over KF/ $\gamma$ -alumina  
4.4 mmol g $^{-1}$



Initial Pressure of  $^{35}\text{SOF}_2 = 300$  Torr

Figure 5.30 Reaction of  $^{35}\text{SOF}_2$  with MF/ $\gamma$ -alumina, Surface Count Rate V Composition

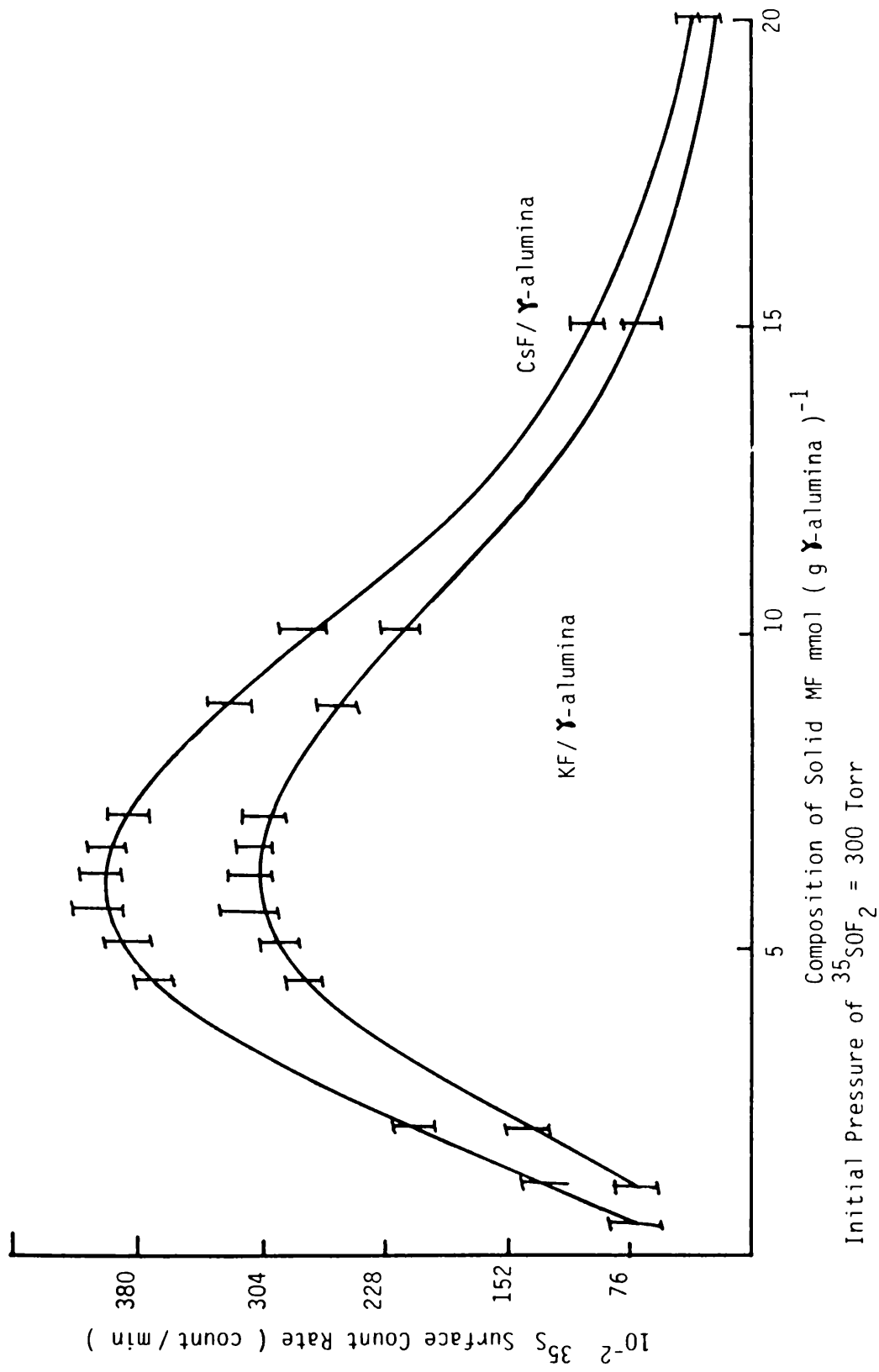
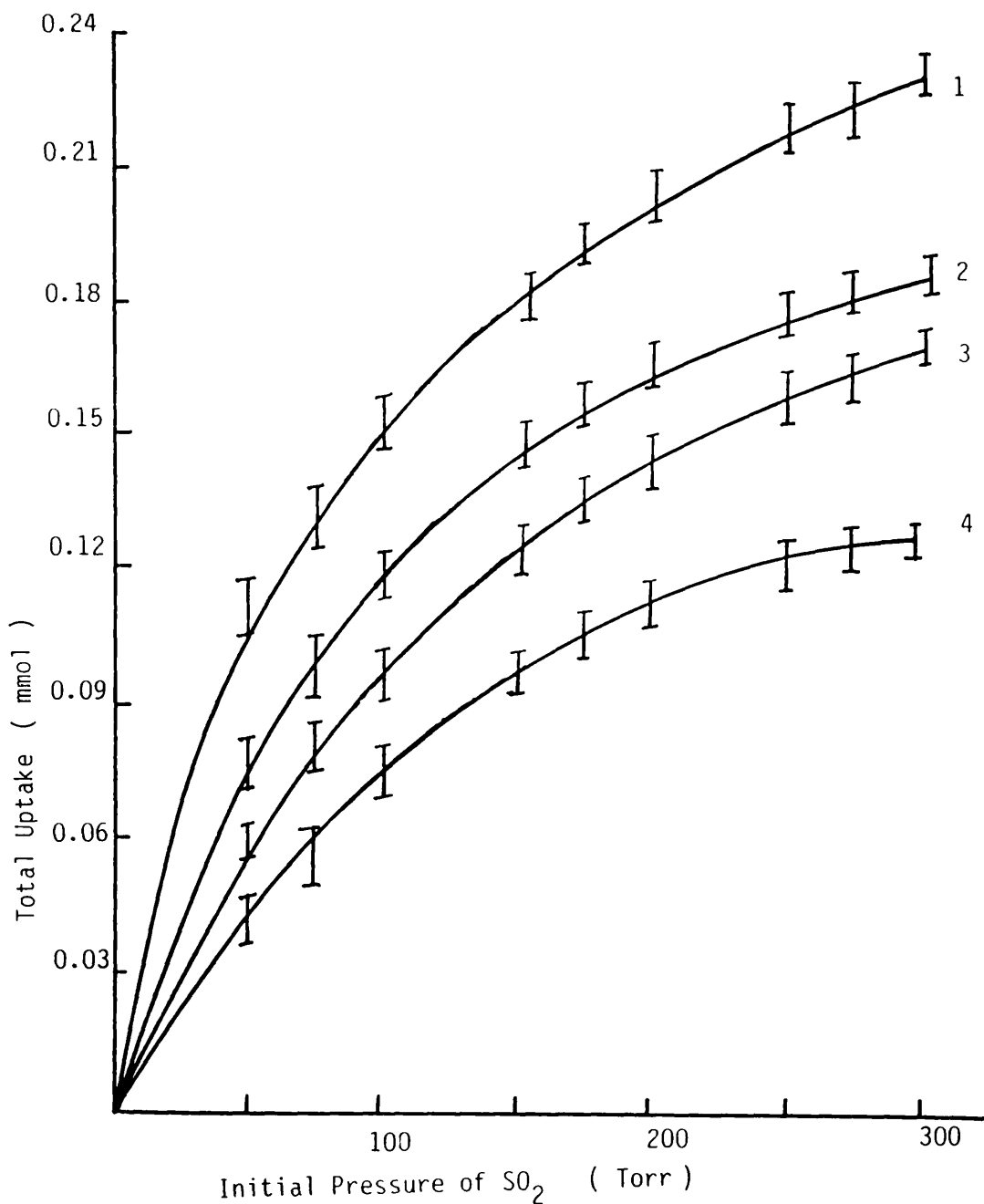


Figure 5.31 Reaction of  $\text{SO}_2$  with MF/ $\gamma$ -alumina  
 Total Uptake  $\bar{V}$  Initial Pressure of  $\text{SO}_2$



KF/ $\gamma$ -alumina	Composition	CsF/ $\gamma$ -alumina
2	$4.4 \text{ mmol g}^{-1}$	1
4	$8.8 \text{ mmol g}^{-1}$	3

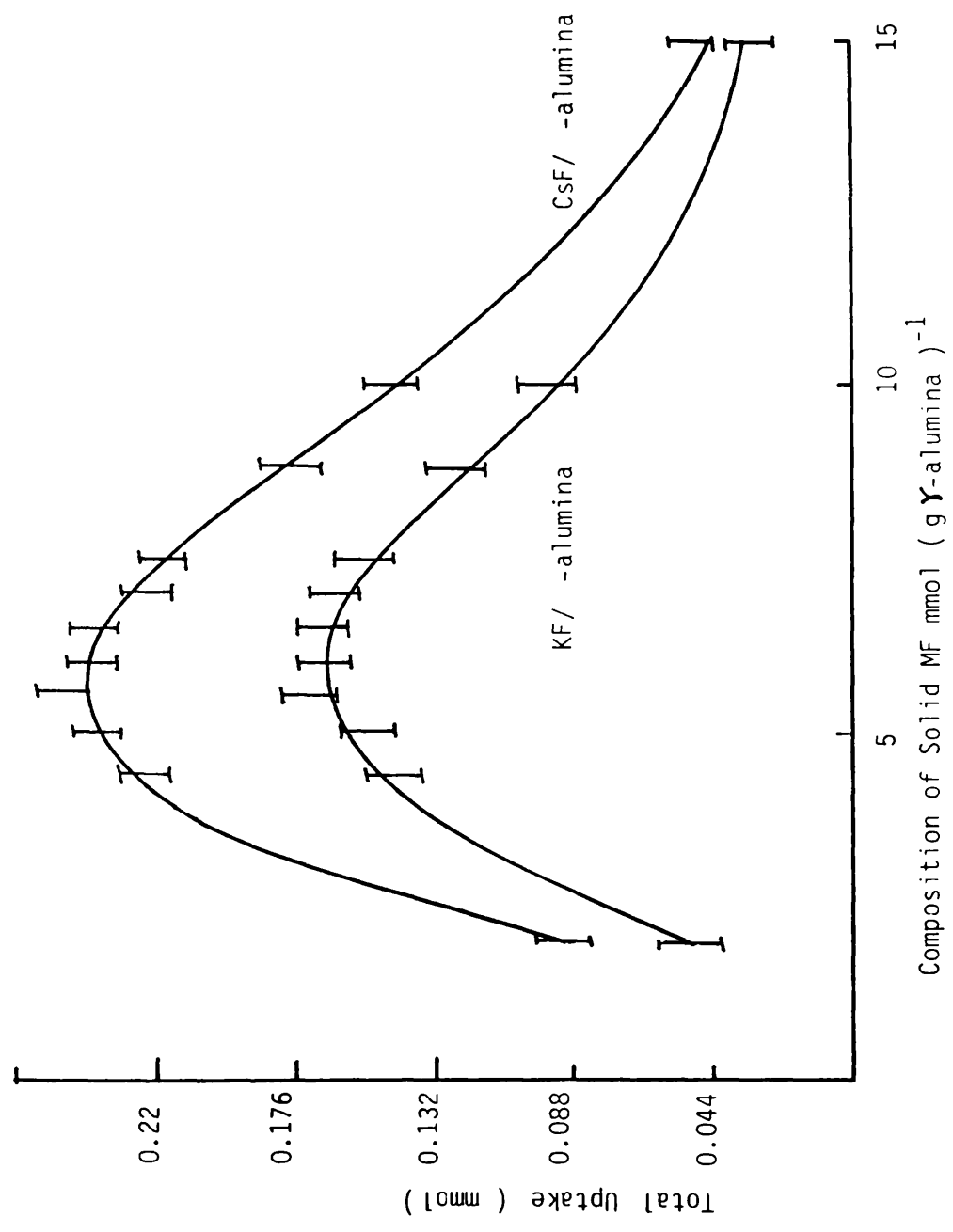
Table 5.23 The Manometric Study of the Adsorption of Sulphur Dioxide by Supported Metal Fluoride

Composition mmol g <sup>-1</sup>	CSF/ $\gamma$ -Alumina		KF/ $\gamma$ -Alumina	
	Total Uptake (mmol)	Retained Gas (mmol)	Total Uptake (mmol)	Retained Gas (mmol)
2.0	0.14 ± 0.01	0.06 ± 0.003	0.1 ± 0.01	0.04 ± 0.003
4.4	0.23 ± 0.01	0.10 ± 0.004	0.16 ± 0.01	0.064 ± 0.004
5.0	0.24 ± 0.02	0.103 ± 0.006	0.18 ± 0.02	0.07 ± 0.006
5.5	0.25 ± 0.02	0.11 ± 0.009	0.19 ± 0.02	0.08 ± 0.009
6.0	0.23 ± 0.03	0.10 ± 0.009	0.17 ± 0.01	0.065 ± 0.009
8.8	0.15 ± 0.02	0.06 ± 0.002	0.12 ± 0.01	0.04 ± 0.002
15.0	0.07 ± 0.01	0.018 ± 0.002	0.04 ± 0.01	0.008 ± 0.002

Initial pressure

300 Torr.

Figure 5.32 Reaction of SO<sub>2</sub> with MF/ γ-alumina, Total Uptake V Composition



Initial Pressure of SO<sub>2</sub> = 310 Torr

reactions studied, the interactions involving supported caesium fluoride were greater than those involving supported potassium fluoride under the same conditions.

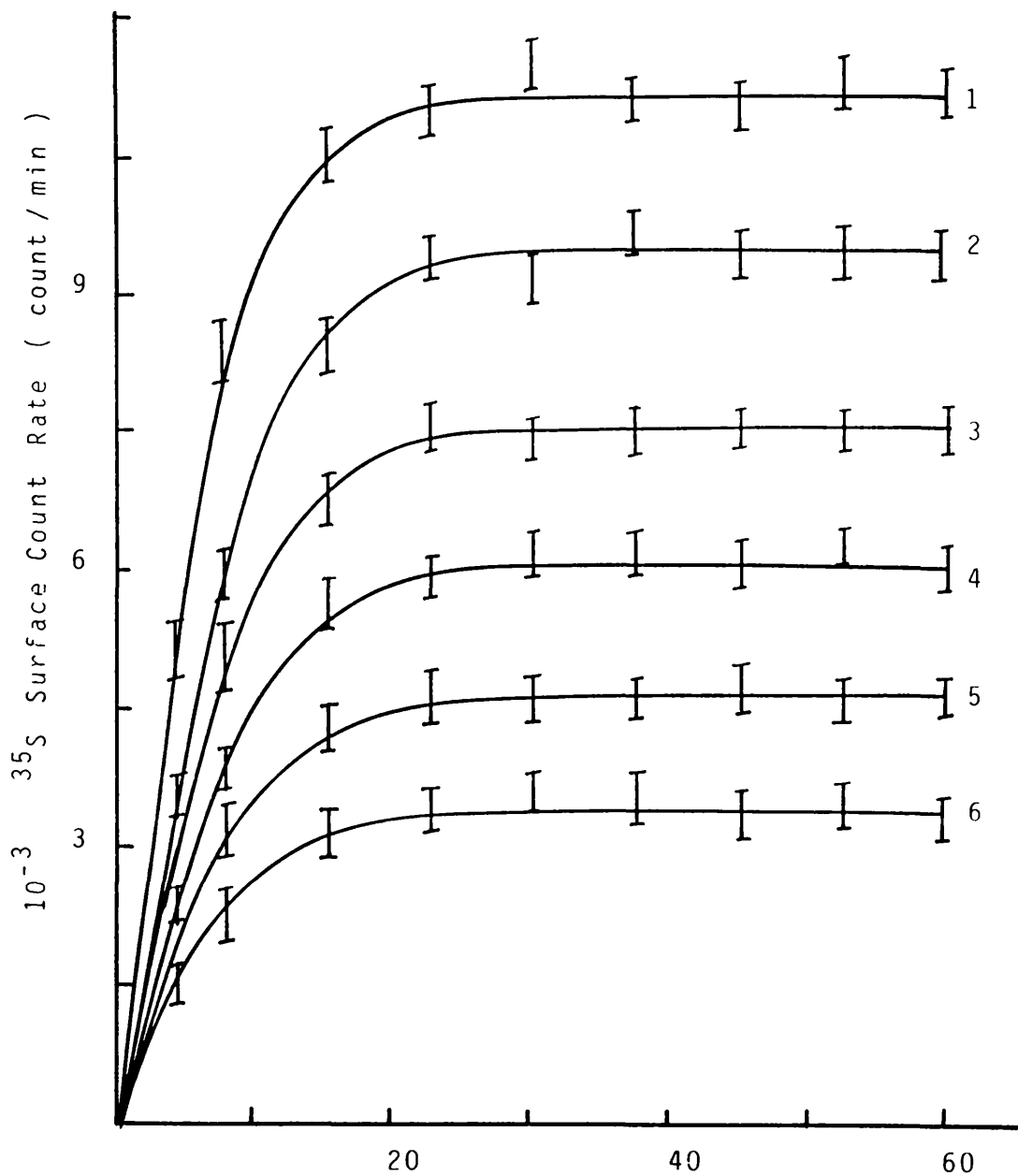
In each case the infra-red spectrum of the supported metal fluoride in the range 2.0-10.0 mmol $g^{-1}$  after reaction with sulphur dioxide at room temperature, showed very strong bands at 594 and 1193  $cm^{-1}$ . These two bands were assigned to the fluorosulphite anion,  $SO_2F^-$ . The infra-red spectrum of KF/ $\gamma$ -alumina 10.0 mmol $g^{-1}$  after the room temperature reaction with sulphur dioxide was identical to that given in Table 5.18.

#### 5.3.10 REACTIONS OF [ $^{35}S$ ]-SULPHUR LABELLED SULPHUR DIOXIDE WITH CAESIUM OR POTASSIUM FLUORIDE SUPPORTED ON $\gamma$ -ALUMINA

The reaction between [ $^{35}S$ ]-sulphur labelled sulphur dioxide and supported metal fluorides across the composition range 0.6-20.0 mmol $g^{-1}$  was studied at different initial pressures in the range 10-300 Torr. Each reaction was followed for 60 min, before the removal of the [ $^{35}S$ ]-sulphur labelled sulphur dioxide from the counting cell. Plots of the [ $^{35}S$ ]-sulphur surface count rate of the supported metal fluoride, 4.4, 5.5 and 8.8 mmol $g^{-1}$  versus time at initial pressures of [ $^{35}S$ ]-sulphur labelled sulphur dioxide of 60, 160 and 240 Torr are given in Figs. 5.33 - 5.35. The surface count rate increased rapidly until a constant level was reached after 20 min. When the [ $^{35}S$ ]-sulphur labelled sulphur dioxide was removed from the counting vessel by condensation at 77K, the surface count rate dropped to ca 40-27% of the original total surface count rate of the supported metal fluoride, 4.4-8.8 mmol $g^{-1}$ . The major surface species was evidently weakly adsorbed with ca 40-27% of the total surface

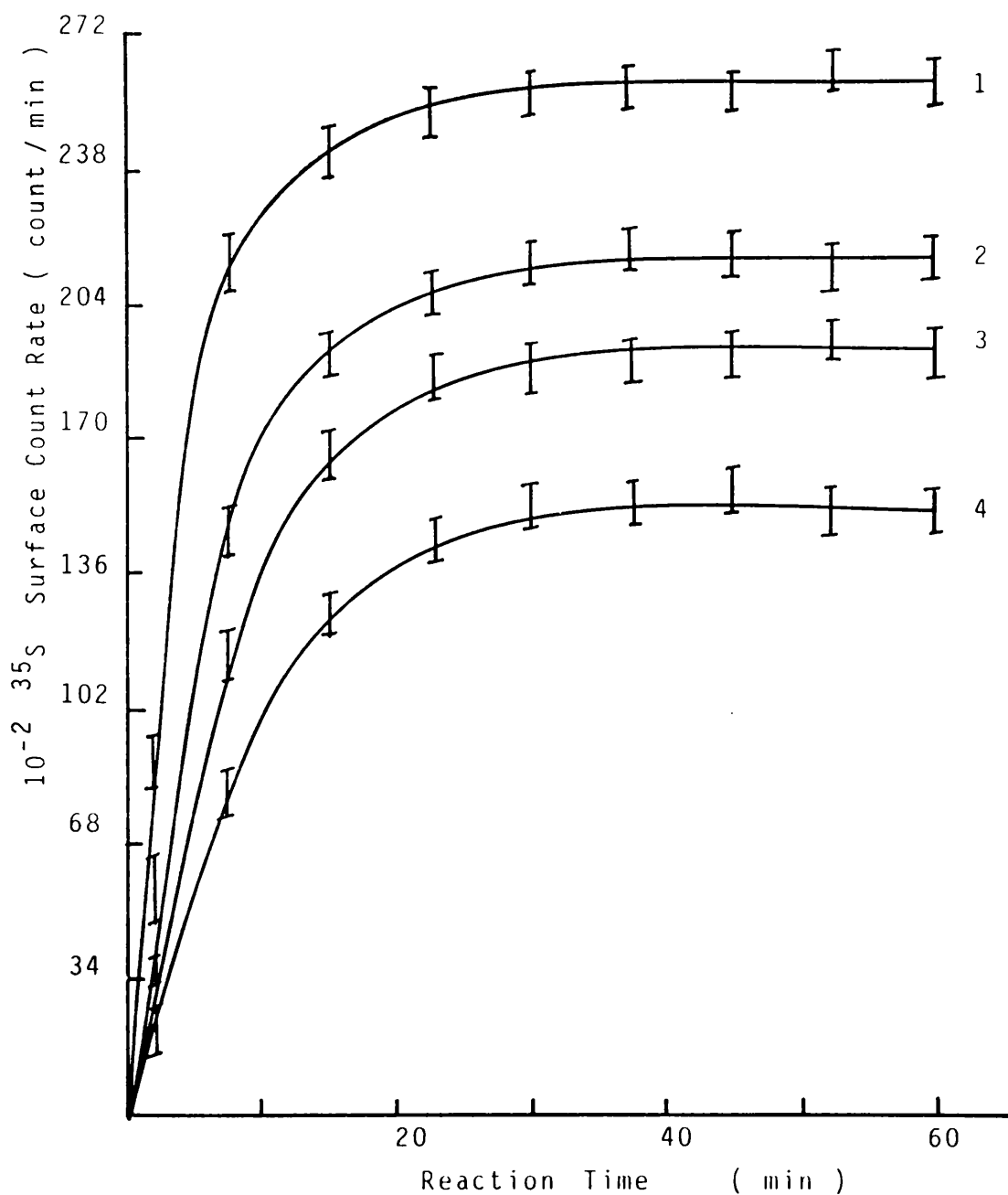


Figure 5.33 Reaction of  $^{35}\text{SO}_2$  with MF/  $\gamma$ -alumina  
 Surface Count Rate  $\nu$  Reaction Time  
 Initial Pressure of  $^{35}\text{SO}_2 = 60$  Torr



KF/ $\gamma$ -alumina	Reaction Time (min)	Composition	CsF/ $\gamma$ -alumina
3	20	$5.5 \text{ mmol g}^{-1}$	1
4	40	$4.4 \text{ mmol g}^{-1}$	2
6	60	$8.8 \text{ mmol g}^{-1}$	5

Figure 5.34 Reaction of  $^{35}\text{SO}_2$  with MF/ $\gamma$ -alumina  
 Surface Count Rate  $\propto$  Reaction Time  
 Initial Pressure of  $^{35}\text{SO}_2 = 160$  Torr



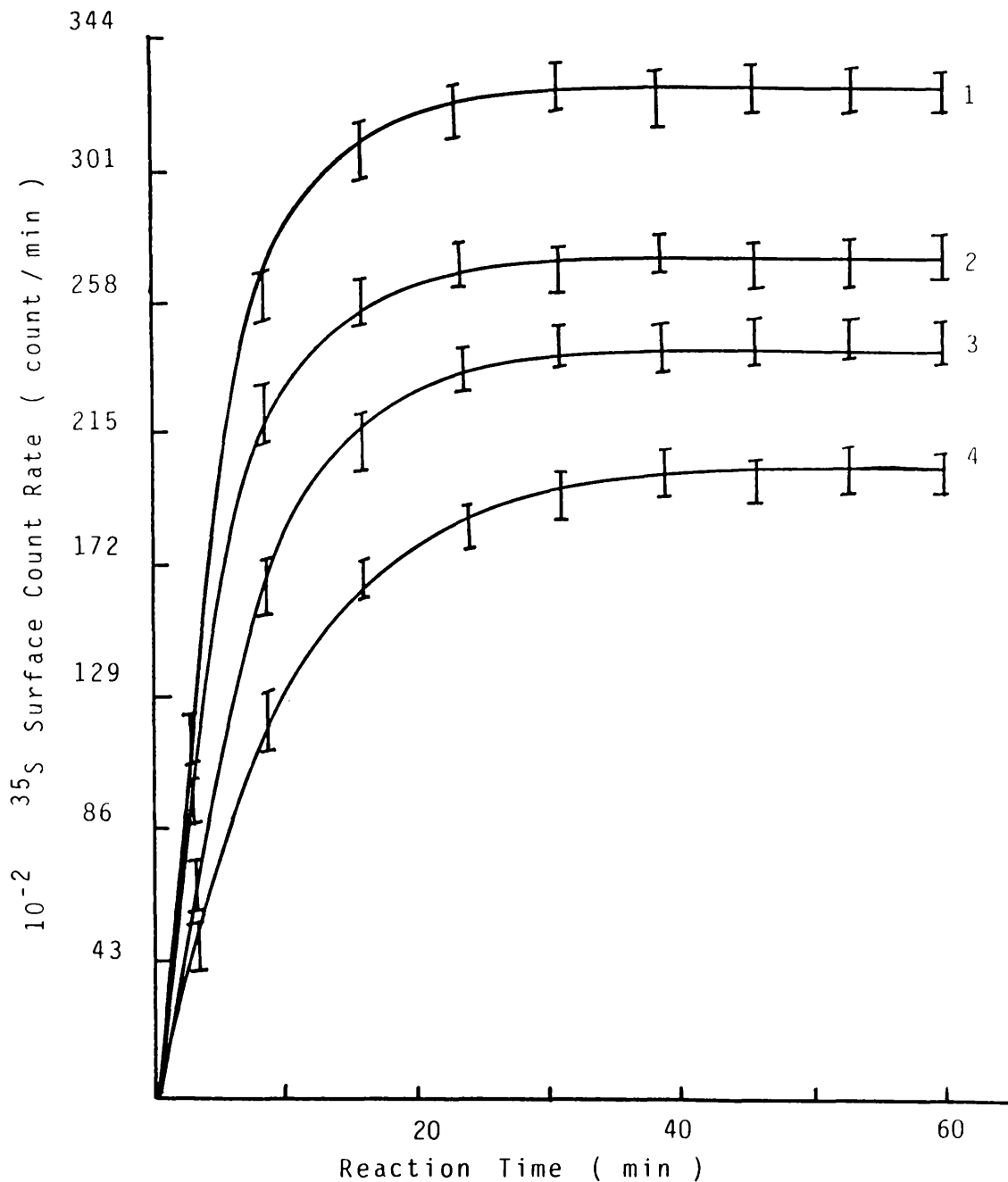
KF/ $\gamma$ -alumina	Composition	CsF/ $\gamma$ -alumina
2	4.4 mmol g <sup>-1</sup>	1
4	8.8 mmol g <sup>-1</sup>	3

Figure 5.35

Reaction of  $^{35}\text{SO}_2$  with MF/ $\gamma$ -alumina

Surface Count Rate  $\sqrt{\text{Reaction Time}}$

Initial Pressure of  $^{35}\text{SO}_2 = 240 \text{ Torr}$



KF/ $\gamma$ -alumina	Composition	CsF/ $\gamma$ -alumina
2	$4.4 \text{ mmol g}^{-1}$	1
4	$8.8 \text{ mmol g}^{-1}$	3

count rate being due to a permanently retained species. The results obtained are given in Tables 5.24-5.27 and shown in Figs. 5.36-5.38 for the 4.4 and 8.8 mmol g<sup>-1</sup> materials. The surface count rate of the supported metal fluoride in the presence of gas or after pumping at room temperature and the overall uptake, were dependent on the initial pressure of [<sup>35</sup>S]-sulphur labelled sulphur dioxide in the range 10-300 Torr. Pumping the solid for 5 days under vacuum at room temperature after the removal of the gas phase had no effect in the final surface count rate, but the surface count rate of the supported metal fluoride decreased to background when the solid was heated to 373K under vacuum, or was exposed to aliquots of water vapour.

When [<sup>35</sup>S]-sulphur labelled sulphur dioxide was readmitted into the counting cell containing a sample of the supported metal fluoride which had been exposed to [<sup>35</sup>S]-sulphur labelled sulphur dioxide, the surface count rate returned to its original value. After the removal of gas at room temperature, the surface count rate dropped to the original level. Further adsorption/desorption cycles followed the same pattern. The results obtained for the supported metal fluoride, 4.4 mmol g<sup>-1</sup> are shown in Figs. 5.39 and 5.40.

The surface count rates in the presence of gas or after pumping at room temperature and the total uptake of gas varied with the composition of the supported metal fluoride as shown in Figs. 5.41-5.43, and were at a maximum for a given pressure at 5.5 mmol g<sup>-1</sup>. The surface count rate of the supported metal fluoride, 20.0 mmol g<sup>-1</sup> after the removal of [<sup>35</sup>S]-sulphur labelled sulphur dioxide from the counting cell at room temperature was equivalent to background.

Table 5.24 Results of Reaction between [<sup>35</sup>S]-Sulphur Labelled Sulphur Dioxide and Supported Caesium Fluoride,  
4.4 mmol g<sup>-1</sup>

Initial Pressure (Torr)	Total Drop in the Gas Count Rate Count min <sup>-1</sup>	Total Uptake of Gas mmol	Surface Count Rate Count min <sup>-1</sup>	Surface Count Rate after Removal of Gas Count min <sup>-1</sup>
10.4 ± 0.5	346 ± 117	0.011 ± 0.006	2096 ± 129	839 ± 119
20.3 ± 0.5	503 ± 122	0.016 ± 0.006	3030 ± 154	1216 ± 143
40.1 ± 0.5	1070 ± 131	0.034 ± 0.006	6481 ± 181	2587 ± 167
60.8 ± 0.5	1603 ± 152	0.051 ± 0.006	9683 ± 243	3874 ± 194
80.8 ± 0.5	2047 ± 182	0.065 ± 0.006	12376 ± 281	4953 ± 243
100.6 ± 0.5	2515 ± 247	0.08 ± 0.006	15203 ± 337	6084 ± 281
120.1 ± 0.5	3050 ± 289	0.097 ± 0.006	18404 ± 367	7378 ± 329
140.2 ± 0.5	3584 ± 346	0.114 ± 0.006	21704 ± 441	8665 ± 377
160.2 ± 0.5	4056 ± 377	0.13 ± 0.006	24556 ± 498	9809 ± 417
180.8 ± 0.5	4402 ± 421	0.14 ± 0.006	26562 ± 576	10641 ± 451
200.0 ± 0.5	4685 ± 463	0.15 ± 0.006	28364 ± 684	11330 ± 489
220.2 ± 0.5	5125 ± 509	0.163 ± 0.006	30974 ± 719	12389 ± 547
240.2 ± 0.5	5596 ± 562	0.175 ± 0.006	33826 ± 798	13533 ± 583
260.8 ± 0.5	5722 ± 613	0.182 ± 0.006	34687 ± 877	13839 ± 641
280.3 ± 0.5	6288 ± 647	0.20 ± 0.006	37953 ± 982	15204 ± 689
300.2 ± 0.5	6634 ± 693	0.211 ± 0.006	40036 ± 1097	16042 ± 733

Sample Weight 0.5g, 1.32 mmol of CsF.

Table 5.25 Results of Reaction between [<sup>35</sup>S]-Sulphur Labelled Sulphur Dioxide and Supported Caesium Fluoride, 8.8 mmol g<sup>-1</sup>

Initial Pressure (Torr)	Total Drop in the Gas Count Rate Count min <sup>-1</sup>	Total Uptake of Gas mmol	Surface Count Rate Count min <sup>-1</sup>	Surface Count Rate after Removal of Gas Count min <sup>-1</sup>
10.4 ± 0.5	220 ± 101	0.007 ± 0.006	943 ± 103	266 ± 68
20.9 ± 0.5	377 ± 121	0.012 ± 0.006	1607 ± 129	451 ± 77
40.1 ± 0.5	628 ± 132	0.02 ± 0.006	2692 ± 153	752 ± 89
60.8 ± 0.5	1067 ± 160	0.034 ± 0.006	4553 ± 187	1278 ± 102
80.7 ± 0.5	1382 ± 182	0.044 ± 0.006	5895 ± 227	1656 ± 147
100.1 ± 0.5	1538 ± 223	0.049 ± 0.006	6579 ± 264	1841 ± 181
120.1 ± 0.5	1978 ± 247	0.063 ± 0.006	8391 ± 291	2345 ± 221
160.3 ± 0.5	2512 ± 277	0.08 ± 0.006	10761 ± 345	3006 ± 243
180.4 ± 0.5	2795 ± 319	0.09 ± 0.006	11920 ± 383	3344 ± 277
200.8 ± 0.5	3454 ± 356	0.11 ± 0.006	14802 ± 452	4136 ± 316
220.8 ± 0.5	4082 ± 391	0.13 ± 0.006	17291 ± 490	4887 ± 348
240.6 ± 0.5	4270 ± 442	0.136 ± 0.006	18215 ± 577	5112 ± 383
260.5 ± 0.5	4396 ± 487	0.14 ± 0.006	18829 ± 623	5261 ± 412
280.5 ± 0.5	4459 ± 525	0.142 ± 0.006	19099 ± 689	5337 ± 451
300.3 ± 0.5	4490 ± 557	0.144 ± 0.006	19239 ± 773	5376 ± 483

Sample Weight 0.5g, 1.88 mmol of CsF.

Table 5.26 Results of Reaction between [<sup>35</sup>S]-Sulphur Labelled Sulphur Dioxide and Supported Potassium Fluoride, 4.4 mmol g<sup>-1</sup>

Initial Pressure (Torr)	Total Drop in the Gas Count Rate Count min <sup>-1</sup>	Total Uptake of Gas mmol	Surface Count Rate Count min <sup>-1</sup>	Surface Count Rate after Removal of Gas Count min <sup>-1</sup>
10.3 ± 0.5	311 ± 111	0.009 ± 0.006	1820 ± 123	699 ± 103
20.1 ± 0.5	472 ± 127	0.015 ± 0.006	2770 ± 154	1058 ± 123
40.9 ± 0.5	850 ± 147	0.027 ± 0.006	4985 ± 196	1910 ± 151
60.0 ± 0.5	1258 ± 167	0.041 ± 0.006	7383 ± 221	2829 ± 184
80.0 ± 0.5	1762 ± 181	0.056 ± 0.006	10302 ± 251	3956 ± 213
100.2 ± 0.5	2203 ± 202	0.071 ± 0.006	12895 ± 284	4946 ± 232
120.0 ± 0.5	2454 ± 247	0.078 ± 0.006	14373 ± 347	5513 ± 276
140.3 ± 0.5	2831 ± 289	0.09 ± 0.006	16594 ± 363	6357 ± 323
160.9 ± 0.5	3115 ± 347	0.1 ± 0.006	18245 ± 431	6993 ± 341
180.7 ± 0.5	3650 ± 400	0.12 ± 0.006	21347 ± 483	8196 ± 381
200.3 ± 0.5	3870 ± 417	0.123 ± 0.006	22636 ± 541	8689 ± 409
220.8 ± 0.5	4184 ± 441	0.133 ± 0.006	24520 ± 591	9399 ± 445
240.9 ± 0.5	4562 ± 488	0.145 ± 0.006	26767 ± 637	10244 ± 463
260.2 ± 0.5	4814 ± 519	0.153 ± 0.006	28256 ± 699	10811 ± 507
280.7 ± 0.5	4908 ± 541	0.156 ± 0.006	28754 ± 752	11025 ± 517
300.9 ± 0.5	5097 ± 556	0.162 ± 0.006	29909 ± 813	11447 ± 553

Sample Weight 0.38g, 1.32 mmol of KF.

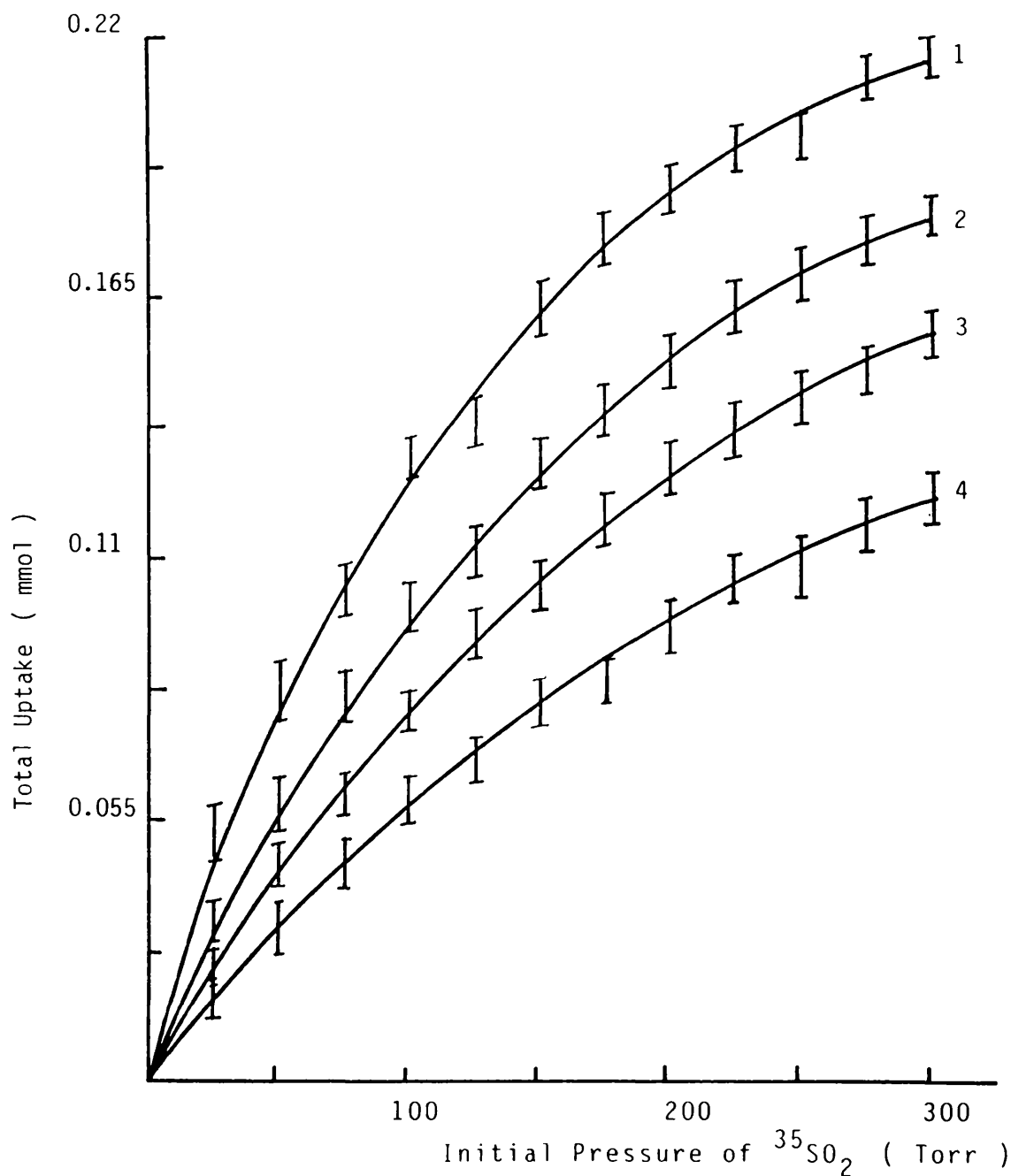
Table 5.27 Results of Reaction between [<sup>35</sup>S]-Sulphur Labelled Sulphur Dioxide and Supported Potassium Fluoride, 8.8 mmolg<sup>-1</sup>

Initial Pressure (Torr)	Total Drop in the Gas Count Rate Count min <sup>-1</sup>	Total Uptake of Gas mmol	Surface Count Rate Count min <sup>-1</sup>	Surface Count Rate after Removal of Gas Count min <sup>-1</sup>
10.7 ± 0.5	202 ± 86	0.007 ± 0.006	768 ± 107	212 ± 53
20.3 ± 0.5	418 ± 111	0.013 ± 0.006	1627 ± 127	436 ± 69
40.3 ± 0.5	803 ± 123	0.025 ± 0.006	3042 ± 131	840 ± 87
60.7 ± 0.5	1156 ± 147	0.036 ± 0.006	4389 ± 152	1208 ± 91
80.4 ± 0.5	1541 ± 168	0.048 ± 0.006	5881 ± 161	1612 ± 107
100.1 ± 0.5	1926 ± 184	0.06 ± 0.006	7135 ± 189	2012 ± 131
120.4 ± 0.5	2119 ± 226	0.066 ± 0.006	8247 ± 221	2216 ± 173
140.9 ± 0.5	2536 ± 247	0.079 ± 0.006	10013 ± 250	2652 ± 191
160.8 ± 0.5	2825 ± 283	0.088 ± 0.006	10653 ± 277	2952 ± 211
180.4 ± 0.5	3017 ± 317	0.094 ± 0.006	11505 ± 347	3152 ± 241
200.8 ± 0.5	3274 ± 347	0.102 ± 0.006	12755 ± 389	3424 ± 276
220.3 ± 0.5	3467 ± 381	0.108 ± 0.006	13176 ± 439	3627 ± 291
240.3 ± 0.5	3659 ± 404	0.114 ± 0.006	13870 ± 482	3825 ± 319
260.2 ± 0.5	3853 ± 427	0.12 ± 0.006	14635 ± 519	4023 ± 327
280.3 ± 0.5	3981 ± 451	0.124 ± 0.006	14746 ± 577	4163 ± 368
300.2 ± 0.5	4109 ± 501	0.128 ± 0.006	15616 ± 601	4296 ± 391

Sample Weight 0.32g, 1.88 mmol of KF.

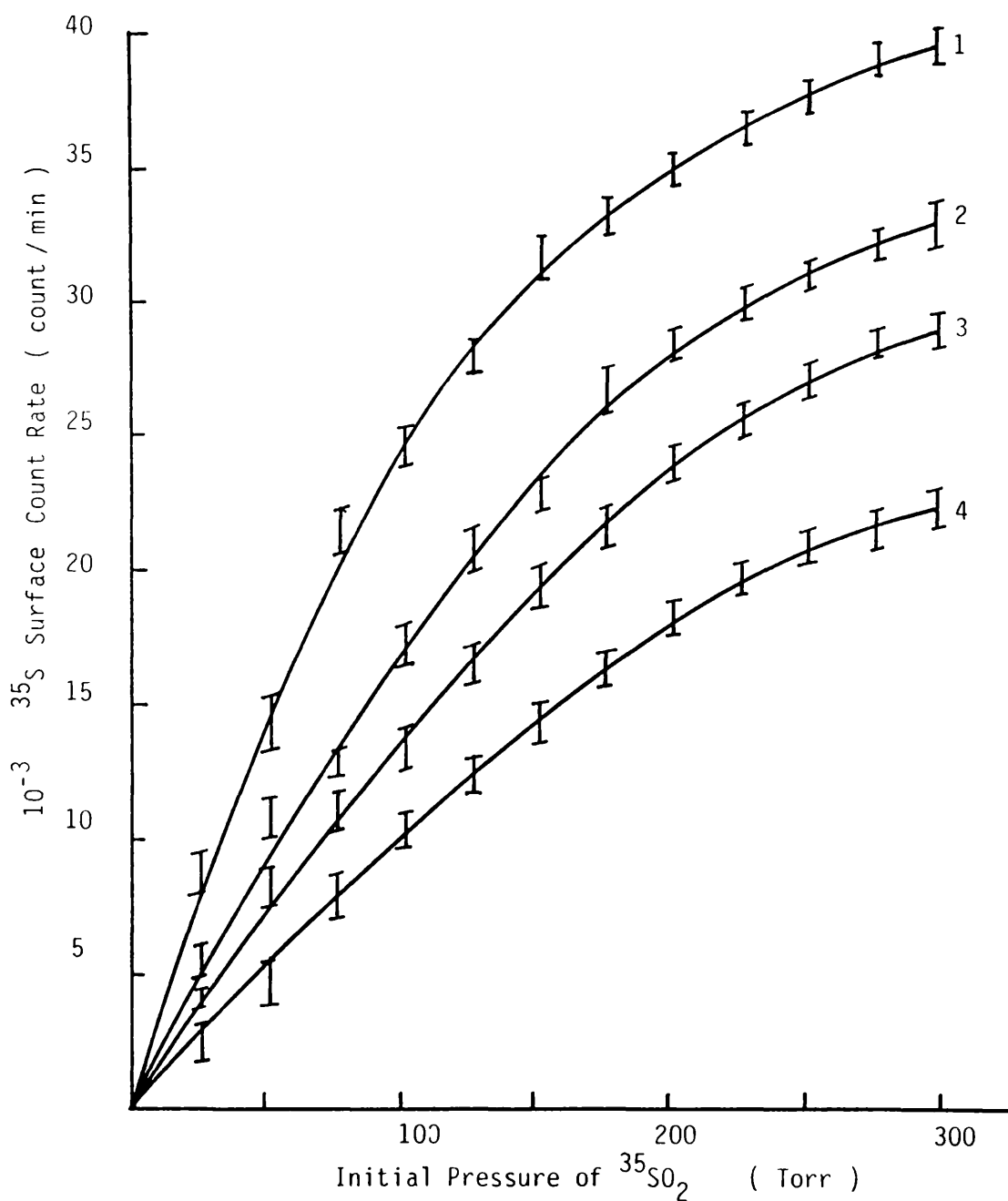


Figure 5.36 Reaction of  $^{35}\text{SO}_2$  with MF/ $\gamma$ -alumina  
 Total Uptake  $\bar{v}$  Initial Pressure of  $^{35}\text{SO}_2$



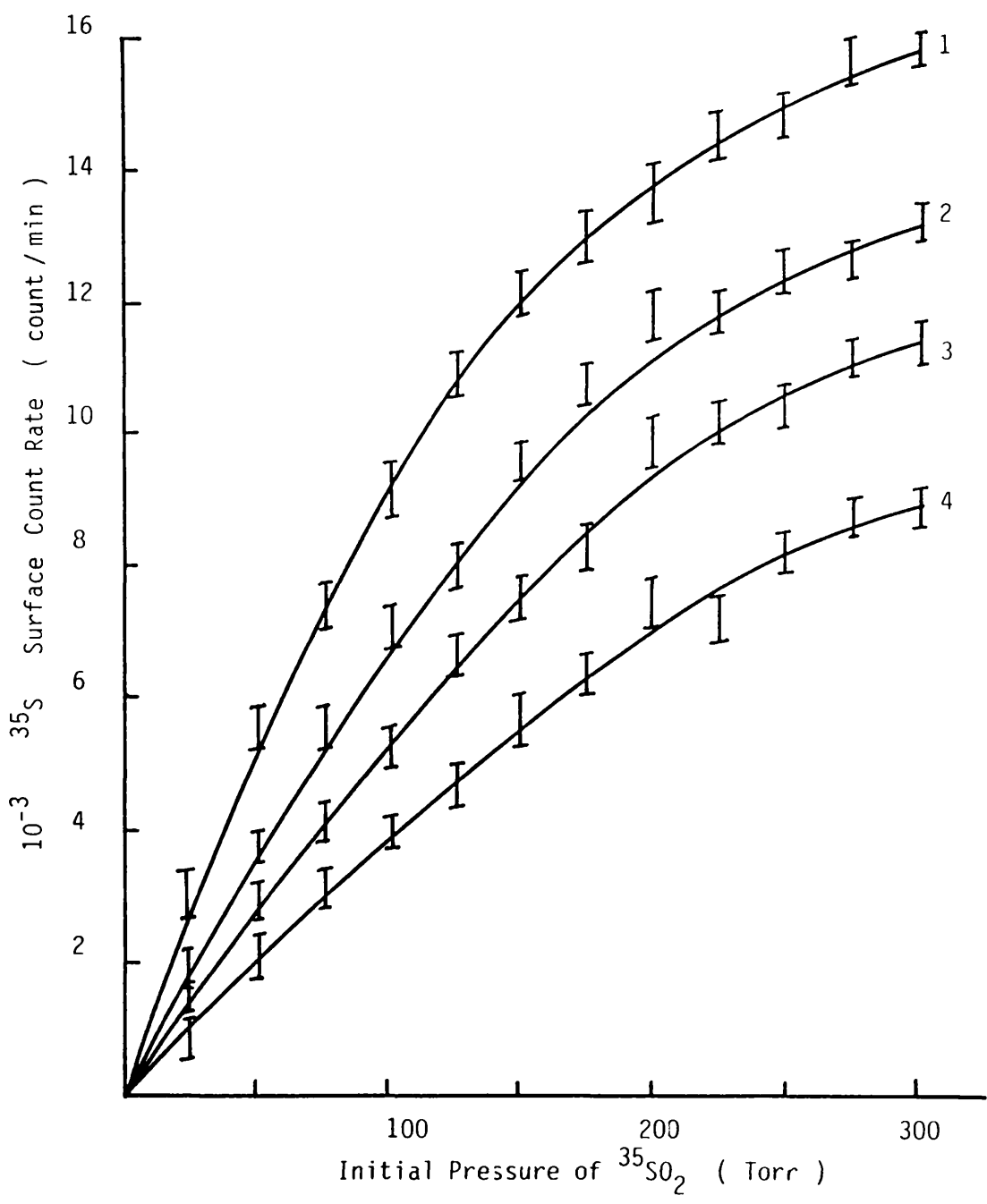
KF/ $\gamma$ -alumina	Composition	CsF/ $\gamma$ -alumina
2	$4.4 \text{ mmol g}^{-1}$	1
4	$8.8 \text{ mmol g}^{-1}$	3

Figure 5.37 Reaction of  $^{35}\text{SO}_2$  with MF/ $\gamma$ -alumina  
 Surface Count Rate  $\propto$  Initial Pressure of  $^{35}\text{SO}_2$



KF/ $\gamma$ -alumina	Composition	CsF/ $\gamma$ -alumina
2	$4.4 \text{ mmol g}^{-1}$	1
4	$8.8 \text{ mmol g}^{-1}$	3

Figure 5.38 Reaction of  $^{35}\text{SO}_2$  with MF/ $\gamma$ -alumina  
 Surface Count Rate after removal of gas Initial Pressure



KF/ $\gamma$ -alumina	Composition	CsF/ $\gamma$ -alumina
2	$4.4 \text{ mmol g}^{-1}$	1
4	$8.8 \text{ mmol g}^{-1}$	3

Figure 5.39 Adsorption/Desorption Cycle of  $^{35}\text{SO}_2$  over CsF/ $\gamma$ -alumina  
4.4 mmol g $^{-1}$

Initial Pressure of  $^{35}\text{SO}_2 = 310$  Torr

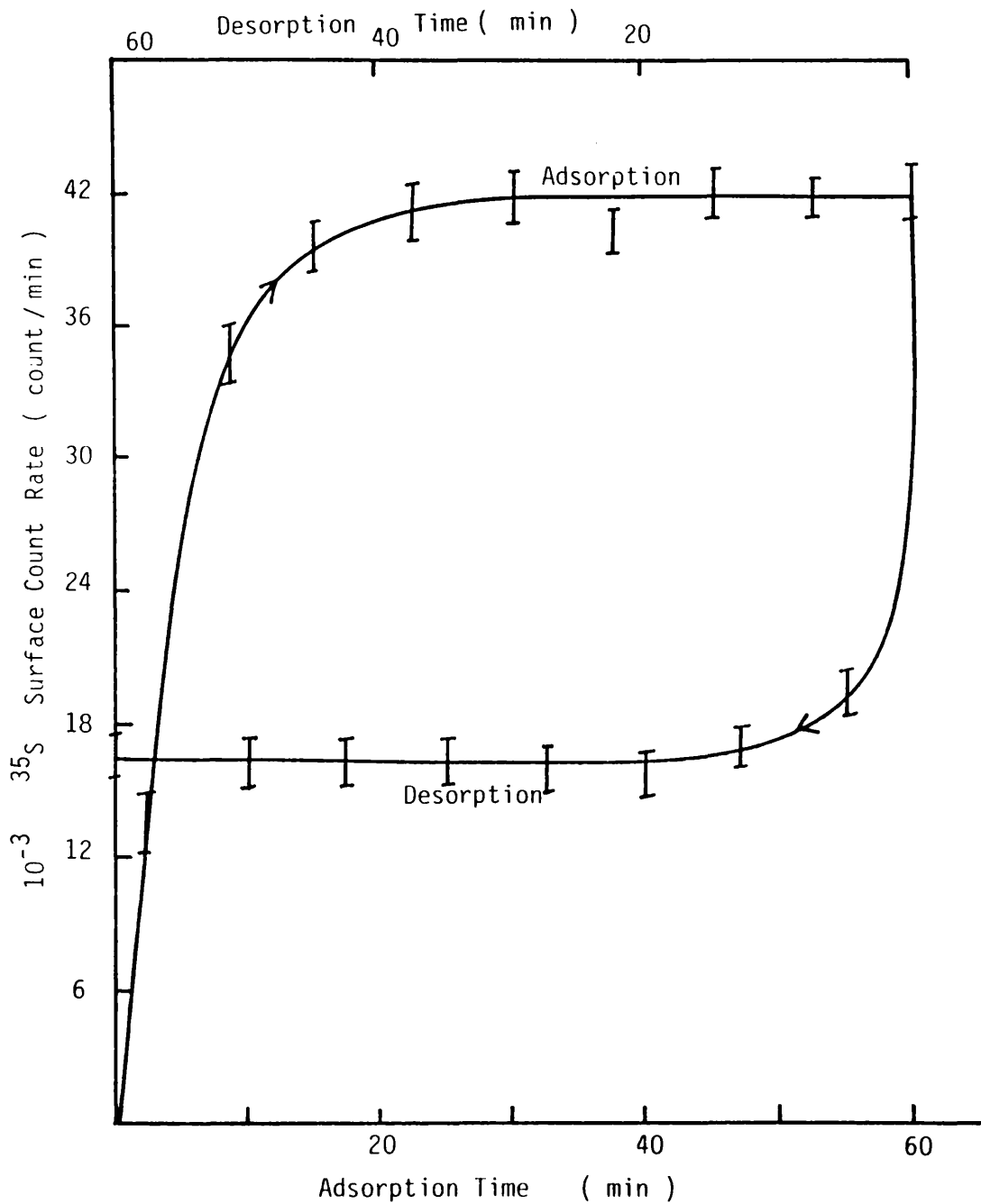


Figure 5.40 Adsorption/Desorption Cycle of  $^{35}\text{S}\text{O}_2$  over KF/ $\gamma$ -alumina  
 $4.4 \text{ mmol g}^{-1}$ , Initial Pressure of  $^{35}\text{S}\text{O}_2 = 310 \text{ Torr}$

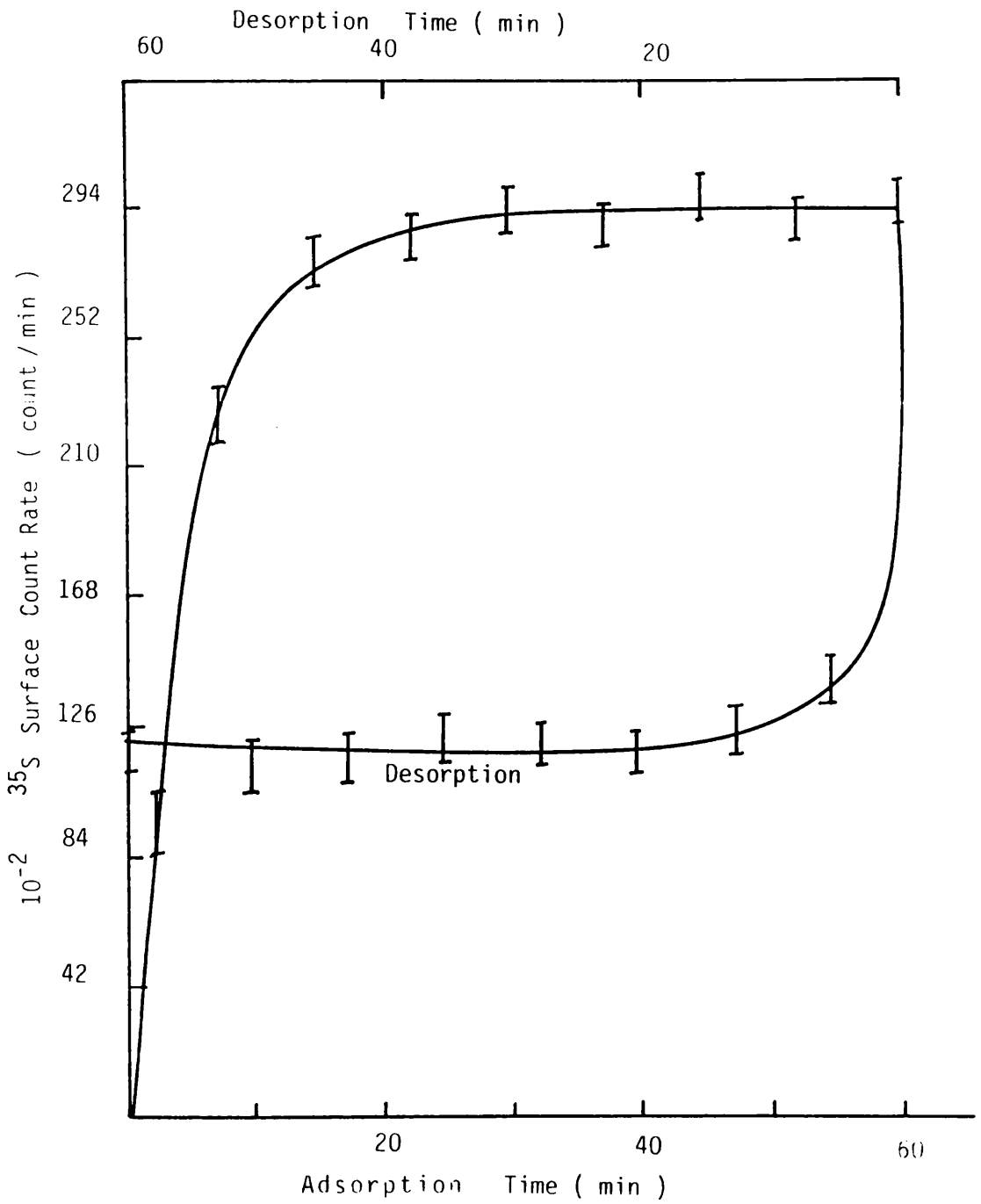


Figure 5.41 Reaction of  $^{35}\text{SO}_2$  with MF/ $\gamma$ -alumina , Total Uptake V Composition

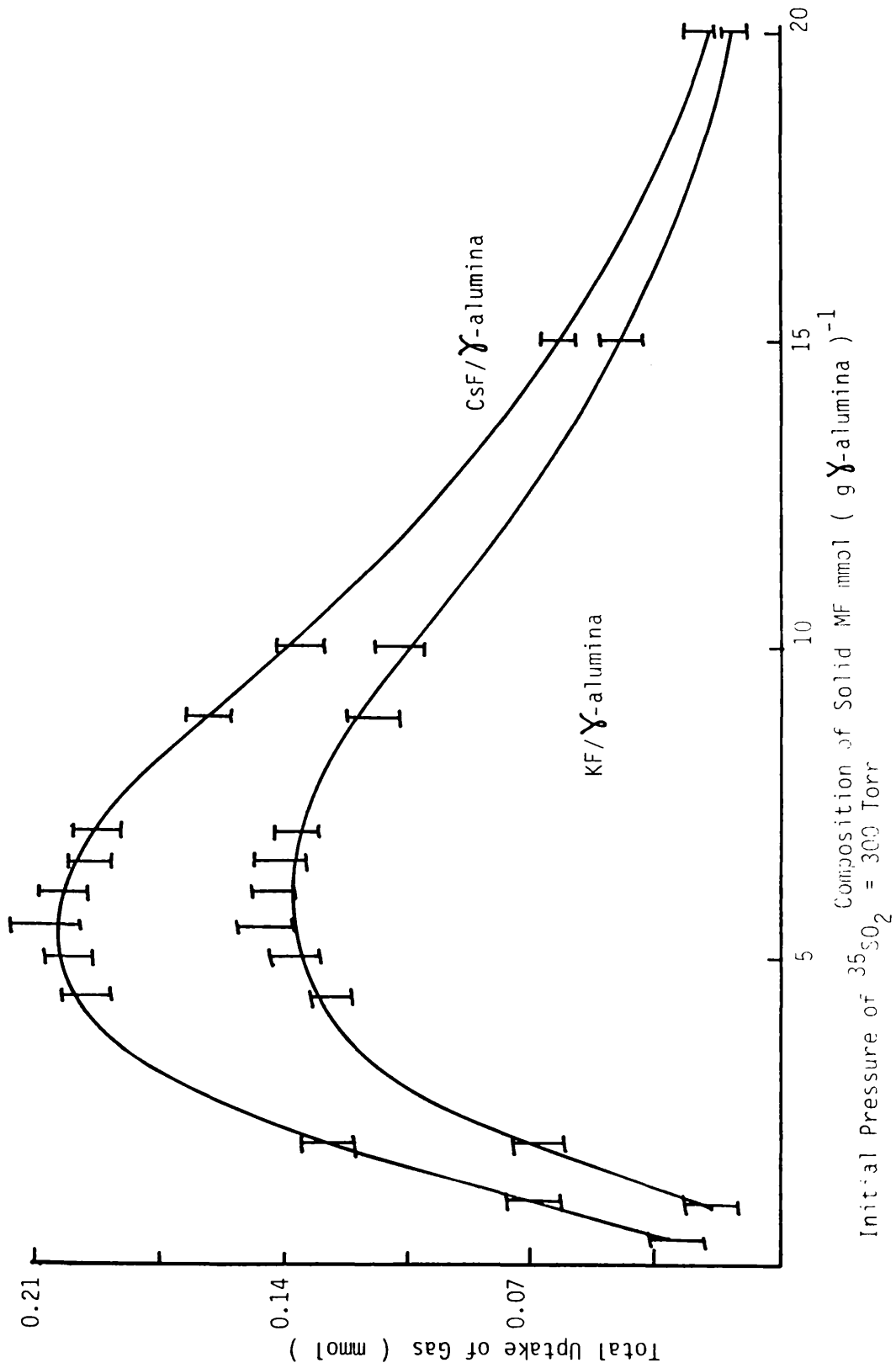


Figure 5.42 Reaction of  $^{35}\text{S}\text{O}_2$  with MF/ $\gamma$ -alumina, Surface Count Rate V Composition  
 Initial Pressure of  $^{35}\text{S}\text{O}_2 = 300$  Torr

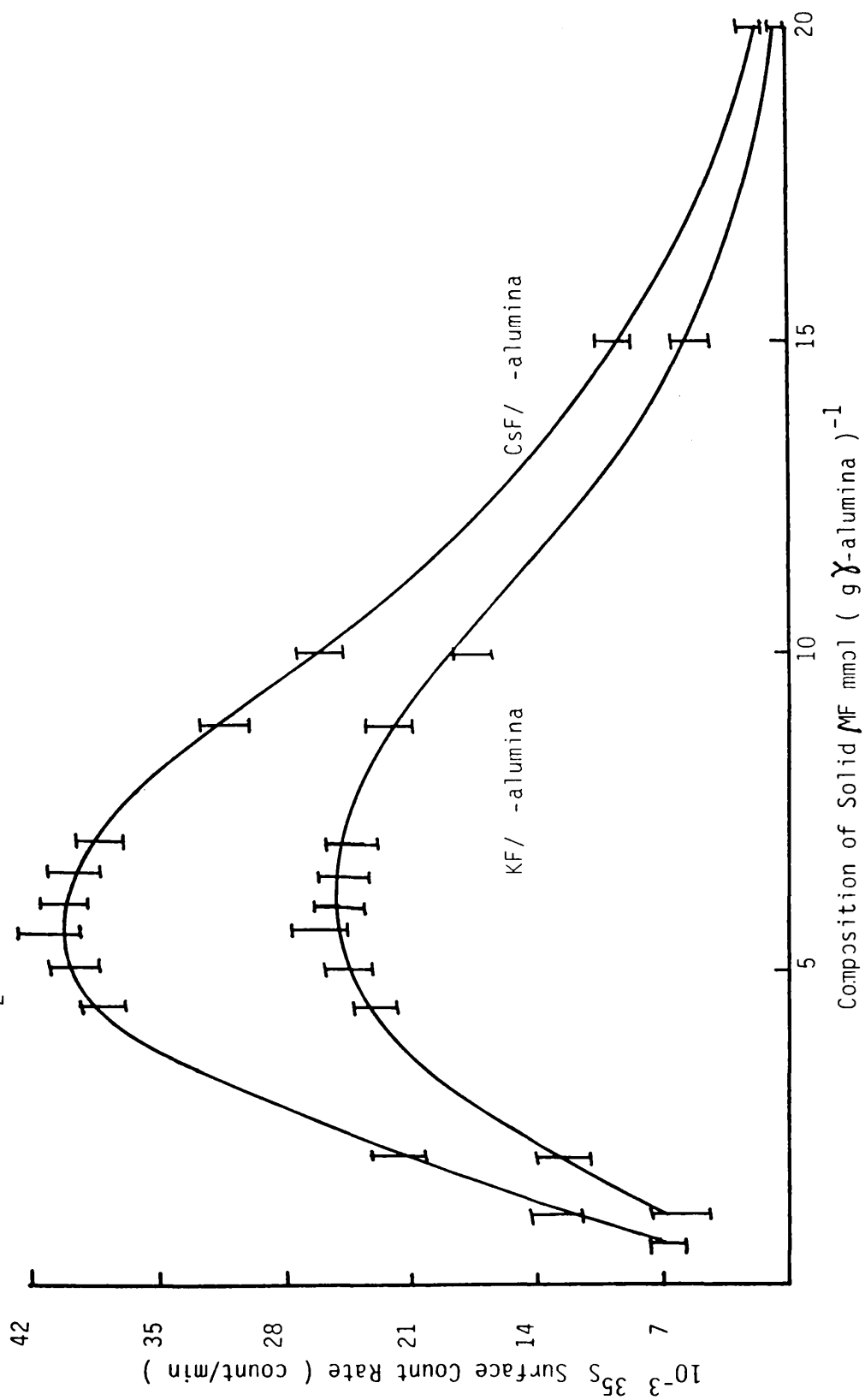
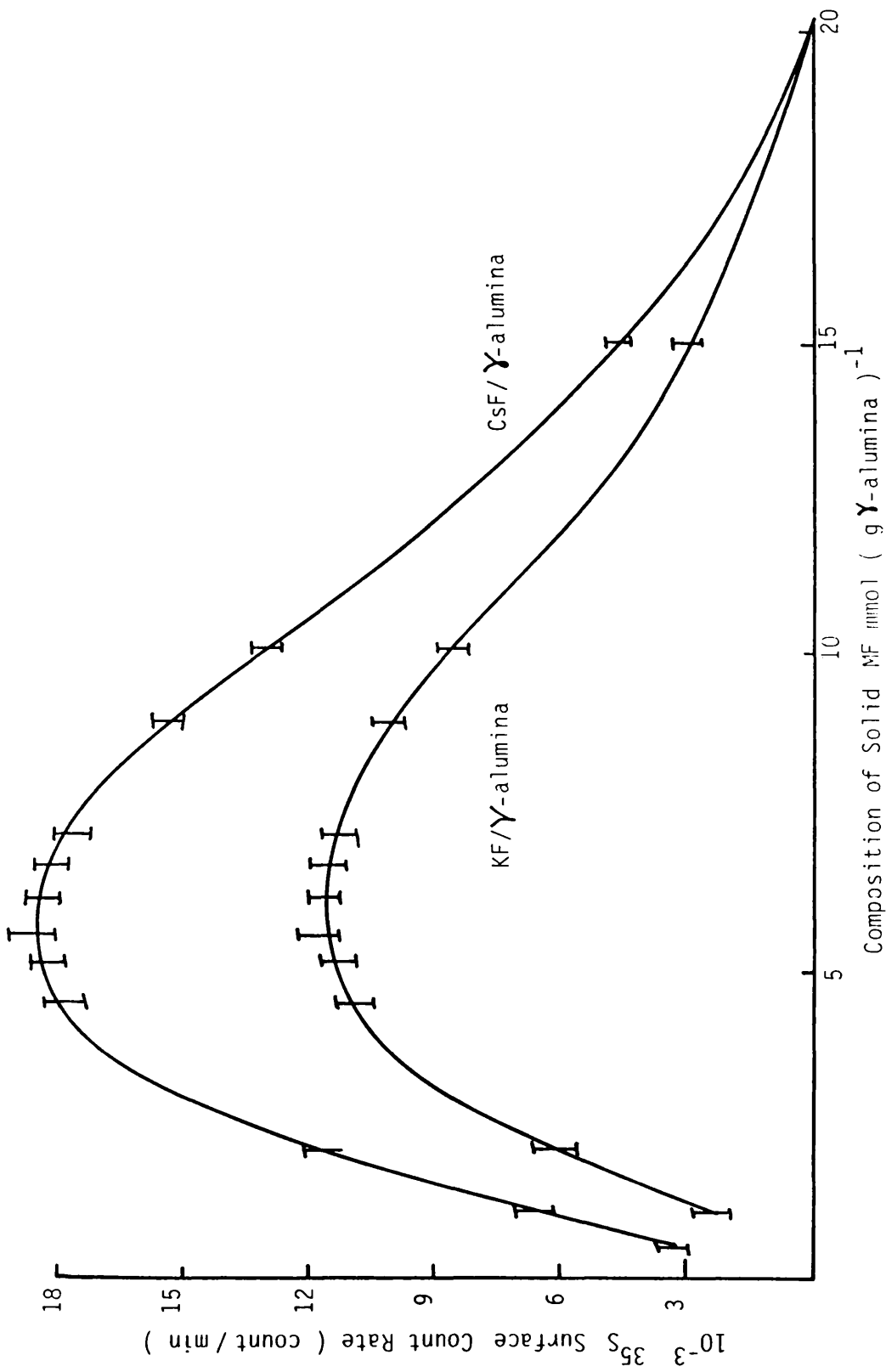


Figure 5.43 Reaction of  $^{35}\text{SO}_2$  with MF/ $\gamma$ -alumina, Surface Count Rate after Removal of Gas  $\gamma$  Composition





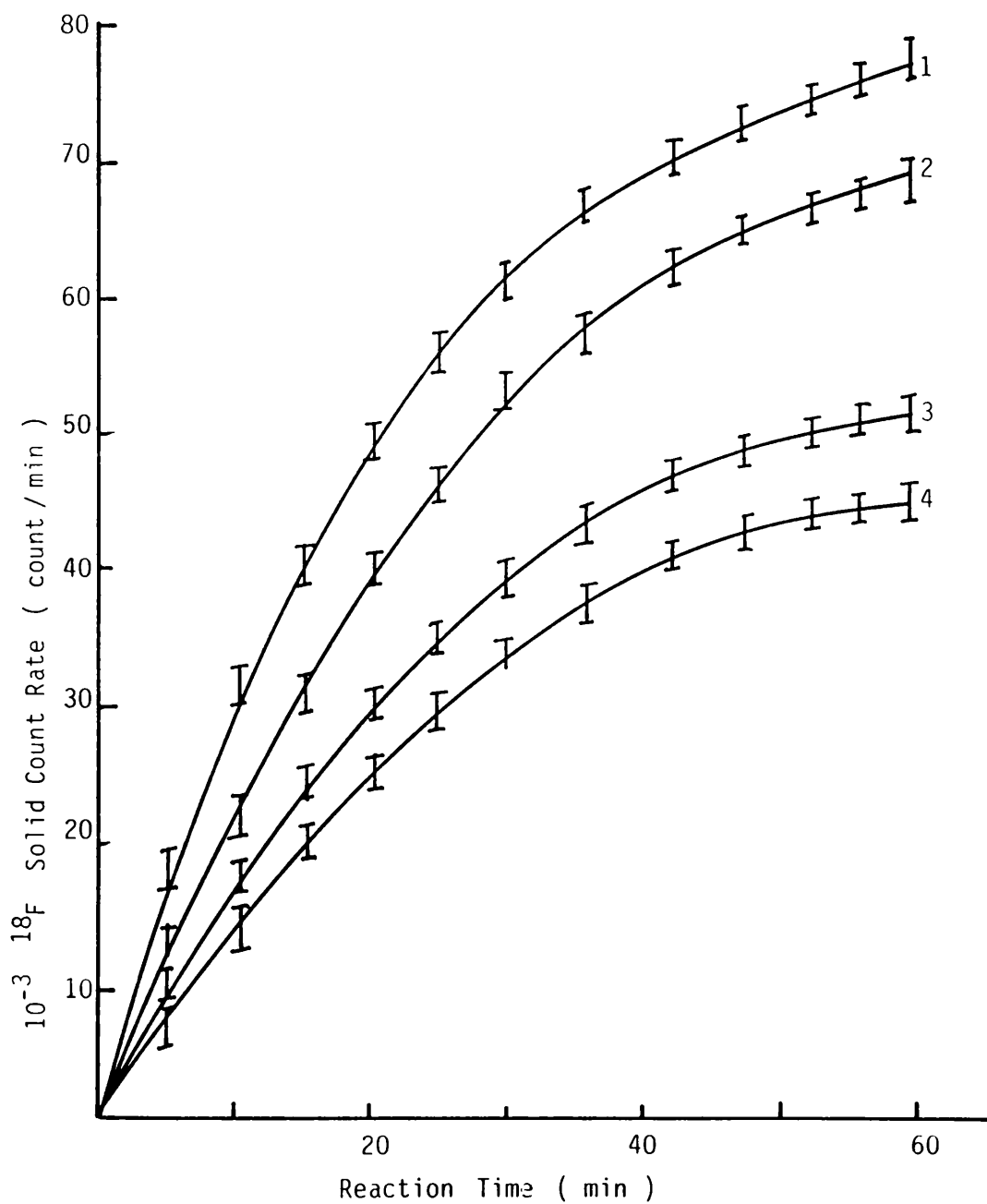
5.3.11 REACTIONS OF [<sup>18</sup>F]-FLUORINE LABELLED THIONYL FLUORIDE WITH CAESIUM OR POTASSIUM FLUORIDE SUPPORTED ON  $\gamma$ -ALUMINA

The admission of [<sup>18</sup>F]-fluorine labelled thionyl fluoride (usually 300 Torr which was equivalent to 1.0 mmol in the reaction vessel) to a sample of the supported metal fluoride, resulted in a rapid growth in the solid count rate over the first 30 min, followed by a slower increase thereafter. Typical results are shown in Fig. 5.44. The removal of the gas phase at room temperature from the reaction vessel led to a very small decrease in the total [<sup>18</sup>F]-fluorine solid count rate, indicating the retention of most of the [<sup>18</sup>F]-fluorine activity by the supported metal fluoride. The [<sup>18</sup>F]-fluorine solid count rates of the supported metal fluoride in the presence of gas and after pumping at room temperature were both dependent on the initial pressure of [<sup>18</sup>F]-fluorine labelled thionyl fluoride, in that, an increase in the initial pressure of [<sup>18</sup>F]-fluorine labelled thionyl fluoride in the range 40-560 Torr, led to an increase in the solid count rate. The results obtained are shown in Fig. 5.45 for the 4.4 and 8.8 mmolg<sup>-1</sup> materials. The solid count rate was also dependent on the composition of the solid; it decreased with increasing the metal fluoride loadings in the range 0.6-15.0 mmolg<sup>-1</sup>. The results are shown in Fig. 5.46. Estimation of the specific count rates of [<sup>18</sup>F]-fluorine labelled thionyl fluoride before and after the reaction with the supported metal fluoride showed that they were equal within the experimental error. This means that the [<sup>18</sup>F]-fluorine solid count rate was due to the uptake of [<sup>18</sup>F]-fluorine labelled thionyl fluoride or to the hydrolysis of [<sup>18</sup>F]-fluorine labelled thionyl fluoride and not due to [<sup>18</sup>F]-fluorine exchange between thionyl fluoride and the

**Figure 5.44** Reaction of  $\text{SO}_2^{18}\text{F}$  with MF/ $\gamma$ -alumina

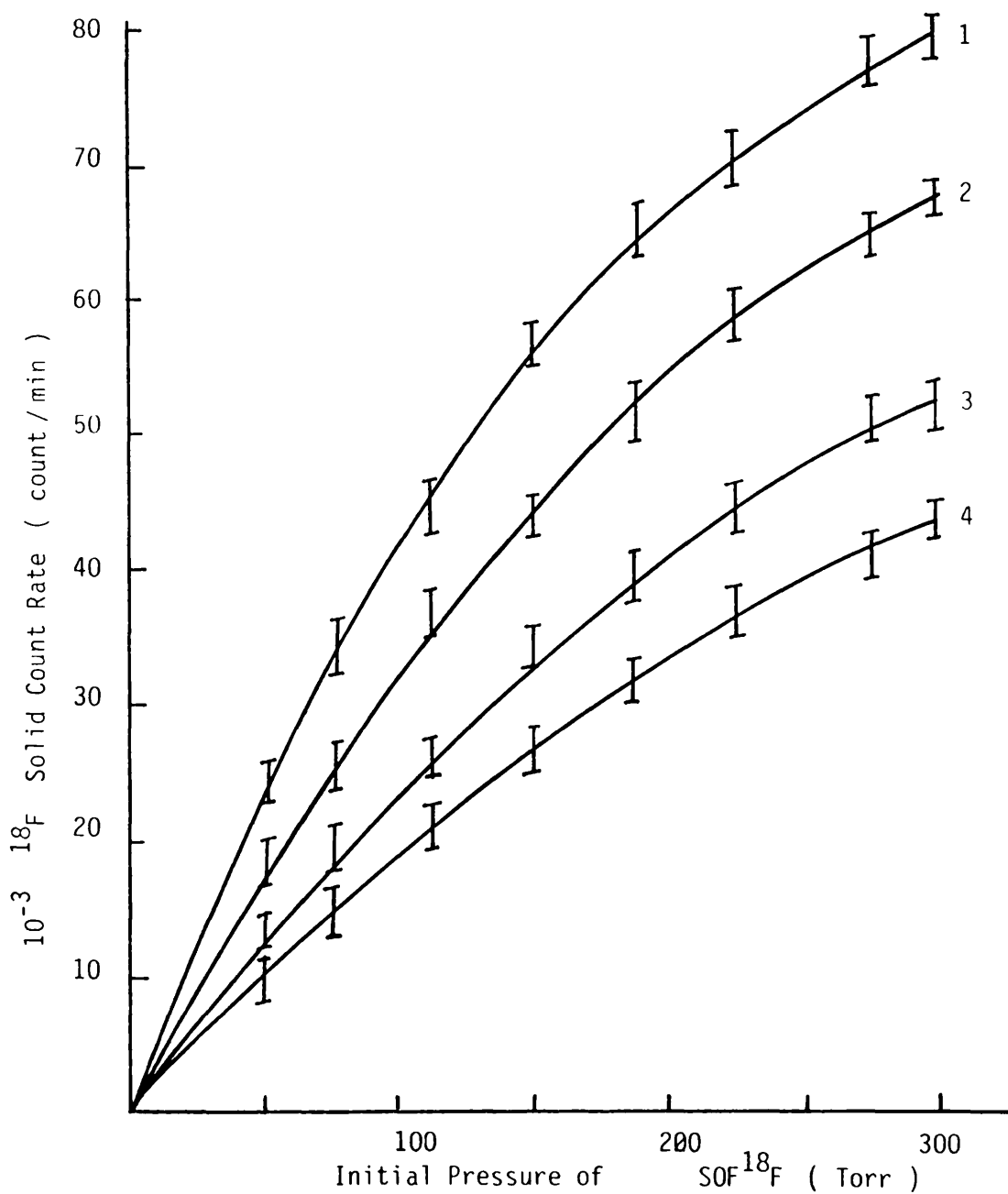
Solid Count Rate  $\checkmark$  Reaction Time

Initial Pressure = 300 Torr



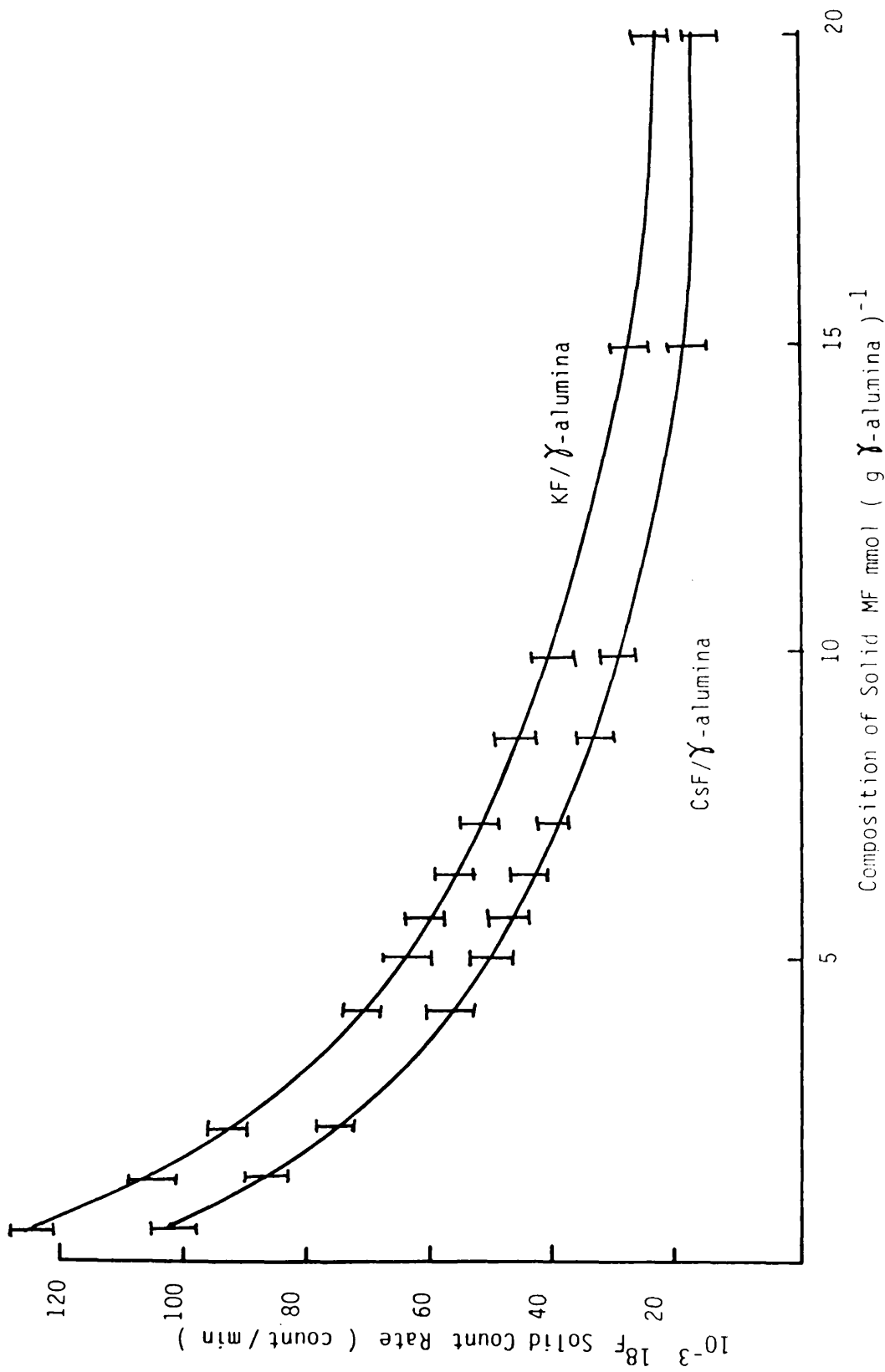
KF/ $\gamma$ -alumina	Composition	CsF/ $\gamma$ -alumina
1	4.4 mmol g <sup>-1</sup>	2
3	8.8 mmol g <sup>-1</sup>	4

Figure 5.45 Reaction of  $\text{SO}_2^{18}\text{F}$  with MF/ $\gamma$ -alumina  
 Solid Count Rate  $\propto$  Initial Pressure of  $\text{SO}_2^{18}\text{F}$

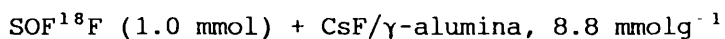


KF/ $\gamma$ -alumina	Composition	CsF/ $\gamma$ -alumina
1	$4.4 \text{ mmol g}^{-1}$	2
3	$8.8 \text{ mmol g}^{-1}$	4

Figure 5.46 Reaction of  $\text{SO}_2^{18}\text{F}$  with MF/ $\gamma$ -alumina, Solid Count Rate vs Composition



supported metal fluoride. To illustrate the method used to treat the data obtained, an example is given for the system



$$0.5\text{g} \equiv 1.88 \text{ mmol CsF}$$

Initial specific count rate of  $\text{SOF}^{18}\text{F} = 37951 \pm 291 \text{ count min}^{-1}$   
(mg atom F)<sup>-1</sup>

After reaction:-

Solid count rate =  $40896 \pm 169 \text{ count min}^{-1}$

Count rate of volatile materials =  $35738 \pm 307 \text{ count min}^{-1}$

Radiochemical balance =  $\frac{5738 + 40896}{75902} \times 100 = 101\%$

Composition of volatile products after reaction, from the infra-red study, section 5.3.5:-

0.47 mmol  $\text{SO}_2$

0.5 mmol  $\text{SO}_2$

Retained quantity as  $\text{SO}_2\text{F}^{\cdot}$  from the [<sup>35</sup>S]-sulphur study, section 5.3.8 and the manometric study section 5.3.6 was 0.03 mmol.

Specific count rate of  $\text{SOF}^{18}\text{F}$  after reaction =

$$\frac{35758 \pm 307}{0.47 \times 2} = 38036 \pm 326 \text{ count min}^{-1} (\text{mg atom F})^{-1}$$

As no [<sup>18</sup>F]-fluorine exchange had occurred in the system, the solid count rate due to [<sup>18</sup>F]-fluorine results from hydrolysis of 0.5 mmol of thionyl fluoride and 0.03 mmol retention of sulphur dioxide as  $\text{SO}_2\text{F}^{\cdot}$ , should be equal to =  $(0.03+0.5) \times 75902 = 40228 \text{ count min}^{-1}$ . This value is in good agreement with the experimental value. The results obtained are given in Tables

5.28-5.31. The admission of inactive thionyl fluoride to a sample of the supported metal fluoride pretreated with [ $^{18}\text{F}$ ]-fluorine labelled thionyl fluoride, had no effect on the solid count rate.

#### **5.3.12 REACTIONS OF [ $^{18}\text{F}$ ]-FLUORINE LABELLED SULPHUR TETRAFLUORIDE WITH CAESIUM OR POTASSIUM FLUORIDE SUPPORTED ON $\gamma$ -ALUMINA**

The admission of [ $^{18}\text{F}$ ]-fluorine labelled sulphur tetrafluoride (300 Torr, 1.0 mmol) to a sample of the supported metal fluoride, resulted in a rapid growth in the solid count rate over the first 30 min, followed by a slower increase thereafter. Plots of the [ $^{18}\text{F}$ ]-fluorine solid count rate versus time are given in Figs. 5.47 and 5.48. When the volatile products were removed at room temperature from the reaction vessel, a very small decrease in the solid count rate was observed. The [ $^{18}\text{F}$ ]-fluorine solid count rate varied with the initial pressure of [ $^{18}\text{F}$ ]-fluorine labelled sulphur tetrafluoride in the range 40-560 Torr, in that, it was increased by increasing the initial pressure. The results obtained are shown schematically in Fig. 5.49 for the supported metal fluorides, 4.4 and 8.8 mmol g<sup>-1</sup>. The solid count rate was dependent on the composition of the solid in the range 0.6-20.0 mmol g<sup>-1</sup>. The increase in the metal fluoride loading resulted in a decrease in the solid count rate. The results obtained are shown in Fig. 5.50. The admission of inactive sulphur tetrafluoride to a sample of the supported metal fluoride treated with [ $^{18}\text{F}$ ]-fluorine labelled sulphur tetrafluoride, led to a decrease in the solid count rate. The results obtained from the supported metal fluoride, 4.4 and 8.8 mmol g<sup>-1</sup> are given in Table 5.32.

Table 5.28 Results of Reaction between [ $^{18}\text{F}$ ]-Fluorine Labelled Thionyl Fluoride and  $\text{CsF}/\gamma\text{Alumina}$ ,  $4.4\text{mmol g}^{-1}$

Sample Weight $\text{g, mmol}$ of $\text{CsF}$	Quantity of Gas Torr mmol	Initial Specific Count Rate $\text{Count min}^{-1}$ (mg atom F) $^{-1}$	Final Specific Count Rate After Reaction $\text{Count min}^{-1}$ (mg atom F) $^{-1}$	Final Solid Count Rate	
				Experimental	Calculated
0.5 $\pm$ 0.01 1.32 $\pm$ 0.06	300 $\pm$ 2 1.0 $\pm$ 0.06	39793 $\pm$ 193	39790 $\pm$ 211	61897 $\pm$ 314	62983
0.5 $\pm$ 0.01 1.32 $\pm$ 0.06	300 $\pm$ 2 1.0 $\pm$ 0.06	43700 $\pm$ 91	43791 $\pm$ 119	67411 $\pm$ 219	67892
0.5 $\pm$ 0.01 1.32 $\pm$ 0.06	300 $\pm$ 2 1.0 $\pm$ 0.06	33671 $\pm$ 122	33729 $\pm$ 249	52593 $\pm$ 197	53110
0.5 $\pm$ 0.01 1.32 $\pm$ 0.06	300 $\pm$ 2 1.0 $\pm$ 0.06	36691 $\pm$ 203	36799 $\pm$ 183	56670 $\pm$ 219	56447

Table 5.29 Results of Reaction between [ $^{18}\text{F}$ ]-Fluorine Labelled Thionyl Fluoride and  $\text{KF}/\gamma\text{Alumina}$ ,  $4.4\text{mmol g}^{-1}$

Sample Weight $\text{g, mmol}$	Quantity of Gas Torr mmol	Initial Specific Count Rate $\text{Count min}^{-1}$ (mg atom F) $^{-1}$	Final Specific Count Rate After Reaction $\text{Count min}^{-1}$ (mg atom F) $^{-1}$	Final Solid Count Rate	
				Experimental	Calculated
$0.38 \pm 0.01$ $1.33 \pm 0.06$	$300 \pm 2$ $1.0 \pm 0.06$	$39793 \pm 193$	$39863 \pm 317$	$63861 \pm 191$	$64591$
$0.38 \pm 0.01$ $1.33 \pm 0.06$	$300 \pm 2$ $1.0 \pm 0.06$	$43700 \pm 91$	$43631 \pm 147$	$69921 \pm 217$	$69092$
$0.38 \pm 0.01$ $1.33 \pm 0.06$	$300 \pm 2$ $1.0 \pm 0.06$	$33671 \pm 122$	$33637 \pm 197$	$54360 \pm 320$	$54892$
$0.38 \pm 0.01$ $1.33 \pm 0.06$	$300 \pm 2$ $1.0 \pm 0.06$	$36691 \pm 203$	$36781 \pm 171$	$58949 \pm 211$	$59574$



Table 5.30 Results of Reaction between [<sup>18</sup>F]-Fluorine Labelled Thionyl Fluoride and CsF/γAlumina, 8.8mmol g<sup>-1</sup>

Sample Weight g, mmol of CsF	Quantity of Gas Torr mmol	Initial Specific Count Rate Count min <sup>-1</sup> (mg atom F) <sup>-1</sup>	Final Specific Count Rate After Reaction Count min <sup>-1</sup> (mg atom F) <sup>-1</sup>	Experimental		Calculated
				Final Solid Count Rate Count min <sup>-1</sup>	Count min <sup>-1</sup>	
0.5 ± 0.01 1.88 ± 0.06	300 ± 2 1.0 ± 0.06	37951 ± 291	38036 ± 325	40896 ± 169		40228
0.5 ± 0.01 1.88 ± 0.06	300 ± 2 1.0 ± 0.06	35739 ± 207	35681 ± 243	38000 ± 171		38197
0.5 ± 0.01 1.88 ± 0.06	300 ± 2 1.0 ± 0.06	40793 ± 198	40833 ± 290	43821 ± 217		44032
0.5 ± 0.01 1.88 ± 0.06	300 ± 2 1.0 ± 0.06	38341 ± 212	38000 ± 314	40004 ± 183		40218

Table 5.31 Results of Reaction between [ $^{18}\text{F}$ ]-Fluorine Labelled Thionyl Fluoride and  $\text{KF}/\gamma\text{Alumina}$ ,  $8.8\text{mmol g}^{-1}$

Sample Weight $\text{g}/\text{mmol}$	Quantity of Gas Torr $\text{mmol}$	Initial Specific Count Rate $\text{Count min}^{-1}$ (mg atom F) $^{-1}$	Final Specific Count Rate After Reaction $\text{Count min}^{-1}$ (mg atom F) $^{-1}$	Final Solid Count Rate	
				Experimental	Calculated
1.32 $\pm$ 0.01	300 $\pm$ 2	37951 $\pm$ 291	37839 $\pm$ 207	48103 $\pm$ 137	47723
1.88 $\pm$ 0.06	1.0 $\pm$ 0.06				
1.32 $\pm$ 0.01	300 $\pm$ 2	35739 $\pm$ 207	36013 $\pm$ 331	44831 $\pm$ 223	45379
1.88 $\pm$ 0.06	1.0 $\pm$ 0.06				
1.32 $\pm$ 0.01	300 $\pm$ 2	40793 $\pm$ 198	40903 $\pm$ 263	50991 $\pm$ 493	51474
1.88 $\pm$ 0.06	1.0 $\pm$ 0.06				
1.32 $\pm$ 0.01	300 $\pm$ 2	38341 $\pm$ 212	38781 $\pm$ 193	48971 $\pm$ 361	48217
1.88 $\pm$ 0.06	1.0 $\pm$ 0.06				

Figure 5.47 Reaction of  $SF_3^{18}F$  with  $CsF/\gamma$ -alumina,  $4.4 \text{ mmol g}^{-1}$   
Solid Count Rate  $\nu$  Reaction Time  
Initial Pressure of  $SF_3^{18}F = 300 \text{ Torr}$

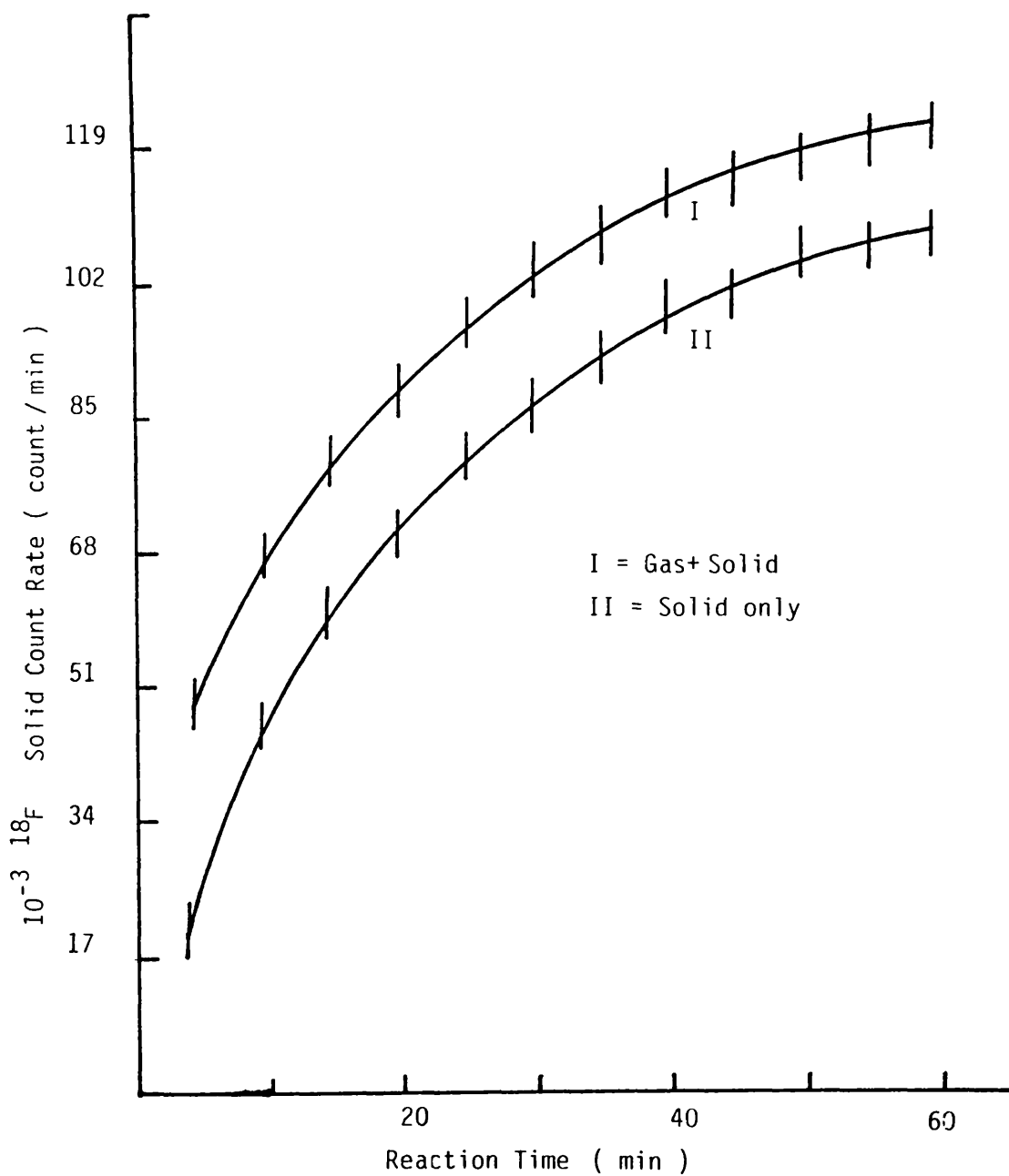


Figure 5.48 Reaction of  $SF_3^{18}F$  with  $KF/\gamma$ -alumina,  $4.4 \text{ mmol g}^{-1}$ , Solid Count Rate  $\nu$  Reaction Time  
 Initial Pressure of  $SF_3^{18}F = 300 \text{ Torr}$

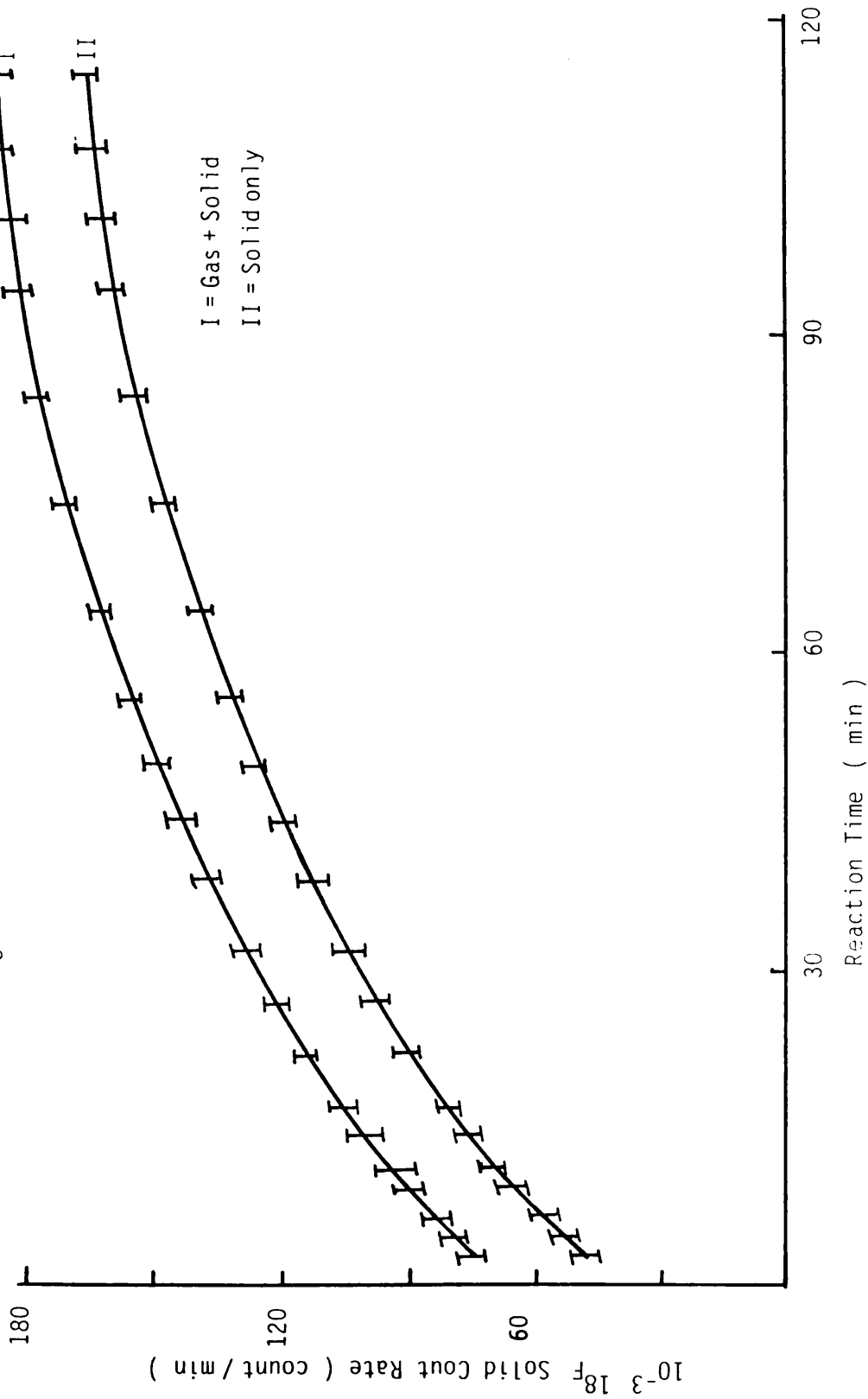
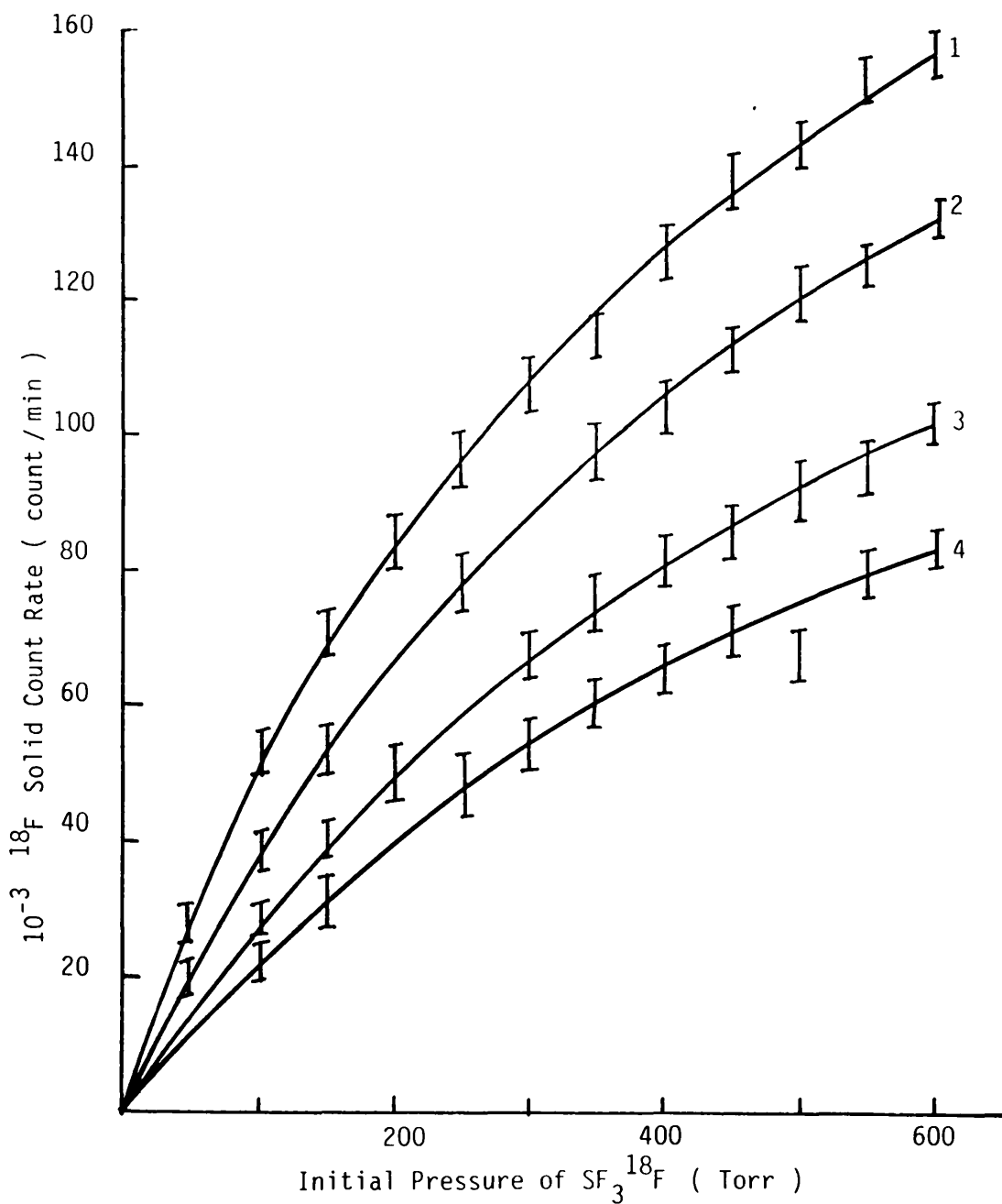


Figure 5.49 Reaction of  $SF_3^{18}F$  with MF/ $\gamma$ -alumina  
 Solid Count Rate  $\nu$  Initial Pressure



KF/ $\gamma$ -alumina	Composition	CsF/ $\gamma$ -alumina
1	$4.4 \text{ mmol g}^{-1}$	2
3	$8.8 \text{ mmol g}^{-1}$	4

Figure 5.50 Reaction of  $SF_3^{18}F$  with MF/ $\gamma$ -alumina, Solid Count Rate  $\nu$  Composition

Initial Pressure of  $SF_3^{18}F = 300$  Torr

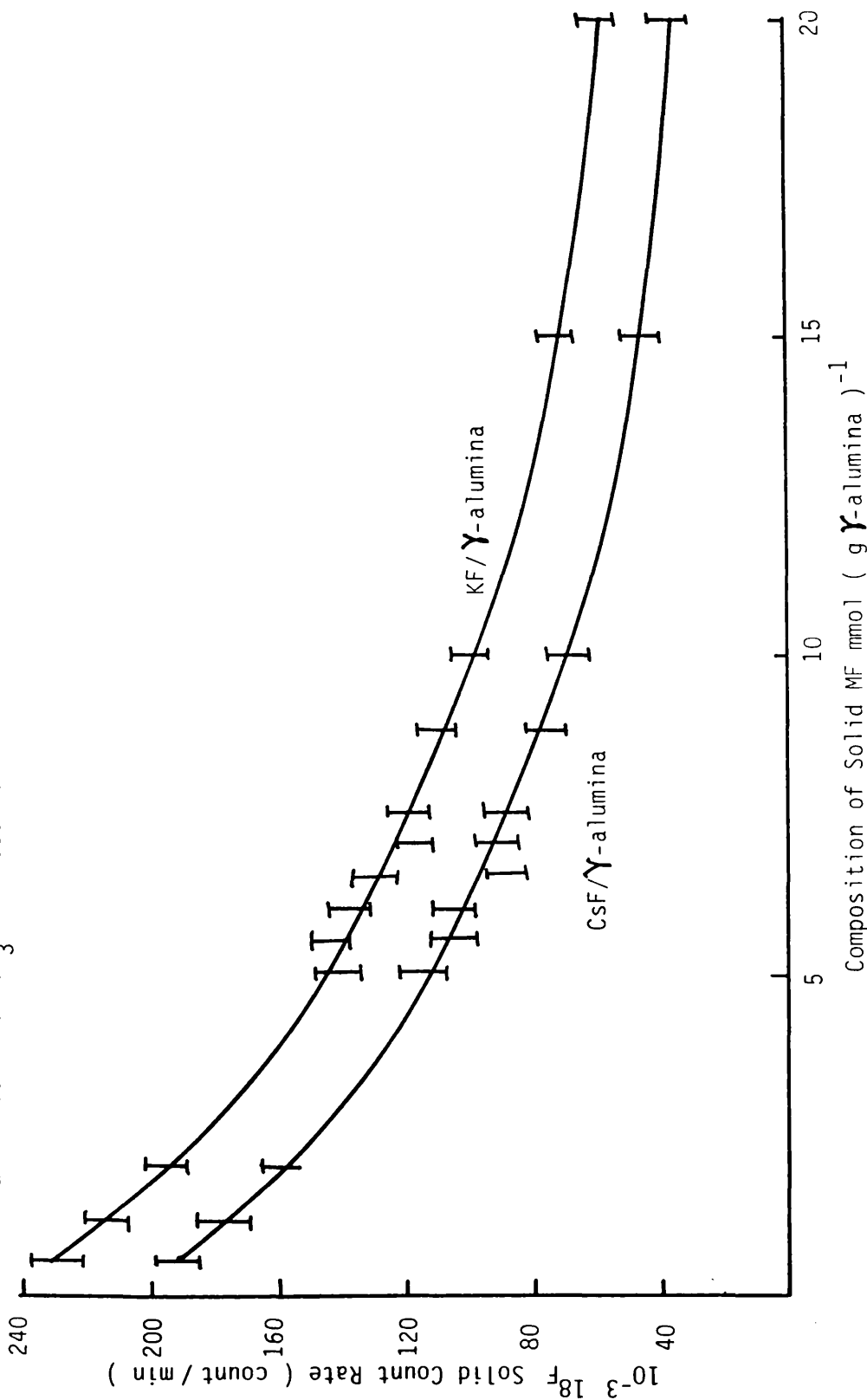


Table 5.32 Reactions between Sulphur Tetrafluoride and MF/ $\gamma$ Alumina pretreated with [ $^{18}\text{F}$ ]-Fluorine Labelled Sulphur Tetrafluoride

Material	Solid Count Rate Before Reaction Count $\text{min}^{-1}$	Solid Count Rate After Reaction Count $\text{min}^{-1}$	Gas Count Rate After Reaction Count $\text{min}^{-1}$	Ratio %	Solid After Solid Before
CsF/ $\gamma$ -alumina 4.4 $\text{mmol g}^{-1}$	120617 $\pm$ 312	108555 $\pm$ 413	12763 $\pm$ 214		90
	128010 $\pm$ 93	112649 $\pm$ 213	17691 $\pm$ 193		88
	118963 $\pm$ 198	108256 $\pm$ 161	11600 $\pm$ 279		91
	121332 $\pm$ 150	109199 $\pm$ 93	12471 $\pm$ 109		90
KF/ $\gamma$ -alumina 4.4 $\text{mmol g}^{-1}$	126293 $\pm$ 373	109875 $\pm$ 219	15819 $\pm$ 133		87
	134564 $\pm$ 132	121108 $\pm$ 193	14053 $\pm$ 219		90
	123786 $\pm$ 89	112645 $\pm$ 93	11592 $\pm$ 300		91
	127577 $\pm$ 410	113544 $\pm$ 311	14632 $\pm$ 100		89
CsF/ $\gamma$ -alumina 8.8 $\text{mmol g}^{-1}$	84903 $\pm$ 93	71319 $\pm$ 131	14593 $\pm$ 331		84
	94312 $\pm$ 173	80165 $\pm$ 293	13843 $\pm$ 139		85
	97293 $\pm$ 201	78807 $\pm$ 93	19082 $\pm$ 100		81
	88819 $\pm$ 147	73720 $\pm$ 167	15699 $\pm$ 214		83
KF/ $\gamma$ -alumina 8.8 $\text{mmol g}^{-1}$	90411 $\pm$ 312	73233 $\pm$ 193	17293 $\pm$ 201		81
	99841 $\pm$ 193	79873 $\pm$ 157	20368 $\pm$ 143		80
	103861 $\pm$ 295	88282 $\pm$ 291	15993 $\pm$ 159		85
	95793 $\pm$ 209	79508 $\pm$ 313	15923 $\pm$ 219		83

Estimation of the specific count rates before and after the reaction of [ $^{18}\text{F}$ ]-fluorine labelled sulphur tetrafluoride and the supported metal fluoride,  $8.8 \text{ mmol g}^{-1}$ , showed that due to [ $^{18}\text{F}$ ]-fluorine labelled sulphur tetrafluoride had decreased, but the specific count rate of [ $^{18}\text{F}$ ]-fluorine labelled thionyl fluoride was equivalent to the specific count rate of [ $^{18}\text{F}$ ]-fluorine labelled sulphur tetrafluoride before the reaction based on the results obtained from the reaction between [ $^{18}\text{F}$ ]-fluorine labelled thionyl fluoride and supported metal fluorides. The calculation is now shown in detail for experiments 1 in Tables 5.33 and 5.35.

$\text{SF}_4$  1.0 mmol + CsF/ $\gamma$ -alumina,  $4.4 \text{ mmol g}^{-1}$ ,  $0.5 \text{ g} \equiv 1.32 \text{ mmol}$  of CsF

Initial specific count rate of  $\text{SF}_3^{18}\text{F} = 38551 \pm 103 \text{ count min}^{-1}$

$$(\text{mg atom F})^{-1}$$

$$= 154204 \text{ count min}^{-1} \text{ mmol}^{-1}$$

After reaction:

Solid count rate =  $120617 \pm 312 \text{ count min}^{-1}$

Count rate of volatile products =  $35506 \pm 217 \text{ count min}^{-1}$

Composition of volatile products after reaction based on the results obtained from the infra-red study:

0.46 mmol  $\text{SOF}_2$

0.40 mmol  $\text{SO}_2$

Retained quantity as  $\text{SF}_5^-$  and  $\text{SO}_2\text{F}^-$  based on the manometric and [ $^{35}\text{S}$ ]-sulphur studies was 0.14 mmol.

The radiochemical balance =  $\frac{35506 + 120617}{154204} \times 100 = 101\%$

The specific count rate of  $\text{SOF}^{18}\text{F} = \frac{35506}{0.46 \times 2} = 38593 \pm 236$

$\text{count min}^{-1} (\text{mg atom F})^{-1}$



As no [ $^{18}\text{F}$ ]-fluorine exchange had occurred in the system, the solid count rate due to [ $^{18}\text{F}$ ]-fluorine results from hydrolysis of 0.86 mmol of sulphur tetrafluoride to yield 0.46 mmol and 0.40 mmol of the respective thionyl fluoride and sulphur dioxide, and 0.14 mmol retained as  $\text{SF}_5^-$  and  $\text{SO}_2\text{F}^-$ , should be equal to

$$= 154204 \times (0.4 + 0.14) + 38551 \times 2 \times 0.46 = 118737 \text{ count min}^{-1}$$

This value is in good agreement with the experimental value.

This method is now generated to include the supported metal fluoride,  $8.8 \text{ mmolg}^{-1}$  systems in which sulphur tetrafluoride was recovered after reaction. The fluorine exchange was calculated based on the assumptions:

- 1) Hydrolysis of sulphur tetrafluoride is fast.
- 2) All the fluorine atoms involved in the system are exchangeable.

An example is given below.

$\text{SF}_4$  (1.0 mmol + CsF/ $\gamma$ -alumina,  $8.8 \text{ mmolg}^{-1}$ )

$$0.5 \equiv 1.88 \text{ mmol CsF}$$

$$\begin{aligned} \text{Initial specific count rate of } \text{SF}_3^{18}\text{F} &= 35955 \pm 79 \text{ count min}^{-1} \\ & \quad (\text{mg atom F})^{-1} \\ &= 143820 \text{ count min}^{-1} \text{ mmol}^{-1} \end{aligned}$$

After reaction:

$$\text{Solid count rate} = 84903 \pm 176 \text{ count min}^{-1}$$

$$\text{Count rate of volatile products} = 59598 \pm 194 \text{ count min}^{-1}$$

$$\text{Radiochemical balance} = \frac{84903 + 59598}{143820} \times 100 = 101\%$$

Composition of volatile products after reaction based on the results obtained from the infra-red study:

0.11 mmol  $\text{SF}_4$

0.64 mmol  $\text{SOF}_2$

0.19 mmol SO<sub>2</sub>

Retained quantity of sulphur tetrafluoride as SF<sub>5</sub><sup>-</sup> and SO<sub>2</sub>F<sup>-</sup> based on the manometric and [<sup>35</sup>S]-sulphur studies was 0.06 mmol. As no [<sup>18</sup>F]-fluorine exchange had occurred in the thionyl fluoride system, therefore:

$$\text{Activity in SOF}^{18}\text{F} = 35955 \times 2 \times 0.64 = 46022 \text{ count min}^{-1}$$

$$\text{Activity in SF}_3^{18}\text{F} = 59598 - 46022 = 13576 \text{ count min}^{-1}$$

$$\text{Specific count rate of SF}_3^{18}\text{F} \text{ after reaction} = \frac{13576}{4 \times 0.11}$$

$$30855 \text{ count min}^{-1} (\text{mg atom F})^{-1}$$

For a total exchange in the system, SF<sub>3</sub><sup>18</sup>F/CsF/γ-alumina, 8.8 mmolg<sup>-1</sup>

$$S_{\infty} = \frac{35955 \times 4}{1.88 + 4 \times 1.0} = 24459 \text{ count min}^{-1} (\text{mg atom F})^{-1}$$

The fraction exchanged is calculated using equation 2.12

$$f = \frac{S_o - S_t}{S_o - S_{\infty}} = \frac{35955 - 30855}{35955 - 24459} \times 100 = 44\%$$

For a 44% exchange, the drop in the specific count rate

$$= 35955 - 30855 = 5100 \text{ count min}^{-1} (\text{mg atom F})^{-1}$$

The total drop in the SF<sub>3</sub><sup>18</sup>F count rate after reaction

$$= 5100 \times 4 \times 0.11 = 2244 \text{ count min}^{-1}$$

The solid count rate due to [<sup>18</sup>F]-fluorine results from, 44% exchange, hydrolysis of 0.83 mmol of sulphur tetrafluoride to yield 0.64 and 0.19 mmol of thionyl fluoride and sulphur dioxide respectively and 0.06 mmol retained as SF<sub>5</sub><sup>-</sup> and SO<sub>2</sub>F<sup>-</sup>, should be:

$$2244 + 35955 \times 2 \times 0.64 + 35955 \times 4 \times (0.19 + 0.06) =$$

$$84221 \text{ count min}^{-1}$$

This value is in good agreement with the experimental value.

This method is used throughout this work and the results

obtained for the supported metal fluoride, 4.4 and 8.8 mmolg<sup>-1</sup> are given in Tables 5.33-5.36.

**5.4 THE REACTIONS INVOLVING VOLATILE CARBON CONTAINING PROBE MOLECULES WITH CAESIUM OR POTASSIUM FLUORIDE SUPPORTED ON  $\gamma$ -ALUMINA**

**5.4.1 INFRA-RED ANALYSIS OF THE HYDROLYSIS OF CARBONYL FLUORIDE OVER  $\gamma$ -ALUMINA SUPPORTED CAESIUM OR POTASSIUM FLUORIDE**

The infra-red spectrum of the volatile products after the room temperature reaction between carbonyl fluoride and supported metal fluorides showed very strong bands due to carbon dioxide and carbonyl fluoride, but no evidence for anhydrous hydrogen fluoride. Bands identified in the infra-red spectrum of the volatile material obtained from the reaction of carbonyl fluoride (200 Torr) with the supported caesium fluoride, 4.4 mmolg<sup>-1</sup> are given in Table 5.37.

The composition of the gas products after reaction between carbonyl fluoride and the supported metal fluoride was dependent on the metal fluoride loading. The results are given in Tables 5.38 and 5.39 for the supported metal fluorides, 4.4 and 8.8 mmolg<sup>-1</sup> and the best data were converted to mole ratios and are given in Table 5.40.

**5.4.2 MANOMETRIC STUDY OF REACTIONS OF CARBONYL FLUORIDE WITH  $\gamma$ -ALUMINA SUPPORTED CAESIUM OR POTASSIUM FLUORIDE**

The uptakes of carbonyl fluoride and/or its hydrolysis product carbon dioxide by supported metal fluoride were studied manometrically using the constant volume manometer across the composition range at different initial pressures of carbonyl

Table 5.33 Results of Reactions between [ $^{18}\text{F}$ ]-Fluorine Labelled Sulphur Tetrafluoride with  $\text{CsF}/\gamma\text{Alumina}$ ,  $4.4\text{mmol g}^{-1}$

Sample Weight $\text{g}_{\gamma\text{mmol}}$ of $\text{CsF}$	Quantity of $\text{SF}_3^{18}\text{F}$ Torr mmol	Specific Count Rate of $\text{SF}_3^{18}\text{F}$ Before Reaction Count $\text{min}^{-1}$ (mg atom F) $^{-1}$	Specific Count Rate of $\text{SOF}^{18}\text{F}$ After Reaction Count $\text{min}^{-1}$ (mg atom F) $^{-1}$	Solid Count Rate Count $\text{min}^{-1}$	Experimental	Calculated
0.5 $\pm$ 0.01 1.32 $\pm$ 0.06	300 $\pm$ 2 1.0 $\pm$ 0.06	38551 $\pm$ 103	38593 $\pm$ 173	120617 $\pm$ 312	118737	
0.5 $\pm$ 0.01 1.32 $\pm$ 0.06	300 $\pm$ 2 1.0 $\pm$ 0.06	41312 $\pm$ 195	41289 $\pm$ 107	128010 $\pm$ 93	129817	
0.5 $\pm$ 0.01 1.32 $\pm$ 0.01	300 $\pm$ 2 1.0 $\pm$ 0.06	37953 $\pm$ 113	37998 $\pm$ 153	118963 $\pm$ 198	119876	
0.5 $\pm$ 0.01 1.32 $\pm$ 0.06	300 $\pm$ 2 1.0 $\pm$ 0.06	39031 $\pm$ 148	38976 $\pm$ 153	121332 $\pm$ 150	120765	
0.5 $\pm$ 0.01 1.32 $\pm$ 0.06	300 $\pm$ 2 1.0 $\pm$ 0.06	40773 $\pm$ 199	40772 $\pm$ 136	126961 $\pm$ 173	128973	

Table 5.34 Results of Reactions between [<sup>18</sup>F]-Fluorine Labelled Sulphur Tetrafluoride with KF/γAlumina, 4.4mmol g<sup>-1</sup>

Sample Weight g, mmol of KF	Quantity of SF <sub>3</sub> <sup>18</sup> F Torr mmol	Specific Count Rate of SF <sub>3</sub> <sup>18</sup> F Before Reaction Count min <sup>-1</sup> (mg atom F) <sup>-1</sup>	Specific Count Rate of SOF <sup>18</sup> F After Reaction Count min <sup>-1</sup> (mg atom F) <sup>-1</sup>	Solid Count Rate Count min <sup>-1</sup>	Experimental	Calculated
0.38 ± 0.01	300 ± 2	38551 ± 103	38503 ± 213	126293 ± 373	127981	
1.33 ± 0.06	1.0 ± 0.06					
0.38 ± 0.01	300 ± 2	41312 ± 195	41376 ± 151	134564 ± 132	135417	
1.33 ± 0.06	1.0 ± 0.06					
0.38 ± 0.01	300 ± 2	37953 ± 113	37955 ± 91	123786 ± 89	122887	
1.33 ± 0.06	1.0 ± 0.06					
0.38 ± 0.01	300 ± 2	39031 ± 148	39112 ± 156	127577 ± 410	127976	
1.33 ± 0.06	1.0 ± 0.06					
0.38 ± 0.01	300 ± 2	40773 ± 199	40723 ± 215	133447 ± 231	134092	
1.33 ± 0.06	1.0 ± 0.06					

Table 5.35 Results of Reactions between [ $^{18}\text{F}$ ]-Fluorine Labelled Sulphur Tetrafluoride with  $\text{CsF}/\gamma\text{Alumina}$ ,  $8.8\text{mmol g}^{-1}$

Sample Weight $\text{g, mmol}$	Quantity of $\text{SF}_3^{18}\text{F}$ Torr $\text{mmol}$	Specific Count Rate of $\text{SF}_3^{18}\text{F}$ Before Reaction $\text{Count min}^{-1}$ (mg atom F) $^{-1}$	Specific Count Rate $\text{SF}_3^{18}\text{F}$ After Reaction $\text{Count min}^{-1}$ (mg atom F) $^{-1}$	Solid Count Rate $\text{Count min}^{-1}$		Fraction Exchanged %
				Experimental	Calculated	
0.5 $\pm$ 0.01 1.88 $\pm$ 0.01	300 $\pm$ 2 1.0 $\pm$ 0.06	35955 $\pm$ 79	30089 $\pm$ 195	84903 $\pm$ 176	84221	44 $\pm$ 1
0.5 $\pm$ 0.01 1.88 $\pm$ 0.06	300 $\pm$ 2 1.0 $\pm$ 0.06	39731 $\pm$ 164	33761 $\pm$ 213	94312 $\pm$ 173	95217	47 $\pm$ 1
0.5 $\pm$ 0.01 1.88 $\pm$ 0.06	300 $\pm$ 2 1.0 $\pm$ 0.06	41495 $\pm$ 203	35523 $\pm$ 131	97293 $\pm$ 201	97596	43 $\pm$ 1
0.5 $\pm$ 0.01 1.88 $\pm$ 0.06	300 $\pm$ 2 1.0 $\pm$ 0.06	37939 $\pm$ 193	31874 $\pm$ 96	88819 $\pm$ 479	88479	40 $\pm$ 1

Table 5.36 Results of Reactions between [ $^{18}\text{F}$ ]-Fluorine Labelled Sulphur Tetrafluoride with KF/ $\gamma$ Alumina,  $8.8\text{mmol g}^{-1}$

Sample Weight $\text{g, mmol}$	Quantity of $\text{Sf}_3^{18}\text{F}$ Torr $\text{mmol}$	Specific Count Rate of $\text{SF}_3^{18}\text{F}$ Before Reaction $\text{Count min}^{-1} (\text{mg atom F})^{-1}$	Specific Count Rate $\text{SF}_3^{18}\text{F}$ After Reaction $\text{Count min}^{-1} (\text{mg atom F})^{-1}$	Solid Count Rate		Fraction Exchanged %
				Experimental	Calculated	
0.32 $\pm$ 0.01 1.88 $\pm$ 0.06	300 $\pm$ 2 1.0 $\pm$ 0.06	35955 $\pm$ 79	32161 $\pm$ 99	90411 $\pm$ 312	91007	31 $\pm$ 1
0.32 $\pm$ 0.01 1.88 $\pm$ 0.06	300 $\pm$ 2 1.0 $\pm$ 0.06	39731 $\pm$ 164	35920 $\pm$ 163	99841 $\pm$ 193	99576	30 $\pm$ 1
0.32 $\pm$ 0.01 1.88 $\pm$ 0.06	300 $\pm$ 2 1.0 $\pm$ 0.06	41495 $\pm$ 203	36585 $\pm$ 237	103861 $\pm$ 295	104792	24 $\pm$ 1
0.32 $\pm$ 0.01 1.88 $\pm$ 0.06	300 $\pm$ 2 1.0 $\pm$ 0.06	37939 $\pm$ 193	33694 $\pm$ 171	95793 $\pm$ 209	95117	27 $\pm$ 1

**Table 5.37**    **Infra-Red Spectrum of the Volatile products after Reaction between Carbonyl Fluoride and CsF/ $\gamma$ -Alumina 4.4 mmol g<sup>-1</sup>**

This Work	Literature [173]	
	COF <sub>2</sub>	CO <sub>2</sub>
2349		3349 $\nu_5$
1931	1928 $\nu_1$ (A <sub>1</sub> )	
1246	1249 $\nu_4$ (B <sub>2</sub> )	
967	965 $\nu_2$ (A <sub>1</sub> )	
776	774 $\nu_6$ (B <sub>1</sub> )	
669		667 $\nu_2$
663	626 $\nu_5$ (B <sub>2</sub> )	
	584 $\nu_3$ (A <sub>1</sub> )	



Table 5.38 Infra-red Analysis of the Volatile Products after Reaction between Carbonyl Fluoride and Supported Caesium Fluoride prepared from Aqueous Solution

Solid mmol <sup>-1</sup>	Gas Admitted to infra-red cell		Composition of Gas Products in the Infra-red Cell			
	Torr	mmol	Torr	mmol	Torr	mmol
						CO <sub>2</sub>
						COF <sub>2</sub>
	15.2 ± 0.5	0.044 ± 0.002	3.9 ± 0.2	0.011 ± 0.0006	11.7 ± 0.2	0.0034 ± 0.0006
	17.3 ± 0.5	00.5 ± 0.002	4.4 ± 0.2	0.013 ± 0.0006	12.4 ± 0.2	0.0036 ± 0.0006
4.2	16.3 ± 0.5	0.047 ± 0.002	4.6 ± 0.2	0.013 ± 0.0006	11.8 ± 0.2	0.0034 ± 0.0006
	15.4 ± 0.5	00.44 ± 0.002	3.8 ± 0.2	0.011 ± 0.0006	12.1 ± 0.2	0.0035 ± 0.0006
	14.8 ± 0.5	0.043 ± 0.002	3.4 ± 0.2	0.001 ± 0.0006	11.5 ± 0.2	0.0033 ± 0.0006
	15.6 ± 0.5	00.45 ± 0.002	8.6 ± 0.2	0.025 ± 0.0006	8.1 ± 0.2	0.0023 ± 0.0006
	17.4 ± 0.5	0.05 ± 0.002	8.8 ± 0.2	0.025 ± 0.0006	9.1 ± 0.2	0.0026 ± 0.0006
	16.6 ± 0.5	00.48 ± 0.002	9.5 ± 0.2	0.027 ± 0.0006	8.0 ± 0.2	0.0023 ± 0.0006
8.8	14.6 ± 0.5	00.42 ± 0.002	7.4 ± 0.2	0.021 ± 0.0006	7.4 ± 0.2	0.0021 ± 0.0006
	15.4 ± 0.5	0.044 ± 0.002	7.5 ± 0.2	0.022 ± 0.0006	7.6 ± 0.2	0.0022 ± 0.0006

Table 5.39 Infra-red Analysis of the Volatile Products after Reaction between Carbonyl Fluoride and Supported Potassium Fluoride Prepared from Aqueous Solution

Solid mmolg <sup>-1</sup>	Gas Admitted to infra-red cell		Composition of Gas Products in the Infra-red Cell			
	Torr	mmol	Torr	mmol	Torr	mmol
			COF <sub>2</sub>			
			CO <sub>2</sub>			
	16.3 ± 0.5	0.047 ± 0.002	3.7 ± 0.2	0.011 ± 0.0006	13.1 ± 0.2	0.0038 ± 0.0006
	15.6 ± 0.5	00.45 ± 0.002	2.9 ± 0.2	0.018 ± 0.0006	13.1 ± 0.2	0.0038 ± 0.0006
4.4	17.8 ± 0.5	0.051 ± 0.002	3.4 ± 0.2	0.01 ± 0.0006	14.0 ± 0.2	0.004 ± 0.0006
	14.8 ± 0.5	00.43 ± 0.002	3.0 ± 0.2	0.019 ± 0.0006	12.2 ± 0.2	0.0035 ± 0.0006
	15.2 ± 0.5	0.044 ± 0.002	3.2 ± 0.2	0.009 ± 0.0006	11.7 ± 0.2	0.0034 ± 0.0006
	15.7 ± 0.5	00.45 ± 0.002	6.0 ± 0.2	0.017 ± 0.0006	10.5 ± 0.2	0.003 ± 0.0006
	14.5 ± 0.5	0.042 ± 0.002	4.4 ± 0.2	0.013 ± 0.0006	9.2 ± 0.2	0.0026 ± 0.0006
8.8	15.2 ± 0.5	00.44 ± 0.002	5.4 ± 0.2	0.016 ± 0.0006	10.1 ± 0.2	0.0029 ± 0.0006
	17.4 ± 0.5	00.5 ± 0.002	7.0 ± 0.2	0.02 ± 0.0006	10.0 ± 0.2	0.0029 ± 0.0006
	16.8 ± 0.5	0.048 ± 0.002	5.5 ± 0.2	0.016 ± 0.0006	10.2 ± 0.2	0.0029 ± 0.0006

**Table 5.40 Infra-red Analysis of the Gas Products after Reaction between Carbonyl Fluoride and Supported Metal Fluoride**

Composition of Solid $\text{mmol g}^{-1}$ MF/ $\gamma$ -Alumina	Composition of Gas Products mole %			
	$\text{COF}_2$		$\text{CO}_2$	
	M = Cs	M = K	M = Cs	M = K
2.0	$10 \pm 3$	$8 \pm 2$	$90 \pm 3$	$92 \pm 4$
4.4	$25 \pm 4$	$20 \pm 5$	$75 \pm 6$	$80 \pm 3$
5.0	$28 \pm 6$	$23 \pm 7$	$72 \pm 5$	$77 \pm 8$
5.5	$35 \pm 7$	$29 \pm 6$	$65 \pm 7$	$71 \pm 5$
8.8	$50 \pm 3$	$35 \pm 3$	$50 \pm 4$	$65 \pm 3$
15.0	$67 \pm 6$	$61 \pm 7$	$33 \pm 9$	$39 \pm 8$

fluoride. The uptakes of gas by supported metal fluorides, 4.4 and 8.8 mmolg<sup>-1</sup> were totally dependent upon the initial pressure of carbonyl fluoride in the range 40-300 Torr. The increase in the initial pressure led to an increase in the uptake of gas. The results obtained for supported metal fluoride, 4.4 and 8.8 mmolg<sup>-1</sup> are given in Table 5.41 and shown schematically in Fig. 5.51. The uptake of volatile carbon containing compounds was also dependent on the composition of the solid, in that, the uptake was increased by increasing metal fluoride loading in the range 1.1-5.5 mmolg<sup>-1</sup>, then decreased in the range 5.5-15.0 mmolg<sup>-1</sup>. The results obtained are shown in Fig. 5.52 at an initial pressure of carbonyl fluoride of 300 Torr. Under the same conditions, the interactions involving supported caesium fluoride were greater than those involving supported potassium fluoride.

In each experiment studied, the infra-red spectrum of the supported metal fluoride in the composition range 2.0-10.0 mmolg<sup>-1</sup>, after reaction with carbonyl fluoride showed very strong bands due to trifluoromethoxide (COF<sub>3</sub>)<sup>-</sup> anion, but there was no evidence for other compounds, eg. the CO<sub>2</sub>F<sup>-</sup> anion. The infra-red spectrum of the supported potassium fluoride, 10.0 mmolg<sup>-1</sup> (0.2g) after reaction with carbonyl fluoride (100 Torr) is given in Table 5.42.

#### 5.4.3 REACTIONS OF [<sup>14</sup>C]-CARBON LABELLED CARBONYL FLUORIDE WITH CAESIUM OR POTASSIUM FLUORIDE SUPPORTED ON γ-ALUMINA

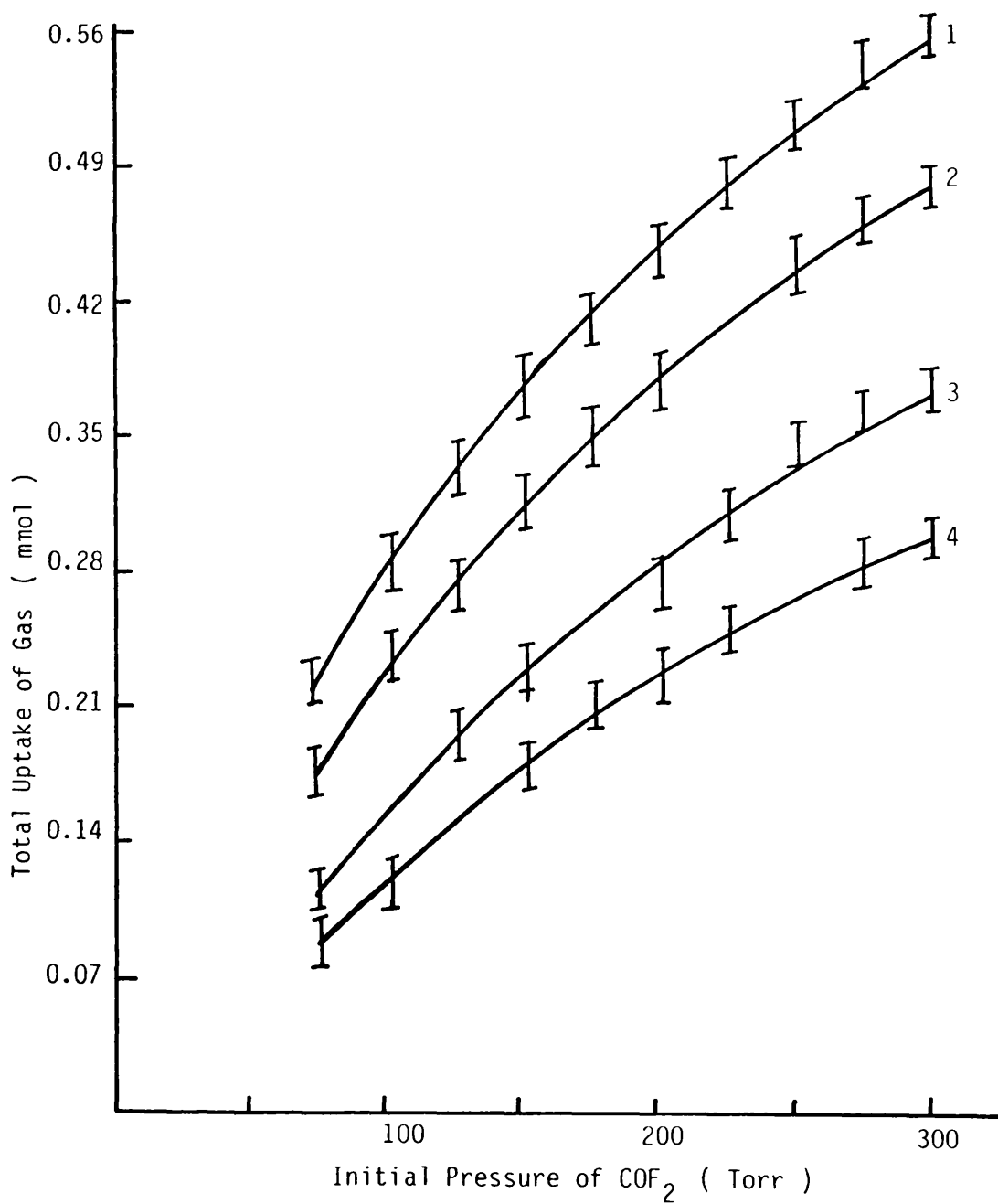
The reaction between [<sup>14</sup>C]-carbon labelled carbonyl fluoride and metal fluorides was studied at different initial pressures in the range 10-300 Torr across the composition range 0.6-20.0

**Table 5.41 Monometric Study of the Uptake of Carbonyl Fluoride by Supported Metal Fluoride**

A (mmol) total uptake  
 B (mmol) retained gas

Initial Pressure Torr	CsF/ $\gamma$ -Alumina				KF/ $\gamma$ -Alumina			
	4.4 mmol g <sup>-1</sup>		8.8 mmol g <sup>-1</sup>		4.4 mmol g <sup>-1</sup>		8.8 mmol g <sup>-1</sup>	
	A	B	A	B	A	B	A	B
40 ± 0.5	0.14 ± 0.002	0.05 ± 0.005	0.10 ± 0.002	0.03 ± 0.003	0.13 ± 0.002	0.04 ± 0.004	0.06 ± 0.01	0.01 ± 0.003
60 ± 0.5	0.20 ± 0.002	0.083 ± 0.005	0.15 ± 0.002	0.04 ± 0.003	0.18 ± 0.002	0.06 ± 0.004	0.01 ± 0.01	0.02 ± 0.003
80 ± 0.5	0.23 ± 0.002	0.13 ± 0.005	0.19 ± 0.002	0.06 ± 0.003	0.21 ± 0.002	0.08 ± 0.004	0.12 ± 0.01	0.03 ± 0.003
120 ± 0.5	0.32 ± 0.002	0.14 ± 0.005	0.25 ± 0.002	0.07 ± 0.003	0.27 ± 0.002	0.10 ± 0.004	0.16 ± 0.01	0.04 ± 0.003
140 ± 0.5	0.35 ± 0.002	0.16 ± 0.005	0.29 ± 0.002	0.09 ± 0.003	0.30 ± 0.002	0.11 ± 0.004	0.18 ± 0.01	0.04 ± 0.003
160 ± 0.5	0.37 ± 0.002	0.18 ± 0.005	0.30 ± 0.002	0.01 ± 0.003	0.32 ± 0.002	0.12 ± 0.004	0.19 ± 0.01	0.05 ± 0.003
220 ± 0.5	0.47 ± 0.002	0.20 ± 0.005	0.34 ± 0.002	0.11 ± 0.003	0.37 ± 0.002	0.14 ± 0.004	0.26 ± 0.01	0.07 ± 0.003
240 ± 0.5	0.48 ± 0.002	0.22 ± 0.005	0.35 ± 0.002	0.11 ± 0.003	0.40 ± 0.002	0.15 ± 0.004	0.27 ± 0.01	0.07 ± 0.003
280 ± 0.5	0.50 ± 0.002	0.23 ± 0.005	0.36 ± 0.002	0.12 ± 0.003	0.41 ± 0.002	0.16 ± 0.004	0.28 ± 0.01	0.07 ± 0.003
300 ± 0.5	0.53 ± 0.002	0.24 ± 0.005	0.37 ± 0.002	0.12 ± 0.003	0.42 ± 0.002	0.16 ± 0.004	0.30 ± 0.01	0.08 ± 0.003

Figure 5.51 Reaction of  $\text{COF}_2$  with  $\text{MF}/\gamma$ -alumina  
 Total Uptake  $\nu$  Initial Pressure



$\text{KF}/\gamma$ -alumina	Composition	$\text{CsF}/\gamma$ -alumina
2	$4.4 \text{ mmol g}^{-1}$	1
4	$8.8 \text{ mmol g}^{-1}$	3

Figure 5.52 Reaction of  $\text{COF}_2$  with  $\text{MF}/\gamma\text{-alumina}$ , Total Uptake  $V$  Composition, Initial Pressure of  $\text{COF}_2 = 300$  torr

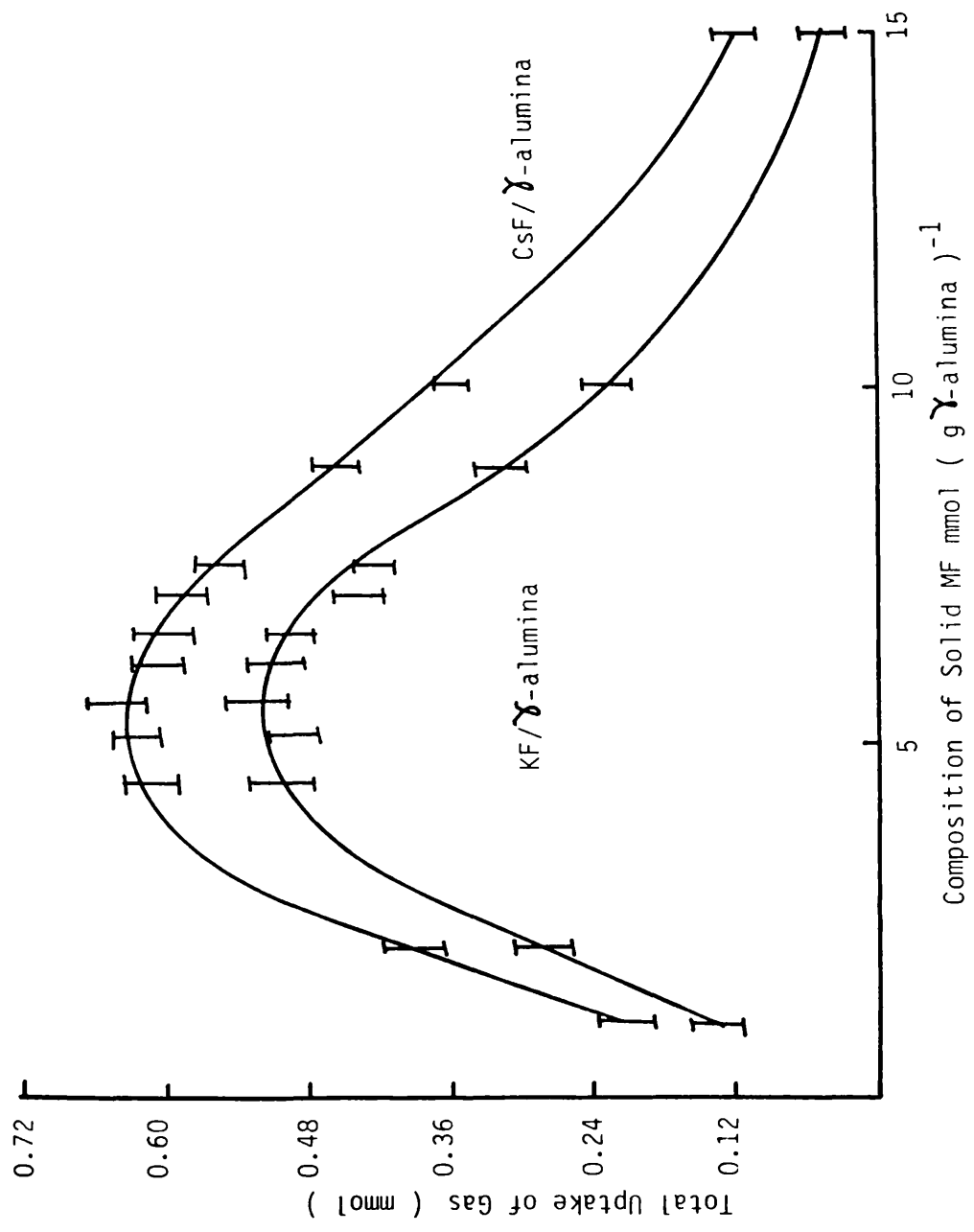


Table 5.42 Infra-Red Spectrum of the Supported Potassium Fluoride after Reaction with Carbonyl Fluoride,  $8.8 \text{ mmol g}^{-1}$

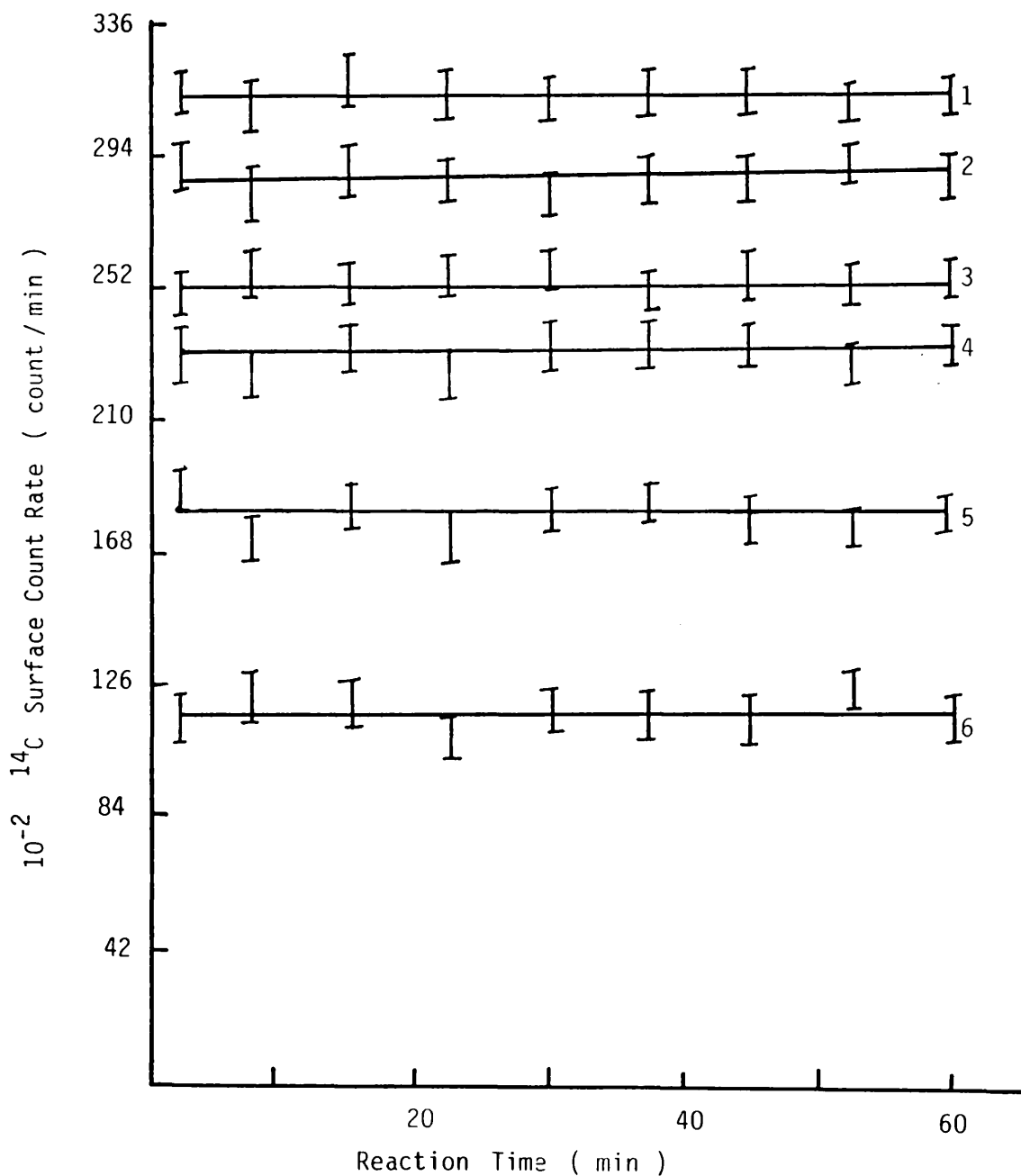
This Work	Literature 41, 47	
	CsCOF <sub>3</sub>	CsCO <sub>2</sub> F
		1749 $\nu_4$ (B <sub>2</sub> ) CO Str
1561	1560 $\nu_1$ (A <sub>1</sub> ) CO Str	
		1316 $\nu_2$ (A <sub>1</sub> ) CO Str
962	960 $\nu_4$ (E) CF <sub>3</sub> assym Str	
		883 $\nu_1$ (A <sub>1</sub> ) CF Str
813	813 $\nu_2$ (A <sub>1</sub> ) CF <sub>3</sub> assym Str	
596	595 $\nu_3$ (A <sub>1</sub> ) CF <sub>3</sub> sym def	
570	574 $\nu_5$ (E) OCF def	
420	423 $\nu_6$ (E) assym CF <sub>3</sub>	



mmolg<sup>-1</sup>. The [<sup>14</sup>C]-carbon surface count rates of the supported metal fluoride, 4.4, 5.5 and 8.8 mmolg<sup>-1</sup> as fraction of time are shown in Figs. 5.53-5.55, using initial pressures of [<sup>14</sup>C]-carbon labelled carbonyl fluoride of 60, 160 and 240 Torr. The surface reaction between [<sup>14</sup>C]-carbon labelled carbonyl fluoride and supported metal fluorides was complete before the first count rate was taken, and the surface count rate remained constant throughout the experiment. When [<sup>14</sup>C]-carbon labelled volatile products were removed from the counting vessel by condensation at 77K, the surface count rate dropped to ca 46-20% of the original surface count rate. This indicated that, ca 54-80% of the [<sup>14</sup>C]-carbon surface count rate was dependent upon there being a pressure of [<sup>14</sup>C]-carbon labelled carbonyl fluoride in the counting vessel with ca 46-20% being permanently retained. The results of these reactions are given in Tables 5.43-5.46 and shown schematically in Figs. 5.56-5.58. The surface count rates and the total uptake of gas were dependent upon the initial pressure of [<sup>14</sup>C]-carbon labelled carbonyl fluoride. Pumping the solid for 3 days under vacuum at room temperature after the removal of the volatile products had no effect on the final surface count rate, but the [<sup>14</sup>C]-carbon surface count rate decreased to background when the solid was heated to 393 under vacuum or was exposed to aliquots of water vapour.

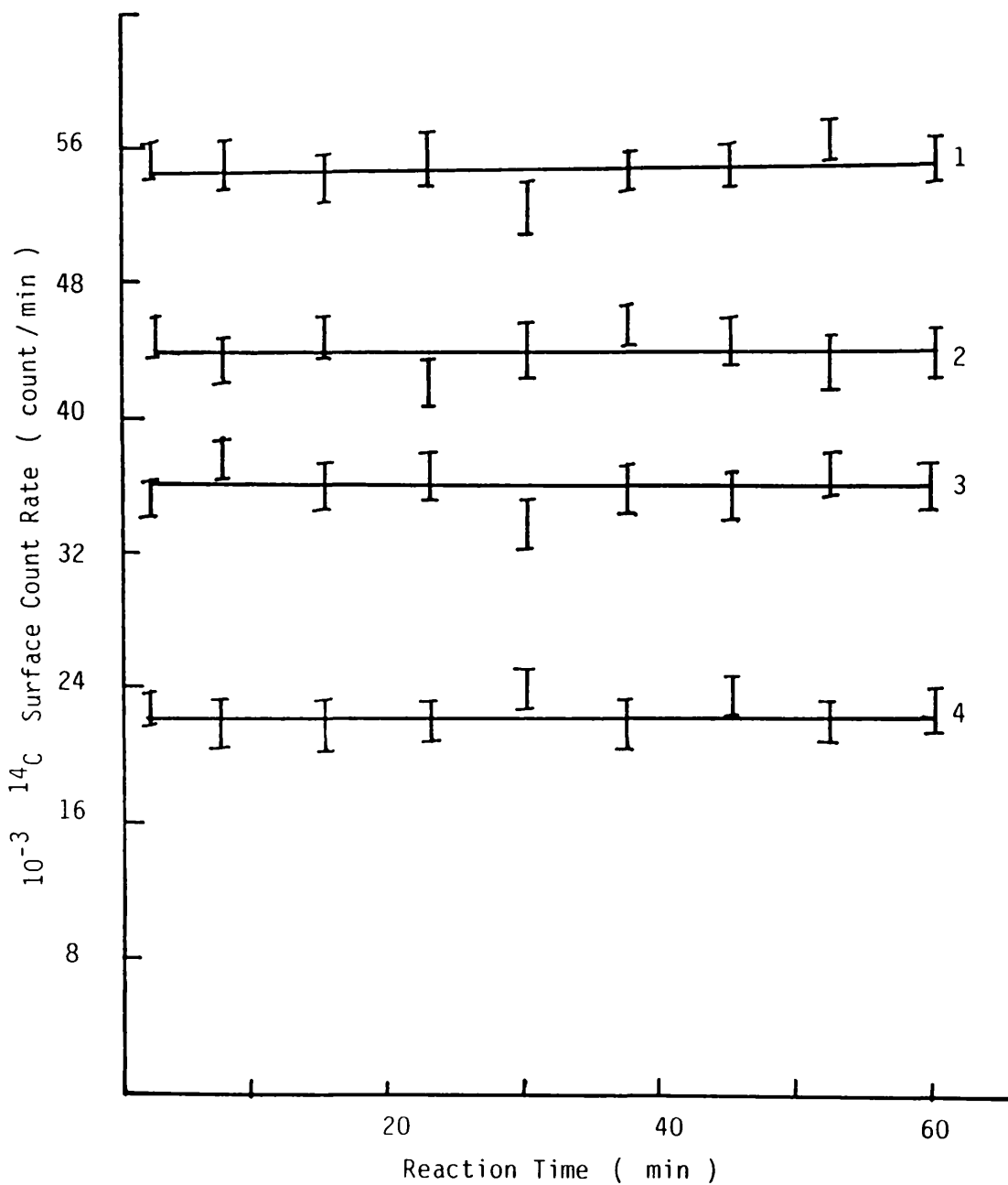
The readmission of [<sup>14</sup>C]-carbon labelled carbonyl fluoride to a sample of supported metal fluoride which had been treated with [<sup>14</sup>C]-carbon labelled carbonyl fluoride resulted in an increase in the surface count rate to its original value during the first admission and the removal of [<sup>14</sup>C]-carbon labelled volatile products at room temperatures decreased the surface

Figure 5.53 Reaction  $^{14}\text{COF}_2$  with MF/ $\gamma$ -alumina  
 Surface Count Rate  $\propto$  Reaction Time  
 Initial Pressure of  $^{14}\text{COF}_2 = 60$  Torr



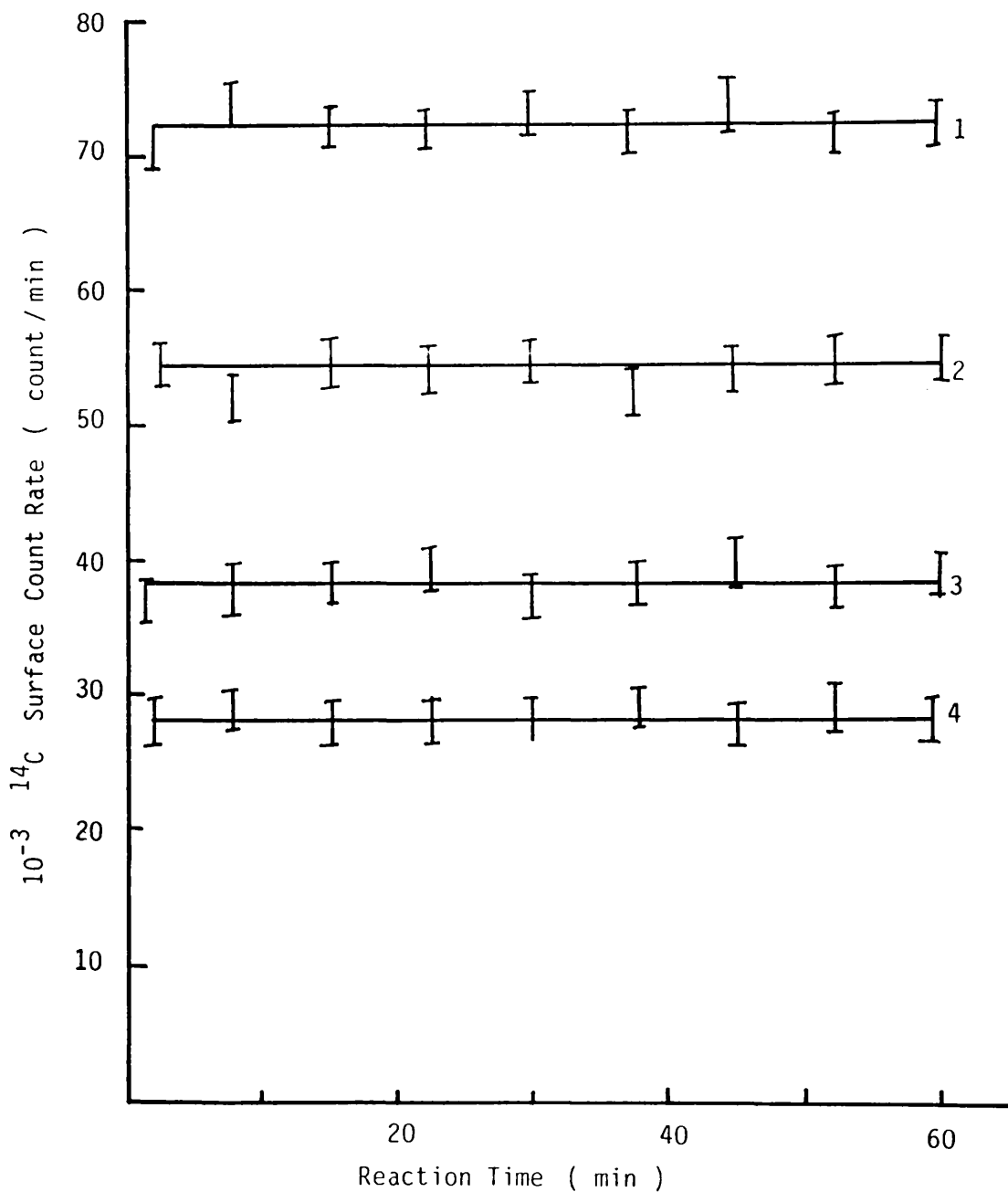
KF/ $\gamma$ -alumina	Composition	CsF/ $\gamma$ -alumina
3	5.5 mmol g <sup>-1</sup>	1
4	4.4 mmol g <sup>-1</sup>	2
6	8.8 mmol g <sup>-1</sup>	5

Figure 5.54 Reaction of  $^{14}\text{COF}_2$  with MF/ $\gamma$ -alumina  
 Surface Count Rate  $\propto$  Reaction Time  
 Initial Pressure of  $^{14}\text{COF}_2$  = 160 Torr



KF/ $\gamma$ -alumina	Composition	CsF/ $\gamma$ -alumina
2	4.4 mmol g <sup>-1</sup>	1
4	8.8 mmol g <sup>-1</sup>	3

Figure 5.55 Reaction of  $^{14}\text{COF}_2$  with MF/ $\gamma$ -alumina  
 Surface Count Rate  $\propto$  Reaction Time  
 Initial Pressure of  $^{14}\text{COF}_2 = 240$  Torr



KF/ $\gamma$ -alumina	Composition	CsF/ $\gamma$ -alumina
2	4.4 mmol g <sup>-1</sup>	1
4	8.8 mmol g <sup>-1</sup>	3

Table 5.43 Results of Reaction between [<sup>14</sup>C]-Carbon Labelled Carbonyl Fluoride with Supported Caesium Fluoride, 4.4 mmolg<sup>-1</sup>

Initial Pressure (Torr)	Total Drop in the Gas Count Rate Count min <sup>-1</sup>	Total Uptake of Gas mmol	Surface Count Rate Count min <sup>-1</sup>	Surface Count Rate after Removal of Gas Count min <sup>-1</sup>
10.2 ± 0.5	1190 ± 103	0.061 ± 0.006	8856 ± 211	4072 ± 153
20.7 ± 0.5	1357 ± 117	0.069 ± 0.006	10082 ± 232	4640 ± 161
40.4 ± 0.5	2713 ± 128	0.14 ± 0.006	20431 ± 261	9288 ± 187
60.7 ± 0.5	3937 ± 137	0.12 ± 0.006	28922 ± 286	13472 ± 221
70.1 ± 0.5	4277 ± 148	0.22 ± 0.006	32030 ± 329	14640 ± 235
80.9 ± 0.5	4772 ± 156	0.24 ± 0.006	35753 ± 341	16328 ± 361
90.7 ± 0.5	5113 ± 173	0.26 ± 0.006	37553 ± 373	17496 ± 301
120.6 ± 0.5	6259 ± 181	0.32 ± 0.006	46709 ± 391	21416 ± 333
140.5 ± 0.5	6677 ± 193	0.34 ± 0.006	49029 ± 431	22848 ± 354
150.6 ± 0.5	7303 ± 229	0.37 ± 0.006	54715 ± 452	24992 ± 384
160.8 ± 0.5	7589 ± 247	0.38 ± 0.006	54561 ± 499	25976 ± 421
170.9 ± 0.5	7904 ± 299	0.40 ± 0.006	59139 ± 527	27056 ± 457
180.3 ± 0.5	8243 ± 352	0.42 ± 0.006	62095 ± 543	28208 ± 483
200.7 ± 0.5	8601 ± 401	0.43 ± 0.006	64087 ± 589	29456 ± 517
220.2 ± 0.5	9025 ± 456	0.46 ± 0.006	67058 ± 654	30840 ± 547
240.8 ± 0.5	9545 ± 484	0.48 ± 0.006	71246 ± 696	32664 ± 566
260.8 ± 0.5	9807 ± 543	0.49 ± 0.006	73201 ± 773	33560 ± 593
280.8 ± 0.5	10120 ± 591	0.51 ± 0.006	74308 ± 881	34632 ± 671
300.3 ± 0.5	10433 ± 673	0.53 ± 0.006	77719 ± 997	35704 ± 717

Sample Weight 0.5g, 1.32 mmol of CsF.

**Table 5.44 Results of Reaction between [<sup>14</sup>C]-Carbon Labelled Carbonyl Fluoride with Supported Caesium Fluoride, 8.8 mmol g<sup>-1</sup>**

Initial Pressure (Torr)	Total Drop in the Gas Count Rate Count min <sup>-1</sup>	Total Uptake of Gas mmol	Surface Count Rate Count min <sup>-1</sup>	Surface Count Rate after Removal of Gas Count min <sup>-1</sup>
10.3 ± 0.5	437 ± 84	0.037 ± 0.006	3936 ± 153	1140 ± 67
20.9 ± 0.5	1451 ± 103	0.013 ± 0.006	7790 ± 181	2298 ± 74
30.6 ± 0.5	2047 ± 106	0.10 ± 0.006	11392 ± 209	3210 ± 89
40.5 ± 0.5	2530 ± 111	0.13 ± 0.006	13812 ± 229	4008 ± 97
60.8 ± 0.5	3307 ± 112	0.17 ± 0.006	18147 ± 245	5244 ± 104
70.7 ± 0.5	3574 ± 117	0.18 ± 0.006	19518 ± 273	5658 ± 119
80.3 ± 0.5	3813 ± 129	0.19 ± 0.006	21186 ± 296	6132 ± 123
100.9 ± 0.5	4542 ± 133	0.23 ± 0.006	24753 ± 313	7188 ± 147
120.0 ± 0.5	5025 ± 141	0.25 ± 0.006	26967 ± 329	7818 ± 163
140.3 ± 0.5	5585 ± 173	0.28 ± 0.006	30603 ± 333	8844 ± 179
160.6 ± 0.5	6031 ± 197	0.30 ± 0.006	32928 ± 372	9408 ± 217
180.0 ± 0.5	6328 ± 227	0.32 ± 0.006	34611 ± 391	9948 ± 247
200.7 ± 0.5	6526 ± 247	0.33 ± 0.006	35634 ± 431	10188 ± 296
220.9 ± 0.5	6813 ± 263	0.34 ± 0.006	37756 ± 462	10188 ± 331
240.5 ± 0.5	6962 ± 301	0.35 ± 0.006	38675 ± 489	10806 ± 356
260.8 ± 0.5	7186 ± 347	0.36 ± 0.006	39399 ± 519	11376 ± 398
280.8 ± 0.5	7334 ± 385	0.37 ± 0.006	40171 ± 543	11538 ± 441
300.7 ± 0.5	7447 ± 445	0.38 ± 0.006	41259 ± 597	11790 ± 493

Sample Weight 0.5g, 1.88 mmol of CsF.

**Table 5.45 Results of Reaction between [<sup>14</sup>C]-Carbon Labelled Carbonyl Fluoride with Supported Potassium Fluoride, 4.4 mmol g<sup>-1</sup>**

Initial Pressure (Torr)	Total Drop in the Gas Count Rate Count min <sup>-1</sup>	Total Uptake of Gas mmol	Surface Count Rate Count min <sup>-1</sup>	Surface Count Rate after Removal of Gas Count min <sup>-1</sup>
10.7 ± 0.5	1079 ± 101	0.053 ± 0.006	6603 ± 184	2380 ± 103
20.3 ± 0.5	1584 ± 115	0.08 ± 0.006	9982 ± 210	3591 ± 113
40.6 ± 0.5	2713 ± 123	0.14 ± 0.006	18011 ± 229	6496 ± 129
60.8 ± 0.5	3564 ± 131	0.18 ± 0.006	23353 ± 253	8533 ± 152
80.7 ± 0.5	4356 ± 143	0.22 ± 0.006	29032 ± 274	10430 ± 186
100.4 ± 0.5	4772 ± 151	0.24 ± 0.006	32175 ± 307	11424 ± 228
120.5 ± 0.5	5544 ± 167	0.28 ± 0.006	36764 ± 331	13272 ± 243
140.6 ± 0.5	5861 ± 173	0.30 ± 0.006	38969 ± 357	14028 ± 274
160.3 ± 0.5	6534 ± 184	0.33 ± 0.006	43362 ± 372	15645 ± 321
180.8 ± 0.5	6732 ± 199	0.34 ± 0.006	44695 ± 399	16114 ± 343
200.3 ± 0.5	7128 ± 211	0.36 ± 0.006	47404 ± 432	17066 ± 386
220.7 ± 0.5	7524 ± 229	0.38 ± 0.006	49949 ± 457	18011 ± 439
240.8 ± 0.5	7781 ± 241	0.39 ± 0.006	51670 ± 503	18627 ± 463
260.4 ± 0.5	8039 ± 247	0.40 ± 0.006	53093 ± 596	19243 ± 496
280.9 ± 0.5	8177 ± 352	0.41 ± 0.006	54227 ± 652	19579 ± 527
300.7 ± 0.5	8356 ± 417	0.42 ± 0.006	55573 ± 759	20006 ± 572

Sample Weight 0.38g, 1.32 mmol of KF.

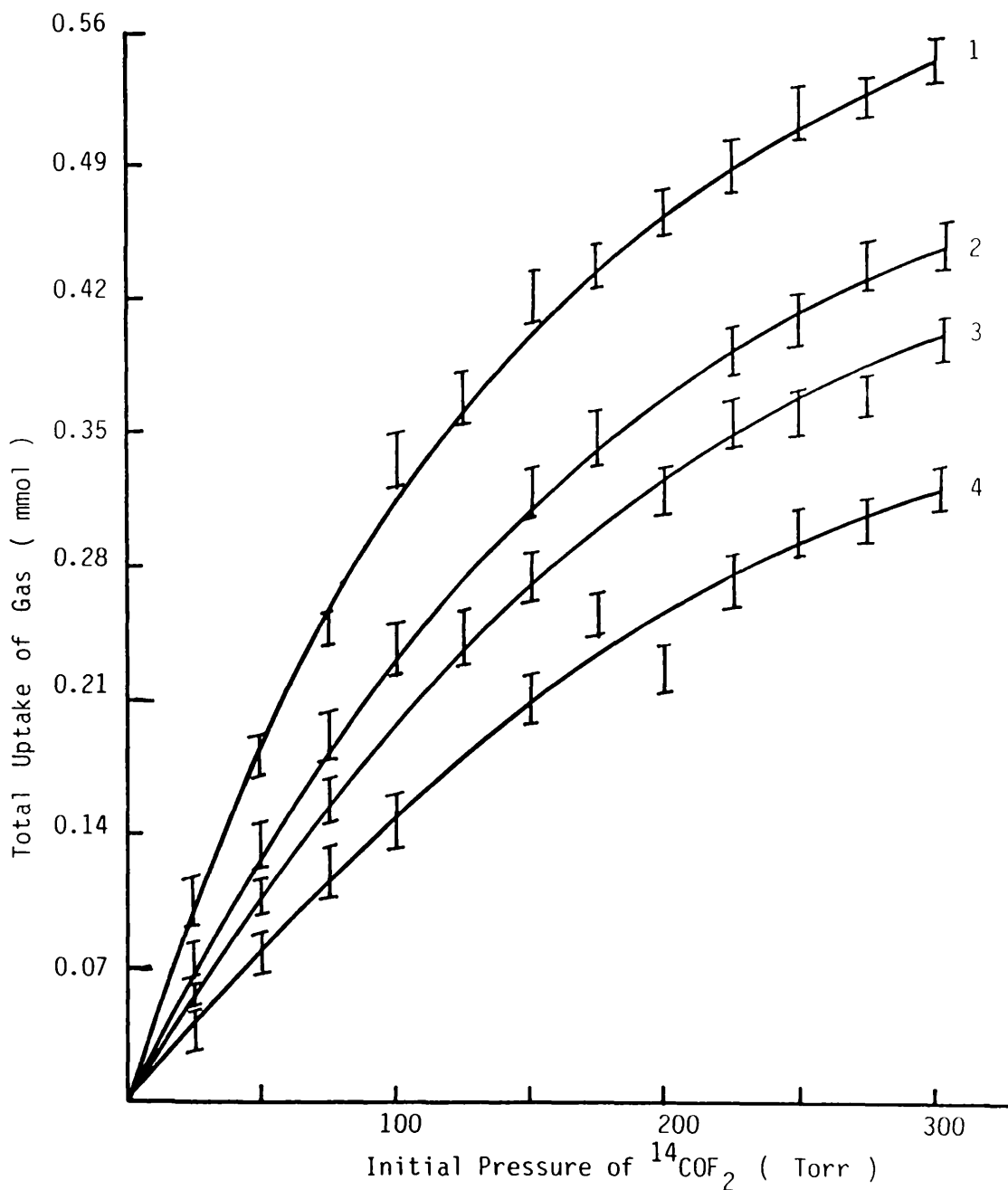
Table 5.46 Results of Reaction between [<sup>14</sup>C]-Carbon Labelled Carbonyl Fluoride with Supported Potassium Fluoride, 8.8 mmol g<sup>-1</sup>

Initial Pressure (Torr)	Total Drop in the Gas Count Rate Count min <sup>-1</sup>	Total Uptake of Gas mmol	Surface Count Rate Count min <sup>-1</sup>	Surface Count Rate after Removal of Gas Count min <sup>-1</sup>
10.6 ± 0.5	455 ± 64	0.023 ± 0.006	2165 ± 103	540 ± 53
20.3 ± 0.5	752 ± 93	0.038 ± 0.006	3586 ± 118	895 ± 69
40.7 ± 0.5	1287 ± 103	0.065 ± 0.006	6102 ± 129	1530 ± 74
60.4 ± 0.5	2020 ± 128	0.10 ± 0.006	9597 ± 143	2400 ± 83
80.1 ± 0.5	2376 ± 142	0.12 ± 0.006	11506 ± 173	2820 ± 97
100.4 ± 0.5	3128 ± 169	0.16 ± 0.006	15336 ± 196	3715 ± 104
120.5 ± 0.5	3208 ± 189	0.17 ± 0.006	15596 ± 216	3795 ± 113
140.5 ± 0.5	3722 ± 216	0.19 ± 0.006	17615 ± 223	4420 ± 127
160.7 ± 0.5	3960 ± 238	0.20 ± 0.006	18877 ± 244	4700 ± 143
180.8 ± 0.5	4554 ± 253	0.23 ± 0.006	21579 ± 260	5410 ± 159
200.0 ± 0.5	4752 ± 282	0.24 ± 0.006	22105 ± 289	5645 ± 193
220.7 ± 0.5	5089 ± 333	0.26 ± 0.006	24361 ± 331	6045 ± 240
240.1 ± 0.5	5177 ± 357	0.27 ± 0.006	24839 ± 343	6185 ± 289
260.9 ± 0.5	5544 ± 374	0.28 ± 0.006	26230 ± 397	6585 ± 317
280.3 ± 0.5	5742 ± 437	0.29 ± 0.006	27813 ± 443	6820 ± 353
300.7 ± 0.5	5999 ± 479	0.30 ± 0.006	28495 ± 487	7125 ± 381

Sample Weight 0.32g, 1.88 mmol of KF.



Figure 5.56 Reaction of  $^{14}\text{COF}_2$  with MF/ $\gamma$ -alumina  
 Total Uptake  $\bar{V}$  Initial Pressure of  $^{14}\text{COF}_2$

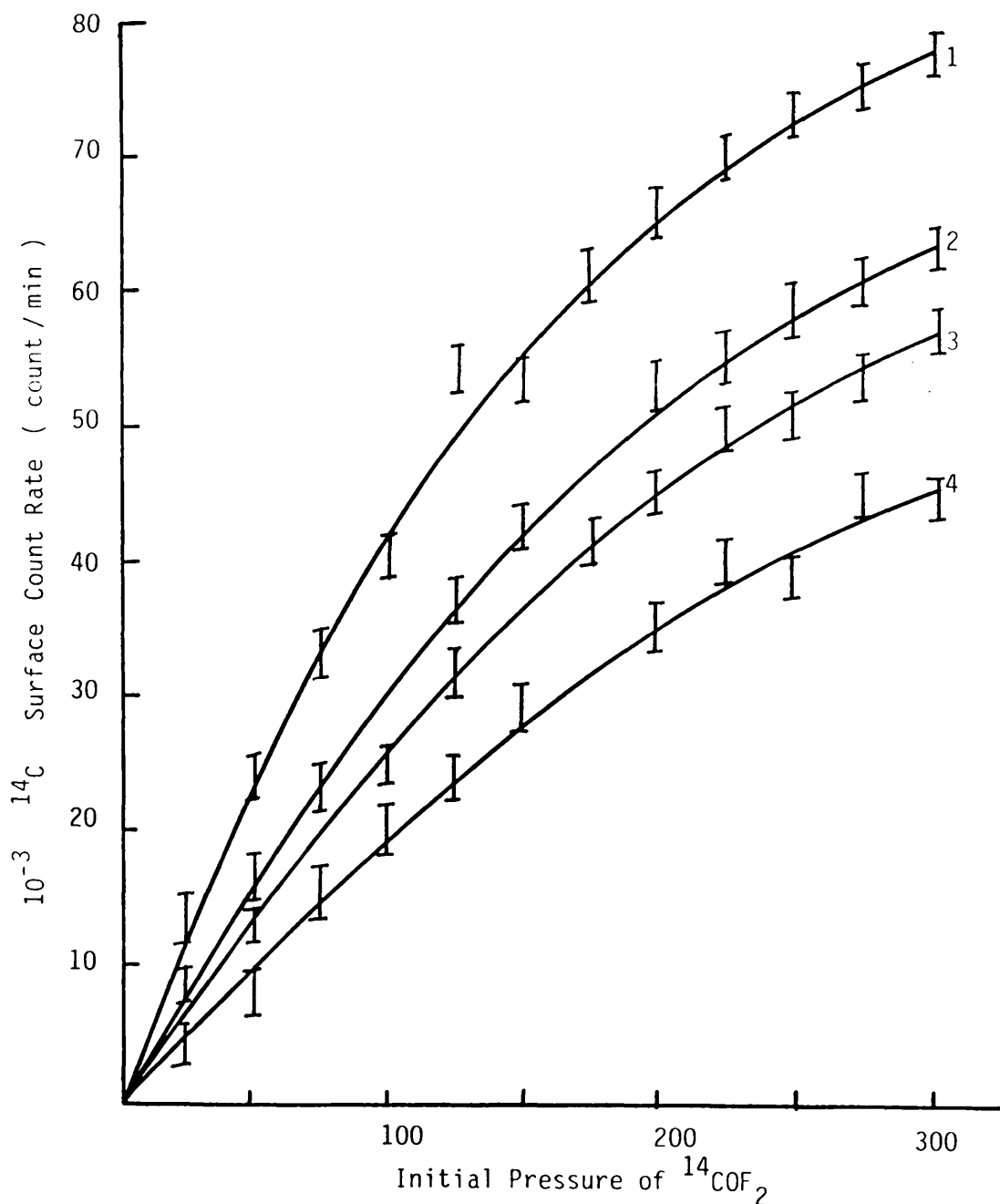


KF/ $\gamma$ -alumina	Composition	CsF/ $\gamma$ -alumina
2	4.4 mmol g <sup>-1</sup>	1
4	8.8 mmol g <sup>-1</sup>	3

Figure 5.57

Reaction of  $^{14}\text{COF}_2$  with MF/ $\gamma$ -alumina

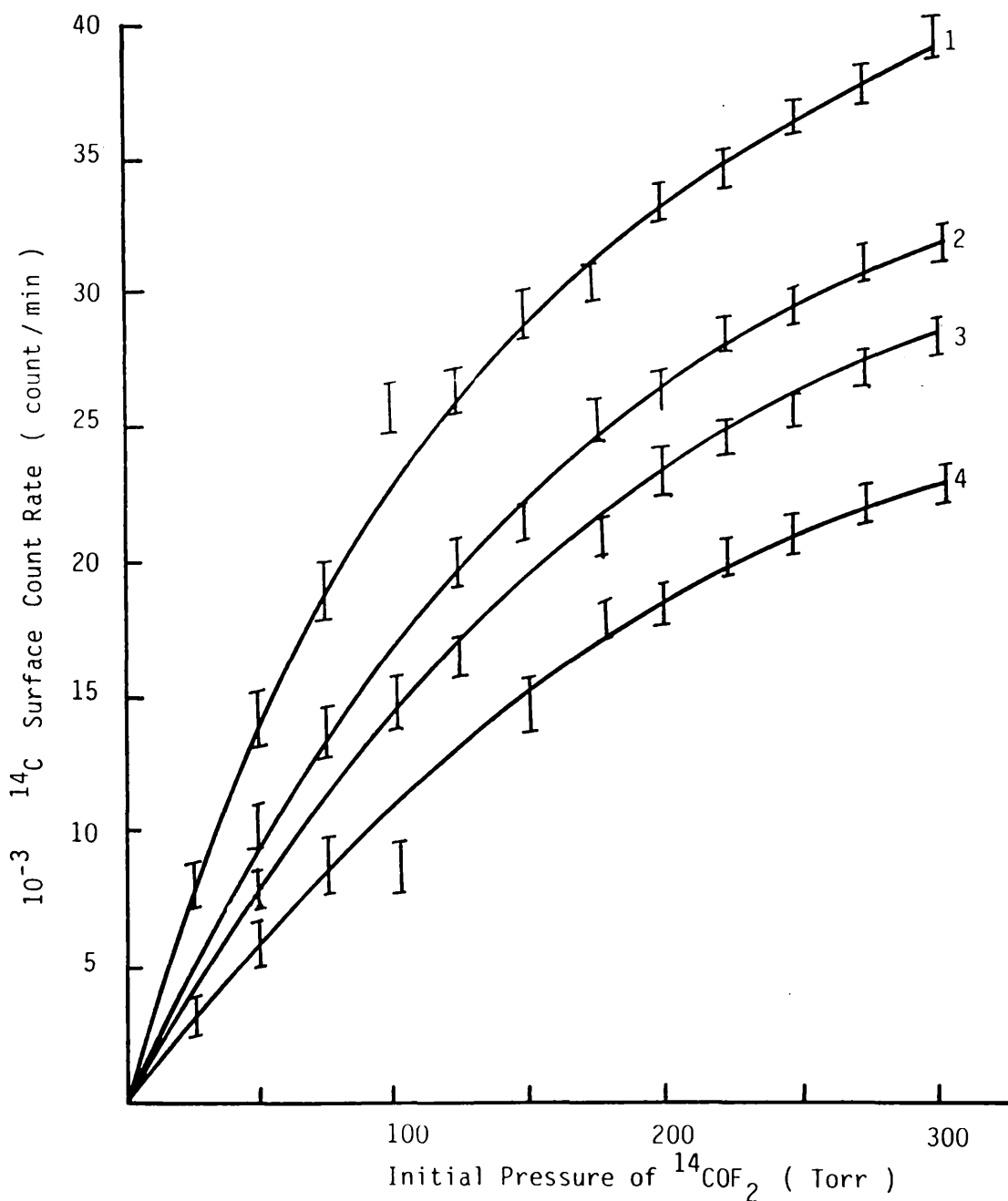
Surface Count Rate  $\nu$  Initial Pressure of  $^{14}\text{COF}_2$



KF/ $\gamma$ -alumina	Composition	CsF/ $\gamma$ -alumina
2	$4.4 \text{ mmol g}^{-1}$	1
4	$8.8 \text{ mmol g}^{-1}$	3

Figure 5.58

Reaction of  $^{14}\text{COF}_2$  with MF/ $\gamma$ -alumina  
 Surface Count Rate after Removal of Gas  $\sqrt$  Initial Pressure



KF/ $\gamma$ -alumina	Composition	CsF/ $\gamma$ -alumina
2	$4.4 \text{ mmol g}^{-1}$	1
4	$8.8 \text{ mmol g}^{-1}$	3

count rate to its original level. Further adsorption/desorption cycles had no effect in the surface count rates.

The [ $^{14}\text{C}$ ]-carbon surface count rate varied with the composition of the supported metal fluoride as shown in Fig. 5.59, and was at a maximum for a given pressure at  $5.5 \text{ mmol g}^{-1}$ . The surface count rate of the supported metal fluoride,  $20.0 \text{ mmol g}^{-1}$  after the removal of the gas phase at room temperature was equivalent to background.

#### 5.4.4 REACTIONS OF [ $^{14}\text{C}$ ]-CARBON LABELLED CARBON DIOXIDE WITH CAESIUM OR POTASSIUM FLUORIDE SUPPORTED ON $\gamma$ -ALUMINA

The reaction between [ $^{14}\text{C}$ ]-carbon labelled carbon dioxide and supported metal fluorides,  $4.4$  and  $8.8 \text{ mmol g}^{-1}$  was studied at different initial pressures in the range 10-300 torr. Plots of the [ $^{14}\text{C}$ ]-carbon surface count rate of the supported metal fluoride,  $4.4$  and  $8.8 \text{ mmol g}^{-1}$  are shown in Figs. 5.60-5.62, using initial pressures of [ $^{14}\text{C}$ ]-carbon labelled carbon dioxide of 60, 160 and 240 Torr. For each pressure studied, the surface count rate was constant throughout the experiment. On removal of [ $^{14}\text{C}$ ]-carbon labelled carbon dioxide from the counting cell, there was a very small surface count rate remaining. This clearly indicated that ca 94-96% of the [ $^{14}\text{C}$ ]-carbon surface count rate was dependent on there being a pressure of

carbon dioxide in the counting vessel with ca 6-4% being permanently retained. The results obtained are shown in Fig. 5.63. The surface count rate in the presence of gas and the total uptake of gas by the supported metal fluoride were dependent on the initial pressure of [ $^{14}\text{C}$ ]-carbon labelled carbon

Figure 5.59 Reaction of  $^{14}\text{COF}_2$  with MF/ $\gamma$ -alumina, Surface Count Rate V Composition, Initial Pressure = 300 Torr

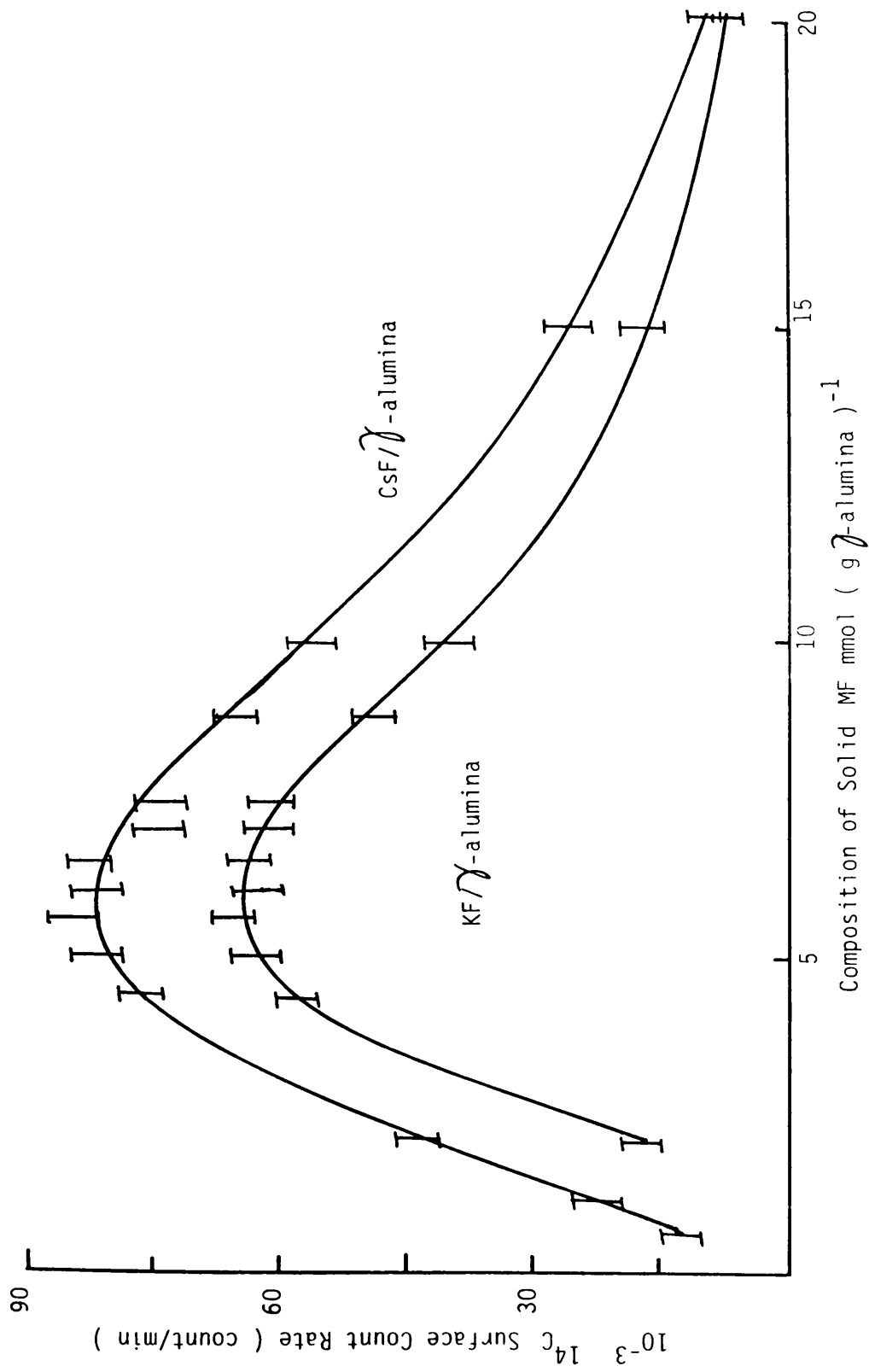
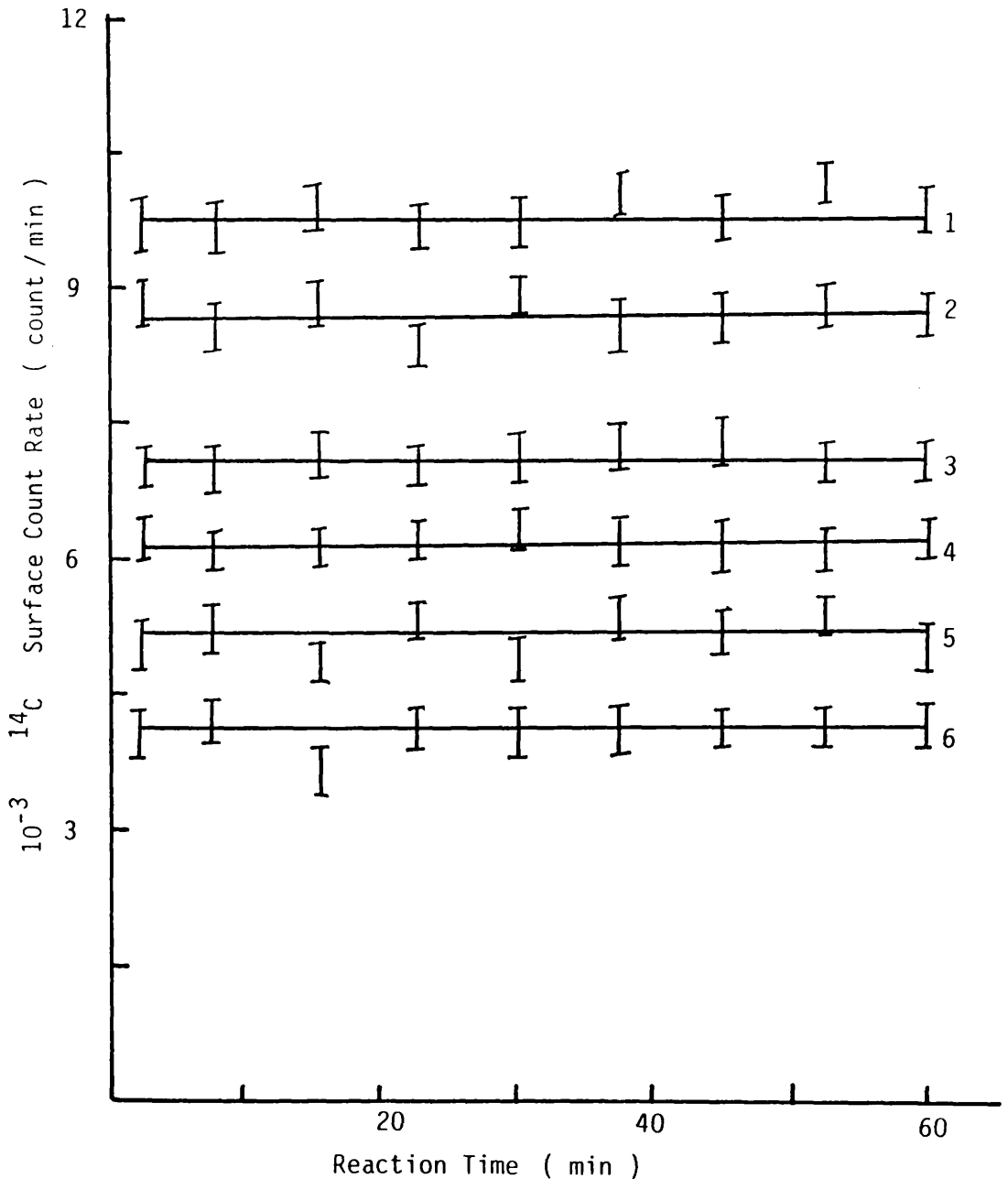
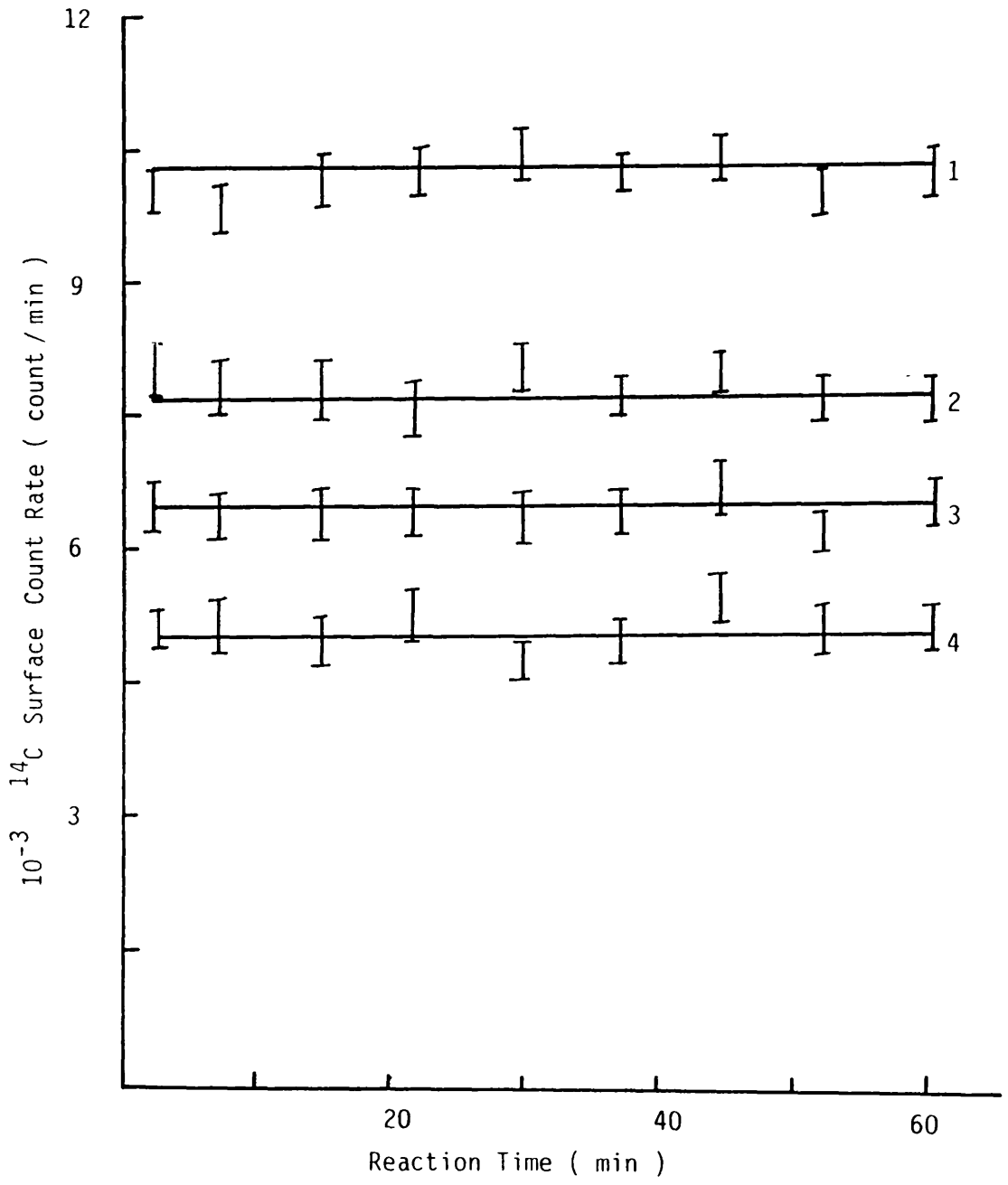


Figure 5.60 Reaction of  $^{14}\text{CO}_2$  with MF/ $\gamma$ -alumina  
 Surface Count Rate  $\propto$  Reaction Time  
 Initial Pressure of  $^{14}\text{CO}_2 = 60$  Torr



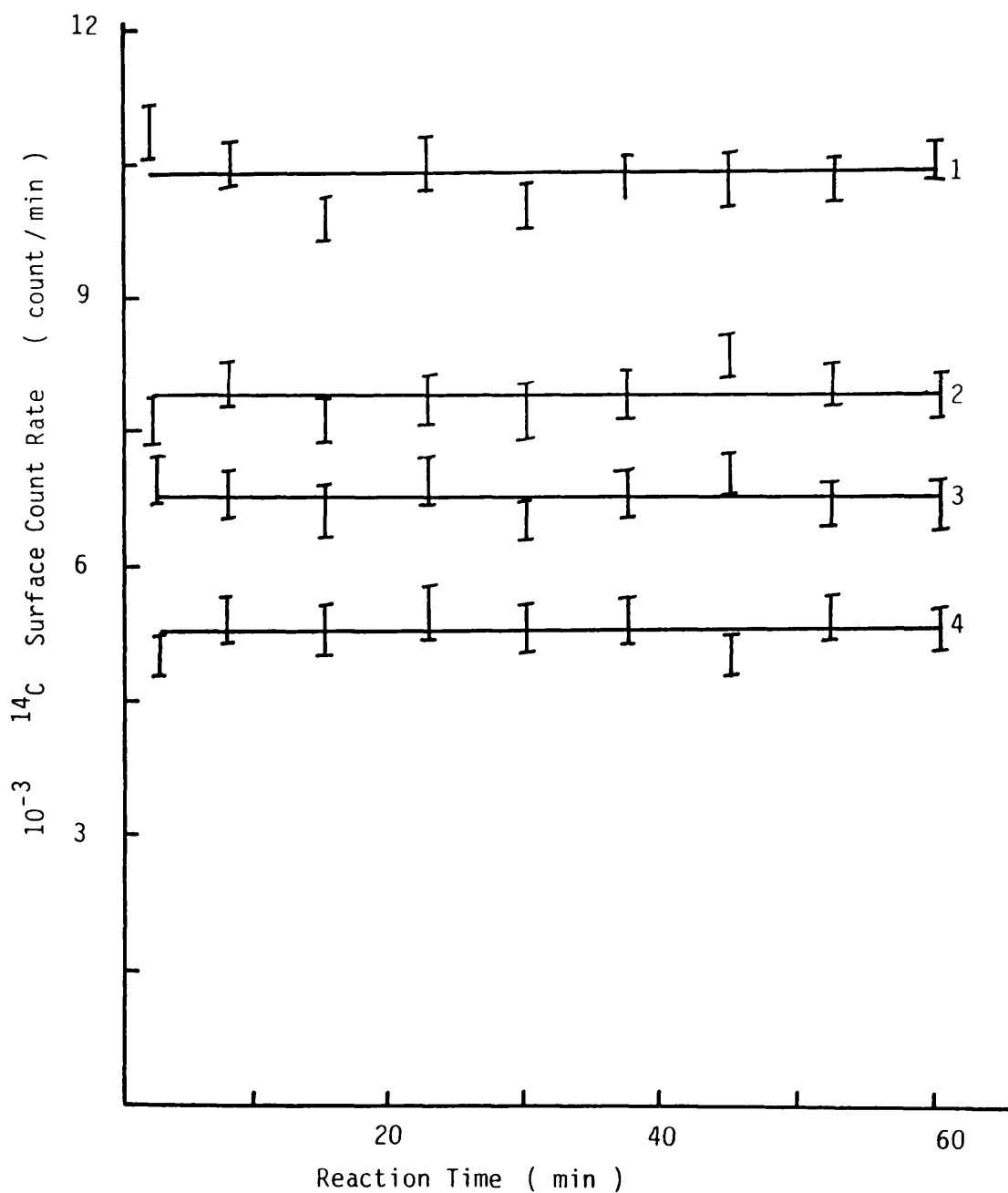
KF/ $\gamma$ -alumina	Composition	CsF/ $\gamma$ -alumina
3	5.5 mmol g <sup>-1</sup>	1
4	4.4 mmol g <sup>-1</sup>	2
6	8.8 mmol g <sup>-1</sup>	5

Figure 5.61 Reaction of  $^{14}\text{CO}_2$  with MF/ $\gamma$ -alumina  
 Surface Count Rate  $\propto$  Reaction Time  
 Initial Pressure of  $^{14}\text{CO}_2 = 160$  Torr



KF/ $\gamma$ -alumina	Composition	CsF/ $\gamma$ -alumina
2	$4.4 \text{ mmol g}^{-1}$	1
4	$8.8 \text{ mmol g}^{-1}$	3

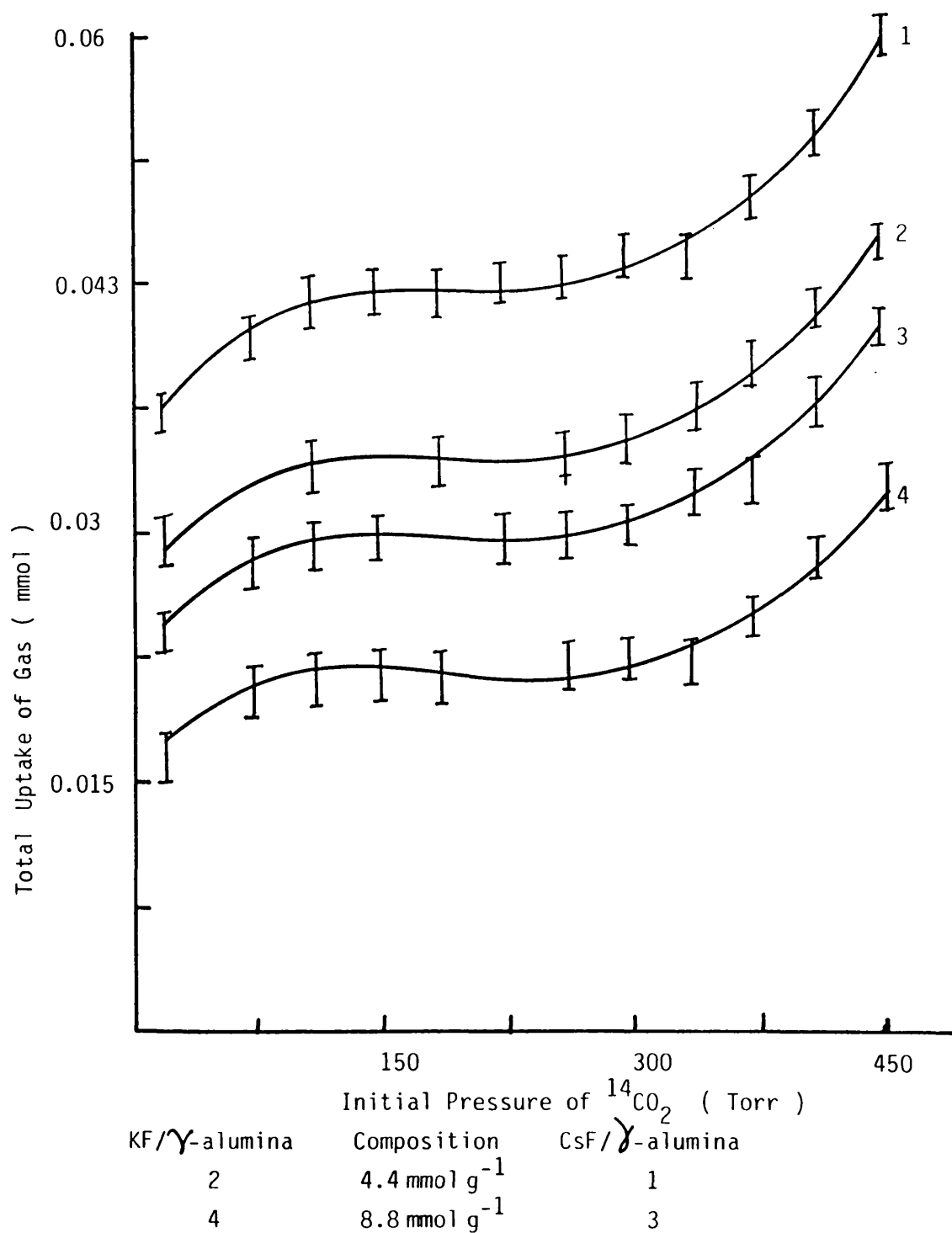
Figure 5.62 Reaction of  $^{14}\text{CO}_2$  with MF/ $\gamma$ -alumina  
 Surface Count Rate  $\nu$  Reaction Time  
 Initial Pressure of  $^{14}\text{CO}_2 = 240$  Torr



KF/ $\gamma$ -alumina	Composition	CsF/ $\gamma$ -alumina
2	$4.4 \text{ mmol g}^{-1}$	1
4	$8.8 \text{ mmol g}^{-1}$	3



Figure 5.63 Reaction of  $^{14}\text{CO}_2$  with MF/ $\gamma$ -alumina  
 Total Uptake  $\bar{V}$  Initial Pressure of  $^{14}\text{CO}_2$



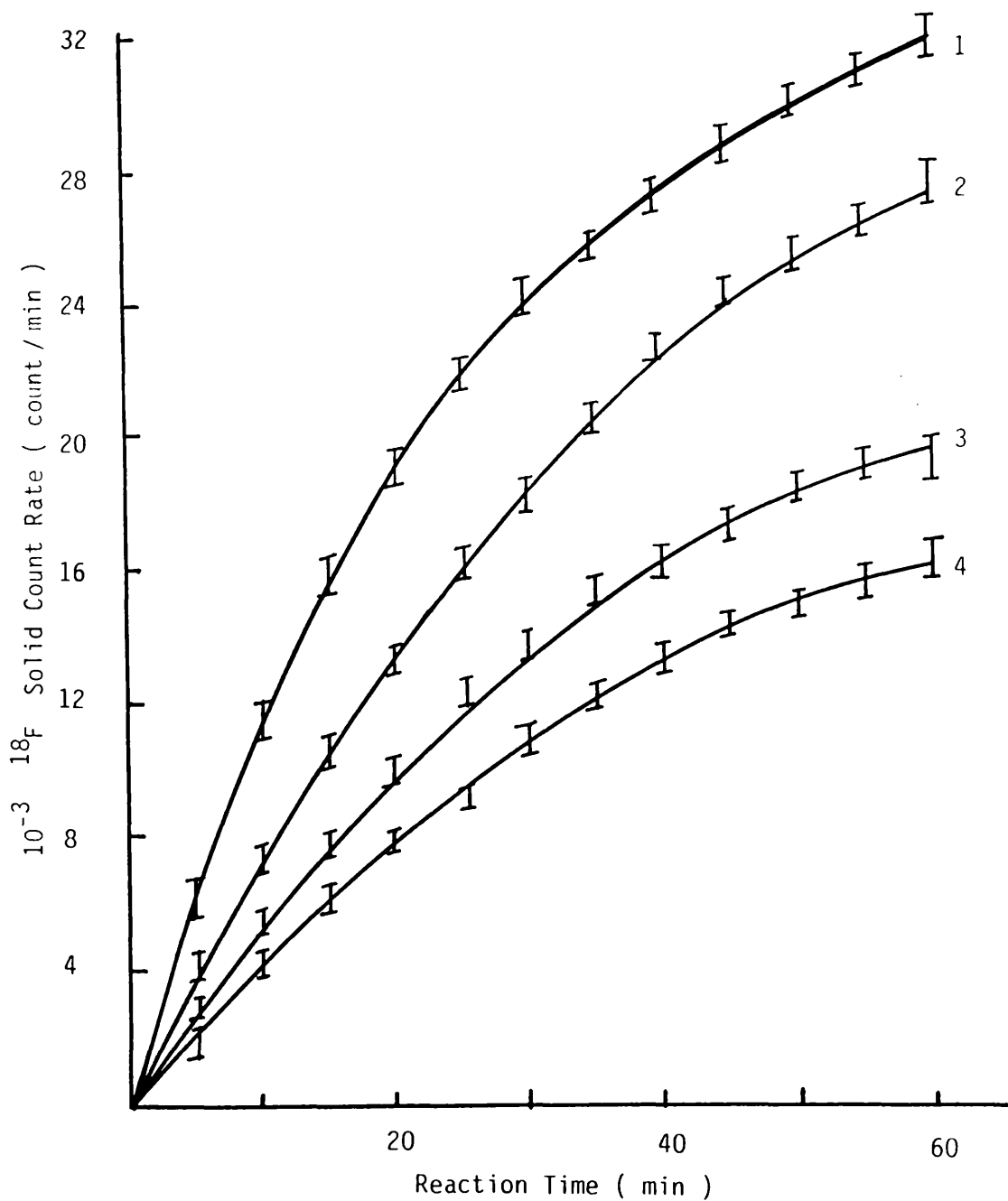
dioxide, but the [ $^{14}\text{C}$ ]-carbon surface count rate after the removal of gas at room temperature was independent of the initial pressure. Pumping the solid for 5 days under vacuum at room temperature after the removal of [ $^{14}\text{C}$ ]-carbon labelled carbon dioxide had no effect in the final count rate, but the [ $^{14}\text{C}$ ]-carbon surface count rate decreased to background when the solid was heated to 393K under vacuum, or was exposed to aliquots of water vapour.

The infra-red spectrum of the solid after reaction with carbon dioxide did not reveal any bands due to the addition of fluoride ions to carbon dioxide.

#### 5.4.5 REACTIONS OF [ $^{18}\text{F}$ ]-FLUORINE LABELLED CARBONYL FLUORIDE WITH CAESIUM OR POTASSIUM FLUORIDE SUPPORTED ON $\gamma$ -ALUMINA

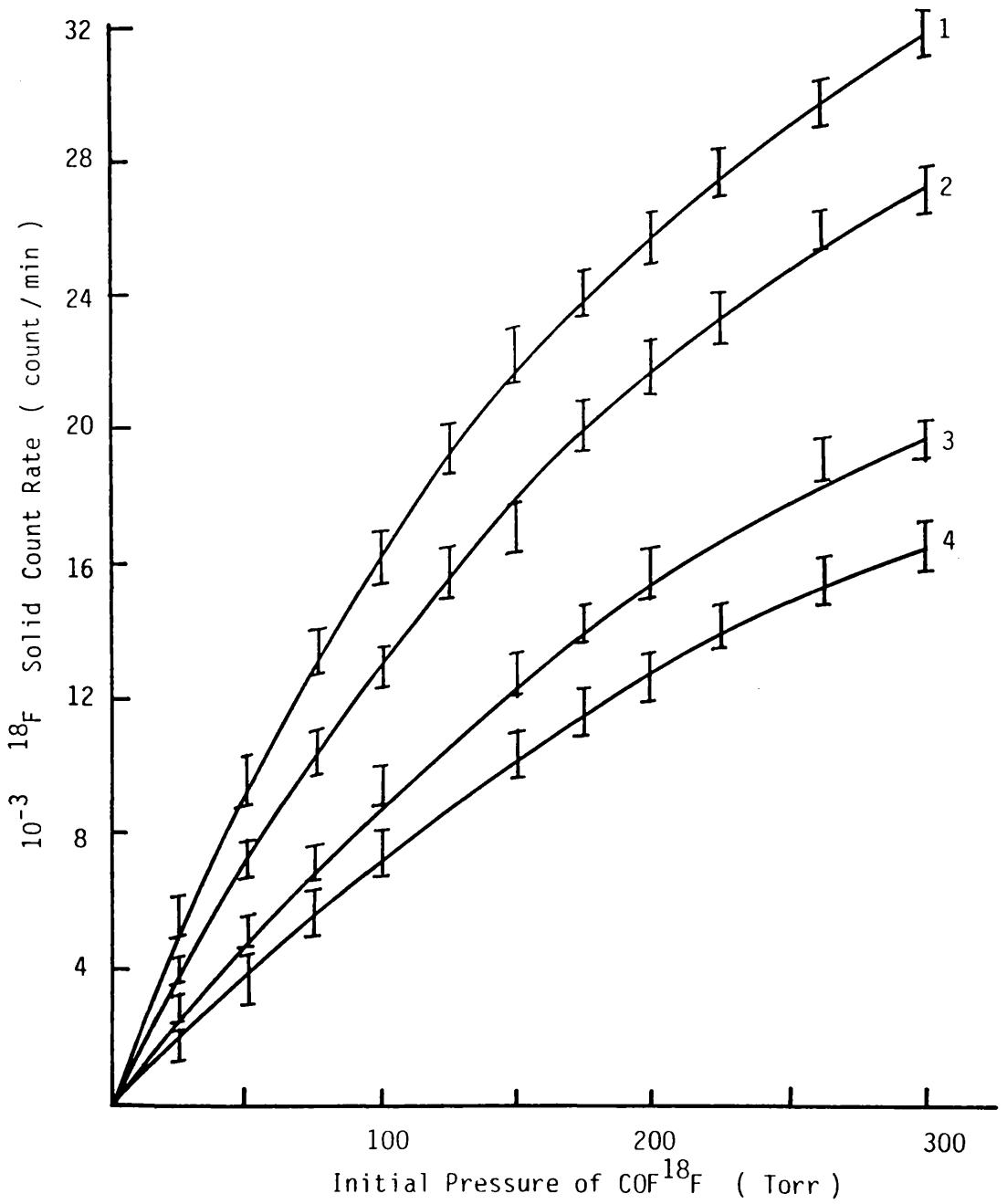
The admission of [ $^{18}\text{F}$ ]-fluorine labelled carbonyl fluoride to a sample of supported metal fluoride, led to a rapid initial increase in the solid count rate over the first 30 min, followed by a second period in which the growth was much slower. The [ $^{18}\text{F}$ ]-fluorine solid count rates of the supported metal fluoride, 4.4 and 8.8  $\text{mmol g}^{-1}$  are shown in Fig. 5.64. The removal of the volatile products at room temperature from the counting vessel resulted in a very small decrease in the final solid count rate. The solid count rate was dependent on the initial pressure of [ $^{18}\text{F}$ ]-fluorine labelled carbonyl fluoride in the range 50-580 Torr, in that, the increase in the initial pressure led to an increase in the solid count rate. The results obtained for the supported metal fluoride, 4.4 and 8.8  $\text{mmol g}^{-1}$  are shown in Fig. 5.65. The [ $^{18}\text{F}$ ]-fluorine solid count rate was also dependent on the composition of the solid in the range 0.6-20.0  $\text{mmol g}^{-1}$ . The

Figure 5.64 Reaction of  $\text{COF}^{18}\text{F}$  with  $\text{MF}/\gamma$ -alumina  
 Solid Count Rate  $\propto$  Reaction Time  
 Initial Pressure of  $\text{COF}^{18}\text{F}$  = 300 Torr



$\text{KF}/\gamma$ -alumina	Composition	$\text{CsF}/\gamma$ -alumina
1	$4.4 \text{ mmol g}^{-1}$	2
3	$8.8 \text{ mmol g}^{-1}$	4

Figure 5.65 Reaction of  $\text{COF}^{18}\text{F}$  with  $\text{MF}/\gamma\text{-alumina}$   
 Solid Count Rate  $\propto$  Initial Pressure of  $\text{COF}^{18}\text{F}$



KF/ $\gamma$ -alumina	Composition	CsF/ $\gamma$ -alumina
1	$4.4 \text{ mmol g}^{-1}$	2
3	$8.8 \text{ mmol g}^{-1}$	4

increase in metal fluoride loading resulted in a decrease in the [ $^{18}\text{F}$ ]-fluorine surface count rate. The results obtained are shown in Fig. 5.66. When inactive carbonyl fluoride was admitted to a sample of supported metal fluoride which had been exposed to [ $^{18}\text{F}$ ]-fluorine labelled carbonyl fluoride, a decrease in the solid count rate was observed. The results obtained for the 4.4 and 8.8  $\text{mmol g}^{-1}$  samples are summarised in Table 5.47. Estimation of the specific count rate of [ $^{18}\text{F}$ ]-fluorine labelled carbonyl fluoride before and after reaction using the same method described in section 5.3.12, showed that, the specific count rate of [ $^{18}\text{F}$ ]-fluorine labelled carbonyl fluoride after reaction had decreased. The data obtained were treated as described in section 5.3.13 and an example is given for the system;

$\text{COF}^{18}\text{F}$  (1.0 mmol) + CsF/ $\gamma$ -alumina, 4.4  $\text{mmol g}^{-1}$  0.5 = 1.32 mmol  
Initial specific count rate of  $\text{COF}^{18}\text{F}$  =  $14598 \pm 133 \text{ count min}^{-1}$   
(mg atom F) $^{-1}$

After reaction:

Solid count rate =  $23889 \pm 139 \text{ count min}^{-1}$

Count rate of volatile materials =  $4797 \pm 45 \text{ count min}^{-1}$

Radiochemical balance =  $\frac{23889 + 4797}{14598 \times 2} \times 100 = 98\%$

Composition of volatile products after reaction, from the infra-red study;

0.19  $\text{COF}_2$

9.57  $\text{CO}_2$

Retained quantity as  $\text{COF}_3^{\overline{}}$  from the [ $^{14}\text{C}$ ]-carbon and manometric study was 0.24 mmol.

Specific count rate of  $\text{COF}^{18}\text{F}$  after reaction

$\frac{4797}{0.19 \times 2} \pm 45 = 12624 \pm 119 \text{ count min (mg atom F)}^{-1}$

Figure 5.66

Reaction of  $\text{COF}^{18}\text{F}$  with  $\text{MF}/\gamma\text{-alumina}$ , Solid Count Rate  $\gamma$  Composition

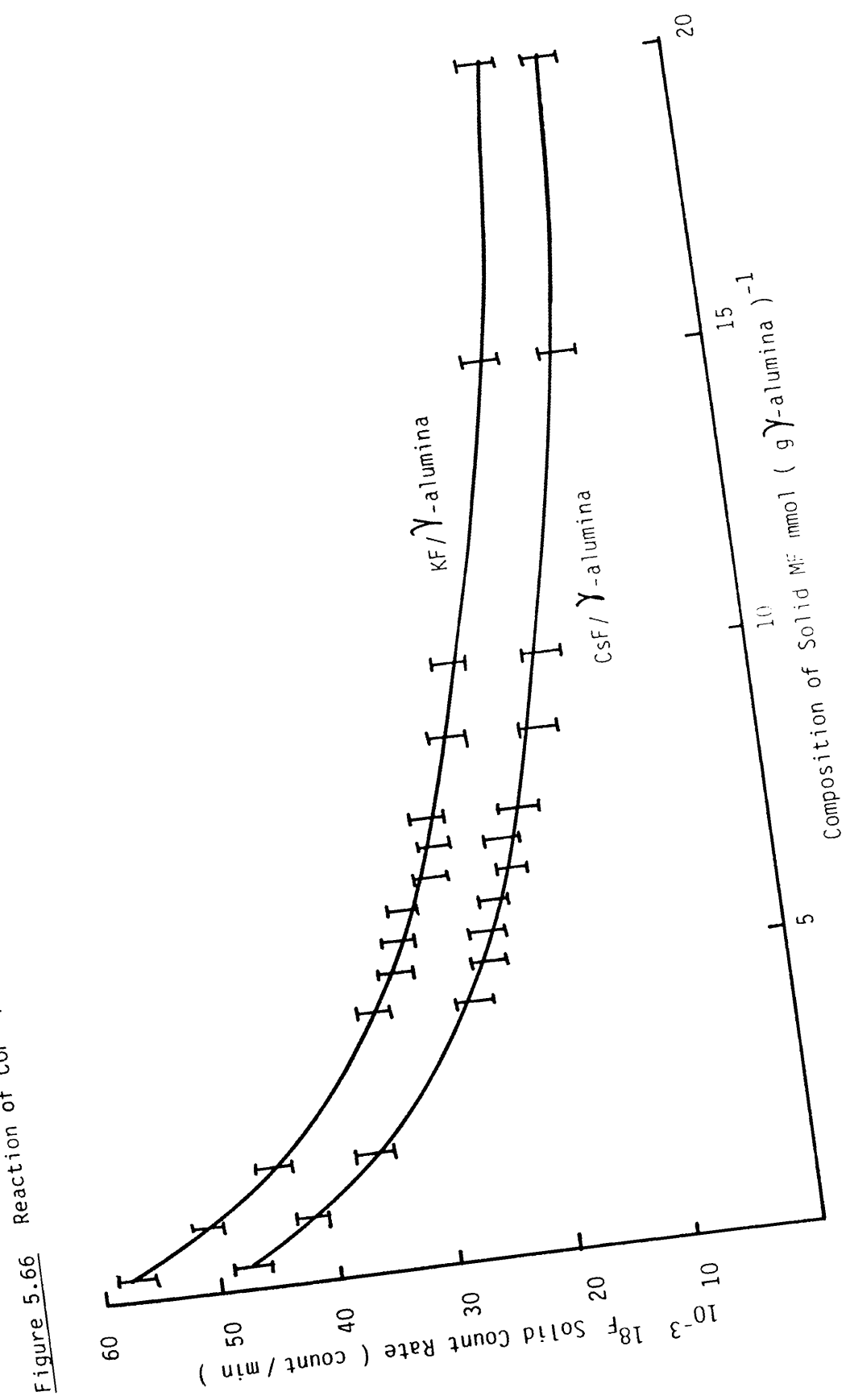


Table 5.47 Results of Reaction between Carbonyl Fluoride and MF/ $\gamma$ Alumina which had been exposed to [ $^{18}\text{F}$ ]-Fluorine Labelled Carbonyl Fluoride

Composition of Solid $\text{mmol g}^{-1}$	Run	CsF/ $\gamma$ -alumina				KF/ $\gamma$ alumina			
		Solid Count Rate Before Reaction	Solid Count Rate After Reaction	Gas Count Rate After Reaction	Solid Count Rate Before Reaction	Solid Count Rate After Reaction	Gas Count Rate After Reaction	Solid Count Rate After Reaction	
4.4	1	23889 $\pm$ 139	20066 $\pm$ 131	4391 $\pm$ 131	24996 $\pm$ 113	20993 $\pm$ 181	3093 $\pm$ 107		
	2	24045 $\pm$ 113	20438 $\pm$ 291	3209 $\pm$ 99	23499 $\pm$ 119	19974 $\pm$ 150	3193 $\pm$		
	3	18417 $\pm$ 191	15286 $\pm$ 103	3433 $\pm$ 189	20175 $\pm$ 201	17350 $\pm$ 203	3013 $\pm$ 79		
	4	21443 $\pm$ 267	18012 $\pm$ 120	3891 $\pm$ 73	22800 $\pm$ 164	19380 $\pm$ 193	3461 $\pm$ 131		
8.8	1	15375 $\pm$ 193	13992 $\pm$ 105	1784 $\pm$ 100	19161 $\pm$ 217	17861 $\pm$ 167	1594 $\pm$ 93		
	2	18417 $\pm$ 179	16575 $\pm$ 136	1893 $\pm$ 93	20769 $\pm$ 203	19003 $\pm$ 131	1631 $\pm$ 123		
	3	18405 $\pm$ 133	16380 $\pm$ 154	2000 $\pm$ 73	22389 $\pm$ 219	20503 $\pm$ 163	1931 $\pm$ 98		
	4	17354 $\pm$ 189	15619 $\pm$ 169	1936 $\pm$ 131	20981 $\pm$ 182	19168 $\pm$ 293	1769 $\pm$ 136		

For a total exchange in the system,  $\text{COF}^{18}\text{F}/\text{CsF}/\gamma\text{-alumina}$ , 4.4  $\text{mmol g}^{-1}$ ,  $\text{SCD} = \frac{14598 \times 2}{1.32 \times 1 + 1 \times 2} = 8794 \text{ count min}^{-1} (\text{mg atom F})^{-1}$

The fraction exchanged is calculated using equation 2.12

$$f = \frac{S_0 - S_t}{S_0 - \text{SCD}} = \frac{14598 - 12624}{14598 - 8794} \times 100 = 34\%$$

For a 34% exchange, the drop in the specific count rate  
 $= 14598 - 12624 = 1974 \text{ count min}^{-1} (\text{mg atom F})^{-1}$

The total drop in the  $\text{COF}^{18}\text{F}$  count rate after reaction  
 $= 1974 \times 2 \times 0.19 \times 750 \text{ count min}^{-1}$

The solid count rate due to [ $^{18}\text{F}$ ]-fluorine results 34% exchange hydrolysis of 0.57 mmol of carbonyl fluoride and 0.24 mmol retained as  $\text{COF}_3^-$ , should be

$$750 + 14598 \times 2 \times (0.24 + 0.57) = 24399 \text{ count min}^{-1}$$

This is in good agreement with the experimental value.

This method is used throughout this work and the results obtained from the supported metal fluoride, 4.4 and 8.8  $\text{mmol g}^{-1}$  are given in Tables 5.48-5.51.

## 5.5 REACTIONS INVOLVING ANHYDROUS HYDROGEN FLUORIDE WITH CAESIUM OR POTASSIUM FLUORIDE SUPPORTED ON $\gamma$ -ALUMINA

### 5.5.1 MANOMETRIC STUDY OF REACTIONS OF ANHYDROUS HYDROGEN FLUORIDE WITH CAESIUM OR POTASSIUM FLUORIDE SUPPORTED ON $\gamma$ -ALUMINA

The procedure used in these experiments was similar to that described in section 5.2, but experiments were carried out in a Monel metal vacuum line, Fig. 2.4. The change in the pressure was measured using a pressure gauge connected to the system. The saturation of the solid was achieved by the admission of successive aliquots of anhydrous hydrogen fluoride into the reactor containing the solid until no further decrease in the



Table 5.48 Results of Reactions between [<sup>18</sup>F]-Fluorine Labelled Carbonyl Fluoride and CsF/γAlumina, 4.4mmol g<sup>-1</sup>

Quantity of Solid g, mmol of CsF	Quantity of Gas Torr mmol	Initial Specific Count Rate Count min <sup>-1</sup> (mg atom F) <sup>-1</sup>	Final Specific Count Rate Count min <sup>-1</sup> (mg atom F) <sup>-1</sup>	Solid Count Rate		Fraction Exchanged %
				Experimental	Calculated	
0.5 ± 0.01	300 ± 2	14598 ± 133	12624 ± 119	23889 ± 139	2	34 ± 1
1.32 ± 0.01	1.0 ± 0.06					
0.5 ± 0.01	300 ± 2	14028 ± 316	12134 ± 169	24045 ± 113	24682	34 ± 1
1.32 ± 0.06	1.0 ± 0.06					
0.5 ± 0.01	300 ± 2	11690 ± 189	10155 ± 136	18417 ± 191	19057	33 ± 1
1.32 ± 0.06	1.0 ± 0.06					
0.5 ± 0.01	300 ± 2	13611 ± 214	11825 ± 303	21443 ± 267	21763	33 ± 1
1.32 ± 0.06	1.0 ± 0.06					

Table 5.49 Results of Reactions between [<sup>18</sup>F]-Fluorine Labelled Carbonyl Fluoride and KF/γAlumina, 4.4mmol g<sup>-1</sup>

Quantity of Solid g, mmol of KF	Quantity of Gas Torr mmol	Initial Specific Count Rate Count min <sup>-1</sup> (mg atom F) <sup>-1</sup>	Final Specific Count Rate Count min <sup>-1</sup> (mg atom F) <sup>-1</sup>	Solid Count Rate Count min <sup>-1</sup>		Fraction Exchanged %
				Experimental	Calculated	
0.38 ± 0.01	300 ± 2	14598 ± 133	13030 ± 291	24996 ± 113	25756	27 ± 1
1.32 ± 0.01	1.0 ± 0.06					
0.38 ± 0.01	300 ± 2	14028 ± 316	12521 ± 187	23499 ± 119	23573	27 ± 1
1.32 ± 0.06	1.0 ± 0.06					
0.38 ± 0.01	300 ± 2	11690 ± 189	10482 ± 167	20175 ± 201	20813	26 ± 1
1.32 ± 0.06	1.0 ± 0.06					
0.38 ± 0.01	300 ± 2	13611 ± 214	12150 ± 160	22800 ± 164	22932	28 ± 1
1.32 ± 0.06	1.0 ± 0.06					

Table 5.50 Results of Reactions between [ $^{18}\text{F}$ ]-Fluorine Labelled Carbonyl Fluoride and CsF/ $\gamma$ Alumina,  $8.8\text{mmol g}^{-1}$

Quantity of Solid of CsF	Quantity of Gas Torr mmol	Initial Specific Count Rate $\text{Count min}^{-1} (\text{mg atom F})^{-1}$	Final Specific Count Rate $\text{Count min}^{-1} (\text{mg atom F})^{-1}$	Solid Count Rate $\text{Count min}^{-1}$		Fraction Exchanged %
				Experimental	Calculated	
0.5 $\pm$ 0.01	300 $\pm$ 2	13408 $\pm$ 177	12234 $\pm$ 203	15375 $\pm$ 193	15732	18 $\pm$ 1
1.88 $\pm$ 0.01	1.0 $\pm$ 0.06					
0.5 $\pm$ 0.01	300 $\pm$ 2	14904 $\pm$ 237	13531 $\pm$ 139	18417 $\pm$ 179	18723	19 $\pm$ 1
1.88 $\pm$ 0.06	1.0 $\pm$ 0.06					
0.5 $\pm$ 0.01	300 $\pm$ 2	15497 $\pm$ 107	14147 $\pm$ 143	18405 $\pm$ 133	17987	18 $\pm$ 1
1.88 $\pm$ 0.06	1.0 $\pm$ 0.06					
0.5 $\pm$ 0.01	300 $\pm$ 2	13963 $\pm$ 246	12677 $\pm$ 171	17354 $\pm$ 189	17746	19 $\pm$ 1
1.88 $\pm$ 0.06	1.0 $\pm$ 0.06					

Table 5.51 Results of Reactions between [<sup>18</sup>F]-Fluorine Labelled Carbonyl Fluoride and KF/γAlumina, 8.8mmolg<sup>-1</sup>

Quantity of Solid g,mmol of KF	Quantity of Gas Torr mmol	Initial Specific Count Rate Count min <sup>-1</sup> (mg atom F) <sup>-1</sup>	Final Specific Count Rate Count min <sup>-1</sup> (mg atom F) <sup>-1</sup>	Solid Count Rate Count min <sup>-1</sup>		Fraction Exchanged %
				Experimental	Calculated	
0.32 ± 0.01	300 ± 2	13408 ± 177	12431 ± 161	19161 ± 217	19623	15 ± 1
1.88 ± 0.01	1.0 ± 0.06					
0.32 ± 0.01	300 ± 2	14904 ± 237	13892 ± 151	20769 ± 203	21314	14 ± 1
1.88 ± 0.06	1.0 ± 0.06					
0.32 ± 0.01	300 ± 2	15497 ± 107	14369 ± 134	22389 ± 219	22012	16 ± 1
1.88 ± 0.06	1.0 ± 0.06					
0.32 ± 0.01	300 ± 2	13963 ± 246	13016 ± 184	20981 ± 182	21947	14 ± 1
1.88 ± 0.06	1.0 ± 0.06					

pressure was observed. The total uptake of anhydrous hydrogen fluoride by the supported metal fluoride is given in Table 5.52. The interactions involving supported potassium fluoride were greater than those involving supported caesium fluoride under the same conditions. In each case, the infra-red spectrum of the supported metal fluoride after reaction with anhydrous hydrogen fluoride showed very strong absorption bands were attributed to the hydrogendifluoride anion ( $\text{HF}_2^-$ ). The infra-red spectrum of the supported potassium fluoride,  $4.4 \text{ mmol g}^{-1}$  after reaction with anhydrous hydrogen fluoride is given in Table 5.53.

#### 5.5.2 REACTIONS OF [ $^{18}\text{F}$ ]-FLUORINE LABELLED ANHYDROUS HYDROGEN FLUORIDE WITH CAESIUM OR POTASSIUM FLUORIDE SUPPORTED ON $\gamma$ -ALUMINA

The admission of [ $^{18}\text{F}$ ]-fluorine labelled anhydrous hydrogen fluoride to the supported metal fluoride (pellets) resulted in an increase in the solid count rate before reaching a constant value after 25 min. The admission of another quantity of [ $^{18}\text{F}$ ]-fluorine labelled anhydrous hydrogen fluoride to the solid followed the same pattern. This procedure was repeated until no further increase in the solid count rate was observed. Results obtained are shown in Fig. 5.67. The specific count rate of [ $^{18}\text{F}$ ]-fluorine labelled anhydrous hydrogen fluoride recovered after the saturation of the supported metal fluoride decreased and the fraction exchanged was calculated using equation 2.12. The results are given in Tables 5.54-5.57. The admission of inactive anhydrous hydrogen fluoride to a sample of supported metal fluoride treated with [ $^{18}\text{F}$ ]-fluorine labelled anhydrous hydrogen

Table 5.52 The Monometric Results of Reaction between Anhydrous Hydrogen Fluoride and Supported Metal Fluoride

Supported Metal Fluoride (mmol g <sup>-1</sup> )		Total Uptake of HF (mmol g <sup>-1</sup> )
CsF/ $\gamma$ -alumina	4.4	8.2 $\pm$ 0.8
KF/ $\gamma$ -alumina	4.4	11.4 $\pm$ 0.9
CsF/ $\gamma$ -alumina	8.8	5.3 $\pm$ 0.7
KF/ $\gamma$ -alumina	8.8	6.4 $\pm$ 0.8

**Table 5.53**    **The Infra-red Spectrum of Solid KF/ $\gamma$ alumina After Reaction with Anhydrous Hydrogen Fluoride**

<b>This Work</b>	<b>Literature KHF<sub>2</sub> 37</b>	<b>Assignment</b>
2043	2060	$\nu_3 + \nu_1$
1843	1870	$\nu_2 + \nu_1$
1468	1425	$\nu_3$
1236	1230	$\nu_2$

Figure 5.67 Reaction of  $\text{H}^{18}\text{F}$  with MF/ $\gamma$ -alumina  
 Solid Count Rate  $\propto$  Quantity of  $\text{H}^{18}\text{F}$  Admitted  
 Sample Weight = 0.28 g

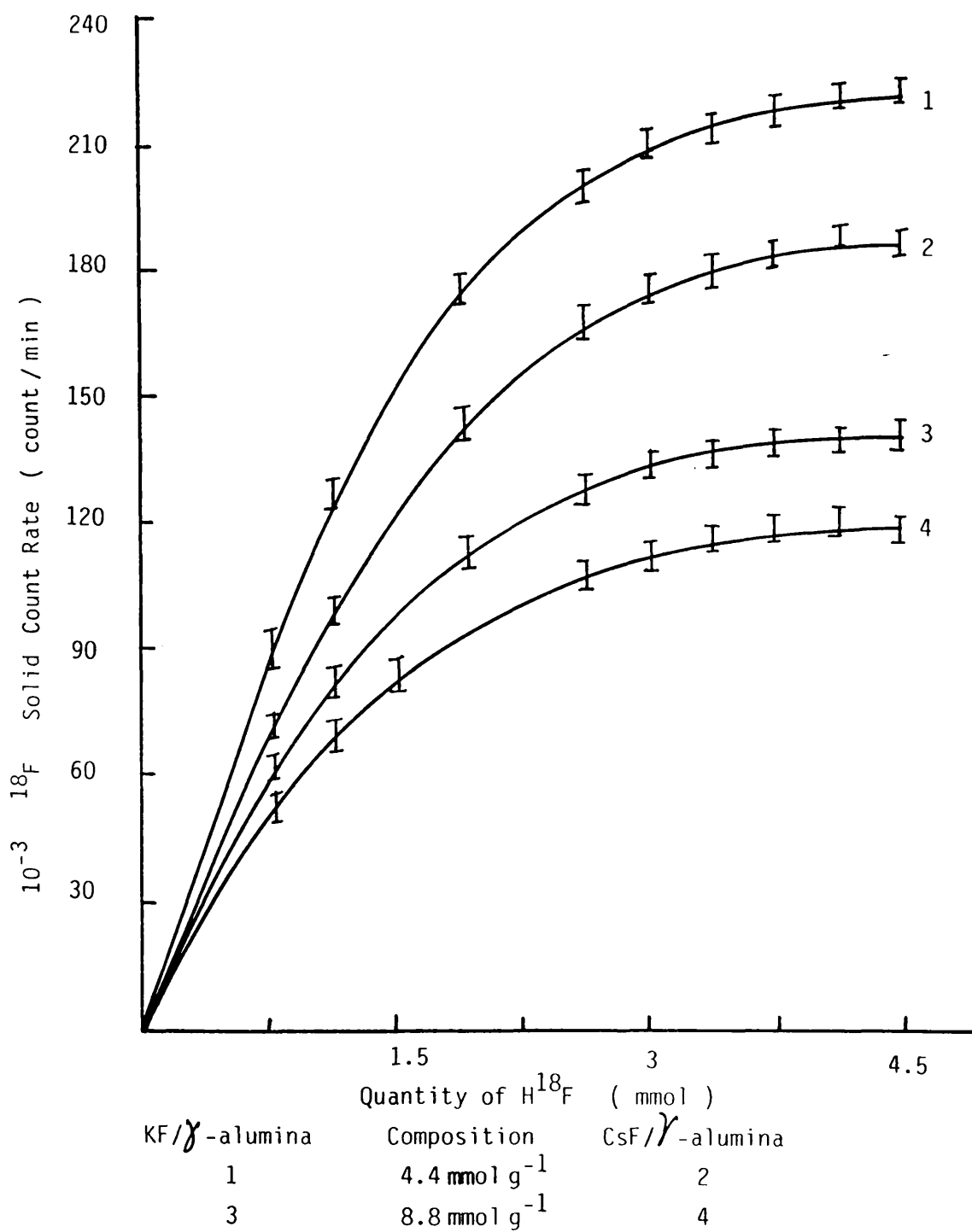




Table 5.54 Results of Reactions between [<sup>18</sup>F]-Fluorine Labelled Anhydrous Hydrogen Fluoride and CsF/γAlumina, 4.4mmolg<sup>-1</sup>

Quantity of Solid g, mmol of CsF	Quantity of Gas Torr mmol	Initial Specific Count Rate of H <sup>18</sup> F Count min <sup>-1</sup> (mg atom F) <sup>-1</sup>	Final Specific Count Rate of H <sup>18</sup> F Count min <sup>-1</sup> (mg atom F) <sup>-1</sup>	Solid Count Rate		Fraction Exchanged %
				Experimental	Calculated	
0.12 ± 0.01 0.316 ± 0.01	4 ± 0.05	233204 ± 128	218178 ± 197	247597 ± 217	248240	88 ± 1
0.12 ± 0.01 0.316 ± 0.01	3 ± 0.05	156713 ± 189	143271 ± 219	172196 ± 284	171538	90 ± 1
0.12 ± 0.01 0.316 ± 0.01	3 ± 0.05	134312 ± 191	122920 ± 173	137006 ± 284	137769	89 ± 1
0.12 ± 0.01 0.316 ± 0.01	3 ± 0.05	163712 ± 173	150140 ± 151	195140 ± 196	194261	87 ± 1

Table 5.55 Results of Reactions between [ $^{18}\text{F}$ ]-Fluorine Labelled Anhydrous Hydrogen Fluoride and KF/ $\gamma$ -Alumina,  $4.4\text{mmol g}^{-1}$

Quantity of Solid g, mmol of KF	Quantity of Gas Torr mmol	Initial Specific Count Rate of $\text{H}^{18}\text{F}$ Count $\text{min}^{-1}$ (mg atom F) $^{-1}$	Final Specific Count Rate of $\text{H}^{18}\text{F}$ Count $\text{min}^{-1}$ (mg atom F) $^{-1}$	Solid Count Rate		Fraction Exchanged %
				Experimental	Calculated	
$0.12 \pm 0.01$ $0.42 \pm 0.01$	$4 \pm 0.05$	$233204 \pm 128$	$213924 \pm 196$	$342183 \pm 297$	$343776$	$87 \pm 1$
$0.12 \pm 0.01$ $0.42 \pm 0.01$	$3 \pm 0.05$	$156713 \pm 189$	$139200 \pm 276$	$230006 \pm 396$	$230974$	$91 \pm 1$
$0.12 \pm 0.01$ $0.42 \pm 0.01$	$3 \pm 0.05$	$134312 \pm 191$	$119467 \pm 169$	$186807 \pm 284$	$187793$	$90 \pm 1$
$0.12 \pm 0.01$ $0.42 \pm 0.01$	$3 \pm 0.05$	$163712 \pm 173$	$145819 \pm 267$	$229793 \pm 184$	$230243$	$89 \pm 1$

Table 5.56 Results of Reactions between [<sup>18</sup>F]-Fluorine Labelled Anhydrous Hydrogen Fluoride and CsF/γAlumina, 8.8mmol g<sup>-1</sup>

Quantity of Solid g, mmol of CsF	Quantity of Gas Torr mmol	Initial Specific Count Rate of H <sup>18</sup> F Count min <sup>-1</sup> (mg atom F) <sup>-1</sup>	Final Specific Count Rate of H <sup>18</sup> F Count min <sup>-1</sup> (mg atom F) <sup>-1</sup>	Solid Count Rate Count min <sup>-1</sup>		Fraction Exchanged %
				Experimental	Calculated	
0.12 ± 0.01 0.45 ± 0.01	3 ± 0.05	136312 ± 189	132223 ± 160	103593 ± 219	102935	23 ± 1
0.12 ± 0.01 0.45 ± 0.06	3 ± 0.05	142911 ± 173	138437 ± 263	95899 ± 307	96557	24 ± 1
0.12 ± 0.01 0.45 ± 0.06	3 ± 0.05	149813 ± 156	145709 ± 143	98347 ± 285	97562	21 ± 1
0.12 ± 0.01 0.45 ± 0.06	3 ± 0.05	146413 ± 199	141638 ± 176	105356 ± 197	106014	25 ± 1

Table 5.57 Results of Reactions between [ $^{18}\text{F}$ ]-Fluorine Labelled Anhydrous Hydrogen Fluoride and KF/ $\gamma$ Alumina,  $8.8\text{mmol g}^{-1}$

Quantity of Solid g, mmol of KF	Quantity of Gas Torr mmol	Initial Specific Count Rate of $\text{H}^{18}\text{F}$ $\text{Count min}^{-1} (\text{mg atom F})^{-1}$	Final Specific Count Rate of $\text{H}^{18}\text{F}$ $\text{Count min}^{-1} (\text{mg atom F})^{-1}$	Solid Count Rate		Fraction Exchanged %
				Experimental	Calculated	
$0.12 \pm 0.01$ $0.7 \pm 0.01$	$3 \pm 0.05$	$136312 \pm 189$	$129865 \pm 183$	$120034 \pm 296$	$119245$	$25 \pm 1$
$0.12 \pm 0.01$ $0.7 \pm 0.01$	$3 \pm 0.05$	$142911 \pm 173$	$136422 \pm 197$	$115365 \pm 384$	$116023$	$24 \pm 1$
$0.12 \pm 0.01$ $0.7 \pm 0.01$	$3 \pm 0.05$	$149813 \pm 156$	$144144 \pm 297$	$121873 \pm 213$	$120994$	$20 \pm 1$
$0.12 \pm 0.01$ $0.7 \pm 0.01$	$3 \pm 0.05$	$146413 \pm 199$	$140596 \pm 235$	$120889 \pm 193$	$121920$	$21 \pm 1$

fluoride led to a decrease in the solid count rate after the removal of the gas phase. The results are given in Table 5.58. The results of the reaction between [ $^{18}\text{F}$ ]-fluorine labelled supported metal fluoride and anhydrous hydrogen fluoride are given in Table 5.59. These showed that the specific count rates of [ $^{18}\text{F}$ ]-fluorine labelled anhydrous hydrogen fluoride obtained after reaction with the supported metal fluoride,  $4.4 \text{ mmol g}^{-1}$  were higher than those obtained after reaction with the supported metal fluoride,  $8.8 \text{ mmol g}^{-1}$ .

Table 5.58 Summary of Results of Reaction between Anhydrous Hydrogen and Metal Fluoride Supported on  $\gamma$ Alumina which had been treated with [ $^{18}\text{F}$ ]-Fluorine Labelled Anhydrous Hydrogen Fluoride

Composition of Solid $\text{mmol g}^{-1}$	Run	CsF/ $\gamma$ -alumina				KF/ $\gamma$ alumina			
		Solid Count Rate Before Reaction	Solid Count Rate After Reaction	Gas Count Rate After Reaction	Solid Count Rate Before Reaction	Solid Count Rate After Reaction	Gas Count Rate After Reaction	Solid Count Rate After Reaction	
4.4	1	247597	190650	57839	342183	239528	98375		
	2	172196	125703	47319	230006	170204	57309		
	3	137006	102754	32101	186807	132633	57183		
	4	195140	144404	53977	229793	172345	54911		
8.8	1	103593	84946	19731	120034	97227	23993		
	2	95899	79596	17709	115365	94599	193164		
	3	98347	82611	16391	121873	99936	200000		
	4	105356	87445	19368	120889	97920	23841		

**Table 5.59 Results of Reaction of [ $^{18}\text{F}$ ]-Fluorine Labelled Supported Metal Fluoride and Anhydrous Hydrogen Fluoride**

Compositon of Solid $\text{mmol g}^{-1}$	Solid before Reaction	Solid After Reaction	Gas After Reaction count $\text{min}^{-1} \text{mmol}^{-1}$
Supported CsF, 4.4	473856 $\pm$ 219	289630 $\pm$ 483	197393 $\pm$ 492
Supported CsF, 8.8	678373 $\pm$ 263	574009 $\pm$ 391	91775 $\pm$ 497
Supported KF, 4.4	347147 $\pm$ 396	201345 $\pm$ 426	135976 $\pm$ 397
Supported KF, 8.8	496976 $\pm$ 411	416429 $\pm$ 374	89596 $\pm$ 419

## CHAPTER SIX



REACTIONS OF PROBE MOLECULES WITH  $\gamma$ -ALUMINA CALCINED TO 523 K AND  $\gamma$ -ALUMINA FLUORINATED WITH SULPHUR TETRAFLUORIDE THIONYL FLUORIDE, CARBONYL FLUORIDE OR ANHYDROUS HYDROGEN FLUORIDE.

6.1 INTRODUCTION

The reactions of the probe molecules, sulphur tetrafluoride thionyl fluoride, sulphur dioxide, carbonyl fluoride, carbon dioxide and anhydrous hydrogen fluoride with  $\gamma$ -alumina calcined to 523 K or  $\gamma$ -alumina fluorinated with sulphur tetrafluoride, thionyl fluoride, carbonyl fluoride or anhydrous hydrogen fluoride at room temperature, are reported in this chapter. The fluorinated  $\gamma$ -alumina materials were characterized prior to the examination of the catalytic activity of the metal fluoride supported on fluorinated  $\gamma$ -alumina which are to be described in detail in Chapter seven.

6.2 EXPERIMENTAL

The saturation of the surface was achieved by the admission of one of the fluorinating agents, e.g. sulphur tetrafluoride to a sample of calcined  $\gamma$ -alumina. The volatile products were removed and a second quantity of sulphur tetrafluoride admitted. This procedure was repeated until no hydrolysis products were observed. The total quantity of sulphur tetrafluoride hydrolysed was calculated from the composition of the volatile products after each step by means of infra-red spectroscopy as described in chapter five. The total uptake of fluorine was calculated from the quantities of thionyl fluoride and sulphur dioxide formed; for each mmol of thionyl fluoride or sulphur dioxide formed it was assumed that 2 and 4 mg atom fluorine respectively were retained by the surface. The [ $^{18}\text{F}$ ]-fluorine labelled volatile products were counted as their adducts or at 77 K

as described in chapter two.

### 6.3 REACTIONS OF PROBE MOLECULES WITH $\gamma$ -ALUMINA PREVIOUSLY CALCINED TO 523 K.

#### 6.3.1 REACTION OF SULPHUR DIOXIDE WITH $\gamma$ -ALUMINA

The admission of [ $^{35}\text{S}$ ]-sulphur labelled sulphur dioxide to a sample of the uncalcined  $\gamma$ -alumina led to a very slow growth in [ $^{35}\text{S}$ ]-sulphur activity on the surface over a period of 3 h. The removal of the [ $^{35}\text{S}$ ]-sulphur labelled sulphur dioxide from the system resulted in an immediate loss of the surface radioactivity. However the reaction of [ $^{35}\text{S}$ ]-sulphur labelled sulphur dioxide with  $\gamma$ -alumina previously calcined to 523 K exhibited different behaviour; the growth of the [ $^{35}\text{S}$ ]-sulphur surface count rate was faster than that obtained for the nonactivated  $\gamma$ -alumina although no apparent equilibrium was observed. Removal of the [ $^{35}\text{S}$ ]-sulphur labelled sulphur dioxide from the system did not result in the removal of all the surface radioactivity from  $\gamma$ -alumina; ca 13% of the total radioactivity was retained. This surface count rate was not removed by the admission of successive pulses of water vapour or by heating the sample below 723 K under vacuum. Plots of the surface count rate as a function of time are shown in Fig 6.1. The surface count rate of the calcined  $\gamma$ -alumina was dependent upon the initial pressure of [ $^{35}\text{S}$ ]-sulphur labelled sulphur dioxide as shown in Fig 6.2. In each experiment studied, infra-red spectroscopic analysis of the gas phase indicated that sulphur dioxide was the only gas present.

Figure 6.1 Reaction of  $^{35}\text{SO}_2$  with  $\gamma$ -alumina  
 $^{35}\text{S}$  Surface  $\nu$  Time  
Initial pressure = 300 Torr

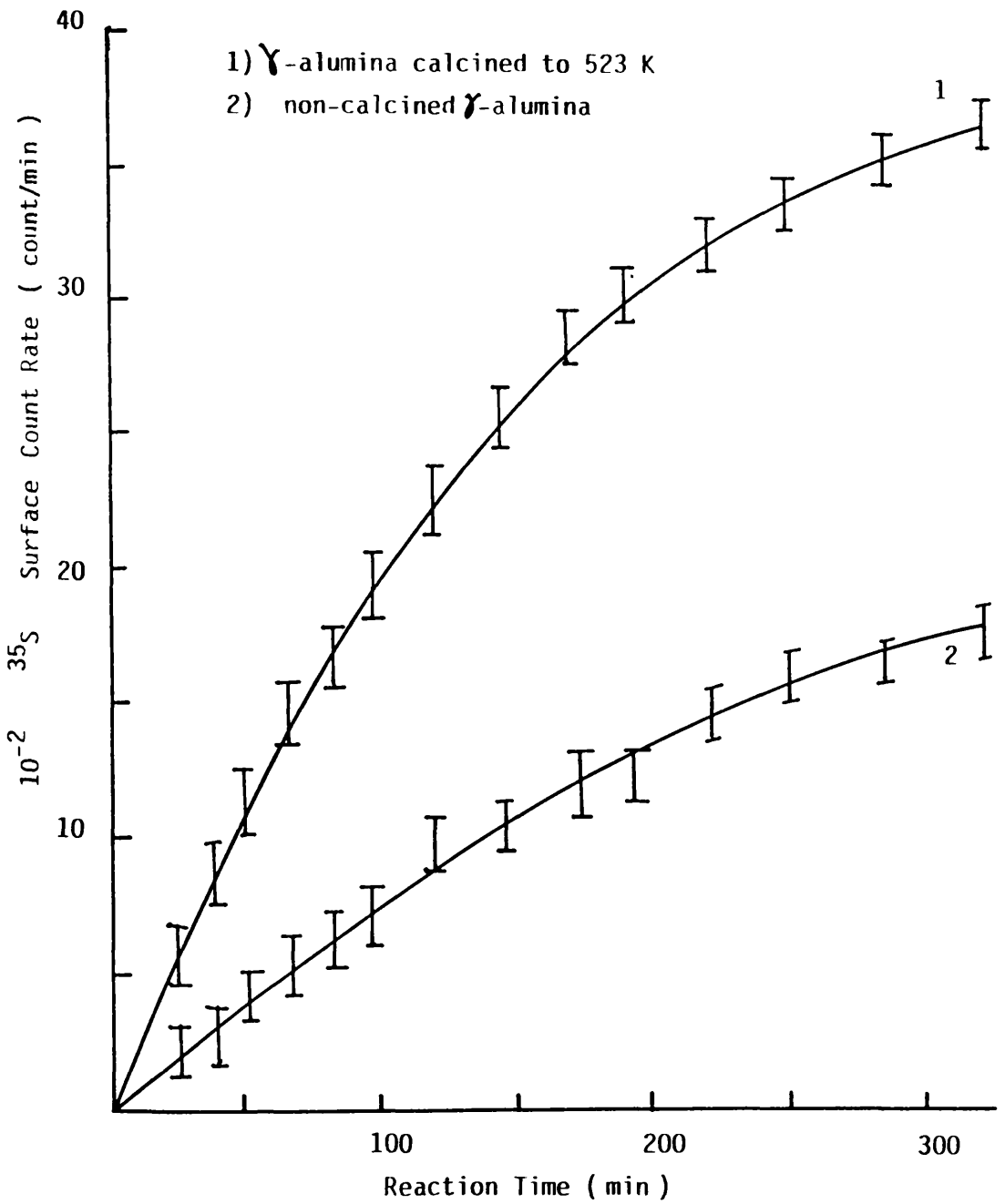
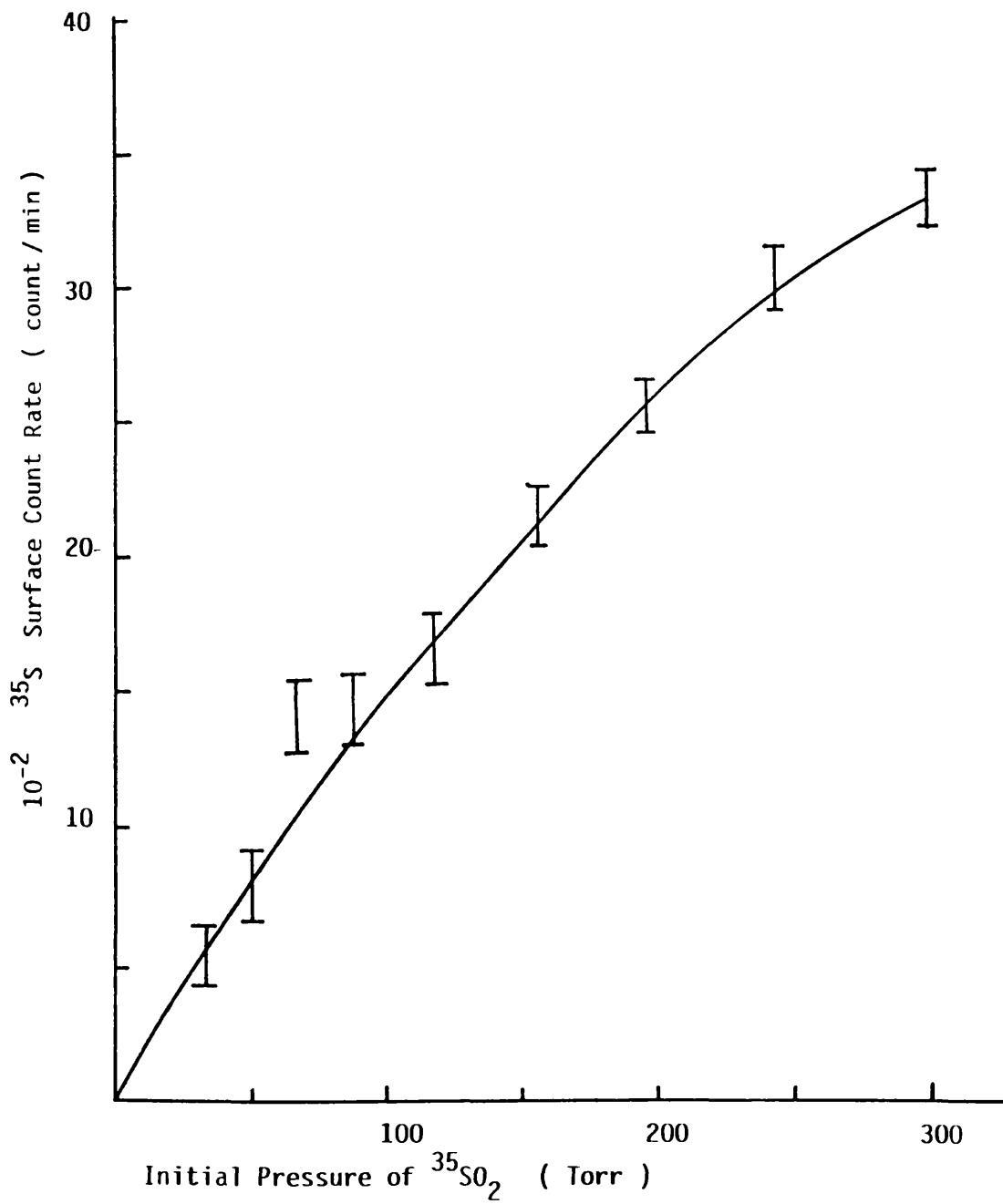


Figure 6.2 Reaction of  $^{35}\text{SO}_2$  with  $\gamma$ -alumina  
 $^{35}\text{S}$  Surface Count Rate  $\nu$  Pressure

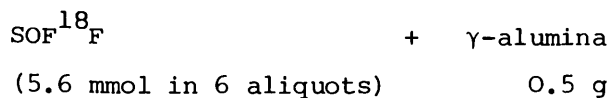


6.3.2 REACTION OF THIONYL FLUORIDE WITH  $\gamma$ -ALUMINA PREVIOUSLY  
CALCINED TO 523 K.

The admission of thionyl fluoride to  $\gamma$ -alumina calcined to 523 K led to the formation of sulphur dioxide. No evidence for the production of anhydrous hydrogen fluoride in the gas phase was obtained. The volatile products after the saturation of the surface of  $\gamma$ -alumina were analysed by infra-red spectroscopy and the composition and hence the total fluorine uptake was calculated. The results are given in Table 6.1.

When [ $^{35}\text{S}$ ]-sulphur labelled thionyl fluoride was admitted to a sample of  $\gamma$ -alumina no [ $^{35}\text{S}$ ]-sulphur activity was obtained from the surface. The volatile products were removed and a further quantity of fresh [ $^{35}\text{S}$ ]-sulphur labelled thionyl fluoride admitted, even in this case, also no [ $^{35}\text{S}$ ]-sulphur uptake by the surface was detected. Further admissions had no effect on the surface of  $\gamma$ -alumina.

The admission of [ $^{18}\text{F}$ ]-fluorine labelled thionyl fluoride to a sample of  $\gamma$ -alumina previously calcined to 523 K resulted in a rapid increase in the solid count rate over the first 50 min, followed by a constant value thereafter. The admission of further quantities of [ $^{18}\text{F}$ ]-fluorine labelled thionyl fluoride to  $\gamma$ -alumina after the removal of the volatile products showed the same behaviour, as shown in Fig. 6.3. The total uptake of fluorine was calculated as shown below:



$$\text{Initial specific count rate of SOF}^{18}\text{F} = 26979 \pm 268 \text{ count min}^{-1} \text{ (mg atom F)}^{-1}$$

**Table 6.1 The Infra-red Analysis of the Gas Products of the Reaction of Thionyl Fluoride with  $\gamma$ -alumina calcined to 523K**

Total $\text{SOF}_2$ Admitted (mmol)	Composition of Gas Products (mmol)		Total Fluorine Uptake by $\gamma$ -alumina mg atom fluorine/g
	$\text{SOF}_2$	$\text{SO}_2$	
$10.9 \pm 0.2$	$2.4 \pm 0.1$	$7.8 \pm 0.1$	$15.6 \pm 0.5$
$11.8 \pm 0.2$	$3.8 \pm 0.1$	$7.6 \pm 0.1$	$15.2 \pm 0.5$
$12.0 \pm 0.2$	$4.6 \pm 0.1$	$7.1 \pm 0.1$	$14.2 \pm 0.5$
$11.1 \pm 0.2$	$3.6 \pm 0.1$	$8.0 \pm 0.1$	$16.0 \pm 0.5$

Weight of  $\gamma$ -alumina 1.0g

Thionyl Fluoride admitted was the total in 6 aliquots

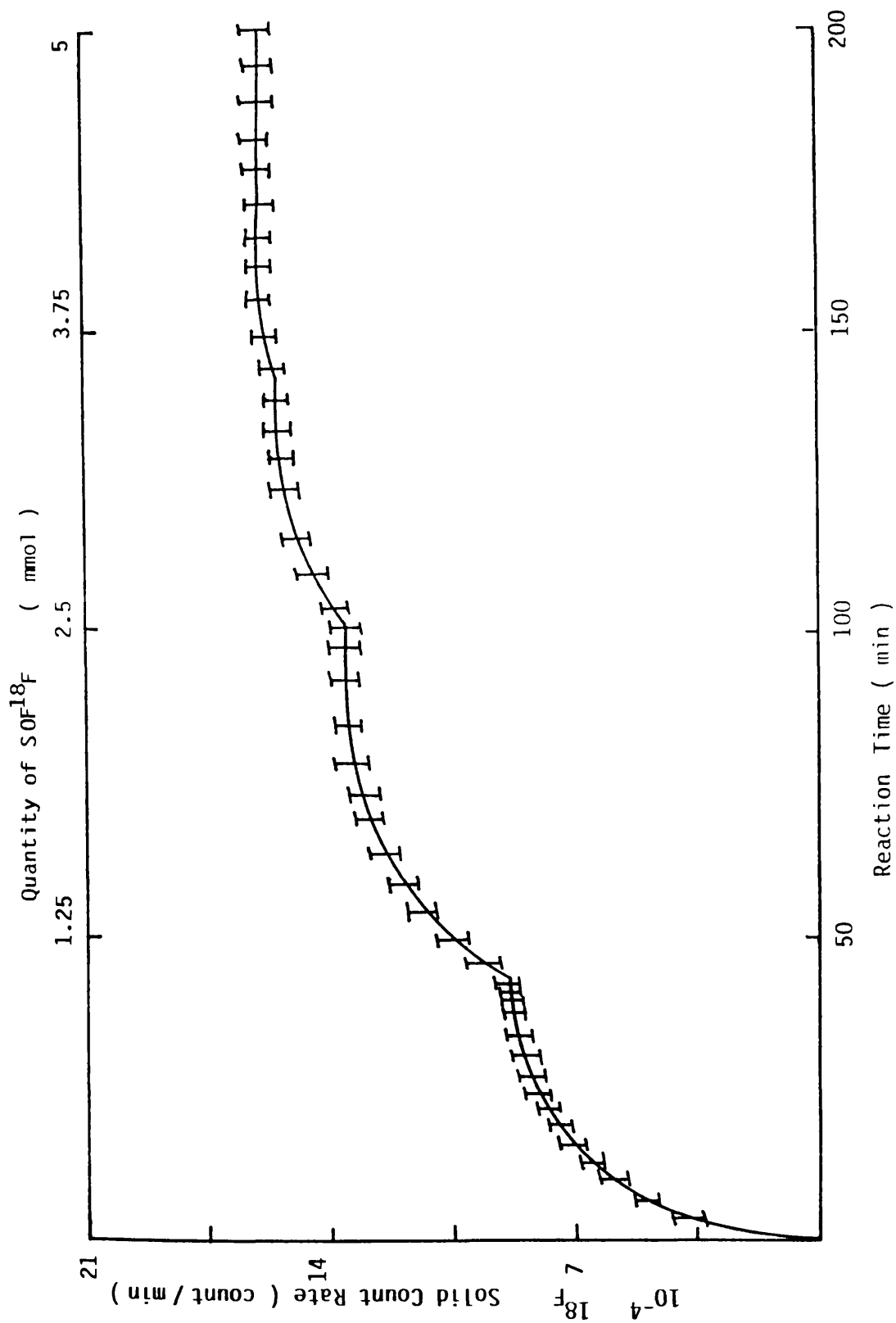


Figure 6.3 Reaction of SOF<sup>18</sup>F with calcined  $\gamma$ -alumina

After reaction

Count rate of volatile products counted at 77 K

$$= 103963 \pm 316 \text{ count min}^{-1}$$

Count rate of solid

$$= 199105 \pm 280 \text{ count min}^{-1}$$

$$\text{Radiochemical balance} = \frac{103963 + 199105}{26979 \times 2 \times 5.6} \times 100 = 100\%$$

The uptake of fluorine in terms of mg atom fluorine

calculated from the solid count rate

$$= \frac{199105}{26979} \pm 280 = 7.4 \pm 0.01 \text{ mg atom fluorine}$$

The uptake was also calculated from the count rate of the gas phase. The only fluorine containing volatile product after reaction was thionyl fluoride, therefore the quantity of thionyl fluoride after reaction was estimated as follows:

$$\text{Quantity of SOF}^{18}\text{F} = \frac{103963}{2 \times 26979} = 1.93 \text{ mmol}$$

The quantity of thionyl fluoride hydrolysed = 5.6 - 1.93 = 3.67 mmol the total uptake of fluoride by 0.5 g of  $\gamma$ -alumina was therefore 7.3 mg atom fluoride.

The results obtained are given in Table 6.2. The data obtained showed that the total uptake of fluorine by  $\gamma$ -alumina was ca 15 mg atom fluorine  $\text{g}^{-1}$ .



Table 6.2 Results of Reactions of [<sup>18</sup>F]-Fluorine Labelled Thionyl Fluoride with γAlumina calcined to 523K

Total Quantity of SO <sup>18</sup> FF Used mmol	Initial Specific Count of SO <sup>18</sup> FF Count min <sup>-1</sup> (mg atom F) <sup>-1</sup>	Final Gas Count of SO <sup>18</sup> FF Count min <sup>-1</sup>	Solid Count Rate After Reaction Count min <sup>-1</sup>	Total Uptake of Fluorine (mg atom Fluorine)	From the Solid Count Rate	From the Gas Count Rate
5.6 ± 0.2	26979 ± 268	103963 ± 316	199105 ± 280	7.4 ± 0.5	7.4 ± 0.5	7.3 ± 0.5
5.2 ± 0.2	25003 ± 166	701001 ± 216	189523 ± 307	7.5 ± 0.5	7.5 ± 0.5	7.6 ± 0.5
5.9 ± 0.2	24788 ± 187	98969 ± 187	193842 ± 188	7.8 ± 0.5	7.8 ± 0.5	7.8 ± 0.5
5.8 ± 0.2	25976 ± 299	101819 ± 208	193973 ± 206	7.5 ± 0.5	7.5 ± 0.5	7.4 ± 0.5

Sample Weight 0.5g

SO<sup>18</sup>FF counted at 77K

Thionyl Fluoride admitted in 6 aliquots

6.3.3 REACTION OF SULPHUR TETRAFLUORIDE AND  $\gamma$ -ALUMINA PREVIOUSLY  
CALCINED TO 523 K.

Hydrolysis of sulphur tetrafluoride took place at the surface of  $\gamma$ -alumina to form thionyl fluoride and sulphur dioxide. The volatile products after the saturation of the surface of  $\gamma$ -alumina were analysed by infra-red spectroscopy and the composition and hence the total uptake of fluorine was calculated. The results obtained are given in Table 6.3.

The admission of [ $^{35}\text{S}$ ]-sulphur labelled sulphur tetrafluoride into the system resulted in a growth of the [ $^{35}\text{S}$ ]-sulphur activity on the surface of  $\gamma$ -alumina over the first 18 min before reaching a constant level. The removal of [ $^{35}\text{S}$ ]-sulphur labelled volatile products from the system led to the removal of the surface adsorbed species as shown by the surface count rate falling to the background. If the [ $^{35}\text{S}$ ]-sulphur labelled sulphur tetrafluoride was re-admitted into the counting cell, the surface count was significantly increased, but the evacuation of the gas phase again resulted in the complete removal of the surface radioactivity with no indication of the formation of any permanently retained species. Further adsorption/desorption cycles exhibited similar characteristics to those described above, as shown in Fig 6.4.

The admission of [ $^{18}\text{F}$ ]-fluorine labelled sulphur tetrafluoride to a sample of  $\gamma$ -alumina led to a rapid initial rise in the solid count rate over the first 30 min followed by a constant value thereafter. The gas phase was removed and a fresh quantity of [ $^{18}\text{F}$ ]-fluorine labelled sulphur tetrafluoride was admitted and the increase in the solid count rate was followed with time. This procedure was

Table 6.3 The Infra-red Analysis of the Volatile Products of the Reaction of Sulphur Tetrafluoride with calcined  $\gamma$ -alumina

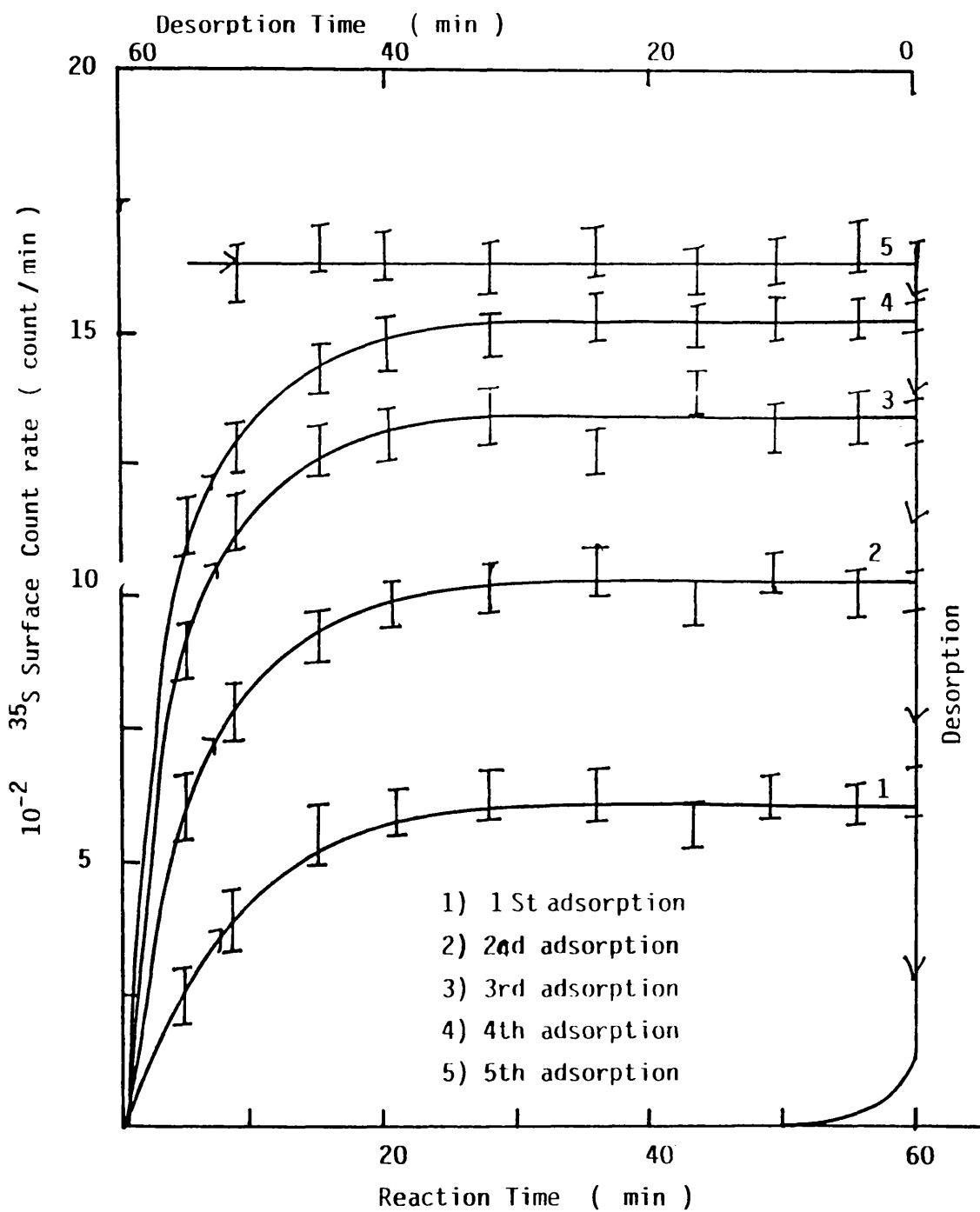
Total SF <sub>4</sub> Admitted (mmol)	Composition of Gas Products (mmol)			Total Fluorine Uptake by $\gamma$ -alumina mg atom fluorine/g
	SF <sub>4</sub>	SOF <sub>2</sub>	SO <sub>2</sub>	
6.8 ± 0.2	2.1 ± 0.1	2.6 ± 0.1	2.4 ± 0.1	14.8 ± 0.5
7.0 ± 0.2	1.7 ± 0.1	2.6 ± 0.1	2.5 ± 0.1	15.2 ± 0.5
8.1 ± 0.2	3.1 ± 0.1	2.3 ± 0.1	2.84 ± 0.1	15.8 ± 0.5
6.7 ± 0.2	1.8 ± 0.1	2.3 ± 0.1	2.5 ± 0.1	14.6 ± 0.5

Quantity of  $\gamma$ -alumina = 1.0g

Sulphur Tetrafluoride admitted was in 6 aliquots

Figure 6.4 Adsorption / Desorption Cycles of  $^{35}\text{SF}_4$  on  $\gamma$ -alumina

$^{35}\text{S}$  Surface Count Rate  $\propto$  Reaction Time  
Initial Pressure of  $^{35}\text{SF}_4 = 300$  Torr



repeated until no further increase in the solid count rate was observed as shown in Fig. 6.5. Since the initial specific count rate of [ $^{18}\text{F}$ ]-fluorine labelled sulphur tetrafluoride was known, the total uptake of fluorine by the  $\gamma$ -alumina could be calculated as follows:-



$$\text{Initial specific count rate of SF}_3^{18}\text{F} = \frac{23931+166}{\text{(mg atom F)}^{-1}} \text{ count min}^{-1}$$

After the reaction, the volatile products were counted in the presence of pyridine at 77 K, then the volatile material was removed at 195 K and counted separately at 77 K.

$$\text{Total activity in the volatile product} = 164973+417 \text{ count min}^{-1}$$

$$\text{Activity in SF}_3^{18}\text{F.pyridine} = 100389+251 \text{ count min}^{-1}$$

$$\text{Activity in SO}^{18}\text{FF at 77 K} = 59159+264 \text{ count min}^{-1}$$

$$\text{Activity in solid} = 183072+319 \text{ count min}^{-1}$$

$$\text{Radiochemical balance} = \frac{183072 + 164973}{23931 \times 4 \times 3.6} \times 100 = 101\%$$

The total uptake of fluorine

$$\text{From the solid} = \frac{183072}{23931} = 7.65 \text{ mg atom fluorine}$$

The composition of the volatile products after reaction was calculated as shown below:

$$\text{Quantity of SF}_4 = \frac{100389}{4 \times 23931} = 1.0 \text{ mmol}$$

$$\text{Quantity of SOF}_2 = \frac{59159}{2 \times 23931} = 1.24 \text{ mmol}$$

The quantity of sulphur dioxide was therefore calculated as follows:

$$\text{quantity of SO}_2 = 3.6 - (1.0 + 1.24) = 1.36 \text{ mmol}$$

The total uptake of fluorine by  $\gamma$ -alumina was therefore:-

$$1.24 \times 2 + 1.36 \times 4 = 7.92 \text{ mg atom fluorine.}$$

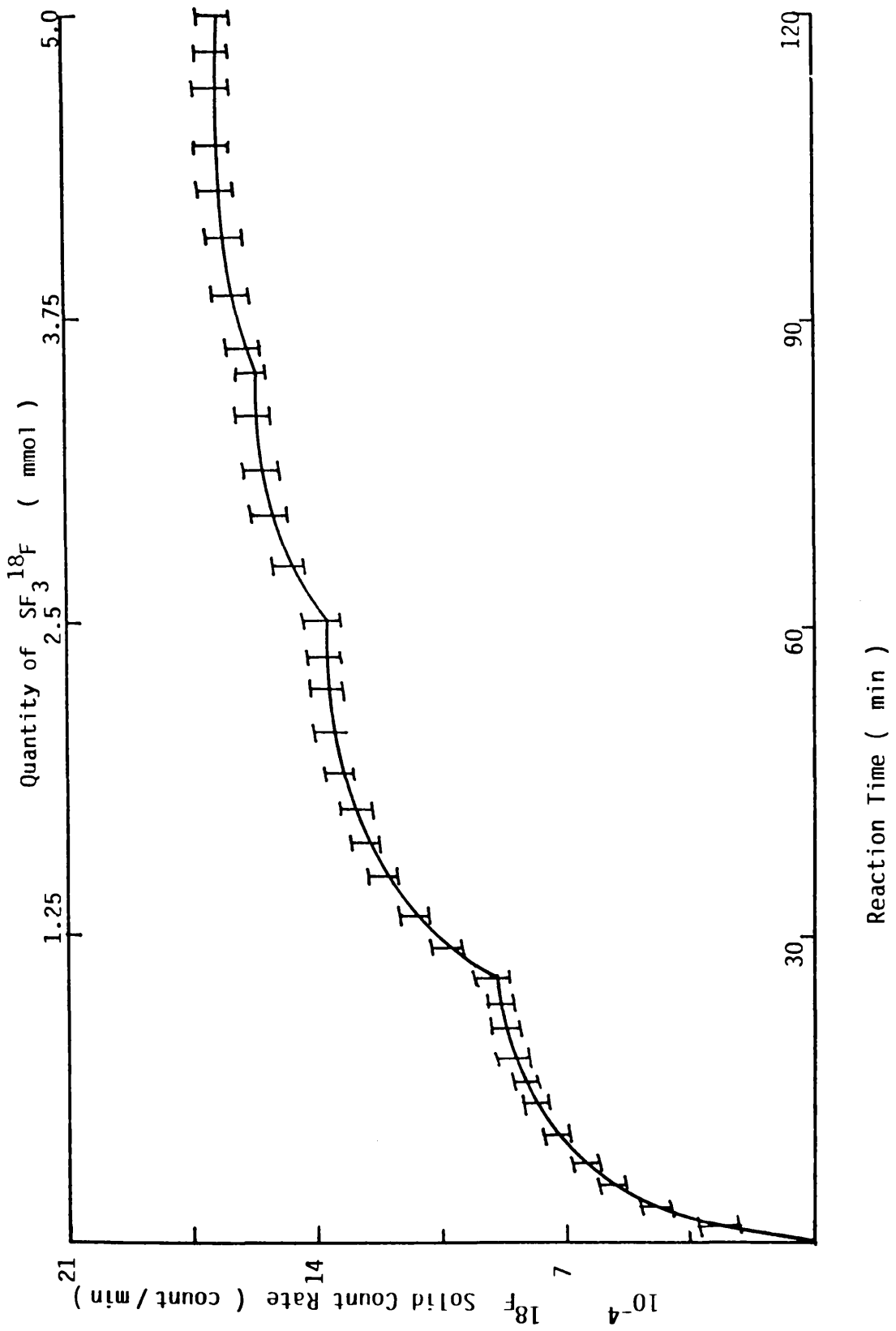


Figure 6.5 Reaction of  $\text{SF}_3^{18}\text{F}$  with calcined  $\gamma$ -alumina

The results obtained from 4 experiments are given in Table 6.4.

The three sets of data were in very good agreement, thus indicating that the total uptake of fluorine by  $\gamma$ -alumina calcined to 523 K was ca 15 mg atom fluorine (g  $\gamma$ -alumina)<sup>-1</sup>.

#### 6.3.4 REACTION OF CARBON DIOXIDE WITH $\gamma$ -ALUMINA

The reaction of [<sup>14</sup>C]-carbon labelled carbon dioxide with non-activated or calcined  $\gamma$ -alumina exhibited similar characteristics to those obtained from the reaction involving [<sup>35</sup>S]-sulphur labelled sulphur dioxide with non-activated or calcined  $\gamma$ -alumina. The variation in [<sup>14</sup>C]-carbon surface count rate as a function of time is shown in Fig. 6.6. In each reaction studied, the permanently retained species on the surface of calcined  $\gamma$ -alumina, was not removed by water vapour or by heating the solid below 693 K. Analysis of the volatile products by the infra-red spectroscopy indicated that carbon dioxide was the only gas present.

#### 6.3.5 REACTION OF CARBONYL FLUORIDE WITH $\gamma$ -ALUMINA CALCINED TO 523 K.

The room temperature reaction of carbonyl fluoride with  $\gamma$ -alumina calcined to 523 K resulted in the formation of carbon dioxide. The composition of the volatile products was calculated by means of infra-red spectroscopy and hence the total uptake of fluorine by  $\gamma$ -alumina. The results obtained are given in Table 6.5.

The experiments involving [<sup>14</sup>C]-carbon labelled carbonyl fluoride showed that there was no [<sup>14</sup>C]-carbon laydown on the surface of  $\gamma$ -alumina calcined to 523 K. However, the admission

Table 6.4 Results of Reactions of [ $^{18}\text{F}$ ]-Fluorine Labelled Sulphur Tetrafluoride with  $\gamma$ Alumina calcined to 523K

Total Quantity of $\text{SF}_4$ admitted mmol	Initial Specific Count of $\text{SF}_3^{18}\text{F}$ $\text{Count min}^{-1} (\text{mg atom F})^{-1}$	$\text{SF}_3^{18}\text{F}$		Solid Count Rate After Reaction $\text{Count min}^{-1}$	Total Uptake of Fluorine (mg atom Fluorine)	From the Gas Count Rate
		Final Gas Count Rate $\text{Count min}^{-1}$	$\text{SOF}^{18}\text{F}$			
$3.6 \pm 0.2$	$23931 \pm 211$	$100389 \pm 251$	$59159 \pm 264$	$183072 \pm 319$	$7.6 \pm 0.5$	$7.9 \pm 0.5$
$4.0 \pm 0.2$	$24623 \pm 183$	$157993 \pm 361$	$54417 \pm 136$	$181964 \pm 263$	$7.4 \pm 0.5$	$7.3 \pm 0.5$
$4.2 \pm 0.2$	$23073 \pm 247$	$156213 \pm 263$	$50523 \pm 291$	$170971 \pm 281$	$7.4 \pm 0.5$	$7.8 \pm 0.5$
$4.0 \pm 0.2$	$22989 \pm 199$	$138561 \pm 189$	$56093 \pm 147$	$173797 \pm 189$	$7.5 \pm 0.5$	$7.6 \pm 0.5$

Sample Weight 0.5g

$\text{SF}_3^{18}\text{F}$  counted as  $\text{SF}_4$  Pyridine

$\text{SOF}^{18}\text{F}$  counted at 77K

$\text{SF}_4$  admitted in 4 aliquots



Figure 6.6 Reaction of  $^{14}\text{CO}_2$  with calcined  $\gamma$ -alumina  
 $^{14}\text{C}$  Surface Count rate V Reaction Time  
Initial Pressure of = 300 Torr

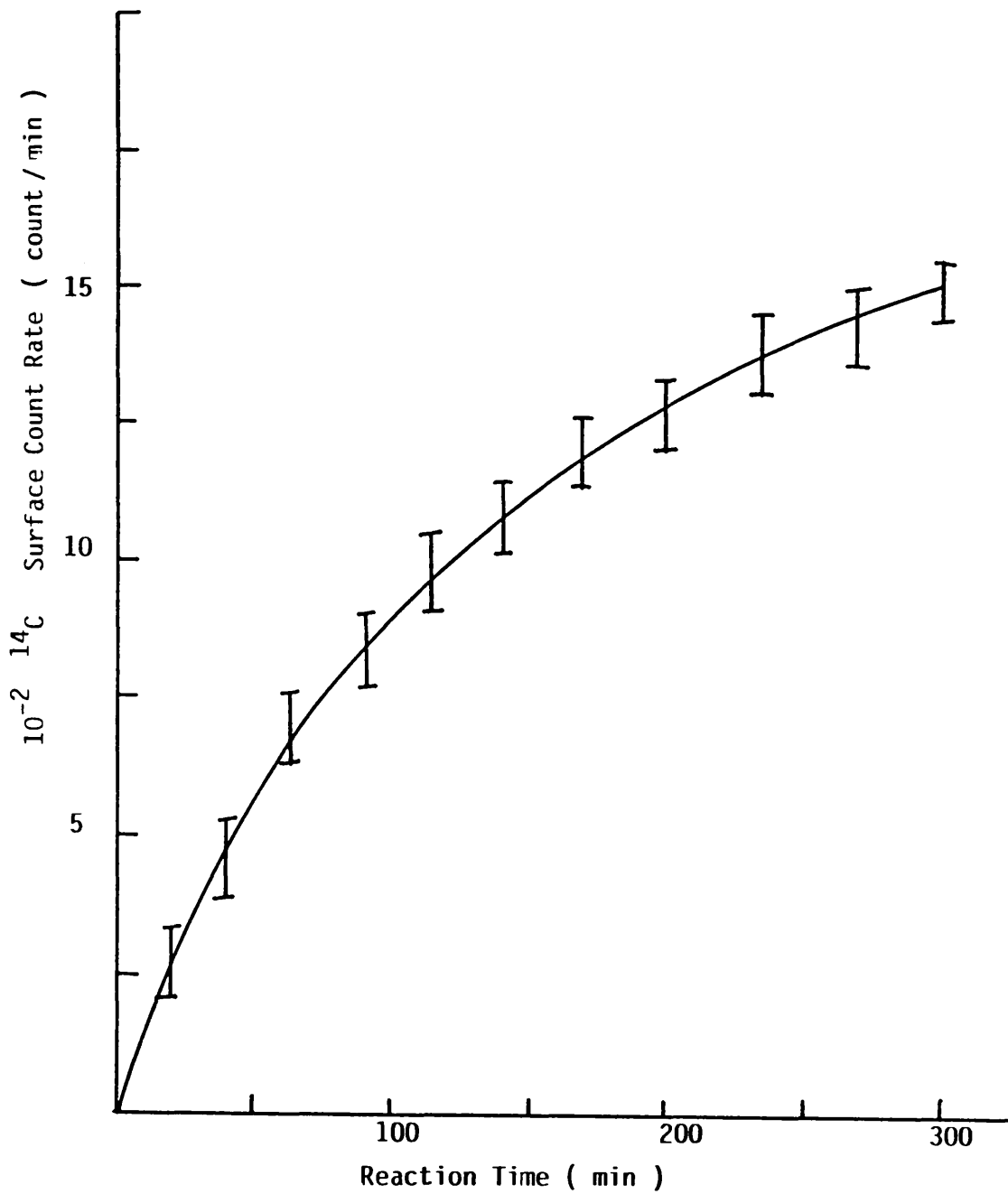


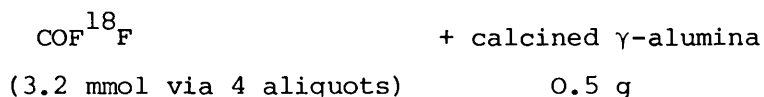
Table 6.5 The Infra-red Analysis of the Gas Products of the Reaction Between Carbonyl Fluoride with  $\gamma$ -alumina calcined to 523K

Total COF <sub>2</sub> Admitted (mmol)	Composition of Gas Products (mmol)		Total Fluorine Uptake by $\gamma$ -alumina mg atom fluorine/g
	COF <sub>2</sub>	CO <sub>2</sub>	
7.8 ± 0.2	3.1 ± 0.1	4.2 ± 0.1	8.4 ± 0.5
5.8 ± 0.2	1.5 ± 0.1	3.8 ± 0.1	7.6 ± 0.5
6.0 ± 0.2	2.4 ± 0.1	4.0 ± 0.1	8.0 ± 0.5
6.3 ± 0.2	2.7 ± 0.1	4.1 ± 0.1	8.2 ± 0.5

Quantity of  $\gamma$ -alumina 1.0g

Carbonyl Fluoride admitted was the total in 5 aliquots

of [ $^{18}\text{F}$ ]-fluorine labelled carbonyl fluoride to a sample of calcined  $\gamma$ -alumina resulted in a rapid rise in the solid count rate. A plot of the [ $^{18}\text{F}$ ]-fluorine solid count rate as a function of time and quantity of [ $^{18}\text{F}$ ]-fluorine labelled carbonyl fluoride is shown in Fig. 6.7. The total uptake of fluorine was therefore calculated as described in section 6.3.2 and an example is given as follows:-



$$\text{Initial specific count rate of COF}^{18}\text{F} = 18932 \pm 227 \text{ count min}^{-1} \text{ (mg atom F)}^{-1}$$

After reaction

$$\text{Solid count rate} = 83490 \pm 289 \text{ count min}^{-1}$$

Count rate of volatile products as a complex with CsF in MeCN

$$= 39989 \pm 208 \text{ count min}^{-1}$$

Radiochemical balance

$$\frac{39989 + 83490}{18932 \times 2 \times 3.2} \times 100 = 102\%$$

The total uptake of fluorine

$$\text{From the solid count rate} = \frac{83490 \pm 289}{18932} = 4.41 \pm 0.02 \text{ mg atom fluorine}$$

From the volatile products count rate:-

$$\text{The quantity of COF}^{18}\text{F} \text{ after reaction} = \frac{39989}{18932 \times 2} = 1.06 \text{ mmol}$$

$$\text{The quantity of CO}_2 \text{ in the volatile products} = 3.2 - 1.06 = 2.14 \text{ mmol}$$

The total uptake of fluorine by  $\gamma$ -alumina was therefore

$$2.14 \times 2 = 4.28 \text{ mg atom fluorine}$$

The results obtained from 4 experiments are given in Table 6.6. The data obtained show that the total uptake of fluorine by  $\gamma$ -alumina calcined to 523 K was ca 8.5 mg atom fluorine (g  $\gamma$ -alumina) $^{-1}$ .

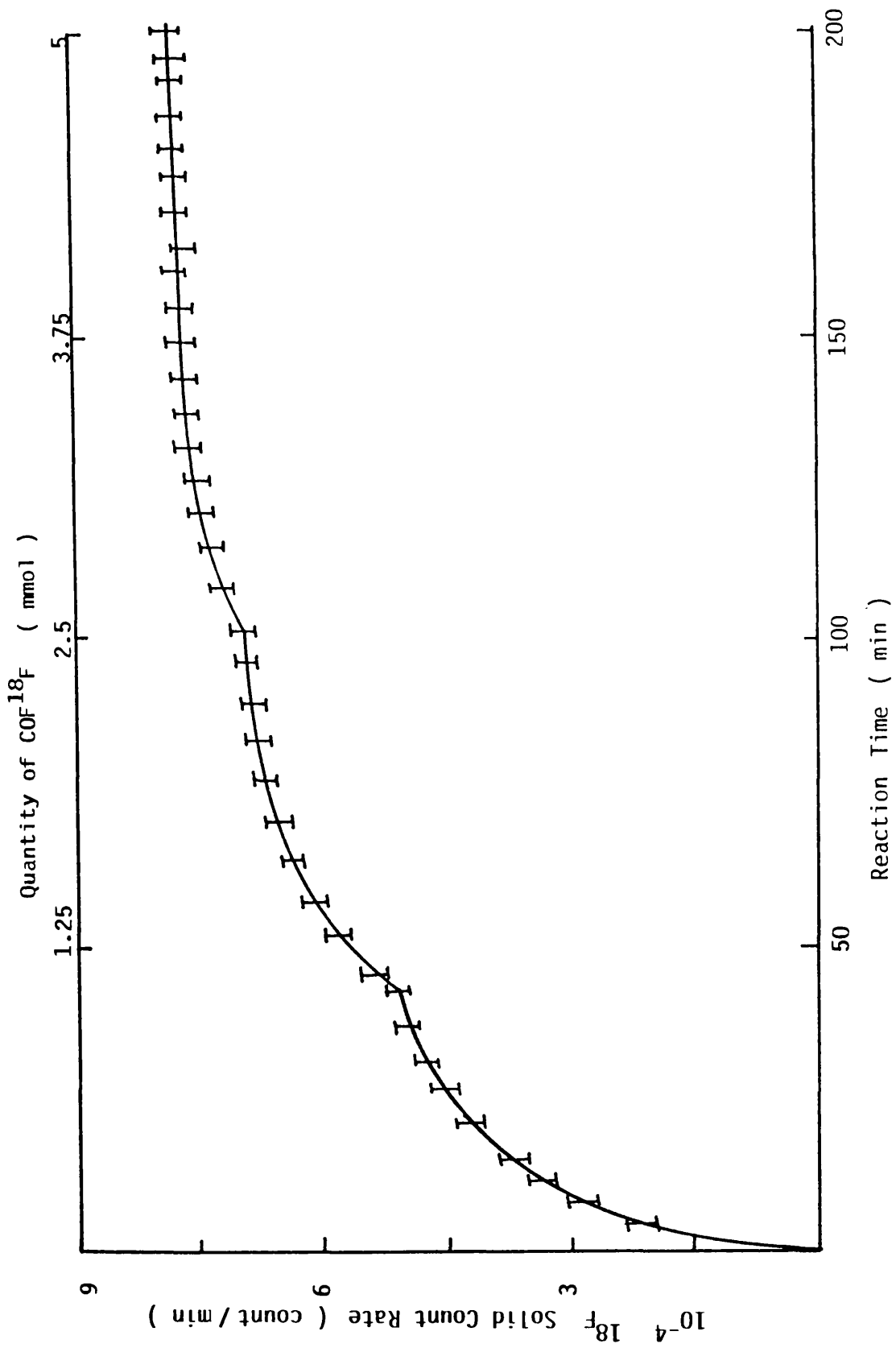


Figure 6.7 Reaction of  $\text{COF}^{18}\text{F}$  with calcined  $\gamma$ -alumina

Table 6.6 Results of Reactions of [<sup>18</sup>F]-Fluorine Labelled Carbonyl Fluoride with  $\gamma$ Alumina calcined to 523K

Total Quantity of COF <sub>2</sub> Used mmol	Initial Specific Count of CO <sup>18</sup> FF Count min <sup>-1</sup> (mg atom F) <sup>-1</sup>	Final Gas Count of CO <sup>18</sup> FF Count min <sup>-1</sup>	Solid Count Rate After Reaction Count min <sup>-1</sup>	Total Uptake of Fluorine (mg atom Fluorine)	
				From the Solid Count Rate	From the Gas Count Rate
3.2 ± 0.2	18932 ± 227	39989 ± 208	83490 ± 289	4.4 ± 0.5	4.3 ± 0.5
3.6 ± 0.2	17327 ± 185	51402 ± 157	73293 ± 137	4.2 ± 0.5	4.2 ± 0.5
4.0 ± 0.2	17763 ± 209	61993 ± 217	80999 ± 142	4.6 ± 0.5	4.5 ± 0.5
3.4 ± 0.2	16301 ± 180	42759 ± 269	66997 ± 198	4.1 ± 0.5	4.2 ± 0.5

Sample Weight 0.5g

SO<sup>18</sup>FF counted at 77K

Thionyl Fluoride admitted in 6 aliquots

6.3.6 REACTION OF ANHYDROUS HYDROGEN FLUORIDE WITH  $\gamma$ -ALUMINA  
CALCINED TO 523 K.

The reaction of anhydrous hydrogen fluoride with  $\gamma$ -alumina calcined to 523 K was studied using [ $^{18}\text{F}$ ]-fluorine labelled anhydrous hydrogen fluoride and the conventional manometric method. The total uptake of anhydrous hydrogen fluoride by  $\gamma$ -alumina at room temperature was measured using the procedure described in Chapter five (5.2). The results of 10 experiments are given in Table 6.7.

When [ $^{18}\text{F}$ ]-fluorine labelled anhydrous hydrogen fluoride was admitted to  $\gamma$ -alumina calcined to 523 K, the [ $^{18}\text{F}$ ]-fluorine count rate of the solid increased rapidly over the first 15 min before reaching a constant level after 25 min. The admission of further quantities of [ $^{18}\text{F}$ ]-fluorine labelled anhydrous hydrogen fluoride resulted in similar behaviour. This procedure was repeated until no further increase in the solid count rate was observed. The results obtained from 14 experiments are given in Table 6.8. The results showed that the total uptake of fluorine by  $\gamma$ -alumina was ca 9 mg atom fluorine  $\text{g}^{-1}$ .

6.4 REACTIONS OF PROBE MOLECULES WITH  $\gamma$ -ALUMINA FLUORINATED WITH  
SULPHUR TETRAFLUORIDE, THIONYL FLUORIDE, CARBONYL FLUORIDE OR  
ANHYDROUS HYDROGEN FLUORIDE.

6.4.1 REACTIONS OF CARBON DIOXIDE AND SULPHUR DIOXIDE WITH  $\gamma$ -ALUMINA  
FLUORINATED WITH SULPHUR TETRAFLUORIDE, THIONYL FLUORIDE,  
CARBONYL FLUORIDE OR ANHYDROUS HYDROGEN FLUORIDE.

When [ $^{35}\text{S}$ ]-sulphur labelled sulphur dioxide was allowed to react with fluorinated  $\gamma$ -alumina, the [ $^{35}\text{S}$ ]-sulphur radioactivity increased very slowly on the surface with time. The removal of the

Table 6.7 The Results of the Manometric Study of the Uptake of Anhydrous Hydrogen Fluoride by  $\gamma$ -alumina calcined to 523K

Total Quantity of AHF Used (mmol)	Total Uptake (mmol)
10.4 $\pm$ 1.0	8.9 $\pm$ 0.5
10.3 $\pm$ 1.0	8.7 $\pm$ 0.5
11.0 $\pm$ 1.0	9.2 $\pm$ 0.5
9.8 $\pm$ 1.0	9.0 $\pm$ 0.5
10.6 $\pm$ 1.0	9.3 $\pm$ 0.5
10.7 $\pm$ 1.0	8.8 $\pm$ 0.5
11.2 $\pm$ 1.0	8.9 $\pm$ 0.5
10.7 $\pm$ 1.0	9.4 $\pm$ 0.5
11.4 $\pm$ 1.0	8.6 $\pm$ 0.5
11.0 $\pm$ 1.0	9.2 $\pm$ 0.5

Sample weight 1.0g

**Table 6.8** Summary of Results of Reactions between [<sup>18</sup>F]-Fluorine Labelled Anhydrous Hydrogen Fluoride and  $\gamma$ Alumina calcined to 523K

Total Quantity of H <sup>18</sup> F Used mmol	Initial Specific Count of H <sup>18</sup> F Count min <sup>-1</sup> mmol <sup>-1</sup>	Final Gas Count of AHF Count min <sup>-1</sup>	Solid Count Rate After Reaction Count min <sup>-1</sup>	Total Uptake of AHF (mmol)
2.1 ± 0.1	98376 ± 219	116253 ± 417	88538 ± 297	0.9 ± 0.01
2.2 ± 0.1	78982 ± 136	103609 ± 296	73453 ± 326	0.93 ± 0.01
1.8 ± 0.1	83603 ± 296	75117 ± 237	73570 ± 164	0.88 ± 0.01
2.3 ± 0.1	82736 ± 317	137612 ± 182	71980 ± 103	0.87 ± 0.01
2.0 ± 0.1	69393 ± 241	73971 ± 297	65923 ± 152	0.95 ± 0.01
1.8 ± 0.1	73785 ± 255	60012 ± 183	70833 ± 166	0.96 ± 0.01
1.9 ± 0.1	74939 ± 389	74293 ± 197	69693 ± 272	0.93 ± 0.01
2.0 ± 0.1	75967 ± 247	76931 ± 207	73689 ± 289	0.97 ± 0.01
1.9 ± 0.1	98376 ± 219	96867 ± 284	87555 ± 236	0.89 ± 0.01
2.3 ± 0.1	78982 ± 136	106263 ± 346	69504 ± 317	0.88 ± 0.01
2.2 ± 0.1	83603 ± 296	107699 ± 176	80259 ± 247	0.96 ± 0.01
1.7 ± 0.1	82736 ± 317	76002 ± 248	72807 ± 187	0.88 ± 0.01
2.4 ± 0.1	69393 ± 241	111294 ± 274	57596 ± 169	0.83 ± 0.01
2.7 ± 0.1	73785 ± 255	134837 ± 175	67882 ± 261	0.92 ± 0.01
1.7 ± 0.1	74939 ± 389	59854 ± 273	70443 ± 116	0.94 ± 0.01
3.3 ± 0.1	75967 ± 247	187042 ± 296	70649 ± 367	0.93 ± 0.01

Sample Weight 0.10g  
H<sup>18</sup>F counted as CsF.HF



gas phase led to an immediate drop of the surface count rate to background. A typical experiment is shown in Fig. 6.8. However, the reactions involving [ $^{14}\text{C}$ ]-carbon labelled carbon dioxide showed different behaviour from that described above; no uptake of [ $^{14}\text{C}$ ]-carbon was observed at room temperature even at high pressure of [ $^{14}\text{C}$ ]-carbon labelled carbon dioxide.

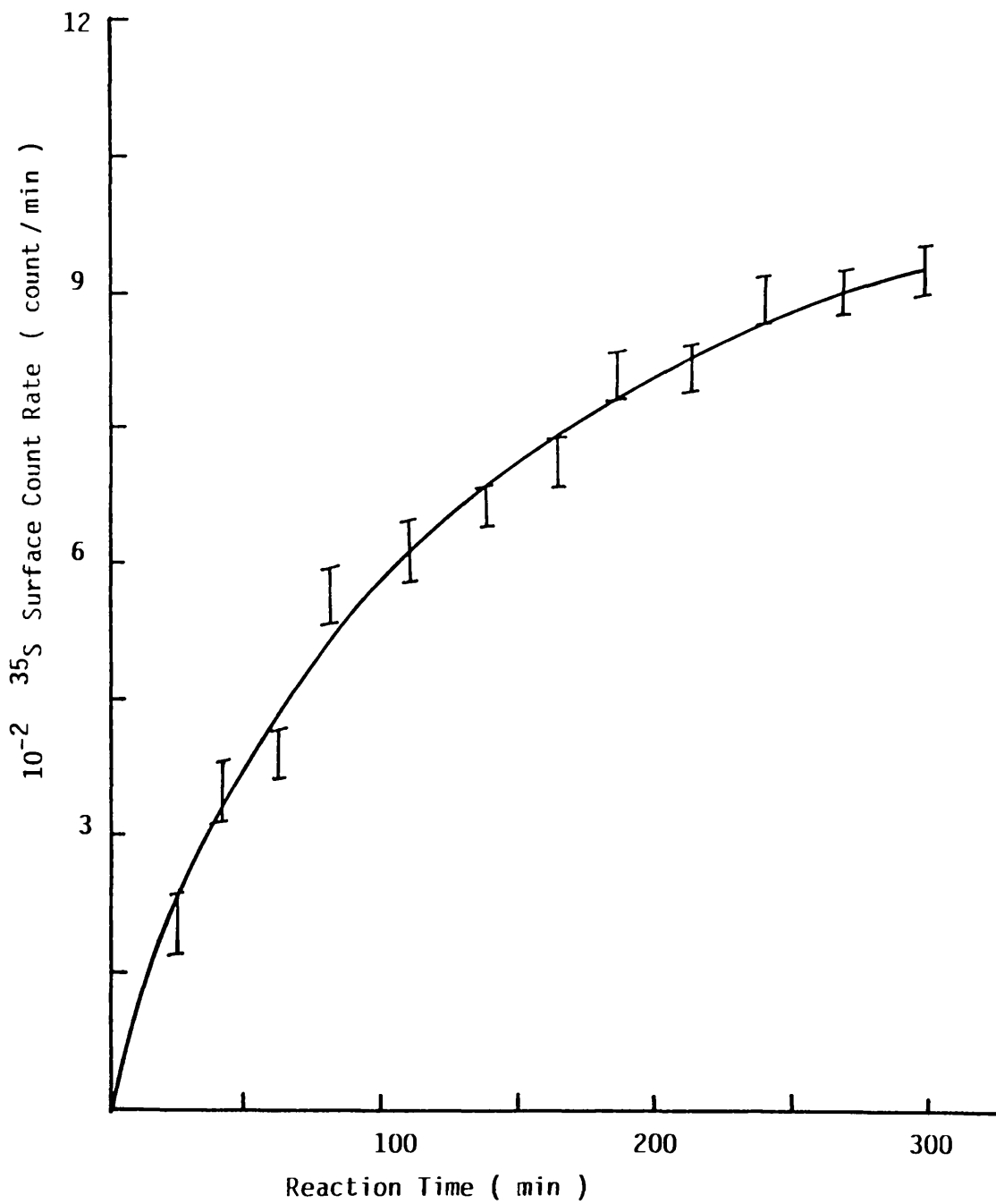
6.4.2 REACTIONS OF CARBONYL FLUORIDE AND THIONYL FLUORIDE WITH  $\gamma$ -ALUMINA FLUORINATED WITH SULPHUR TETRAFLUORIDE, THIONYL FLUORIDE OR ANHYDROUS HYDROGEN FLUORIDE.

The individual experiments using [ $^{14}\text{C}$ ]-carbon, [ $^{18}\text{F}$ ]-fluorine and [ $^{35}\text{S}$ ]-sulphur labelled carbonyl fluoride or thionyl fluoride showed that neither uptake of [ $^{14}\text{C}$ ]-carbon or of [ $^{35}\text{S}$ ]-sulphur nor [ $^{18}\text{F}$ ]-fluorine exchange occurred in the individual reactions of carbonyl fluoride or thionyl fluoride with fluorinated  $\gamma$ -alumina.

6.4.3 REACTION OF SULPHUR TETRAFLUORIDE WITH  $\gamma$ -ALUMINA FLUORINATED WITH SULPHUR TETRAFLUORIDE, THIONYL FLUORIDE, CARBONYL FLUORIDE OR ANHYDROUS HYDROGEN FLUORIDE.

The room temperature reactions of sulphur tetrafluoride and  $\gamma$ -alumina fluorinated with sulphur tetrafluoride, thionyl fluoride, carbonyl fluoride or anhydrous hydrogen fluoride were studied using [ $^{18}\text{F}$ ]-fluorine and [ $^{35}\text{S}$ ]-sulphur labelled sulphur tetrafluoride. When [ $^{35}\text{S}$ ]-sulphur labelled sulphur tetrafluoride was admitted to a sample of fluorinated  $\gamma$ -alumina, the [ $^{35}\text{S}$ ]-sulphur count rate increased rapidly over the first 5 min before reaching a constant value thereafter. Under the same conditions and using the same initial pressure of [ $^{35}\text{S}$ ]-sulphur labelled sulphur tetrafluoride, the

Figure 6.8 Reaction of  $^{35}\text{SO}_2$  with  $\gamma$ -alumina fluorinated with  $\text{SF}_4$   
 $^{35}\text{S}$  Surface Count Rate  $\nu$  Reaction Time



[<sup>35</sup>S]-sulphur surface count rate of  $\gamma$ -alumina pretreated with sulphur tetrafluoride or thionyl fluoride was higher than those obtained for  $\gamma$ -alumina pretreated with carbonyl fluoride or anhydrous hydrogen fluoride. The [<sup>35</sup>S]-sulphur surface count rates recorded over fluorinated  $\gamma$ -alumina are given in Table 6.9. The removal of the gas phase from the system led to a drop in the surface count rate to the background level. If the same pressure of [<sup>35</sup>S]-sulphur was re-admitted to the counting vessel, the surface count rate followed the same pattern as that previously described. On removal of the gas phase no surface counts remained. The [<sup>35</sup>S]-sulphur surface count rate of the fluorinated  $\gamma$ -alumina was dependent on the initial pressure of [<sup>35</sup>S]-sulphur labelled sulphur tetrafluoride as shown in Fig. 6.9

The admission of [<sup>18</sup>F]-fluorine labelled sulphur tetrafluoride to a sample of fluorinated  $\gamma$ -alumina resulted initially in a rapid rise in the solid count rate over the first 40 min followed by slower increase thereafter. The specific count rate of [<sup>18</sup>F]-fluorine labelled sulphur tetrafluoride decreased after reaction, indicating that fluorine exchange occurred. The fraction exchanged was calculated using equations 2.11 and 2.12 and the results are given in Table 6.10. The fact that identical values were obtained using these two different equations for each reaction means that there was no retention of sulphur tetrafluoride by fluorinated  $\gamma$ -alumina and the [<sup>18</sup>F]-fluorine solid count rate was due to the fluorine exchange alone.

Table 6.9 Reaction of [ $^{35}\text{S}$ ] Sulphur Labelled Sulphur Tetrafluoride with Fluorinated  $\gamma$ -alumina

Time	[ $^{35}\text{S}$ ] Sulphur Surface Count Rate (count min $^{-1}$ )			
	I	II	III	IV
2	4857 $\pm$ 317	4857 $\pm$ 390	2392 $\pm$ 391	2296 $\pm$ 361
6	4912 $\pm$ 371	4976 $\pm$ 352	2411 $\pm$ 362	2387 $\pm$ 374
14	4863 $\pm$ 391	4795 $\pm$ 391	2301 $\pm$ 317	2493 $\pm$ 317
20	4892 $\pm$ 327	4877 $\pm$ 354	2297 $\pm$ 352	2307 $\pm$ 361
26	4737 $\pm$ 317	4797 $\pm$ 363	2385 $\pm$ 361	2389 $\pm$ 357
32	4903 $\pm$ 311	4902 $\pm$ 371	2372 $\pm$ 373	2296 $\pm$ 318
38	4982 $\pm$ 391	4887 $\pm$ 353	2409 $\pm$ 394	2356 $\pm$ 310
44	4807 $\pm$ 327	4809 $\pm$ 329	2318 $\pm$ 354	2388 $\pm$ 342
50	4796 $\pm$ 316	4796 $\pm$ 318	2397 $\pm$ 342	2427 $\pm$ 392
56	4892 $\pm$ 333	4807 $\pm$ 377	2303 $\pm$ 357	2397 $\pm$ 314
62	4873 $\pm$ 347	4865 $\pm$ 362	2389 $\pm$ 365	2374 $\pm$ 367

Quantity of Solid 0.5g

I  $\gamma$ -alumina treated with  $\text{SF}_4$

II  $\gamma$ -alumina treated with  $\text{SOF}_2$

III  $\gamma$ -alumina treated with  $\text{COF}_2$

IV  $\gamma$ -alumina treated with AHF

Initial pressure of  $^{35}\text{SF}_4 = 300$  Torr

Figure 6.9 Reaction of  $^{35}\text{SF}_4$  with fluorinated  $\gamma$ -alumina

$^{35}\text{S}$  Surface Count Rate  $\propto$  Initial Pressure

- 1)  $\text{SF}_4$  treated  $\gamma$ -alumina
- 2)  $\text{COF}_2$  treated  $\gamma$ -alumina

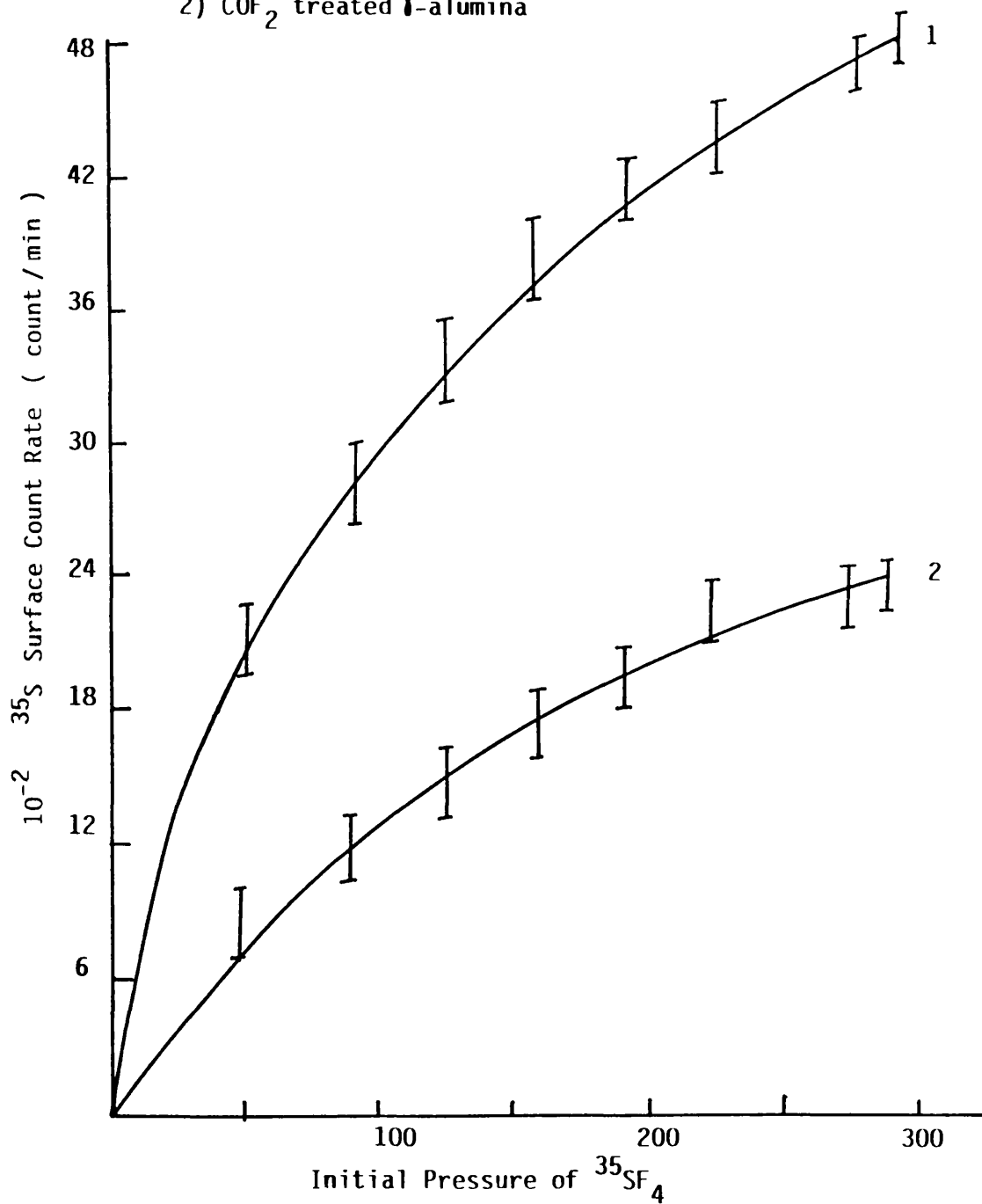


Table 6.10 Results of Reactions of [<sup>18</sup>F]-Fluorine Labelled Sulphur Tetrafluoride γAlumina Fluorinated with Probe Molecules

Material	Sample Weight of mmol	Quantity of F <sub>3</sub> <sup>18</sup> F Torr mmol	Starting Specific Count Rate of SF <sub>3</sub> <sup>18</sup> F Count min <sup>-1</sup> (mg atom F) <sup>-1</sup>	Specific Count Rate of SF <sub>3</sub> <sup>18</sup> F After Reaction Count min <sup>-1</sup> (mg atom F) <sup>-1</sup>	Solid Count Rate After Reaction Count min <sup>-1</sup>	Fraction Exchanged
FI	0.5 ± 0.01	3.00 ± 2	35768 ± 217	25925 ± 185	38585 ± 307	0.42
	7.6 ± 0.06	1.0 ± 0.06				0.41
FII	0.5 ± 0.01	3.00 ± 2	35768 ± 217	26394 ± 276	38297 ± 184	0.40
	7.6 ± 0.06	1.0 ± 0.06				0.40
FIII	0.5 ± 0.01	3.00 ± 2	32791 ± 300	23552 ± 108	36217 ± 273	0.42
	7.6 ± 0.06	1.0 ± 0.06				0.42
FIII	0.5 ± 0.01	3.00 ± 2	32791 ± 300	23768 ± 211	36813 ± 148	0.43
	7.6 ± 0.06	1.0 ± 0.06				0.43
FIII	0.5 ± 0.01	3.00 ± 2	36803 ± 285	28271 ± 276	33785 ± 157	0.45
	4.25 ± 0.06	1.0 ± 0.06				0.44
FIII	0.5 ± 0.01	3.00 ± 2	36803 ± 285	28651 ± 189	33260 ± 237	0.43
	4.25 ± 0.06	1.0 ± 0.06				0.44
FIV	0.5 ± 0.01	3.00 ± 2	37917 ± 187	30273 ± 208	29964 ± 176	0.38
	4.52 ± 0.06	1.0 ± 0.06				0.37
FIV	0.5 ± 0.01	3.00 ± 2	37917 ± 187	30072 ± 167	32321 ± 244	0.39
	4.52 ± 0.06	1.0 ± 0.06				0.40

FI γ-alumina treated with Sulphur Tetrafluoride

FII γ-alumina treated with Thionyl Fluoride

FIII γ-alumina treated with Carbonyl Fluoride

FIV γ-alumina treated with Anhydrous Hydrogen Fluoride

6.4.4 REACTION OF  $^{18}\text{F}$  LABELLED ANHYDROUS HYDROGEN FLUORIDE WITH  
FLUORINATED  $\gamma$ -ALUMINA

Reactions of anhydrous hydrogen fluoride with fluorinated  $\gamma$ -alumina were studied using [ $^{18}\text{F}$ ]-fluorine labelled anhydrous hydrogen fluoride. The admission of [ $^{18}\text{F}$ ]-fluorine labelled anhydrous hydrogen fluoride to a sample of fluorinated  $\gamma$ -alumina resulted in a rapid growth in the solid count rate over the first 40 min, then a constant value thereafter. The [ $^{18}\text{F}$ ]-fluorine count rate recorded for solid  $\gamma$ -alumina pretreated with carbonyl fluoride or anhydrous hydrogen fluoride was higher than those recorded with  $\gamma$ -alumina pretreated with sulphur tetrafluoride or thionyl fluoride, under the same conditions. The fraction exchanged was calculated using equations 2.11 and 2.12. The values obtained from these two different equations for each experiment were identical. This was consistent with that, no retention of anhydrous hydrogen fluoride by fluorinated  $\gamma$ -alumina and the increase in the solid count rate was due totally to [ $^{18}\text{F}$ ]-fluorine exchange. The fraction exchanged was 0.98, 0.99, 0.58 and 0.57 respectively, for  $\gamma$ -alumina pretreated with anhydrous hydrogen fluoride, carbonyl fluoride, sulphur tetrafluoride and thionyl fluoride after reaction with [ $^{18}\text{F}$ ]-fluorine labelled anhydrous hydrogen fluoride. The results obtained are given in Table 6.11.

The admission of [ $^{18}\text{F}$ ]-fluorine labelled anhydrous hydrogen fluoride to a sample of anhydrous aluminium(III) fluoride preactivated at 395 K under vacuum, showed that no [ $^{18}\text{F}$ ]-fluorine activity was incorporated into the solid. This means that there was no reaction between anhydrous hydrogen fluoride and anhydrous aluminium(III) fluoride. However, a solid aluminium(III) fluoride sample

**Table 6.11 Results of Reactions of [<sup>18</sup>F]-Fluorine Labelled Anhydrous Hydrogen Fluoride and  $\gamma$ -Alumina Fluorinated with Probe Molecules**

Material	Sample Weight Of mmol	Quantity of F <sub>3</sub> <sup>18</sup> F Torr mmol	Specific Count Rate of H <sup>18</sup> F Count min <sup>-1</sup> mmol <sup>-1</sup>		Solid Count Rate After Reaction Count min <sup>-1</sup>	Fraction Exchanged	
			Initial	Final		Eq 2.11	Eq 2.12
FI	0.5 ± 0.01	1 ± 0.06	134961 ± 321	65786 ± 243	71250 ± 251	0.58	0.59
	7.6 ± 0.06						
FII	0.5 ± 0.01	1 ± 0.06	134961 ± 321	66978 ± 204	65944 ± 193	0.57	0.56
	7.6 ± 0.06						
FIII	0.5 ± 0.01	1 ± 0.06	123035 ± 275	58885 ± 163	66075 ± 205	0.59	0.60
	7.6 ± 0.06						
FIII	0.5 ± 0.01	1 ± 0.06	123035 ± 275	59972 ± 189	61172 ± 193	0.58	0.57
	7.6 ± 0.06						
FIII	0.5 ± 0.01	1 ± 0.06	127219 ± 172	25262 ± 178	10515 ± 148	0.99	1.0
	4.25 ± 0.06						
FIII	0.5 ± 0.01	1 ± 0.06	127219 ± 172	23202 ± 183	102976 ± 197	1.01	1.0
	4.25 ± 0.06						
FIV	0.5 ± 0.01	1 ± 0.06	125932 ± 259	24876 ± 306	105098 ± 178	0.99	0.99
	4.52 ± 0.06						
FIV	0.5 ± 0.01	1 ± 0.06	125932 ± 259	25907 ± 147	97023 ± 176	0.97	0.96
	4.52 ± 0.06						
FV	$\gamma$ -alumina treated with Sulphur Tetrafluoride $\gamma$ -alumina treated with Thionyl Fluoride $\gamma$ -alumina treated with Carbonyl Fluoride $\gamma$ -alumina treated with Anhydrous Hydrogen Fluoride						



was exposed to water vapour in the reactor for 1 h, at the end of which the solid was pumped in situ for 1 h. When the solid was then exposed to gaseous [ $^{18}\text{F}$ ]-fluorine labelled anhydrous hydrogen fluoride a significant surface count rate was detected on the solid. In all these experiments involving aluminium(III) fluoride exposed to water vapour [ $^{18}\text{F}$ ]-fluorine exchange occurred; the extent of the exchange was not complete. The results obtained are given in Table 6.12 based on the assumption that all the fluorines are exchangeable in the case of aluminium(III) fluoride which had been exposed to water vapour before reaction.

Table 6.12 Results of Reactions of [<sup>18</sup>F]-Fluorine Labelled Anhydrous Hydrogen Fluoride with Aluminium (III) Fluoride

Material	Sample Weight g mmol	Quantity of H <sup>18</sup> F Torr mmol	Specific Count Rate of H <sup>18</sup> F Count min <sup>-1</sup> mmol <sup>-1</sup>		Solid Count Rate After Reaction Count min <sup>-1</sup>	Fraction Exchanged	
			Initial	Final		Eq 2.11	Eq 2.12
FV	0.5 ± 0.01	1 ± 0.06	137281 ± 319	137387 ± 417	53 ± 7	0	0
	5.95 ± 0.06						
FVI	0.5 ± 0.01	1 ± 0.06	132147 ± 284	132261 ± 317	101 ± 17	0	0
	5.95 ± 0.06						
FV	0.5 ± 0.01	1 ± 0.06	129797 ± 410	24430 ± 291	101048 ± 417	0.86	0.85
	5.95 ± 0.06						
FVI	0.5 ± 0.01	1 ± 0.06	138962 ± 381	21027 ± 382	126953 ± 296	0.90	0.91
	5.95 ± 0.06						
FV	0.5 ± 0.01	1 ± 0.06	130662 ± 302	23386 ± 432	114367 ± 397	0.87	0.88
	5.95 ± 0.06						

FV Anhydrous aluminium (III) fluoride

FVI Anhydrous aluminium (III) fluoride exposed to water vapour

## CHAPTER SEVEN

CATALYTIC ACTIVITY OF CAESIUM OR POTASSIUM FLUORIDE SUPPORTED  
ON  $\gamma$ -ALUMINA FLUORINATED AT ROOM TEMPERATURE.

7.1 INTRODUCTION

The reaction of sulphur tetrafluoride and chlorine monofluoride in the presence of caesium or potassium fluoride supported on  $\gamma$ -alumina prepared from aqueous or non-aqueous solution or by mixing the solids together under nitrogen, and treated by various inorganic fluorinating agents, is reported in this chapter.

7.2 EXPERIMENTAL

The procedure used for the radiotracer experiments was the same as that described in Chapter 5. Where appropriate, reaction mixtures containing, chlorine monofluoride, sulphur tetrafluoride and sulphur chloride pentafluoride, were analysed by separating them into their individual components by low temperature, trap-to-trap distillation, chlorine monofluoride being identified by vapour pressure and sulphur tetrafluoride and sulphur chloride pentafluoride by their infra-red spectra and molecular weight determination after transfer to a Pyrex vacuum system.

Due to the large number of solids used to catalyse the chlorofluorination of sulphur tetrafluoride by chlorine monofluoride, code numbers are used for classification as follows:

- MFAI MF/ $\gamma$ -alumina prepared from aqueous solution and fluorinated with sulphur tetrafluoride.
- MFAII MF/ $\gamma$ -alumina prepared from aqueous solution and fluorinated with thionyl fluoride.

MFAlIII MF/ $\gamma$ -alumina prepared from aqueous solution and fluorinated with carbonyl fluoride.

MFAlIV MF/ $\gamma$ -alumina prepared from aqueous solution and fluorinated with anhydrous hydrogen fluoride.

MFAV MF/ $\gamma$ -alumina prepared from aqueous solution and fluorinated with sulphur dioxide then anhydrous hydrogen fluoride.

MFNI-  
MFNV are the codes of MF/ $\gamma$ -alumina prepared from non-aqueous solution and treated as described above.

MFDI-  
MFDV are the codes of MF/ $\gamma$ -alumina prepared by mixing the two solids together at room temperature and treated as described above.

M = Caesium or Potassium

A = Aqueous

N = Non-aqueous

D = Dry preparation

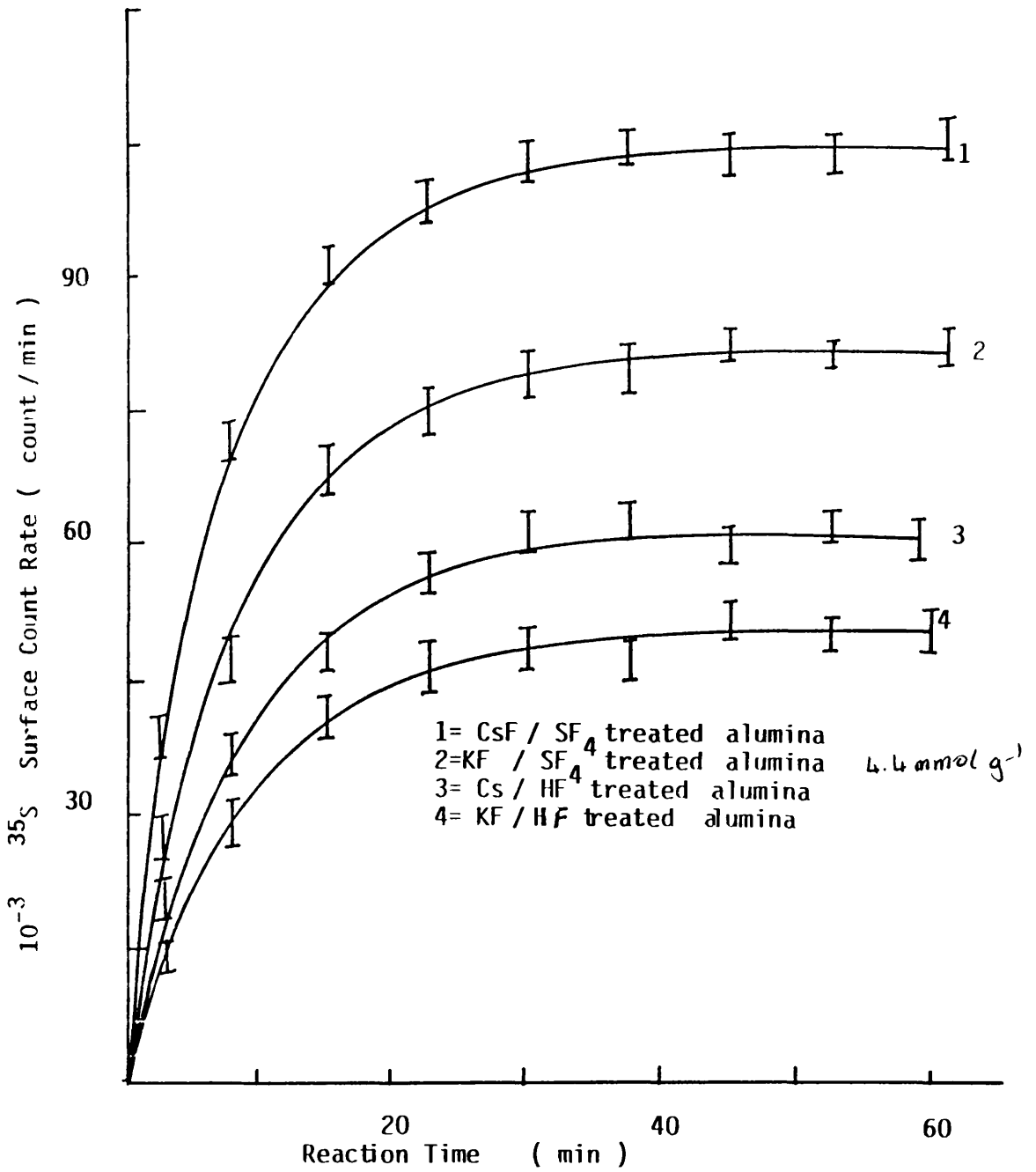
### 7.3 REACTIONS OF SULPHUR AND CHLORINE CONTAINING SPECIES WITH CAESIUM OR POTASSIUM FLUORIDE SUPPORTED ON FLUORINATED $\gamma$ -ALUMINA.

Before the oxidative addition of sulphur tetrafluoride by chlorine monofluoride utilising metal fluoride supported on fluorinated  $\gamma$ -alumina as a catalyst was carried out, the separate reactions of chlorine monofluoride and sulphur tetrafluoride and the product sulphur chloride pentafluoride with metal fluoride supported on  $\gamma$ -alumina fluorinated at room temperature were studied and are updated below.

7.3.1 REACTION OF SULPHUR TETRAFLUORIDE WITH CAESIUM OR  
POTASSIUM FLUORIDE SUPPORTED ON  $\gamma$ -ALUMINA FLUORINATED  
AT ROOM TEMPERATURE.

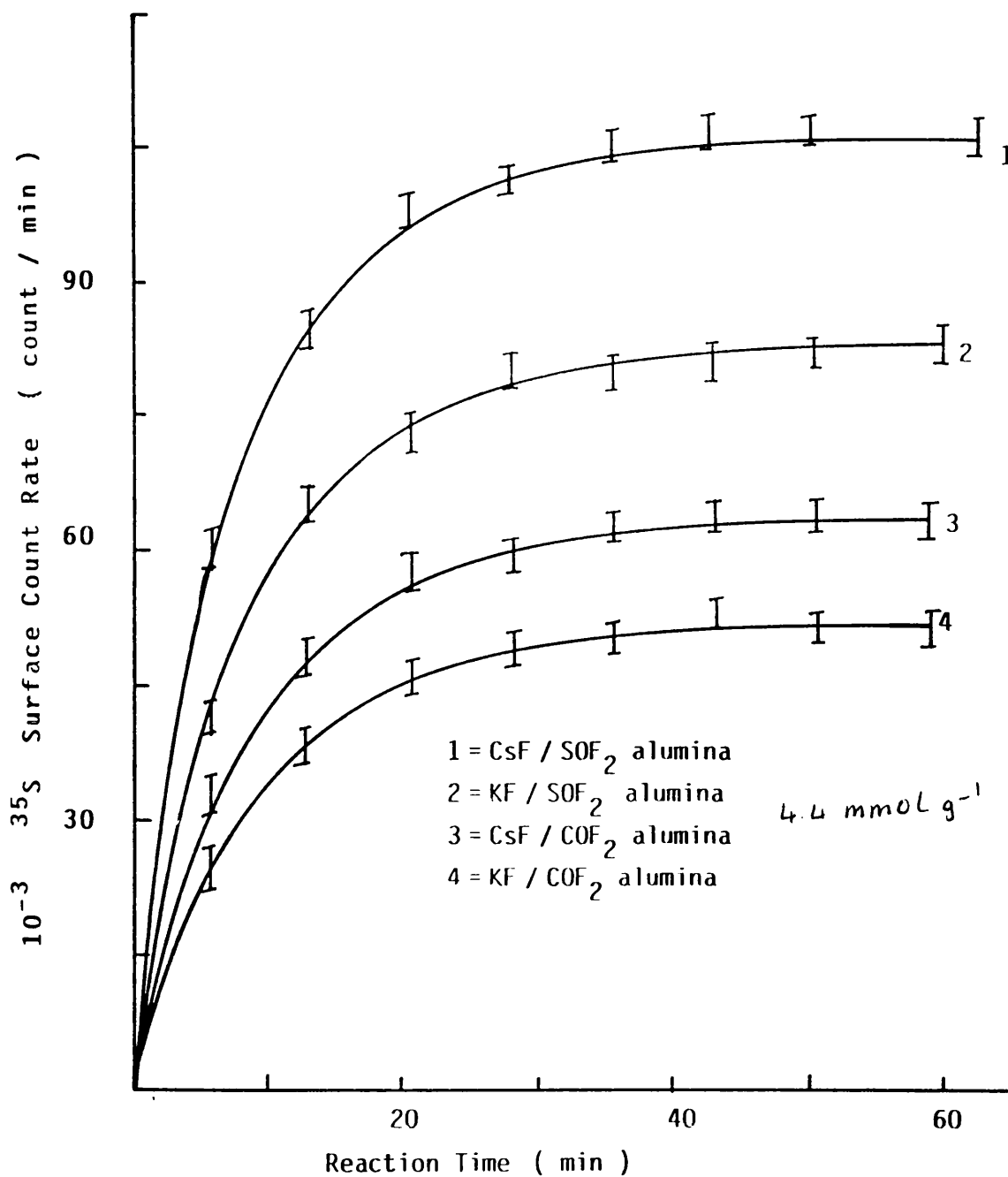
The room temperature reaction between sulphur tetrafluoride and the metal fluoride supported on fluorinated  $\gamma$ -alumina prepared and treated in various ways, was studied using [ $^{35}\text{S}$ ]-sulphur labelled sulphur tetrafluoride. The growth of the [ $^{35}\text{S}$ ]-sulphur count rate on the surface of the supported metal fluoride was followed with time in each experiment, and plots are given in Figs. 7.1 - 7.3 for initial reactant pressures of 300 Torr. The behaviour of sulphur tetrafluoride towards metal fluoride supported on fluorinated  $\gamma$ -alumina was similar to that towards metal fluoride supported on  $\gamma$ -alumina as reported in Chapter 5, but no hydrolysis of sulphur tetrafluoride was observed in any case except with MFA, MFN or MFD(III) (carbonyl fluoride fluorinated materials) where the formation of thionyl fluoride took place, and in consequence, work using these materials was discontinued. Under the same conditions, the samples MFA and MFN(I,II and V) appeared to take up more [ $^{35}\text{S}$ ]-sulphur labelled sulphur tetrafluoride, but the [ $^{35}\text{S}$ ]-sulphur surface count rate after desorption of [ $^{35}\text{S}$ ]-sulphur labelled sulphur tetrafluoride at room temperature was identical to that reported for metal fluoride supported on  $\gamma$ -alumina. The adsorption/desorption cycles of [ $^{35}\text{S}$ ]-sulphur labelled sulphur tetrafluoride by fluorinated  $\gamma$ -alumina supported metal fluoride had no effect on the initial surface count rate in the presence of gas or after desorption as shown in Fig. 7.4. Less uptake

Figure 7.1 Reaction of  $^{35}\text{SF}_4$  with MF/fluorinated alumina prepared from aqueous solution Surface count rate



Initial pressure of  $^{35}\text{SF}_4 = 300$  Torr

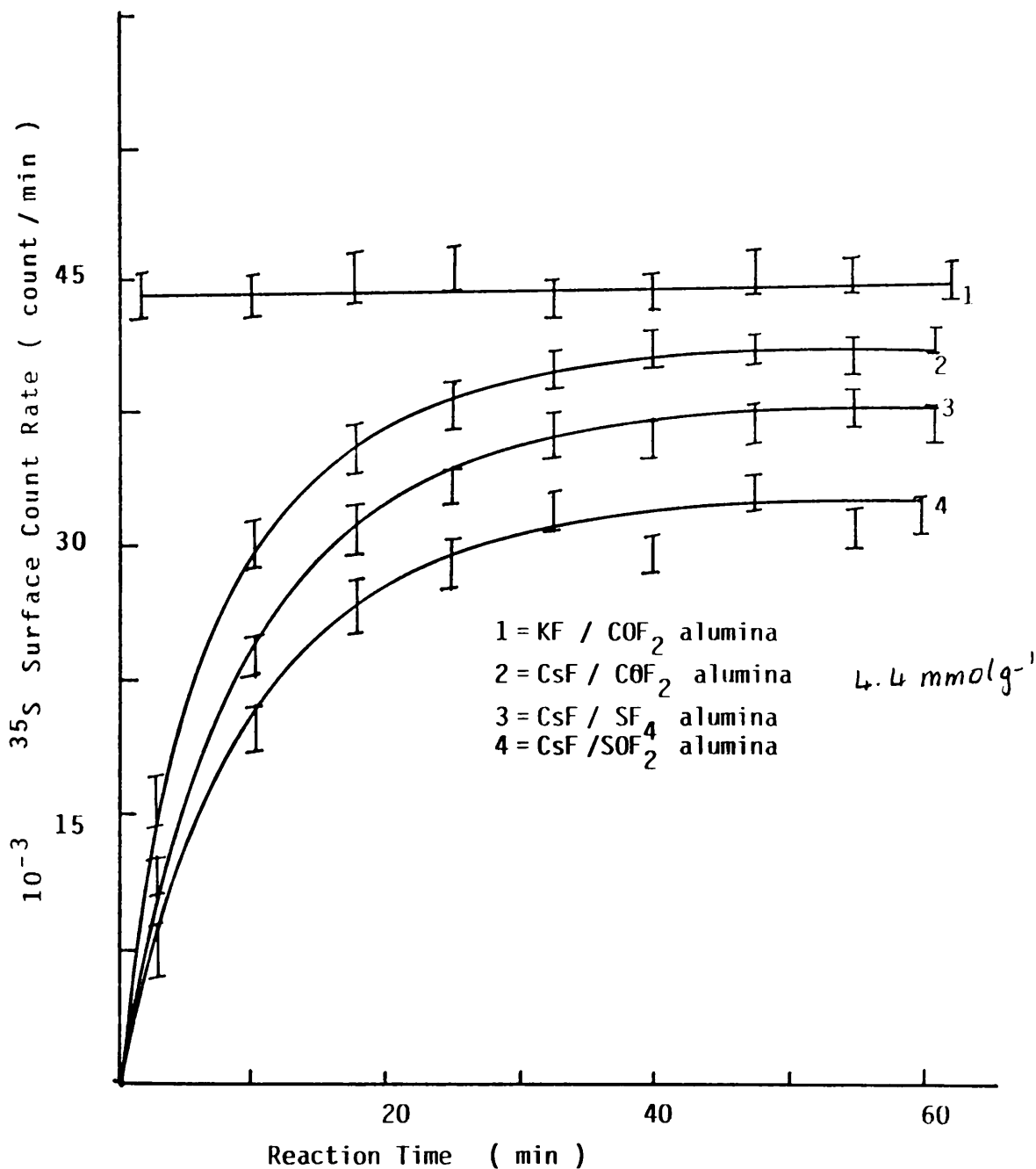
Figure 7.2 Reaction of  $^{35}\text{SF}_4$  with MF / fluorinated alumina prepared from nonaqueous solution Surface count rate



Initial pressure of  $^{35}\text{SF}_4 = 300$  Torr

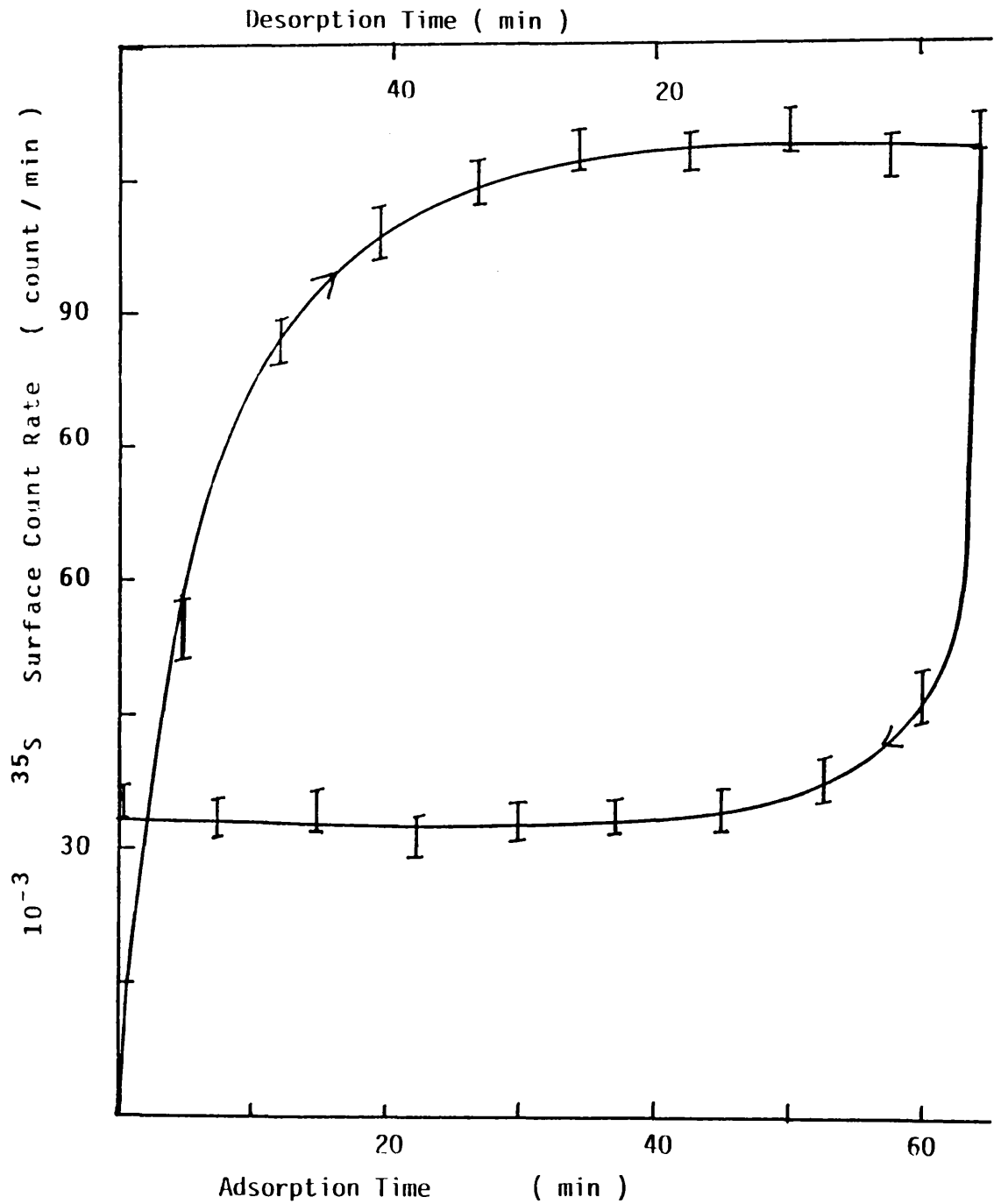


Figure 7.3 Reaction of  $^{35}\text{SF}_4$  with MF / fluorinated alumina prepared from dry reaction Surface count rate



Initial pressure of  $^{35}\text{SF}_4 = 300$  Torr

Figure 7.4  $^{35}\text{SF}_4$  adsorption / desorption at MFA I  $4.4 \text{ mmol g}^{-1}$



Initial pressure of  $^{35}\text{SF}_4 = 300 \text{ Torr}$

of [ $^{35}\text{S}$ ]-sulphur labelled sulphur tetrafluoride by MFN or MFA (IV) than the values reported in Chapter 5 was observed. The reactions involving MFD (I-V) showed different behaviour, in that under the same conditions and using the same initial pressure of [ $^{35}\text{S}$ ]-sulphur labelled sulphur tetrafluoride, the [ $^{35}\text{S}$ ]-sulphur surface count rate in the presence of gas and after desorption was different from one sample to another. Sometimes no retention of radioactivity was observed. The results are shown in Table 7.1. Since the uptake of sulphur tetrafluoride by MFD (I-V) was not reproducible, work utilising MFD (I-V) catalyst samples was discontinued.

### 7.3.2 REACTION BETWEEN SULPHUR CHLORIDE PENTAFLUORIDE AND CAESIUM OR POTASSIUM FLUORIDE SUPPORTED ON FLUORINATED $\gamma$ -ALUMINA.

The admission of [ $^{35}\text{S}$ ]-sulphur or [ $^{36}\text{Cl}$ ]-chlorine labelled sulphur chloride pentafluoride into the counting cell containing a sample of a catalyst led to a very small uptake of radioactivity by the surface. However, this was completely removed by evacuation at room temperature. The [ $^{35}\text{S}$ ]-sulphur and [ $^{36}\text{Cl}$ ]-chlorine surface count rates of MFA and MFN (I, II and V) as a function of time are shown in Figs. 7.5 and 7.6. The [ $^{35}\text{S}$ ]-sulphur surface count rate was independent of the initial pressure of [ $^{35}\text{S}$ ]-sulphur labelled sulphur chloride pentafluoride in the range 50 - 300 Torr.

Table 7.1      The [<sup>35</sup>S]-Sulphur Surface Count Rate of Caesium  
or Potassium Fluoride Supported on  $\gamma$ -Alumina  
Prepared under Dry Conditions and Treated by  
Sulphur Tetrafluoride.

Run	Batch	Sample	Surface Count Rate			
			M = Cs		M = K	
			A	B	A	B
1	1	1	9832	2910	4321	2131
2		2	4117	32	961	11
3		3	6911	797	1937	39
1	2	1	1039	0	8372	2093
2		2	7834	2341	3737	174
1	3	1	3241	67	5796	1997
2		2	8327	3031	1796	30
3		3	2032	983	531	0
1	4	1	5741	1349	8397	2137
2		2	1000	17	634	0

Sample Weight    M = Cs    0.5g                      M = K 0.38g (1.32 mmol)

Initial pressure    300 Torr.

Figure 7.5 Reaction of  $^{35}\text{SF}_5\text{Cl}$  with MF / fluorinated alumina prepared from aqueous solution Surface count rate

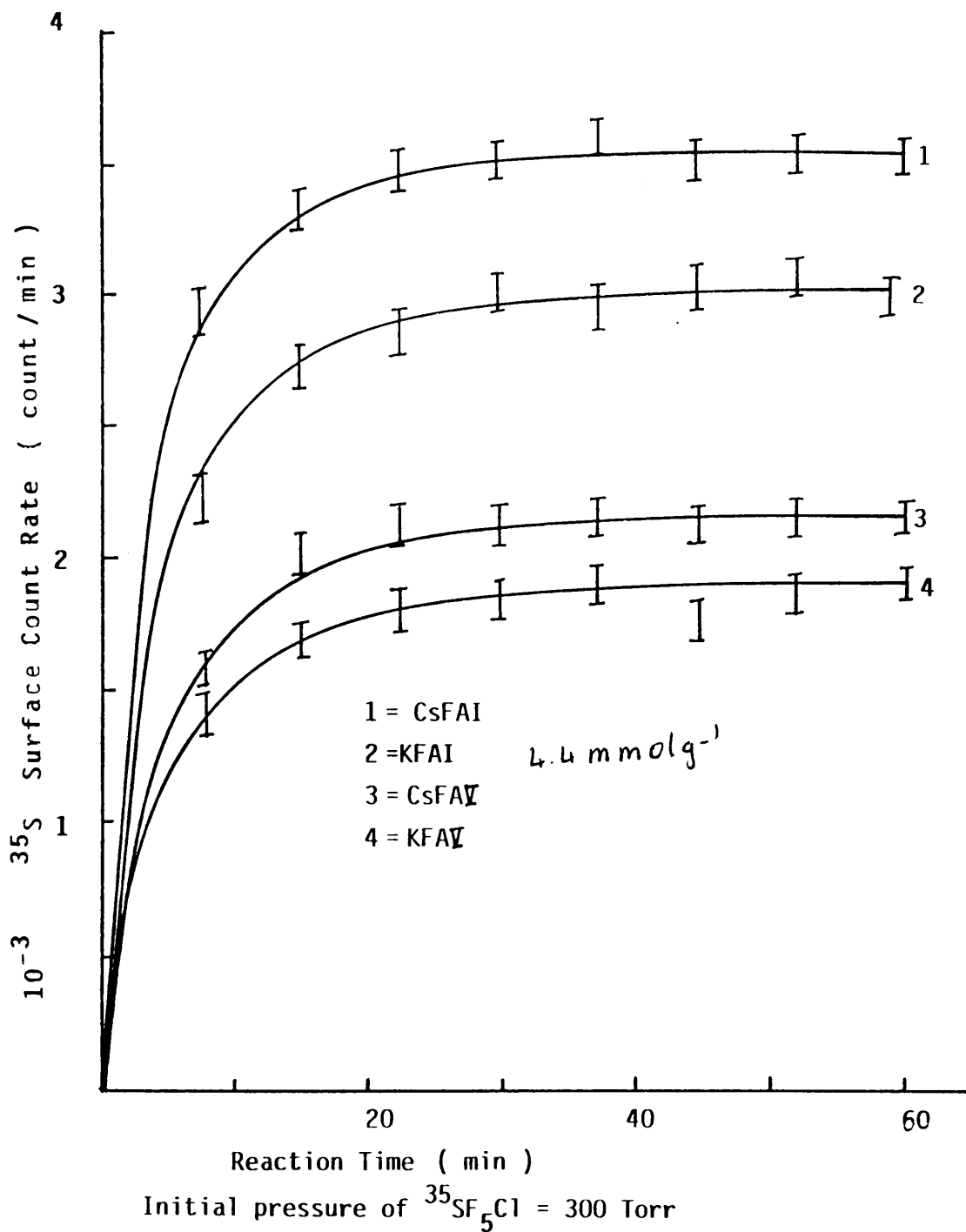
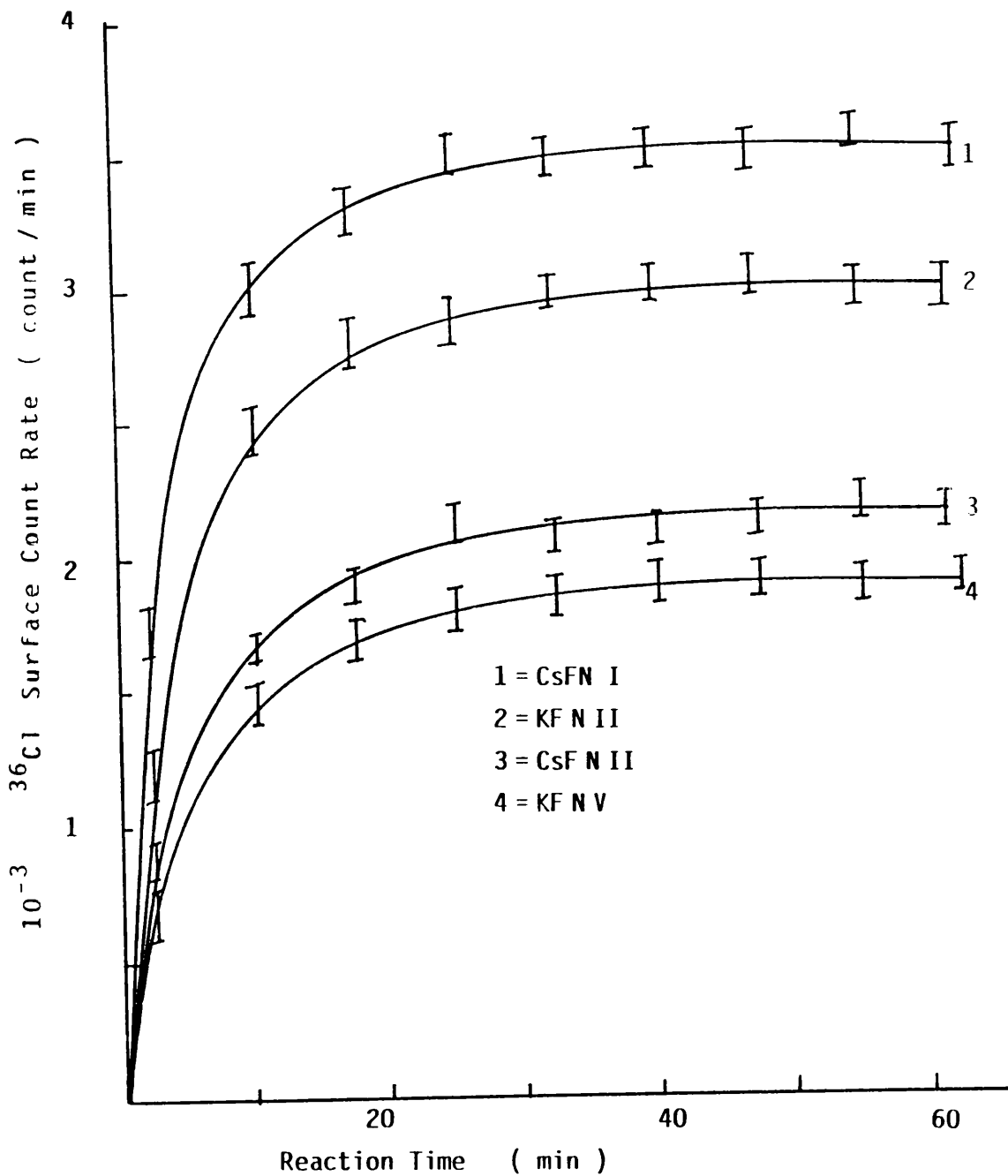


Figure 7.6 Reaction of  $SF_5^{36}Cl$  with MF / fluorinated alumina prepared from nonaqueous solution Surface count rate

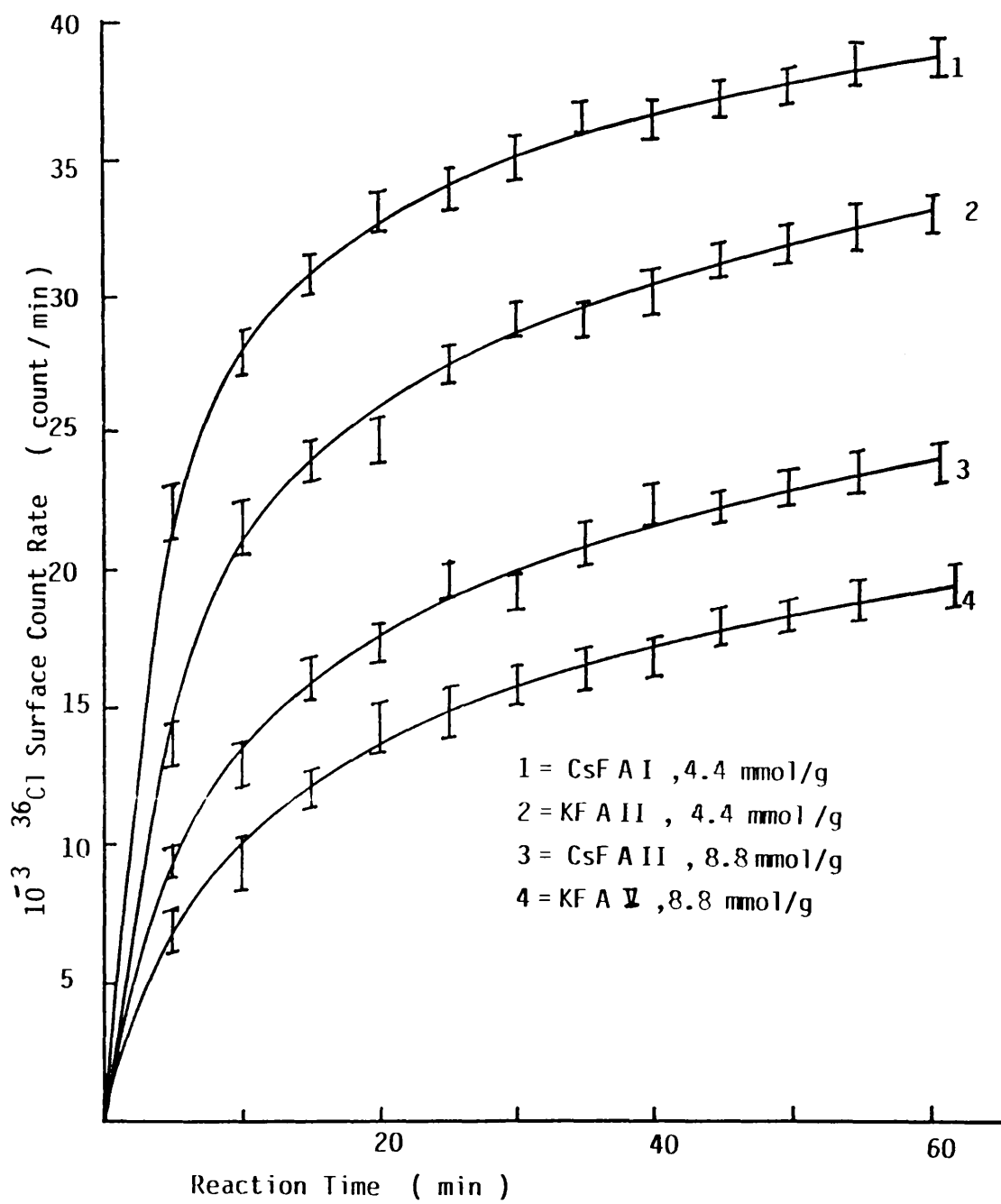


Initial pressure of  $SF_5^{36}Cl$  = 300 Torr

7.3.3 REACTION BETWEEN CHLORINE MONOFLUORIDE AND CAESIUM  
OR POTASSIUM FLUORIDE SUPPORTED ON FLUORINATED  
 $\gamma$ -ALUMINA.

The reaction between chlorine monofluoride and caesium or potassium fluoride supported on  $\gamma$ -alumina prepared from aqueous or non-aqueous solution and treated with various inorganic agents, across the composition range, 0.6 - 20.0 mmol g<sup>-1</sup>, was studied using [<sup>36</sup>Cl]-chlorine labelled chlorine monofluoride and by conventional manometric methods at initial gas pressures in the range 10 - 300 Torr. In each experiment the admission of [<sup>36</sup>Cl]-chlorine labelled chlorine monofluoride to a sample of MFA or MFN (I, II or V) resulted in a rapid initial growth in the [<sup>36</sup>Cl]-chlorine count rate on the surface of the solid over the first 5 min followed, therefore, by a relatively slow process. Plots of the [<sup>36</sup>Cl]-chlorine count rate of the surface of MFA and MFN (I, II and V), 4.4 and 8.8 mmol g<sup>-1</sup> using initial pressures of 60 and 160 Torr are given in Figs. 7.7 and 7.8. When the gas phase was removed at room temperature, no decrease in the surface count rate was observed. Re-admission of a similar quantity or further additions of [<sup>36</sup>Cl]-chlorine labelled chlorine monofluoride had no effect on the initial [<sup>36</sup>Cl]-chlorine count rate of the surface. Thus, the uptake of chlorine monofluoride was irreversible at room temperature, in contrast to the behaviour of [<sup>35</sup>S]-sulphur labelled sulphur tetrafluoride, where weakly absorbed and permanently retained species were both present. This surface activity was removed at 553 K or by the admission of water vapour.

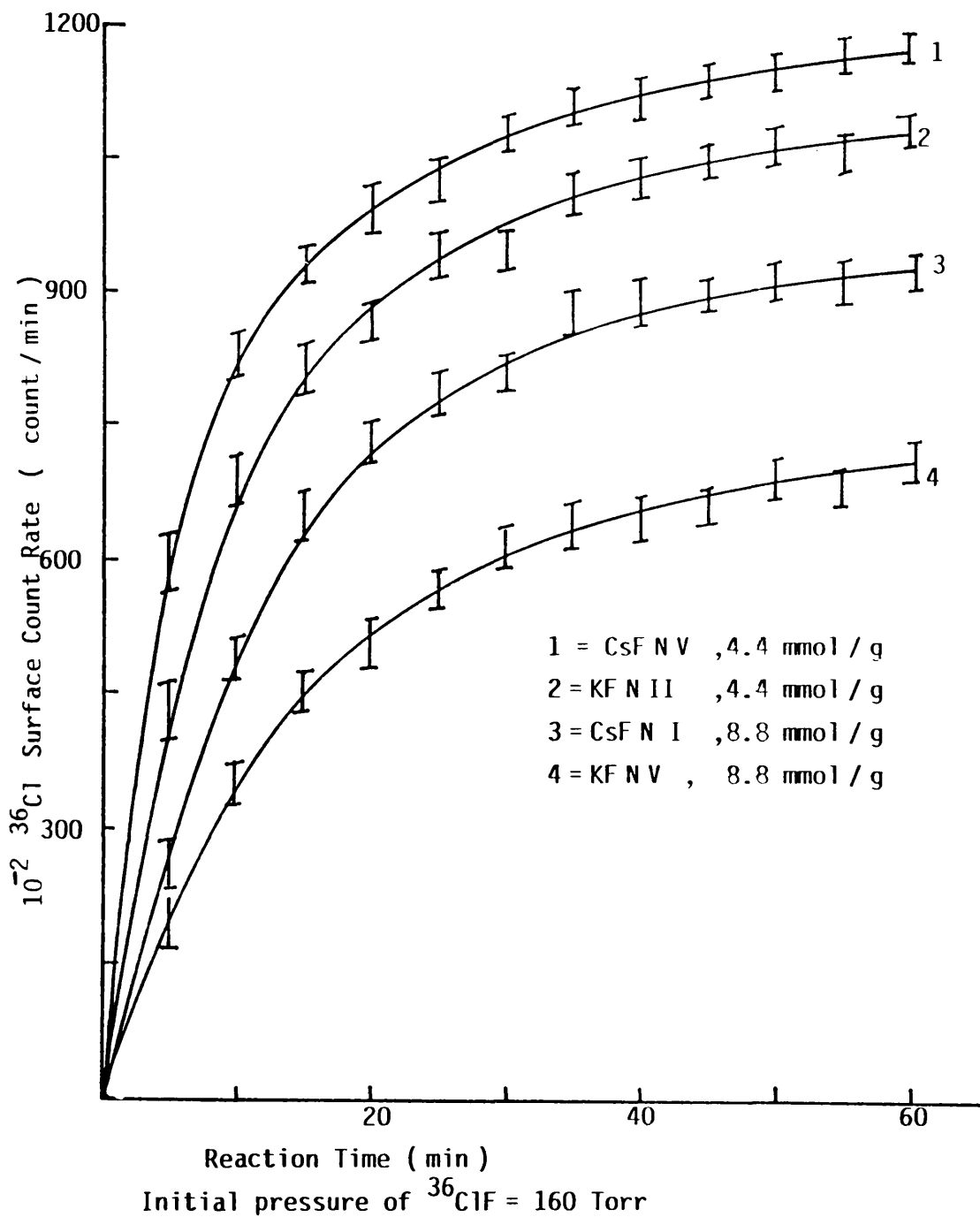
Figure 7.7 Reaction of  $^{36}\text{ClF}$  with MF / fluorinated alumina prepared from aqueous solution. Surface count rate



Initial pressure of  $^{36}\text{ClF}$  = 60 Torr



Figure 7.8 Reaction of  $^{36}\text{ClF}$  with MF / fluorinated alumina prepared from nonaqueous solution, Surface count rate



The total uptake and the  $[^{36}\text{Cl}]$ -chlorine surface count rate were dependent on the initial pressure of  $[^{36}\text{Cl}]$ -chlorine labelled chlorine monofluoride; they varied linearly with the initial pressure in the range 10-300 Torr. The results obtained for FMAI 4.4 and 8.8  $\text{mmol g}^{-1}$  are given in Tables 7.2 - 7.5 and shown schematically in Figs. 7.9 and 7.10.

The reaction between  $[^{36}\text{Cl}]$ -chlorine labelled chlorine monofluoride and metal fluoride supported on fluorinated  $\gamma$ -alumina was studied across the composition range 0.6 - 20.0  $\text{mmol g}^{-1}$ . The behaviour of  $[^{36}\text{Cl}]$ -chlorine labelled chlorine monofluoride was similar to that obtained from the probe molecule reactions, reported in chapter five. The total uptake of  $[^{36}\text{Cl}]$ -chlorine labelled chlorine monofluoride and the surface count rate obtained were completely dependent upon the composition of the solids used; the increase in the metal fluoride loading in the range 0.6 - 5.5  $\text{mmol g}^{-1}$ , resulted in an increase in both the total uptake and the surface count rate, but further increase in the metal fluoride loading in the range 5.5 - 20.0  $\text{mmol g}^{-1}$  led to a very sharp decrease in the total uptake and in the surface count rate.

The removal of the gas phase had no effect on the  $[^{36}\text{Cl}]$ -chlorine surface count rate. The surface count rate of MFA or MFN 20.0  $\text{mmol g}^{-1}$  recorded during reaction with  $[^{36}\text{Cl}]$ -chlorine labelled chlorine monofluoride at any initial pressure studied was equivalent to the background. This means, there was no uptake of  $[^{36}\text{Cl}]$ -chlorine monofluoride by this material. The  $[^{36}\text{Cl}]$ -chlorine surface count rate of MFA and MFN (I, II and V) are shown schematically in Figs. 7.11 and 7.12 for the cases where an initial pressure of  $[^{36}\text{Cl}]$ -chlorine labelled

**Table 7.2 Summary of Results of Reaction of [<sup>36</sup>Cl] Chlorine Monofluoride with Caesium Fluoride Supported on γ-alumina Prepared from Aqueous Solution and Treated with Sulphur Tetrafluoride (CsFAI, 4.4 mmol g<sup>-1</sup>)**

Initial Pressure (Torr)	Total Uptake		Total Drop in Gas		Surface Count Rate		Surface Count Rate	
	Gas	mmol	Count Rate	Count min <sup>-1</sup>	Count min <sup>-1</sup>	Count min <sup>-1</sup>	after Removal of Gas	Count min <sup>-1</sup>
10 ± 1	0.024 ± 0.001		914 ± 31		8239 ± 182		8219 ± 93	
20 ± 1	0.052 ± 0.001		1981 ± 45		1783 ± 267		1784 ± 133	
40 ± 1	0.083 ± 0.001		3162 ± 56		28468 ± 337		2846 ± 169	
60 ± 1	0.112 ± 0.001		4267 ± 65		38417 ± 392		3840 ± 196	
80 ± 1	0.187 ± 0.001		7125 ± 84		64123 ± 506		6437 ± 254	
100 ± 1	0.233 ± 0.001		8877 ± 94		79902 ± 565		79833 ± 283	
120 ± 1	0.223 ± 0.001		8496 ± 92		76450 ± 553		76454 ± 276	
140 ± 1	0.322 ± 0.001		12268 ± 111		110428 ± 665		110409 ± 332	
160 ± 1	0.341 ± 0.001		12992 ± 114		116933 ± 684		116877 ± 341	
180 ± 1	0.373 ± 0.001		14211 ± 119		127909 ± 715		127894 ± 358	
200 ± 1	0.441 ± 0.001		16802 ± 130		151228 ± 778		151235 ± 389	
220 ± 1	0.483 ± 0.001		18402 ± 136		165622 ± 814		165697 ± 409	
240 ± 1	0.511 ± 0.001		19431 ± 139		174881 ± 837		174883 ± 418	
260 ± 1	0.562 ± 0.001		21412 ± 146		192719 ± 878		192732 ± 439	
280 ± 1	0.602 ± 0.001		22936 ± 151		206437 ± 909		206449 ± 454	
300 ± 1	0.643 ± 0.001		24498 ± 157		220483 ± 939		220521 ± 470	

Sample Weight 0.5g

Experimental time 60 mins

Table 7.3 Summary of Results of Reaction of [<sup>36</sup>Cl] Chlorine Monofluoride with Caesium Fluoride Supported on γ-alumina Prepared from Aqueous Solution and Treated with Sulphur Tetrafluoride (CsFAl, 8.8 mmol g<sup>-1</sup>)

Initial Pressure (Torr)	Total Uptake Gas mmol	Total Drop in Gas Count Rate Count min <sup>-1</sup>	Surface Count Rate Count min <sup>-1</sup>	Surface Count Rate after Removal of Gas Count min <sup>-1</sup>
10 ± 1	0.015 ± 0.001	572 ± 24	5430 ± 149	5423 ± 74
20 ± 1	0.038 ± 0.001	1448 ± 38	13753 ± 230	13779 ± 117
40 ± 1	0.061 ± 0.001	2324 ± 48	22081 ± 299	22107 ± 149
60 ± 1	0.103 ± 0.001	3924 ± 63	37284 ± 396	37278 ± 193
80 ± 1	0.117 ± 0.001	4458 ± 67	42357 ± 419	42359 ± 206
100 ± 1	0.153 ± 0.001	5829 ± 76	55389 ± 479	55333 ± 235
120 ± 1	0.187 ± 0.001	7125 ± 84	67688 ± 541	67602 ± 260
140 ± 1	0.206 ± 0.001	7849 ± 89	74563 ± 551	74597 ± 273
160 ± 1	0.266 ± 0.001	10135 ± 101	96282 ± 628	96311 ± 310
180 ± 1	0.273 ± 0.001	10401 ± 102	98816 ± 633	98803 ± 314
200 ± 1	0.315 ± 0.001	12002 ± 110	114023 ± 679	114311 ± 338
220 ± 1	0.316 ± 0.001	12040 ± 110	114382 ± 679	114337 ± 338
240 ± 1	0.345 ± 0.001	13145 ± 115	124871 ± 709	124933 ± 353
260 ± 1	0.400 ± 0.001	15240 ± 123	144780 ± 783	144332 ± 380
280 ± 1	0.425 ± 0.001	16193 ± 127	153837 ± 789	153897 ± 392
300 ± 1	0.453 ± 0.001	17259 ± 131	163967 ± 811	163875 ± 405

Sample Weight 0.5g

Experimental time 60 mins

**Table 7.4 Summary of Results of Reaction of [<sup>36</sup>Cl] Chlorine Labelled Chlorine Monofluoride with Potassium Fluoride Supported on γ-alumina Prepared from Aqueous Solution and Treated with Sulphur Tetrafluoride (KFAI, 4.4 mmol.g<sup>-1</sup>)**

Initial Pressure (Torr)	Total Uptake		Total Drop in Gas		Surface Count Rate after Removal of Gas Count min <sup>-1</sup>	Surface Count Rate Count min <sup>-1</sup>
	Gas	mmol	Count Rate Count min <sup>-1</sup>	Count min <sup>-1</sup>		
10 ± 1	0.015 ± 0.001		572 ± 24		5313 ± 143	5307 ± 73
20 ± 1	0.040 ± 0.001		1524 ± 39		14179 ± 238	14163 ± 119
30 ± 1	0.045 ± 0.001		1715 ± 42		15945 ± 252	15909 ± 126
40 ± 1	0.071 ± 0.001		2705 ± 50		25167 ± 317	25192 ± 158
60 ± 1	0.098 ± 0.001		3745 ± 62		34834 ± 374	34895 ± 187
80 ± 1	0.151 ± 0.001		5753 ± 75		53508 ± 463	53536 ± 231
100 ± 1	0.165 ± 0.001		6287 ± 76		58469 ± 483	58426 ± 242
120 ± 1	0.211 ± 0.001		8039 ± 79		74763 ± 546	74738 ± 273
140 ± 1	0.240 ± 0.001		9144 ± 96		85049 ± 583	85197 ± 292
160 ± 1	0.285 ± 0.001		10859 ± 104		100982 ± 635	100873 ± 311
180 ± 1	0.315 ± 0.001		12002 ± 110		111613 ± 668	111514 ± 334
200 ± 1	0.360 ± 0.001		13716 ± 115		127567 ± 716	127634 ± 357
220 ± 1	0.388 ± 0.001		14783 ± 119		137483 ± 743	137597 ± 371
240 ± 1	0.428 ± 0.001		16307 ± 127		151696 ± 779	151653 ± 389
260 ± 1	0.455 ± 0.001		17336 ± 129		161226 ± 803	161274 ± 402
280 ± 1	0.481 ± 0.001		18326 ± 136		170438 ± 825	170437 ± 413
300 ± 1	0.525 ± 0.001		20003 ± 143		186022 ± 863	186008 ± 423

Sample Weight 0.38g  
Experimental time 60 mins

Table 7.5 Summary of Results of Reaction of [<sup>36</sup>Cl] Chlorine Labelled Chlorine Monofluoride with Caesium Fluoride Supported on γ-alumina Prepared from Aqueous Solution and Treated with Sulphur Tetrafluoride (KFAl, 8.8 mmol.g<sup>-1</sup>)

Initial Pressure (Torr)	Total Uptake Gas mmol	Total Drop in Gas Count Rate Count min <sup>-1</sup>	Surface Count Rate Count min <sup>-1</sup>	Surface Count Rate after Removal of Gas Count min <sup>-1</sup>
10 ± 1	0.011 ± 0.001	419 ± 20	4024 ± 127	4001 ± 63
20 ± 1	0.021 ± 0.001	800 ± 28	7682 ± 175	7693 ± 88
40 ± 1	0.048 ± 0.001	1829 ± 43	17563 ± 264	17398 ± 132
60 ± 1	0.069 ± 0.001	2629 ± 51	25246 ± 318	25322 ± 159
80 ± 1	0.102 ± 0.001	3886 ± 62	37316 ± 386	37306 ± 193
100 ± 1	0.120 ± 0.001	4572 ± 68	43898 ± 419	43927 ± 210
120 ± 1	0.146 ± 0.001	5563 ± 74	53409 ± 462	53476 ± 231
140 ± 1	0.173 ± 0.001	6591 ± 81	63283 ± 503	63294 ± 252
160 ± 1	0.193 ± 0.001	7353 ± 86	70592 ± 531	70615 ± 266
180 ± 1	0.223 ± 0.001	8496 ± 92	81569 ± 571	81597 ± 286
200 ± 1	0.248 ± 0.001	9449 ± 97	90715 ± 601	90733 ± 301
220 ± 1	0.255 ± 0.001	9716 ± 98	93286 ± 611	93282 ± 305
240 ± 1	0.305 ± 0.001	11621 ± 107	111567 ± 668	111711 ± 334
260 ± 1	0.336 ± 0.001	12802 ± 113	122903 ± 701	122977 ± 351
280 ± 1	0.345 ± 0.001	13145 ± 115	126192 ± 710	126122 ± 355
300 ± 1	0.370 ± 0.001	14097 ± 119	135331 ± 736	135289 ± 368

Sample Weight 0.32g  
Experimental time 60 mins

Figure 7.9 Reaction of  $^{36}\text{ClF}$  with MF / fluorinated alumina  
Surface count rate  $\nu$  initial pressure

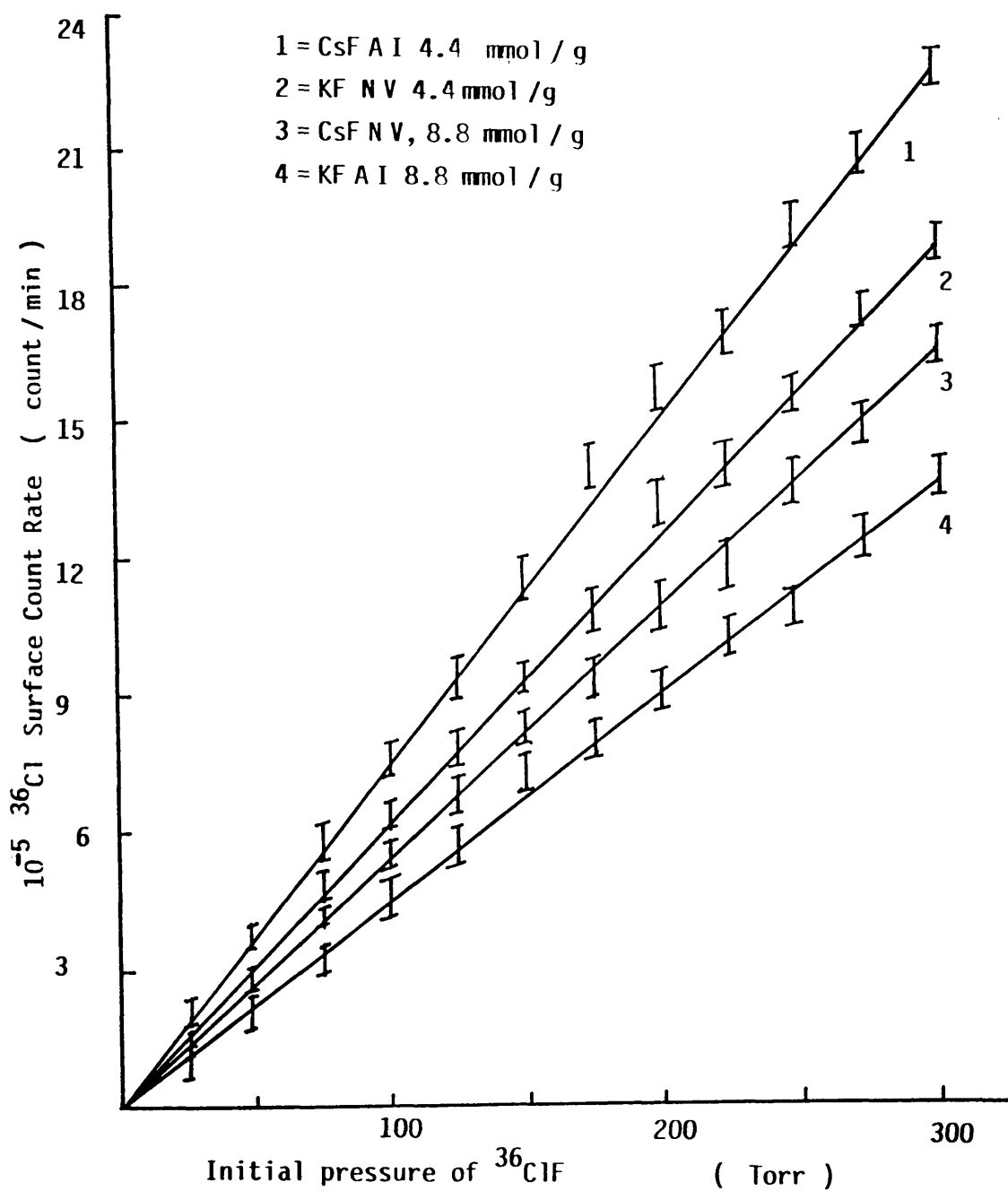
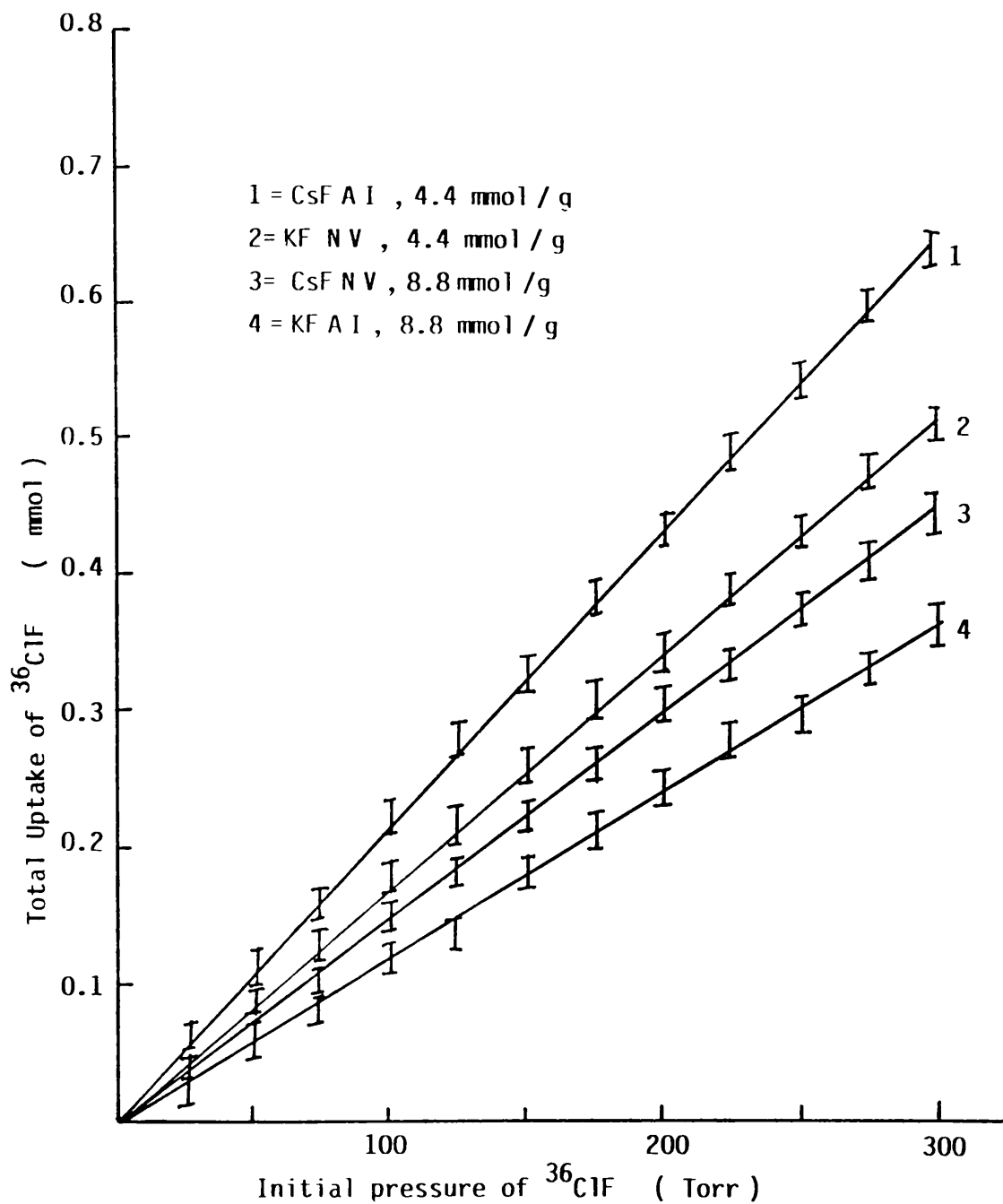


Figure 7.10 Reaction of  $^{36}\text{ClF}$  with MF / fluorinated alumina  
Total uptake vs initial pressure





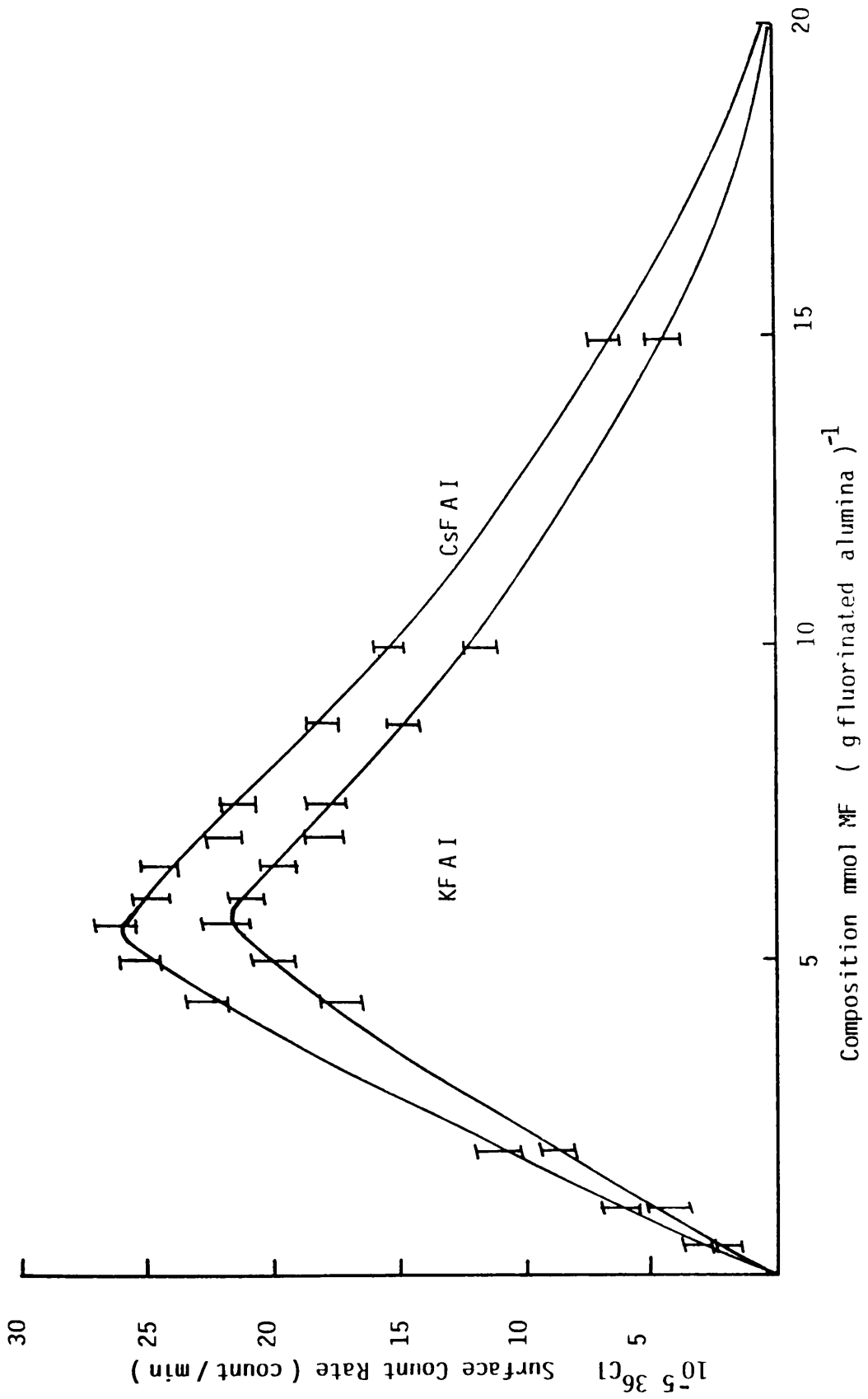


Figure 7.11 Reaction of  $^{36}\text{ClF}$  with MF A I Surface count rate v composition

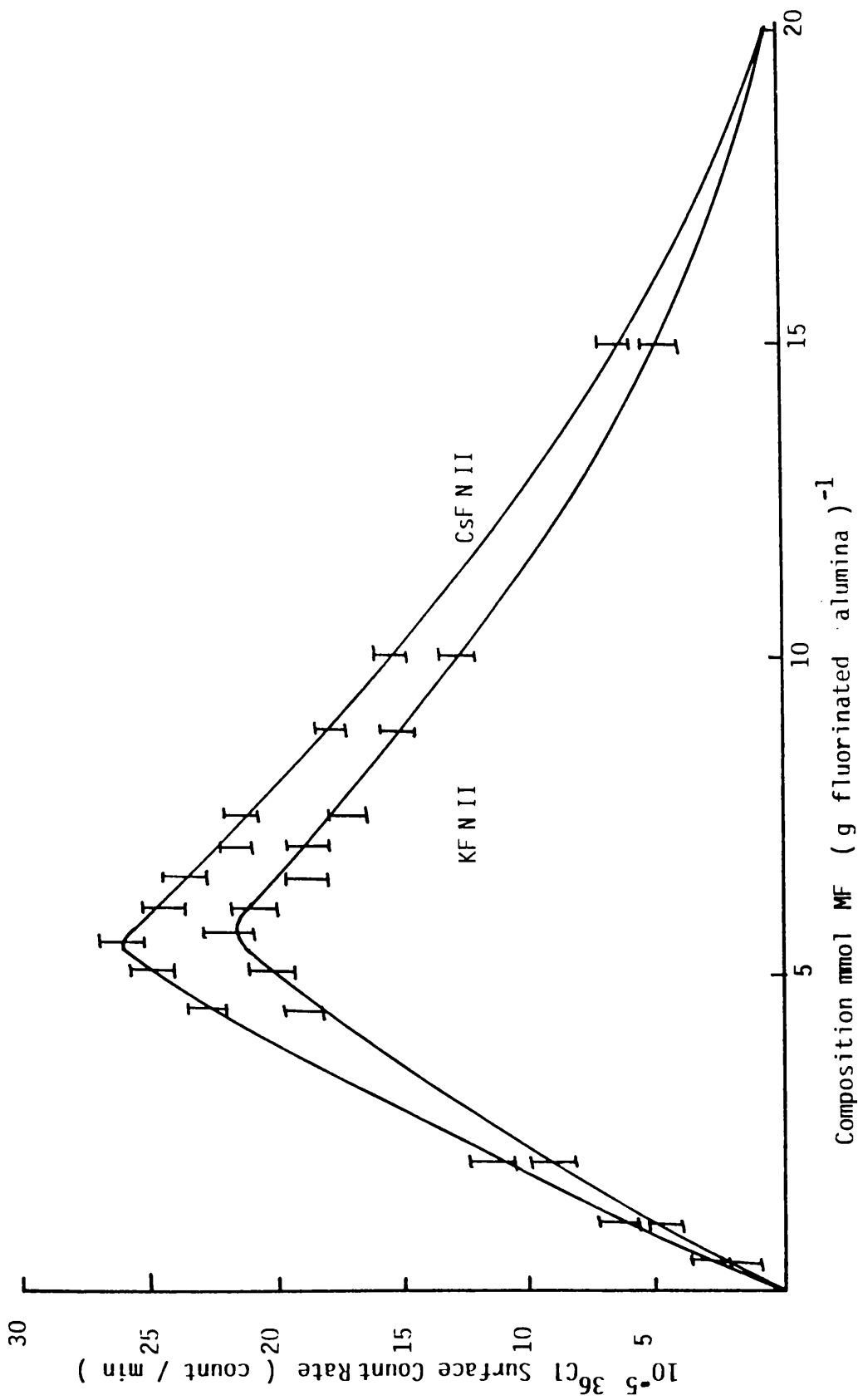


Figure 7.12 Reaction of  $^{36}\text{ClF}$  with MF N II Surface Count Rate vs Composition

chlorine monofluoride of 300 Torr was used.

The uptake of chlorine monofluoride by MFA and MFN (I,II and V) was studied at different initial pressures using the constant volume manometer similar to that used for anhydrous hydrogen fluoride experiments as described in chapter five, section 5.1. The results obtained were identical to those obtained using the radiotracer method and are shown in Fig. 7.13 for solids in the composition range  $0.6 - 15.0 \text{ mmol g}^{-1}$ . The two sets of data showed very good agreement and confirmed that the reaction between chlorine monofluoride and metal fluoride supported on fluorinated  $\gamma$ -alumina was dependent upon the initial pressure of gas and the composition of the solid, and that the uptake of chlorine monofluoride was irreversible at room temperature, even after overnight evacuation, but could be reversed by heating at 523 K.

In some experiments the infra-red and Raman spectra of the solid after reaction were obtained and are listed in Table 7.6. The infra-red spectrum showed bands at 643, 502 and  $483 \text{ cm}^{-1}$  which were attributed to the difluorochlorate(I) anion, but only one very sharp line was observed in the Raman spectrum at  $482 \text{ cm}^{-1}$  which was also attributed to the difluorochlorate(I) anion.

#### 7.4 THE OXIDATIVE ADDITION OF CHLORINE MONOFLUORIDE TO SULPHUR TETRAFLUORIDE IN THE PRESENCE OF METAL FLUORIDE SUPPORTED ON FLUORINATED $\gamma$ -ALUMINA

The reaction between sulphur tetrafluoride and chlorine monofluoride in the presence of metal fluoride supported on fluorinated  $\gamma$ -alumina was studied using [ $^{35}\text{S}$ ]-sulphur labelled sulphur tetrafluoride and [ $^{36}\text{Cl}$ ]-chlorine labelled chlorine

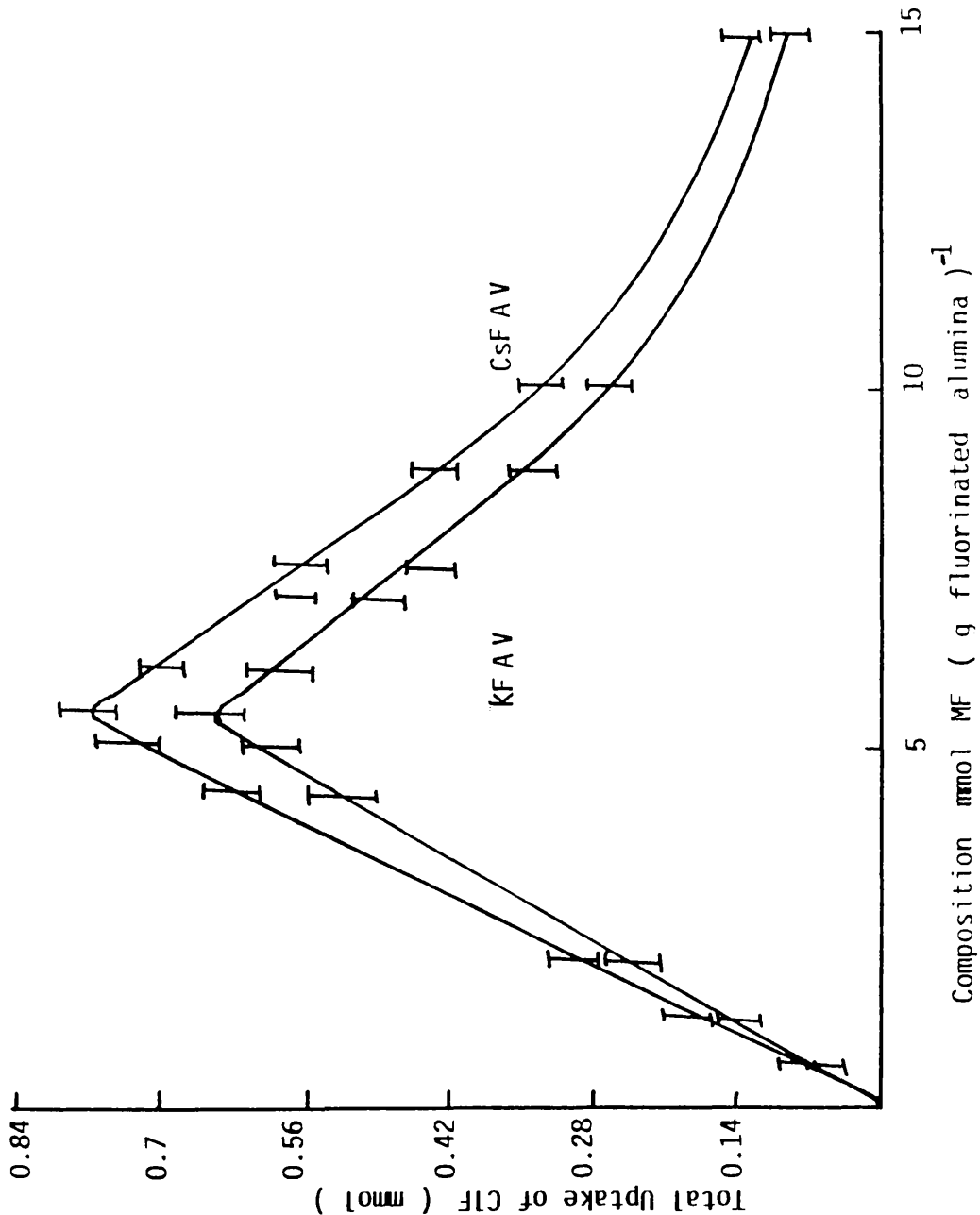


Figure 7.13 Manometric study of the reaction of ClF with MF AV  
 Total uptake v Composition

**Table 7.6 The Vibrational Spectra for C<sub>2</sub>F/Fluorinated  $\gamma$ -alumina After Reaction with Chlorine Monofluoride**

This Work		Literature 21, 22	
IR	Raman	IR	Raman
483	482	478 $\nu_1$	475 $\nu_1$
502		510 $\nu_1$	
643		630 $\nu_3$	

monofluoride and by the conventional manometric technique.

7.4.1 THE REACTION OF SULPHUR TETRAFLUORIDE WITH METAL FLUORIDE  
SUPPORTED ON FLUORINATED  $\gamma$ -ALUMINA PRETREATED WITH  
CHLORINE MONOFLUORIDE.

A sample of metal fluoride supported on fluorinated  $\gamma$ -alumina MFA or MFN (I,II or V) was allowed to react with chlorine monofluoride (662 Torr, 5.0 mmol) at ambient temperature for 2 h. After the removal of the gas phase, sulphur tetrafluoride (662 Torr, 5.0 mmol) was admitted to the pretreated sample and left at room temperature for 1.5 h. The gas phase was removed and analysed; a small quantity of sulphur chloride pentafluoride was obtained. The analysis showed that the extent of uptake of sulphur tetrafluoride was considerably enhanced by the pre-adsorption of chlorine monofluoride. The reaction of sulphur tetrafluoride with metal fluoride supported on fluorinated  $\gamma$ -alumina pretreated by chlorine monofluoride was carried out several times, using the same sample of catalyst. The results obtained for MFAI 5.5 mmol g<sup>-1</sup>, using ca 2 g of catalyst and 5.0 mmol chlorine monofluoride and 5.0 mmol sulphur tetrafluoride for each experiment are shown in Table 7.7. The results of the five cycles studied, the composition of the solids corresponded to the mole ratios metal fluoride:chlorine monofluoride:sulphur tetrafluoride, 5.98:3.2:3.26 and 5.98:2.53:2.6 for CsFAI and KFAI 5.5 mmol g<sup>-1</sup> respectively. Sulphur chloride pentafluoride was not formed by pumping these solids at room temperature, but was evolved by pumping at 333 K. Further heating of the solids at 393 K for 5 h resulted in the production of 2.1 and 1.4 mmol of sulphur chloride pentafluoride respectively. When the solids heated at 473 K more sulphur chloride pentafluoride was formed. Displacement of the retained quantity of chlorine

Table 7.7 Repeated Addition of Chlorine Monofluoride (662 Torr, 5.0 mmol), Then Sulphur Tetrafluoride (662 Torr, 5.0 mmol) to MFAI 5.5 mmol<sup>-1</sup> (5.98 mmol)

Run	Gas Added	MFAI 5.5 mmol <sup>-1</sup>					
		M = Cs			M = K		
		Time(h)	Gas Retained	SF <sub>5</sub> Cl	Time(h)	Gas Retained	SF <sub>5</sub> Cl
1	ClF	2.0	1.23	-	2.0	0.84	-
	SF <sub>4</sub>	5.0	1.24	0.31	5.0	0.89	0.22
2	ClF	2.0	1.21	0.03	2.0	0.88	0.04
	SF <sub>4</sub>	5.0	1.20	0.41	5.0	0.79	0.19
3	ClF	1.5	1.19	0.32	1.5	0.79	0.23
	SF <sub>4</sub>	5.0	1.21	0.28	5.0	0.86	0.18
4	ClF	2.0	1.18	0.33	2.0	0.82	0.19
	SF <sub>4</sub>	3.0	1.20	0.42	4.0	0.82	0.20
5	ClF	2.0	1.21	0.31	2.0	0.84	0.17
	SF <sub>4</sub>	2.0	1.21	0.31	2.0	0.84	0.17

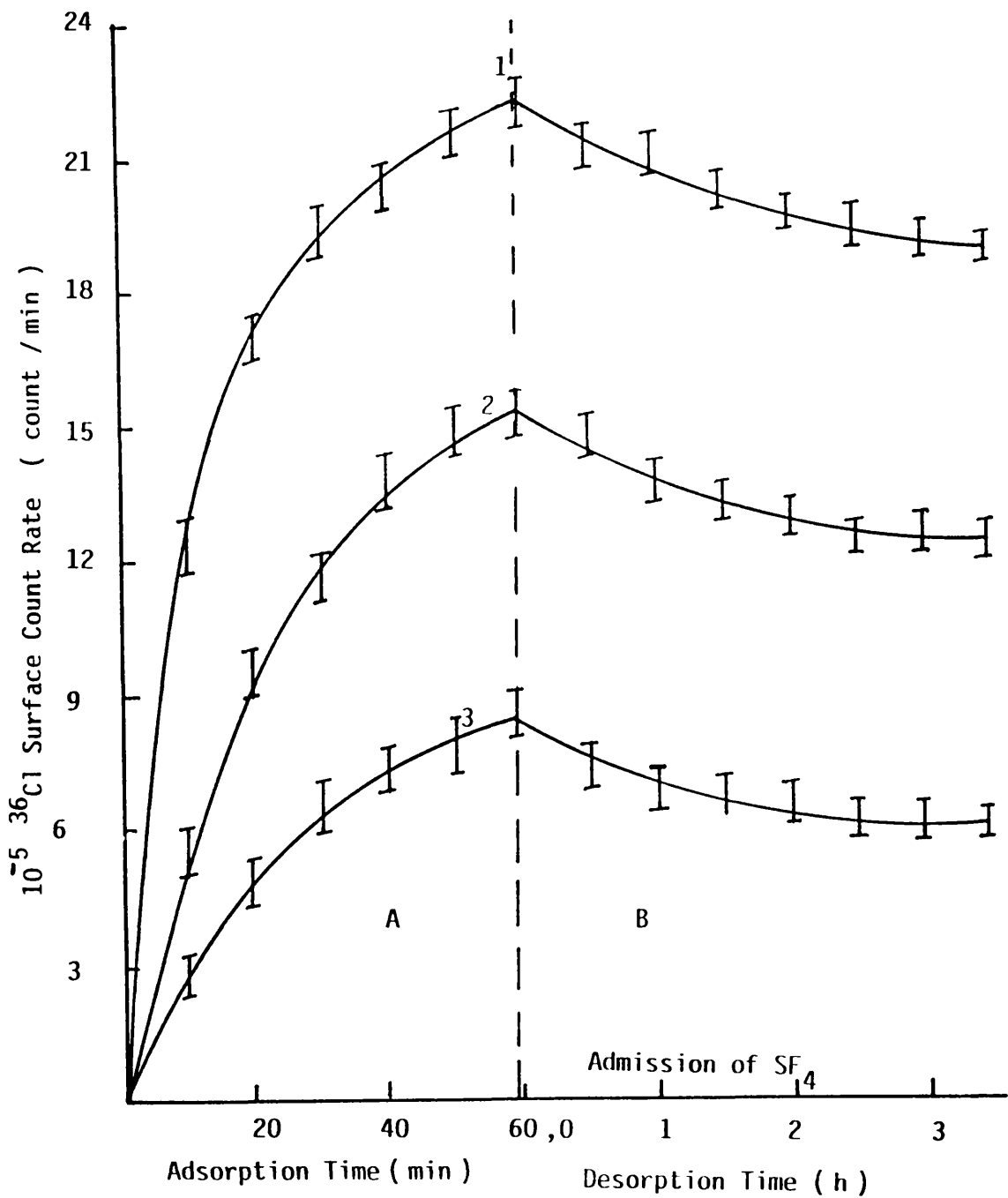
monofluoride from the surface of metal fluoride supported on fluorinated  $\gamma$ -alumina by sulphur tetrafluoride, was not complete as shown by the admission of sulphur tetrafluoride to a sample of MFA or MFN pretreated with [ $^{36}\text{Cl}$ ]-chlorine labelled chlorine monofluoride. The decrease in the [ $^{36}\text{Cl}$ ]-chlorine surface count on admission of sulphur tetrafluoride was equivalent to the quantity of [ $^{36}\text{Cl}$ ]-chlorine labelled sulphur chloride pentafluoride formed. The results obtained for MFA and MFN (I or V)  $4.4 \text{ mmol g}^{-1}$  are shown in Figs. 7.14 - 7.17 using initial pressures of sulphur tetrafluoride of 100, 200 and 300 Torr. These showed that, the release of sulphur chloride pentafluoride in these reactions was independent of the initial pressure of sulphur tetrafluoride.

#### 7.4.2 THE REACTION OF CHLORINE MONOFLUORIDE WITH METAL FLUORIDE SUPPORTED ON FLUORINATED $\gamma$ -ALUMINA PRETREATED WITH SULPHUR TETRAFLUORIDE.

The behaviour of chlorine monofluoride towards metal fluoride supported on fluorinated  $\gamma$ -alumina pretreated with sulphur tetrafluoride showed different characteristics from those observed with the sulphur tetrafluoride reaction. A sample (2.0 g) of the supported metal fluoride on fluorinated  $\gamma$ -alumina was allowed to react with sulphur tetrafluoride (662 Torr, 5.0 mmol) at ambient temperature for 1 h. The gas phase was removed and a quantity of chlorine monofluoride (662 Torr, 5.0 mmol) was admitted to the sample and allowed to stand for 5 h at room temperature. The gas phase was removed, chlorine monofluoride superated by low temperature evacuation and the gas product analysed. A considerable quantity of sulphur chloride pentafluoride was collected, which was equivalent to the quantity of



Figure 7.14  $^{36}\text{Cl}$  Surface Count Rate of CsFAI, 4.4 mmol / g at  
 A) Adsorption of  $^{36}\text{ClF}$ , B) Desorption of  $\text{SF}_5^{36}\text{Cl}$  by the admission  
 of  $\text{SF}_4$



Initial pressure of  $^{36}\text{ClF}$  1) 300, 2) 200, 3) 100 Torr

Figure 7.15  $^{36}\text{Cl}$  Surface Count Rate of  $\text{CsFNY}$ , 4.4 mmol / g at  
 A) Adsorption of  $^{36}\text{ClF}$ , B) Desorption of  $\text{SF}_5^{36}\text{Cl}$  by the  
 admission of  $\text{SF}_4$

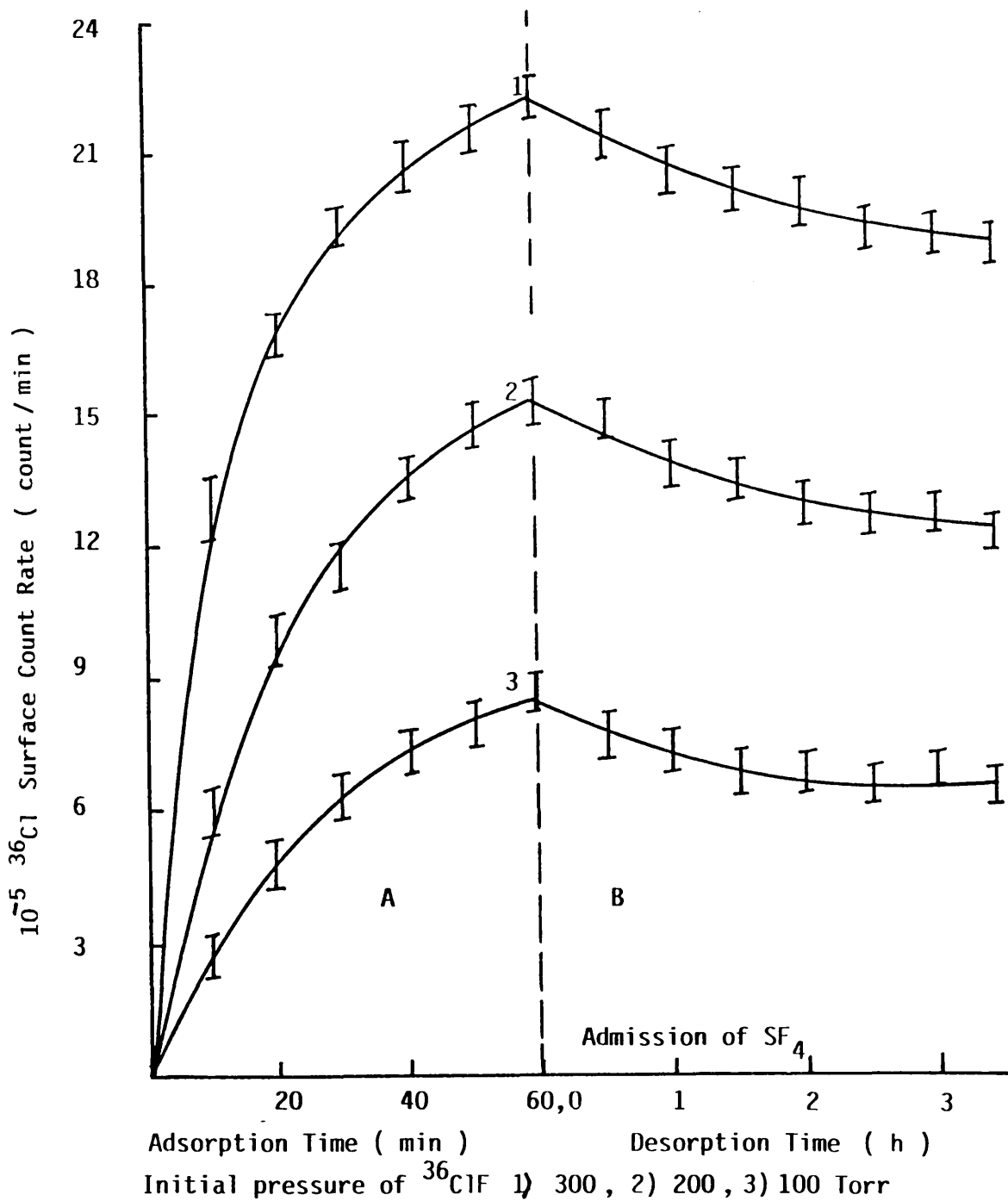


Figure 7.16  $^{36}\text{Cl}$  Surface Count Rate of KFAI, 4.4 mmol/g at  
 A) Adsorption of  $^{36}\text{ClF}_3$ , B) Desorption of  $\text{SF}_5^{36}\text{Cl}$  by the  
 admission of  $\text{SF}_4$

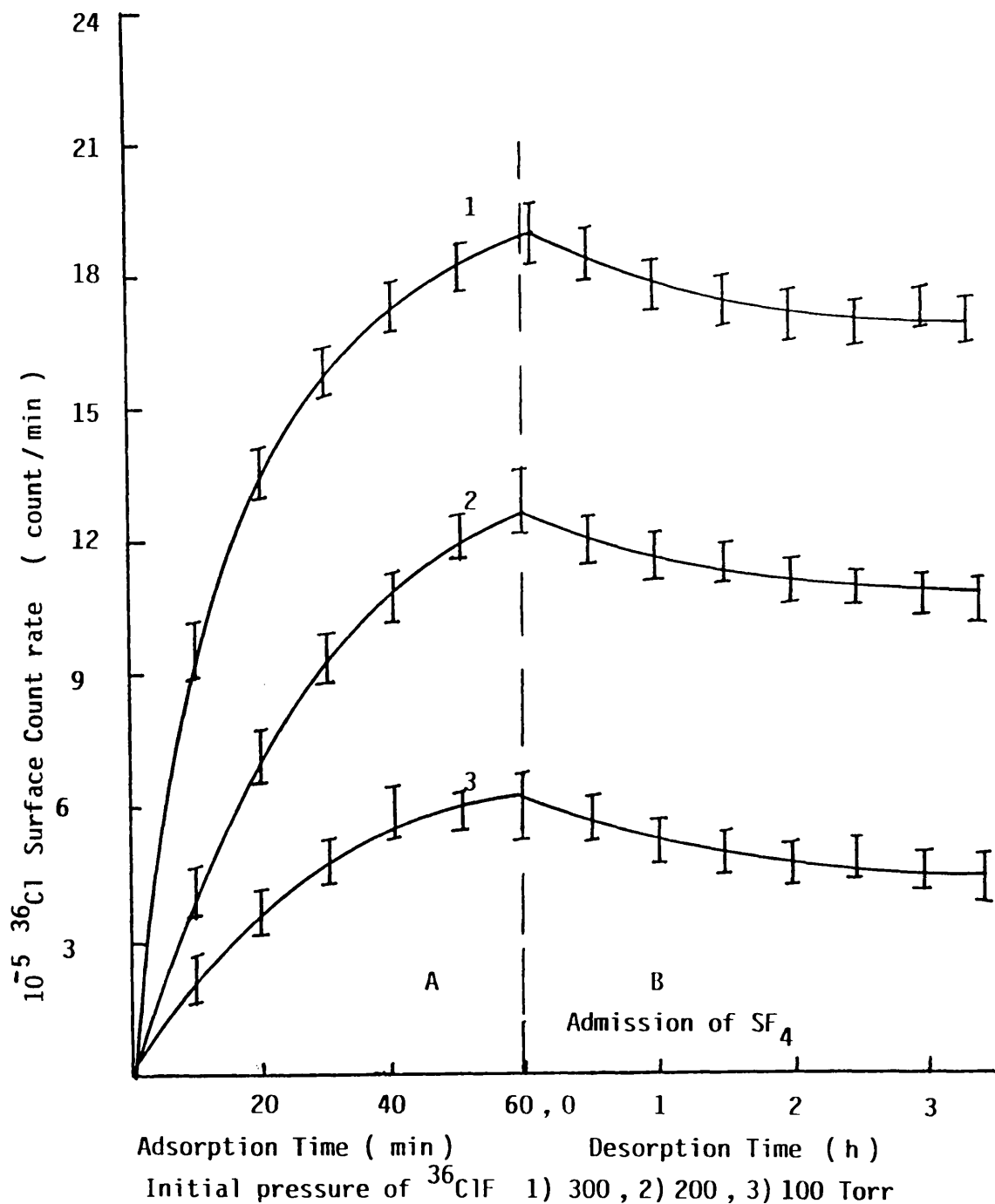
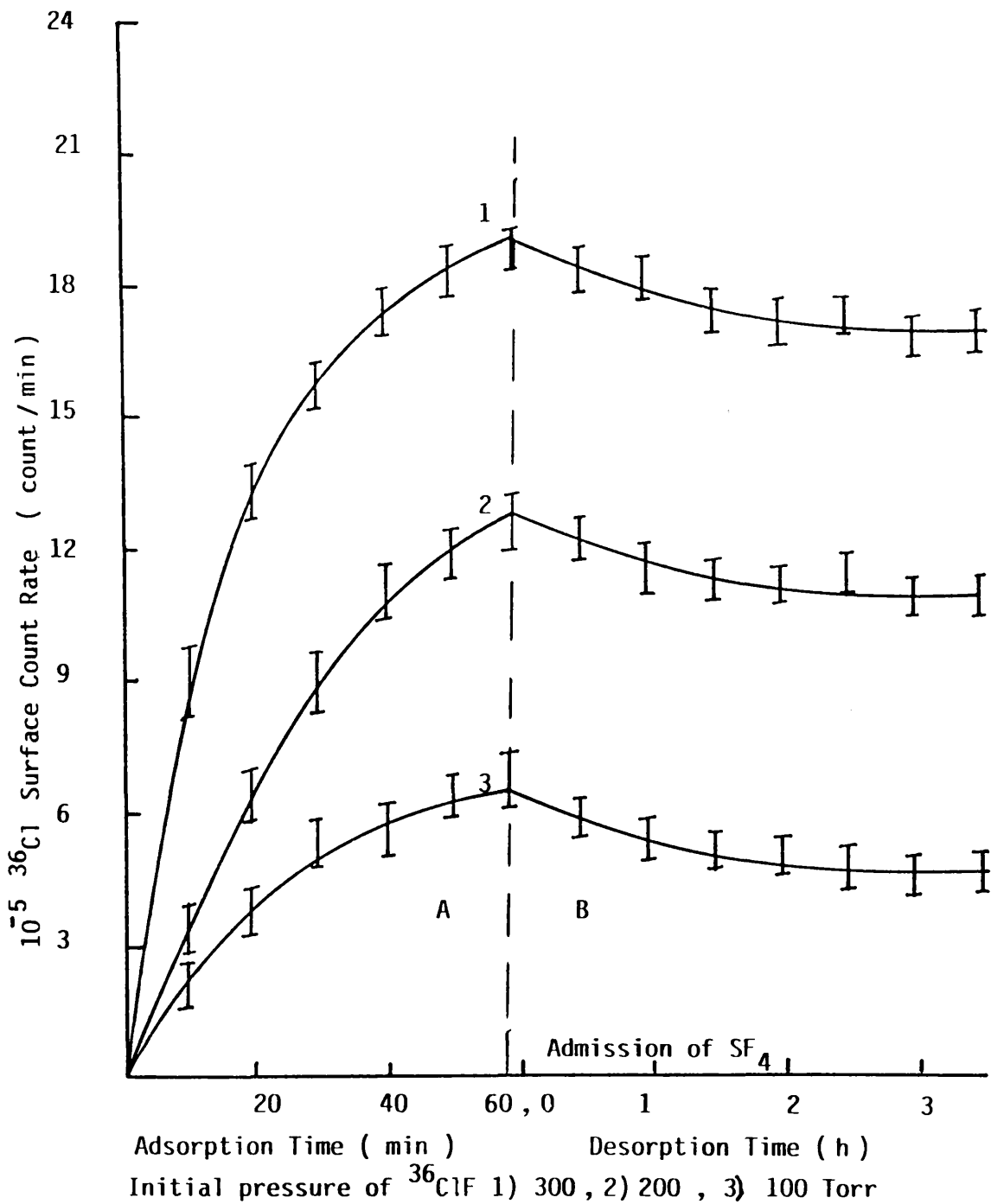


Figure 7.17  $^{36}\text{Cl}$  Surface Count Rate of  $\text{KF N V}$ , 4.4 mmol / g at  
 A) Adsorption of  $^{36}\text{ClF}$  B) Desorption of  $\text{SF}_5^{36}\text{Cl}$  by the  
 admission of  $\text{SF}_4$



sulphur tetrafluoride retained during the first exposure. However, the quantity of chlorine monofluoride recovered was less than expected after correction for the quantity which reacted with the retained sulphur tetrafluoride. Thus, the retention of chlorine monofluoride was observed after the reaction of excess chlorine monofluoride with metal fluoride supported on fluorinated  $\gamma$ -alumina pretreated with sulphur tetrafluoride. The admission of sulphur tetrafluoride to the solid after the removal of chlorine monofluoride led to the formation of a very small quantity of sulphur chloride pentafluoride. The results obtained for 5 cycles are listed in Table 7.8. The compositions of solids corresponded to the mole ratio, metal fluoride:chlorine monofluoride:sulphur tetrafluoride, 5.98:3.21:2.33 and 5.98:2.6:1.89 for CsFAI and KFAI  $5.5 \text{ mmol g}^{-1}$  respectively. The quantity of chlorine monofluoride retained by the catalyst was equal to that presented in section 7.4.1.

In order to investigate the effect of the poisoning of the active sites, the quantity of chlorine monofluoride admitted was equal to the quantity of sulphur tetrafluoride retained during the first exposure. A sample of metal fluoride supported on fluorinated  $\gamma$ -alumina, CsFAI  $5.5 \text{ mmol g}^{-1}$  (2 g, 5.98 mmol) was allowed to react with sulphur tetrafluoride (662 Torr, 5 mmol) at ambient temperature for 1 h. The unreacted sulphur tetrafluoride (557 Torr, 4.2 mmol) was removed at room temperature. Chlorine monofluoride (106 Torr, 0.8 mmol) was then admitted and allowed to stand at room temperature for 3h. The gas product was removed and analysed by infra-red spectroscopy. Bands obtained due to sulphur chloride pentafluoride (105 Torr, 0.79 mmol) were observed. Further cycles exhibited the same pattern, with no retention of gas.

Table 7.8 Repeated Addition of Sulphur Tetrafluoride (662 Torr, 5.0 mmol), Then Chlorine Monofluoride (662 Torr, 5.0 mmol) to MFAI 5.5 mmolg<sup>-1</sup> (5.98 mmol)

Run	Gas Added	MFAI 5.5 mmolg <sup>-1</sup>					
		M = Cs			M = K		
		Time(h)	Gas Retained	SF <sub>5</sub> Cl	Time(h)	Gas Retained	SF <sub>5</sub> Cl
1	SF <sub>4</sub>	2.5	0.66	-	2.5	0.42	-
	ClF	5.0	1.42	0.66	7.5	0.98	0.42
2	SF <sub>4</sub>	5.0	1.35	0.38	3.5	0.88	0.20
	ClF	3.5	1.35	0.32	2.5	0.95	0.17
3	SF <sub>4</sub>	2.5	1.38	0.33	7.5	0.89	0.23
	ClF	6.0	1.38	0.37	6.5	0.88	0.23
4	SF <sub>4</sub>	3.5	1.34	0.39	5.0	0.86	0.22
	ClF	5.5	1.39	0.41	5.5	0.89	0.19
5	SF <sub>4</sub>	2.5	1.35	0.45	3.5	0.88	0.17
	ClF	3.5	1.42	0.44	4.5	0.92	0.21

The results obtained for 5 cycles are given in Table 7.9. A complete displacement of the adsorbed quantity of sulphur tetrafluoride by chlorine monofluoride occurred as shown by the admission of chlorine monofluoride to a sample of metal fluoride supported on fluorinated  $\gamma$ -alumina pretreated with [ $^{35}\text{S}$ ]-sulphur labelled sulphur tetrafluoride, when the decrease in [ $^{35}\text{S}$ ]-sulphur surface count rate on admission of chlorine monofluoride corresponded to the quantity of [ $^{35}\text{S}$ ]-sulphur labelled sulphur chloride pentafluoride formed. On removal of the gas phase, the surface count rate recorded was equivalent to the background of the Geiger-Müller counter. Plots of the [ $^{35}\text{S}$ ]-sulphur surface count rate as a function of time are shown in Figs. 7.18 - 7.21 for MFA or MFN (I or V).

#### 7.4.3 THE REACTION BETWEEN SULPHUR TETRAFLUORIDE AND CHLORINE MONOFLUORIDE IN THE PRESENCE OF METAL FLUORIDE SUPPORTED ON FLUORINATED $\gamma$ -ALUMINA.

The admission of a sulphur tetrafluoride and chlorine monofluoride mixture to a sample of metal fluoride supported on fluorinated  $\gamma$ -alumina at ambient temperature led to a different behaviour from that described in sections 7.4.1 or 7.4.2. The mixtures of sulphur tetrafluoride and chlorine monofluoride (3 - 10.0 mmol) were admitted to a sample of catalyst, MFA or MFN (I, II or V) and kept at room temperature or at 373 K. After 1 h the volatile product was removed, the sulphur chloride pentafluoride separated from unreacted sulphur tetrafluoride and chlorine monofluoride and its yield determined. In the reaction between sulphur tetrafluoride and chlorine monofluoride using a sample of

Table 7.9 Repeated Addition of Sulphur Tetrafluoride (662 Torr, 5.0 mmol), Then Chlorine Monofluoride (147 Torr, 1.11 mmol) to MFAI 5.5 mmol g<sup>-1</sup> (5.98 mmol)

Run	Gas Added	MFAI 5.5 mmol g <sup>-1</sup>					
		M = Cs			M = K		
		Time(h)	Gas Retained	SF <sub>5</sub> Cl	Time(h)	Gas Retained	SF <sub>5</sub> Cl
1	SF <sub>4</sub>	2.0	0.8	-	2.0	0.42	-
	ClF	5.0	-	0.79	5.0	-	0.41
2	SF <sub>4</sub>	2.0	0.83	-	2.0	0.43	-
	ClF	3.0	-	0.82	3.0	-	0.43
3	SF <sub>4</sub>	1.0	0.77	-	1.0	0.40	-
	ClF	5.0	-	0.77	3.0	-	0.40
4	SF <sub>4</sub>	1.0	0.83	-	1.0	0.41	-
	ClF	3.0	-	0.83	3.0	-	0.40
5	SF <sub>4</sub>	2.0	0.84	-	1.0	0.45	-
	ClF	3.0	-	0.84	3.0	-	0.44



Figure 7.18  $^{35}\text{S}$  Surface Count Rate of KFAI, 4.4 mmol/g pretreated with  $^{35}\text{SF}_4$  during reaction with ClF

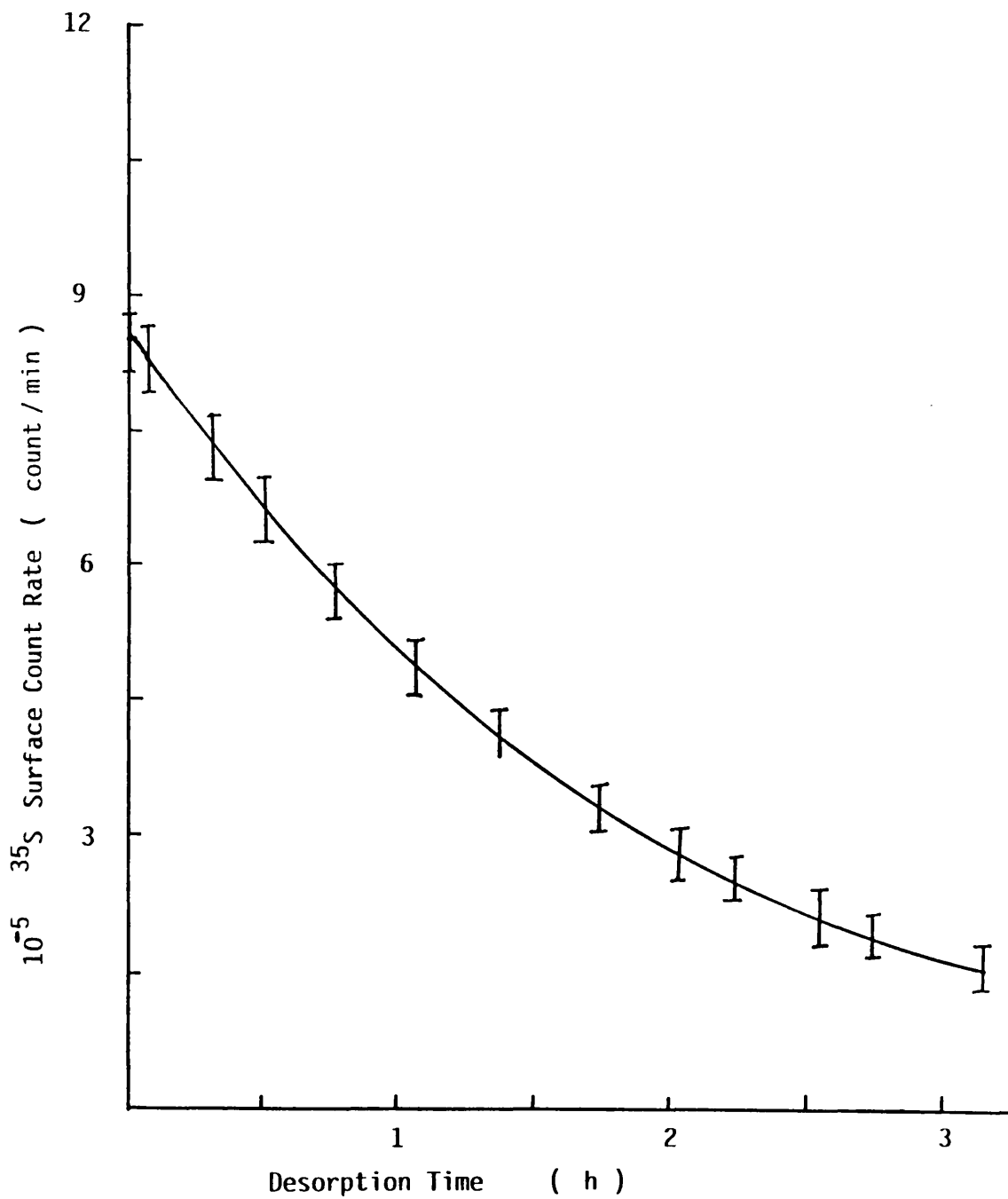


Figure 7.19  $^{35}\text{S}$  Surface Count Rate of  $\text{KF N}\nabla$ , 4.4 mmol / g pretreated with  $^{35}\text{SF}_4$  during reaction with  $\text{Cl}_2$

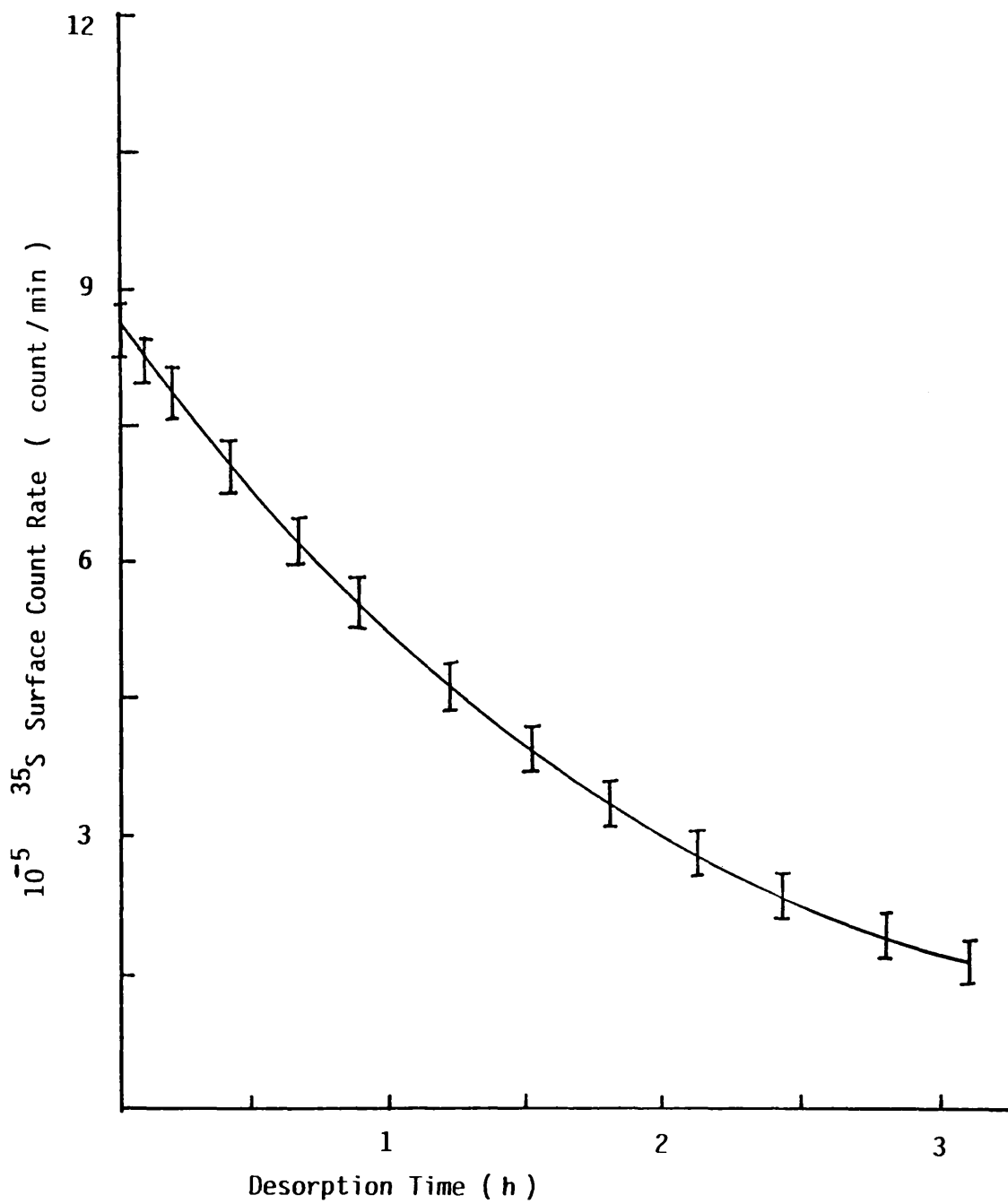


Figure 7.20  $^{35}\text{S}$  Surface Count Rate of CsFAI, 4.4 mmol/g, pretreated with  $^{35}\text{SF}_4$  during reaction with ClF

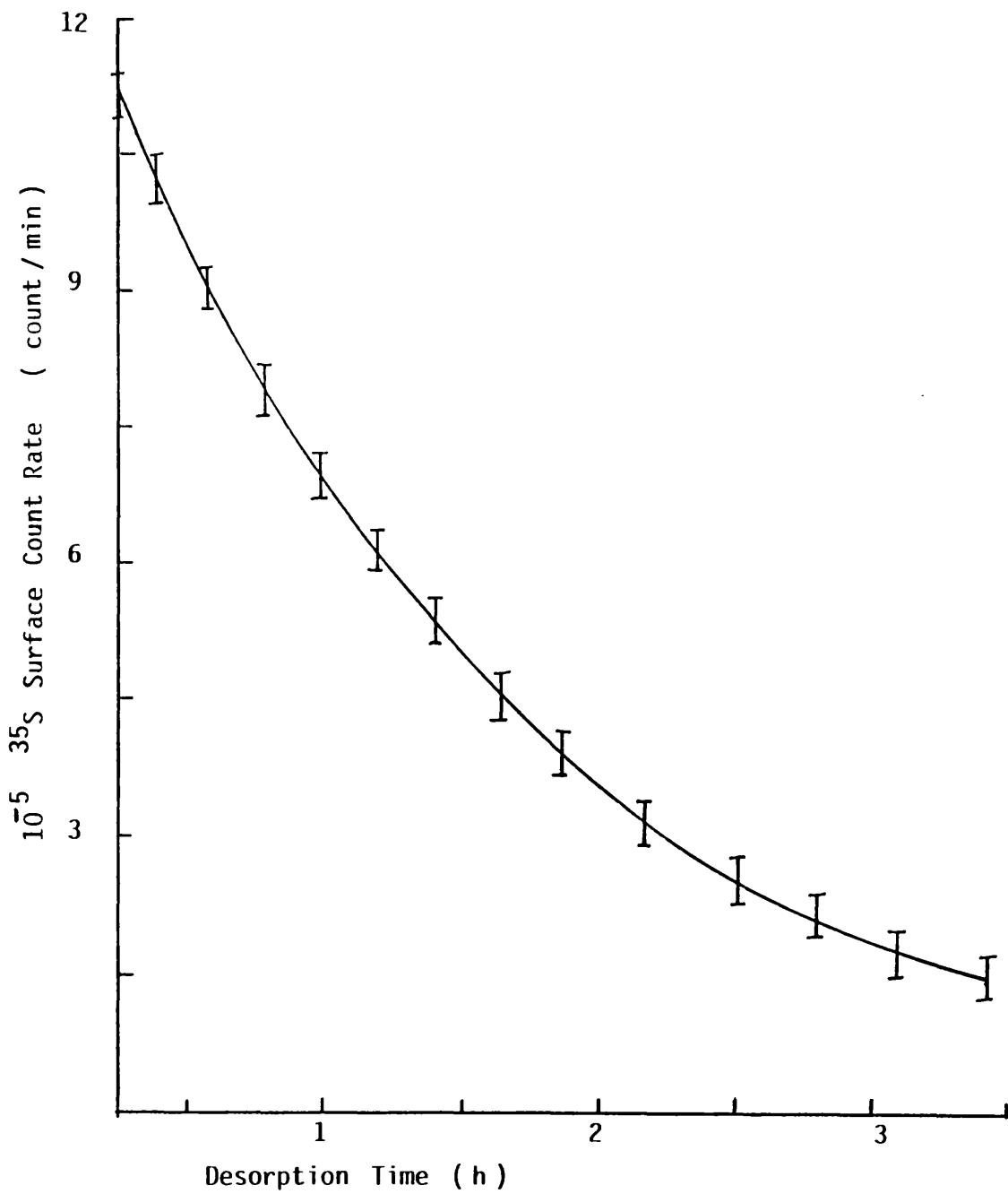
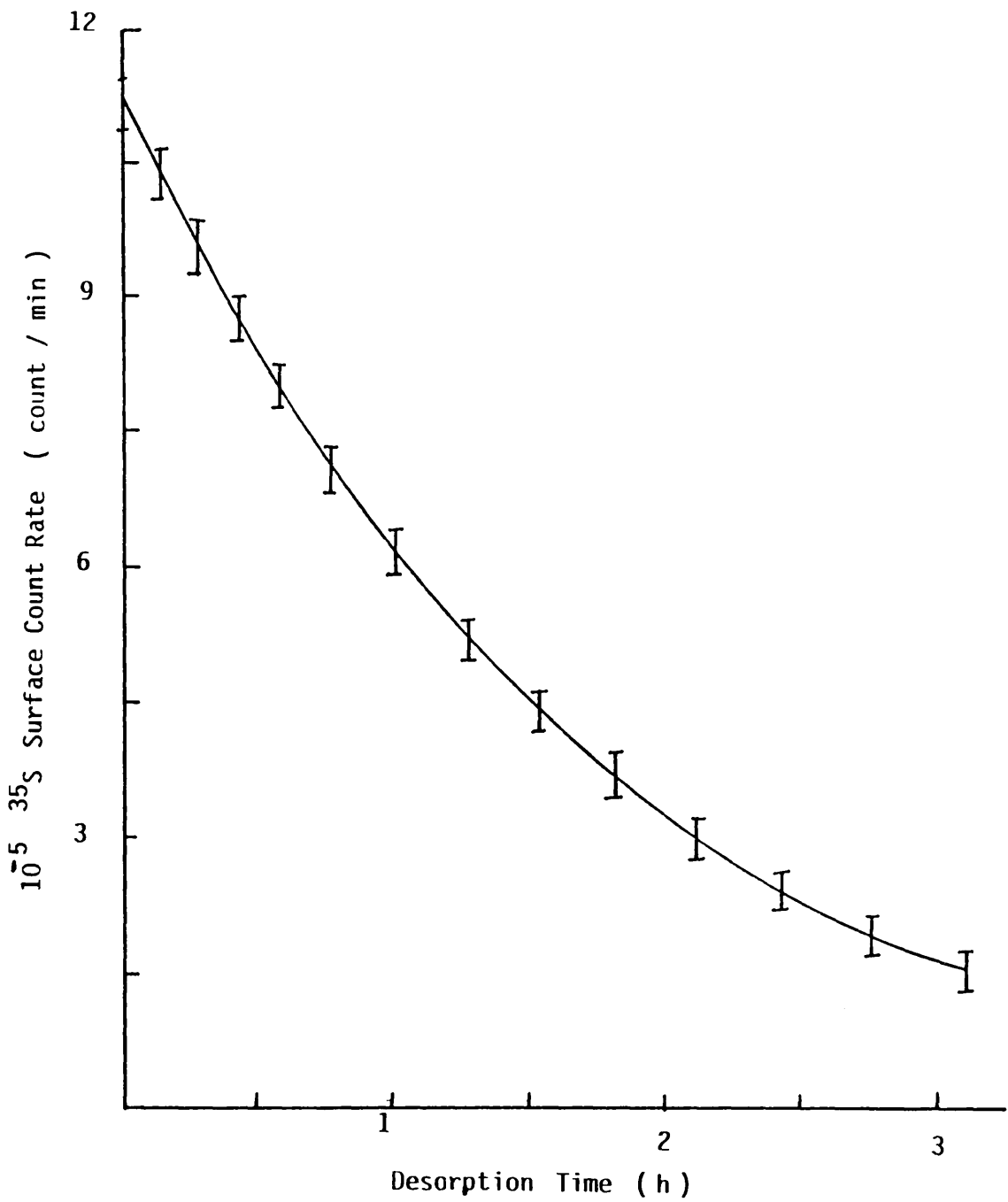


Figure 7.21  $^{35}\text{S}$  Surface Count Rate of  $\text{CsFN}\text{V}$ , 4.4 mmol/g, pretreated with  $^{35}\text{SF}_4$  during reaction with  $\text{ClF}$



MFA III as a catalyst, the formation of sulphonyl halides was observed. In consequence, no more work was carried out, to examine the catalytic activity of the MFA or MFN (III) samples. The infra-red spectrum of the gas product is given in Table 7.10. The yield of sulphur chloride pentafluoride prepared using the MFD samples as catalysts, was not reproducible from a sample to another at the same composition, under the same conditions. For example, the yield was ca 53% using a sample of MFD I  $4.4 \text{ mmol g}^{-1}$  as a catalyst, another sample of the same composition yielded only 12% the third sample yielded 28%. The data collected using the MFD catalysts are summarized in Table 7.11. The samples of MFA or MFN (IV) gave very poor yields at room temperature, ca 15-18%. The results obtained are given in Table 7.12.

The reaction of the mixture of the 1:1 mole ratio of sulphur tetrafluoride and chlorine monofluoride, was examined several times using the same sample of catalyst with no pretreatment between runs. No decrease in the yield of sulphur chloride pentafluoride was observed from reaction to reaction. For example the yield was ca 84% when MFA or MFN (II or V)  $4.4 \text{ mmol g}^{-1}$  was used as a catalyst for 6 reactions. This yield was independent of the total quantity of the 1:1 mole ratio mixture admitted to the catalyst. These reactions showed that, under similar conditions supported caesium fluoride was more reactive than supported potassium fluoride in catalysing the chlorofluorination of sulphur tetrafluoride by chlorine monofluoride at room temperature. The results of 6 experiments using the same catalyst are listed in Tables 7.13-7.16 for the  $4.4$  and  $8.8 \text{ mmol g}^{-1}$  samples.

Table 7.10 The Infra-red Spectrum of the Gas Products after Reaction of  $\text{SF}_4 + \text{ClF}$  with  $\text{CsF}$  AIII  $5.5 \text{ mmol g}^{-1}$

This Work	Literature 215		
	$\text{SO}_2\text{F}_2$	$\text{SO}_2\text{ClF}$	$\text{SO}_2\text{Cl}_2$
1510	1502 $\text{B}_1\nu_6$		
1461		1455 $\text{A}_2\nu_7$	
1427			1434 $\text{B}_1\nu_6$
1277	1269 $\text{A}_1\nu_1$		
1229		1244 $\nu_1$	
1196			1205 $\text{A}_1\nu_1$
859	855 $\text{B}_2\nu_8$		
813		823 $\nu_2$	
637		627 $\nu_3$	
589			582 $\text{B}_2\nu_8$
538	544 $\nu_3$	505 $\nu_4$	
515			
482		480 $\nu_8$	
417			406 $\nu_3$

**Table 7.11 The Yield of Sulphur Chloride Pentafluoride Utilizing the MFD as a Catalyst**

Run	Batch	Sample	Gas Admitted (SF <sub>4</sub> +ClF)mmol	SF <sub>5</sub> Cl mmol	Yield %
1	1	1	10	2.65	53
2	-	2	8	0.48	12
3	-	3	8	1.12	28
4	2	1	6	0.33	11
5	-	2	4	1.06	53
6	3	1	4	0.32	16
7	-	2	7	1.33	39
8	-	3	6	0.24	8

CsFDI 4.4 mmolg<sup>-1</sup>      Sample Weight 2g

Reaction Time 2h.

Table 7.12 The Yield of Sulphur Chloride Pentafluoride Utilizing the CsFA or CsFN(IV)  $5.5 \text{ mmol g}^{-1}$  as a Catalyst

Run	Gas Admitted (ClF+SF <sub>6</sub> )mmol	SF <sub>5</sub> Cl Recovered			
		CsFA		CsFN	
		mmol	%	mmol	%
1	10	0.75	15	0.85	17
2	7	0.63	18	0.67	19
3	6	0.48	16	0.54	18
4	7	0.53	15	0.53	15
5	8	0.68	17	0.64	16
6	5	0.45	18	0.43	17

Similar results were obtained for KFAIV  $5.5 \text{ mmol g}^{-1}$

Sample Weight 2.0g

Experimental time 2h.



**Table 7.13 Results of Reaction of Sulphur Tetrafluoride with Chlorine Monofluoride in the Presence of Caesium Fluoride Supported on Fluorinated  $\gamma$ -alumina, 4.4 mmol g<sup>-1</sup>**

Run	Gas Admitted (ClF+SF <sub>4</sub> ) Torr mmol	Yield of SF <sub>5</sub> Cl (Torr/mmol)					
		CsFA		CsFN			
		I	II	V	I	II	V
1	1589	643	635	596	634	647	609
	12	4.86	4.8	4.5	4.79	4.89	4.60
2	794	330	339	315	320	314	338
	6	2.49	2.56	2.38	2.42	2.37	2.55
3	1059	445	449	433	462	438	437
	8	3.36	3.39	3.27	3.49	3.31	3.30
4	2648	1072	1044	1059	1082	1030	1058
	20	8.1	7.89	8.0	8.17	7.78	7.99
5	1854	751	731	759	727	743	737
	14	5.67	5.52	5.73	5.49	5.61	5.57
6	1324	543	555	515	519	545	551
	10	4.1	4.19	3.89	3.92	4.12	4.16

Yield of sulphur pentafluoride was based on chlorine monofluoride admitted.

**Table 7.14 Results of Reaction of Sulphur Tetrafluoride with Chlorine Monofluoride in the Presence of Potassium Fluoride Supported on Fluorinated  $\gamma$ -alumina, 4.4 mmol g<sup>-1</sup>**

Run	Gas Admitted (ClF+SF <sub>4</sub> ) Torr mmol	Yield of SF <sub>5</sub> Cl (Torr/mmol)					KFN	
		KFA		V				
		I	II	I	II	I	II	V
1	1324	477	397	432	422	406	422	428
	10	3.15	3.0	3.26	3.19	3.07	3.19	3.23
2	1854	593	569	567	565	581	565	597
	14	4.48	4.30	4.28	4.27	4.39	4.27	4.51
3	1059	328	346	307	316	322	316	336
	8	2.48	2.61	2.32	2.39	2.43	2.39	2.54
4	794	258	258	260	248	239	248	242
	6	1.95	1.93	1.96	1.87	1.81	1.87	1.83
5	2648	794	810	759	777	782	777	809
	20	6.0	6.12	5.73	5.87	5.91	5.87	6.11
6	1059	323	332	292	327	312	327	308
	8	2.44	2.51	2.21	2.47	2.36	2.47	2.33

Yield of sulphur pentafluoride was based on chlorine monofluoride admitted.

**Table 7.15 Results of Reaction of Sulphur Tetrafluoride with Chlorine Monofluoride in the Presence of Caesium Fluoride Supported on Fluorinated  $\gamma$ -alumina, 8.8 mmol g<sup>-1</sup>**

Run	Gas Admitted (ClF+SF <sub>4</sub> ) Torr mmol	Yield of SF <sub>5</sub> Cl (Torr/mmol)					CsFN
		I	II	V	I	II	
1	1324	298	293	302	285	303	301
	10	2.25	2.21	2.28	2.15	2.29	2.27
2	794	163	149	171	155	167	153
	6	1.23	1.12	1.29	1.17	1.26	1.15
3	1854	371	375	347	369	361	377
	14	2.8	2.83	2.62	2.79	2.73	2.85
4	2648	596	567	600	568	579	584
	20	4.5	4.28	4.53	4.29	4.37	4.41
5	1059	244	213	237	238	237	225
	8	1.84	1.61	1.79	1.80	1.79	1.70
6	1589	350	352	328	343	334	336
	12	2.64	2.66	2.48	2.59	2.52	2.54

Yield of sulphur pentafluoride was based on chlorine monofluoride admitted.

**Table 7.16** Results of Reaction of Sulphur Tetrafluoride with Chlorine Monofluoride in the Presence of Potassium Fluoride Supported on Fluorinated  $\gamma$ -alumina, 8.8 mmol g<sup>-1</sup>

Run	Gas Admitted (ClF+SF <sub>4</sub> ) Torr mmol	Yield of SF <sub>5</sub> Cl (Torr/mmol)					KFN				
		I	II	V	I	II	I	II	V	I	II
1	794	147	132	122	151	143	142	1.07	1.14	1.08	1.07
	6	1.11	1.0	0.92	1.14	1.08	1.07				
2	1324	252	265	222	229	249	261	1.97	1.73	1.88	1.97
	10	1.9	2.0	1.68	1.73	1.88	1.97				
3	1059	179	162	184	181	171	172	1.30	1.37	1.29	1.30
	8	1.32	1.22	1.39	1.37	1.29	1.30				
4	2648	463	467	449	446	454	461	3.48	3.37	3.43	3.48
	20	3.5	3.53	3.39	3.37	3.43	3.48				
5	1589	294	281	302	287	295	290	2.19	2.17	2.23	2.19
	12	2.22	2.12	2.28	2.17	2.23	2.19				
6	1854	315	322	316	303	324	315	2.38	2.29	2.45	2.38
	14	2.38	2.43	2.39	2.29	2.45	2.38				

Yield of sulphur pentafluoride was based on chlorine monofluoride admitted.

In each reaction, at any pressure studied, no retention of gas by the solid was observed, based on the constancy of the sample weight and the pressure of gas after reaction. The yield of sulphur chloride pentafluoride formed was dependent on the composition of the catalyst in the range  $0.6 - 15.0 \text{ mmol g}^{-1}$ . The yield was increased sharply by increasing the metal fluoride loading and the maximum yield, recorded at MF loadings of  $5.5 \text{ mmol g}^{-1}$  sample was ca 96% and 73% for CsFA and KFA respectively. In the MF loading in the range  $5.5 - 20.0 \text{ mmol g}^{-1}$  the yield of sulphur chloride pentafluoride decreased such that when a sample of MFA or MFN (I, II or V),  $20.0 \text{ mmol g}^{-1}$  was used as a catalyst, little or no sulphur chloride pentafluoride was formed. The lack of the catalytic activity of the  $20.0 \text{ mmol g}^{-1}$  sample is in good agreement with the results obtained in chapter five. The results obtained for the MFA and MFN (I, II and V) across the composition range  $0.6 - 15.0 \text{ mmol g}^{-1}$  are shown in Figs. 7.22 - 7.26.

When a 1:1 mole ratio mixture of sulphur tetrafluoride and chlorine monofluoride was heated with a sample of MFA or MFN at 373 K for 0.5 h, the gas product was a mixture of sulphonyl halides. Neither sulphur chloride pentafluoride nor reactants were observed. The infra-red spectrum of the gas products is given in Table 7.17. When the mixture was allowed to react at room temperature for 2 h in the presence of the catalyst MFA or MFN, which had been previously exposed to the mixture of sulphur tetrafluoride and chlorine monofluoride at 373 K for 0.5 h, no sulphur chloride pentafluoride was formed and only chlorine monofluoride and sulphur tetrafluoride were recovered. This showed that, no reaction occurred between the reactants and the solid.

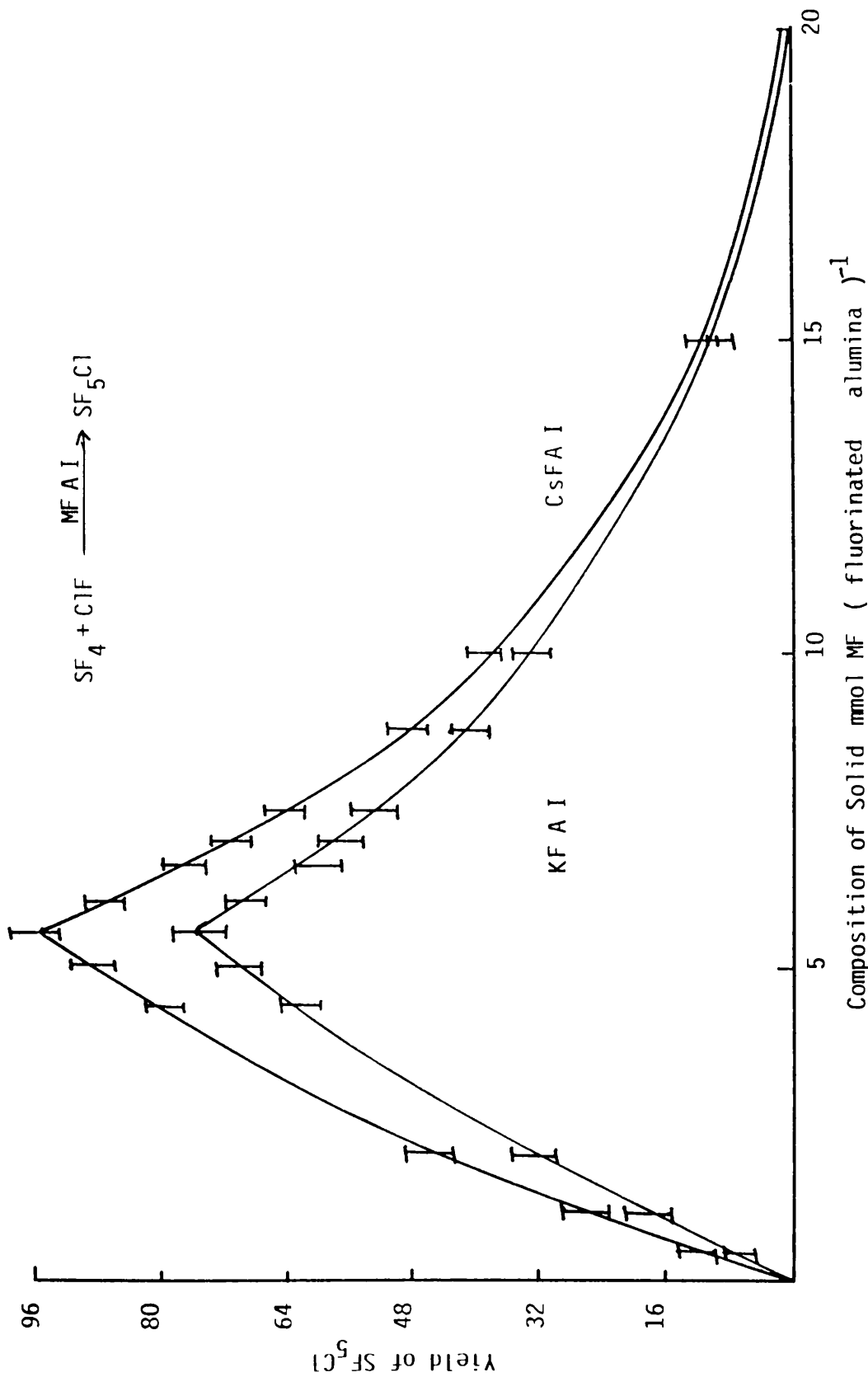


Figure 7.22 Reaction of 1:1 mole ratio of SF<sub>4</sub> + ClF over MFAl

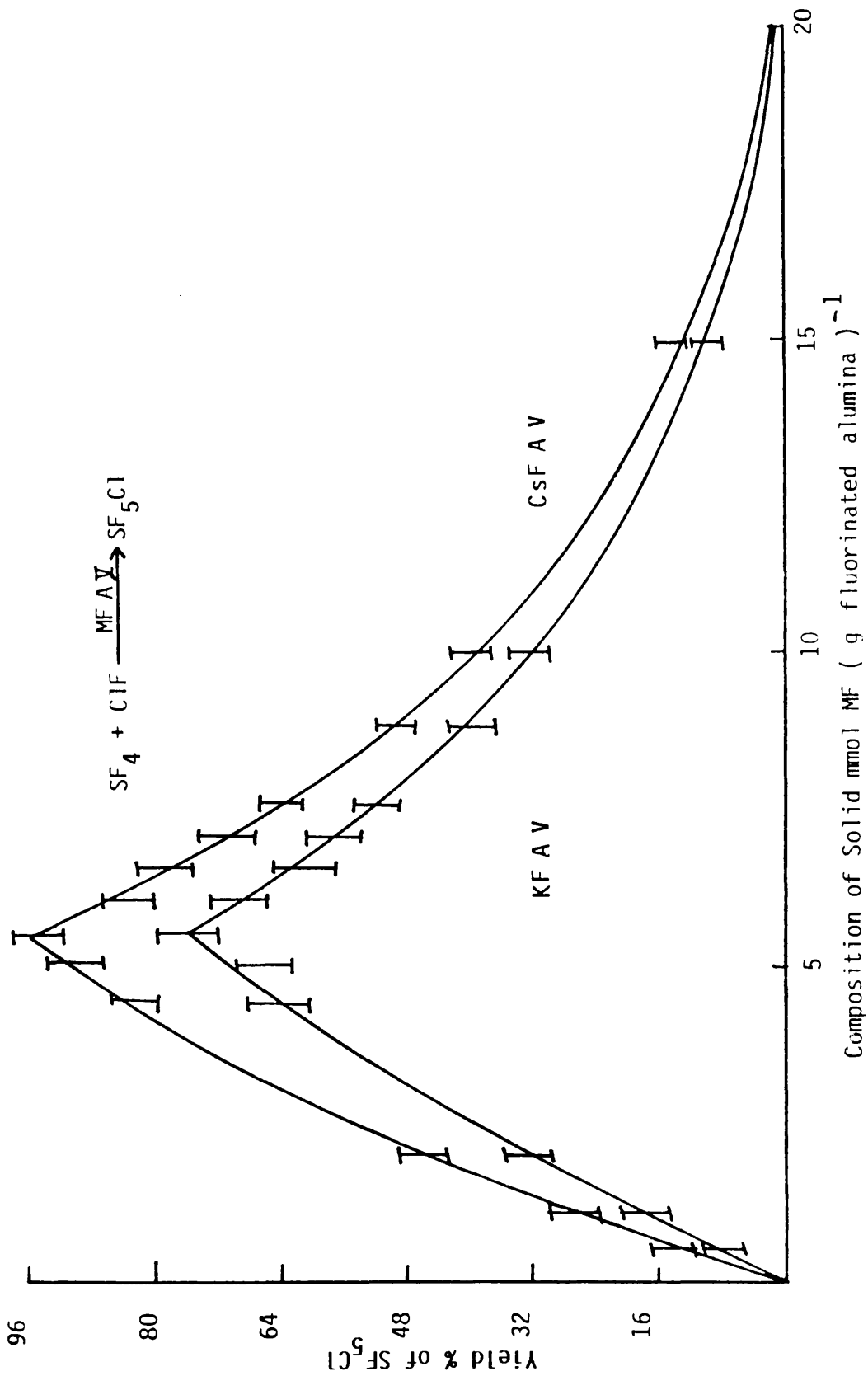


Figure 7.23 Reaction of  $\text{SF}_4 + \text{ClF}$ , 1:1 mole ratio mixture over MF A V

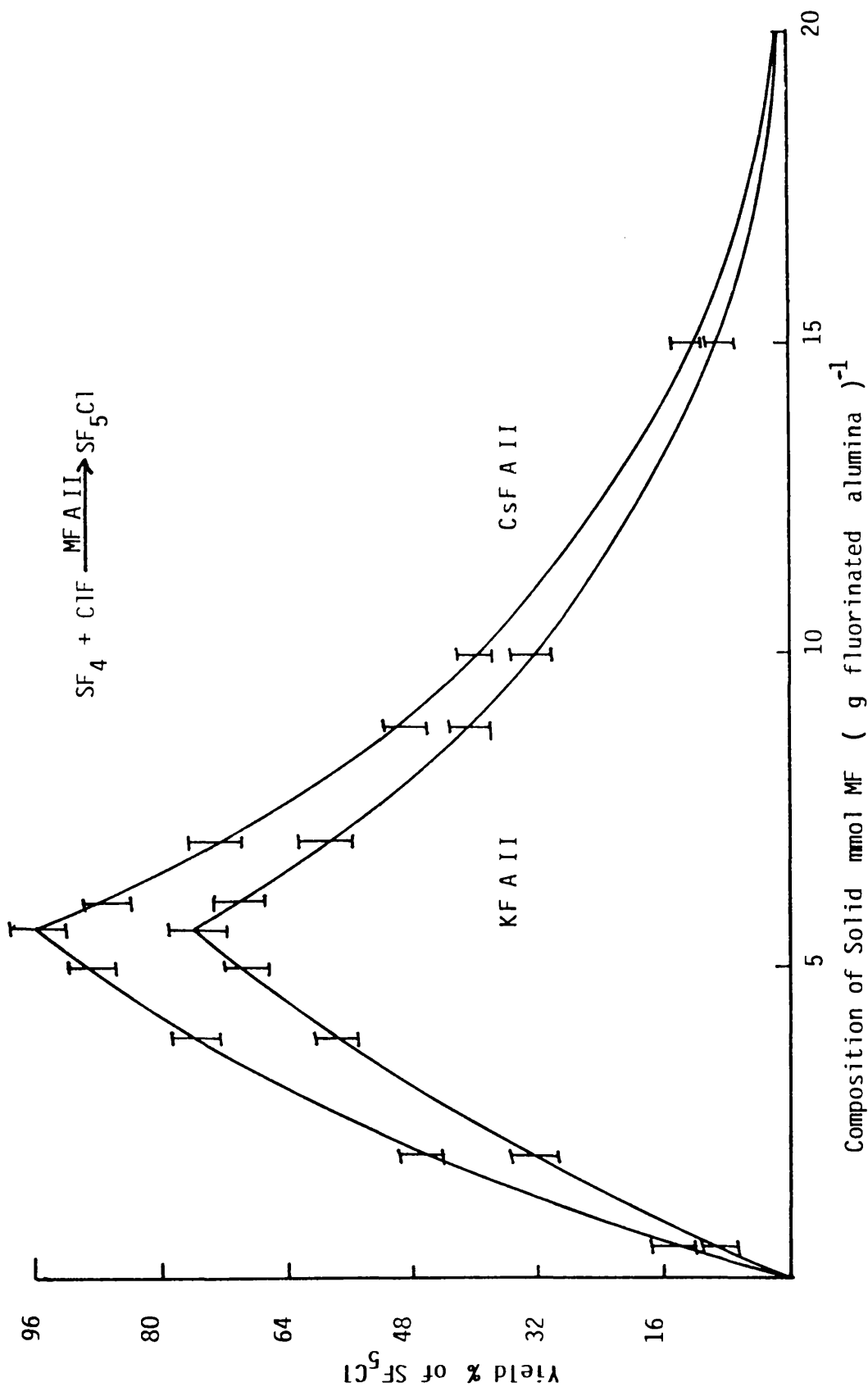


Figure 7.24 Reaction of 1:1 mole ratio mixture of  $SF_4 + ClF$  over MFA II



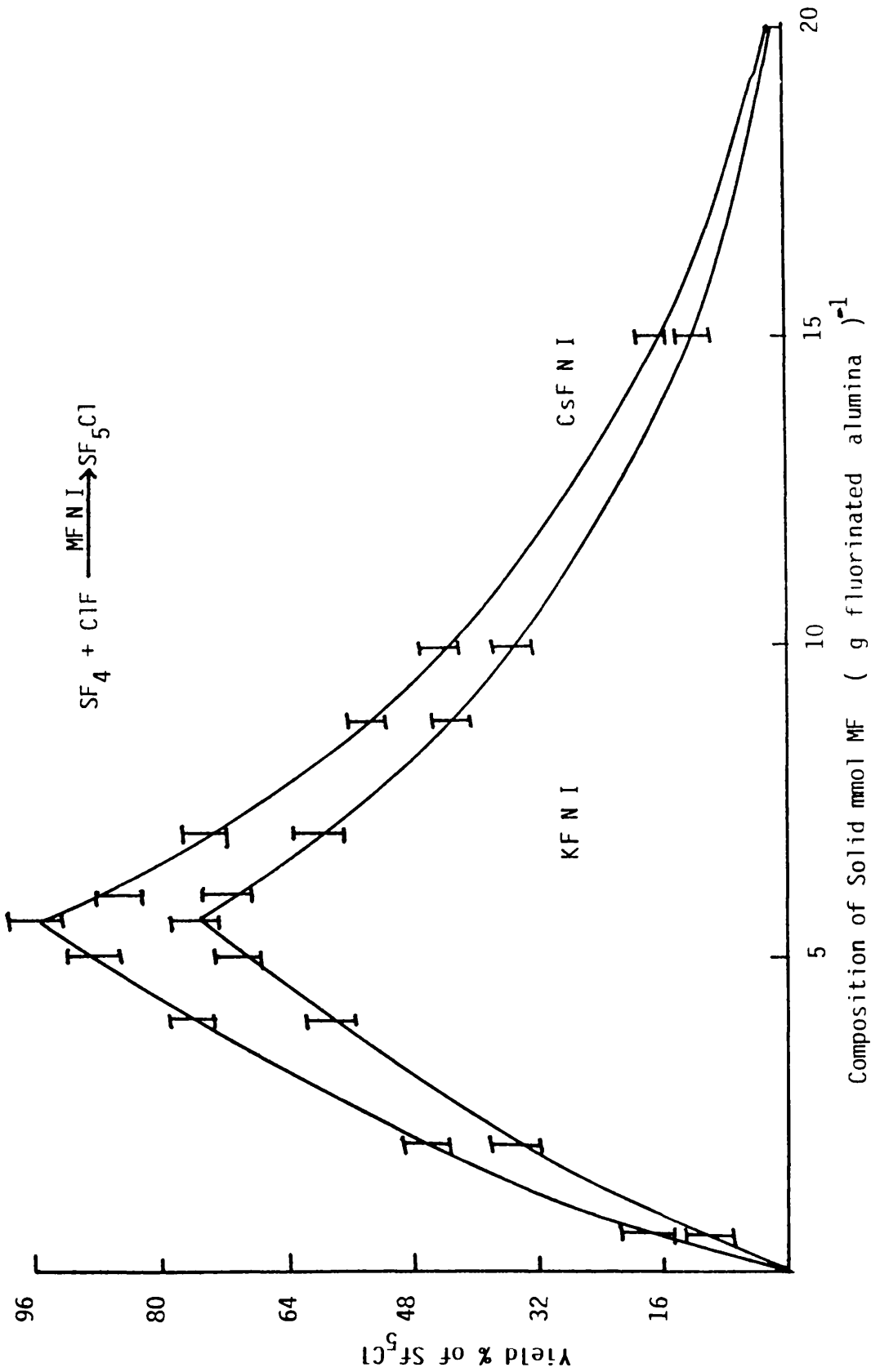


Figure 7.25 Reaction of 1:1 mole ratio of mixture of  $\text{SF}_4 + \text{ClF}$  over MFNI

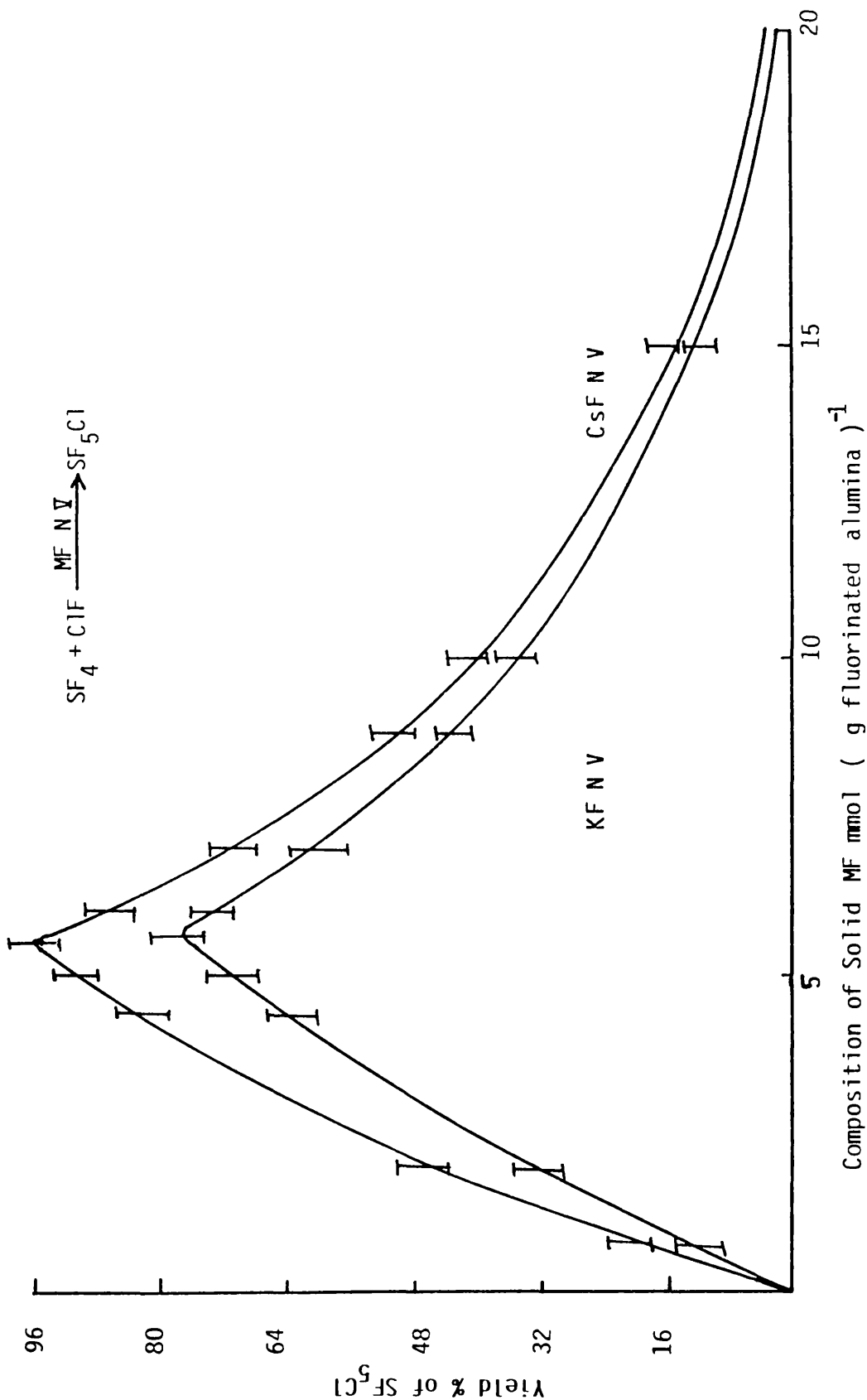


Figure 7.26 Reaction of 1:1 mole ratio of SF<sub>4</sub>+ClF mixture over MF N V

Table 7.17 The Infra-red Spectrum of the Gas Products after Reaction of  $\text{SF}_4 + \text{ClF}$  with  $\text{CsF}$  At  $5.5 \text{ mmol g}^{-1}$  at 373K

This Work	Literature 215		
	$\text{SO}_2\text{F}_2$	$\text{SO}_2\text{ClF}$	$\text{SO}_2\text{Cl}_2$
1510	1502 $B_1\nu_6$		
1461		1455 $A_2\nu_7$	
1427			1434 $B_1\nu_6$
1277	1269 $A_1\nu_1$		
1229		1244 $\nu_1$	
1196			1205 $A_1\nu_1$
859	855 $B_2\nu_8$		
813		823 $\nu_2$	
637		627 $\nu_3$	
589			582 $B_2\nu_8$
538	544 $\nu_3$	505 $\nu_4$	
515			
482		480 $\nu_8$	
417			406 $\nu_3$

The reactions between [ $^{35}\text{S}$ ]-sulphur labelled sulphur tetrafluoride or [ $^{36}\text{Cl}$ ]-chlorine labelled chlorine monofluoride and the sample of MFA or MFN, which had been treated with a mixture of chlorine monofluoride and sulphur tetrafluoride at 373 K for 0.5 h, were studied at room temperature. When [ $^{36}\text{Cl}$ ]-chlorine labelled chlorine monofluoride was admitted to the solid, no [ $^{36}\text{Cl}$ ]-chlorine surface count rate was detected even after 3 h at an initial pressure of 500 Torr. However, admission of [ $^{35}\text{S}$ ]-sulphur labelled sulphur tetrafluoride to the solid led over the first 5 min to a very small [ $^{35}\text{S}$ ]-sulphur surface count rate which thereafter remained constant throughout the experiment. On removal of the gas phase, the surface count rate dropped to the background level. The results obtained from those reactions are given in Table 7.18 for chlorine monofluoride and in Fig. 7.27 for sulphur tetrafluoride.

The competitive adsorption of sulphur tetrafluoride and chlorine monofluoride on metal fluoride supported on fluorinated  $\gamma$ -alumina was studied by keeping one of the reactants constant and varying the other using fresh materials for each experiment. In these reactions, sulphur tetrafluoride was kept constant at 4.0 mmol while the amount of chlorine monofluoride was varied from 0.5 - 4.0 mmol, the yield of sulphur chloride pentafluoride was based on the quantity of chlorine monofluoride and the quantity of the reactants recovered or retained based on the total initial gas admitted. The results obtained from MFA II 4.4 mmol  $\text{g}^{-1}$  are given in Table 7.19 and shown schematically in Fig. 7.28 and 7.29. These clearly show that, the catalysed chlorofluorination of sulphur tetrafluoride by chlorine monofluoride to form sulphur chloride pentafluoride reached a maximum yield, with no retention of gas,

Table 7.18 Reaction of [ $^{36}\text{Cl}$ ]-Chlorine Labelled Chlorine Monofluoride with  $\text{CsFNII}$  ( $4.4 \text{ mmol g}^{-1}$ ) which had been Exposed to A Mixture of Sulphur Tetrafluoride and Chlorine Monofluoride at 373K

Time (min)	Solid + Gas Count Rate Count $\text{min}^{-1}$	Gas Only Count Rate Count $\text{min}^{-1}$	Solid Count Rate Count $\text{min}^{-1}$
2	96456 $\pm$ 311	96456 $\pm$ 311	0
6	96738 $\pm$ 313	96733 $\pm$ 311	3
18	96521 $\pm$ 311	96522 $\pm$ 312	-1
28	96477 $\pm$ 311	96470 $\pm$ 312	7
36	96633 $\pm$ 312	96645 $\pm$ 312	-12
52	96641 $\pm$ 312	96641 $\pm$ 312	0
58	96673 $\pm$ 312	96673 $\pm$ 312	0
68	96571 $\pm$ 312	96578 $\pm$ 312	7
73	96584 $\pm$ 312	96587 $\pm$ 312	-3
89	96649 $\pm$ 312	96654 $\pm$ 312	-5
93	96503 $\pm$ 312	96509 $\pm$ 312	6
120	96483 $\pm$ 311	96492 $\pm$ 312	9
140	96577 $\pm$ 312	96585 $\pm$ 312	8
158	96497 $\pm$ 312	96499 $\pm$ 312	-2
163	96580 $\pm$ 312	96581 $\pm$ 312	-1
181	96511 $\pm$ 312	96511 $\pm$ 312	0

Sample Weight 2.0g

Figure 7.27 Reaction of  $^{35}\text{SF}_4$  with CsF N II, 5.5 mmol / g, pretreated with (ClF +  $\text{SF}_4$ ) mixture at 373 K

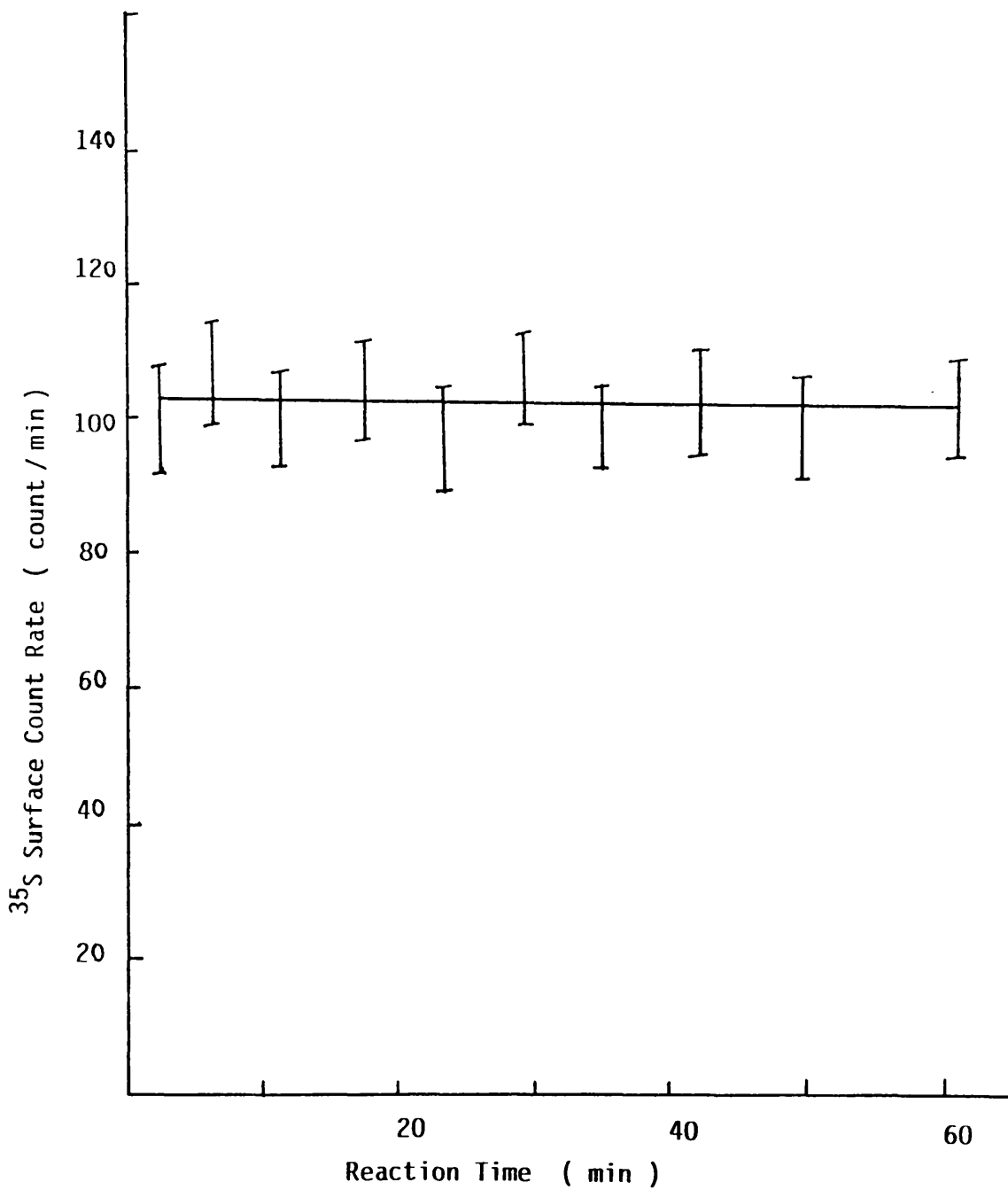


Table 7.19 The Competition Reaction Results of the Reaction of Sulphur Tetrafluoride 4.0 mmol with Chlorine Monofluoride (0.5-4.0 mmol) over MFALL 4.4 mmol g<sup>-1</sup>

CLF Admitted Torr	CsFALL				KFALL			
	Gas Retained (CLF+SF <sub>4</sub> ) Torr mmol	SF <sub>5</sub> Cl Torr mmol	Gas Recovered (CLF+SF <sub>4</sub> ) Torr mmol	Gas Retained (CLF+SF <sub>4</sub> ) Torr mmol	SF <sub>5</sub> Cl Torr mmol	Gas Recovered (CLF+SF <sub>4</sub> ) Torr mmol	Gas Recovered (CLF+SF <sub>4</sub> ) Torr mmol	
18.5	24.7	6.85	12.81	20	5.18	136.14		
0.5	0.67	0.19	3.46	0.54	0.14	3.68		
37	2.59	14.06	131	20	11.1	143		
1.0	0.7	0.38	3.54	0.54	0.3	3.86		
55.5	22.39	22.2	136.71	18.32	17.76	151.46		
1.5	0.61	0.6	3.7	0.50	0.48	4.09		
74	17.76	31.82	140.6	13.32	25.16	158.36		
2	0.48	0.86	3.8	0.30	0.68	4.28		
9.25	14.43	43.33	135.41	12.0	35.15	158.2		
2.5	0.39	1.23	3.66	0.32	0.95	4.28		
111	10.36	63.27	122.1	7.77	49.95	157.33		
3	0.28	1.71	3.3	0.21	1.35	4.25		
129.5	5.55	85.47	101.01	3	67.34	139.82		
3.5	0.15	2.31	2.73	0.08	1.82	3.78		
148	0.0	122.84	50.32	0	91.76	112.48		
4	0	3.32	1.36	0	2.48	3.04		

Figure 7.28 Change in % Composition for  $\text{Si}_4\text{ClH} \longrightarrow \text{Si}_5\text{Cl}$  over  $\text{CsF AlI}$ , 4.4 mmol / g

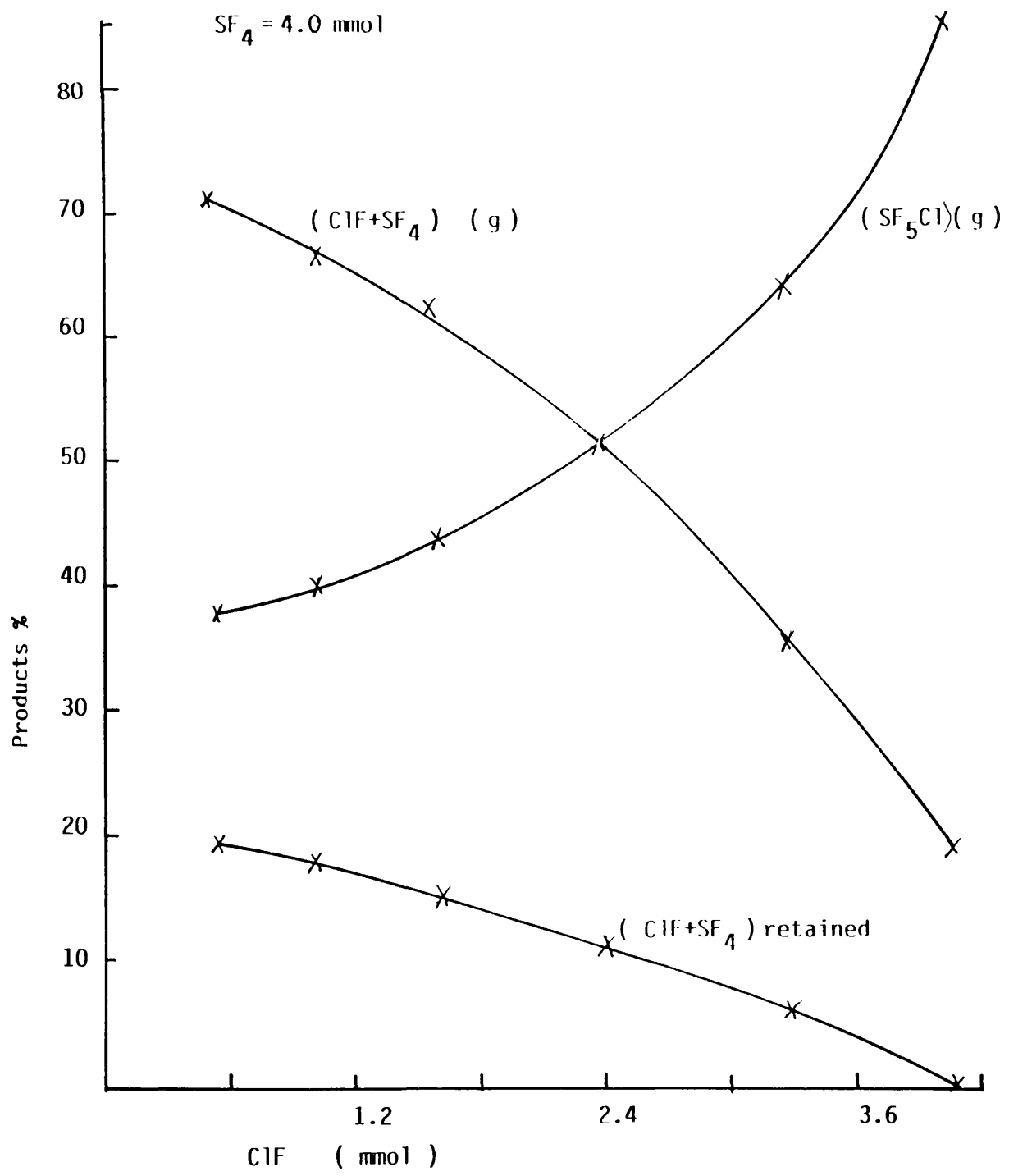
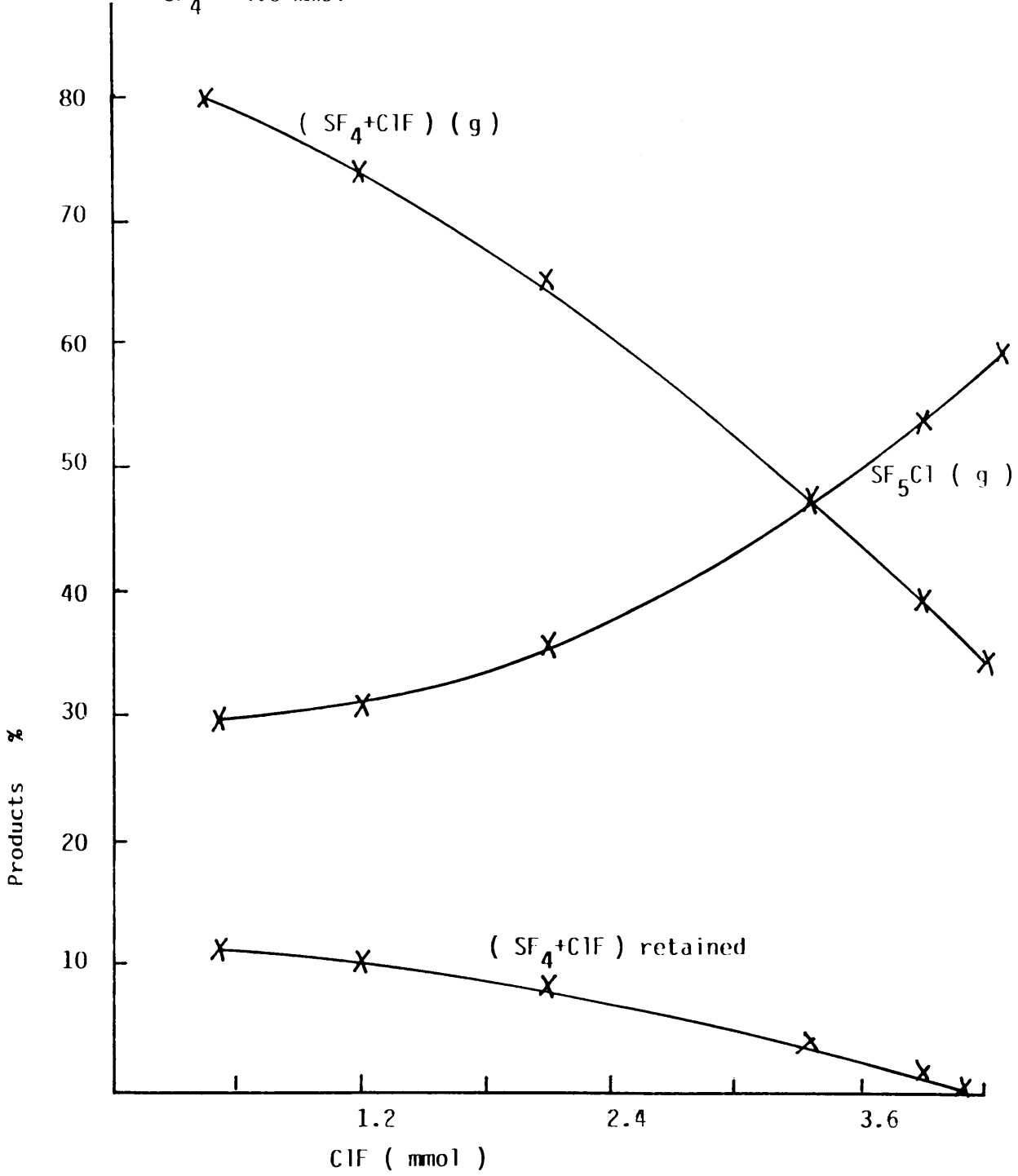




Figure 7.29 Change in % Composition for  $SF_4 + ClF \rightarrow SF_5Cl$  over  $KFAI, 4.4$   
 $mmol/g$

$SF_4 = 4.0 mmol$



when a 1:1 mole ratio mixture was used. When the quantity of chlorine monofluoride in the mixture exceeded  $4.0 \text{ mmol g}^{-1}$ , the fraction of gas retained by the catalyst was markedly increased. The yield of sulphur chloride pentafluoride and the fraction of sulphur tetrafluoride and chlorine monofluoride retained by the catalyst were affected when sulphur tetrafluoride was varied from 0.5 - 4.0 mmol, while the amount of chlorine monofluoride was kept constant at 4.0 mmol. The effect was similar to that described above, but the fraction of sulphur tetrafluoride and chlorine monofluoride retained at low sulphur tetrafluoride concentration was significantly higher than at low chlorine monofluoride concentration. Higher concentrations of sulphur tetrafluoride than those required for a 1:1 mole ratio led to a significant increase in the fraction of sulphur tetrafluoride and chlorine monofluoride retained, but the retention was less than that at higher chlorine monofluoride concentration. The results obtained from MFA II ( $4.4 \text{ mmol g}^{-1}$ ) are given in Table 7.20 and shown schematically in Figs. 7.30 and 7.31. The results obtained from MFN V 4.4 and MFN I 8.8 exhibited similar characteristics to those found with MFA II samples. For each experiment in which the catalyst retained a quantity of gas, heating the solid at 493 K led to complete desorption of sulphur tetrafluoride or chlorine monofluoride. No evidence for desorption of sulphur chloride pentafluoride or other products was obtained.

The nature of the chlorofluorination of sulphur tetrafluoride by chlorine monofluoride on the surface of metal fluoride supported on fluorinated  $\gamma$ -alumina under reaction conditions was studied by

Table 7.20 The Competition Reaction Results of the Reaction of Sulphur Tetrafluoride (0.5-4.0 mmol) with Chlorine Monofluoride 4.0 mmol<sup>-1</sup> over MFAII 4.4 mmol<sup>-1</sup>

SF <sub>4</sub> Admitted Torr	CsFAII			KFAII		
	Gas Retained (ClF+SF <sub>4</sub> ) Torr mmol	SF <sub>5</sub> Cl Torr mmol	Gas Recovered (ClF+SF <sub>4</sub> ) Torr mmol	Gas Retained (ClF+SF <sub>4</sub> ) Torr mmol	SF <sub>5</sub> Cl Torr mmol	Gas Recovered (ClF+SF <sub>4</sub> ) Torr mmol
18.5	33.3	6.85	119.5	26.64	5	129.86
0.5	0.9	0.19	3.23	0.72	0.14	3.51
37	3.33	14.43	127.65	26.0	10.73	137.54
1.0	0.9	0.39	3.45	0.7	0.29	3.72
55.5	32.56	22.76	132.27	26.46	17.76	141.52
1.5	0.88	0.62	3.57	0.72	0.48	3.82
74	26.64	31.1	133.16	2.22	25.16	149.48
2	0.72	0.84	3.60	0.6	0.68	4.04
9.25	21.6	46.25	126.4	16.84	35.15	153.36
2.5	0.58	1.25	3.42	0.46	0.95	4.14
111	15.54	63.27	116.92	12.95	51.1	143.85
3	0.42	1.71	3.16	0.35	1.38	3.89
129.5	8.33	86.77	95.63	5.55	67.34	137.3
3.5	0.23	2.35	2.58	0.15	1.82	3.71
148	0.0	121.36	53.28	0	88.8	118.4
4	0	3.28	1.44	0	2.4	3.2

Figure 7.30 Change in % Composition for  $SF_4 + ClF \longrightarrow SF_5Cl$  over CsF A I

4.4 mmol / g

ClF = 4 mmol

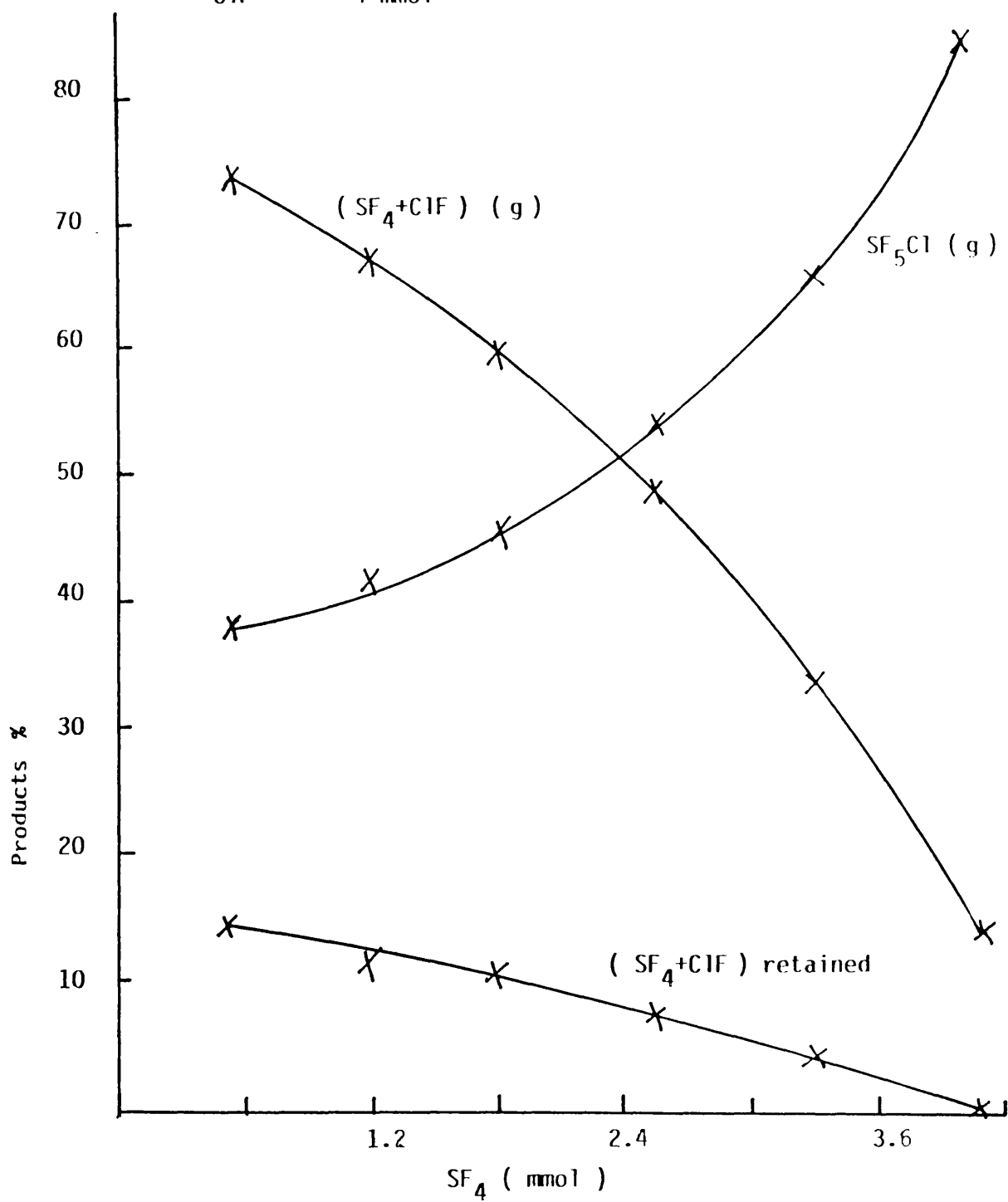
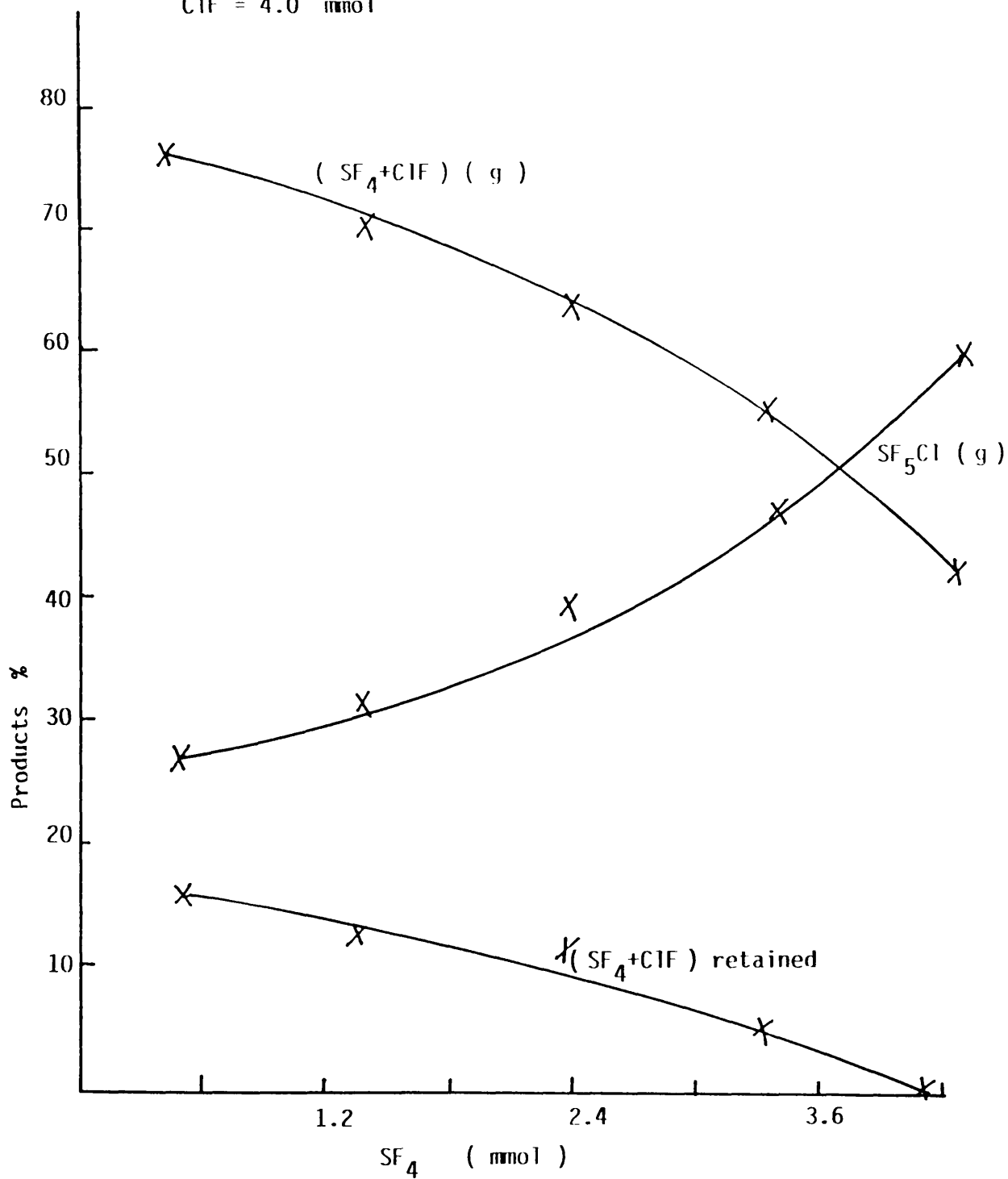


Figure 7.31 Change in % Composition for  $\text{SF}_4 + \text{ClF} \longrightarrow \text{SF}_5\text{Cl}$  over KI Al,  
 4.4 mmol / g  
 ClF = 4.0 mmol



monitoring the [ $^{35}\text{S}$ ]-sulphur or [ $^{36}\text{Cl}$ ]-chlorine count rate of the surface during reaction of [ $^{36}\text{Cl}$ ]-chlorine labelled chlorine monofluoride and sulphur tetrafluoride or [ $^{35}\text{S}$ ]-sulphur labelled sulphur tetrafluoride and chlorine monofluoride mixtures. Each catalyst was examined at least 5 times using different samples from different batches and either 1:1 or 1:2 mole ratio mixtures at different initial pressures in the range 100-600 Torr. The surface count rate was monitored with time for catalysts in the composition range 0.6 - 15.0 mmol g<sup>-1</sup>, particular attention was given to the 4.4, 5.5 and the 8.8 mmol g<sup>-1</sup> MF loadings. In each reaction the data collected from the surface count rates were converted to first and second order plots taking the highest count rate recorded as the surface count rate at time,  $t = 0$ . The slope of the straight line fit was taken as the rate constant (count)<sup>-1</sup>. Admission of 1:1 mole ratio of [ $^{36}\text{Cl}$ ]-chlorine labelled chlorine monofluoride and sulphur tetrafluoride mixture to MFA or MFN (I, II or V) 4.4 mmol g<sup>-1</sup> resulted in an increase in the [ $^{36}\text{Cl}$ ]-chlorine surface count rate at a rate too rapid to be followed accurately. It decreased sharply before reaching a constant value after ca 1.0 h. When the counting cell was evacuated the surface count rate recorded was effectively that of the background. Admission of another mixture to the solid gave results which followed the same patterns as that described above. Results for the [ $^{36}\text{Cl}$ ]-chlorine surface count rate of the MFA I and V and the MFN II 4.4 mmol g<sup>-1</sup> at initial pressures of 370, 444 and 592 Torr are given in Tables 7.21 - 7.26, and shown in Fig 6. 7.32 and 7.33. For each experiment the first order relationship  $\log \text{CR}_0/\text{CR}$  versus time was plotted. In each case the plot was not a straight line, Fig 5. 7.34 and 7.35. This means that the chlorofluorination of sulphur

**Table 7.21** The Results of Reactions of [ $^{36}\text{Cl}$ ]-Chlorine Labelled Chlorine Monofluoride and Sulphur Tetrafluoride in the Presence of CsFAI  $4.4 \text{ mmol g}^{-1}$

Time (min)	Count Rate Count $\text{min}^{-1}$	$\frac{\text{CRo}-\text{CR}}{\text{CRo}} \times 10^5$	Log $\frac{\text{CRo}}{\text{CR}} \times 10^2$
2	40591 $\pm$ 407	0	0
4	26486 $\pm$ 391	1.31	18.54
8	15626 $\pm$ 257	3.94	41.46
12	11082 $\pm$ 217	6.56	56.38
16	8585 $\pm$ 169	9.18	67.47
20	7007 $\pm$ 167	11.8	76.29
24	5919 $\pm$ 157	14.43	83.62
28	5123 $\pm$ 143	17.06	89.9
32	4516 $\pm$ 134	19.68	95.37
36	4038 $\pm$ 126	22.3	100.23
40	3651 $\pm$ 120	24.93	104.6
44	3332 $\pm$ 115	27.55	108.57
48	3064 $\pm$ 112	30.17	112.21
52	2836 $\pm$ 107	32.8	115.57
56	2639 $\pm$ 103	35.43	118.7
60	2600 $\pm$ 102	36.0	119.35
64	2583 $\pm$ 102	36.25	119.63

CRo = 40591 count  $\text{min}^{-1}$

Initial pressure of ( $\text{ClF}+\text{SF}_4$ ) = 370 Torr

**Table 7.22** The Results of Reactions of [<sup>36</sup>Cl]-Chlorine Labelled Chlorine Monofluoride and Sulphur Tetrafluoride in the Presence of CsFAII 4.4 mmol g<sup>-1</sup>

Time (min)	Count Rate Count min <sup>-1</sup>	$\frac{1}{CR} - \frac{1}{CRO} \times 10^5$	Log $\frac{CRO}{CR} \times 10^2$
2	42589 ± 417	0	0
4	27189 ± 330	1.33	19.49
8	15778 ± 251	3.99	43.12
12	11114 ± 211	6.65	58.34
16	8578 ± 185	9.31	69.59
20	6984 ± 166	11.97	78.52
24	5890 ± 156	14.63	85.92
28	5092 ± 142	17.29	92.24
32	4485 ± 133	19.95	97.75
36	4007 ± 125	22.61	102.65
40	3621 ± 119	25.27	107.05
44	3303 ± 114	27.93	111.04
48	3036 ± 112	30.59	114.70
52	2809 ± 106	33.25	118.07
56	2614 ± 102	35.91	121.2
60	2584 ± 102	36.35	121.7
64	2563 ± 101	36.67	122.05

CRO = 42589 count min<sup>-1</sup>

Initial pressure of (ClF+SF<sub>6</sub>) = 444 Torr



**Table 7.23** The Results of Reactions of [<sup>36</sup>Cl]-Chlorine Labelled Chlorine Monofluoride and Sulphur Tetrafluoride in the Presence of CsFNI 4.4 mmol g<sup>-1</sup>

Time (min)	Count Rate Count min <sup>-1</sup>	$\frac{1}{CR} - \frac{1}{CR_0} \times 10^5$	Log $\frac{CR_0}{CR} \times 10^2$
2	48996 ± 443	0	0
4	29771 ± 345	1.32	21.64
8	16681 ± 258	3.95	46.79
12	11586 ± 221	6.59	62.62
16	8875 ± 172	9.23	74.20
20	7193 ± 168	11.86	83.32
24	6046 ± 159	14.50	90.87
28	5215 ± 145	17.13	96.99
32	4585 ± 136	19.77	102.88
36	4090 ± 128	22.40	107.84
40	3692 ± 122	25.04	112.29
44	3365 ± 117	27.68	116.32
48	3091 ± 114	30.31	120.0
52	2858 ± 109	32.95	123.41
56	2658 ± 104	35.58	126.56
60	2602 ± 103	36.39	127.48
64	2564 ± 102	36.96	128.12

CR<sub>0</sub> = 48996 count min<sup>-1</sup>

Initial pressure of (ClF+SF<sub>4</sub>) = 592 Torr

**Table 7.24** The Results of Reactions of [ $^{36}\text{Cl}$ ]-Chlorine Labelled Chlorine Monofluoride and Sulphur Tetrafluoride in the Presence of KFAI 4.4 mmol g $^{-1}$

Time (min)	Count Rate Count min $^{-1}$	$\frac{1}{\text{CR}} - \frac{1}{\text{CRo}} \times 10^5$	Log $\frac{\text{CRo}}{\text{CR}} \times 10^2$
2	25925 $\pm$ 322	0	0
4	21217 $\pm$ 291	0.86	8.7
8	15564 $\pm$ 256	2.57	22.16
12	12289 $\pm$ 219	4.28	32.42
16	10153 $\pm$ 202	5.99	40.71
20	8650 $\pm$ 174	7.70	47.67
24	7534 $\pm$ 170	9.42	53.67
28	6673 $\pm$ 163	11.13	58.94
32	5989 $\pm$ 155	12.84	63.64
36	5432 $\pm$ 147	14.55	67.88
40	4970 $\pm$ 141	16.26	71.74
44	4580 $\pm$ 135	17.98	75.29
48	4247 $\pm$ 130	19.69	78.56
52	3959 $\pm$ 126	21.40	81.61
56	3708 $\pm$ 122	23.11	84.46
60	3487 $\pm$ 118	24.82	87.13
64	3400 $\pm$ 167	25.56	88.22

CRo = 25925 count min $^{-1}$

Initial pressure of (ClF+SF $_4$ ) = 370 Torr

Table 7.25 The Results of Reactions of [ $^{36}\text{Cl}$ ]-Chlorine Labelled Chlorine Monofluoride and Sulphur Tetrafluoride in the Presence of KFAV  $4.4 \text{ mmol g}^{-1}$

Time (min)	Count Rate Count $\text{min}^{-1}$	$\frac{1}{\text{CR}} - \frac{1}{\text{CR}_0} \times 10^5$	Log $\frac{\text{CR}_0}{\text{CR}} \times 10^2$
2	31353 $\pm$ 354	0	0
4	24658 $\pm$ 314	0.87	10.43
8	17279 $\pm$ 263	2.60	25.87
12	13299 $\pm$ 231	4.33	37.25
16	10809 $\pm$ 208	6.06	46.25
20	9105 $\pm$ 191	7.79	53.70
24	7864 $\pm$ 177	9.53	60.06
28	6922 $\pm$ 166	11.26	65.60
32	6181 $\pm$ 157	12.99	70.52
36	5583 $\pm$ 149	14.72	74.94
40	5091 $\pm$ 143	16.45	78.95
44	4678 $\pm$ 136	18.19	82.62
48	4328 $\pm$ 132	19.92	86.0
52	4026 $\pm$ 127	21.65	89.14
56	3763 $\pm$ 123	23.39	92.07
60	3533 $\pm$ 118	25.12	94.81
64	3496 $\pm$ 118	25.41	95.27

$\text{CR}_0 = 31353 \text{ count min}^{-1}$

Initial pressure of  $(\text{ClF} + \text{SF}_4) = 444 \text{ Torr}$

Table 7.26 The Results of Reactions of [ $^{36}\text{Cl}$ ]-Chlorine Labelled Chlorine Monofluoride and Sulphur Tetrafluoride in the Presence of KFNII  $4.4 \text{ mmol g}^{-1}$

Time (min)	Count Rate Count $\text{min}^{-1}$	$\frac{1}{\text{CR}} - \frac{1}{\text{CRo}} \times 10^5$	Log $\frac{\text{CRo}}{\text{CR}} \times 10^2$
2	40791 $\pm$ 404	0	0
4	30289 $\pm$ 348	0.85	12.93
8	19994 $\pm$ 283	2.55	30.97
12	14922 $\pm$ 244	4.25	43.67
16	11903 $\pm$ 218	5.95	53.49
20	9899 $\pm$ 199	7.65	61.50
24	8473 $\pm$ 184	9.35	68.25
28	7407 $\pm$ 172	11.05	74.09
32	6578 $\pm$ 162	12.75	79.25
36	5917 $\pm$ 154	14.45	83.85
40	5376 $\pm$ 147	16.15	88.01
44	4926 $\pm$ 140	17.85	91.81
48	4545 $\pm$ 135	19.55	95.30
52	4219 $\pm$ 130	21.25	98.54
56	3937 $\pm$ 125	22.95	101.53
60	3690 $\pm$ 121	24.65	104.35
64	3613 $\pm$ 120	25.23	105.27

CRo = 40791 count  $\text{min}^{-1}$

Initial pressure of ( $\text{ClF} + \text{SF}_4$ ) = 592 Torr

Figure 7.32 Reaction of  $^{36}\text{Cl} + \text{SF}_4$ , 1:1 mole ratio with CsF Al, 4.4 mmol / g  
Surface Count Rate  $\sqrt{\text{Time}}$   
Pressure of mixture = 592 Torr

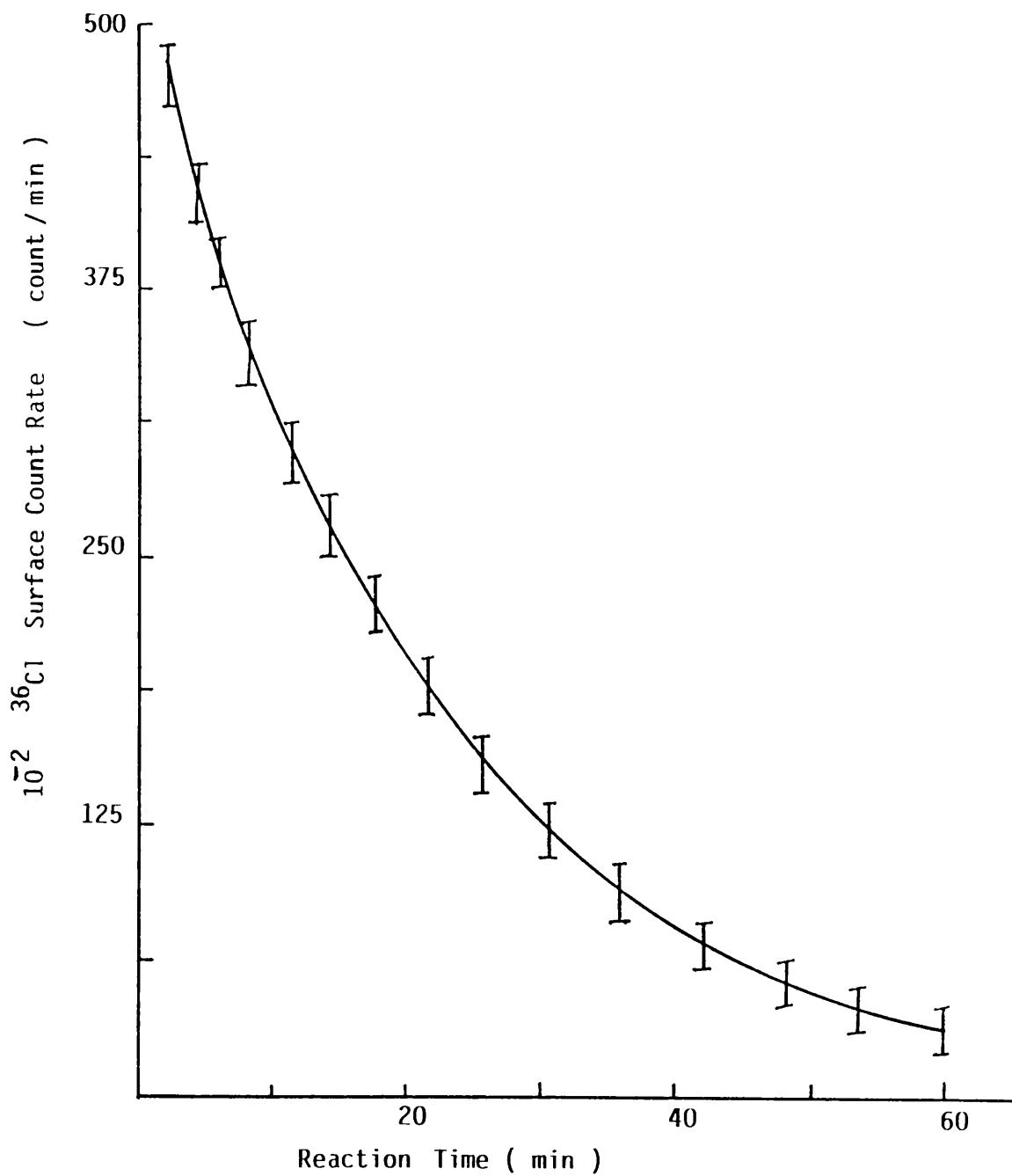


Figure 7.33 Reaction of  $^{36}\text{ClF} + \text{SF}_4$ , 1:1 mole ratio with KF AI, 4.4 mmol/g  
 $^{36}\text{Cl}$  Surface Count Rate V Time  
Pressure of the mixture = 592 Torr

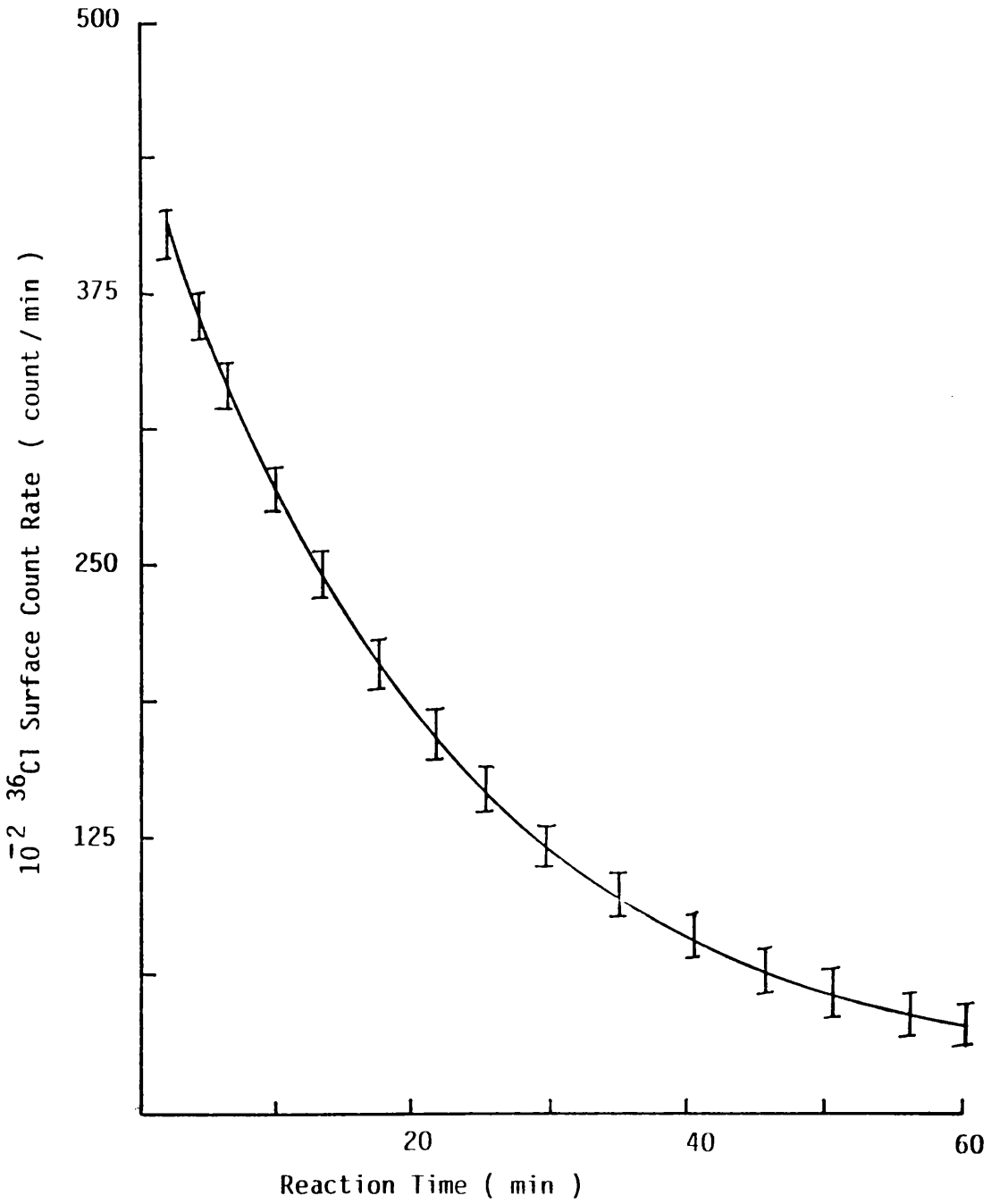


Figure 7.34 Reaction of  $^{36}\text{Cl} + \text{SF}_4$ , 1:1 mole ratio over CsF Al, 4.4 mmol/g  
1st Order Plot

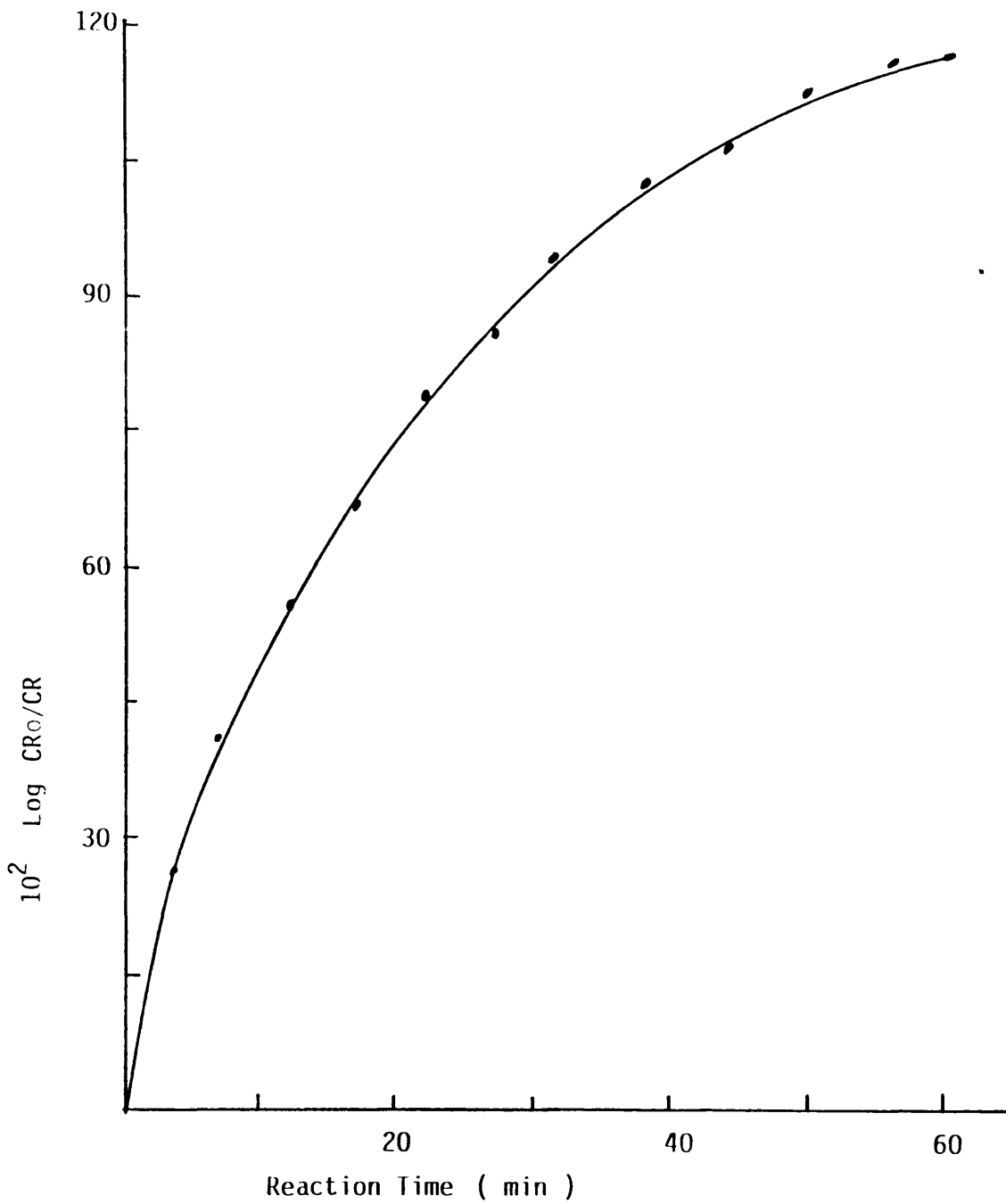
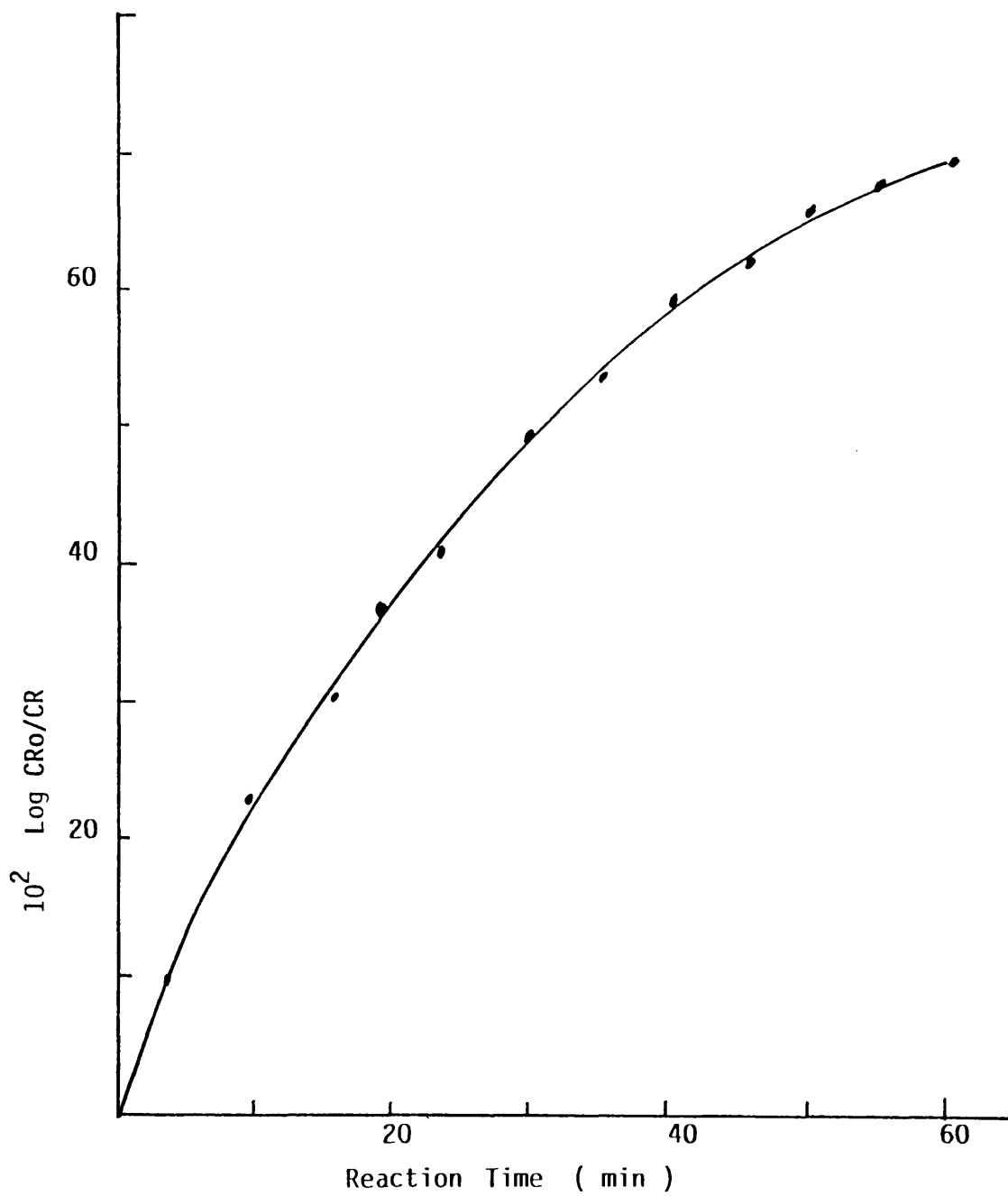


Figure 7.35 Reaction of  $^{36}\text{Cl} + \text{SF}_4$ , 1:1 mole ratio over Kf Al, 4.4 mmol / g  
1st Order Plot





tetrafluoride by chlorine monofluoride does not follow a first order reaction. The second order plots were obtained,

Fig. 7.36 - 7.39, for MFA I and V and MFN II  $4.4 \text{ mmol g}^{-1}$  at the initial pressures studied. These plots gave straight lines with a correlation coefficient  $> 0.999$  and a slope in the range  $6.37 - 6.87 \times 10^{-6} \text{ count}^{-1}$  using CsFA or CsFN. This clearly showed that the chlorofluorination of sulphur tetrafluoride by chlorine monofluoride was a second order reaction providing the mixture had a 1:1 mole ratio composition. The second order rate constant was  $(6.64 \pm 0.17) \times 10^{-6} \text{ count}^{-1}$  using CsFA  $4.4 \text{ mmol g}^{-1}$ . On the other hand admission of a 1:1 mole ratio of chlorine monofluoride and [ $^{35}\text{S}$ ]-sulphur labelled sulphur tetrafluoride to the solid MFA or MFN, exhibited the same characteristics as those described above, in that, the [ $^{35}\text{S}$ ]-sulphur surface count rate increased rapidly then decreased over the first 60 min before reaching a constant value thereafter. On removal of the gas phase from the counting cell the surface radioactivity was completely removed with no indication of the formation of any permanently adsorbed species. The admission of another quantity of the mixture, followed the same pattern as that described above. The results obtained from the MFA I and V and MFN II  $4.4 \text{ mmol g}^{-1}$  at initial pressures of 370, 444 and 600 Torr are summarized in Tables 7.27 - 7.32 and shown schematically in Fig. 7.40 and 7.41. For each experiment a plot of the first order reaction showed that the chlorofluorination of sulphur tetrafluoride by chlorine monofluoride did not follow a first order reaction. The second order plots are shown in Fig. 7.42 and 7.43 for the samples studied at different initial pressures. These plots gave straight lines with correlation coefficients  $> 0.999$  and slopes in the range  $6.39 - 6.81 \times 10^{-6}$

Figure 7.36 Reaction of  $^{36}\text{ClF} + \text{SF}_4$ , 1:1 mole ratio over CsF AI, 4.4 mmol/g  
2nd Order Plot

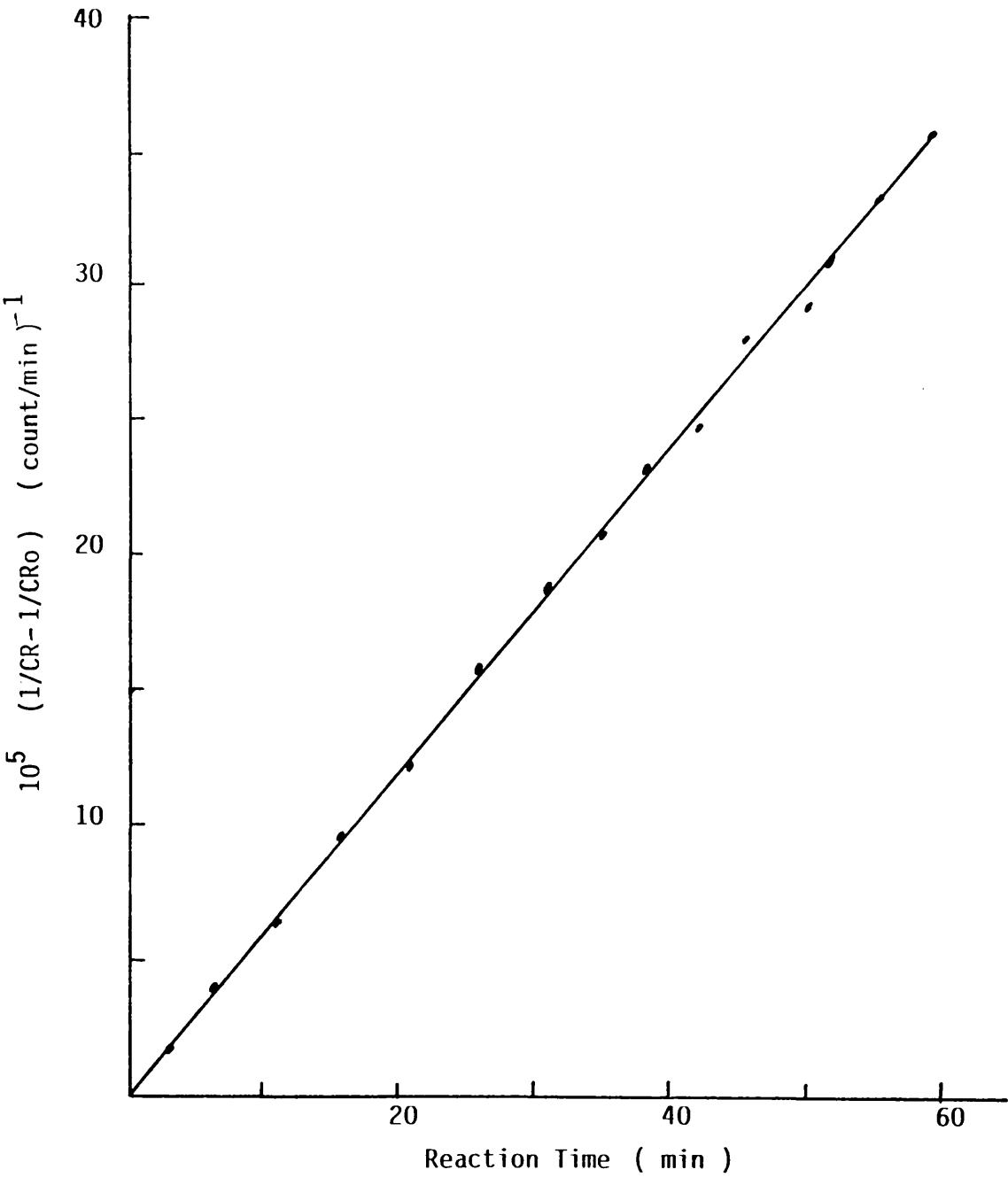


Figure 7.37 Reaction of  $^{36}\text{Cl} + \text{SF}_4$ , 1:1 mole ratio over CsF  $\Lambda$ , 4.4 mmol/g  
2nd Order Plot

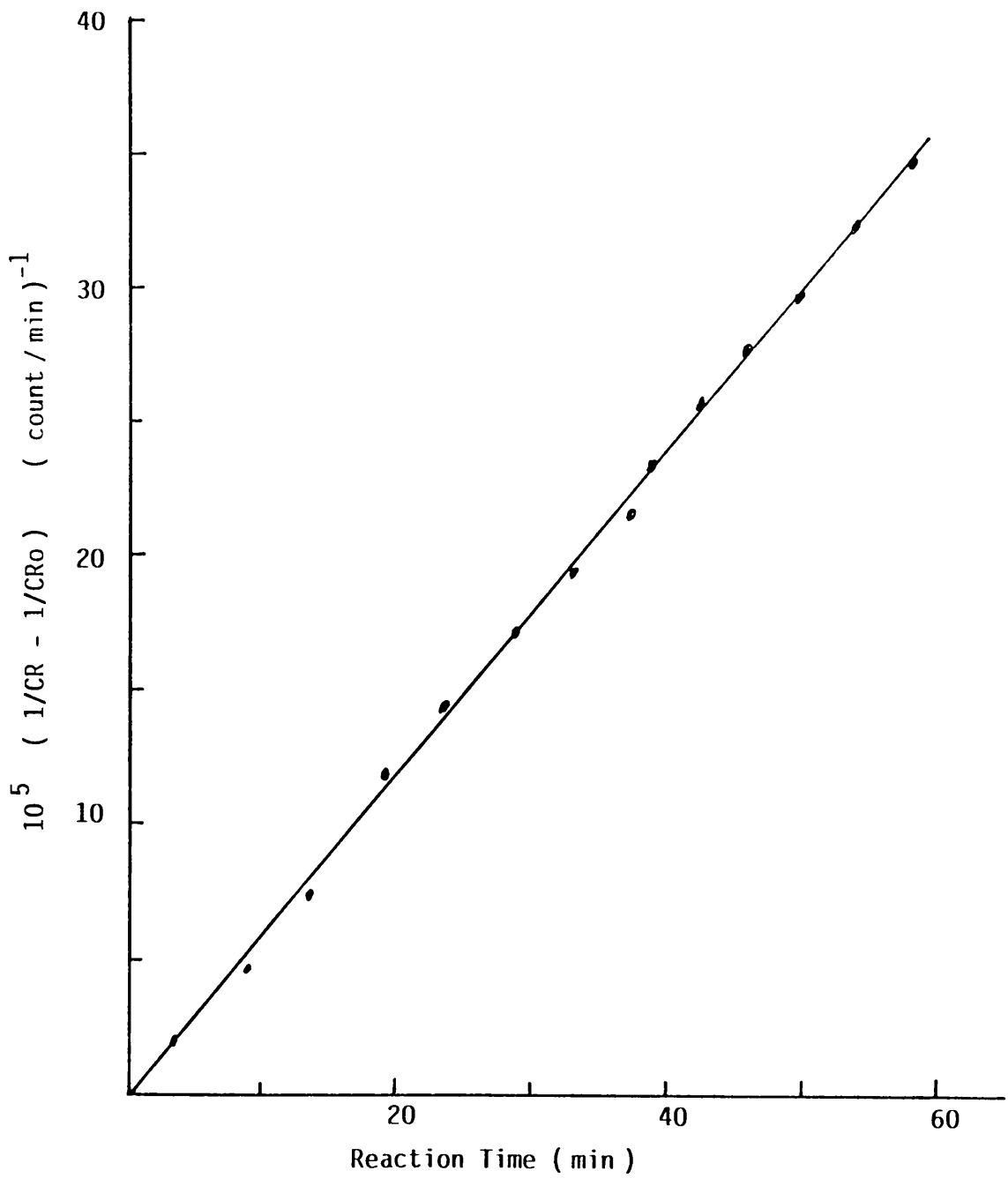
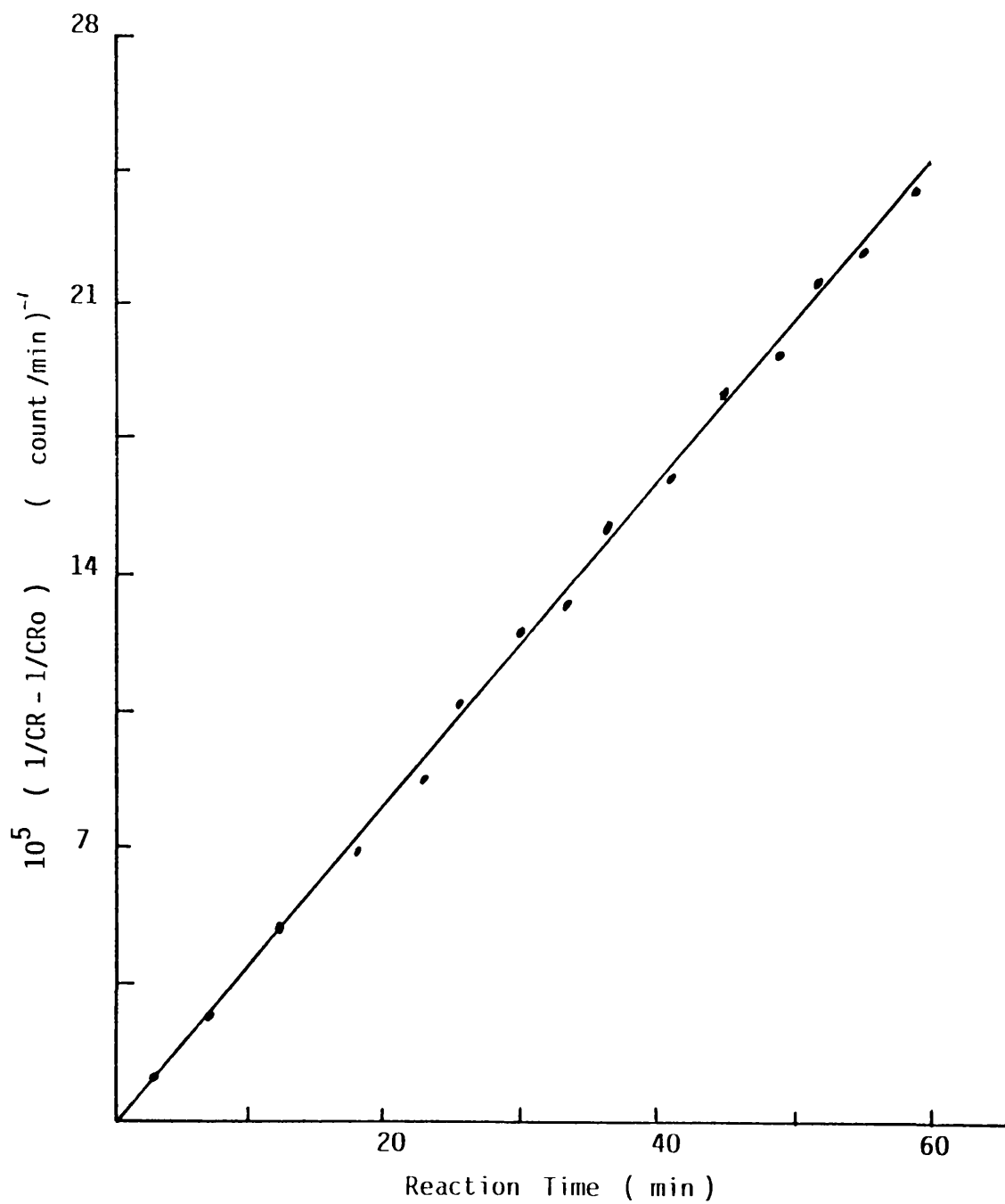


Figure 7.38 Reaction of  $^{36}\text{Cl} + \text{SF}_4$ , 1:1 mole ratio over KFA I, 4.4  
mmol / g  
2nd Order Plot



**Figure 7.39** Reaction of  $^{36}\text{ClF} + \text{SF}_4$ , 1:1 mole ratio over KI AV, 4.4 mmol / g  
2nd Order Plot

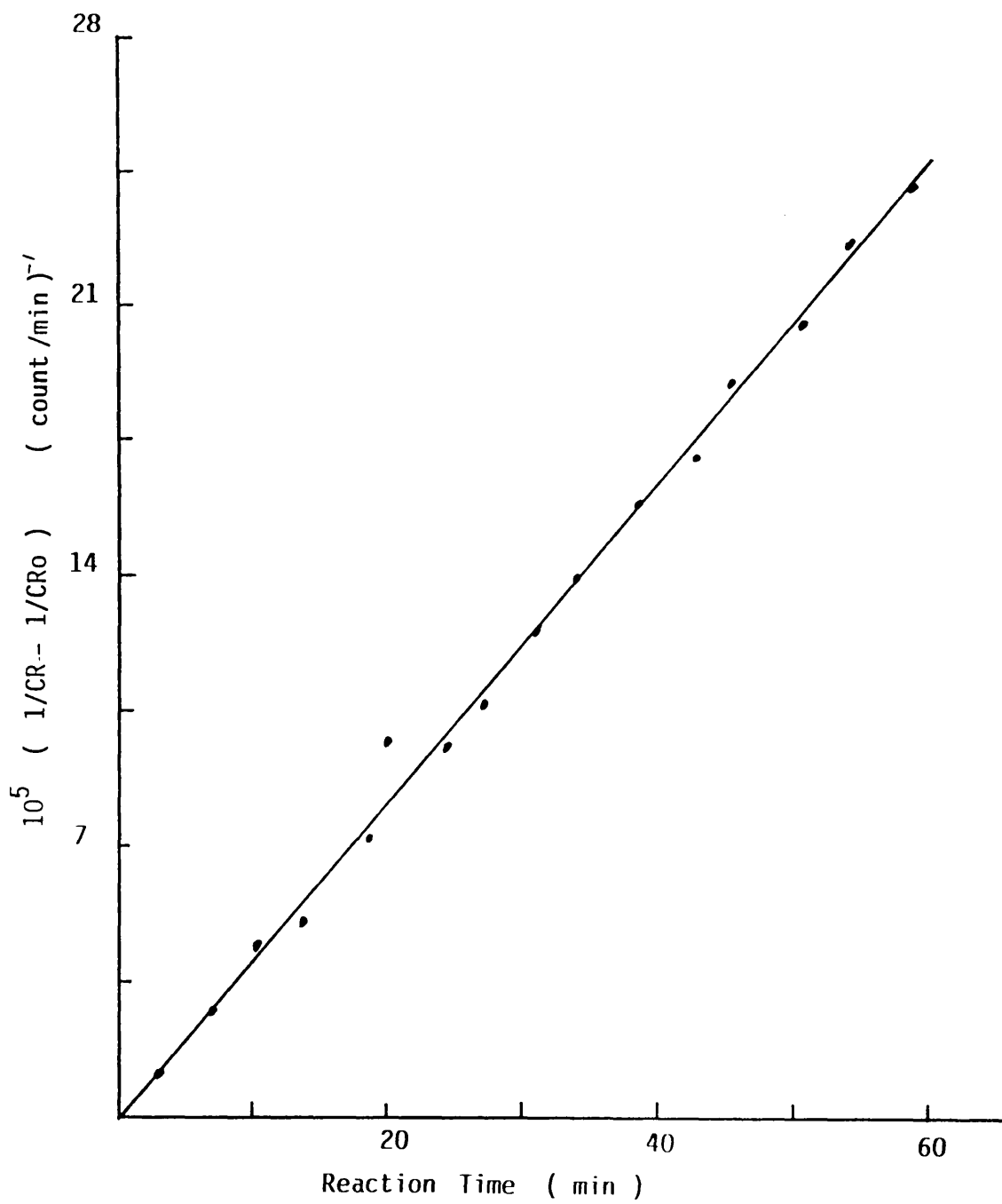


Table 7.27 The Results of Reactions of Chlorine Monofluoride and [<sup>35</sup>S]-Sulphur Labelled Sulphur Tetrafluoride in the Presence of CsFAI 4.4 mmol g<sup>-1</sup>

Time (min)	Count Rate Count min <sup>-1</sup>	$\frac{1}{CR} - \frac{1}{CR_0} \times 10^5$	Log $\frac{CR_0}{CR} \times 10^2$
2	30184 ± 347	0	0
4	21594 ± 294	1.32	14.54
8	13671 ± 235	3.95	34.11
12	10098 ± 201	6.59	47.55
16	7975 ± 179	9.23	57.80
20	6590 ± 162	11.86	66.09
24	5615 ± 150	14.30	73.04
28	4891 ± 140	17.13	79.04
32	4332 ± 132	19.77	84.31
36	3888 ± 125	22.41	89.0
40	3527 ± 119	25.04	93.24
44	3227 ± 114	27.68	97.10
48	2974 ± 108	30.31	100.64
52	2758 ± 105	32.95	103.92
56	2571 ± 101	35.58	109.97
60	2543 ± 101	36.01	107.44
64	2501 ± 100	36.62	108.17

CR<sub>0</sub> = 30184 count min<sup>-1</sup>

Initial pressure of (ClF+SF<sub>4</sub>) = 370 Torr

**Table 7.28** The Results of Reactions of Chlorine Monofluoride and [<sup>35</sup>S]-Sulphur Labelled Sulphur Tetrafluoride in the Presence of CsFAV 4.4 mmol g<sup>-1</sup>

Time (min)	Count Rate Count min <sup>-1</sup>	$\frac{1}{CR} - \frac{1}{CR_0} \times 10^5$	Log $\frac{CR_0}{CR} \times 10^2$
2	36769 ± 384	0	0
4	24632 ± 314	1.34	17.39
8	14837 ± 244	4.02	39.41
12	10616 ± 206	6.70	53.95
16	8292 ± 182	9.34	64.68
20	6766 ± 165	12.06	73.51
24	5727 ± 151	14.74	80.76
28	4965 ± 141	17.42	86.96
32	4382 ± 132	20.1	92.38
36	3922 ± 125	22.78	97.19
40	3549 ± 119	25.46	101.53
44	3240 ± 114	28.14	105.49
48	2982 ± 109	30.81	109.10
52	2760 ± 105	33.51	112.46
56	2570 ± 101	36.19	115.56
60	2563 ± 101	36.91	116.67
64	2557 ± 101	37.17	115.78

CR<sub>0</sub> = 36769 count min<sup>-1</sup>

Initial pressure of (ClF+SF<sub>4</sub>) = 444 Torr

**Table 7.29** The Results of Reactions of Chlorine Monofluoride and [<sup>35</sup>S]-Sulphur Labelled Sulphur Tetrafluoride in the Presence of CsFNII 4.4 mmol g<sup>-1</sup>

Time (min)	Count Rate Count min <sup>-1</sup>	$\frac{1}{CR} - \frac{1}{CR_0} \times 10^5$	Log $\frac{CR_0}{CR} \times 10^2$
2	47481 ± 436	0	0
4	29035 ± 341	1.34	21.36
8	16340 ± 256	4.01	46.33
12	11369 ± 213	6.69	62.01
16	8717 ± 187	9.37	73.62
20	7068 ± 168	12.04	82.72
24	5944 ± 154	14.72	90.24
28	5128 ± 143	17.39	96.96
32	4509 ± 134	20.07	102.24
36	4024 ± 127	22.74	107.19
40	3633 ± 121	25.42	111.63
44	3311 ± 115	28.10	115.66
48	3041 ± 110	30.78	119.35
52	2812 ± 106	33.46	122.75
56	2617 ± 102	36.11	125.87
60	2593 ± 102	36.46	126.27
64	2561 ± 101	36.94	126.81

CR<sub>0</sub> = 47481 count min<sup>-1</sup>

Initial pressure of (ClF+SF<sub>4</sub>) = 600 Torr



**Table 7.30** The Results of Reactions of Chlorine Monofluoride and [<sup>35</sup>S]-Sulphur Labelled Sulphur Tetrafluoride in the Presence of KFAI 4.4 mmol g<sup>-1</sup>

Time (min)	Count Rate Count min <sup>-1</sup>	$\frac{1}{CR} - \frac{1}{CR_0} \times 10^5$	Log $\frac{CR_0}{CR} \times 10^2$
2	20068 ± 283	0	0
4	17161 ± 262	0.84	6.80
8	13307 ± 231	2.53	17.84
12	10866 ± 208	4.22	26.64
16	9182 ± 192	5.91	33.64
20	7950 ± 178	7.6	40.21
24	7009 ± 167	9.28	45.68
28	6268 ± 158	10.97	50.54
32	5668 ± 151	12.66	54.91
36	5173 ± 144	14.35	58.88
40	4758 ± 138	16.03	62.51
44	4404 ± 133	17.72	65.87
48	4099 ± 128	19.41	68.98
52	3834 ± 124	21.10	71.89
56	3600 ± 120	22.79	74.62
60	3581 ± 120	22.94	74.85
64	3562 ± 119	23.09	75.08

CR<sub>0</sub> = 20068 count min<sup>-1</sup>

Initial pressure of (ClF+SF<sub>6</sub>) = 370 Torr

Table 7.31 The Results of Reactions of Chlorine Monofluoride and [<sup>35</sup>S]-Sulphur Labelled Sulphur Tetrafluoride in the Presence of KFAV 4.4 mmol g<sup>-1</sup>

Time (min)	Count Rate Count min <sup>-1</sup>	$\frac{1}{CR} - \frac{1}{CR_0} \times 10^5$	Log $\frac{CR_0}{CR} \times 10^2$
2	23045 ± 304	0	0
4	19167 ± 277	0.88	8.0
8	14340 ± 239	2.63	20.6
12	11456 ± 214	4.39	30.35
16	9537 ± 195	6.15	38.32
20	8169 ± 181	7.9	45.04
24	7144 ± 169	9.66	50.86
28	6348 ± 159	11.41	56.0
32	5711 ± 151	13.17	60.59
36	5191 ± 144	14.92	64.73
40	4757 ± 138	16.68	68.52
44	4390 ± 133	18.44	72.01
48	4076 ± 128	20.19	75.23
52	3804 ± 123	21.95	78.23
56	3566 ± 119	23.70	81.04
60	3509 ± 118	24.16	81.74
64	3491 ± 118	24.33	81.96

CR<sub>0</sub> = 23045 count min<sup>-1</sup>

Initial pressure of (ClF+SF<sub>4</sub>) = 444 Torr

**Table 7.32** The Results of Reactions of Chlorine Monofluoride and [<sup>35</sup>S]-Sulphur Labelled Sulphur Tetrafluoride in the Presence of KFNI 4.4 mmol g<sup>-1</sup>

Time (min)	Count Rate Count min <sup>-1</sup>	$\frac{1}{CR} - \frac{1}{CR_0} \times 10^5$	Log $\frac{CR_0}{CR} \times 10^2$
2	26890 ± 328	0	0
4	21849 ± 296	0.86	9.02
8	15891 ± 252	2.57	22.84
12	12486 ± 223	4.29	33.32
16	10283 ± 203	6.01	41.75
20	8741 ± 187	7.72	48.80
24	7601 ± 174	9.44	54.87
28	6724 ± 164	11.15	60.2
32	6028 ± 155	12.87	64.94
36	5463 ± 148	14.59	69.22
40	4995 ± 141	16.3	73.11
44	4600 ± 136	18.02	76.68
48	4264 ± 131	19.73	79.98
52	3973 ± 126	21.45	83.05
56	3721 ± 122	23.16	85.9
60	3691 ± 122	23.37	86.24
64	3673 ± 121	23.51	86.40

CR<sub>0</sub> = 26890 count min<sup>-1</sup>

Initial pressure of (ClF+SF<sub>4</sub>) = 592 Torr

Figure 7.40 Reaction of  $\text{ClF} + {}^{35}\text{SF}_4$ , 1:1 mole ratio over  $\text{CsFAI}$ , 4.4 mmol/g  
 ${}^{35}\text{S}$  Surface Count Rate V Time

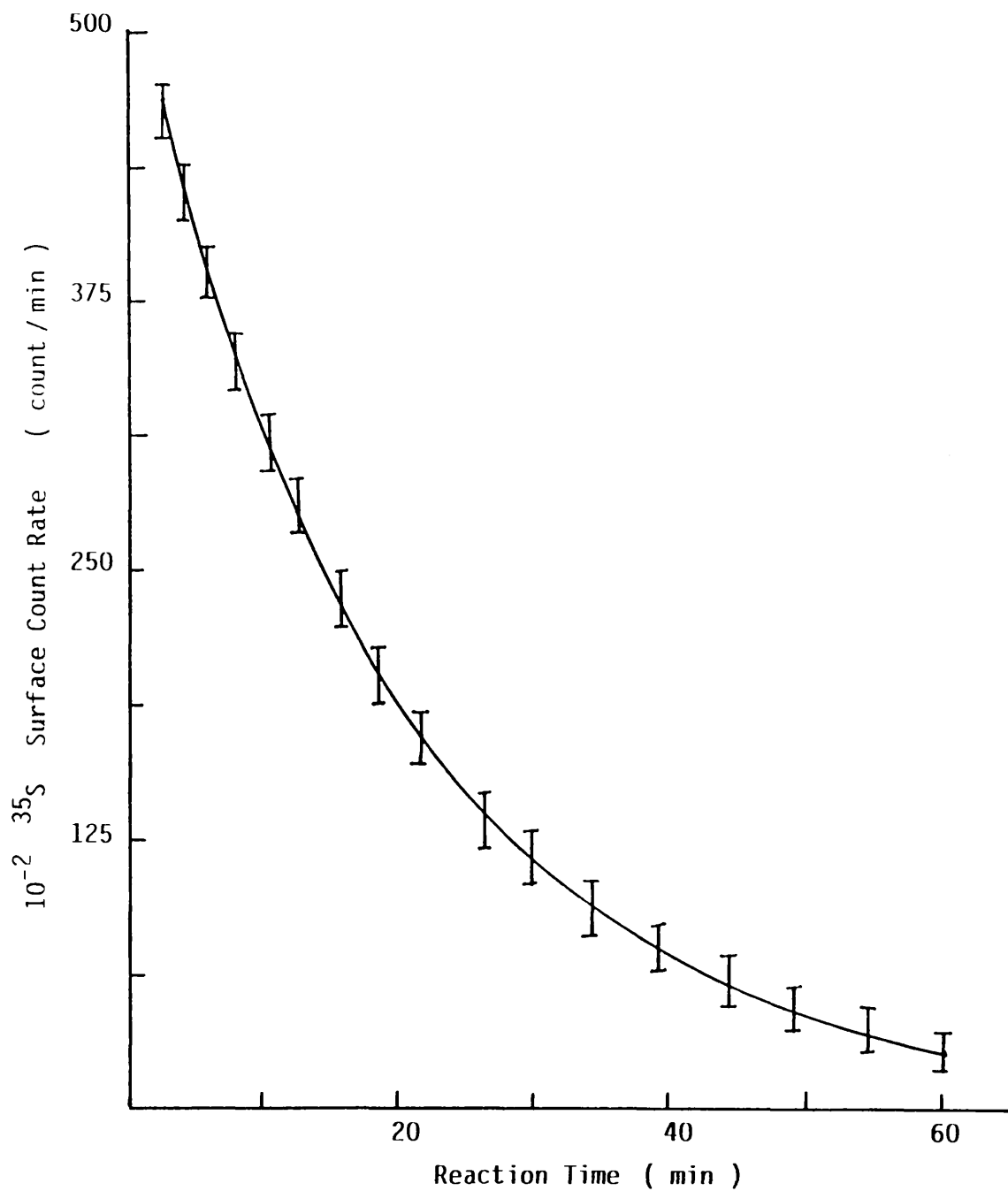


Figure 7.41 Reaction of  $\text{ClF} + {}^{35}\text{SF}_4$ , 1:1 mole ratio over  $\text{KF Al}$ , 4.4 mmol / g  
 ${}^{35}\text{S}$  Surface Count Rate  $\underline{V}$  Time

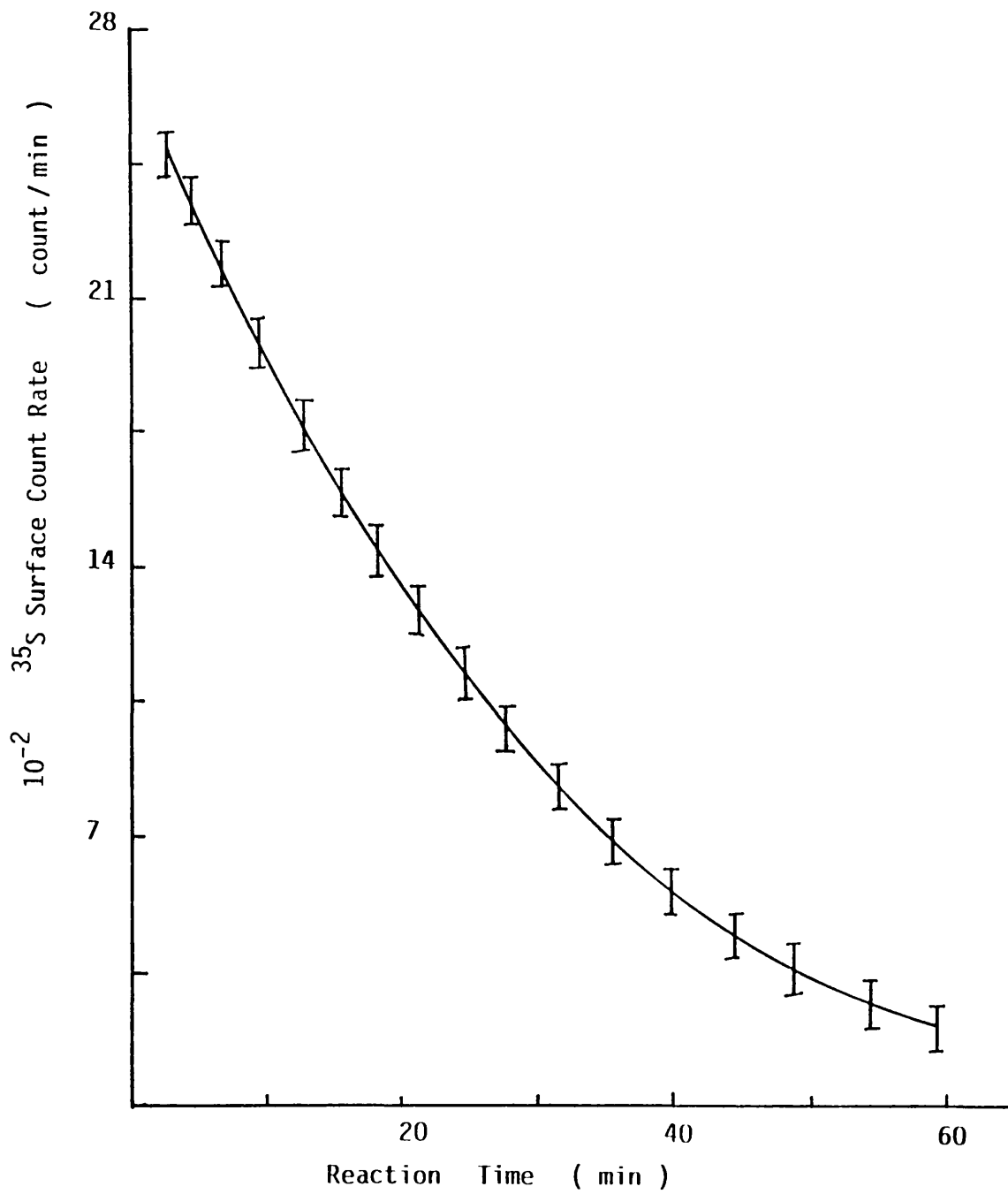


Figure 7.42 Reaction of  $\text{ClF} + {}^{35}\text{SF}_4$ , 1:1 mole ratio CsF AV, 4.4 mmol/g  
2nd Order Plot

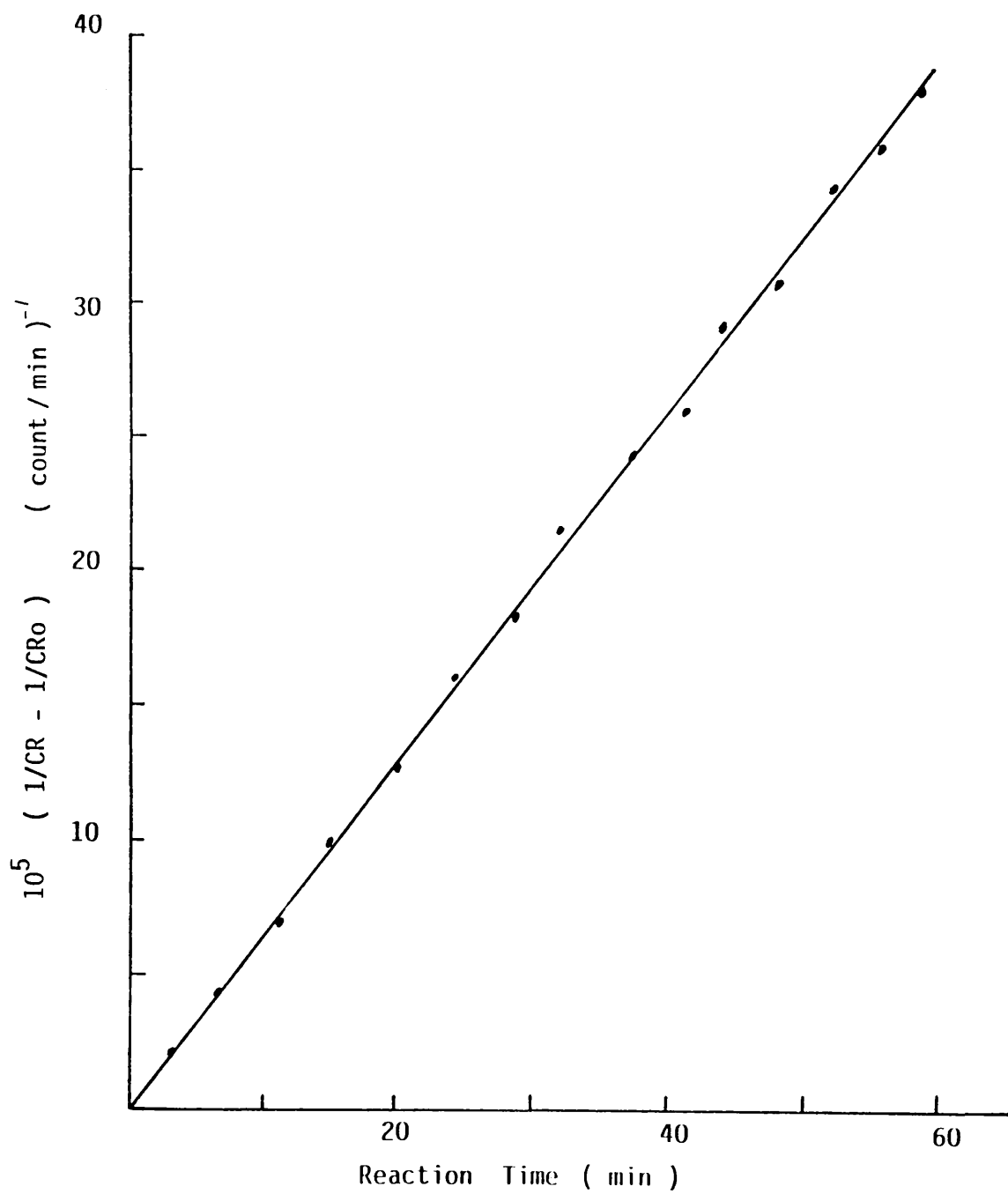
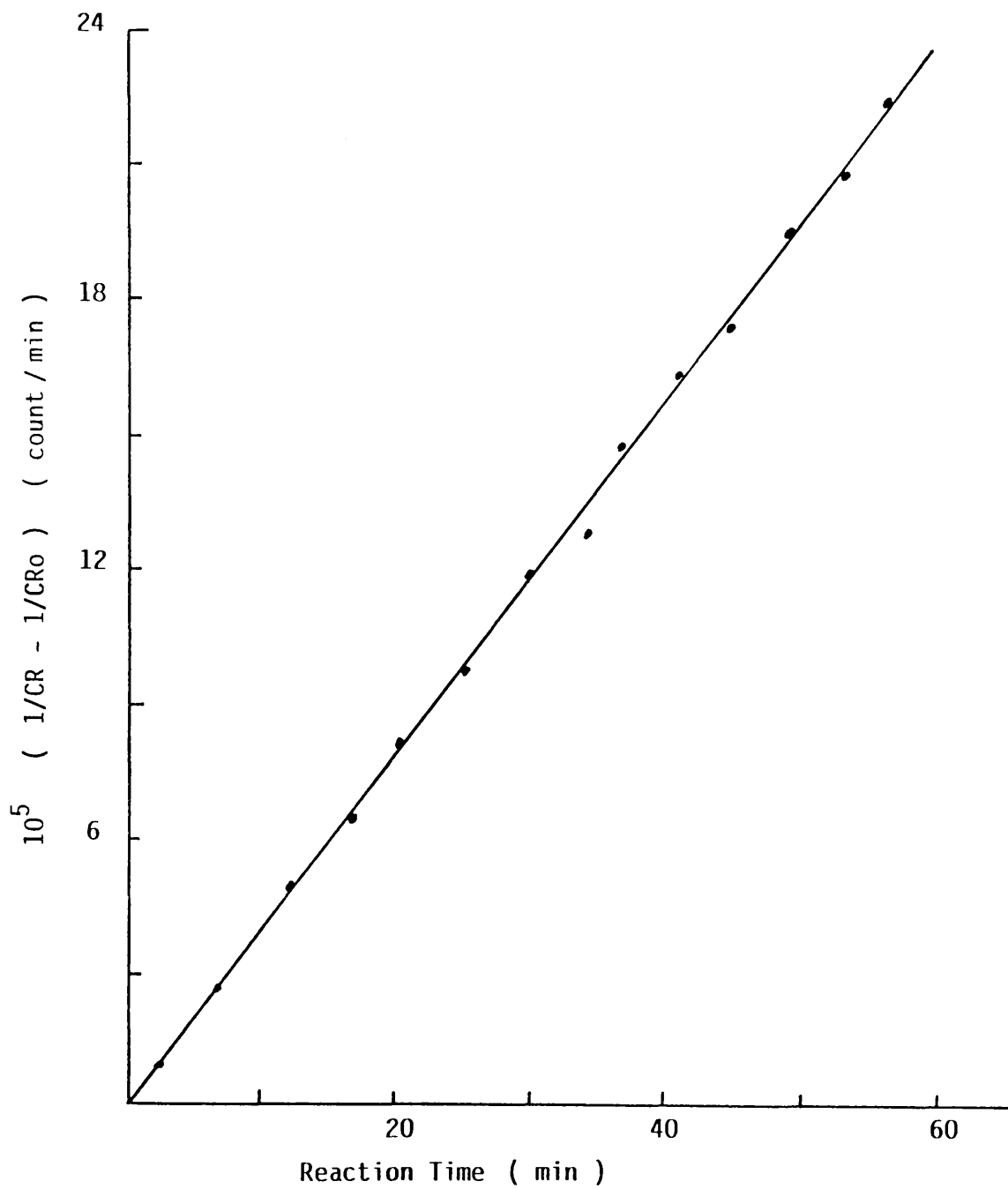


Figure 7.43 Reaction of  $\text{ClF} + {}^{35}\text{SF}_4$ , 1:1 molar ratio over  $\text{KF} \cdot \text{AlF}_3$ , 4.4 mmol/g  
2nd Order Plot



count<sup>-1</sup>, for CsFA or CsFN samples. These results are in good agreement with those obtained from the [<sup>36</sup>Cl]-chlorine experiments. The second order rate constant was  $(6.60 \pm 0.15) \times 10^{-6}$  count<sup>-1</sup> for CsFA or CsFN samples. The results obtained are summarized in Table 7.33.

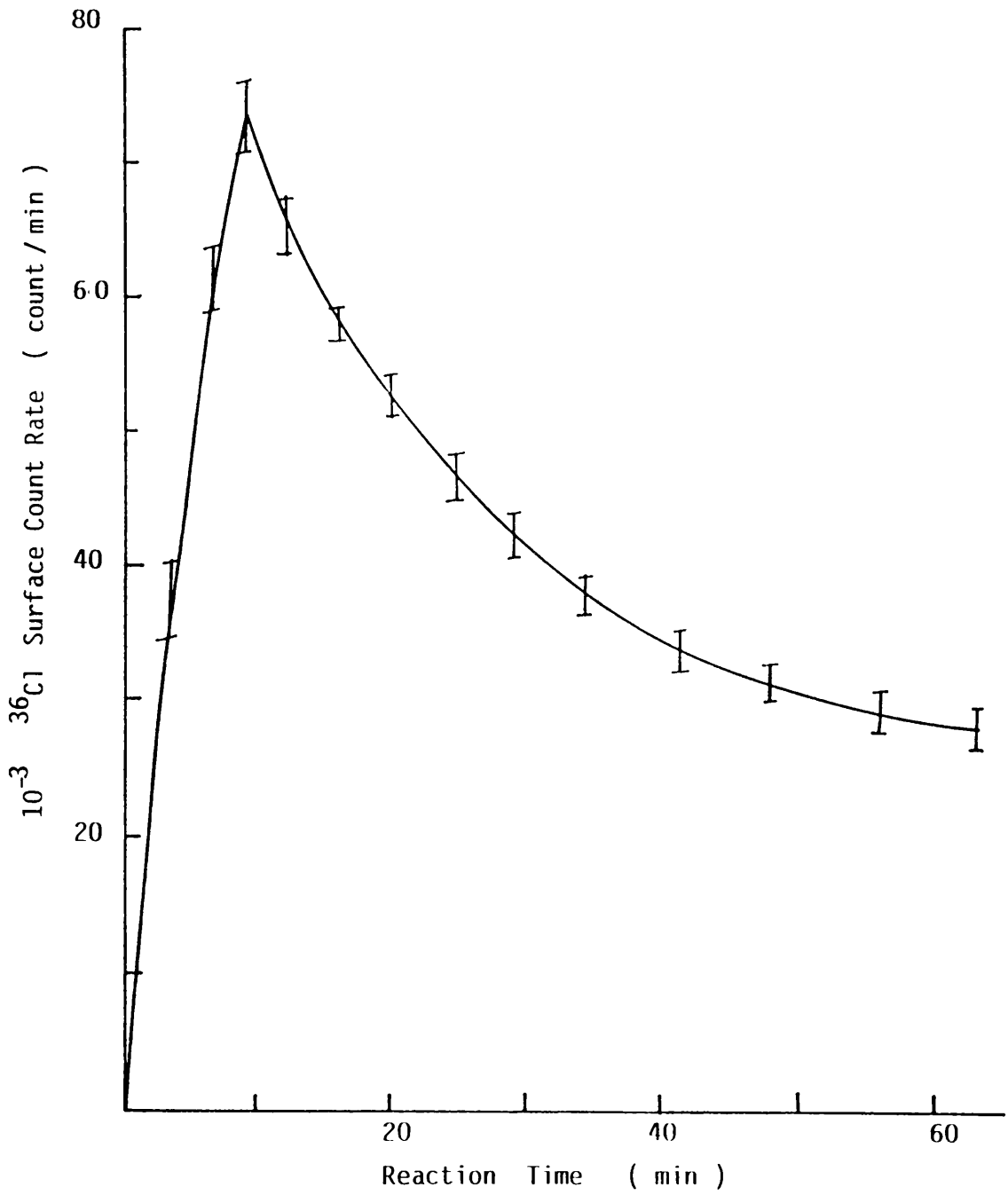
The admission of a 1:2 mole ratio of [<sup>36</sup>Cl]-chlorine labelled chlorine monofluoride and sulphur tetrafluoride to MFA I 4.4 mmol g<sup>-1</sup> showed similar behaviour to that obtained for the 1:1 mole ratio. However, the reaction of 2:1 mole ratio of [<sup>36</sup>Cl]-chlorine labelled chlorine monofluoride and sulphur tetrafluoride with MFA I 4.4 mmol g<sup>-1</sup>, exhibited different behaviour; the [<sup>36</sup>Cl]-chlorine surface count rate increased over the first 10 min then decreased over the next 2 h before reaching a constant value. Evacuation of the system after reaction was complete had no effect upon the final [<sup>36</sup>Cl]-chlorine surface count rate. However, when the solid heated at 473 K under vacuum the surface count rate recorded was equivalent to background. The surface count rate as a function of time is shown in Fig. 7.44. Neither first order nor second order plots gave a straight line. These results show that the 2:1 mole ratio mixture did not follow a second order process, although the yield of sulphur chloride pentafluoride increased. The admission of a 1:1 mole ratio of [<sup>36</sup>Cl]-chlorine labelled chlorine monofluoride and sulphur tetrafluoride mixture to a solid MFA I 4.4 mmol g<sup>-1</sup> which had been treated with a 2:1 mole ratio of [<sup>36</sup>Cl]-chlorine labelled chlorine monofluoride and sulphur tetrafluoride mixture, then heated at 473 K under vacuum for 2 h, exhibited similar behaviour to that described for the 1:1 mole ratio with a



Table 7.33 Second Order Rate Constants for the Reactions  $^{36}\text{ClF} + \text{SF}_4 \rightarrow \text{SF}_5^{36}\text{Cl}$  and  $\text{ClF} + ^{35}\text{SF}_4 \rightarrow ^{35}\text{SF}_5\text{Cl}$  Over MF(A or N)  $4.4 \text{ mmol g}^{-1}$

Initial Pressure of $^{36}\text{ClF}$ or $^{35}\text{SF}_4$ Torr	Second Order Constant (Count) $^{-1}$	
	CsF(A or N) (I,II or V)	KF(A or N) (I,II and V)
74 (ClF)	$6.76 \times 10^{-6}$	$4.2 \times 10^{-6}$
74 (SF <sub>4</sub> )	$6.81 \times 10^{-6}$	$4.19 \times 10^{-6}$
111 (ClF)	$6.37 \times 10^{-6}$	$4.18 \times 10^{-6}$
111 (SF <sub>4</sub> )	$6.49 \times 10^{-6}$	$4.24 \times 10^{-6}$
160 (ClF)	$6.87 \times 10^{-6}$	$4.69 \times 10^{-6}$
160 (SF <sub>4</sub> )	$6.39 \times 10^{-6}$	$4.53 \times 10^{-6}$
185 (ClF)	$6.59 \times 10^{-6}$	$4.28 \times 10^{-6}$
185 (SF <sub>4</sub> )	$6.56 \times 10^{-6}$	$4.22 \times 10^{-6}$
222 (ClF)	$6.7 \times 10^{-6}$	$4.35 \times 10^{-6}$
222 (SF <sub>4</sub> )	$6.65 \times 10^{-6}$	$4.39 \times 10^{-6}$
296 (ClF)	$6.59 \times 10^{-6}$	$4.25 \times 10^{-6}$
296 (SF <sub>4</sub> )	$6.69 \times 10^{-6}$	$4.29 \times 10^{-6}$

Figure 7.44 Reaction of  $^{36}\text{ClF} + \text{Si}$ , 2:1 mole ratio over  $\text{CsI } \Lambda 1$ , 4.4 mmol/g  
 $^{36}\text{Cl}$  Surface Count Rate V Time



fresh sample of catalyst. However, under the same conditions the 1:1 mole ratio reaction showed different behaviour when the solid was not heated to remove the permanently adsorbed [ $^{36}\text{Cl}$ ]-chlorine labelled chlorine monofluoride. The [ $^{36}\text{Cl}$ ]-chlorine surface count rate increased over the first 10 min then decreased over a period of 2 h before reaching a constant value thereafter. The removal of the gas phase from the system had no effect upon the final surface count rate which was higher than that recorded before reaction. Neither first order nor second order plots gave a straight line. Admission of 1:1 mole ratio of [ $^{36}\text{Cl}$ ]-chlorine labelled chlorine monofluoride and sulphur tetrafluoride mixture to MFA I  $4.4 \text{ mmol g}^{-1}$  which had been treated with a 1:2 mole ratio of [ $^{36}\text{Cl}$ ]-chlorine labelled chlorine monofluoride and sulphur tetrafluoride mixture, then heated at 473 K under vacuum for 2 h, exhibited similar behaviour as that described for the 1:1 mole ratio with a fresh sample of MFA I  $4.4 \text{ mmol g}^{-1}$ . However, if the solid was not heated, the 1:1 mole ratio reaction exhibited different behaviour, in that, the surface count rate decreased very slowly over a period of 2 h before reaching a constant value. On removal the gas phase from the system, the [ $^{36}\text{Cl}$ ]-chlorine surface count rate remained constant.

The reaction of the 1:1 mole ratio of [ $^{36}\text{Cl}$ ]-chlorine labelled chlorine monofluoride and sulphur tetrafluoride or chlorine monofluoride and [ $^{35}\text{S}$ ]-sulphur labelled sulphur tetrafluoride in the presence of MFA I was studied across the catalyst composition range  $0.6 - 15.0 \text{ mmol g}^{-1}$ . In each reaction the decrease in both [ $^{36}\text{Cl}$ ]-chlorine and [ $^{35}\text{S}$ ]-sulphur surface count rates occurred according to a second order process with a different rate constant

which was at a maximum at  $5.5 \text{ mmol g}^{-1}$ . For each reaction studied, the removal of the gas phase from the system led to the complete removal of the surface radioactivity with no indication of the formation of any permanently adsorbed species. Plots of the [ $^{36}\text{Cl}$ ]-chlorine and [ $^{35}\text{S}$ ]-sulphur surface count rates are given in Fig. 7.45 and 7.46 across the composition range  $0.6 - 15.0 \text{ mmol g}^{-1}$ . The second order rate constants are given in Table 7.34

Figure 7.45 Reaction of  $^{36}\text{ClF} + \text{SF}_4$  1:1 mole ratio over

$^{36}\text{Cl}$  Surface Count Rate  $\nu$  Time

- 1) CsF A I , 8.8 mmol/g
- 2) CsF A I , 1.1 mmol/g
- 3) CsF A I , 2.0 mmol/g
- 4) CsF N II , 4.4 mmol/g
- 5) CsF A V , 5.5 mmol/g

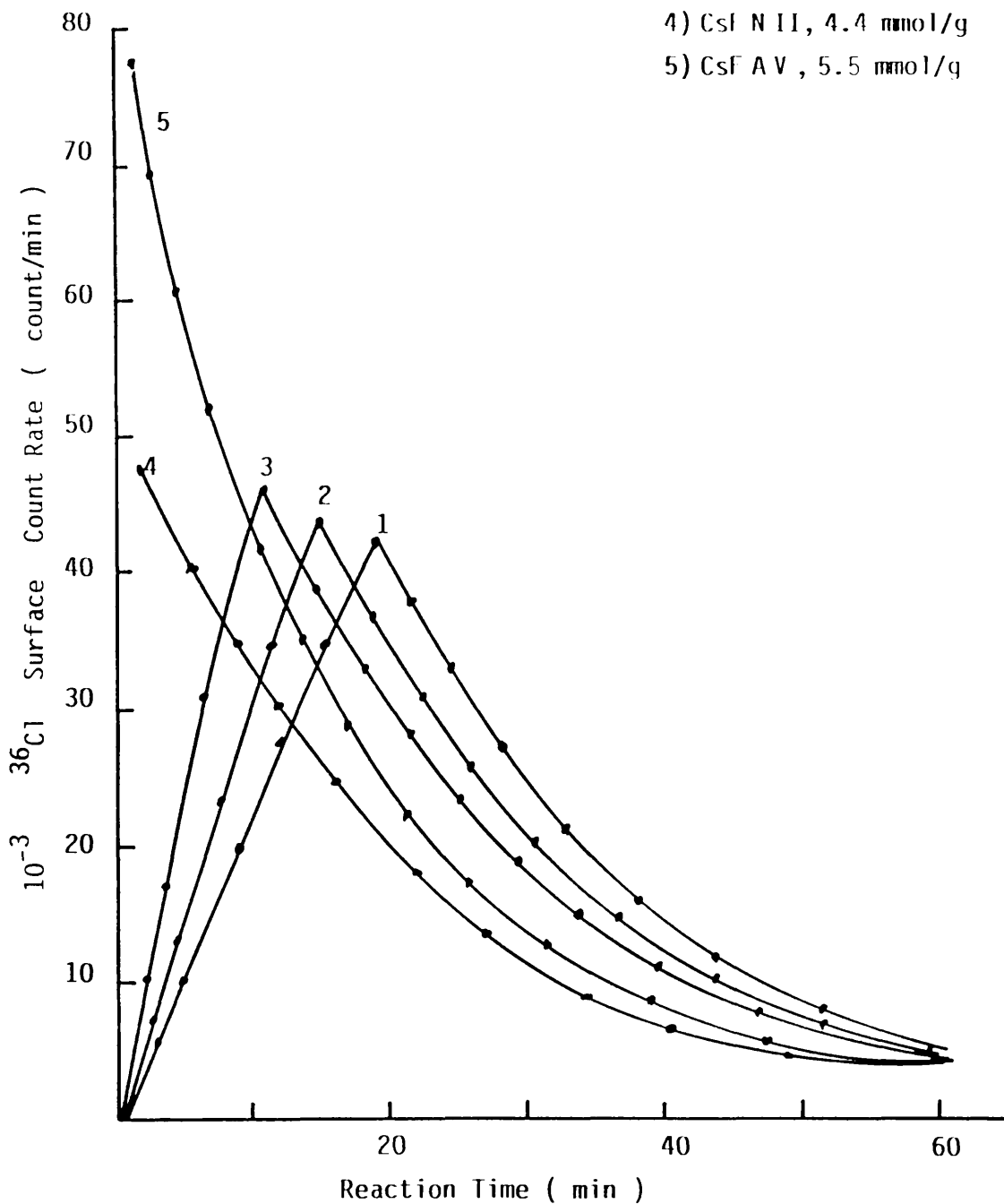


Figure 7.46 Reaction of  $\text{ClF} + {}^{35}\text{SiF}_4$ , 1:1 mole ratio over  
 ${}^{35}\text{S}$  Surface Count Rate V. Time

- 1) CsF A I , 8.8 mmol/g
- 2) CsF A I , 1.1 mmol/g
- 3) CsF A I , 2.0 mmol/g
- 4) CsF N II , 4.4 mmol/g
- 5) CsF A V , 5.5 mmol/g

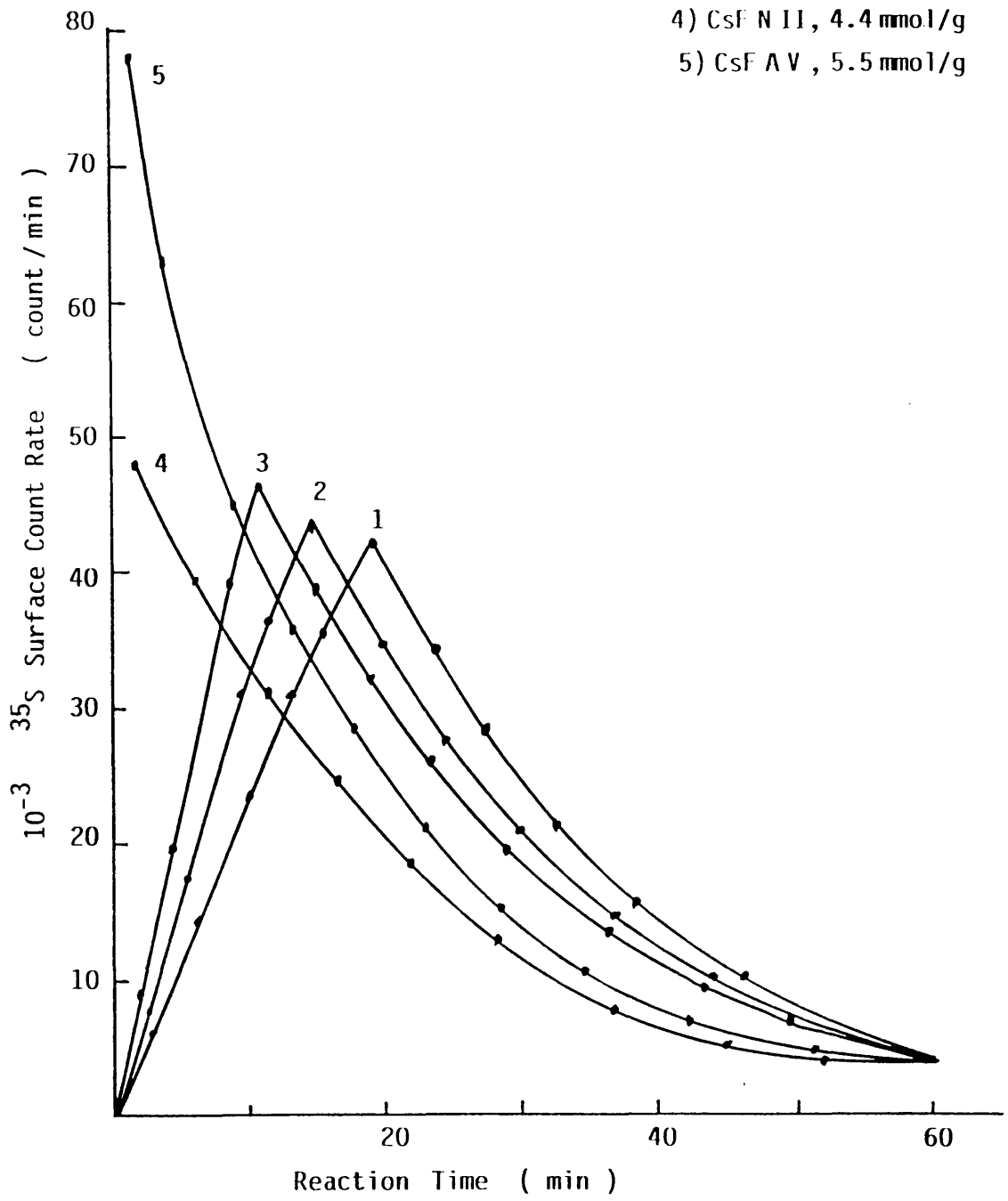


Table 7.34 Second Order Constant of ClF+SF<sub>4</sub> --> SF<sub>5</sub>Cl

Material Used <sup>35</sup> SF <sub>4</sub> or <sup>36</sup> ClF Torr	Composition mmol/g	Second Order Constant (Count) <sup>-1</sup> x 10 <sup>6</sup>	
		CsF(A or N)	KF(A or N)
ClF	0.6	3.3 ± 0.1	-
SF <sub>4</sub>		3.4 ± 0.1	-
ClF	1.1	3.9 ± 0.2	-
SF <sub>4</sub>		3.8 ± 0.2	-
ClF	2.0	4.52 ± 0.5	2.96 ± 0.2
SF <sub>4</sub>		4.6 ± 0.6	2.80 ± 0.2
ClF	4.4	6.6 ± 0.2	4.3 ± 0.2
SF <sub>4</sub>		6.5 ± 0.2	4.4 ± 0.2
ClF	5.0	7.28 ± 0.4	5.23 ± 0.4
SF <sub>4</sub>		7.42 ± 0.5	5.1 ± 0.5
ClF	5.5	7.87 ± 0.5	5.96 ± 0.5
SF <sub>4</sub>		7.8 ± 0.4	5.91 ± 0.7
ClF	6.0	6.8 ± 0.4	4.93 ± 0.5
SF <sub>4</sub>		6.7 ± 0.4	5.1 ± 0.5
ClF	7.5	4.35 ± 0.3	3.6 ± 0.4
SF <sub>4</sub>		4.28 ± 0.4	3.5 ± 0.4
ClF	8.8	3.33 ± 0.4	2.19 ± 0.3
SF <sub>4</sub>		3.41 ± 0.3	2.29 ± 0.3
ClF	15.5	1.21 ± 0.2	1.18 ± 0.2
SF <sub>4</sub>		1.29 ± 0.3	-

Sample Weight 2g

## CHAPTER EIGHT



## DISCUSSION

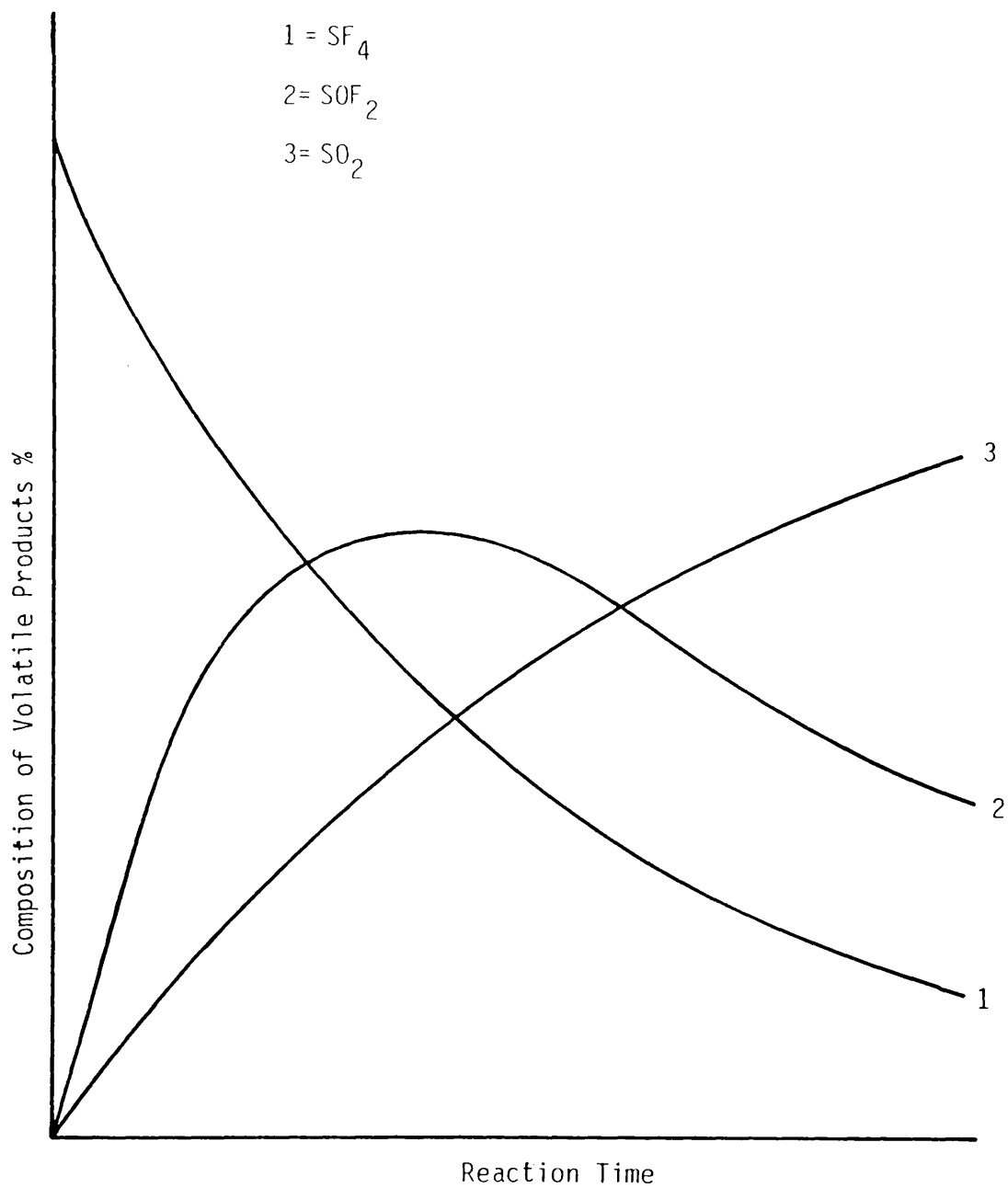
### 8.1 CHARACTERIZATION OF SUPPORTED METAL FLUORIDE

As a result of the work presented in Chapters 4 - 7, it has been shown that sulphur tetrafluoride reacts exothermically with supported metal fluorides to form thionyl fluoride, sulphur dioxide and species containing Al-F bonds, but there is no evidence for anhydrous hydrogen fluoride in the gas phase. The hydrolysis of thionyl fluoride at the surface to give sulphur dioxide occurs less exothermically and less rapidly as shown in Fig 8.1. Studies using  $^{35}\text{S}$  -sulphur labelled volatile sulphur-containing probe molecules, sulphur tetrafluoride, thionyl fluoride or sulphur dioxide show that there are two distinct species present in the surface of the supported metal fluoride in the range 0.6 - 15.0 mmol g<sup>-1</sup>. Only one species appears to be present on the surface at the composition 20.0 mmol g<sup>-1</sup> for each system. The permanently retained species which is not removed by pumping at room temperature can be removed by heating to 395 K under vacuum or by exposure of the surface to water vapour at room temperature. The other species is weakly adsorbed and can be removed at room temperature.

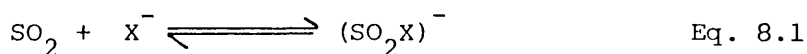
The infra-red and Raman spectra of the supported metal fluorides after reaction with sulphur tetrafluoride show the presence of pentafluorosulphate and fluorosulphite anions. The infra-red spectrum of the solids after reaction with thionyl fluoride or sulphur dioxide show the presence of the fluorosulphite anion. There is no evidence for the trifluorosulphite anion.

The heterogeneous, room temperature reaction between sulphur tetrafluoride and an unsupported metal fluoride (caesium or potassium

Figure 8.1 Hydrolysis of  $\text{SF}_4$  over  $\gamma$ -alumina



fluoride) is conveniently followed using radiotracer methods. The major surface species is weakly adsorbed sulphur tetrafluoride, pentafluorosulphate anion being a minor species. By analogy with this work it is suggested that the major, weakly adsorbed species on the supported metal fluorides are weakly adsorbed sulphur tetrafluoride, thionyl fluoride and sulphur dioxide molecules since the permanently retained species are pentafluorosulphate and fluorosulphite anions. The pentafluorosulphate anion has  $C_{4v}$  symmetry<sup>74</sup> as shown in Fig. 8.2. A possible structure for the fluorosulphite anion on the surface is shown in Fig. 8.3. The basis for the suggestion is as follows; the ultraviolet and the infra-red spectra of mixtures of halide ions in liquid sulphur dioxide have been interpreted in terms of the formation of  $X^- \dots SO_2$  complexes.<sup>216</sup> They have been characterized in the solid state in some cases; for example the infra-red spectrum of potassium fluorosulphite (the  $KF \dots SO_2$  complex) has been interpreted in terms of an  $F^- SO_2$  anion of pyramidal, Cs, structure.<sup>217</sup> The formation of  $F^- \dots SO_2$  complex in different solvents has been examined. The stoichiometry of the complex was suggested to be 1:1 and the equilibrium shown in equation 8.1 was proposed. Studies of anions containing both oxygen and fluorine have suggested that cation



coordination occurs through the fluorine or fluorines rather than the oxygen.<sup>218</sup> Furthermore, an infra-red study of the oxygen-18 labelled fluorosulphite anion, demonstrates conclusively the presence of two equivalent oxygen atoms.<sup>52</sup>

Infra-red spectrum of solid solvates which have an  $SO_2:X^-$

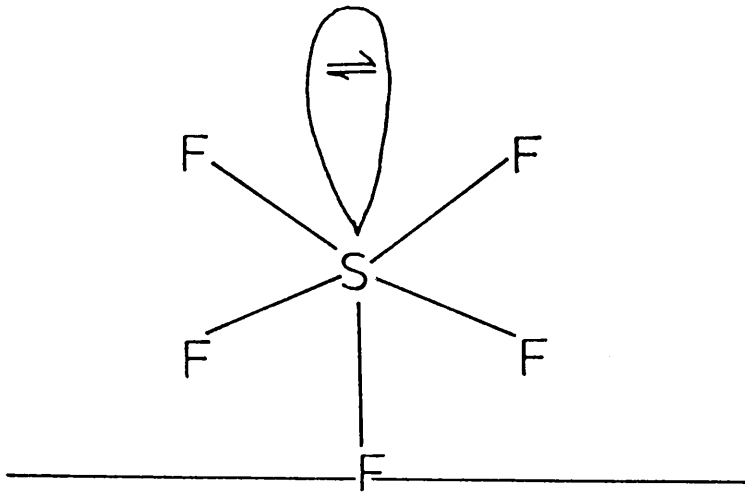


Figure 8.2 The Structure of  $\text{SF}_5^-$

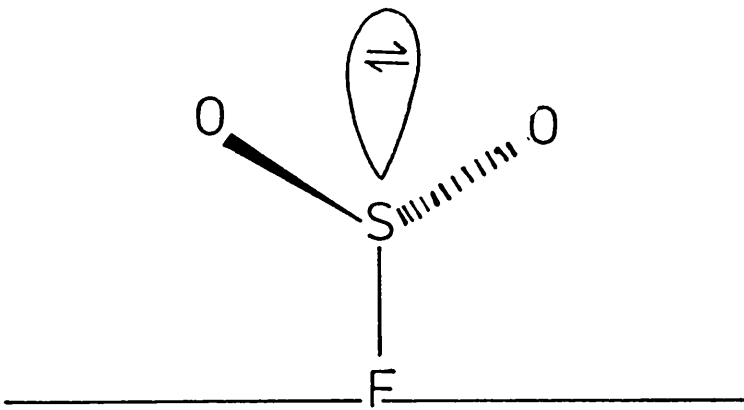


Figure 8.3 The Structure of  $\text{SO}_2\text{F}^-$

mole ratio  $\gg 1:1$  possess two additional bands in the S-O stretching region. It is proposed that these bands may be attributed to the presence of a  $2:1, \text{SO}_2:\text{X}$  complex, although higher complexes cannot be entirely ruled out.<sup>216</sup> Complexes of this type are not likely to be found in the present work since the quantities of permanently retained  $\text{SO}_2$  were very small.

The structures proposed for sulphur tetrafluoride weakly adsorbed on the surface of the supported metal fluoride are shown in Figs. 8.4 and 8.5. These two possible structures are derived from the structure of the pentafluorosulphate anion. Sulphur tetrafluoride may be adsorbed with the sulphur lone pair in an equatorial or an axial position as shown in Figs. 8.4 and 8.5 respectively. Since the pentafluorosulphate has been characterized having  $\text{C}_{4v}$  symmetry, this weakly adsorbed species is more likely to have the structure shown in Fig 8.4 with the lone pair in an axial position.

One possible structure proposed for the weakly adsorbed thionyl fluoride on the surface of the supported metal fluoride is shown in Fig. 8.6. In the present work, studies involving  $^{18}\text{F}$ -fluorine and  $^{35}\text{S}$ -sulphur labelled thionyl fluoride with unsupported caesium or potassium fluoride, activated by formation and subsequent thermal decomposition of their  $1:1$  adducts with hexafluoroacetone to increase their surface areas<sup>206</sup> show that thionyl fluoride interacts weakly with the surface. There is no evidence for any radioactivity retained by the solid after the removal of the gas phase at room temperature. The infra-red and Raman spectra of the supported or unsupported caesium or potassium fluoride after reaction with thionyl fluoride at room temperature or

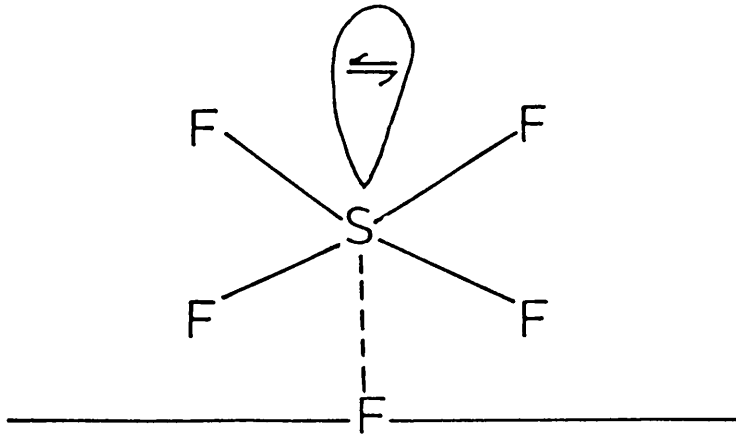


Figure 8.4 The Structure of  $SF_4$  Adsorbed

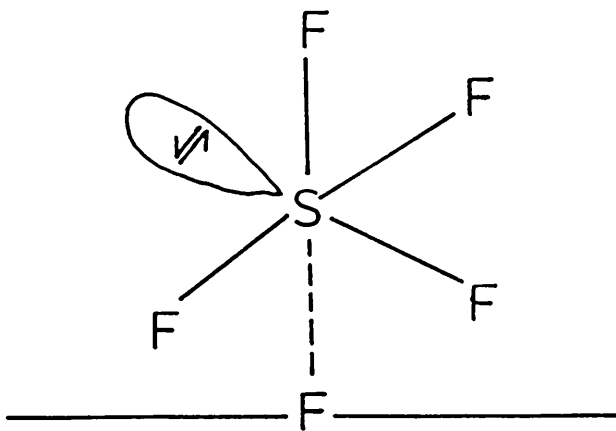


Figure 8.5 The Structure of  $SF_4$  Adsorbed

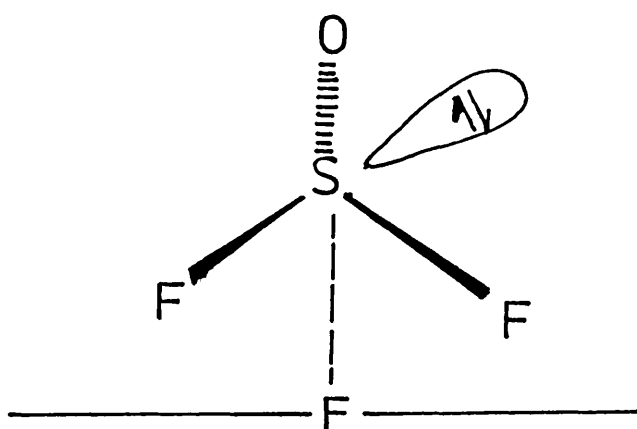


Figure 8.6 The Structure of  $\text{SOF}_2$  Weakly Adsorbed

at 373 K do not show any evidence for the trifluorosulphite anion.

The uptakes of sulphur tetrafluoride, thionyl and sulphur dioxide by the supported metal fluoride vary with the initial pressure of the volatile material in the range 10-300 Torr, and the metal fluoride loading in the composition range 0.6 - 20.0 mmol g<sup>-1</sup>. In each case the overall uptake is at a maximum at the 5.5 mmol g<sup>-1</sup>.

The room temperature reaction of carbonyl fluoride with the supported metal fluorides leads to the formation of carbon dioxide and species containing Al-F bonds, but there is no evidence for anhydrous hydrogen fluoride in the gas phase. Reactions of <sup>14</sup>C - carbon labelled volatile carbon containing probe molecules carbonyl fluoride or carbon dioxide with the supported metal fluoride are rapid. There are two distinct species present on the surface in the composition range 0.6 - 15.0 mmol g<sup>-1</sup>, but only one species at the 20.0 mmol g<sup>-1</sup> for each system. One is permanently retained. It is not removed by pumping at room temperature but it is removed by heating to 373 K under vacuum or by exposure of the surface to water vapour at room temperature. The other species which is removed by pumping at room temperature is weakly adsorbed.

The infra-red spectra of the supported metal fluorides after reaction with carbonyl fluoride show the presence of trifluoromethoxide anion.

The heterogeneous, room temperature reaction of carbonyl fluoride and an unsupported metal fluoride shows the presence of two species, permanently retained as trifluoromethoxide and weakly adsorbed molecule of carbonyl fluoride.<sup>47</sup> The <sup>14</sup>C -carbon experiments provide direct evidence for an interaction between carbon dioxide and



the surface of unsupported caesium fluoride activated with hexafluoroacetone, but the extent of any reaction that occurs, for example formation of the fluoroformate anion, is too small for product identification.

The observed behaviour is consistent with previous lack of success in preparing caesium fluoroformate from reactions between caesium fluoride and carbon dioxide under various conditions,<sup>45</sup> although the infra-red spectrum of the matrix-isolated ion pair  $\text{Cs}^+\text{FCO}_2^-$  has been reported.<sup>219</sup> Similarly to this work the major surface species is weakly adsorbed molecules of carbonyl fluoride and carbon dioxide and the permanently retained species is trifluoromethoxide anion. The structure of the trifluoromethoxide anion has been characterized having  $\text{C}_{3v}$  symmetry.<sup>42</sup>

The uptake of volatile carbon containing probe molecules, carbonyl fluoride and carbon dioxide by the supported metal fluoride depends on the initial pressure of the volatile materials and the metal fluoride loading in the composition range, 0.6 - 20.0 mmol  $\text{g}^{-1}$ . The overall uptake is at a maximum at the 5.5 mmol  $\text{g}^{-1}$  for each system. The increase in the metal fluoride loading in the range, 5.5 - 20.0 mmol  $\text{g}^{-1}$ , leads to less uptake and less hydrolysis of carbonyl fluoride. The complete removal of the  $^{14}\text{C}$ -carbon radioactivity from the surface of the supported metal fluoride, 20.0 mmol  $\text{g}^{-1}$  simply by pumping the system at room temperature is observed.

The individual reactions of probe molecules with the supported metal fluoride indicate that, fluoride ions are the major active sites on the surface of  $\gamma$ -alumina at all compositions  $\leq$

5.5 MF mmol (g  $\gamma$ -alumina)<sup>-1</sup>. The complete removal of the <sup>35</sup>S -sulphur or <sup>14</sup>C -carbon radioactivity from the surface of the supported metal fluoride, 20.0 mmol g<sup>-1</sup> is consistent with the absence of fluoride ions. It is suggested that at the 20.0 mmol g<sup>-1</sup>, fluoride ions react with  $\gamma$ -alumina during the calcination process to form Al-F species. Reactions using <sup>18</sup>F -fluorine labelled thionyl fluoride and the supported metal fluoride show that no fluorine exchange occurs. The absence of observable fluorine exchange in the system is simply explained by the fact that, the weakly adsorbed molecules of thionyl fluoride are adsorbed in such a way that fluorine from the supported metal fluoride is not equivalent to the two fluorines from the thionyl fluoride molecule. In the reactions of the supported metal fluoride, 8.8 mmol g<sup>-1</sup> and <sup>18</sup>F -fluorine labelled sulphur tetrafluoride, the fluorine exchange occurs. There are several possible explanations for this exchange. The weakly adsorbed sulphur tetrafluoride molecule is adsorbed in such a way as to make the fluorine from the supported metal fluoride equivalent to the four fluorines from sulphur tetrafluoride. The individual or the mixture equivalences between pentafluorosulphate or fluorosulphite and sulphur tetrafluoride adsorbed on the supported metal fluoride may account for the fluorine exchange although no fluorine exchange is observed in the case of the unsupported metal fluoride, at room temperature. Or the fluorine exchange between sulphur tetrafluoride and the Al-F species formed at high loadings that is above 5.5. mmol g<sup>-1</sup>. The absence of the fluorine exchange in the SF<sub>4</sub>/MF (M = Cs or K), system at room temperature is due to the retained pentafluorosulphate anion being coordinatively saturated and in the weakly adsorbed state the sulphur-fluorine bonds of the adsorbed sulphur tetrafluoride retain their integrity. This means, at no

time during the reaction, the four sulphur-fluorine bonds of the sulphur tetrafluoride are equivalent to the bond between sulphur tetrafluoride and the supported metal fluoride. However, the fluorine exchange between  $^{18}\text{F}$ -fluorine labelled sulphur tetrafluoride and caesium fluoride at 323 and 423 K is reported by Fraser et al,<sup>188</sup> who quoted fractions exchanged of 0.018 and 0.2 respectively. A recent study of this system by the same workers,<sup>220</sup> reported a complete fluorine exchange, if the caesium fluoride is reground between each cycle of the pretreatment process.

The weakly adsorbed sulphur tetrafluoride molecules, retain their integrity even at high temperatures; the fluorines never become equivalent at the same time and the exchange is not possible. In this work no fluorine exchange is observed in the  $\text{SF}_4/\text{K}_3\text{AlF}_6$ ,  $\text{SF}_4/\text{K}_2\text{AlF}_5$  or  $\text{SF}_4/\text{NH}_4\text{AlF}_4$  systems at room temperature or at 373 K. So that, the formation of the Al-F species does not account for the fluorine exchange quoted in the  $\text{SF}_4/\text{MF}$   $\gamma$ -alumina system. The possibility of the equivalence between pentafluorosulphate and sulphur tetrafluoride adsorbed on the surface of the supported metal fluoride seems to be the most likely mechanism, based on the thermal properties of the anion formed. Pentafluorosulphate anion is stable at room temperature and decomposes below 423 K.

The overall reaction of the volatile sulphur containing probe molecules, sulphur tetrafluoride, thionyl fluoride and sulphur dioxide with the supported metal fluoride is shown in Fig. 8.7

The reaction of  $^{18}\text{F}$ -fluorine labelled carbonyl fluoride with the supported metal fluoride leads to the fluorine exchange. The exchange cannot occur via the weakly adsorbed molecules of carbonyl fluoride, because the species formed at the surface of the supported

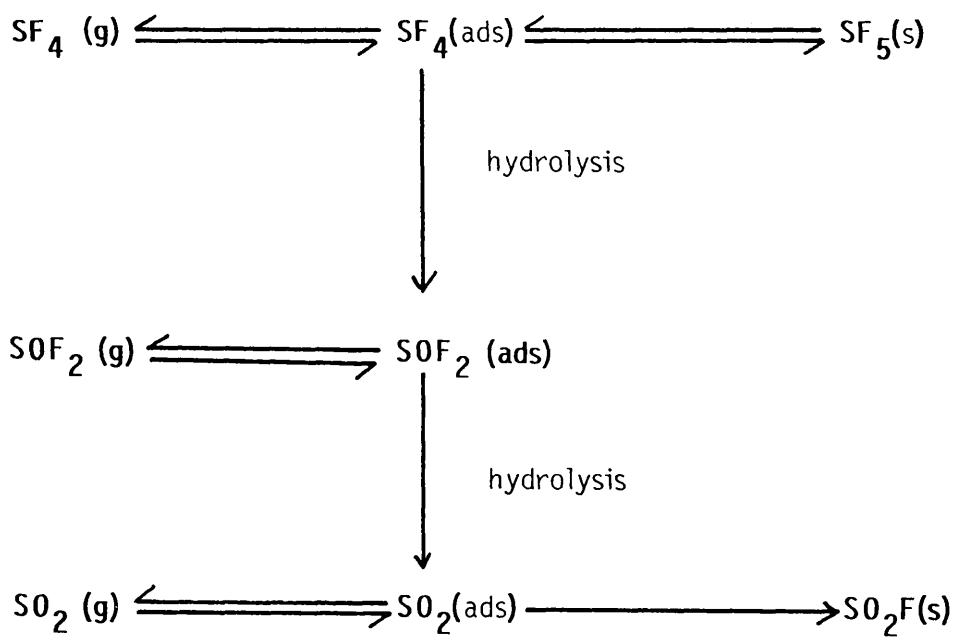


Figure 8.7 Reaction of Volatile Sulphur Containing Probe Molecules with Supported Metal Fluoride

metal fluoride is not adsorbed in such a way as to allow all the fluorines to become equivalent. Evidence for this is supplied by a matrix-isolation study by B.S. Ault<sup>221</sup> in which he reported the formation of an unusual complex from the reaction of formaldehyde with caesium fluoride in an argon mixture. This reaction does not give rise to the expected fluoride ion transfer and formation of the  $\text{CH}_2\text{FO}^-$  anion. There is no evidence for the C-F stretching mode, and the C=O stretching mode is shifted by only  $50\text{-}60\text{ cm}^{-1}$  compared with a shift of  $400\text{ cm}^{-1}$  when trifluoromethoxide is formed from carbonyl fluorides. This suggests that the fluoride ion interacting weakly with the carbon centre of the formaldehyde, but not forming a bond. A similar type of reaction may occur between the weakly adsorbed carbonyl fluoride and the supported metal fluoride, but this does not account for the fluorine exchange, because there is no point at which all the fluorines become equivalent.

The possibility of equivalence between trifluoromethoxide and carbonyl fluoride adsorbed on the surface of the supported metal fluoride seems the more likely mechanism.

These results are in good agreement with those reported by Fraser et al,<sup>220</sup> who observed a fluorine exchange in the  $\text{COF}_2/\text{CsF}$  system at 288, 323 and 423 K. A recent study<sup>222</sup> of the  $\text{COF}_2/\text{CsF}$  system at room temperature quotes 27% exchange. In this work, the fractions exchanged quoted during the reaction of  $^{18}\text{F}$ -fluorine labelled carbonyl fluoride and the supported metal fluoride,  $4.4\text{ mmol g}^{-1}$  were higher than those quoted for the  $8.8\text{ mmol g}^{-1}$  samples.

This is consistent with the loss of the metal fluorides at high loadings.

The overall reaction of volatile carbon containing probe molecules with the supported metal fluoride is given in Fig. 8.8

The reaction of anhydrous hydrogen fluoride with the supported metal fluoride leads to both uptake and fluorine exchange. The great extent of the uptake is accounted for by the formation of oligomeric hydrogen fluoride species on the surface of the supported metal fluoride. Anhydrous hydrogen fluoride is known to exist in neutral oligomers of the form  $(\text{HF})_n$  and charged oligomers of the type  $(\text{HF})_n \text{F}^-$ . Both neutral and charged oligomeric species are strongly hydrogen bonded. Redington,<sup>223</sup> in recent analysis of  $(\text{HF})_n$  oligomers, determined the energy of the hydrogen bond in  $(\text{HF})_2$  to be  $23 \pm 2 \text{ k J mol}^{-1}$ . An ion cyclotron resonance determination of fluoride binding energies to Brønsted acids<sup>224</sup> yielded a value of  $163 \pm 4 \text{ K J mol}^{-1}$  for the hydrogen bond energy in  $\text{HF} \cdot \text{F}^-$ . The stronger hydrogen bond in  $\text{HF} \cdot \text{F}^-$  is a result of the great electronegativity and small size of fluorine.

The uptake and the fluorine exchange during reactions of anhydrous hydrogen fluoride with the supported metal fluoride,  $4.4 \text{ mmol g}^{-1}$  was higher than those recorded at the  $8.8 \text{ mmol g}^{-1}$ . This behaviour may be due to the decrease in the quantity of metal fluoride as a result of the fluoridehydroxylation of  $\gamma$ -alumina during the preparation process.

In all systems studied the surface coverage is dependent on the initial pressure of the probe molecule in the range 10-300 Torr in contrast with the unsupported metal fluorides in which the surface coverage is independent of the initial pressure above 20 Torr. This

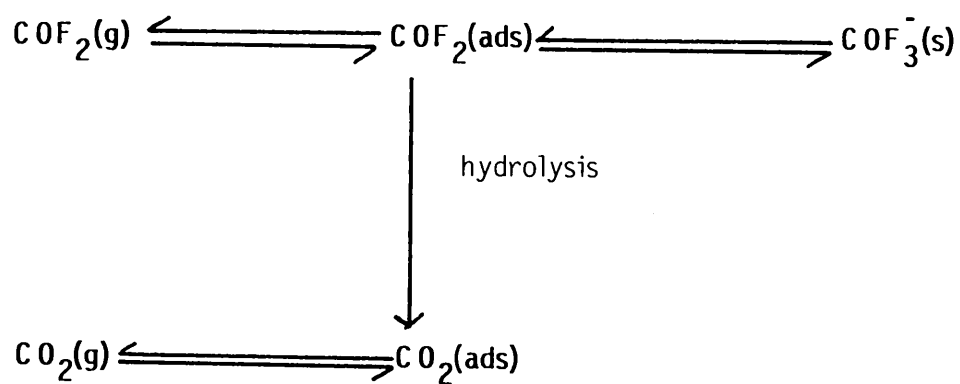


Figure 8. 8 The Overall Reaction involving Volatile Carbon Containing Probe Molecules

different behaviour may be due to the different surface sites which are metal fluoride particles in the former at  $\leq 5.5 \text{ mmol g}^{-1}$  and fluoride ions in the latter.

The uptake of each of the probe molecules by caesium or potassium fluoride supported on  $\gamma$ -alumina are shown in Figs. 8.9 -8.12 . The extent of the uptake of gas by the supported metal fluoride is related to the Lewis acidity of the gas, that is the stronger the Lewis acid, the greater the uptake. The fluoride ion affinities of the various materials used are given in Table 8.1. The order of uptake of gas by the supported metal fluorides is not so easily explained, because other factors such as, the sintering which occurs during reaction, and the shape of the gas can also be involved in the rate of the reaction of a gas with a solid.

## 8.2 CHARACTERIZATION OF FLUORINATED $\gamma$ -ALUMINA

The reaction of  $^{35}\text{S}$ -sulphur labelled sulphur dioxide with non-calcined or calcined  $\gamma$ -alumina results in the formation of two distinct species in the latter but one only in the former. The weakly adsorbed species which is present on the surface of  $\gamma$ -alumina is easily removed by pumping at room temperature, but the permanently retained species on the surface of calcined  $\gamma$ -alumina is not removed at room temperature or by the exposure to water vapour or even by heating under vacuum below 753 K. A recent study provides some information about the structure of the adsorbed sulphur dioxide. This species is proposed <sup>228</sup> to have the structure of sulphite on the basis of the similarity of its infra-red spectrum with that observed in the adsorption of sulphur dioxide on magnesium oxide. <sup>228</sup> Adsorption



Figure 8.9 Reaction of Lewis Acids with CsF/Alumina

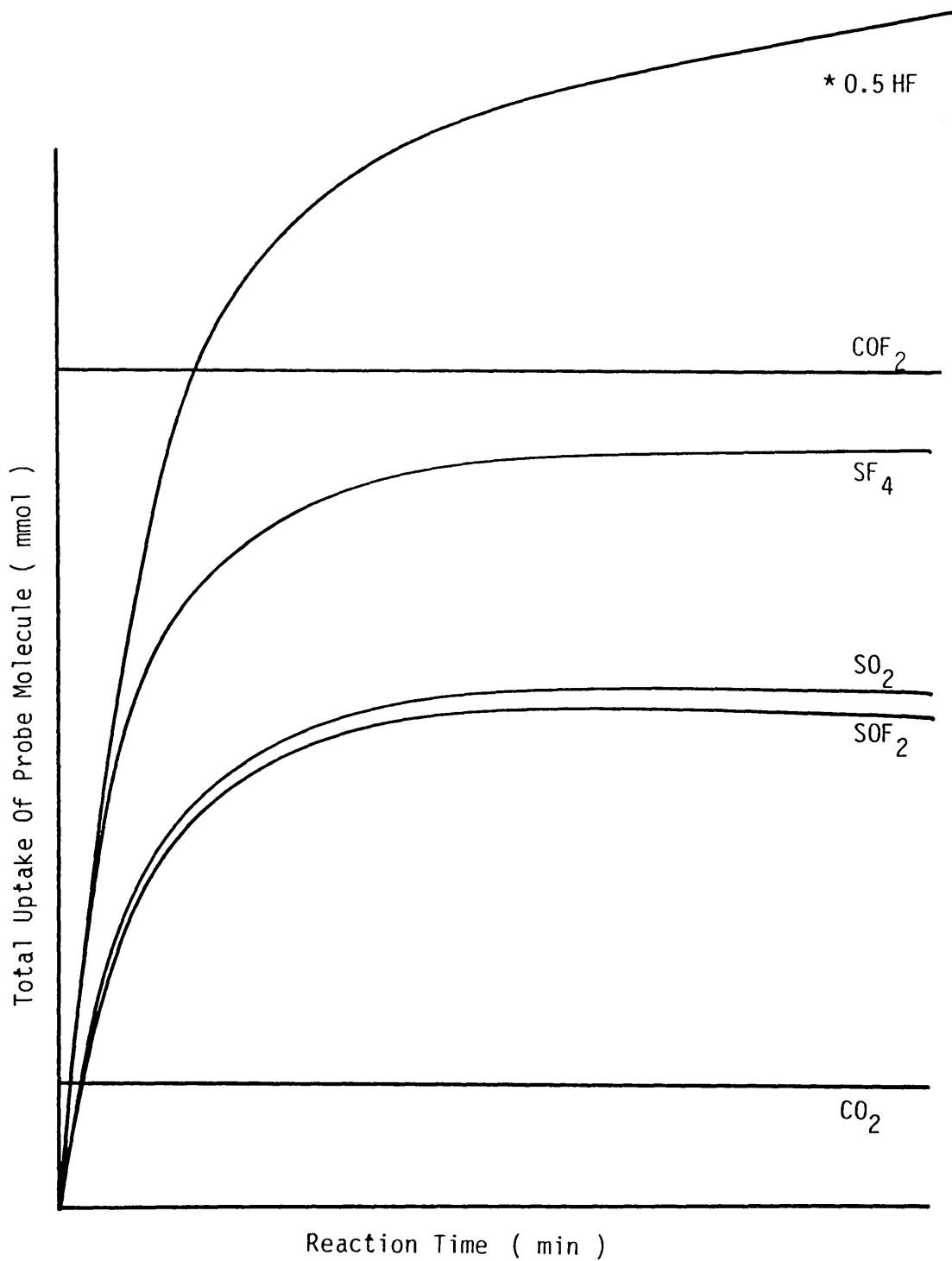


Figure 8.10 Reaction of Lewis Acids with KF/ $\gamma$ -alumina

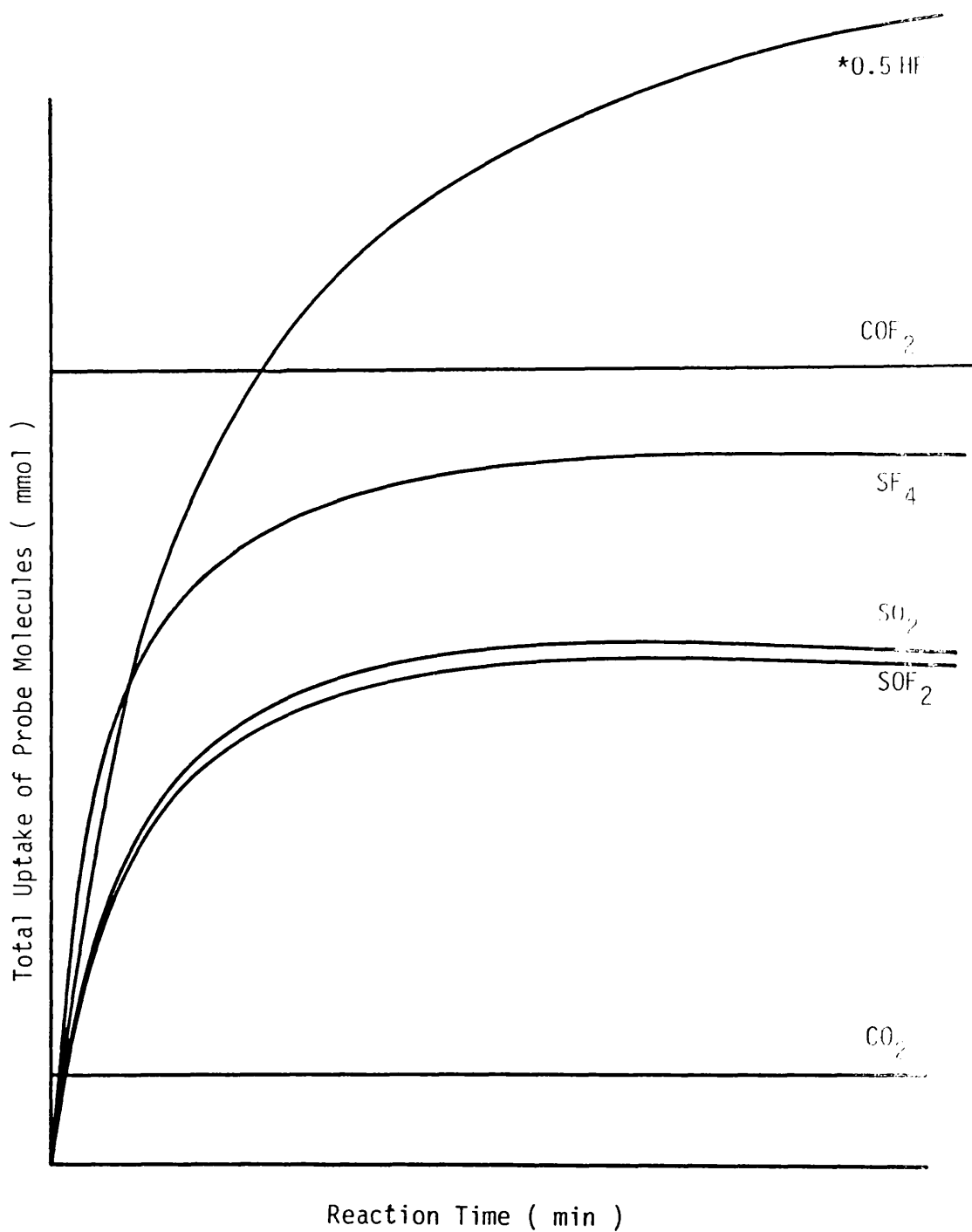


Figure 8.11 Reaction of Lewis Acids with CsF/alumina

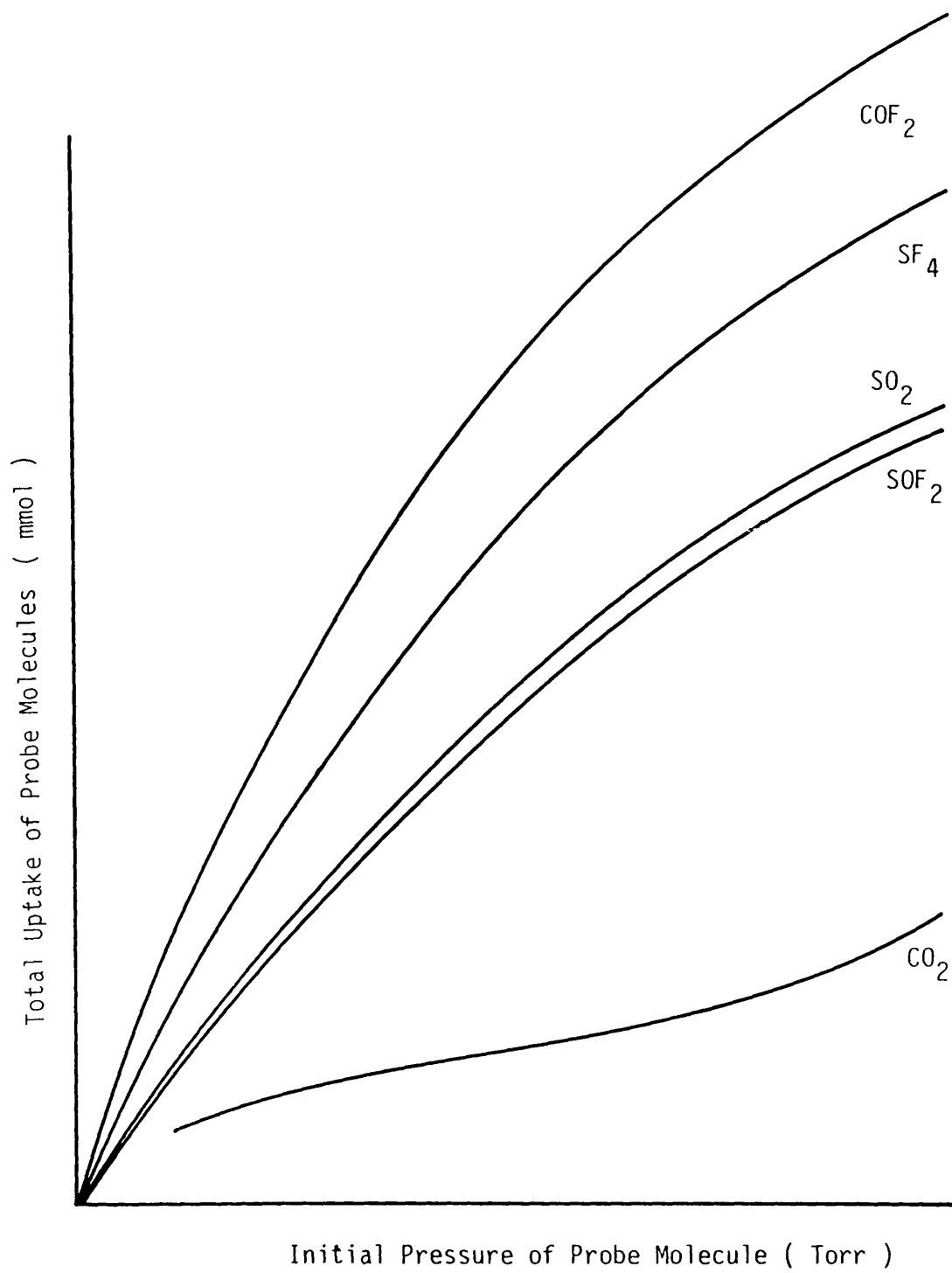


Figure 8.12 Reaction of Lewis Acids with KF/ $\gamma$ -alumina

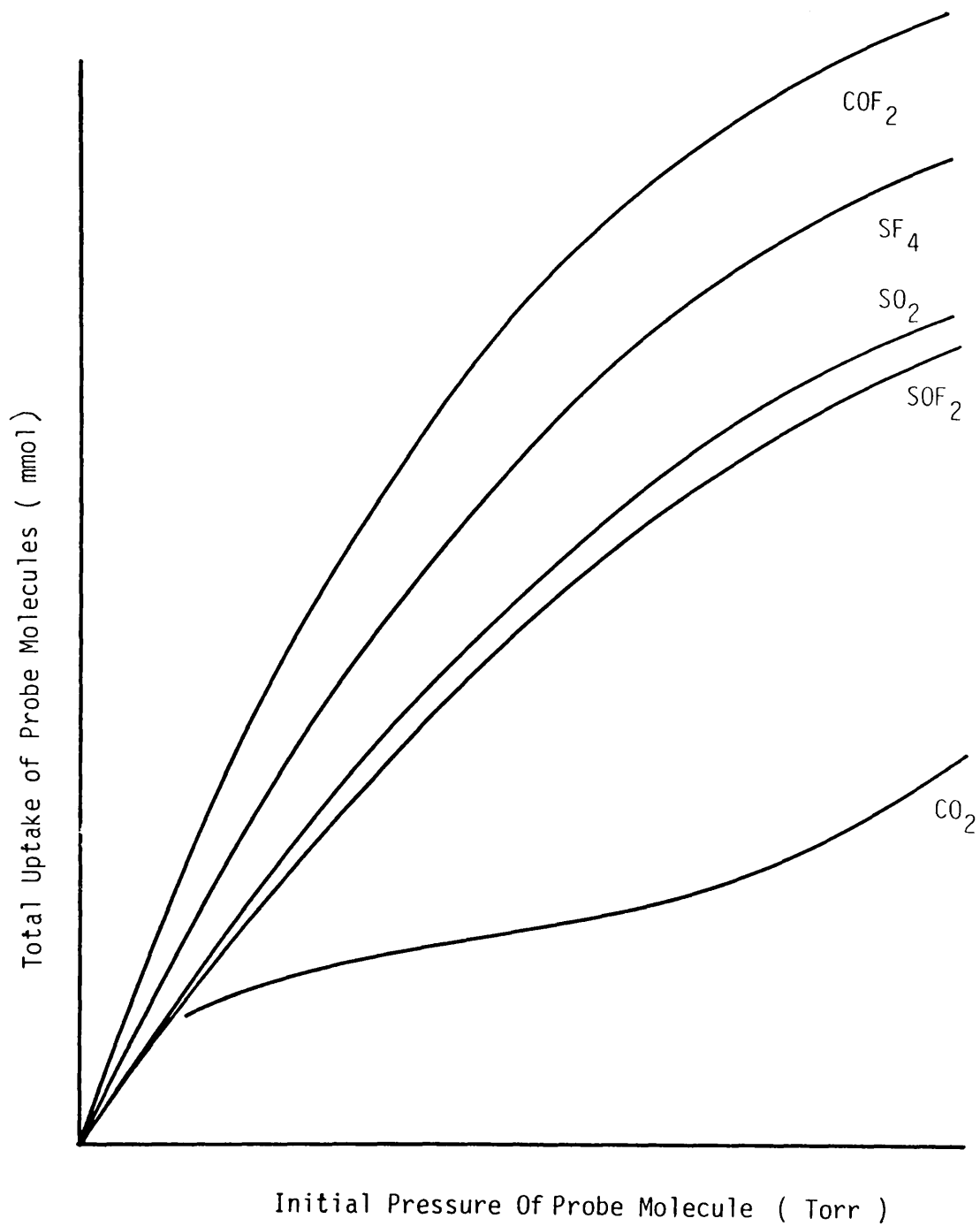


Table S.1 Fluoride Ion Affinity

Material	( FA ) Kcal/mol	Ref
SF <sub>4</sub>	-46	225
SO <sub>2</sub>	-12.3	225
COF <sub>2</sub>	-35	226
CO <sub>2</sub>	-33	226
HF	-55	227
ClF	-83	227

in the form of a sulphite bound to the alumina via the sulphur atom is consistent with the observation<sup>229</sup> that sulphite coordination via sulphur would shift the S-O stretching band to higher frequencies than in the free sulphite ion (967, 933  $\text{cm}^{-1}$ ), whereas coordination via the oxygen would shift the same band to lower frequencies. It is therefore suggested that sulphur dioxide adsorption on the basic sites of the  $\gamma$ -alumina to yield a surface species. This adsorbed species could then bond to an oxygen atom from the surface of  $\gamma$ -alumina to form a strongly adsorbed species. The complete removal of the  $^{35}\text{S}$ -sulphur radioactivity from the surface of non-calcined  $\gamma$ -alumina, at room temperature is consistent with the absence of the basic sites on the fully hydrated surface of  $\gamma$ -alumina.

The room temperature adsorption of  $^{14}\text{C}$ - carbon labelled carbon dioxide by non-calcined or calcined  $\gamma$ -alumina is observed. The removal of the gas phase at room temperature resulted in an instant removal of the  $^{14}\text{C}$ -carbon radioactivity from the surface of the former, but not from that of the latter. This shows that two distinct species are present on the surface of calcined  $\gamma$ -alumina and only one on that of non-calcined  $\gamma$ -alumina. One which is weakly adsorbed is removed by pumping at room temperature and one which is permanently retained is not removed at room temperature or by the exposure to water vapour. This observation is in good agreement with the results obtained by Solymosi et al<sup>230</sup> who reported the presence of carbonate bands during the adsorption at 300-400 K. A recent study<sup>231</sup> shows that carbon dioxide exists in both relatively strongly adsorbed and weakly adsorbed state on the surface of  $\gamma$ -alumina. Similarly to this work, the weakly adsorbed

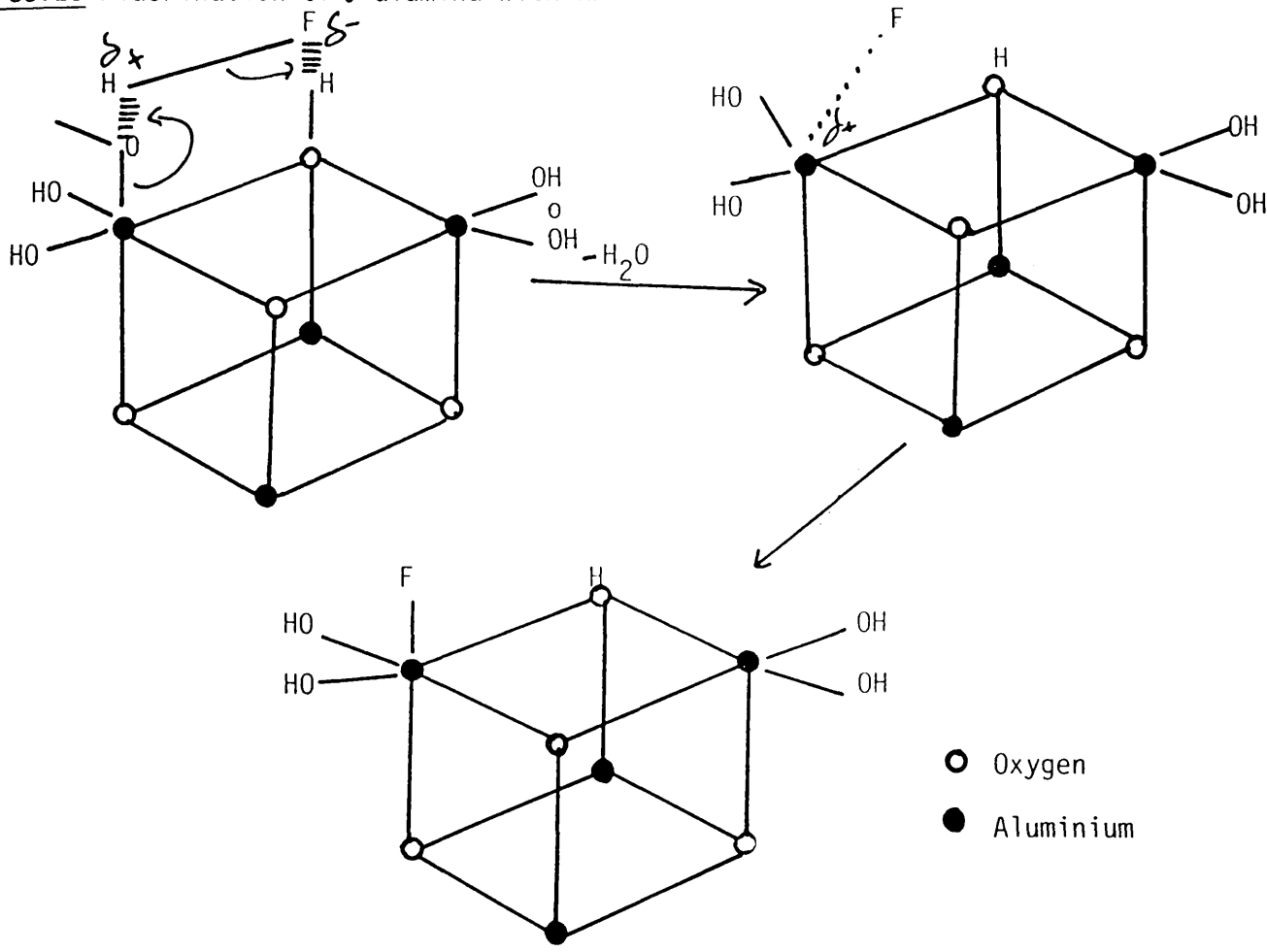
species is suggested to be an adsorbed molecule of carbon dioxide and the permanently retained species is a carbonate anion.

The adsorption of anhydrous hydrogen fluoride by  $\gamma$ -alumina calcined to 523 K is consistent with the proposed scheme shown in Fig. 8.13 using the Al-o-Al arrangement from Fig. 1.20. The weakly adsorbed hydroxyl groups can be displaced by anhydrous hydrogen fluoride to form a monofluorinated coordinatively saturated aluminium as shown in the proposed scheme, Fig. 8.13.

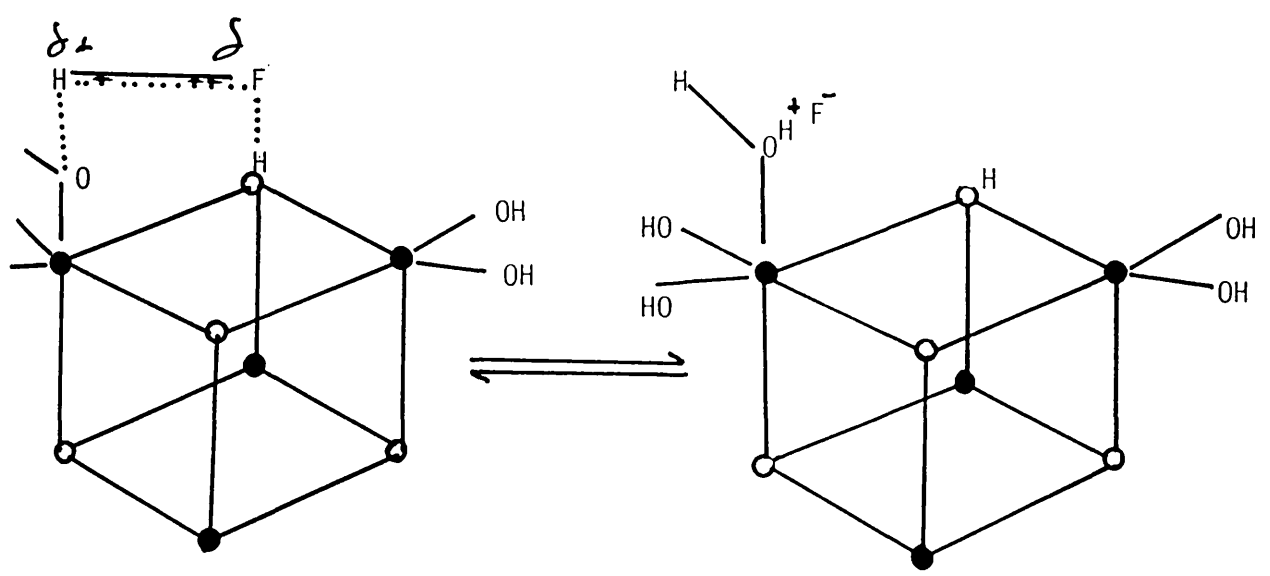
A complete exchange is observed during reaction of  $^{18}\text{F}$  - fluorine labelled anhydrous hydrogen fluoride with  $\gamma$ -alumina pretreated with anhydrous hydrogen fluoride or carbonyl fluoride, but only 60% in the case of  $\gamma$ -alumina pretreated with sulphur tetrafluoride or thionyl fluoride. This exchange is accounted for by the dissociation of the HF molecules at the fluorine sites. As the gas phase molecule approaches the exchange site, coulombic attraction arising from hydrogen bonding minimises the conformational energy between the fluorinated surface and the substrate when alignment of hydrogen fluoride molecule is achieved a concerted exchange results. It is proposed that the reverse action is possible when the hydrogen on the bridging oxygen is retained, Fig. 8.14 .

Evidence presented in Chapter 6, indicates that there is no  $^{18}\text{F}$  -fluorine exchange during reaction of  $^{18}\text{F}$  -fluorine labelled anhydrous hydrogen fluoride and anhydrous aluminium(III) fluoride, but a complete exchange is observed if the solid is first exposed to water vapour. Several hydrates of aluminium(III) fluoride are known. The most stable hydrate appears to be  $\text{AlF}_3 \cdot 3\text{H}_2\text{O}$ , which exists in two structurally different forms,  $\alpha$  and  $\beta$ . 232

Figure 8.13 Fluorination of  $\gamma$ -alumina with HF

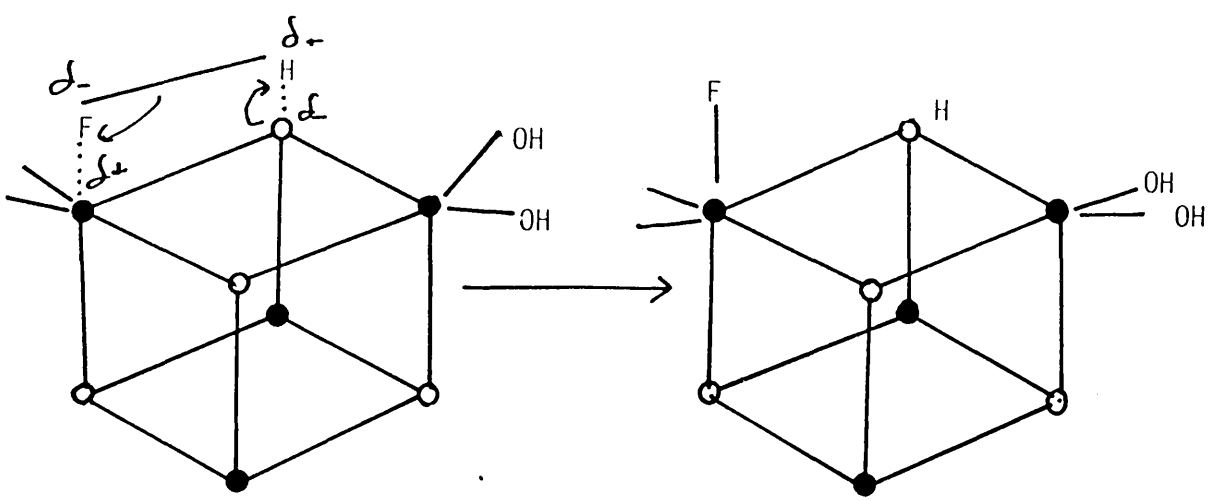


Displacement of Surface Hydroxyl Groups by Hydrogen Fluoride



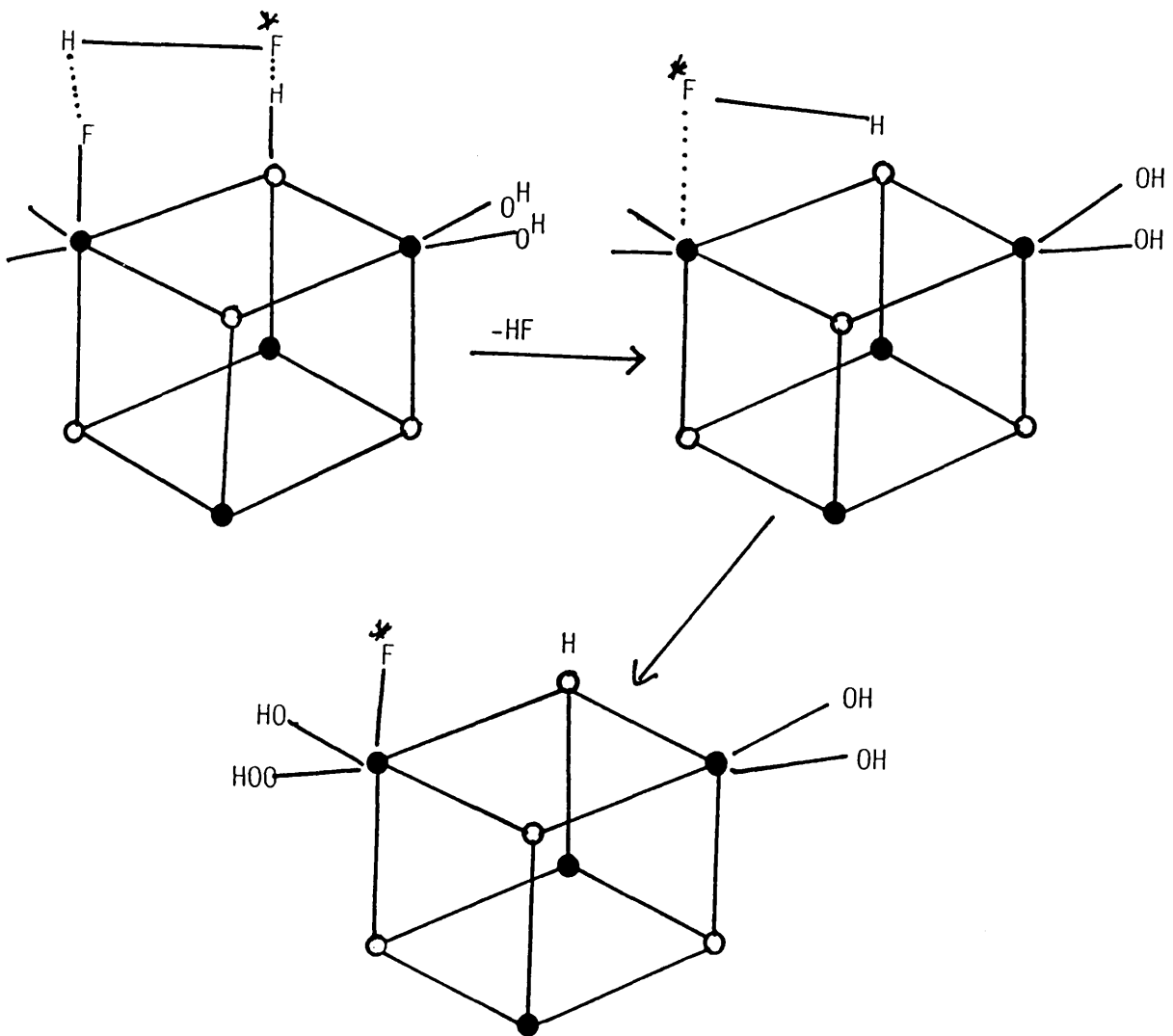
Complex Formation where the Hydroxyl Group is Strongly Bonded to the Surface





Dissociative Adsorption of Hydrogen Fluoride at Coordinatively Unsaturated Surface Aluminium

Figure 8.14 Exchange of  $H^*F$  with  $HF/\gamma$ -alumina



The gelatinous precipitate of aluminium fluoride formed when hydrofluoric acid is added to a solution of an aluminium salt approximates to the  $\text{AlF}_3 \cdot 3\text{H}_2\text{O}$  composition. Two other hydrates,  $\text{AlF}_3 \cdot 9\text{H}_2\text{O}$  and  $\text{AlF}_3 \cdot 0.5\text{H}_2\text{O}$  are also definitely established. A hydrate  $\text{AlF}_3 \cdot \text{H}_2\text{O}$  occurs in nature as the mineral fluellite. Two acid fluorides,  $\text{AlF}_3 \cdot 3\text{HF} \cdot 6\text{H}_2\text{O}$  and  $\text{AlF}_3 \cdot 3\text{HF} \cdot 3\text{H}_2\text{O}$ , have been identified as solid phases in the system  $\text{AlF}_3\text{-HF-H}_2\text{O}$ .<sup>233</sup> In the present work, it is suggested that the fluorine exchange occurred via similar species to those in the system  $\text{AlF}_3/\text{HF}/\text{H}_2\text{O}$ .

The fluorination of  $\gamma$ -alumina by anhydrous hydrogen fluoride or carbonyl fluoride leads to a less uptake of fluorine and a complete exchange with  $^{18}\text{F}$ -fluorine labelled anhydrous hydrogen fluoride, comparable with sulphur tetrafluoride or thionyl fluoride treated  $\gamma$ -alumina which leads to a more uptake of fluorine and less exchange with  $^{18}\text{F}$ -fluorine labelled anhydrous hydrogen fluoride. The fluorination of  $\gamma$ -alumina by sulphur tetrafluoride or thionyl fluoride proceeds via the formation of thionyl fluoride and sulphur dioxide in the former and sulphur dioxide in the latter with no detectable sulphur laydown from the sulphur tetrafluoride or thionyl fluoride treatment. The different behaviour between the reactions involving  $\gamma$ -alumina treated with anhydrous hydrogen fluoride or carbonyl fluoride and the reactions involving  $\gamma$ -alumina treated with thionyl fluoride or sulphur tetrafluoride, is due to the presence of different sites on the surface of the fluorinated  $\gamma$ -alumina.

The exchange of anhydrous  $^{18}\text{F}$ -fluorine labelled hydrogen fluoride with sulphur tetrafluoride or thionyl fluoride treated  $\gamma$ -alumina results in ca 60% of the fluorine content of the  $\gamma$ -alumina being labile. (Chapter Six). This labile fluorine is shown to

originate from the fluorination of  $\gamma$ -alumina with hydrogen fluoride. The residual ca 40% is proposed to be associated with another site which is not exchangeable with anhydrous hydrogen fluoride.

The reaction of  $^{18}\text{F}$ -fluorine labelled sulphur tetrafluoride with  $\gamma$ -alumina treated with any of the fluorinating agents results in ca 40% exchange. A similar result was obtained in a radio-tracer study of the reactions of sulphur tetrafluoride with aluminium(III) fluoride or chromium(III) fluoride.<sup>234</sup> In this work 20% and 30% exchange is observed respectively and it is proposed that the exchange occurred via the  $\text{SF}_3^+$ . It is therefore reasonable to assume that a similar species is involved in these reactions.

### 8.3 CATALYTIC ACTIVITY OF METAL FLUORIDE SUPPORTED ON FLUORINATED $\gamma$ -ALUMINA.

The room temperature reaction between chlorine monofluoride and sulphur tetrafluoride in the presence of the metal fluoride supported on  $\gamma$ -alumina prepared from aqueous or non-aqueous solution and treated with sulphur tetrafluoride, thionyl fluoride, sulphur dioxide then anhydrous hydrogen fluoride or anhydrous hydrogen fluoride, leads to the formation of sulphur chloride pentafluoride. The low yield observed when the metal fluoride supported on  $\gamma$ -alumina treated with anhydrous hydrogen fluoride used as a catalyst is due to the presence of the hydrogen difluoride anions which are not catalytically active towards the chlorofluorination of sulphur tetrafluoride. The yield of sulphur chloride pentafluoride varies with the metal fluoride loading of the supported metal fluoride on fluorinated  $\gamma$ -alumina (MFA or MFN - I, II or V),  $0.6 - 20.0 \text{ mmol g}^{-1}$  and is at a maximum at

the 5.5 mmol g<sup>-1</sup>. Further increase in the metal fluoride loading in the range 5.5 - 20.0 mmol g<sup>-1</sup> leads to poor yields of sulphur chloride pentafluoride as shown in Fig. 8.15-8.18. This behaviour is accounted for by the loss of the active sites on the surface of the catalyst which is in turn due to the reaction of the metal fluoride particles with the  $\gamma$ -alumina to form the hexafluoroaluminate salts (M<sub>3</sub>AlF<sub>6</sub>).

The results presented in Chapter Seven using the surface concentrations of chlorine monofluoride and sulphur tetrafluoride by monitoring the activity of the surface during reaction of <sup>36</sup>Cl -chlorine labelled chlorine monofluoride and sulphur tetrafluoride or chlorine monofluoride and <sup>35</sup>S -sulphur labelled sulphur tetrafluoride 1:1 mole ratio mixtures, indicate that the formation of sulphur chloride pentafluoride is a true surface reaction involving adsorbed chlorine monofluoride and sulphur tetrafluoride. The generally accepted mechanism for the caesium fluoride catalysed chlorofluorination of sulphur tetrafluoride involves the formation of CsSF<sub>5</sub> which is then oxidised with chlorine monofluoride to give sulphur chloride pentafluoride. This mechanism is shown to be incorrect, in that the oxidative chlorofluorination of sulphur tetrafluoride in the presence of the catalyst is much faster than the chlorofluorination of the sulphur tetrafluoride treated supported metal fluoride on fluorinated  $\gamma$ -alumina complex as shown in Figs. 8.19-8.22, and described in detail in Chapter Seven. Kolta and co-workers<sup>83</sup> reported that, this mechanism is incorrect in that such a mechanism does not take into account the reaction between chlorine monofluoride and the caesium fluoride. The results presented in this work are in good agreement with those reported by Kolta and co-workers<sup>83</sup> using activated caesium fluoride as a catalyst. A similar mechanism is therefore

Figure 8.15 Reaction of SF<sub>4</sub> and ClF over MFAI

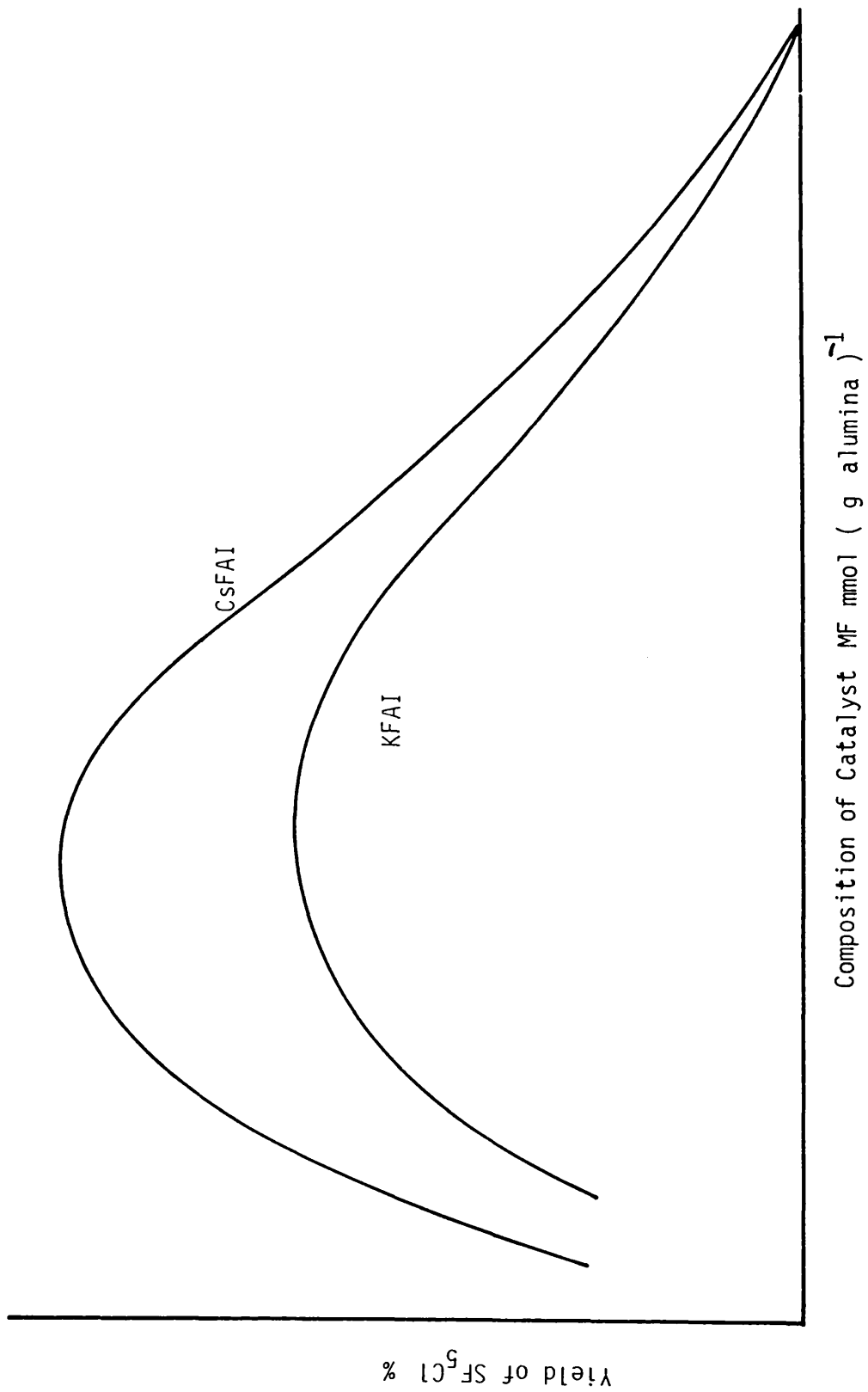


Figure 8.16 Reaction of  $SF_4$  and CIF over MFAV

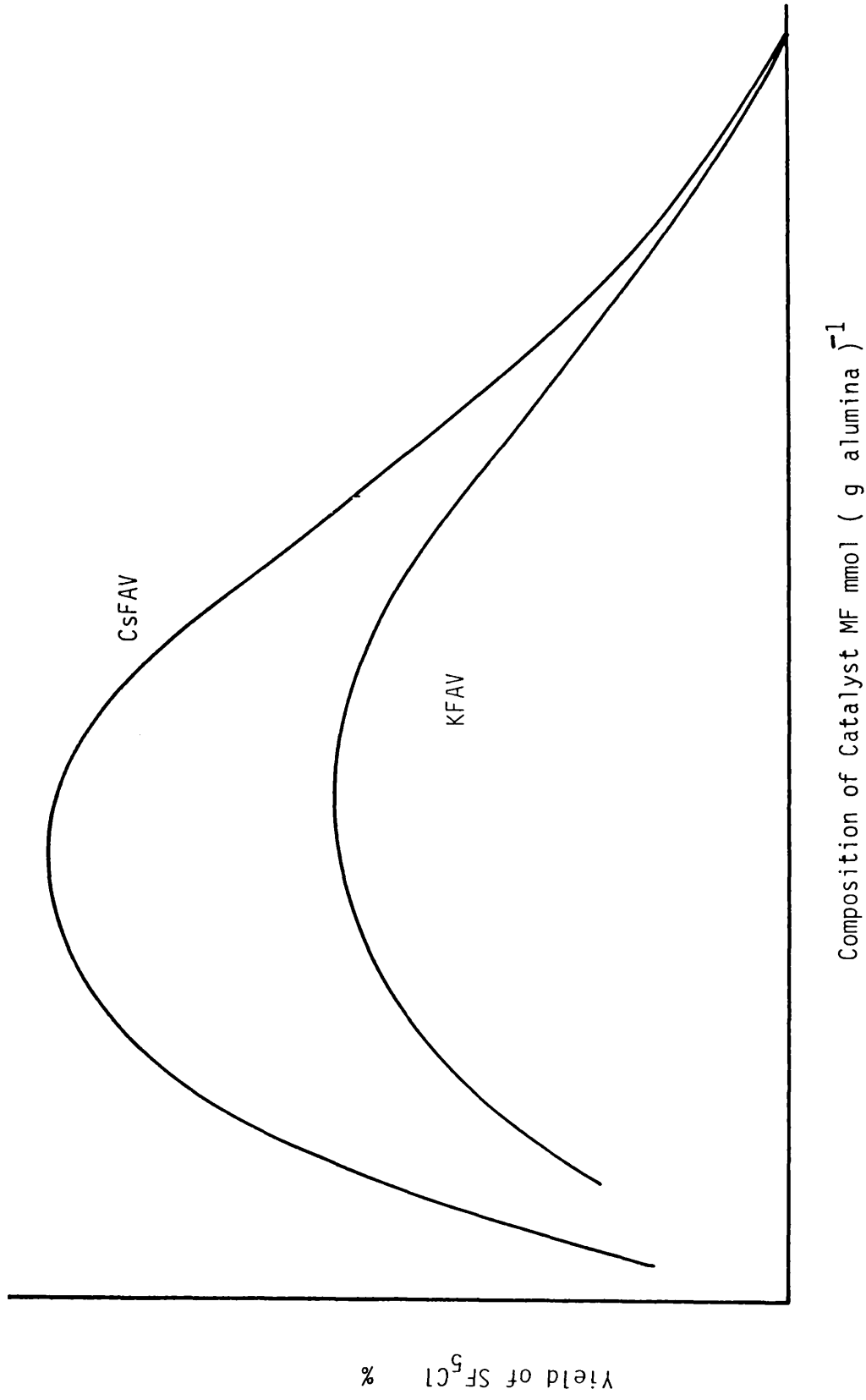


Figure 8.17 Reaction of  $SF_4$  and  $ClF$  over  $MFNII$

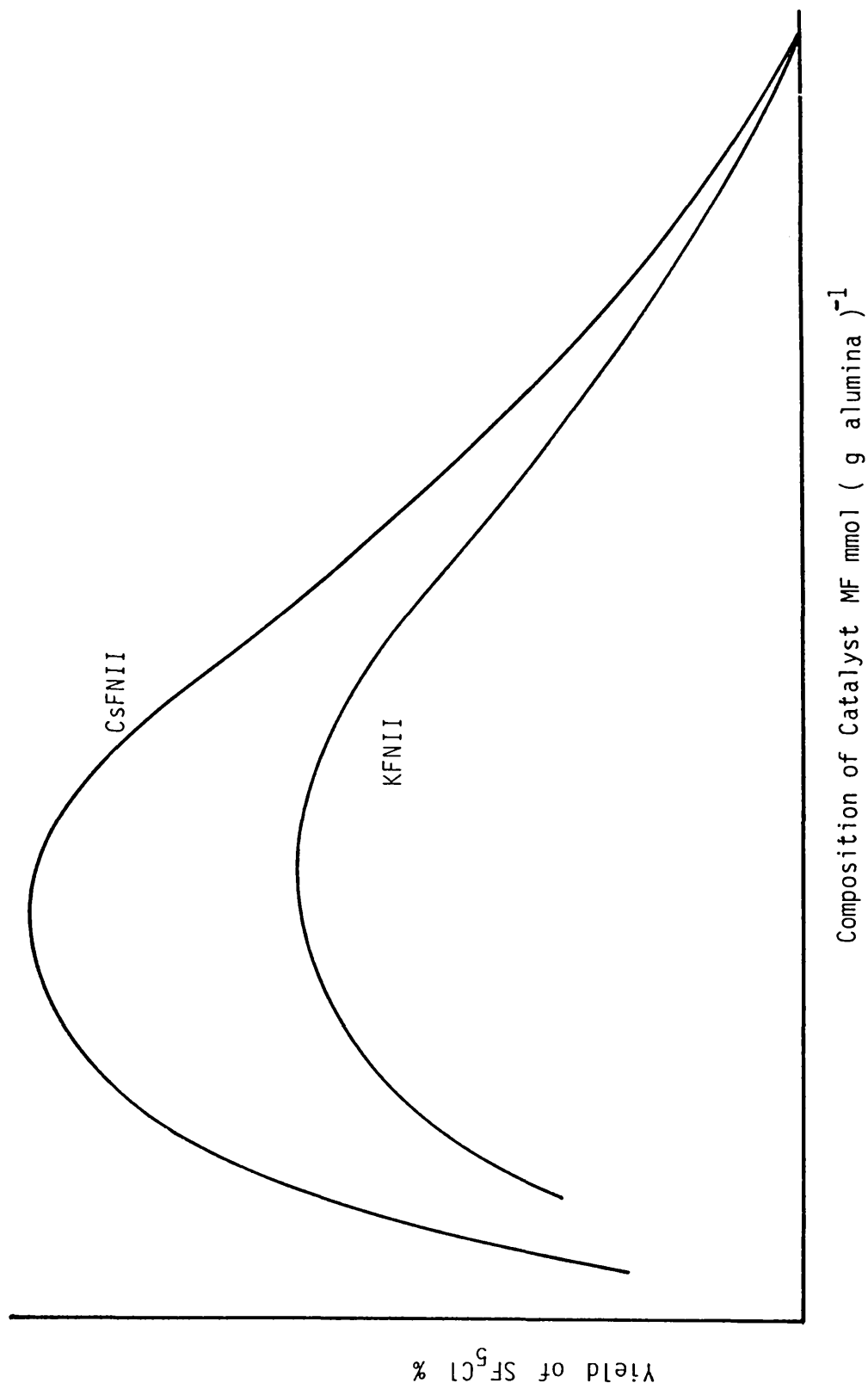


Figure 8.18 Reaction of  $SF_4$  and  $ClF$  Over  $MF/$  fluorinated  $\gamma$ -alumina

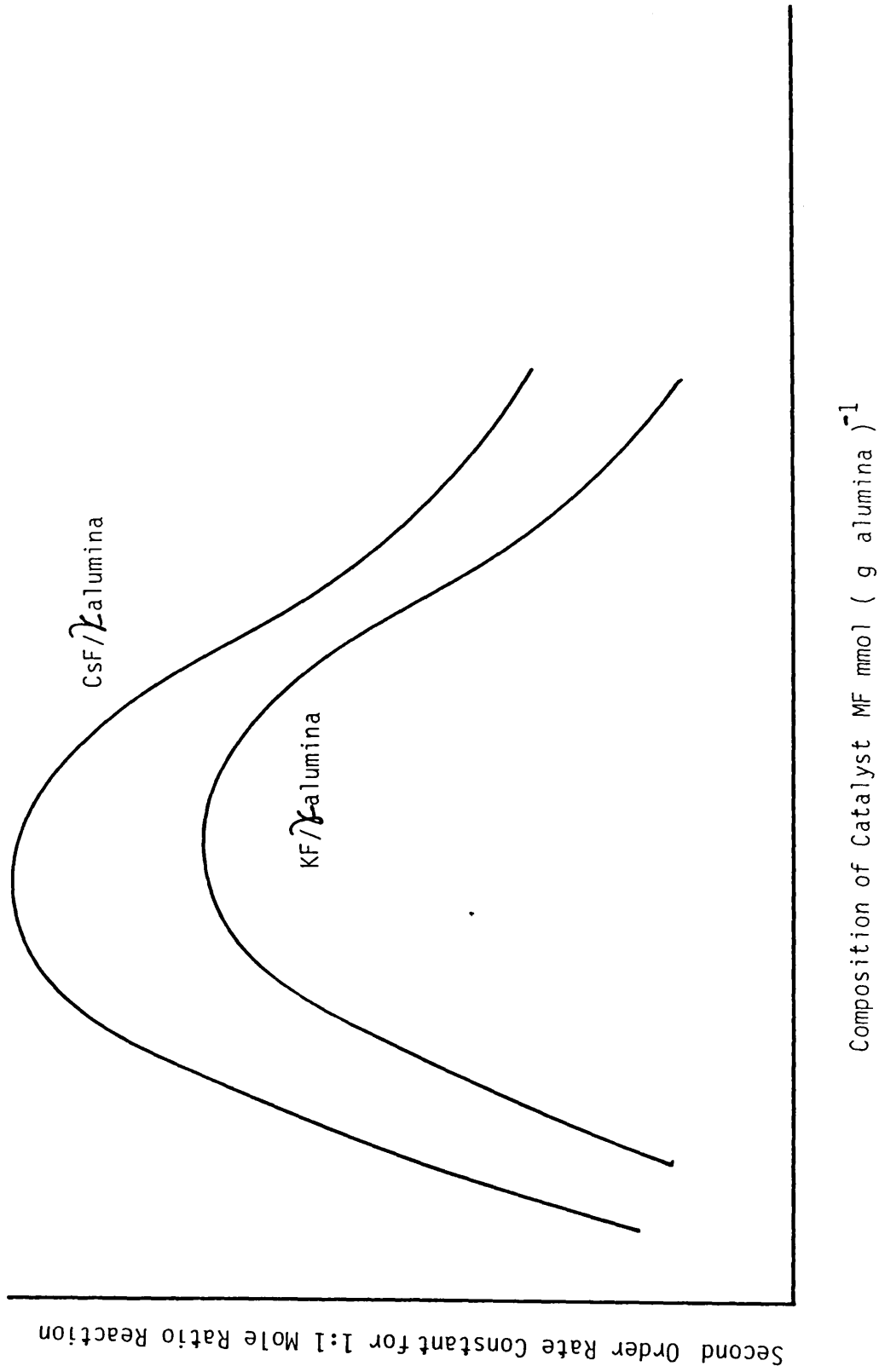




Figure 8.19 Reaction of  $^{35}\text{SF}_4 + \text{ClF}$  over CsF/ fluorinated alumina

$^{35}\text{S}$  Surface Count Rate  $\underline{\text{v}}$  Reaction Time

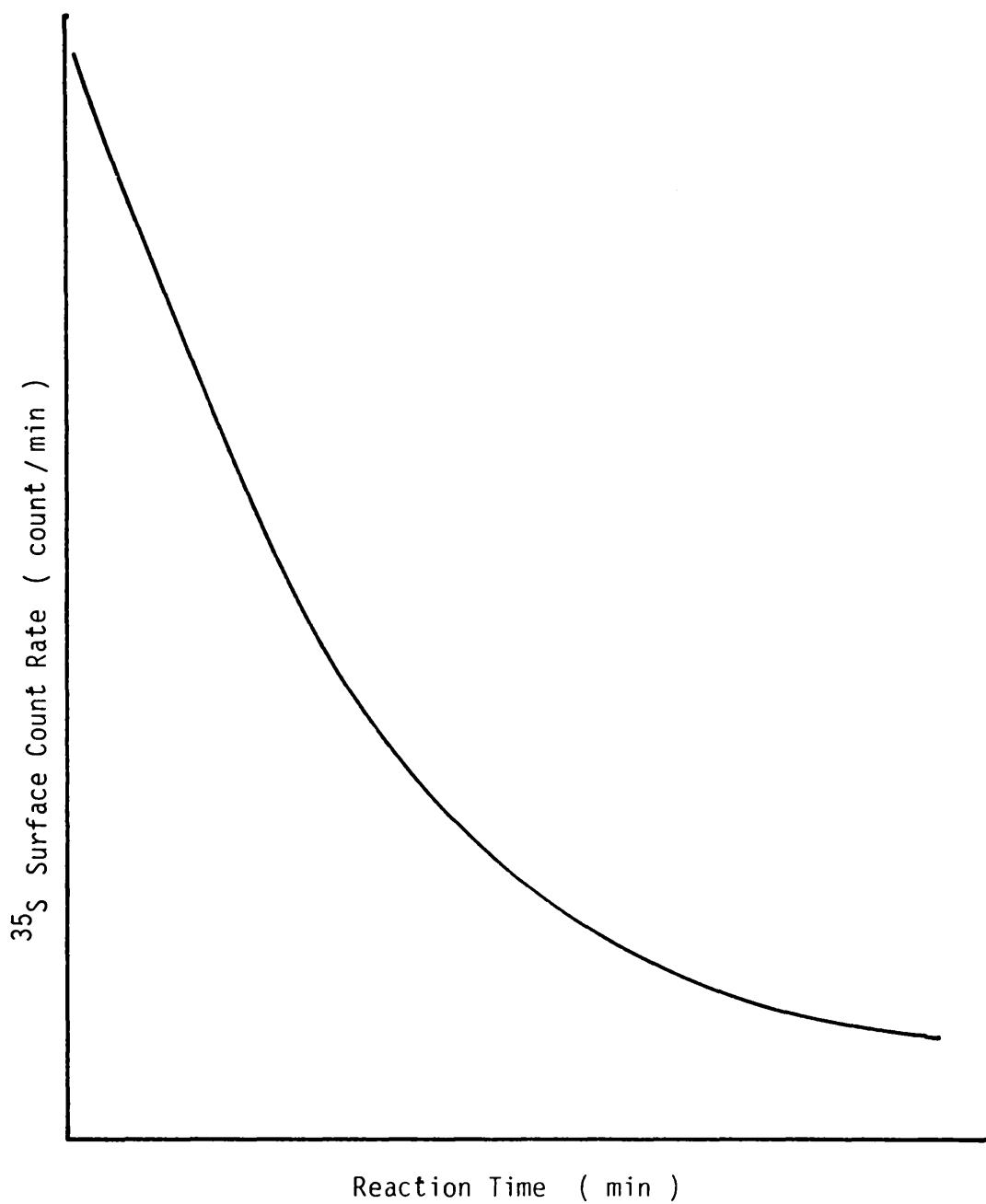


Figure 8.20 Reaction of  $SF_4 + {}^{36}ClF$  over CsF/ fluorinated  $\gamma$ -alumina

${}^{36}Cl$  Surface Count Rate  $\underline{v}$  Reaction Time

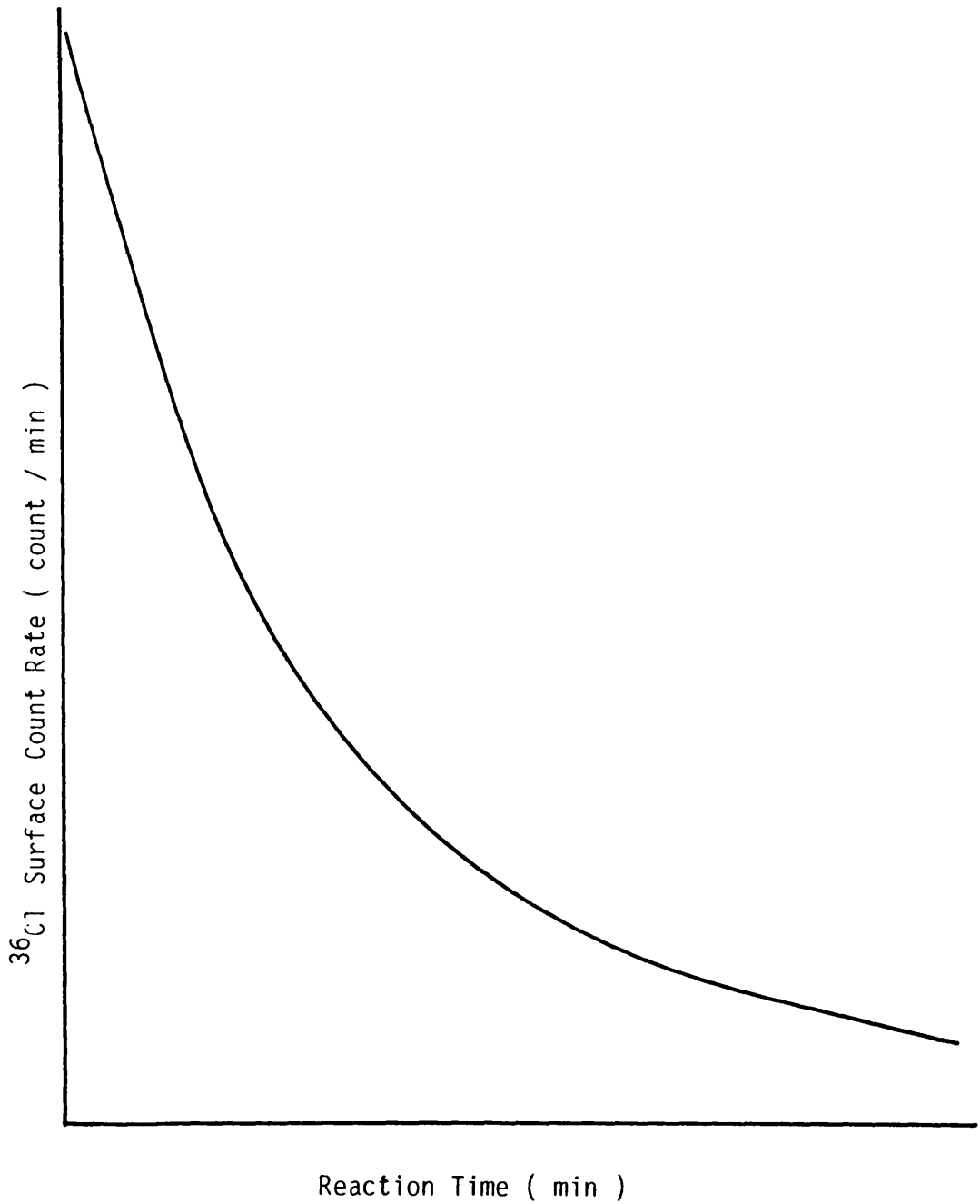


Figure 8.21 Reaction of ClF with  $^{35}\text{SF}_4$  treated catalyst

$^{35}\text{S}$  Surface Count Rate  $\underline{v}$  reaction Time

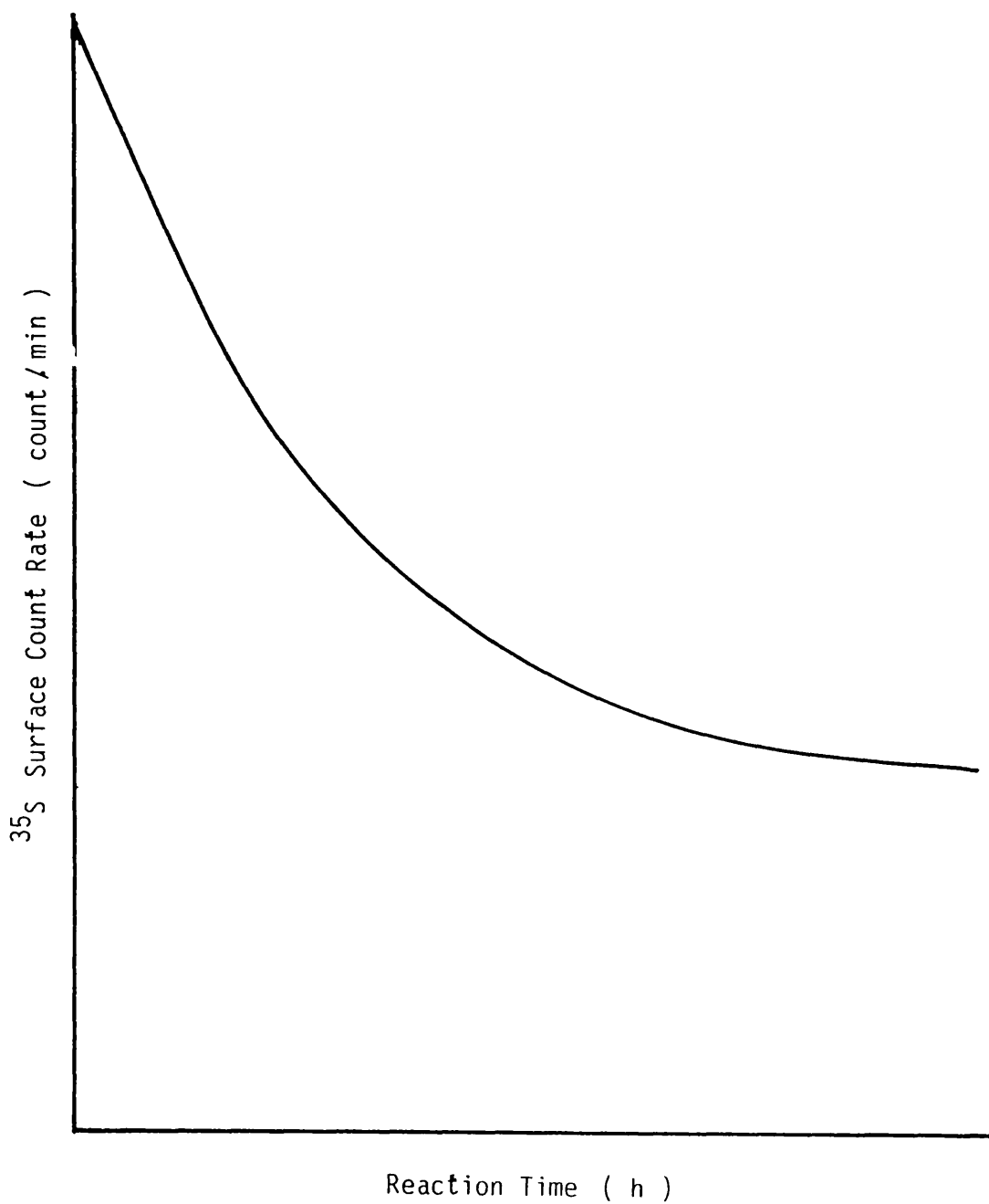
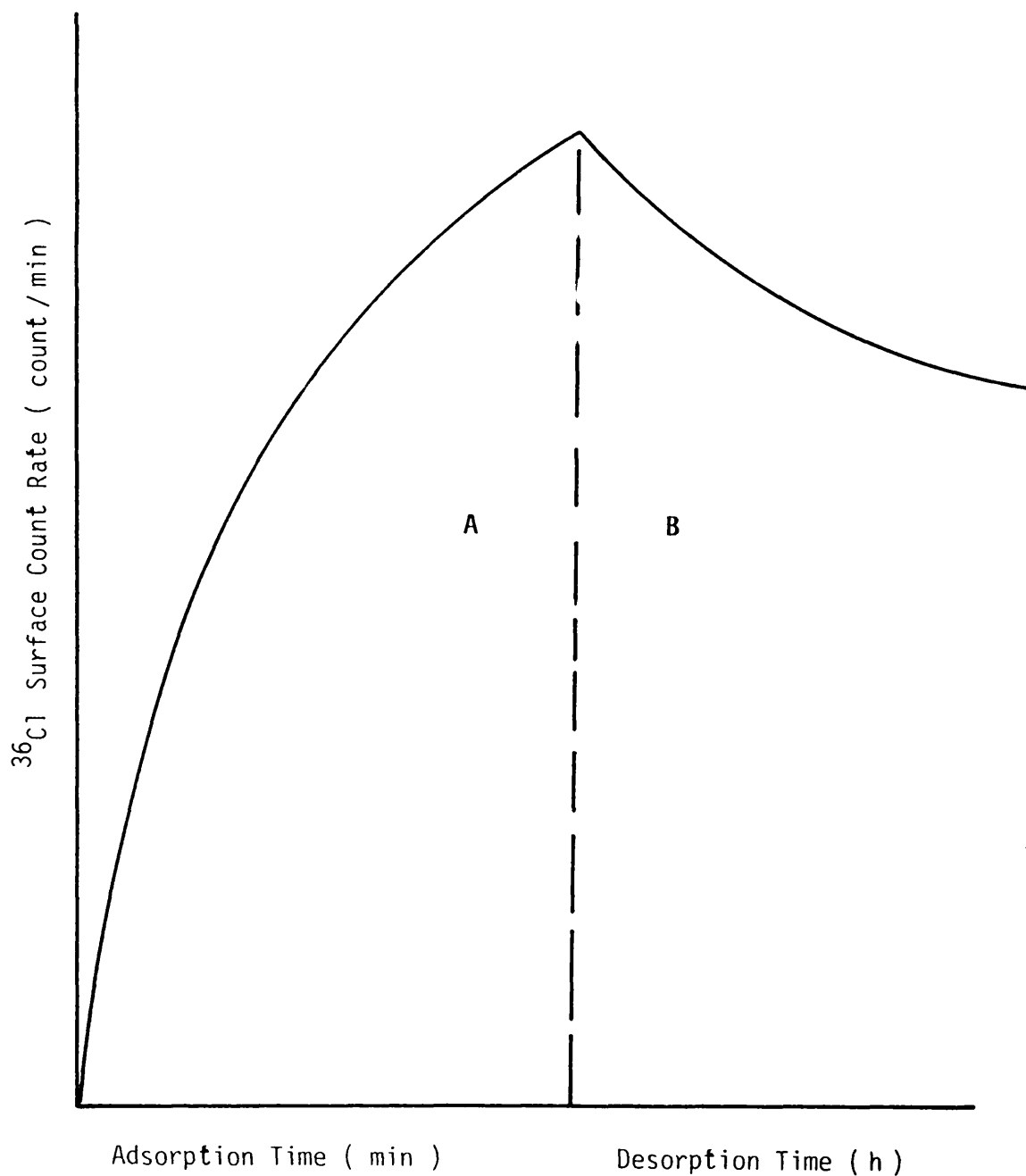
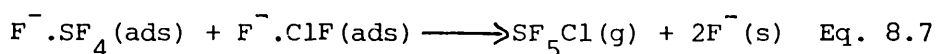
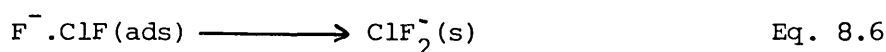
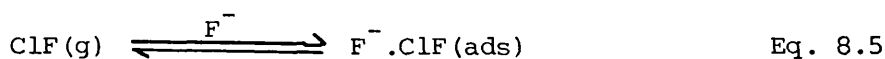
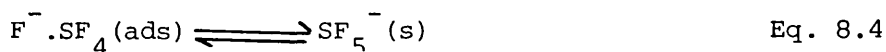
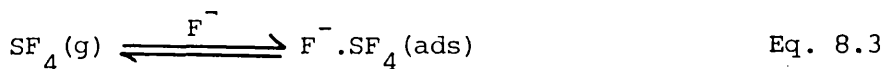


Figure 8.22 Reaction of  $SF_4$  with  $^{36}ClF$  treated catalyst

A = Adsorption of  $^{36}ClF$  B = Desorption of  $SF_5^{36}Cl$  by admission of  $SF_4$



proposed for the catalytic effect of the supported metal fluoride on fluorinated  $\gamma$ -alumina and is given in equations 8.3 - 8.7



where  $\text{F}^- \cdot \text{SF}_4(\text{ads})$  and  $\text{F}^- \cdot \text{ClF}(\text{ads})$  represent the surface adsorbed states of sulphur tetrafluoride and chlorine monofluoride respectively and involve a relatively weak chemical interaction between the substrate and the surface. For a given composition across the metal fluoride loading in the range 0.6 - 15.0 mmol  $\text{g}^{-1}$ , and under the same conditions, supported caesium fluoride is more reactive catalysts than supported potassium fluoride.

The results presented in Chapter Seven show that the reaction of  $^{36}\text{Cl}$ -chlorine labelled chlorine monofluoride with the supported metal fluoride on fluorinated  $\gamma$ -alumina is rapid at room temperature and the removal of the gas phase has no effect on the final surface activity. This means that there is only one species present on the surface of the catalyst. This species is permanently retained at room temperature, but it is removed by heating to 423 K under vacuum. The infra-red and Raman spectra of the solid after reaction of the catalyst with chlorine monofluoride show bands assigned for the

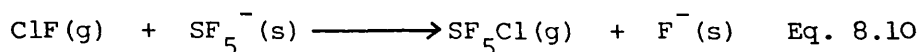
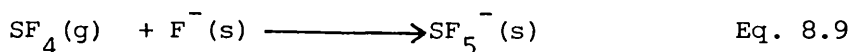
difluorochlorates(I) anion. The difluorochlorates(I) of caesium, rubidium and potassium are successfully prepared by metathetical reaction or direct interaction of chlorine monofluoride with the corresponding metal fluoride.<sup>22</sup> The infra-red spectrum of the caesium difluorochlorate in the range 4000 - 400  $\text{cm}^{-1}$  shows its strongest absorption at 636  $\text{cm}^{-1}$ , in agreement with the 635  $\text{cm}^{-1}$  value for the asymmetric stretching of the difluorochlorate(I) anion in the nitrosyl difluorochlorate.<sup>21</sup> Based on the suggested linearity of the difluorochlorate anion in nitrosyl difluorochlorate, a similar structure is assumed for the difluorochlorate(I) anion in the alkali metal difluorochlorates(I). The evidence for the formation of a  $\text{M}^+\text{FClF}^-$  ion pair is reported from infra-red and Raman spectroscopic studies of the reaction between metal fluoride and chlorine monofluoride in an argon matrix at 15 K.<sup>235</sup>

Similar retention of  $^{35}\text{S}$ -sulphur labelled sulphur tetrafluoride is observed, although the quantities retained are considerably less than the quantities of chlorine monofluoride retained. Furthermore, unlike chlorine monofluoride retention, which leads to catalyst poisoning, there is no evidence to suggest that the retained sulphur tetrafluoride acts as a catalyst poison.

The admission of sulphur tetrafluoride to chlorine monofluoride pretreated catalyst leads only to a very small yields of sulphur chloride pentafluoride, relative to those obtained when reactants were admitted simultaneously to the catalyst. However, there is a marked increase in the extent of retention of sulphur tetrafluoride when the catalyst is pretreated with chlorine monofluoride. This observation is in good agreement with those reported by Kolta et al<sup>83</sup> who suggested that the  $(\text{Cs}^+\text{ClF}_2^--\text{SF}_4)$  entity exists as a stable species on the

catalyst, which only decomposes slowly to caesium fluoride and sulphur chloride pentafluoride at elevated temperatures.

The admission of chlorine monofluoride to sulphur tetrafluoride pretreated catalyst leads to the complete conversion of the sulphur tetrafluoride retained to sulphur chloride pentafluoride over longer times than that required when reactants are admitted simultaneously to the catalyst. This observation indicates that reactions of the type, equations 8.9 and 8.10 can occur



to a very small extent, but do not account for the overall reaction.

Since the chlorofluorination of sulphur tetrafluoride by chlorine monofluoride is a base catalysed reaction, it is strongly stressed that the active basic sites of the caesium or potassium fluoride supported on fluorinated  $\gamma$ -alumina are fluoride ions dispersed on the surface of  $\gamma$ -alumina at all compositions,  $\leq 5.5$  mmol  $\text{g}^{-1}$ . At higher loading,  $> 5.5$  mmol  $\text{g}^{-1}$  the catalyst loses its reactivity. This behaviour is accounted for by the reaction between fluoride ions and  $\gamma$ -alumina to form Al-F containing species which are not catalytically active in the present system. The reaction of chlorine monofluoride and sulphur tetrafluoride over MFAI at 373 K leads to the formation of sulphoryl chlorofluorides but no sulphur chloride pentafluoride or reactants are observed.

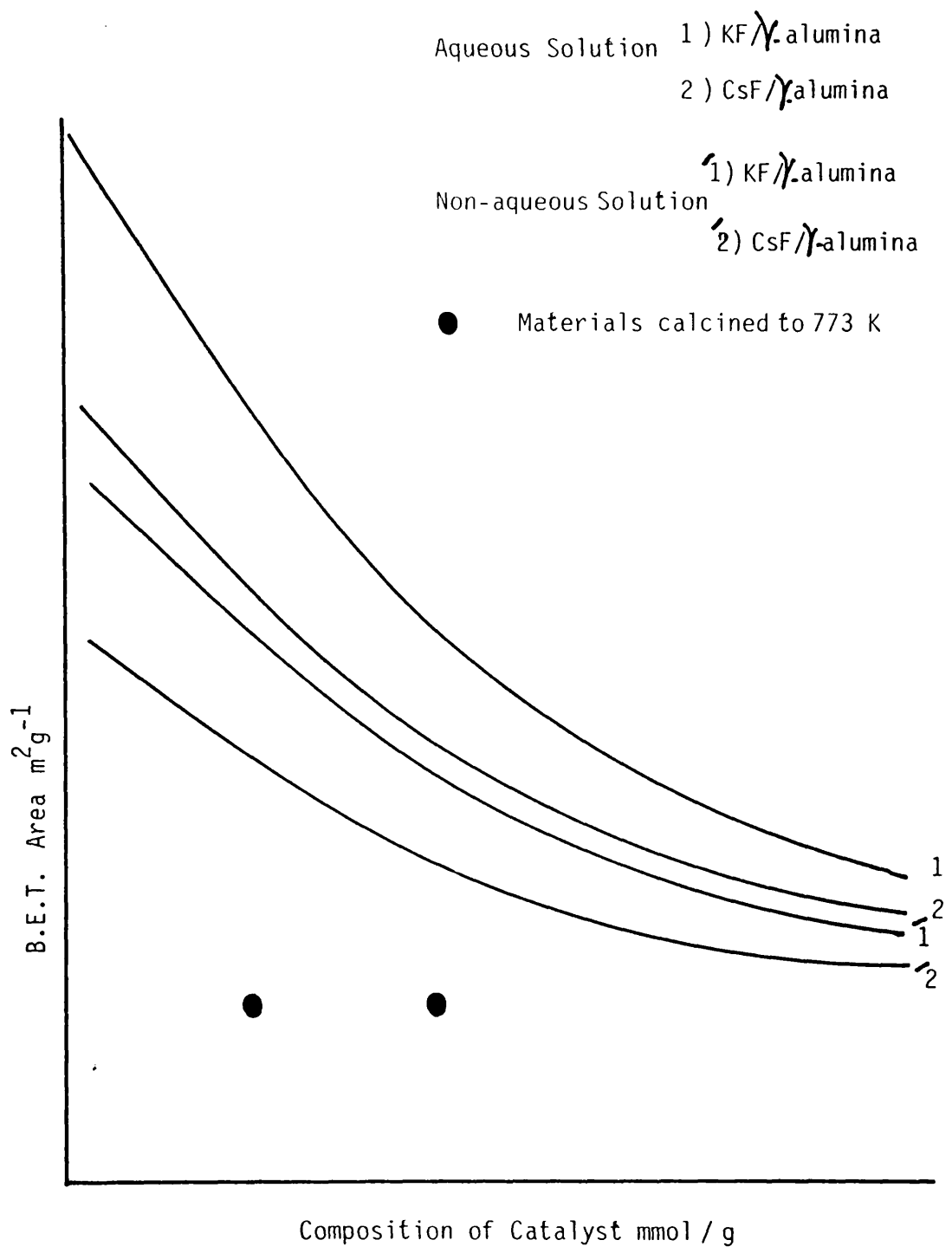
#### 8.4 THE PHYSICAL EXAMINATION OF THE SUPPORTED METAL FLUORIDE.

The calcination of  $\gamma$ -alumina to 523 K leads to an increase in the B.E.T. area whilst the subsequent impregnation of caesium or potassium fluoride on to  $\gamma$ -alumina or the room temperature fluorination of the calcined  $\gamma$ -alumina reduced the B.E.T area of these materials. The reduction in the B.E.T area for the supported metal fluoride, with increased the metal fluoride loading in the range 0.6 - 20.0 mmol g<sup>-1</sup> is observed. The supported metal fluoride calcined to 773 K under vacuum, shows a sharp drop in the B.E.T area for both the 4.4 and 8.8 mmol g<sup>-1</sup> materials as shown in Fig. 8.23 . This drop is attributed to the formation of hexafluoroaluminate which blocks some pores at the surface of  $\gamma$ -alumina. For a given composition, the B.E.T area of the supported caesium fluoride is smaller than that obtained for the potassium fluoride. This is consistent with the size of the cation, caesium or potassium which is believed to block some pores at the surface of  $\gamma$ -alumina. The formation of hexafluoroaluminate particularly at high metal fluoride loading reduces the B.E.T area of the material.

The B.E.T area of the supported metal fluoride prepared from non-aqueous solution, exhibits similar characteristics to those described above, but for a given composition, a small B.E.T area is recorded as shown in Fig.8.23. This different behaviour is attributed to the ~~smaller~~ hydroxyl groups coverage of the surface of the supported metal fluoride prepared from non-aqueous solution compared with that of the material prepared from aqueous solution. However, the B.E.T area of the supported metal fluoride prepared by mixing the metal fluoride with  $\gamma$ -alumina under nitrogen atmosphere



Figure 8.23 B.E.T. Area of MF/ $\gamma$ -alumina



is not reproducible from sample to sample for a given composition.

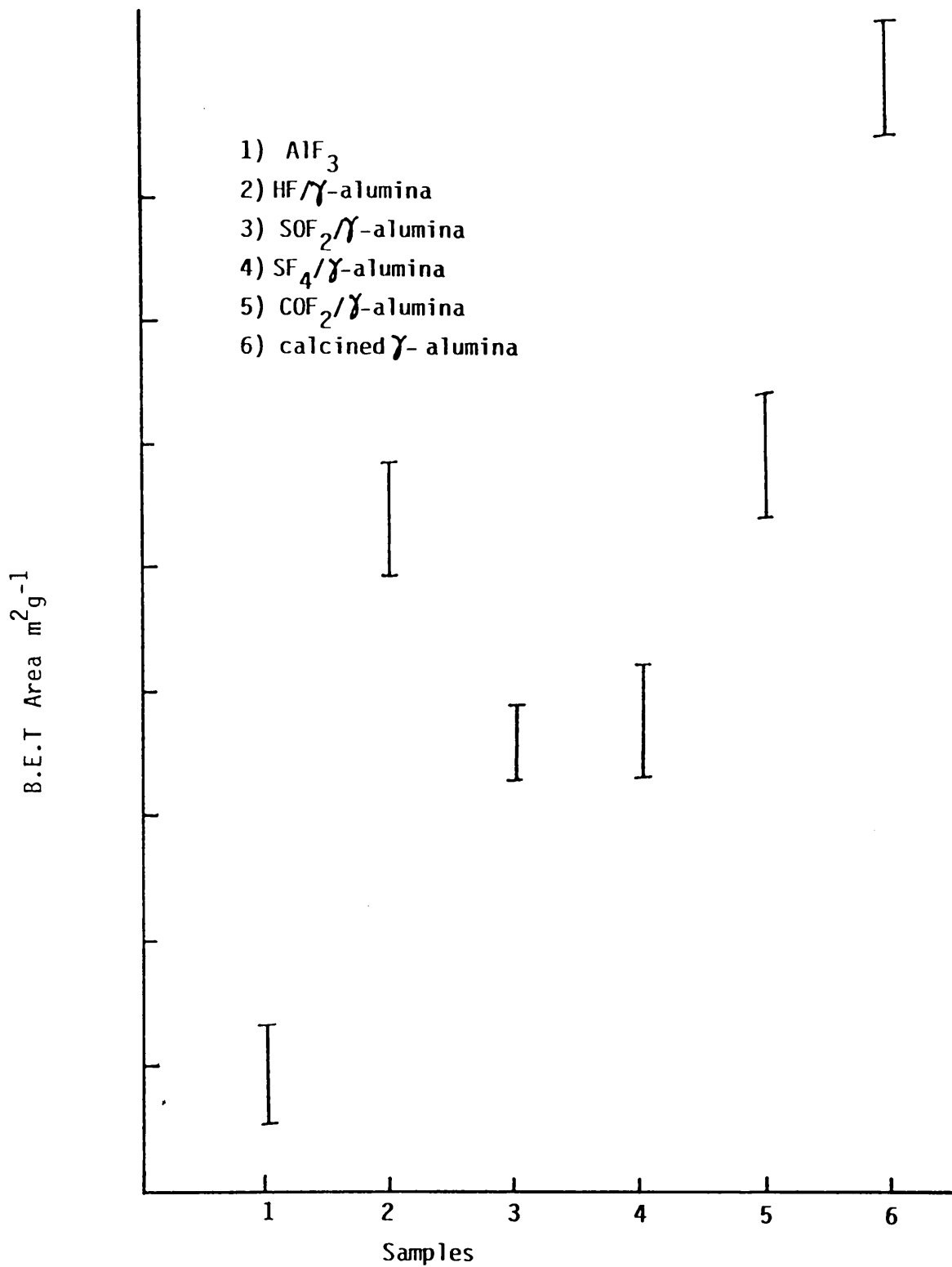
The room temperature treatment of  $\gamma$ -alumina calcined to 523 K, by sulphur tetrafluoride, thionyl fluoride, carbonyl fluoride or anhydrous hydrogen fluoride results in a reduction in the B.E.T area of the materials, as shown in Fig. 8.24

The x-ray diffraction shows very sharp lines attributed to the metal fluoride and  $\gamma$ -alumina at low metal fluoride loading,  $\leq 5.5 \text{ mmol g}^{-1}$ , but lines due to the hexafluoroaluminate anion are clearly observed at loading,  $> 5.5 \text{ mmol g}^{-1}$ . The absence of the metal fluoride lines in the  $20.0 \text{ mmol g}^{-1}$  samples in the x-ray diffraction spectra is consistent with the reaction of most of the metal fluoride to form the metal hexafluoroaluminate ( $M_3AlF_6$ ).

The transmission electron microscopy clearly shows the presence of potassium fluoride particles at loadings,  $\leq 5.5 \text{ mmol g}^{-1}$  but not at higher loadings. However there is no evidence for potassium hexafluoroaluminate at the surface of the supported metal fluoride,  $8.8 \text{ mmol g}^{-1}$  in the areas examined.

The strong absorption band at ca  $580 \text{ cm}^{-1}$  in the infra-red spectrum of the supported metal fluoride,  $> 5.5 \text{ mmol g}^{-1}$ , is similar to the Al-F stretch band of hexafluoroaluminate. This finding, supports the suggestion that heating promoters, fluoro-dehydroxylates  $\gamma$ -alumina and hence the formation of hexafluoroaluminate particularly at high metal fluoride loading.

Figure 8.24 B.E.T Area of fluorinated  $\gamma$ -alumina



The results of the  $^{27}\text{Al}$  MAS-NMR of the supported metal fluoride show that the impregnation of metal fluoride on to  $\gamma$ -alumina results in a shift upfield of the signals arising from tetrahedral and octahedral aluminium environments. The shielding of aluminium is consistent with the metal fluoride loading in the composition range  $4.4 - 20.0 \text{ mmol g}^{-1}$ . These results do not show any evidence for aluminium(III) fluoride, tetrafluoroaluminate or pentafluoroaluminate in the supported metal fluoride across the composition range  $4.4 - 20.0 \text{ mmol g}^{-1}$ . However due to the small chemical shifts recorded for the aluminium octahedral environment, it is not possible to justify the hexafluoroaluminate species in the material examined.

The infra-red, the  $^{27}\text{Al}$  MAS-NMR and the powder x-ray diffraction spectra and the transmission electron microscopy of the metal fluoride supported on fluorinated  $\gamma$ -alumina,  $4.4 \text{ mmol g}^{-1}$  which is exposed to 1:1 mole ratio mixture of sulphur tetrafluoride and chlorine monofluoride at 373 K, clearly show the presence of the metal tetrafluoroaluminate. There are two possible explanations for the formation of this. The first is the direct fluorodehydroxylation of the catalyst at 373 K with chlorine monofluoride and/or sulphur tetrafluoride, the second is the formation of sulphur chloride pentafluoride followed by the subsequent fluorodehydroxylation of the catalyst resulting in the demolition of the catalytically active sites.

## CHAPTER NINE

## CONCLUSIONS

It is found that experimentally by physical methods e.g. the B.E.T, infra-red,  $^{27}\text{Al}$  MAS-NMR and structural properties, powder X-ray diffraction of the supported metal fluorides depend on their composition. The B.E.T. area of these materials decreases by increasing the metal fluoride loading in the range 0.6 - 20.0 mmol  $\text{g}^{-1}$ , and for a given composition, the B.E.T area of these materials prepared from aqueous solution is larger than those obtained from the materials prepared from non-aqueous solution. However, the materials prepared by simply mixing the metal fluoride and  $\gamma$ -alumina under nitrogen atmosphere, have irreproducible B.E.T. area. This behaviour is accounted for by the fact that the metal fluoride is not dispersed homogeneously on the surface of the  $\gamma$ -alumina. The powder x-ray diffraction and the infra-red spectroscopy clearly show the presence of  $\text{M}_3\text{AlF}_6$  in all samples above 5.5 mmol  $\text{g}^{-1}$ . Transmission electron microscopy is particularly useful, below 5.5 mmol  $\text{g}^{-1}$  potassium fluoride particles are detected while at higher loadings formation of Al-F phases are observed. These species are suggested to be  $\text{K}_3\text{AlF}_6$ .

Sulphur tetrafluoride and thionyl fluoride are exothermically hydrolysed at the surface of the supported metal fluoride, to give thionyl fluoride and sulphur dioxide in the former and sulphur dioxide in the latter. There is no evidence for anhydrous hydrogen fluoride present in the volatile products. Apparently anhydrous hydrogen fluoride formed, is retained by the supported metal fluoride.

Radiotracer studies of the reaction of [ $^{35}\text{S}$ ]-sulphur labelled sulphur tetrafluoride, thionyl fluoride or sulphur dioxide with the supported metal fluoride show that two distinct species are present

on the surface. One which is weakly adsorbed is removed at room temperature by pumping and one which is permanently retained is not removed at room temperature, but is removed at 395 K or by the exposure to water vapour. These species are proposed to be weakly adsorbed molecules of sulphur tetrafluoride, thionyl fluoride and sulphur dioxide and permanently retained pentafluorosulphate and fluorosulphate anions. The uptake of sulphur containing probe molecules by the supported metal fluoride is in the order  $SF_4 > SO_2 \sim SOF_2$ , across the composition range 0.6 - 20.0 mmol g<sup>-1</sup>, and is at a maximum at 5.5 mmol g<sup>-1</sup>. [<sup>18</sup>F]-Fluorine exchange is observed in the reaction of sulphur tetrafluoride and the supported metal fluoride and is suggested to occur via the pentafluorosulphate anion.

Carbonyl fluoride is hydrolysed at the surface of the supported metal fluoride to give carbon dioxide but there is no evidence for anhydrous hydrogen fluoride present in the volatile products.

The reaction of [<sup>14</sup>C]-carbon labelled carbonyl fluoride shows that two distinct species are present in the surface of the supported metal fluoride. The permanently retained species is proposed to be trifluoromethoxide anion and the weakly adsorbed is adsorbed molecules of carbonyl fluoride and carbon dioxide. The uptake of carbonyl fluoride by the supported metal fluoride varies with the metal fluoride loading and is at a maximum at 5.5 mmol g<sup>-1</sup>. The formation of the trifluoromethoxide species is proposed to be responsible for the [<sup>18</sup>F]-fluorine exchange observed in the system. The uptake of anhydrous hydrogen fluoride by the supported metal fluoride and the complete [<sup>18</sup>F]-fluorine exchange

observed in these systems is consistent with the formation of hydrogen fluoride oligomers of the type  $(\text{HF})_n$  and  $(\text{HF})_n\text{F}^-$ .

It is concluded that caesium or potassium fluoride supported on  $\gamma$ -alumina does not owe its basic activity to the formation of caesium or potassium hydroxide and/or aluminate during preparation. Weinstock et al<sup>154</sup> who have recently noted the presence of potassium hexafluoroaluminate in an unspecified sample of potassium fluoride supported on  $\gamma$ -alumina and stated that 'fluoride ion has little or no direct role in the enhanced reactivity', and potassium hydroxide and/or aluminate are the agents responsible, are seriously in error. Caesium or potassium fluoride supported on  $\gamma$ -alumina owes its efficient and versatile reactivity as a heterogeneous super base to at least two possible mechanisms: dispersion of the metal fluoride particles on the surface of  $\gamma$ -alumina giving co-ordinately unsaturated fluoride ions, or the co-operative action of fluoride ion and the hydrated or the unhydrated  $\gamma$ -alumina surface.

The fluorination of  $\gamma$ -alumina by anhydrous hydrogen fluoride or carbonyl fluoride results in surface fluorine which is chemically bound to the surface and is labile to exchange with anhydrous hydrogen fluoride at 293 K. The fluorination of  $\gamma$ -alumina surface by the sulphur tetrafluoride or thionyl fluoride treatment at room temperature resulted in two forms of fluorine on the surface. One form of the surface fluorine is labile to exchange with anhydrous hydrogen fluoride and is ca 60%. The other form of the surface fluorine is not labile to exchange with anhydrous hydrogen fluoride and is ca 40%.

There is no reaction between anhydrous hydrogen fluoride and dry anhydrous aluminium(III) fluoride, but a total exchange is quoted



in the system if anhydrous aluminium(III) is first exposed to water vapour. It is therefore concluded that the fluorination of  $\gamma$ -alumina by anhydrous hydrogen fluoride, carbonyl fluoride, sulphur tetrafluoride or thionyl fluoride at room temperature does not form anhydrous aluminium(III) fluoride.

Terminal hydroxyl groups present on the surface of  $\gamma$ -alumina supported metal fluoride are removed by treatment with sulphur tetrafluoride, thionyl fluoride, or sulphur dioxide then anhydrous hydrogen fluoride. The resulting materials, caesium or potassium fluoride supported on fluorinated  $\gamma$ -alumina, are efficient catalysts for chlorofluorination of sulphur tetrafluoride by chlorine monofluoride catalytic activity is at a maximum at  $5.5 \text{ mmol g}^{-1}$  and poisoning by chlorine monofluoride appeared to be less important than was the case for unsupported caesium fluoride. The materials prepared from non-aqueous solution; from heptafluoroisopropoxide salts, and fluorinated with sulphur tetrafluoride, thionyl fluoride or sulphur dioxide then anhydrous hydrogen fluoride, exhibit similar characteristics to those prepared from aqueous solution. The catalytically active sites at the surface of the catalyst are fluoride ions, by which the reactants are adsorbed to form  $\text{SF}_4 \cdot \text{F}^- (\text{ads})$  and  $\text{ClF} \cdot \text{F}^- (\text{ads})$ . The subsequent reaction of these species gives sulphur chloride pentafluoride, leaving two vacant active sites on the surface of the catalyst for further adsorptions.

APPENDIX I

The analogous impregnation of thalium (I) fluoride on to  $\gamma$ -alumina from aqueous solution results in a very dark coloured solid after the removal of the bulk of water at 70°C. The fluorination of this material by sulphur tetrafluoride or thionyl fluoride at room temperature results in a colourless solid. However, the exposure of the surface to the moisture at room temperature leads to a change in colour to black.

No chemical reactions or physical examination are attempted to characterize this material in the present work.

What is the nature of this material? Does this material behave the same as supported caesium or potassium fluoride as far as the chlorofluorination of sulphur tetrafluoride by chlorine monofluoride is concerned? Or does it behave similar to the unsupported thalium fluoride which is not catalytically active?

APPENDIX II

The dehydrohalogenation of halo-olefins is Lewis acid or Lewis base catalysed reaction. In this context, in an attempt to dehydrochlorinate 1,1,1 trichloroethane by caesium or potassium fluoride supported on fluorinated  $\gamma$ -alumina, large quantities of the volatile product is retained. Small quantities of hydrogen chloride and 1,1 dichloroethane are observed in the gas phase. After the removal of the volatile products at room temperature, the colour of the catalyst is changed to very dark black. What is the nature of this material?

REFERENCES

1. (a) J. Berzelius, Jahres-Bericht Uber die Fortschritte der Physichem Wissenschaften., Tubingen., 1836, pp. 243;  
(b) P. Emmett, Crit. Rev. Solid State Sci., 1974, 4, 127.
2. D.R. Oldroyd, J. Chem. Educ., 1973, 50, 450.
3. Davy's papers on chlorine are collected together in the Elementary Nature of Chlorine Alembic Club Reprints, N.9., Edinburgh, 1953; R. Siegfried, J. Chem. Educ., 1959, 36, 568.
4. B.H. Maham, 'University Chemistry' 3rd Ed., 1975, Addison-Wesley Publishing Company, Berkeley, pp 204-251.
5. S. Arrhenius, Z. Phys. Chem., 1887, 1, 631.
6. J.N. Brønsted, Rec. Trav. Chim., 1923, 42, 718.
7. T.M. Lowry, Chem. Ind., 1923, 42, 43.
8. G.N. Lewis, J. Franklim Inst., 1938, 226, 293.
9. R.G. Pearson, J. Chem. Educ., 1968, 45, 581, 643.
10. F.C. Nachood and E.A. Braude, "Determination of Organic Structures by Physical Methods" Academic Press, New York, 1955 Vol. 1.
11. A.F. Scott 'Survey of Progress in Chemistry' Academic Press, New York, 1969, Vol. 5.
12. A.F. Clifford, H.C. Beachell and W.M. Jack, J. Inorg. Nucl. Chem., 1957, 5, 57.
13. S. Brownstein, Can.J. Chem., 1969, 47, 605.
14. T.C. Rhyne and J.G. Dillard, Inorg. Chem., 1971, 10, 730.
15. O. Ruff, Angew. Chem., 1933, 46, 739.
16. L. Pauling "The Nature of the Chemical Bond", 3rd Ed., pp 81, 85, 90, 102, 177, 288. Cornell University Press, Ithaca, New York.

17. D.A. Gilbert, A. Roberts and P.A. Griswold, Phys. Rev. 1959, 76, 1723.
18. J. Murray, J. Chem. Soc., 1959, 1884.
19. H.S. Booth and J.T. Pinkston, Chem. Rev., 1947, 41, 421.
20. H.S. Booth and J.T. Pinkston 'Fluorine Chemistry' 1950. Ed. J.H. Simons, Academic Press, INC., London, Vol. 1, pp. 189.
21. K.O. Christe and J.P. Guertin, Inorg. Chem., 1965, 4, 905.
22. K.O. Christe and J.P. Guertin, Inorg. Chem., 1965, 4, 1785.
23. I.G. Ryss, 'The Chemistry of Fluorine and Its Inorganic Compounds', State Publishing House for Scientific, Technical and Chemical Literature, Moscow, 1956, English Translation, Vol. 1, 1960, p. 217.
24. M.E. Weeks and H.M. Leicester., Discovery of the Elements 7th Ed. Journal of Chemical Education, Easton Pa., 1968, pp 727.
25. J.R. Partington 'A History of Chemistry, Vol. 3, Macmillan, London 1962, p. 213; and Historical and Industrial Discovery of Elements. Chem. Ind. (Lond)., 1941, 60, 109.
26. J.W. Mellor, 'A Comprehensive Treatise on Inorganic and Theoretical Chemistry, Vol. 2, Longmans, Green, London, 1922, p.3.
27. (a) C.E. Vanderzee and W.W. Rodenberg, J. Chem. Thermodyn., 1970, 2, 461; (b) E.V. Frank and W. Spalthoff, Z. Elektrochem, 1957 61, 348.
28. W. Strohmeier and G. Briegleb, Z. Elektrochem, 1953, 57, 662.
29. Y. Duff and W. Holzer, J. Chem. Phys., 1974, 60, 2175.
30. J. Janzen and L.S. Bartell, J. Chem. Phys., 1969, 50, 3611.

31. R.L. Redington, J. Phys. Chem., 1982, 86, 552.
32. L. Andrews and G.L. Johnson, J. Phys. Chem., 1984, 88, 425.
33. Demelin Handbook of Inorganic Chemistry, 8th Ed., Fluorine Supplement, D. Koschel Ed., Springer-Verlag, Berlin, 1982, 3, 330.
34. A. Azman, A. OcVirk, D. Hadzi, P.A. Giguère and M. Schneider, Can. J. Chem., 1967, 45, 1347.
35. I. Gennick, K.M. Harm<sup>ON</sup> and M.M. PotVin, Inorg. Chem., 1977, 16, 2033.
36. J.H. Clark, J. Emsley, D.J. Jones and R.E. Overill, J. Chem. Soc. Dalton Trans., 1981, 1219.
37. J.A. Ibers, J. Chem. Phys., 1964, 40, 402.
38. O.D. Gupta and J.M. Shreeve, J. Chem. Soc. Chem. Commun., 1984, 416.
39. P.E. Aldrich and W.A. Sheppard, J. Org. Chem., 1964, 29, 11.
40. M.E. Redwood and C.J. Willis, Can J. Chem., 1965, 43, 1893.
41. K.O. Christe, E.C. Curtis and C.J. Schack, Spectrochim. Acta., 1975, 31A, 1035.
42. W.B. Farnham, B.E. Smart, W.J. Middleton, J.C. Calabrese and D.A. Dixon, J. Am. Chem. Soc., 1985, 107, 4565.
43. J.N. Butler "Catalytic Activation of Carbon Dioxide".  
Developed from a symposium sponsored by the Division of Colloid and Surface Chemistry at the 191st Meeting of the American Chemical Society, New York, 1986, pp 9 - 15.
44. E. Martineau and J.B. Milne, J. Chem. Soc. Chem. Commun., 1971, 1327.
45. L. Lawlor and J. Passmore, Inorg. Chem., 1979, 18, 2923.

46. S.J. David and B.S. Ault, Inorg. Chem., 1985, 24, 1238.
47. K.W. Dixon, Ph.D. Thesis, University of Glasgow, 1986.
48. T. Mahmood and J.M. Shreeve, Inorg. Chem., 1985, 24, 1395;  
R. Muller and D. Mross, Z. Anorg. Allgem. Chem., 1963, 324,  
78-89.
49. F.A. Cotton and G. Wilkinson "Advanced Inorganic Chemistry",  
4th Ed., Wiley-Interscience; New York, 1980, pp 537-39.
50. J.R. Morton and K.F. Preston, Chem. Phys. Lett., 1973,  
18, 98.
51. J.R. Morton and K.F. Preston, J. Chem. Phys., 1973, 58,  
2657.
52. K. Garber and B. Ault, Inorg. Chem., 1983, 22, 2509.
53. G.S.H. Chen and J. Passmore, J. Chem. Soc., Dalton., 1979,  
1257.
54. J-Y. Claves and R.J. Gillespie, J. Am. Chem. Soc., 1977,  
99, 1788.
55. P.W. Schenk and R. Steudel, "Inorganic Sulphur Chemistry",  
Edited by G. Nickless, Elsevier Publishing Company, 1968,  
pp 369 - 418.
56. B.P. Dailey, S. Golden and E.B. Wilson, Phys. Rev., 1947,  
72, 871.
57. V. Schomaker and D.P. Stevenson, J. Am. Chem. Soc., 1940,  
62, 1270.
58. M. H. Sirvetz, J. Chem. Phys., 1951, 19, 938.
59. R.R. Lucchese, K. Haber and H.F. Schaefer, J. Am. Chem.  
Soc., 1976, 98, 7617.
60. P. G. Eller and G.J. Kubas, Inorg. Chem., 1978, 17, 894.
61. P.E. Peterson, R. Brockington and D.W. Vidrine, J. Am.  
Chem. Soc., 1976, 98, 2660.

62. O. Ruff and C. Thiel, Ber., 1905, 38, 549.
63. (a) C.W. Tullock, F.S. Fawcett, W.C. Smith and D.D. Coffman, J. Am. Chem. Soc., 1960, 82, 539; (b) F.S. Fawcett and C.W. Tullock, Inorg. Synth., 1963, 7, 119; (c) F. Nyman and H.L. Roberts, J. Chem. Soc., 1962, 3180; (d) R.E. Elmer and R. E. Booth, U.S. Patent 4,082,839 (1978), C.A. 89, 26943, (1978); (e) C. Lau and J. Passmore, J. Fluorine Chem., 1975, 6, 77; (f) W. Luckinger, Thesis, Techn. Hochschule, Breslau, 1936, pp 23; (g) F. Brown and P.L. Robinson, J. Chem. Soc., 1955, 3147; (h) G.A. Silvey and G.H. Cady, J. Am. Chem. Soc., 1952, 74, 5792.
64. J. Nicholls, Ph.D. Thesis, Durham University, 1958.
65. J.D. Vaughn and E.L. Muetterties, J. Phys. Chem., 1960, 64, 1787.
66. R.E. Dodd, L.A. Woodward and H.L. Roberts, Trans. Faraday Soc., 1956, 52, 1052.
67. F.A. Cotton, J.W. George and J. S. Vaughn, J. Chem. Phys., 1958, 28, 994; E.L. Muetterties and W.D. Philips, J. Am. Chem. Soc., 1959, 81, 1084.
68. W.M. Tolles and W.D. Gwinn, J. Chem. Phys., 1962, 36, 1119.
69. D.D. Gibler, C.J. Adams, M. Fischer, A. Zalkin and N. Bartlett, Inorg. Chem., 1972, 11, 2325.
70. F. Seel and O. Detmer, Z. Anorg. Allgen. Chem., 1959, 301, 113.
71. C. Smith, Angew. Chem. Intern. Ed. Engl., 1962, 1, 467.
72. R. Tunder and B. Siegel, J. Inorg. Nucl. Chem., 1963, 25, 1097.



73. C.W. Tullock, D.D. Coffman and E.L. Muetterties, J. Am. Chem. Soc., 1964, 86, 357.
74. G.M. Begun, W.H. Fletcher and D.F. Smith, J. Chem. Phys., 1965, 42, 2236.
75. L.F. Drullinger and J.E. Griffiths, Spectrochim. Acta., 1971, 27(A), 1793.
76. (a) W.R. Hasek, W.C. Smith and V.A. Engelhardt, J. Am. Chem. Soc., 1960, 82, 543; (b) R.J. Harder and W.C. Smith J. Am. Chem. Soc., 1961, 83, 3422; (c) D.E. Applequist and R. Searle, J. Org. Chem., 1964, 29, 987; (d) W.R. Hasek, Org. Synth., 1961, 41, 104; (e) J. Tadanier and W. Cole, J. Org. Chem., 1961, 26, 2436; (f) W.C. Smith J. Am. Chem. Soc., 1960, 82, 6176.
77. (a) D.T. Sauer and J.M. Shreeve, J. Fluorine Chem., 1971/1972, 1, 1; (b) A.L. Opegard, W.C. Smith, E.L. Muetterties and V.A. Engelhardt, J. Am. Chem. Soc., 1960, 82, 3835; (c) R.D.W. Kemmitt and D.W.A. Sharp, J. Chem. Soc., 1961, 2496; (d) W.C. Smith and V.A. Engelhardt, J. Am. Chem. Soc., 1960, 82, 3838; (e) D.A. Jones, J. Cryst. Growth, 1976, 34, 149.
78. C.J. Schack, U.S. Patent, 3,649,222 (1972), C.A. 1972, 77, 22415.
79. H.L. Roberts, "Inorganic Sulphur Chemistry", Edited by G. Nickless, Elsevier Publishing Company, 1968, pp 420-454.
80. J.M. Shreeve, "Sulphur in Organic and Inorganic Chemistry", Edited by A. Senning, Marcel Dekker, INC., New York and Basel, Vol. 4, pp 131 - 191.

81. J. Steward, L. Kegley, H.F. White and G.L. Gard.,  
J. Org. Chem., 1969, 34, 760; H.W. Sidebottom, J.M.  
Tedder and J.C. Walton, J. Chem. Soc. Chem. Commun., (D),  
1970, 253; H.W. Sidebottom, J.M. Tedder and J.C. Walton,  
Trans. Faraday Soc., 1970, 66, 2038; R.E. Banks, R.N.  
Haszeldine and W.D. Morton, J. Chem. Soc., (C), 1969, 1947.
82. C.J. Schack, R.D. Wilson and M.G. Warner, J. Chem. Soc.  
Commun., 1969, 1110.
83. G. Kolta, G. Webb and J.M. Winfield, Applied Catal., 1982,  
2, 257.
84. A.K. Barbour, L.J. Belf and M.W. Buxton, "Advances in  
Fluorine Chemistry", M. Stacey, J.C. Tatlow, A.G. Sharp  
Eds., Vol. 3, Butterworths, London, 1963, pp 181 - 270.
85. G.G. Yakobson and V.M. Vlasov, Synth., 1976, 652.
86. J.J. Berzelius, Traite de Chemie, 1838, 1, 553.
87. I.L. Knunyants, O.A. Kildisheva and I.P. Detrov.,  
J. Ger. Chem., 1949, 19, 95; C.A. 1949, 43, 6163.
88. G.G. Yakobson, Ph.D. Thesis, Moscow, 1958; G.G.  
Yakobson and N.N. Vorozhtsov, Zh. Vses. Khim. Ova., 1961,  
6, 360, C.A., 1961, 55.27172.
89. G.G. Yakobson and N.E. Akhmetova, Synth., 1983, 169.
90. J.H. Clark, Chem. Rev., 1980, 80, 429.
91. I. Naray-Szabo, "Inorganic Crystal Chemistry", Published  
by Akademiai Kiado, Budapest, 1969, pp 192.
92. M. Hudlicky, "Chemistry of Organic Fluorine Compounds",  
2. Ed., Ellis Horwood Ltd., Halsted Press, J. Wiley and  
Sons, 1976, pp 24-35.
93. R.W.G. Wyckoff, Crystal Structures, 2 Ed. Vol 1,  
Interscience Publishers, J. Wiley & Sons, 1963, pp 85.

94. A.F. Wells, "Structural Inorganic Chemistry", 5 Ed., Clarendon Press, Oxford, 1984, pp 238 - 241.
95. H. Yasuda, H. Midorikawa and S. Aoyama, Sci. Papers. Inst. Phys. Chem. Res. Jpn., 1959, 53, 19; C.A. 1960, 54, 3192.
96. S. Kambe and H. Yasuda, Bull. Chem. Soc. Jpn., 1968, 41, 1444.
97. K. Midorikawa, S. Kambe and H. Yasuda, Japanese Patent., 1971, 7143368; C.A. 1972, 76, 45713.
98. R.H. Wollenberg and S.J. Miller, Tetrahedron Lett., 1978, 3219.
99. A.N. Nesmeyanov, K.A. Pecherskaya and G.Y. Uretskaya, Bull. Acad. Sci. U.R.S.S., Classe Sci. Chim., 1948, 240; C.A. 1948, 42, 4924.
100. N.N. Vorozhtsov and G.G. Yakobson, Zh. Obshch. Khim., 1958, 28, 40; C.A. 1958, 52, 12784
101. L. Rand, W. Wagner, P.O. Warner and L.R. Kovac, J. Org. Chem., 1962, 27, 1034.
102. D.J. Burton and F.E. Herkes, J. Org. Chem., 1968, 33, 1854.
103. H.J. Hagemeyer and M.B. Edwards, U.S. Patent, 1959, 2,899,413 C.A., 1959, 53, 23096; H.W. Cooper, U.S. Patent, 1962, 3,038,892; C.A. 1962, 57, 6142.
104. K. Okazaki, Makromol. Chem., 1961, 43, 74; K. Okazaki, Kogyo Kagaku Zasshi, 1962, 65, 966; C.A., 1963, 58, 4653.
105. N.L. Madison, British Patent, 1969, 1,141,265; C.A. 1969, 70, 69360.
106. C.I. Merrill, U.S. Patent, 1972, 3,658,872; C.A., 1972, 77, 101 176.
107. C.I. Merrill and N.L. Madison, U.S. Patent, 1970, 3,549,711; C.A., 1971, 74, 99456.

108. A.G. Pitman and W.L. Wasley, U.S. Patent, 1969, 3,484,470;  
C.A. 1970, 72, 43849.
109. D..E. Gould, L.R. Anderson, D.E. Young and W.B. Fox,  
J. Am. Chem. Soc., 1969, 91, 1310.
110. D.L. Cocke, E.D. Johnson and R.P. Merrill, Catal. Rev. Sci.  
Eng., 1984, 26, 163.
111. P. Ratnasamy and S. Sivasanker, Catal. Rev. Sci. Eng.,  
1980, 22, 401.
112. J.M. Thomas and R.M. Lambert, "Characterization of  
Catalysts", Wiley, New York, 1980.
113. H. Knozinger and P. Ratnasamy, Catal. Rev. Sci. Eng.,  
1978, 17, 31.
114. F.S. Stone, 'Chemistry and Chemical Engineering of  
Catalytic Processes', Ed. R. Prins and G.C.A. Schuit,  
(Nato. Adv. Study E39, 1980).
115. B.C. Gates, J.R. Katzer and G.A. Schuit, 'Chemistry of  
Catalytic Processes', McGraw - Hill Chemical Engineering  
Series, 1979, 184.
116. H. Topscoe, R. Candia, N.Y. Topscoe and B. Clausen,  
Bull. Soc. Chim. Belg., 1984, 93, 783.
117. T. Pasryjczak and P. Zienlinski , React. Kinet. Catal. Lett.,  
1982, 20, (3-4), 357; L. Gonzaler Tejuca, K. Alka, S.  
Namba and J. Turkevich, J. Phys. Chem., 1977, 81, 1399.
118. J.M. Zowtiak, G.D. Weatherbee and C.H. Bartholomew, J.  
Catal., 1983, 82, 230; G.D. Weatherbee and C.H. Bartholomew,  
J. Catal., 1984, 87, 55.
119. Z. Paal and P.G. Menon, Catal. Rev. Sci. Eng., 1983, 25(2),  
229.

120. R. Uma, R. Venkatachalam and J.C. Kuria c o s e . ,  
Catalysis, Proceedings of the 5th International Congress  
on Catalysis, Ed. J.W. Hightower, Elsevier Publishing  
Company, INC., Vol. 1, pp 11-245.
- 121 U. Steinike, Z. Anorg. Allg. Chem., 1965, 338, 78;  
V.A. Dzis'ho, M. Kolovertnova, T.S. Kinnikova and Y.O.  
Bulgakova, Kinet. Katal., 1966, 7, 655.
122. K. Pohl and G. Rubentisch, Chem. Technol., 1966, 18, 496;  
H. Duken, P. Fink and E. Pilz, ibid., 1966, 18, 490.
123. J.H. DeBoer, J.M.H. Fortuin, B.C. Lippens and W.H. Meijs,  
J. Catal., 1963, 2, 1.
124. G.M. Schwab and H. Kral, "Proc. 3rd Catal", Vol. 1,  
1965, p 433.
125. J.A.N. Scott, B.D. Flockhart and R.C. Pink, Proc. Chem.  
Soc., 1964, 139.
126. B.D. Flockhart, C. Naccake, J.A.N. Scott and R.C. Pink,  
J. Chem. Soc. Chem. Commun., 1965, 238.
127. (a) J.J. Kipling, D.B. Peakall, J. Chem. Soc., 1957, 834;  
F.C. Frany, Ind. Eng. Chem., 1946, 38, 129; (b) H.P.  
Rooksby, 'X-Ray Identification and Crystal Structure of Clay  
Minerals', the Mineralogical Soc. London, 1951.
128. H. Krishner, Ber. dt. Keram. Ges., 1966, 43, 479.
129. B.C. Lippens and J.J. Steggerdo 'Physical and Chemical  
Aspects of Adsorbents and Catalysts', London, New York,  
Academic Press, 1970, pp 171.
130. B.C. Lippens, "Structure and Texture of Aluminas", Thesis,  
Delft University of Technology, The Netherlands, 1961.
131. H. Saalfed, Neues Jb. Miner. Abh., 1960, 95, 1.

132. L.L. van Reijen, Thesis, Technical University of Eindhoven, The Netherland, 1964.
133. C.S. John and M.S. Scurrrell, "Catalysis Specialist Periodical Reports", Vol. 1. Chemical Society, London, 1977, p 136.
134. H. R. Gerberich, F.E. Lutinski and W.K. Hall, J. Catal 1966, 6, 209.
135. F.P.J.M. Kerkhof, J.C. Oudejans, J.A. Moulijn and E.R.A. Matulewicz, J. Colloid Interface Sci., 1980, 77, 120.
136. A.K. Ghosh, and R.A. Kydd, Catal. Rev. Sci. Eng., 1985, 27, 539.
137. J.M. Melot, F.T. Boulet and A. Foucaud, Tetrahedron, 1988, 44, 2215.
138. F.A. Cotton and G. Wilkinson, 'Advanced Inorganic Chemistry', J. Wiley and Sons, 4th Ed., 1980, 329.
139. L.E. Oomes, J.H. deBoer and B.C. Lippens, 'Reactivity of Solids', Editor J.H. deBoer, Elsevier, Amsterdam, 1961, pp 317 - 320.
140. B.C. Lippens, Chem. Weekbl., 1966, 62, 336.
141. M.K.B. Day and V.J. Hill, J. Phys. Chem., 1953, 57, 946; J.F. Brown, D. Clark and W.W. Elliott, J. Chem. Soc., 1953, 84; H. Krishnaer, Ber. dt. Keram. Ges., 1966, 43, 479.
142. A.F. Wells, 'Structural Inorganic Chemistry' 3rd Ed., Oxford Press, London, 1962, 556.
143. H. Jagodzinski and H. Saalfeld, Z. Kristallogr., 1958, 110, 197.
144. B. Peri, J. Phys. Chem., 1965, 69, 211-239.
145. S. Soled, J. Catal., 1983, 81, 252; H. Kawakami and S. Yoshida, J.Chem.Soc.Faraday Trans II, 1985, 81, 1129.

146. G.H. Posner, Angew. Chem. Int. Ed. Engl., 1978, 17, 487-496; D.C. Bailey and S.H. Langer, Chem. Rev., 1981, 81, 109-148.
147. P. Laszlo, Acc. Chem. Rev., 1986, 19, 121.
148. J. Yamawaki and T. Ando, Chem. Lett., 1979, 755.
149. J.H. Clark, D.G. Cork and H.W. Gibbs, J. Chem. Soc. Perkin Trans. I., 1983, 2253.
150. G. Rosini, E. Marotta, R. Ballini and M. Petrini, Synthesis, 1986, 237.
151. D.E. Bergbreiter and J.J. Lalonde, J. Org. Chem., 1987, 52, 1601.
152. G.G. Rao, Synth. Commun., 1982, 12, 177; D. Villemin, J. Chem. Soc Chem. Commun., 1983, 1092; D. Villemin, Chem. Ind. (London), 1985, 166; A. Benalloum and D. Villemin, Synth. Commun., 1989, 19, 2567.
153. T. Ando, S.J. Brown, J.H. Clark, D.G. Cork, T. Hanafusa, J. Ichihara, J.M. Miller and M.S. Robertson, J. Chem. Soc. Perkin Trans. II, 1986, 1133.
154. L.M. Weinstock, J.M. Stevenson, S.A. Tomellini, S.H. Pan, T. Utne, R.B. Jobson and D.F. Reinhold, Tetrahedron Lett., 1986, 27, 3845.
155. T. Ando, J.H. Clark, D.G. Cork, T. Hanafusa, J. Ichihara and T. Kimura, Tetrahedron Lett., 1987, 28, 1421.
156. R.I. Hedge and M.A. Barteau; J. Catal, 1989, 120, 387; V. R. Choudhary, Ind. Eng. Chem. Prod. Res. Dev., 1977, 16, 14.
157. D.G. McBeth, Ph.D. Thesis, Glasgow University, 1987.
158. L. de Broglie, Philos. Mag., 1924, 47, 446.

159. E. Ruska, Z. Phys., 1934, 87, 580; J. Hillier and F.G. Ramberg, J. Appl. Phys., 1947, 18, 48.
160. J.M. Winfield, J. Fluorine Chem., 1984, 25, 91.
161. M. Walter and L. Ramaley, Anal. Chem., 1973, 45, 165.
162. C.J. Schack and R.D. Wilson, Synth. React. Inorg. Met. Org. Chem., 1973, 3, 393.
163. H. Schmitz and H.J. Schumacher, Z. Naturforsch A., 1947, 2, 359.
164. C. M. Suter, E.J. Lawson and P.G. Smith, J. Am. Chem. Soc., 1939, 61, 161.
165. D.W.A. Sharp, Adv. Fluorine Chem., 1960, 1, 68.
166. G.C. Finger and R.F. Oesterling, J. Am. Chem. Soc., 1956, 78, 2593.
167. G. Balz and G. Schiemann, Ber., 1927, 60, 1186.
168. J. Vanderryn, J. Chem. Phys., 1959, 30, 331; B.P. Susz and J.J. Wuhrmann, Helv. Chim. Acta, 1957, 40, 722.
169. F. Moissan, Bull. Soc. Chim. France, 1930, 3, 29.
170. G. Kolta, G. Webb and J.M. Winfield, J. Fluorine Chem., 1981/1982, 19, 89.
171. J.E. Griffiths, Spectrochim. Acta, Part A., 1967, 23, 2145.
172. F.S. Fawcett, C.W. Tullock and D.D. Coffman, J. Am. Chem. Soc., 1962, 84, 4275.
173. P.D. Mallinson, D.C. McKean, J.H. Holloway and I.A. Oxtan, Spectrochim Acta., 1975, 31A, 143.
174. C.W. Tullock and D.D. Coffman, J. Org. Chem., 1960, 25, 2016.
175. J.K. O'Loane and M.K. Wilson, J. Chem. Phys., 1955, 23, 1313.
176. H.M. Haendler, F.A. Johnson and D.S. Crocket, J. Am. Chem. Soc., 1958, 80, 2662.



177. R. Stodolski and L. Kolditz, Z. Chem., 1986, 26, 187.
178. Joint Committee on Powder Diffraction Standards. File No. 3-615 Fiche No. I-12-E9.
179. Joint Committee on Powder Diffraction Standards. File No. 3-122. Fiche No. I-11-D4
180. Joint Committee on Powder Diffraction Standard. File No. 14-69. Fiche No. I-56-E12.
181. Joint Committee on Powder Diffraction Standard. File No. 20-77. Fiche No. I-117-E10.
182. F. Joliot and I. Curie, Nature, 1934, 133, 201.
183. M.F. Dove and D.B. Sowerby, "Halogen Chemistry", V. Gutman Ed., Academic Press, London, New York, 1967, 1, 41.
184. G.T. Seaborg, Chem. Rev., 1940, 27, 199.
185. G. Hevesy, Trans. Faraday Soc., 1938, 34, 841.
186. H.A.C. McKay, Nature, 1938, 142, 997.
187. R.M. Adams, R.B. Bernstein and J.J. Katz, J. Chem. Phys., 1954, 22, 13.
188. C.J.W. Fraser, D.W.A. Sharp, G. Webb and J.M. Winfield, J. Chem. Soc. Dalton Trans, 1972, 2226.
189. J.D. Mahoney and S.S. Markowitz, J. Inorg. Nucl. Chem., 1964, 26, 907.
190. A.H. Snell, Phys. Rev., 1937, 51, 143.
191. A.F. Cotton and G. Wilkinson 'Advances in Inorganic Chemistry', 5th Ed, Wiley Interscience, New York, 1988, p. 546; J.M. Winfield, J. Fluorine Chem., 1980, 16, 1.
192. J.P. De Kleijn, J. Fluorine Chem., 1977, 10, 341.
193. J. Nazoki, M. Iwamoto and T. Ido, Int. J. Appl. Radiat Isolt, 1974, 25, 393.

194. R.J. Nickles, R.D. Hichwa, M.E. Doube, G.D. Hutchins and D.D. Congdon, Int. J. Appl. Radiot. Isot., 1983, 34, 625.
195. R.M. Lambrecht, R. Neisinckx and A.P. Wolf, Int. J. Appl. Radiot Isot., 1978, 29, 175.
196. G. Nickless, 'Inorganic Sulphur Chemistry', Elsevier Publ. Comp. (G. Nickless, ed), London, 1968, p.4.
197. E.S. Woodhouse and T.H. Norris, J. Inorg. Nucl. Chem., 1968, 30, 1373.
198. G. Friedlander, J.W. Kennedy, E.S. Macias and J.M. Miller, Nuclear and Radiochemistry, 3rd ed., 1981, Wiley Interscience, New York.
199. A.S. Al-Ammar and G. Webb, J. Chem. Soc. Faraday, Trans I, 1978, 74, 195.
200. D.K. Padma, J. Fluorine Chem, 1974, 4, 441.
201. M. Azeem and R.J. Gillespie, J. Inorg. Nucl. Chem., 1966, 28, 1791.
202. R.B. Bernstein and T.I. Taylor, Science, 1947, 106, 498.
203. W. Kwasnik, 'Handbook of Preparative Inorganic Chemistry' Ed. G. Brauer, Vol. 1, Academic Press (London) Ltd, London 2nd Ed., 1963, p. 208.
204. M.E. Redwood and C.J. Willis, Can. J. Chem., 1967, 45, 389.
205. D.A.C. Compton, J.D. Goddard, S.C. Hsi, W.F. Murphy and D.M. Rayner, J. Phys. Chem., 1984, 88, 356.
206. G.A. Kolta, G. Webb and J.M. Winfield, J. Fluorine Chem, 1979, 14, 331.
207. T. Takeuchi, D. Myatani, Y. Takoda and K. Okamoto, J. Phys. Chem, 1972, 76, 2625.
208. I. Langmuir, J. Am. Chem. Soc., 1916, 38, 2221.

209. S. Brunauer, P.H. Emmett and E. Teller, J. Am. Chem. Soc., 1938, 60, 309.
210. R. Staritzky and S. Asprey, Anal. Chem., 1957, 29, 984.
211. National Bureau of Standards (U.S) Mono. 25 Sect. 3 (1964).
212. Suranson and Tatge, J.C. Fel. Reports, NBS, 1950.
213. R. McMillan, J.S. Brinen and G.L. Haller, J.Catal., 1986; 97, 243; G.L. Haller, M. McMillan and J.B.J.S. Brinen, J.Prep. Div. Pet. Chem. Am. Chem. Soc., 1984, 29, 939; B.C. Gerstein, Anal. Chem., 1983, 55, 781A, 899A.
214. D. Muller, W. Gessner, H.J. Berens and G. Scheller, Chem. Phys. Lett., 1981, 59; J.J. Depuech, in "NMR" of Newly Accessible Nuclei," P. Laszlo, Ed. Vol.2, P153, Academic Press, New York, 1983.
215. T. Birchall and J. Gillespie, Spectrochim. Acta, 1966, 22, 681.
216. D. F. Burow, Inorg. Chem., 1972, 11, 573.
217. E. A. Robinson, D.S. Lavery and S. Weller, Spectrochim. Acta., 1969(A), 25, 151.
218. B.S. Ault, J. Phys. Chem. 1980, 84 3448.
219. B.S. Ault, Inorg. Chem., 1982, 21, 756.
220. C.J.W. Fraser, D.W.A. Sharp, G. Webb and J.M. Winfield, J. Chem. Research (m), 1978; 0311.
221. S.B.H. Bach and B.S. Ault, Inorg. Chem., 1984, 23, 4394.
222. K.W. Dixon and J.M. Winfield, J. Chem. Soc. Dalton t Trans., 1989, 937.
223. R.L. Redington, J. Phys. Chem., 1982, 86, 552.
224. J.W. Larson and T.B. McMahon, J. Am. Chem. Soc., 1983, 105 2944.
225. J.C. Haartz and D.H. McDanial, J. Am. Chem. Soc., 1973, 95 8562.

226. T.B. McMahon and C.J. Northcot, Can. J. Chem., 1978, 56, 1069.
227. G. Glockler, "Fluorine Chemistry", Ed. J.H. Simons, 1950, Vol. I, pp 319-368 Academic Press INC, Publishers New York, N.Y.
228. K.W. Nam and G.R. Gavalas, Applied Catal., 1989, 55, 193.
229. F.A. Cotton and R. Francis, J. Am. Chem. Soc., 1960, 82, 2986.
230. F. Solymosi, A. Erdohelyi, and M. Lancz, J. Catal., 1985, 95, 567.
231. E. Susan, PhD Thesis, University of Glasgow, 1986.
232. H.J. Emeleus, "Fluorine Chemistry", Ed. J.H. Simons, 1950, Vol. I, pp 1-72 Academic Press INC, Publishers New York.
233. I. Tananav, Bull. Acad. Belg., 1985, 29, 874.
234. K.W. Dixon, M.F. Ghorab, and J.M. Winfield, J. Fluorine Chem., 1987, 37 357.
235. B.S. Ault and L. Andrews, Inorg. Chem., 1977, 16, 202.

